FABRICATION OF POLYMER-METAL NANOCOMPOSITES WITH COMPLEX POLYMERIC MATRICES FOR BACTERICIDAL AND CATALYTIC APPLICATIONS

BERTA DOMÈNECH GARCIA

March 2014

Fabrication of polymer-metal nanocomposites with complex polymeric matrices for bactericidal and catalytic applications.

Berta Domènech Garcia

Tesi Doctoral

Doctorat en Química

Directors: Maria Muñoz Tapia, Dmitri N. Muraviev, Jorge Macanás de Benito

Departament de Química
Facultat de Ciències

2014

Memòria presentada per aspirar al Grau de Doctor per

Berta Domènech Garcia

Vist i plau

Dra. Maria Muñoz Tapia **Dr. Dmitri N. Muraviev** **Dr. Jorge Macanás de Benito**

Bellaterra (Cerdanyola del Vallès), 27 de març de 2014

Un tesi és un treball ple de mans implicades.

L'esforç de tots i cadascun dels que hem aconseguit que tiri endavant.

Que demostra que entre tots, podem.

Que demostra que entre tots, sumem.

Aquesta tesi és, per tant, un treball ple de gratitud a les mans implicades.

A TU. GRÀCIES.

This work presented here has been possible thanks to the project *Nuevo material nanocomposite para el tratamiento combinado de aguas*. (ACC1Ó, *Departament d'Innovació, Universitats i Empresa de la Generalitat de Catalunya*, Spain) (VALTEC-09-2-0056), developed under the supervision of Dr. Dmitri Muraviev, Prof. Maria Muñoz Tapia and Dr. Jorge Macanás de Benito, and executed within *Grup de Tècniques de Separació* and *Grup de Sensors i Biosensors* from the *Departament de Química* (Universitat Autònoma de Barcelona, Barcelona, Spain).

Part of this work has also been possible thanks to the financing received during a 3 month PhD stage by the group headed by Prof. Jean-François Lahitte and Prof. Jean-Christophe Remigy in the Department of *Génie des Interfaces & Milieux Divisés* in the *Laboratoire de Génie Chimique* (Université Toulouse III, Paul Sabatier, Toulouse, France).

Special thanks are given to Prof. Jordi Mas and MSc. Núria Vigués from *Departament de Genètica i Microbiologia* (Universitat Autònoma de Barcelona, Barcelona, Spain) and to Prof. Fernando Carrillo from *Institut d'investigació Tèxtil i Cooperació Industrial de Terrassa* (INTEXTER) (Universitat Politècnica de Catalunya, Terrassa, Spain) for their specific collaborations in different parts of the work.

A muns pares.

General Index i
Abbreviations v
Resum ix
Summary x

GENERAL INDEX

1 INTRODUCTION 1
1.1. Green Chemistry 2
1.2. Nanotechnology 3
1.2.1. Historical evolution 4
1.3. Nanoobjects and Metal Nanoparticles 7
1.3.1. General properties of MNPs 8
1.3.2. Synthetic methods 9
1.3.2.1. Stability challenge 13
1.3.2.2. Toxicity concerns 14
1.3.2.3. Stability agents and the “polymeric solution” 15
1.4. Intermatrix Synthesis 19
1.4.1. General principles 19
1.4.2. Requirements of the parent polymers: limitations 24
1.4.3. Precursor-matrix interactions 24
1.5. Polymeric matrices 31
1.5.1. Polymeric films 32
1.5.1.1. Nafion 39
1.5.1.2. Poly(arylsulfones) 42
1.5.2. Polyurethane foams 46
1.5.3. Textile fiber polymers 47
1.6. Polymer-metal nanocomposites 50
1.6.1. Nanocomposite films 51
1.6.1.1. Nafion nanocomposites 51
1.6.1.2. Poly(arylsulfones) nanocomposites 52
1.6.2. Nanocomposite polyurethane foams 52
1.6.3. Nanocomposite textile fibers 53
1.7. Nanocomposite characterization techniques 53
1.8. Nanocomposite Applications 57
1.8.2. Fuel cells 60
1.8.3. Amperometric sensors 62

1.8.4. Water treatment 64
1.8.4.1. Catalytic degradation of toxic compounds in water 64
1.8.4.2. Bactericidal and anti-biofouling applications 67
1.9. References 69

2 OBJECTIVES 85

3 RESULTS AND DISCUSSION 87
3.1 Synthesis, adequacy and characterization of the polymeric Matrices 90
3.1.1. Synthesis and characterization of polymeric films 91
3.1.1.1. Sulfonated and non sulfonated PPSU 91
3.1.1.2. Sulfonated and non sulfonated PES-C 94
3.1.2. Nafion films 108
3.1.3. Adequacy and characterization of polyurethane foams 109
3.1.4. Textile fibers 113
3.2 Synthesis and characterization of Nanocomposites containing Polymer Stabilized Metal Nanoparticles 113
3.2.1. Synthesis and characterization of Nanocomposite polymeric films 113
3.2.1.1. Synthesis and characterization of PdNPs in polymeric films 113
3.2.1.2. Synthesis and characterization of AgNPs in polymeric films 121
3.2.1.3. Stability of the AgNPs in polymeric films 124
3.2.1.4. Unexpected patterns in Nafion films 127
3.2.2. Synthesis and characterization of Nanocomposite Polyurethane foams 131
3.2.2.1. Synthesis and characterization of AgNPs in Polyurethane foams 131
3.2.2.2. Stability of the AgNPs in Polyurethane foams 133
3.2.3. Synthesis and characterization of Nanocomposite Textile fibers 136
3.2.4. Comparison of the NCs developed 141
3.3 Nanocomposite applications 142
3.3.1. Catalytic reduction of nitroaromatic compounds in water 143
3.3.1.1. Palladium-nanocomposite polymeric films 143
3.3.1.2. Silver-nanocomposite polymeric films 151
3.3.1.3. Silver-nanocomposite polyurethane foams 154
3.3.1.4. Silver-nanocomposite textile fibers 159
3.3.1.5. Comparison of the Catalytic performance of the NCs developed 160
3.3.2. Bactericidal and anti-biofouling applications 161
3.3.2.1. Silver-nanocomposite polymeric films 163

3.3.2.2. Silver-nanocomposite polyurethane foams 165
3.3.2.3. Comparison of the bactericidal performance of the developed NCs 166
3.4 References 167

4 CONCLUSIONS 175

ANNEX A

A1. Catalysis Today (2012), 193, 1, 158-164.
A2. Procedia Engineering (2012), 44, 1264-1267.
A3. Ion Exchange Technologies (2012), InTech.
A4. Nanoscale Research Letters (2013), 8, 238.
A5. Solvent Extraction and Ion Exchange (2013), (In press)
A6. Nanocomposites: Synthesis, Characterization and Applications (2013), Nova Science Publishers, Inc.
A7. Microbial pathogens and strategies for combating them science, technology and education (2013), FORMATEX Research Center.

ANNEX B

B1. Nanoscale Research Letters (2011), 6, 406.
B2. Chemical Communications (2014), (In press)
B3. Polymers for advanced technologies, (Submitted)

ABBREVIATIONS

4-ap	p-aminophenol
4-np	p-nitrophenol
AgNP	silver nanoparticle
BM	blend membrane
CA	cellulose acetate
CFU	colony forming unit
COC	chlorinated organic compound
COT	cotton
DEE	Donnan exclusion effect
DMF	N,N-dimethylformaide
DMSO	dimethyl sulfoxide
EW	equivalent weight
FTIR-ATR	Fourier Transform Infrared Attenuated Reflectance spectroscopy
GECE	graphite-epoxy composite electrodes
ICP-AES	Inductively Coupled Plasma Atomic Emission Spectroscopy
ICP-MS	Inductively Coupled Plasma Mass Spectroscopy
IEC	ion exchange capacity
IMS	Intermatrix Synthesis
Lp	hydraulic permeanility
LR	Liesegang rings
MNP	metal nanoparticle
MOF	metal-organic framework
MWU	matrix water uptake
NC	nanocomposite
NMP	N-methylpyrolidone

NMR	Nuclear magnetic resonance spectroscopy
NP	nanoparticle
P	pressure
PA	polyamide
PAN	polyacrylonitrile
PCB	polychlorinated biphenyl
PdNP	palladium nanoparticle
PEMFC	proton exchange membrane fuel cells
PES	polyethersulfone
PES-C	polyethersulfone with Cardo group
PET	polyester
PMNC	polymer-metal nanocomposite
POMs	polyoxometalate
POSS	polyhedral oligomeric silsesquioxane
PPSU	polyphenylsulfone
PSMNP	polymer-stabilized metal nanoparticle
PSU	polysulfone
PTFE	polytetrafluoroethylene
PU	polyurethane
PUFs	polyurethane foams
PVP	poly(N)vinyl-2-pyrrolidone
SAXS	small-angle X-ray scattering
SCF	supercritical fluid
SD	sulfonation degree
SEM	Scanning Electron Microscopy
SPEEK	poly(etherether ketone)
SPES-C	sulfonated polyethersulfone with Cardo group

SPPSU	sulfonated polyphenylsulfone
T	temperature
TCE	trichloroethylene
TEM	Transmission Electron Microscopy
T_g	glass transition temperature
UAB	Universitat Autònoma de Barcelona
UPC	Universitat Politècnica de Catalunya
WAXS	wide-angle X-ray scattering

RESUM

D'una manera general, el present treball està enfocat a l'obtenció i l'estudi de nous materials útils per al tractament combinat d'aigües, és a dir, materials capaços d'aconseguir diferents objectius al tractar l'aigua en un sol pas. Aquest propòsit sembla un nínxol d'aplicació molt adient per als materials de mida nanoscòpica, donades les inusuals propietats catalítiques i bactericides que presenten com a conseqüència de la seva mida. No obstant, els nanomaterials, i en especial les nanopartícules metàl·liques (*metal nanoparticles,* MNPs), també tenen limitacions i poden plantejar certs riscos. És per això que cal buscar mecanismes que en garanteixin la seva estabilització, la qual es considera un pas previ clau per la seva manipulació i aplicació futura. Durant els darrers anys s'ha demostrat que l'estabilització de les MNPs en matrius polimèriques permet el desenvolupament de nous materials polimèrics nanocompòsits en els quals les espècies reactives estan altament estabilitzades al temps que s'aconsegueix una fàcil manipulació del conjunt. Des d'un punt de vista pràctic, tant l'elecció com l'adequació de la matriu polimèrica juguen un paper molt important doncs sovint la matriu ha de servir simultàniament de medi de síntesi i d'estabilitzant.

Així, en el present estudi s'ha considerat essencial obtenir, modificar o utilitzar directament diverses matrius polimèriques en la forma de pel·lícules i membranes, espumes i fibres tèxtils, capaces d'incorporar MNPs (concretament de de pal·ladi o plata) mitjançant la metodologia sintètica de la Síntesi Intermatricial (IMS), que inclou dos processos *a priori* senzills: la càrrega del precursor en la matriu polimèrica i la transformació del precursor en nanopartícula (normalment gràcies a una reacció de reducció).

Per a fer-ho, d'una banda s'ha dut a terme la modificació de matrius polimèriques existents (p.e. poliètersulfona tipus Cardo) mitjançant reaccions senzilles de sulfonació amb la finalitat d'aportar els grups ionogènics considerats necessaris per aconseguir la càrrega dels precursors (ions metàl·lics o complexos iònics). D'altra banda, i com a novetat en l'aplicació de la IMS, s'han provat matrius sense grups iònics (com ara espumes de poliuretà i fibres tèxtils), a fi d'avaluar l'aplicabilitat i l'abast real de la tècnica. Els resultats obtinguts han mostrat que és possible sintetitzar AgNPs i PdNPs (tot i que no sempre amb la mateixa quantitat, distribució o mida) en totes les matrius assajades mantenint-ne les propietats inicials.

Allò que es pot considerar com és més interessant és que s'ha demostrat que gairebé la totalitat dels diferents materials desenvolupats ofereixen les desitjades funcionalitats tant en aplicacions catalítiques (més concretament en l'eliminació de compostos nitroaromàtics de l'aigua) com en bactericides (en l'eliminació d'*Eschericha coli* de solucions aquoses).

Finalment, cal remarcar que la caracterització dels nanocompòsits obtinguts en una de les matrius utilitzades (Nafion 117) ha permès aportar nous coneixements en relació a la seva estructura interna, la qual cosa és de gran interès donat que és un material d'altes prestacions i àmpliament utilitzat, per exemple en piles de combustible de membrana polimèrica.

SUMMARY

In general terms, this work is focused on the obtainment and study of new materials useful for the combined treatment of water, it is to say, materials able to achieve different goals when treating water in one single step. In fact, such application seems to the perfect niche for nanosized materials, given their unusual catalytic and bactericidal properties, arising from their size. However, nanomaterials and particularly metal nanoparticles (MNPs) also hold some limitations and may pose certain risks. It is therefore necessary to seek mechanisms that allow guaranteeing their stabilization, which is considered a crucial key point for its future application and handling. Over the past years, it has been shown that the stabilization of MNPs in polymeric matrices allows the development of new polymeric nanocomposites in which the reactive species are highly stabilized while their easy manipulation is achieved. Besides, from a practical point of view, both the choice and the suitability of the polymer matrix play an important role in the development of such nanocomposites, because the matrix is often used simultaneously as a mean for synthesis and stabilization.

Thus, in this study it has been considered essential to obtain, modify, or directly use several polymeric matrices in the form of films and membranes, foams and textile fibers, capable of incorporating MNPs (specifically those made of palladium or silver) by the Intermatrix Synthesis (IMS) procedure, which includes two *a priori* simple processes: the loading/binding of a precursor in the polymer matrix and the transformation of such precursor into nanoparticles (usually through a reduction reaction).

To do so, on one hand the modification of existing polymeric matrices (e.g. polyethersulfone with Cardo group) by simple sulfonation reactions was carried out in order to provide the ionogenic groups, considered necessary to achieve the loading of the MNPs precursors (i.e. metal ions or ionic complexes). Moreover, and as a novelty in the implementation of the IMS, some matrices (such as polyurethane foam and textile fibers) without ionic groups were also tested, so as to assess the real applicability and scope of the technique. The obtained results have shown that it is certainly possible to synthesize AgNPs and PdNPs in all the matrices tested (though not always with the same amount, or size distribution) maintaining their initial properties.

Anyway, what can be considered as the most interesting result is that almost all the different developed materials have exhibited the desired functionality in both catalytic (specifically, the removal of nitroaromatic compounds in water) and bactericidal applications (in the disinfection of *Escherichia coli* from aqueous solutions).

Lastly, it is important to mention that the characterization of the obtained nanocomposites for one of the matrices used (Nafion 117), has shed some light about its internal structure, which is of great interest as this matrix is a high performance material, widely used, for example, in polymeric membrane fuel cells.

> *There's plenty of room at the bottom.*
> (R. Feynman)

1 INTRODUCTION

The present work is focused on the obtainment and optimization of new systems for wastewater treatment and for catalytic purposes via the development of polymer-metal nanocomposites (PMNCs) with biocide and/or catalytic activity. Since a multidisciplinary approach has been essential to carry out this work, I have considered necessary to provide the reader with an overview of concepts involved. Therefore, this chapter is an attempt to establish the basis so as to further discuss and understand all the different parts implied in the whole study.

Up to now, research in nanosized materials (especially in metal nanoparticles (MNPs)) is in a moment of maximum interest, since due to their unusual electrical, optical and catalytic properties they offer new features differing from both macroscopic materials and isolated atoms.[1] However, within these interesting features there is also a high reactivity, what makes nanoparticles to have a high tendency to self-aggregate and form larger particles, therefore losing the special properties arising from their size. For this reason MNPs stabilization is considered as an important prelude to possible manipulation and further application. In this sense, stabilization of MNPs in polymeric matrices allows the development of new

nanocomposite polymeric materials in which the reactive species are highly stabilized while manipulation is facilitated and the escape to the media controlled.

Nevertheless, from a practical point of view, the development of these new materials become meaningless without a future clear application, since this future application will dictate some of the main requirements of the nanocomposite. In this regard the choice and adequacy of the polymeric matrix play an important role, as it will be explained during the present work. Moreover, thanks to the actual social concerning for the planet, several aspects related to green chemistry thinking are increasingly involved in the development of nanocomposites and have to be taken into account.

1.1. Green Chemistry

Over the last decades of this 21st century a great consideration for the limited resources of the planet has begun. Growing demand for energy, food and materials have put increasing pressure on air and water, arable land, and raw materials. Concern over the ability of natural resources and environmental systems to support the needs and wants of global populations, now and in the future, is part of an emerging awareness of the concept of sustainability.[2] Under this context, it is widely acknowledged that there is a growing need for more environmentally-friendly processes and products. For this reason, the scientists are taking much of the leadership by applying eco-friendly thinking to different topics, such as energy production, global warming, development of clean industrial processes, and so on.[3]

In the chemistry field, this eco-friendly thinking is the so-called Green Chemistry, also known as Sustainable Chemistry, and which consists on the use and development of chemicals and chemical processes in order to reduce or eliminate negative environmental impacts, involving the reduction of waste products, the use of non-toxic components, and the improvement of efficiency.[4, 5] In this sense, the bases of Green Chemistry are being established giving a highly effective approach to problems such as pollution prevention as it applies innovative scientific solutions to real environmental concerns. Thus, Green Chemistry is not only focused in minimizing the potential negative impact of those procedures, but it must also be an additional objective for the general optimization of processes and products. So, in short, the main guiding principle of Green Chemistry is the design of environmentally benign products and processes (*benign by design*).

This concept is embodied in the 12 principles of Green Chemistry[6] which are summarized in **Figure 1.1**, in which the ones highlighted in blue are tackled at more or less extent by the materials and processes of the present thesis.

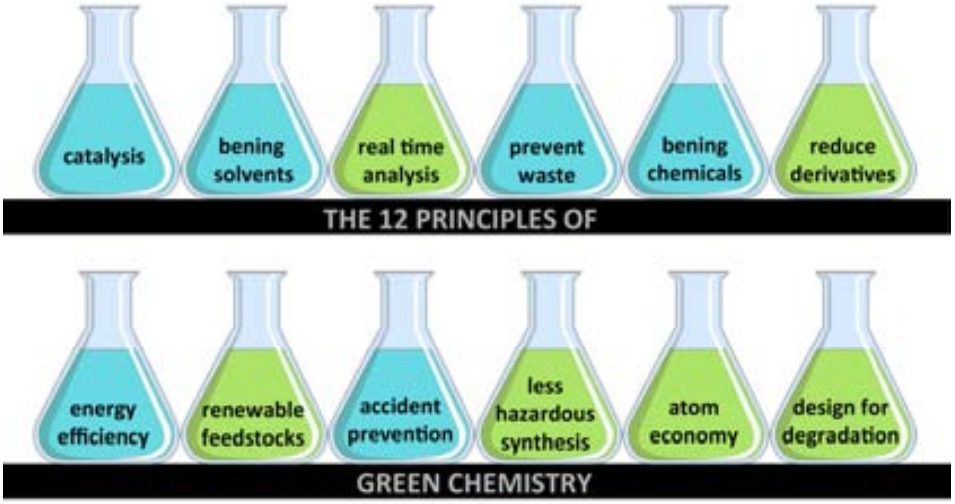

Figure 1.1. The 12 principles of the Green Chemistry.

Just to mention some examples of what Green Chemists are looking for:[7]

- cleaner fuels: free of aromatics, with minimal sulfur content or even those ones converting chemical energy directly to electricity, without production of noxious oxides and particulates;
- solvent-free processes;
- processes preferably using air as oxidant;
- one-step processes in the chemical, petrochemical and pharmaceutical industry;
- industrial processes that minimize consumption of energy, production of waste, or the use of corrosive, explosive, volatile, and non-biodegradable materials.

Some of these needs could be achieved by the use of nanomaterials, since the development of Nanotechnology presents a unique opportunity to offer more sustainable approach such the design of appropriate catalysts; the use of more environmentally friendly low cost species, with high efficiency and that allow an easy separation from the reaction media and the possibility to reuse the catalytic specie without incurring in a loss of the catalytic efficiency;[1] the use of membranes that can help separating the desired chemical reaction products from waste materials; the development of sensors and biosensors with enhancement of both the rate of mass transfer and in the electrocatalytic activity;[8] or the use of alternative energy systems.

1.2. Nanotechnology

Nanotechnology is understood as the study and manipulation of matter on an atomic and molecular scale. In an early definition, Nanotechnology was referred to the fabrication of macroscale products by precisely manipulate atoms and molecules.[9] Up to now, this definition

has been updated, and a more generalized description of Nanotechnology defines it as the manipulation of matter which has at least one dimension sized from 1 to 100 nanometers (nm).[10]

Thus, the principal being of Nanotechnology involves the development of materials, structures, systems and devices which combine the desired properties and functionalities of nanosized building blocks. Under this essence, it comes clear that many scientific disciplines are involved, but, among them, Chemistry and Physics establish the fundamental principles for the development of such materials. In particular, Surface Science has made a giant leap forward thanks to the special properties of nanoscale materials, since when decreasing the particle size, the ratio of surface atoms to volume increase, thus surface effects become much more significant.[11]

1.2.1. Historical evolution

Although Nanotechnology is a relatively new scientific discipline, when doing some research in its historical evolution, it comes clear that the development of its central concepts had happened over a long period of time.

It is not clear when humans first began to take advantage of nanosized materials but it is known that in the 4th century A.D. Roman glassmakers fabricated glasses containing metals in the nanoscale. A clear example of this fact is the *Lycurgus cup* (in British Museum of London), made of soda lime glass which is able to change its colours depending on the incident light: in reflected light the glass turns green, but when the light is shone directly through it, it turns red due to the presence of small amount of silver and gold nanoparticles with diameters of approximately 70 nm.[12] Nevertheless, it was not until the mid-16th century when the potential importance of clusters was first recognized by the chemist Robert Boyle in his *Sceptical Chymist* published in 1661, in which the author criticized the Aristotle's belief of matter composed for four elements: earth, fire, water and air. Instead, Boyle suggested that matter was formed by tiny particles of which combine in various ways forming "corpuscles".[13]

After that, other examples of applications of nanoscale materials (metal colloids) can be found. As a remarkable example, between the 18th and 19th centuries the appearance and development of Photography started creating its own magic. In its beginnings, and after several efforts searching for the perfect photosensible emulsion, photographic films were based on a thin layer of gelatin with supported silver halides (such as AgBr) and a thin layer of transparent cellulose acetate. With the incident light, the halides decomposed producing silver nanoparticles (AgNPs) which were the "pixels" of the photographic image. Around 1883 the

american inventor George Eastman (who later founded the Kodak Corporation) produced the first long flexible photographic film with a paper strip coated with a similar emulsion (with silver halides) what finally made photography really accessible to many.[14]

Although the first reports of cluster species date back from the 1940s,[15] the systematically study of finite aggregates from a few to tens of thousands of atoms that are bounded by different forces (such as metallic, covalent, ionic, hydrogen-bonded or Van der Waals) did not emerged as a separate discipline until the 1980s. Cluster Science was born focusing much of the research in the field in the study of the gradual development of collective phenomena for characterizing a bulk solid. Later on, during the first decade of the 20th century, the advances in interface and colloid science propitiated a great leap forward to the field with the first observations and size measurements of nanoparticles.

Nevertheless, the first observations of the nanometer started earlier. Richard Adolf Zsigmondy was the very first to characterize particles in the range of nanometers in 1914. He made a detailed study of gold sols and other nanomaterials with sizes down to 10 nm using an ultramicroscope capable of visualizing particles much smaller than the light wavelength.[16] In the 1920s, Irving Langmuir and Katharine B. Blodgett introduced the concept of monolayer, a layer of material one molecule thick. And in the early 1950s, Derjaguin and Abrikosova conducted the first measurement of surface forces.[17]

Anyway, it is possible to state that the fundamentals of modern Nanoscience and Nanotechnology date back from the mid-20th century, when scientists began to be aware of the exceptional properties that such materials could have.

In this sense what we can consider as the first inspiration to the nanoscopic world is attributed to the physicist Richard Feynman, who with his lecture "There's Plenty of Room at the Bottom"[15] at an American Physical Society meeting on December 29th 1959, contemplated the possibility to manipulate things on a small scale. In the course of that conference he pointed out that scaling issues would arise from the changing magnitude of various physical phenomena: gravity would become less important and surface tension and Van der Waals attraction would become crucial. After that, the issue was open to debate. But, it was not until 1974 when the word “Nano-technology” appeared in another conference, precisely in a lecture by the japanese scientist Norio Taniguchi from the Tokyo University of Science when describing semiconductor processes, such as thin film deposition and ion beam milling, exhibiting a characteristic control on the nanometer range.[16] Afterwards, the term gained strength, especially when K. Eric Drexler unknowingly used a related term in his 1986 book “Engines of

Creation: The Coming Era of Nanotechnology" to describe what latterly would be known as Molecular Nanotechnology.[9]

Once the conceptual basis of Nanoscience and Nanotechnology was established, it was time to confirm and further develop the field with experimental research. In this sense, it is noteworthy that two major developments finally boosted the discipline: the aforementioned birth and consolidation of cluster science and the invention of the scanning tunneling microscope (developed in 1981 by Gerd Binnig and Heinrich Rohrer at IBM Zurich Research Laboratory), which afterwards led to the appearance of the different electron microscopes used nowadays.[17]

Now in the in the early 2000s, after less than a century in this research field, we are living the beginnings of the use of Nanotechnology in commercial products. In fact, nanoparticles (NPs) properties are already used for developing new products[18] such as paints (where they serve to break down odour substances), on surgical instruments and food packing (in order to keep them sterile), in highly effective sun creams, slow release pharmaceuticals and many others.[19-22] Under this regard, bench-marketing studies on main current industries[18, 23] revealed the key market opportunities that are illustrated in **Figure 1.2** Most of these key market opportunities are, in fact, involving the development of new materials, and, among them, Metal nanoparticles (MNPs) are attracting much of the interest, as will be shown explained afterwards.

Figure 1.2. Possible marketable applications of nanotechnology products in different fields.

Thus, nowadays, the main goal of Nanoscience and Nanotechnology is the creation of useful/functional materials, devices and systems through control of matter on the nanometer length scale and exploitation of novel phenomena and properties (physical, chemical and biological) at that scale. To achieve such goal it is necessary to use a multidisciplinary approach: inputs from physicists, biologists, chemists and engineers are required for the advancement of the understanding in the preparation, application and impact of these new nanotechnologies.

1.3. Nanoobjects and Metal Nanoparticles

Considering a nanoobject as an object in which at least one of its phases has a nanometer size in at least one dimension,[24] it is possible to classify them in three groups: 1D nanometer-size objects (e.g., thin films) , 2D nanometer-size objects (e.g., nanowires, nanorods and nanotubes) or 3D nanometer-size objects (e.g. nanoparticles and/or nanoclusters).

Nanoobjects can be porous materials (with particle sizes in the nanometer range), polycrystalline materials (with nanometer-sized crystallites), materials with surface protrusions separated by nanometric distances, or nanometer-sized metallic clusters.

Among all of these nanoobjects, some of the ones being extensively used nowadays are: Polyhedral oligomeric silsesquioxanes (POSSs), Zeolites are micro- and nano-porous aluminosilicate minerals, Metal-organic frameworks (MOFs), Polyoxometalate (POMs), Carbon-based nano-objects, Enzymes or Dendrimeric structures such the ones shown in **Figure 1.3**.

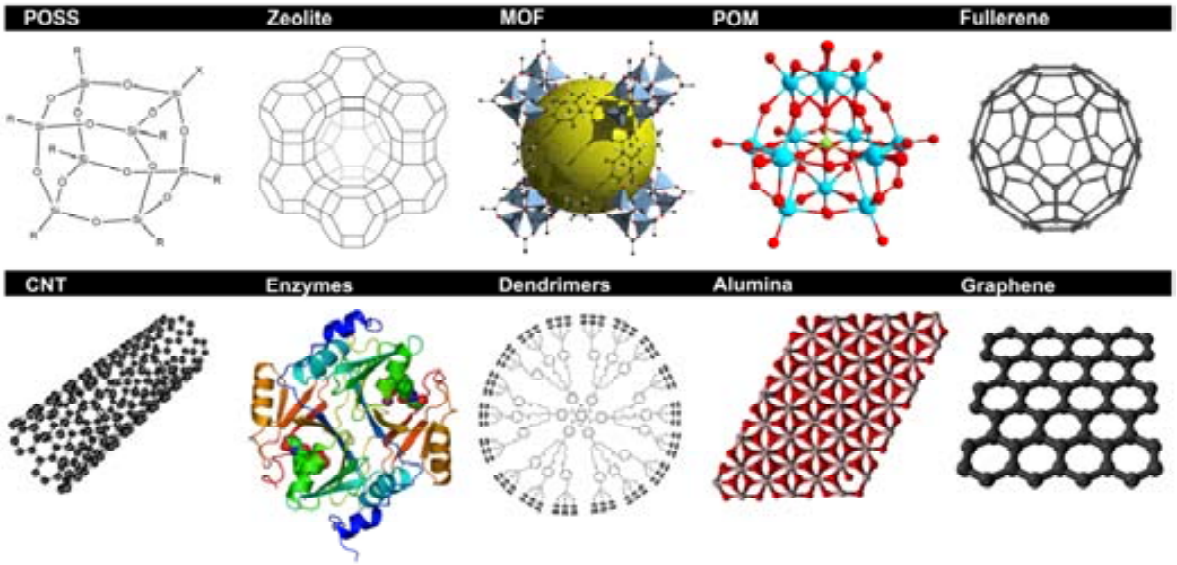

Figure 1.3. Schematic representation of some common nano-objects.

Thus, although there is a myriad of nanoobjects, among those, metal nanoparticles (MNPs) have already made a major impact on the field of Surface Science (including catalysis) due to the appearance of new particular physical and chemical properties.[24, 25]

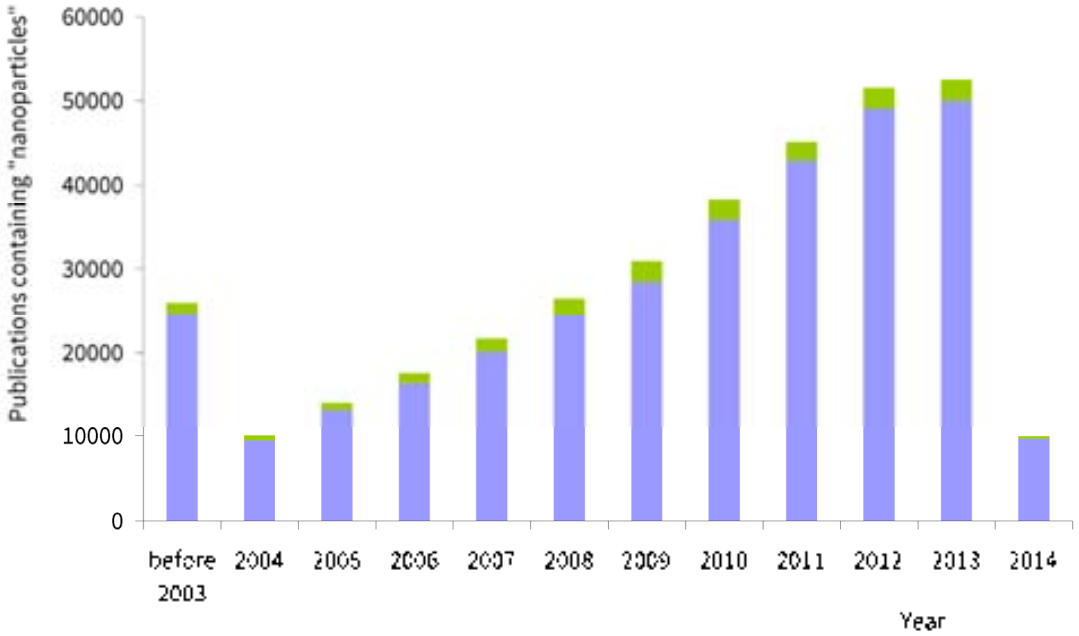

Figure 1.4. Bibliographic analysis based on the search of "nanoparticles" in Scifinder. Blue represents scientific publications (e.g. books, articles, reviews) whereasgreen patents. (According to data obtained in February 2014).

NPs have been and still are a hot topic, as it can be clearly seen in **Figure 1.4** in which the trend in publication regarding the word "nanoparticles" is presented. As observed the number of publications in the subject increases almost linearly due to their wide applications in different fields (such as Medicine, Chemistry, and Physics and so on). Moreover, not only scientific publications have been growing in the last decades but also a huge number of patents have been issued in the last decade (as highlighted in green in the figure above), testifying for the great economic interest of the field.

1.3.1. General properties of MNPs

MNPs are nanometric pieces of metal with particular physical and chemical properties derived from their number of bound metal atoms, what makes them display intermediate electronic energy levels in comparison with molecules or the bulk counterpart. Within the last two decades a new focus has been initiated to control and to better understand these nanometer-size particles what has stimulated a new wave of intensive and more detailed studies of MNPs and of various nanocomposites on their base.

In fact, the reduction of the bulk materials to a nanometric size induces size-dependant effects derivative from:

(i) an increase of the relation surface-volume, what yields to an increase in the total surface area and in the fraction of the species in the surface of the material;

(ii) changes in the electronic structure of the present species in the nanoparticles and in the same nanoparticles;

(iii) changes in the associations (e.g. interatomic distances) of the specie in the nanoparticle and presence of defects;

(iv) confinement and quantic effects (due to the confinement of the charge carriers in a particle of size comparable to the length wave of the electron).

This can be illustrated, for example, by the dependence of gold melting temperature on the size of gold nanoparticles; or by suspensions of Ag nanoparticles with sizes ranging from 40 to 100 nm showing different colours.[26] In addition, there are physical phenomena that do not exist in materials with larger grain sizes, as the general quantum-size effect for optical transitions in semiconductor nanocrystals which occurs in very small nanoparticles (<10 nm) due to the quantum confinement effects inherent in particles of that size.

Since particle size and distribution are the most important characteristics of nanoparticle systems, and taking into account that they determine the in vivo distribution, the biological fate, the toxicity, and their catalytic properties[27] it is a crucial issue to search for an accurate synthesis route that allows us controlling the aforementioned parameters.

1.3.2. Synthetic methods

In general terms there are two main routes for the preparation of MNPs: *top-down* and *bottom-up*.

The *top-down* methods are those that reduce the macroscopic particles to the nanoscale, usually by breaking down a piece of material continually until nanoscopic pieces (with nanometric dimensions) are obtained. The traditional *top-down* methods involve various milling techniques. For MNPs, for example, traditional source material, such as metal oxides, are pulverized using high-energy ball mills equipped with grinding media composed by wolfram carbide or steel. The main problem of this route is that it is not very suitable to prepare uniform particles of very small sizes.[28] In contrast, with the *bottom-up* methods it is possible to obtain uniform particles (usually of different shapes and structures). These methods are usually based on physico-chemical principles of molecular or atomic self-organization, starting from atoms

that can be added (either in solution or gas phase) to form larger particles, either by precipitation or aerogel processes.[28]

Taking a closer look to the preparation of MNPs a good way to classify the different methods of synthesis is by categorizing them as Physical, Physicochemical and Chemical routes (See **Figure 1.5**).[29, 30] As it is shown in **Figure 1.5** MNPs synthetic methodologies include a wide myriad of methods and processes including electrochemical methods, microwave assisted methods or mechano-chemical methods (such us the dry milling method developed by Luque *et al.*[31] among some others.

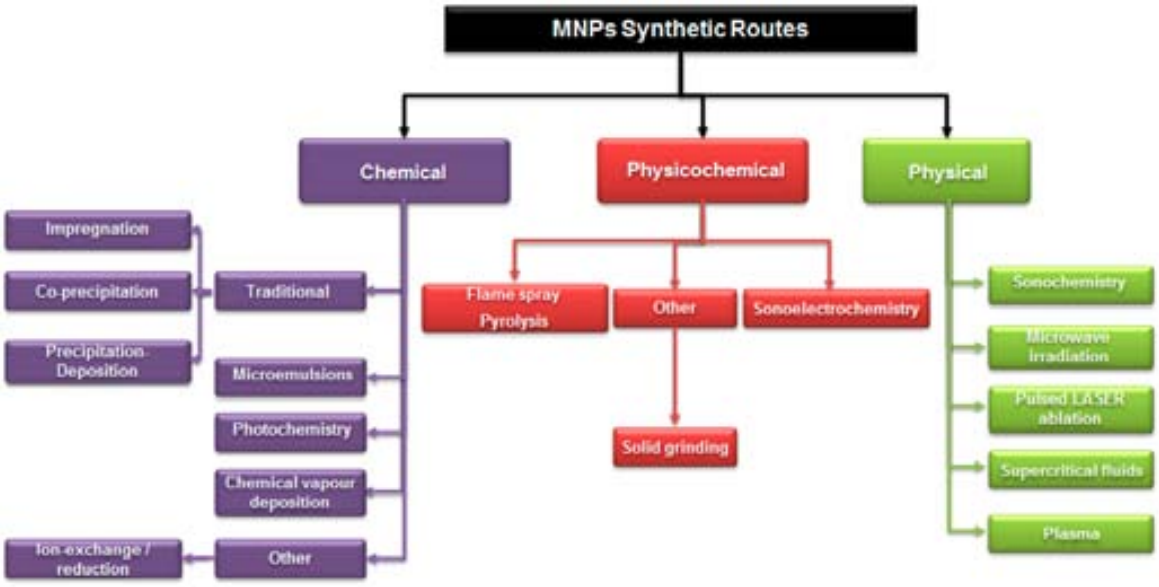

Figure 1.5. Physical, Physicochemical and Chemical routes for the preparation of MNPs.

Anyway, chemical methods are generally cheaper and easier to perform than Physical or Physicochemical ones, since they do not require specific equipment or instruments. Some of the typical Chemical synthetic routes are described below.

- **Co-precipitation:** It is a facile way to synthesize MNPs by a simultaneous precipitation of the metal and the support. For example Barau *et al.*[32] reported the preparation of supported PdNPs on hexagonal mesoporous silica using a sol-gel approach. As a result, well dispersed PdNPs with diameters around 4–5 nm, were found. Co-precipitation is typically used for the production of magnetic MNPs such as iron oxides (either Fe_3O_4 or γ-Fe_2O_3) from aqueous Fe^{2+}/Fe^{3+} salt solutions by the addition of a base under inert atmosphere at room temperature or at elevated temperature. However, metal precursors in solution sometimes interfere with the polymerisation of the material, often resulting in samples with undesirable properties.[30]

- **Precipitation-deposition:** This methodology, initially developed by Haruta *et al*.[33] involves the dissolution of the metal precursor followed by an adjustment of the pH (i.e. 5–10) to achieve a complete precipitation of the metal hydroxide (e.g. $Au(OH)_3$). Afterwards, the hydroxide is calcined and therefore reduced to the elemental metal. Iojoiu *et al*[34]*.* reported the synthesis of different nanostructured catalytic membranes by platinum deposition (by evaporation-crystallisation or by ionic impregnation), and found that the chemical interactions between the platinum precursor an the superficial species was a crucial parameter for choosing the right deposition method, since the intensity and location of those interactions would determine the amount and distribution of the final PtNPs. Another deposition approach is the one reported by Yang *et al.*[35] in which the *in-situ* deposition of PtNPs on bacterial cellulose membranes (BC) was performed in a 3D network structure of BC membrane. Besides, although there are several approaches that can be suitable for a deposition method, usually, these methodologies lack in the control of the size and distribution of the final MNPs, and sometimes require the use an excess of external reductant (e.g. $NaBH_4$, H_2, hydrazine) to ensure the complete formation of MNPs.
- **Impregnation:** This methodology entails the soaking of a porous solid support with a solution containing the metal precursor or even a solution with the preformed MNPs. By this procedure, the MNP precursor, which is normally a salt (e.g. metal nitrate, chloride), is dissolved in the minimum quantity of solvent and then added to a porous support, filling its pores so that a thick paste is formed. Once the solvent is removed the obtained MNPs dispersed depending on the metal, support and loading of the final solid.[32, 36]

By this procedure, Zhang *et al.*[37] reported the formation of MNPs by impregnation of a polymeric support in a supercritical fluid (SCF) solution of the metal precursor. Afterwards, the formation of the MNPs can proceed by three procedures: (i) chemical reduction in the SCF with a reducing agent, such as hydrogen and an alcohol; (ii) thermal reduction in the SCF; or (iii) thermal decomposition in an inert atmosphere or chemical conversion with hydrogen or air after depressurization. Thanks to the low surface tension of SCFs a better penetration and wetting of pores (comparing to liquid solvents) is obtained, and it is also possible to avoid the pore collapse (which can occur on certain structures such as organic and silica aerogels with liquid solvents). Nevertheless, there is still a need for improving the solubility of the organic precursor in the SCF, improve the reduction and find low-cost SCF equipment.

- **Microemulsions:** They are liquid systems consisting of at least ternary mixtures of oil, water and surfactant. In fact, they are heterogeneous (nanostructured) on a molecular scale what can be used for producing functional membranes and polymer nanocomposites.[38] Nano-

sized particles of inorganic materials are generally prepared in Water/Oil microemulsion, and microlatexes (d <50 nm) of polymers from both Oil/Water- and Water/Oil-microemulsion polymerizations.

In a typical run, a solid support is impregnated with a microemulsion containing a dissolved metal salt precursor (in a similar way to that of the previously described traditional chemical impregnation).[39] MNPs obtained by this technique have a more controllable, narrow distribution of crystallites,compared to those obtained through the traditional impregnation.[40] Nevertheless, there are some challenges to overcome, focused on the improvement of the low amount of MNPs produced from a single microemulsion and on the feasibility of recovery and recycling of the liquid phase.[39]

- **Photochemistry:** The photochemical synthetic method generates MNPs through direct photoreduction of a metal precursor (metal salt or complex), or by the reduction of metal ions using photochemically generated intermediates such as excited molecules and radicals (photosensitization). It is, in fact, an attractive tool for the preparation of nanomaterials because of the spatial and temporal control, allowing the fabrication of MNPs in a selected and microscopic region.[41] For example, Scaiano *et al.*[42] found that AuNPs could be easily prepared by irradiating in the UVA region (315–400 nm) a solution of a commercially available benzoin compound (Irgacure-2959) and $AuCl_4$. With irradiances around 40 W/m^2 they obtained in a few minutes AuNPs in the range of 8-40 nm. Hence, since no need for an excess of reducing agents or stabilizers is required, this methods are considered as environmentally-friendly. However, it is still not clear how it is possible to control the size and distribution of the obtained MNPs.
- **Chemical Vapor Deposition:** It is a gas-phase aerosol process for producing high-purity nanoparticles. However, the generated nanoparticles are produced in the form of aggregates due to their coagulation at the high temperature used.[43] In a general run, this procedure involves the sublimation of metals and the posterior growth of the MNPs under high vacuum in the presence of an excess of stabilizing organic solvent (e.g. aromatic hydrocarbons, alkenes and tetrahydrofuran) and/or reducing agent (e.g. H_2).[30] This methodology allow the preparation of MNPs on a wide range of organic and inorganic supports under very mild conditions (<50 ^oC) to afford highly active heterogeneous catalysts,[44] thereby avoiding the formation of large agglomerated nanoparticles from other protocols. Nevertheless, the method is often limited by the vapor pressure of the precursor and mass-transfer-limited kinetics.[30]

Besides all the above mentioned methodologies the simplest and therefore most common way to synthesize MNPs is their precipitation from a solution (aqueous or non aqueous) where the

metal precursor is dissolved. This methodology involves the reduction of metal ions to its zero-valence state using a suitable reducing agent. In the case of chemical reducing agents, alcohols, hydrogen gas, hydrazine and borohydride are frequantly used. A classic example of this can be found in one of the most common methods of producing AuNPs: the citrate reduction of $HAuCl_4$ in water. This was firstly introduced by Turkevich *et al.*[45] and afterwards refined by Frens *et al.*[46] who varied the ratio of reducing agent / stabilizing agent to Au ratio in order to obtain some control over the AuNPs diameter.

Nonetheless, the main drawback which still limits the wide application of MNPs is their insufficient stability dealing with the manipulation of objects in the nanoscale and with their high tendency to self-aggregate.[47]

1.3.2.1. Stability challenge

MNPs are so reactive that when they touch each other, they surfaces fuse, what results in a loss of the nanometric size and in their special properties. These features of nanoparticles, in part determined by the conditions of synthesis, create enormous difficulties in their fabrication and final application.[48]

It is well-established that NPs can aggregate not only as a result of a further manipulation but also during their growth. A typical mechanism of aggregation is the so-called Ostwald ripening which is a growth mechanism where small particles dissolve, and are consumed by larger particles.[49]

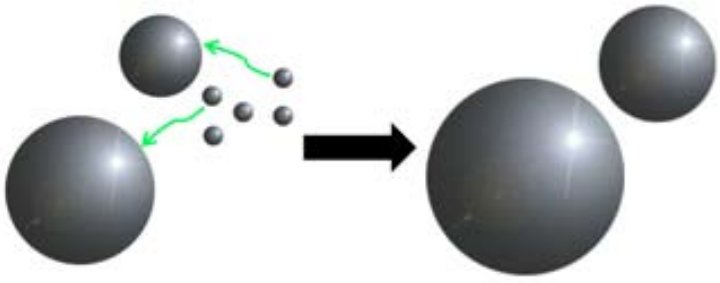

Figure 1.6. Schematic representation of the Ostwald ripening mechanism.

The clearest example of this was reported by Simonsen *et al.*[50] in which time-resolved image series unequivocally revealed that the sintering of PtNPs dispersed on a planar, amorphous Al_2O_3 support exposed to 10 mbar air at 650 °C was mediated by an Ostwald ripening process. A statistical analysis of an ensemble of PtNPs showed that the particle size distributions change shape from an initial Gaussian distribution via a log-normal distribution to a Lifshitz-Slyozov-Wagner distribution.

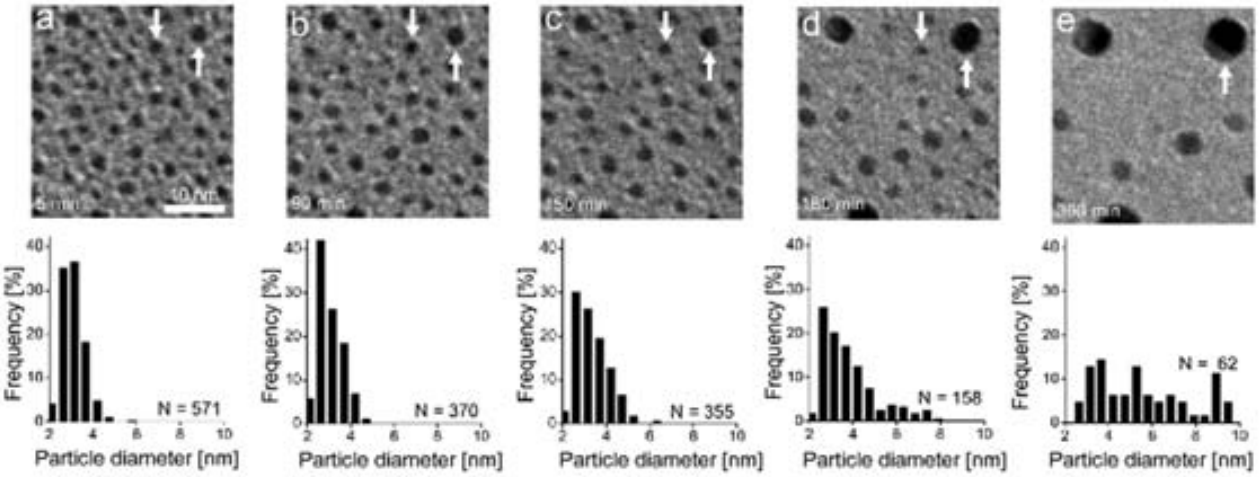

Figure 1.7. Direct observation of Ostwald ripening by TEM. [50]

As a result, the average nanoparticle size increased with time while the particle concentration decreased and their solubility diminished.

Therefore it comes clear that the stabilization of MNPs is a crucial issue and specifically required to prevent their uncontrollable growth, control their final shape and size, and prevent particle aggregation. It is important to remark that these three guidelines are not isolated points, but rather are intrinsically correlated, since a good control on the MNPs growth will lead to a better control on their final size and shape and therefore, to a better final stability *versus* time, in the presence of solvents, and so on.

1.3.2.2. Toxicity concerns

Despite their advantageous properties, MNPs are risky. Even if the use of MNPs seems to open a new window of possibilities in the development of new-age materials, some environmental and health safety risks, sometimes referred as nanotoxicity[51-56] must be intensively considered. The use of engineered NPs in the environment, as a consequence of the development of Nanotechnology, is a serious case of worldwide concern. Accordingly, the use of nanomaterials has come under some scrutiny by both private and public institutions regarding in particular the possible hazards associated with NPs either deliberately or inadvertently produced.[10, 23, 57-60]

Their wide application of engineered NPs, their entry into the environment, and the lack of knowledge regarding their impact on the ecosystem are a growing concern in society because of the possible adverse effects.[58, 60-62] Therefore, detailed understanding and assessment of their source, release, interaction with environment, and possible risks would provide a basis for safer use of NPs with minimal or no hazardous impact on environment.

In this context, new and safe strategies for MNPs applications are pursued. On one hand, since MNPs toxicity is presumed to be size and shape-dependent,[63] controlling these parameters has turned to be a crucial factor during their synthesis. On the other hand, controlling the escape of the NPs to the media, in other words, avoiding a possible exposure to the environment, can bring a second security level. Again, the stabilization plays an important role, and this is why the development of stabilized nanometer sized particles has been intensively chased within this broad field.[48, 64-66]

The prevention of NPs escaping into the environment is very likely the best approach that can be considered as a possible solution by developing environmentally safe polymer–metal nanocomposite materials.

1.3.2.3. Stability agents and the "polymeric solution"

Due to the aforementioned drawbacks such as lack of stability and safety concerns of MNPs uses, a successful synthesis of nanoparticles should involve three main steps: nucleation, growth, and termination by a stabilizing agent through colloidal forces.[66]

The stabilizing agents typically employed are usually molecules that can bind on particle surface and are often denoted as either surfactants, ligands or capping agents: oleylamine, oleic acid, trioctylphosphine, dodecanethiol cetyltrimethylammonium bromide, poly(N)vinyl)2)pyrrolidone) (PVP), polyvinyl alcohol , poly(amido amine), just to name a few. But, for surface applications, the capping agent impedes reactants to approach the metal surface. Moreover, the presence of capping agents also brings an additional complexity to the system, such as uncertain coverage density of capping molecules, non-covalent interaction between capping molecules and reactants, as well as charge transfer at the organic-metal interface.[67]

A typical example of this surface modification can be found in the aforementioned classic preparation of AuNPs by the Turkevich method.[45] By this method, after dissolving $HAuCl_4$, the solution is rapidly stirred while the reducing agent (sodium citrate) is added, causing Au^{3+} ions to be reduced to Au^0. As more and more of these gold atoms form, the solution becomes supersaturated and gold gradually starts to precipitate as AuNPs. During the AuNPs formation, the colloidal particles are surrounded by an electrical double layer formed by adsorbed citrate and chloride ions and cations which are attracted to them. This results in a Coulombic repulsion between particles, impeding their aggregation. The problem lies in the fact that the presence of the stabilizing agent alters the particle surface hindering its reaction properties. In this case, the surface charge of the AuNPs changes from being mostly positive to negative.

Alternatively, the use of polymer-assisted fabrication of inorganic NPs has proved to be one of the most efficient and universal ways to overcome the stability problem of MNPs and to save their properties. MNPs synthesized by this approach exhibit long-time stability against aggregation and oxidation while NPs prepared in the absence of polymers are prone to quick aggregation and oxidation.[48, 68]

That is true, but it is of crucial importance to take a deeper look to the interaction forces acting between nanoparticles in order to understand the exact role of the polymer as the most effective candidate for stabilizing MNPs preventing their aggregation and as solubilizing agents, providing a convenient tool for further manipulation and application. These colloidal forces can be classified in three main types as follows: Van der Waals interactions, electrical double-layer interactions, and steric interactions.[69, 70]

- **The Van der Waals attractive potential** (Φ_{VdW}) between two spherical particles of radius *R* separated a distance *d* is given by the Hamaker equation showed in equation (1-1). This potential increases with an increase in the radius of the NP or with a decrease in center-to-center distance between particles. For particles with diameters between 10-100 nm, the predicted Van de Waals potential is positive, resulting in an attractive force between both particles.[71]

$$\Phi_{VdW} = -\frac{A}{6}\left[\frac{2R^2}{d^2 - 4R^2} + \frac{2R^2}{d^2} + \ln\left(\frac{d^2 - 4R^2}{4R^2}\right)\right] \qquad (1\text{-}1)$$

Where: Φ_{VdW} is the Van der Waals attractive potential,
R is the particle radius,
d is the separation distance between particles,
A is de Hamaker constant.

- **The electrical double-layer interactions** between charged ionic moieties, which are attracted to an oppositely charged interface and, in many cases, form a diffuse layer near the surface.[72]
- **The steric interactions**, due to the adsorption of a polymer in a surface. When two polymer layers overlap at a collision distance between particles, repulsion occurs.[73]

In addition, hydrophobic and solvation forces may be important, because the ordering of solvent molecules close to a surface involves solvation forces.

The mechanism of MNP stabilization with polymers can be explained by two approaches which run simultaneously in the system and influence one another: the substantial increase of

viscosity of the immobilizing media (the polymer matrix), and the decrease of the energy of particle-particle interaction in Polymer Stabilized MNPs (PSMNPs) systems versus non-stabilized MNP dispersions.[74]

In the first approach, the coagulation velocity depends on some factors as the range of attractive forces, the brownian motion velocity, the concentration of colloidal solution and the presence of electrolytes. As follows from the Smoluchowsky equation (1-2) the rate constant of particle coagulation is inversely proportional to the viscosity of the media:[65]

$$k_c = \frac{8 K_B T}{\eta} \qquad (1\text{-}2)$$

Where: k_c is the rate constant of particle coagulation,

η is the viscosity of the media,

K_B stands for the Boltzman constant,

T is the absolute temperature.

Therefore, when increasing the viscosity of the media (by adding a polymeric matrix), the rate constant of particle coagulation decreases.

As it is said before, the second approach is the decrease of the energy of particle-particle interaction in PSMNP systems versus non-stabilized MNP dispersions. The potential energy of attraction between two spherical particles of radius R and minimum distance between their surfaces can be given by the following equation:

$$U_r \approx \frac{A \cdot R}{12\, d} \quad \text{at} \quad R >> d \qquad (1\text{-}3)$$

Where: U_r is the potential energy of attraction,

R is the particle radius,

d is the distance between particles,

A is the Hamaker's constant.

The value of Hamaker constant is known to be close to kT for polymer particles (e.g $6.3 \cdot 10^{-20}$ J for polystyrene), while for the metal dispersions it is far higher ($40 \cdot 10^{-20}$ J for silver).[74]

As a result, the encapsulation of MNPs inside polymeric matrices can be considered as a win–win strategy to cope with the drawbacks of both MNPs stabilisation and manipulation.[75]

From a practical point of view, stabilization of MNPs can be done by different strategies (**Figure 1.8**).

In the *ex-situ* synthesis[30] MNPs are chemically synthesized and their surface is organically passivated. Then, the derivatized NPs are dispersed, using different mechanochemical approaches, into a polymer solution or liquid monomer which is afterwards polymerized in order to obtain the stabilizing polymer shell. First the particles, then the polymer. The presence of such a shell increases the compatibility of the particles with the polymer and simplifies their homogeneous dispersion inside the matrix. However, significant challenges are associated with blending polymers and NPs to afford homogeneous and well dispersed inorganic material within the polymer, and, in some cases, the success of the stabilization is limited by the possibility of re-aggregation of the MNPs along the time. Some of the typical *ex-situ* synthetic methods include the sol-gel synthesis, the grafting, electrostatic deposition and microencapsulation.

On the opposite hand, by the *in-situ* synthesis[76] the monomer is polymerized in solution, with metal ions introduced before or after polymerization and then metal ions in the polymer matrix are reduced chemically, thermally, or by UV irradiation. First the polymer, then the particles. Hereby, MNPs are grown directly in the stabilizer medium yielding a material that can be directly used for a foreseen purpose. For this reason, *in-situ* approaches are getting much attention lately.[77-79] Some of the common *in-situ* methods include thermal methods, sol-gel processing, chemical vapour deposition and co-precipitation techniques. Indeed, the *in-situ* method can be extended to the preparation of many metal–polymer nanocomposites. As an example, Chou *et al.*[80] synthesized AgNPs by reducing $AgNO_3$ with formaldehyde in the presence of PVP of various molecular weights, and demonstrated that the polymeric stabilization efficiency depended not only on the molecular weight of the polymer stabilizer but also on the rate of MNP formation.

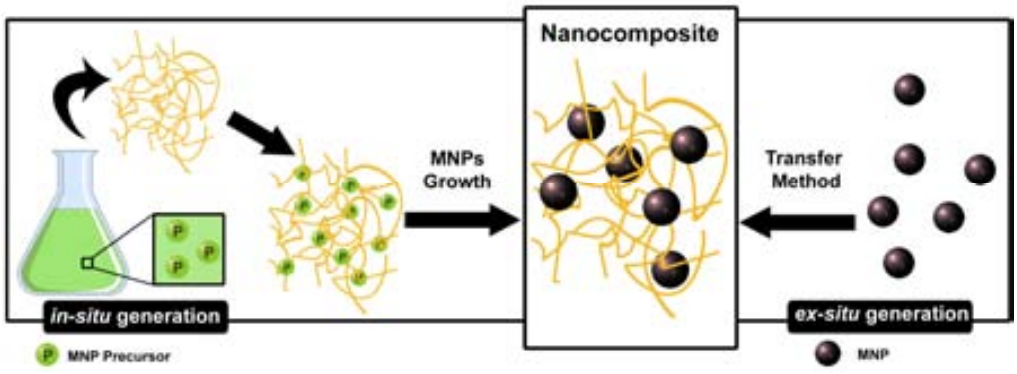

Figure 1.8. Schematic comparison between in-situ and ex-situ methodologies.

During the development of this Thesis work, the *in-situ* preparation of several types of polymer-metal nanocomposites has been achieved by the Intermatrix Synthesis (IMS) approach.

1.4. Intermatrix Synthesis

The ion-exchange synthesis of Metal Nanoparticles (MNPs) refers to a group of methods which can be generally classified as Intermatrix Synthesis (IMS) technique, also known as Matrix Chemistry.[81] The main feature of IMS is the dual function of the matrix, which allows the stabilization of the MNPs to prevent their uncontrollable growth and aggregation and provides a medium for the synthesis.

It is noteworthy that IMS was essentially the first method employed by the humans to incorporate nanoparticles inside inorganic materials. In this sense, one of the oldest nanocomposite materials found is, precisely, the aforementioned *Lycurgus cup*.[12] It is remarkable that Greco-Roman techniques have been used up to modern times: related recipes were described by Arabian authors during the medieval period.[82] During the Renaissance as practical application of alchemical knowledge, and by modern chemists, from the Encyclopedie of Diderot and d'Alembert[83] through to the present day.

Another example is the "lustre pottery"[84] employed at the same time in Asian and European countries by a simple two-step procedure:

1. the immobilization of metal cations (MNP precursors) inside the ceramic matrix.
2. the reduction of metal ions to the zero-valent state with carbon monoxide leading to the formation of MNPs.

Yet, as it has been shown above, humanity had used these methodologies for a long time, the fundamentals of the scientific studies regarding nanofabrication did not appear since the middle of the XIXth. IMS is not an exception. In 1949 the first communication of the IMS was published by Mills and Dickinson.[85] In this pioneered publication the preparation of the anionic resin containing CuNPs ("colloid copper") is described as it is and the use of such nanocomposite material for the removal of oxygen from water. Since that, a great number of researchers focused their efforts to the development to a new class of ion-exchange materials, combining ion-exchange and redox properties (known also as "redoxites" or "electron-ion exchangers").

1.4.1. General principles

This section describes the principles of the IMS in ionic exchange matrices. This technique takes advantage of the *in-situ* approach, and has a wide range of application because of the multiple metal-polymer existing possibilities. Let's consider that even if in the typical IMS approach the number of polymers is reduced to those with ion exchange capacities, the multiple possibilities

remain and a different number of polymer-nanocomposites can be obtained. **Figure 1.9** tries to illustrate the multiple possibilities of this versatile methodology.

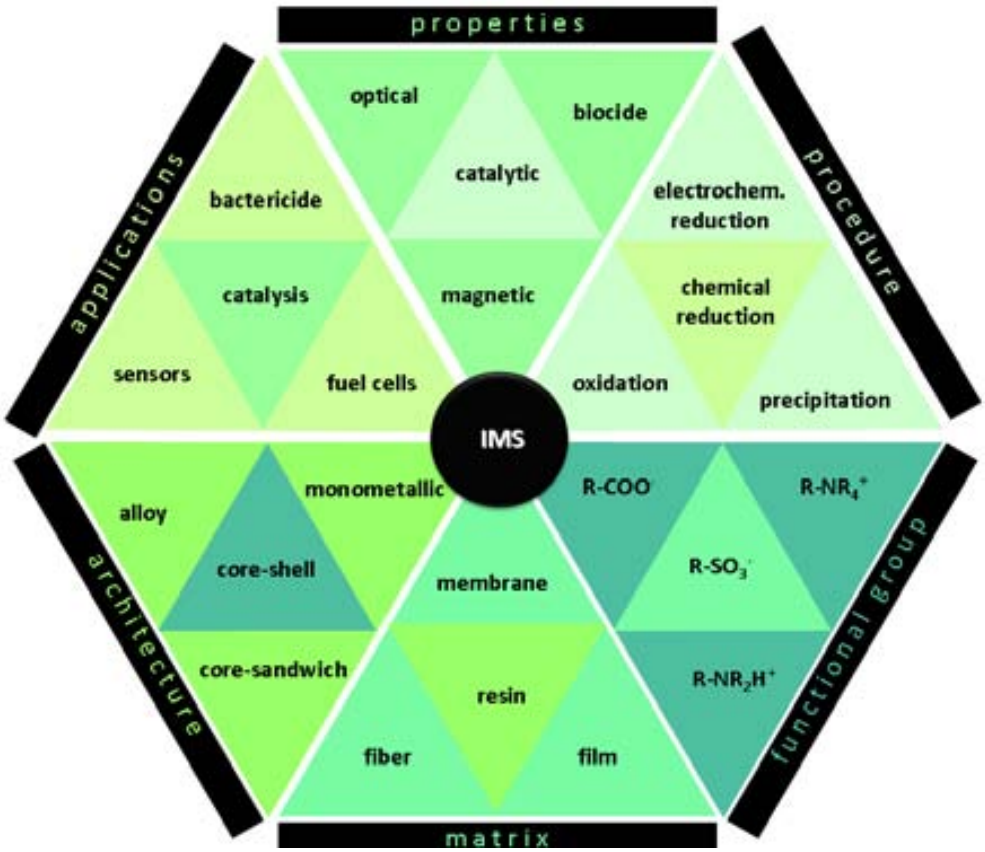

Figure 1.9. Scheme of the multiple possibilities of Intermatrix Synthesis.

The general principles of IMS, valid for any kind of polymer matrix and type of nanoparticle, are based on:

1. the nanoreactor effect: the confinement of the particles by the polymer molecules which allows limiting the the size and particle size distribution; and,
2. the barrier effect: the polymer molecules locally isolate the formation of each single NP preventing the contact between their surfaces and therefore their aggregation.

These guidelines are only achievable if NPs precursors can properly be immobilized in the polymeric matrix. In this sense, ion exchange matrices are the perfect template to retain the ionic species, either metal cations, anions or any kind of coordination compound. It is noteworthy to mention that up to now this synthetic approach has never been utilized for non-ionic polymeric supports. Thus, for the first time, one of the objectives of this work has been to achieve a further development by extending the IMS application to non-ionic matrices for further development.

The first works of our research group based on the IMS procedure[86] were focused on the reduction of metal ions in order to obtain MNPs (PtNPs and CuNPs) inside polymeric matrices with charged groups, such as sulfonated poly(etherether ketone) (SPEEK), for the development of ampertometric sensors. Although in its beginning the reduction was effectuated via electrochemical reduction in the same electrode (which was a suitable procedure for the sensor and biosensor final applications developed at the time),[87] the use of a chemical reducer (such as $NaBH_4$) was also tested, providing really comparable results in terms of MNPs distribution and size and final applications with the electrochemical procedure and, therefore, expanding the applicability of such technique.[86]

The basis of this last approach can be illustrated as two negatively charged sites of the matrix (such as sulfonic group, $-SO_3^-$) efficiently interacting with a divalent metal cation (M_1^{2+}) which afterwards can undergo a chemical reaction (reduction, in this case) yielding to the formation of the MNP.

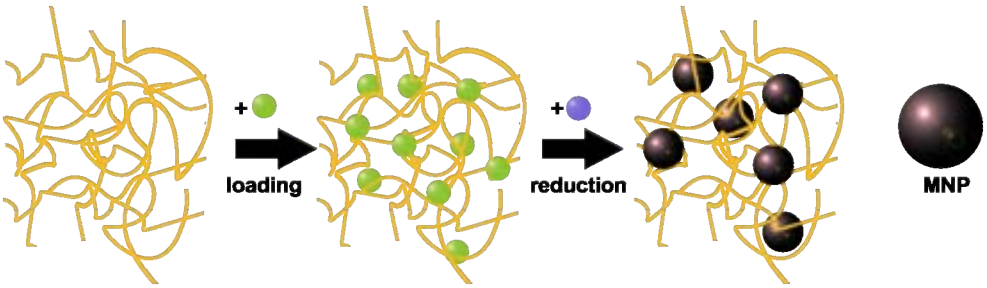

Figure 1.10. Schematic representation of the main two steps of MNPs preparation inside a polymeric ion-exchange matrix by IMS.

These two stages of the IMS can be described by the following equations (equations 1-4 and 1-5) considering the presence of negatively charged groups (X^-). In this case, M_1 stands for a divalent metal (like Pd^{2+}) and R is an organic radical.

$$2(R\text{-}X^- Na^+) + M_1^{2+} \rightleftharpoons (R\text{-}X^-)_2M_1^{2+} + 2\ Na^+ \qquad (1\text{-}4)$$

$$(R\text{-}X^-)_2M_1^{2+} + 2\ NaBH_4 + 6H_2O \longrightarrow 2(R\text{-}X^-Na^+) + 7H_2 + 2B(OH)_3 + M_1^0 \qquad (1\text{-}5)$$

A deeper look in the second stage reveals that the MNPs formation is, indeed, a combination of an ion-exchange reaction and a reduction reaction. Accordingly the reduction of the metal ions to the zero-valent metal takes place in the solution boundary, close to the ion exchange groups:

$$(R\text{-}X^-)_2M_1^{2+} + 2\ Na^+ \rightleftharpoons 2(R\text{-}X^-Na^+) + M_1^{2+} \qquad (1\text{-}6)$$

$$M_1^{2+} + 2BH_4^- + 6H_2O \rightarrow 7H_2 + 2B(OH)_3 + M_1^0 \quad (1\text{-}7)$$

Due to the successful results obtained with this methodology, the next step was focused on widening the use of IMS to obtain new types of nanocomposites. In this sense, it was possible to prepare MNPs of low solubility compounds (e.g. metal sulphides) using metal-loading and precipitation cycles,[88] and the preparation of nanocomposites with much complex MNPs, such as core-shell and core-sandwich structures by following a repetitive procedure.[88, 89]

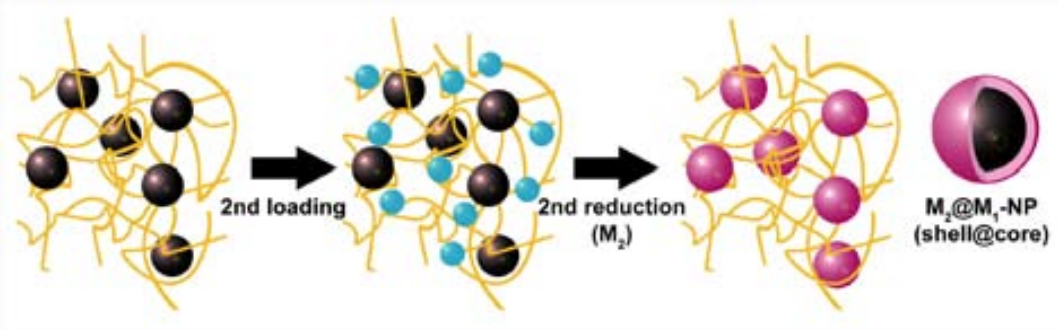

Figure 1.11. Bimetallic core-shell MNPs preparation. Black spheres represent the MNPs obtained after the first loaing-reduction cycle, blue spheres the M_2^{2+} cations and the pink ones the final core-shell MNPs.

Such new structures allowed the modification of the nanocomposite functionality, improve the stability or even a combine properties of the different compounds making their future applications more efficient. Although the final activity of these nanocomposites was usually ruled by the properties of the metal in the shell, it was also found that the properties of the metal core were also important for the final nanocomposite.

In this regard, Ruiz *et al.*[90] obtained CuNPs in SPEEK coated with a shell of platinum group metal of the minimal thickness, what resulted in the protection of Cu core against oxidation while maintaining the sensitivity of core–shell NP-modified sensors at sufficiently high level.

To better understand this procedure, equations (1-8 and 1-9) correspond to the second stage (after the first loading-reduction cycle) of the IMS of core-shell MNPs inside a parent polymeric matrix:

$$2(R\text{-}X^-Na^+) + M_1^0 + M_2^{2+} \rightleftharpoons (R\text{-}X^-)_2M_2^{2+} + M_1^0 + 2\,Na^+ \quad (1\text{-}8)$$

$$((R\text{-}X^-)_2M_2^{2+} + M_1^0 + 2NaBH_4 + 6H_2O \rightarrow 2(R\text{-}X^-Na^+) + 7H_2 + 2B(OH)_3 + M_2@M_1 \quad (1\text{-}9)$$

According to some authors,[91] the second metal ion can act as an oxidizing agent towards the core-metal (M_1^0) resulting in the partial oxidation of the first metal by the following transmetallation (redox) reaction:

$$M_2^{2+} + 2M_1^0 \rightarrow M_1^{2+} + M_2^0@M_1^0 \qquad (1\text{-}10)$$

More recently, Alonso *et al.* worked on the possibility of synthesizing polymer-stabilized core-shell MNPs with a magnetic core made of Co in non-woven fibrous cation-exchange materials [92-94] for bactericide (with Ag-shell) or catalytic (with Pd-shell) applications. The main feature of these magnetic materials was to prevent MNPs to escape by profiting of the embedding of MNPs into organic matrices added to the fact that in case of leakage, MNPs could be easily recovered by using simple magnetic traps.

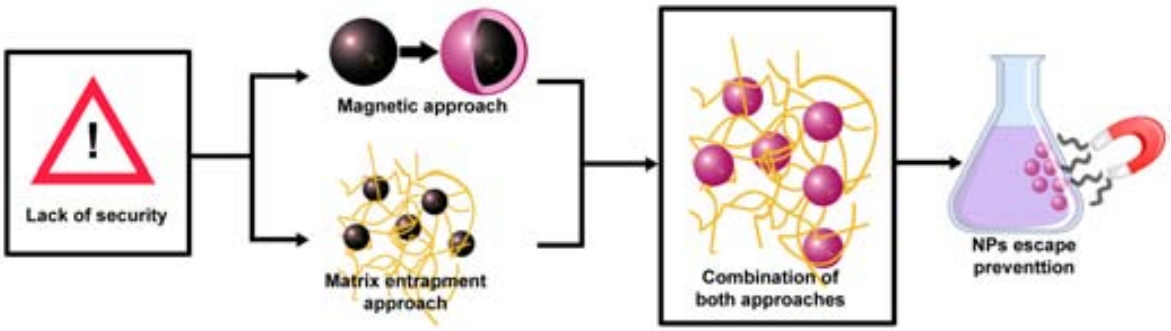

Figure 1.12. Schema describing the concepts involved in the design of magnetic polymer-metal nanocomposites.

Unfortunately, as-prepared fibrous materials were difficult to recover from the media due to their swelling properties. Therefore, with the aim of developing easy-recovery nanocomposites for bactericidal disinfection of water, Alonso *et al.* applied the IMS for the obtainment of Ag@Co into granulated cation-exchange resins. [95, 96]

Lately, when the versatility of the IMS became clear, new approaches peeped out. In this regard, the technique was extended to its use in anion exchange matrices (with cation charged groups). To do so, Alonso *et al.* and Bastos-Arrieta *et al.* used granulated anion-exchange resins with ammine groups (known to stabilize NPs against aggregation without disturbing their properties) capable to immobilize metal complexes (i.e. $[CoCl_4]^{2-}$) or other anions (i.e. BH_4^-). [97, 98]

Thus, up to now, it is possible to state that IMS technique has offered a great varying of synthetic approaches, and, in less or more extent, they all have been tested within the last seven years. However, the single approach that has not been evaluated yet, and which is one of the main objectives of the present work, is the use of non-ionic matrices as hosts for the IMS.

1.4.2. Requirements of the parent polymers: limitations

Many materials can be used as supports for the IMS disregarding their form or shape: granulated beads, fibrous materials or membranes and films. Though, everything is not possible. In all cases, when using the IMS technique it is important to take into account both the polymer properties and the final application of the nanocomposite, as both points dictate certain necessary requirements of the parent matrix to allow the synthesis of MNPs.

For example, when conceiving a nanocomposite for making a sensor or biosensor to be applied in aqueous solutions, the polymer must be obviously insoluble in water. But, at the same time, the polymer has to provide enough permeability towards the analyte under study (ions or molecules). Besides, the polymer must either slightly swell in water or at least be hydrophilic to enhance both the sensor the response rate.

Similarly, if nanocomposites have to be used to modify surfaces (e.g. electrodes), it has to be possible to prepare homogeneous solutions or dispersions in any organic solvent which can be deposited onto the desired surface. This solubility would also allow the characterization via microscopic analysis, electrochemical technique and others.[86]

In this regard, more examples can be drawn, and from all of them, it is possible to extract the main requirements of a polymer to be used as a matrix for the IMS technique. For example, the polymer must bear functional groups which would act as nanoreactors with appropriate distances between the coordinating centers to insure the hopping of charge carriers. It also must be insoluble in water, but it should have an appropriate swelling ratio, since all the reactions involved are carried out in an aqueous media, so species should diffuse through the polymer. Obviously, the polymeric matrix has to be chemically compatible with the surface charge density of the MNPs, and chemically stable to the reactants. Noticeably, low price and availability are also advantageous properties for such polymers even if they are not strictly needed.

The first of the requirements cited (the ion exchange properties) has been, until now, crucial. Nevertheless and as aforementioned, during the development of this thesis work, and as a novelty, the IMS has been applied to both, ion exchange and non-ionic polymeric matrices.

1.4.3. Precursor-matrix interactions

Several processes can take place between the polymeric matrix and the solution containing the reactive species for the IMS procedure. In this sense, mechanisms such as diffusion, ion-

exchange and adsorption have to be certainly considered for the loading step but also for the reaction step.

In this sense, if we want to consider the entry of ions to our polymeric matrix, first thing to evaluate is the diffusion of the ionic specie throughout the matrix.[99, 100]

Let's imagine a system as the one showed in **Figure 1.13**, at a constant temperature and pressure, in which there is the matrix (phase 1) and a solution rich in one of the species we want to immobilize (phase 2) to further form the MNP.

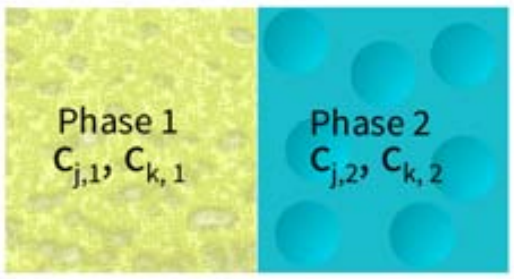

Figure 1.13. Schema of a binary system with 2 components, *j* and *k*.

Each phase contains only substances named *j* and *k* but with different initial molar concentrations: $c_{j,1} \neq c_{j,2}$ and $c_{k,1} \neq c_{k,2}$, where $c_{j,1}$ is the concentration of *j* in phase 1.

When the two phases are in contact, the random molecular motion of *j* and *k* molecules will reduce and ultimately eliminate the concentration differences between the two solutions. This spontaneous decrease in concentration differences is the macroscopic motion of diffusion. If $c_{j,1} < c_{j,2}$, there is a net flow of *j* from phase 2 to phase 1 and a net flow of *k* from phase 1 to 2. This flow continues until the concentrations and chemical potentials of *j* and *k* are constant throughout the system described.

Usually diffusion processes can be described by Fick's law. Fick's first law of diffusion (equation 1-11), shows that the diffusion rate in the x axis is proportional to the contact area between phases and to the concentration gradient.

$$\frac{dn_j}{dt} = -D_{jk} A \frac{dc_j}{dx} \quad \text{and} \quad \frac{dn_k}{dt} = -D_{kj} A \frac{dc_k}{dx} \qquad (1\text{-}11)$$

Where: dn_j/dt is the net rate of flow of *j* (in moles per unit time) across a plane of area *A* perpendicular to the x axis,

dc_j/dx is the value at plane of the rate of change of the molar concentration of *j* with respect to the x coordinate,

D_{jk} is called the (mutual) diffusion coefficient,

A is the contact area between phases.

As time goes on, dc_j/dx at a given plane changes, eventually becoming zero. Diffusion then stops.

The diffusion coefficient D_{jk} is a function of the local state of the system and therefore depends on temperature, pressure, and the local composition of the solution. If the two solutions substantially differ in initial concentrations, then D_{jk} varies substantially with distance x along the diffusion system and with time as the concentrations change, so the experiment yields some sort of complicated average D_{jk} for the concentrations involved. Whereas if the initial concentrations in phase 1 are similar to those in phase 2, the variation of D_{jk} with concentration can be neglected and one obtains a D_{jk} value corresponding to the average composition of 1 and 2.

In liquid solutions, D_{jk} varies strongly with composition and increases as temperature increases. Whereas diffusion coefficients at 1 atm and 25°C are typically 10^{-1} cm^2s^{-1} for gases and 10^{-5} cm^2s^{-1} for liquids; they are extremely small for solids. [100]

Once the ion has diffused thought the matrix, two different sorption phenomena have to be considered: ion exchange and adsorption, in which certain species are selectively transferred from the fluid phase to the surface of the insoluble phase.[101]

Adsorption can be considered as an accumulation of compounds, for example, from fluids on surfaces of solid state bodies. During this enrichment of the solid surface (adsorbent) with the atoms and molecules of the fluid phase (adsorptive) several interactions between both may occur. Although there are major differences in the interaction forces and the kinetics of adsorption onto the surface or inner part of the matrix,[101] adsorption processes are generally distinguished in two different sorption types depending on the nature of the interactions between the adsorbent matrix and the adsorptive.

On one hand, physisorption is commonly a reversible and rapid sorption process. It is mainly based on weak nonspecific interaction forces such as Van der Waals, dipole, dipole-dipole, and dispersion as well as induction forces, which usually are below 50 kJ/mol. For physical adsorption, once a monolayer of adsorbate is formed in the adsorbent surface has formed, intermolecular interactions between adsorbed molecules in the monolayer and the fluid phase molecules can lead to formation of a second layer of adsorbed molecules.

In contrast, in chemisorption a chemical reaction occurs at the surface of the solid, and the adsorptive specie is held to the surface by relatively strong chemical bonds. Accordingly, the interaction forces are much higher and are reported to be in the range of 60-450 kJ/mol. For

chemisorption, once a monolayer of adsorbed molecules covers the solid's surface, no further chemical reaction between the fluid and the solid can occur; although physical adsorption of further layers on top of this chemisorbed monolayer sometimes occurs.[100, 101]

In order to describe the relation between both phases before mentioned (solid and liquid) before a possible ion-exchange process, adsorption isotherms are frequently used (considering a system in a constant temperature). They are empirical models representing the amount of material bound at the surface as a function of the material present in the gas phase and/or in the solution. Even if they have been empirically deduced using gas-solid systems, they can be also applied to fluid-solid systems as the ones implied in this thesis work. The most familiar isotherms presented in **Figure 1.14** and explained below.

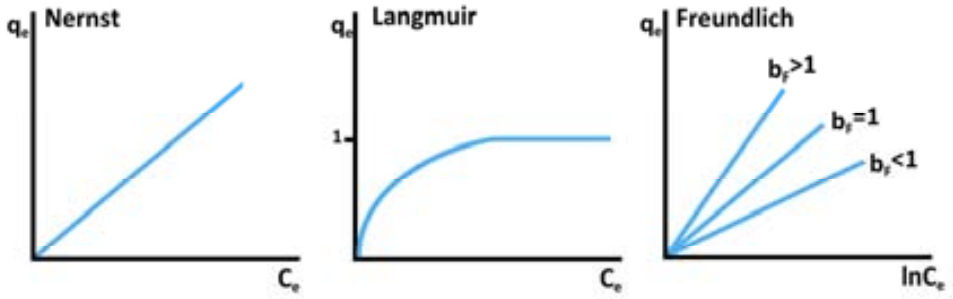

Figure 1.14. Graphical representation of the three main adsorption isotherms.

- **Nernst's Isotherm**: This is the simplest adsorption isotherm (presented in equation 1-12). It assumes that i) all sorption sites are identical and may be occupied and ii) there are no interactions between the compounds bound onto the surface.

$$q_e = K_N C_e \qquad (1\text{-}12)$$

Where q_e (mg/g) is the amount of adsorbate per gram of sorbent at equilibrium

C_e (mg/L) is the equilibrium solute concentration

K_N is a proportionality factor equivalent to the slope of an isotherm, when the surface loading approximates zero.

This isotherm equation cannot be thermodynamically deduced, however due to its good linear adjustment for small concentrations, it is frequently used. For gas adsorption, Henry law is used as special case of Nernst law.

- **Langmuir's Isotherm**: It assumes the physisorption of neutral particles in a solid with uniform surface which is characterized by energetically homogeneous sorption sites. Furthermore, it also assumes the following statements: i) adsorbed molecules don't interact with one another, ii) adsorbed molecules are localized at specific sites, iii) only a monolayer

can be adsorbed, and iv) desorption rate from a particular sorption site is thought to be independent of the occupancy of the neighbour sorption sites.

$$q_e = \frac{Q_{mL} a_L C_e}{1 + a_L C_e} = \frac{K_L C_e}{1 + a_L C_e} \quad (1\text{-}13)$$

Where: Q_{mL} (mg/g) is the monolayer adsorbent capacity under equilibrium conditions, which indicates the maximum concentration retained by the adsorbent surface when it is completely covered by an adsorbate monolayer.

K_L (L/g) and a_L (L/mg) are the Langmuir constants.

q_e (mg/g) is defined as the amount of adsorbate per gram of sorbent at equilibrium,

C_e (mg/L) is the equilibrium solute concentration.

At low concentrations ($a_L C_e << 1$), the Langmuir isotherm can be approximated by the Nernst's isotherm.

- **Freundlich's Isotherm**: In contrast to the Langmuir's equation, the Freundlich's isotherm, which is also very frequently applied (especially for liquid in solids adsorption processes), assumes adsorption onto sorbent surfaces, which are characterized by heterogeneous sorption sites.

$$q_e = K_F C_e^{b_F} \quad (1\text{-}14)$$

Where: q_e (mg/g) is the amount of adsorbate per gram of sorbent at equilibrium,

C_e (mg/L) is the equilibrium solute concentration,

K_F (L/g) is the Freundlich constant describing the adsorption capacity,

b_F is the dimensionless parameter, a measure of the adsorption intensity.

In contrast to the Langmuir isotherm, it cannot be approximated by the Nernst's isotherm at low concentrations and does not result in a saturation value at very high solute concentrations.

Although other isotherms can be used (e.g. Brunauer-Emmett-Teller's , Tempkin, Fowler, Hill-de Boer), those presented here are the simplest models that can be proposed in order to understand and describe solid-liquid adsorption systems.[100, 101]

On the other hand, ion exchange phenomena exhibit numerous similarities with adsorption processes, but there are also some significant differences. In such processes, the species are ions that are not removed from the solution but are replaced by ions bound by the solid phase via electrostatic interactions to achieve electroneutrality. Accordingly, there are two ionic

fluxes, one into the ion exchange particles and the other in the opposite direction out of the polymeric matrix.

In most cases, adsorption and ion exchange phenomena are not differentiated in practical applications, and most theories and models have been approached by using adsorbent resins.[101] In fact, upon the exchange of ionic compounds adsorption also occurs onto the polymeric matrix due to hydrophobic interactions, making the evaluation of ion-exchange data much more complex. Accordingly, differentiation between a pure ion exchange process and a sorption process results to be almost impossible, without further analytical investigations, such as the quantification of counterions released during the process.

Nevertheless, when talking about ion exchanger matrices it is possible to state that functional groups define chemical properties of the polymer matrix, by bearing on surface a negative or positive charge. The different dissociation properties of groups, lead to either strong or weak exchangers (which are recognized similar to that of strong and weak electrolytes). Taking into account that an ion exchanger can be considered as a "reservoir" containing exchangeable counterions, the counterion content in a given amount of material is defined essentially by the amount of charged functional groups which must be compensated by the counterions, and thus is essentially constant. This can be defined by the Ion exchange capacity (IEC):

IEC = amount of functional groups, equivalents / mass of polymer, g (1-15)

Whereas for neutral matrices the driving force for ion transport is the concentration gradient, when talking about charged or ion-exchange matrices, ion transport is also affected by the presence of the fixed charge. In this sense, Teorell[102] and Meyer *et al*.[103] proposed a theory to describe this ion transport, based on two principles: the Donnan exclusion effect (DEE) and the Nernst-Planck equation.

If we consider now an ion-exchange matrix in contact with an ionic solution, it comes clear that during the IMS there are always two species bearing the same charge: the matrix itself and one of the reactants (the reducing agent in cation exchangers; or the metal ion in anion exchangers). This means that there is an electrostatic repulsion between the matrix and one of the species mentioned that impede the penetration inside the polymeric matrix, referred as DEE.[104-106]

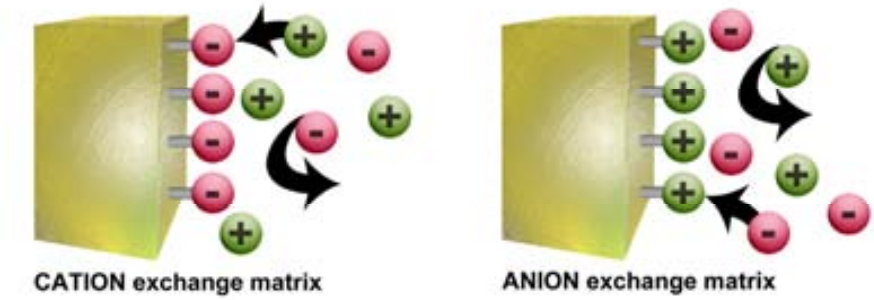

Figure 1.15. Schematic representation of electric interactions between a charged matrix and the ionic solution.

The DEE is based on the inability of co-ions to deeply penetrate inside the polymer when the sign of their charge coincides with that of the polymer functional groups. DEE can be described by thermodynamics allowing us to calculate the chemical potential (μ_i) of the ionic species when an ionic solution is in equilibrium with an ionic matrix. (Equations 1.16-17)

Thus, in the ionic solution itself:

$$\mu_i = \mu_i^0 + RT\ln(m_i) + RT\ln(\gamma_i) + z_iF\psi \qquad (1\text{-}16)$$

And in the matrix:

$$\mu_i^m = \mu^{0m}_i + RT\ln m_i^m + RT\ln\gamma_i^m + z_iF\psi^m \qquad (1\text{-}17)$$

Where: μ_i^0 states for the electrochemical potential in some reference state,

R is the ideal gas constant,

T is the absolute temperature,

m_i is the mobility of the ion,

γ is the activity coefficient of the ion,

z_i is the valence of the ion,

F is Faraday's number (96,485 C/mol),

ψ is the electrical potential (e.g. in Volts).

An ion will tend to diffuse from where its μ_i is higher to where its μ_i is lower, and, when reaching the equilibrium:

$$\mu_i^m = \mu_i \qquad (1\text{-}18)$$

Thus, if the reference states for both phases, the appearance of an electric potential (the Donnan electric potential, E_{Don}) at the surface of a solid is solely determined by the activity of ions in solution, and it can be described by Nernst equation. Moreover, for dilute solutions, since activity can be considered equal to concentration:

$$E_{Don} = \frac{RT}{Fz} \ln\left(\frac{a_{i,m}}{a_i}\right) \approx \frac{RT}{Fz} \ln\left(\frac{c_{i,m}}{c_i}\right) \qquad (1\text{-}19)$$

Where: $RTln(c_{i,m}/c_i)$ is the tendency to diffuse from one phase to another because of the concentration difference: "the concentration force",

E_{don} is the tendency for the ion to diffuse due to the electrical potential difference: "the electrical force".

Consequently, ion penetration inside the ionogenic matrix is balanced by the sum of two driving forces acting in opposite directions: the gradient of the ion concentration and the DEE itself.

Regarding the implications of this in relation to the IMS, the result of these two driving forces usually is the formation of the MNPs mainly near the surface of the polymer matrix. This supposes a really suitable situation for some final applications of the nanocomposites (e.g. catalysis) since MNPs remain maximally accessible for substrates of interest such as chemical reagents or bacteria.[97, 107]

Anyway, even if diffusion, adsorption and ion exchange are the main mechanisms by which we can explain the interactions between the polymeric matrix and the loading solution, other aspects such as are the hydration of the matrix, the ion mobility and the ion hydration and of course, the matrix structure have to be considered in order understand MNPs formation by IMS in such polymeric matrices. In this sense and taking into account that this work is focused on the development of nanocomposite materials from different polymeric matrices, with and without ion exchange sites, next section of this chapter provides a short overview of the matrices employed.

1.5. Polymeric matrices

Even if the number of polymeric matrices is reduced to those accomplishing the aforesaid requirements, a great number of possibilities are, in fact, available to proceed with the successful loading of MNPs via IMs approach. In this sense, resin beds, fibrous materials, films and so on offer a wide range of applicability to the technique. Among all these possible polymer

matrices, this thesis work is mainly focused on the use of cross-linked polymers in the form of commercial or tailored polymeric films, polymeric foams and textile fibers.

Special attention will be focused on those matrices which have been more relevant (in time dedicated and in number of publications), such is the case of polymeric membranes, which are among the better opportunity to apply the nanocomposites successfully so as to obtain the intensification of processes. However, in order to understand the importance of the new materials tackled it is necessary to provide a short overview of membrane and membrane processes.

1.5.1. Polymeric films

The use of polymeric films, specially when applied as membrane filtration materials (described in Section 1.8.1 of this chapter) finds a widespread and ever increasing application in the petrochemical, food and pharmaceutical industries, in biotechnology, and in a variety of environmental applications, including the treatment of contaminated air and water streams. [108]

Organic or polymeric films constitute the wider and most developed field of membranes, from a standpoint of production volume and of its practical applications. The main reason that has led to this situation has to do with the versatility of polymers available, and can be resumed as follows:[109]

- there is a possibility to exert some control over the molecular configurations of polymers, which directly affect permeability and selectivity of the membranes,
- polymers can easily adopt different physical forms, which has an obvious advantage in a technological term, and
- the large variety of existing polymers allows to choose those most interesting to design a particular membrane.

These films can be based either on rubbery or glassy polymers, depending on their glass transition temperature (T_g) which is defined as the temperature at which an amorphous polymer changes from a glassy state to rubbery state. For example, for T_g values below 25 °C the polymer would remain in a liquid-like form at room temperature. In this rubbery state the rotation of the side groups of the polymer chains is freer and allows obtainment membranes with greater flexibility and free volume. As a consequence, glassy polymers have high selectivity and lower permeability, which allow obtainment a high purity, whereas rubbery polymers usually have high permeabilities for gases, but a relatively low selectivity.[110]

A part from the evident need for resistant and efficient polymeric films for the process, other important parameters have to be maximized, such as their permeability and permselectivity, especially when applied in membrane processes. These are strongly influenced by (1) the mobility of polymer chains (as reflected in many cases by the T_g of the polymer), (2) the intersegmental spacing, a measure of the mean free volume of the polymer, and (3) the penetrant polymer interactions (as reflected by the solubility of the penetrant gases in polymers). [110]

In this sense, several works have been focused to achieve simultaneously higher permeability and selectivity, by coupling chain stiffness with an increase of the interchain separation.[111-114] The results lead to the conclusion that substituent mobility rather than the size of the pendant side group is the critical factor in determining free volume and transport properties. In other cases, some efforts have been done to create new materials with significant chemical and thermal resistance.[115-117]

Under these requirements, new research is focused on the development of polymeric films that overcome these typical disadvantages. In this sense, new solvent-resistant polymeric films have been developed.[115, 116] For example, Vanherck *et al*., reported the development of a new solvent stable nanofiltration membrane,[118, 119] which allows the separation of organic mixtures down to a molecular level by simply applying a pressure gradient over a membrane.

Thanks to the great versatility of polymer conformations, polymeric nanocomposite films offer added flexibility over their conventional reactor counterparts. The accurate selection of the polymer molecular configuration and the control of its morphology would lead to the most appropriate membrane for a desired application. Moreover, when applied in industrial processes, polymeric organic membranes developed with polymeric films are usually less expensive than their ceramic or metallic counterparts.[119, 120]

Similarly to the extensive diversity of existing polymers, the methods of preparation of such films are also abundant. This wide range of possibilities allows, in last instance, the obtainment of a great myriad of films with different structures. And since the properties and performance of a membrane depends strongly on its morphology, one of the greatest objectives is precisely controlling and optimizing its formation process.

Methods such as immersion precipitation,[121] interfacial polymerisation,[122] evaporation,[123] plasma polymerisation,[124] and so on are widely used. Nevertheless, the majority of polymeric films are developed via phase separation (also known as phase inversion or phase demixing)

which comes due to a change of the thermodynamic state of the initial homogeneous polymeric solution.[125, 126]

This change of thermodynamic state can be induced by different methods:

- temperature variation;
- differential evaporation of the solvent in a ternary solution polymer / solvent / non-solvent;
- intrusion of a non-solvent in a polymer / solvent binary solution.

This phase inversion causes the creation of two polymeric phases: a poor phase and a rich phase, growing following the mechanisms of nucleation-growth or spinodal decomposition. After liquid-liquid phase separation, the polymer rich phase solidifies forming the film matrix. On the other hand, the poor phase is removed by successive washings and gives way to the pores of the film.[127]

The application of the concept of phase inversion (or separation) to prepare films was first introduced by Loeb and Surirajan in 1959 (with the development of the so-called Loeb-Sourirajan membranes[126]) but it was not fully explained until 1971, when Kesting[128] applied the same thermodynamic principles as all separation processes in such films formations. In all cases, the starting point is a thermodynamically stable solution that is afterwards subjected to such conditions that cause a demixing.

The parameter describing the miscibility of different compounds is the free enthalpy of the mixture, ΔG_m (or Gibbs free energy of the mixture):

$$\Delta G_m = \Delta H_m - T\,\Delta S_m \qquad (1\text{-}20)$$

Where: ΔH_m is the enthalpy of the mixture,

ΔS_m is the entropy of the mixture.

When the free enthalpy of the system polymer/solvent is negative ($\Delta G_m < 0$), the two components are miscible, but once it becomes positive, phase separation happens.

The chemical potential of a compound *i* (μi) in the mixture can be obtained from the expression of the Gibbs free energy of the mixture as follows:

$$\frac{\Delta \mu_i}{RT} = \frac{\partial}{\partial n_i}\left(\frac{\Delta G_m}{RT}\right)\Bigg|_{P,T,n_{i\neq j}} \qquad (1\text{-}21)$$

Where: n_i is the number of mols of the component *i*

R is the ideal gas constant

T is the temperature of the system

Since for a binary system such is a polymer / solvent mixture the entropy of mixing is not very high, a slight increase in the enthalpy of mixing ($\Delta H_m > 0$) can cause phase separation. And this increase in enthalpy of mixing typically occurs when decreasing the temperature. **Figure 1.16-a**, **b** represents the evolution of $\Delta G_m/RT$ as a function of the volume fractions of solvent (ϕ_1) and polymer (ϕ_2) at two different temperatures of a binary system as the one described before.

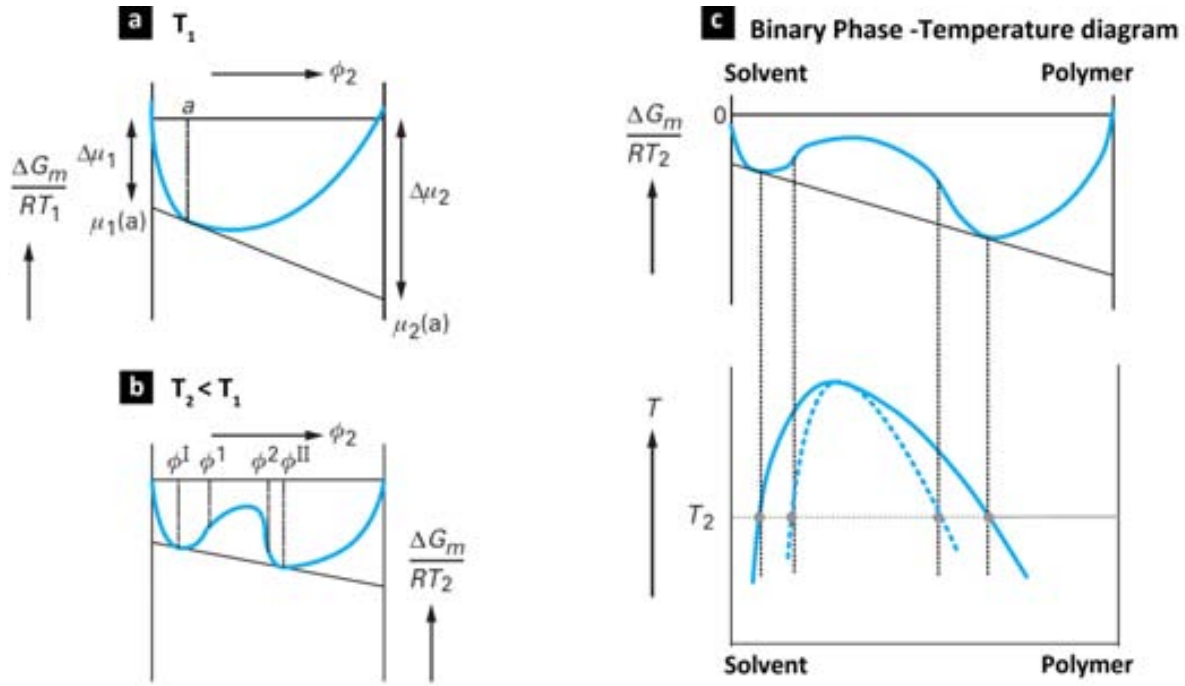

Figure 1.16. (a) and (b) Evolution of $\Delta G_m/RT$ as a function of the composition of a binary system of solvent (ϕ_1) and polymer (ϕ_2) at two different temperatures $T_2 < T_1$ ($\Delta H_m > 0$); (c) Diagram of phase-composition-temperature for a binary system polymer-solvent.[125, 127]

As it can be observed, at T_1 polymer and solvent are miscible in all ratios, and the tangent in one point of the curve (for example *a*) allows identifying the chemical potential of the mixture. When the temperature diminishes, at $T_2 < T_1$, the evolution of ΔG_m presents two minimums for two different polymer volume fractions ϕ^I and ϕ^{II} which are in equilibrium. Any system whose composition ϕ lies between these two values can therefore separate into two phases of composition ϕ^I and ϕ^{II}, respectively (whose ΔG_m is lower than if there was formation of a single homogeneous solution).

For each temperature, the volume fractions of the two minimums of the function studied and of the inflection points (ϕ^1 and ϕ^2) can be determined. When temperature is increased, the domain of immiscibility is generally reduced, and the two points connected by the tangent get closer to each other, collapsing finally in one single point, the critic point.

Figure 1.16-c shows the diagram obtained by relating these volume fractions depending on the temperature into a single diagram. In this figure, the solid curve corresponds to the minimums of the $\Delta G_m / RT$, ϕ^I and ϕ^{II}. It is the so-called the binodal curve, denoting the condition at which two distinct phases may coexist. Whereas the dotted line corresponding to the inflection points of the function studied (ϕ^1 and ϕ^2) is the spinodal curve, denoting the boundary of absolute instability of the solution to decomposition into both phases. The two curves cross at the critical point. When increasing the temperature from this point the polymer and solvent are miscible in all proportions.

In addition to changes in temperature, changes due to the inclusion of a third component, a non-solvent, in the mixture can also cause the demixing of the solution. In order to explain the mechanism of separation in this last case, ternary diagrams as the one showed in **Figure 1.17** are often used.

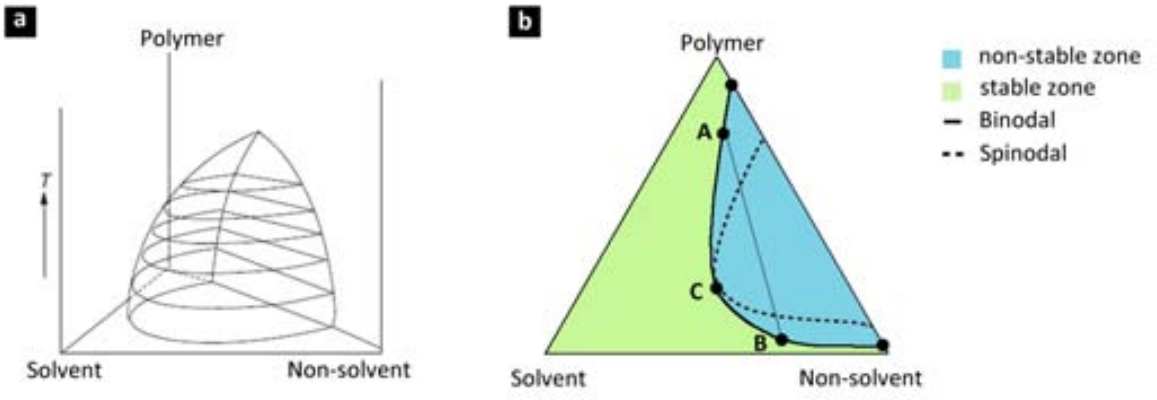

Figure 1.17. Representation of the binodal surface for a ternary system. (a) 3D view at different temperatures; (b) 2D view at a certain temperature, Isothermal ternary diagram.[125, 127]

Figure 1.17–a schematically illustrates the influence of the temperature on such 3D demixing surface for a ternary system as the one described above. As the temperature increases, the surface area of the separation decreases, so, when the temperature is high enough, the compounds are miscible in all proportions.

Figure 1.17–b shows an isothermal cross section (at a certain temperature) of **Figure 1-17-a**. Each vertex of the triangle represents a pure compound (polymer, solvent or non-solvent). A point on one side of the triangle corresponds to a binary mixture and any point within the triangle is a ternary mixture. The binodal curve divides the diagram into two main regions:

homogeneous medium (region of mutual miscibility shown as the one-phase region in green on the diagram) and two-phase medium (region in blue on the diagram, where two phases exist). The straight line (tie line) connects the points of conjugation on the binodal curve which are in equilibrium and have the same chemical potential. A composition within this two-phase region always lies on a tie line and splits into two binary system, one phase rich in polymer (*A*) and the other poor in polymer (*B*).

In this work membranes were obtained by wet phase inversion of a binary mixture of solvent / polymer in a non-solvent, as explained in **Figure 1.18**.

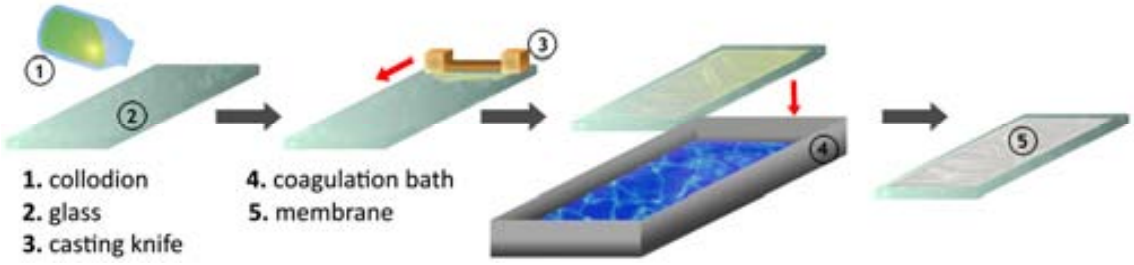

Figure 1.18. Membrane preparation by wet phase inversion.

As it has been already mentioned, it is important to note that the polymers to be used must be capable of retaining ions (MNPs precursors), so during the initial development of this thesis work it was considered essential to necessary to fabricate films with ion exchange positions.

Let's review now the formation and characteristics of ion-exchange membranes.
In its origins, ca. 1939, many researchers focused their efforts to the establishment of the basis of the studies on electrochemical ion exchange films. For example, in 1939 K.H. Meyer, J.F. Sievers and T. Teorell developed the first artificial charged film with the aim to obtain a theory of membrane potential. But it was not until 1950, with the work of M.R.J. Wyllie, W. Juda and M.R.C. McRae, when the first ion exchange film synthesis was published.[129] After these works, studies on ion exchange films, their synthetic methods, modifications, theoretical explanations and applications in industry became very active.[130, 131]

Ion exchange films can be classified via several ways, and usually each classification is used as the interest of the classifier itself. From the morphological point of view, they can be classified by their morphology in two main types: homogenous and heterogeneous films.[131] In an initial

stage of their development, heterogeneous ion exchange films were actively developed by blending and formed as a film finely powdered ion-exchangeable materials and a binder. In a general procedure, cation or anion exchange resins are homogenously blended and heated with a thermoplastic polymer (i.e. polyethylene, polypropylene, etc.) and the mixture is formed as a membrane by pressing or heating. [127] Although these types of films are easily prepared and have a great mechanical strength, their electrochemical properties are lower than the ones facilitated by the homogenous ones in which the fixed charged groups are evenly distributed over the whole membrane polymer matrix. Homogeneity can be achieved thanks to the fact that membrane films can be produced by polymerization or polycondensation of functional monomers such as phenylsulfonic acid with formaldehyde, or by functionalizing a polymer such as polysulfone dissolved in an appropriate solvent by sulfonation and cast into a film.

But the completely homogeneous and the macroscopically heterogeneous ion-exchange films are extreme structures. Most ion-exchange films show a certain degree of heterogeneity on the microscopic scale. Thus, other properties may be considered to classify them. In this regard, according to the distribution and species of the fixed charge (ion exchange groups) it is possible to difference between:[129]

(i) cation exchange films (with functional groups such as $-SO_3^-$, $-COO^-$, $-PO_3^{3-}$);
(ii) anion exchange films (with cationic charged groups such as $-NR_4^+$, $-NH_2^+$, $-NHR^+$);
(iii) amphoteric ion exchange films (with both cation and anion exchange groups);
(iv) bipolar exchange films (bilayer films composed by a cation exchange layer and an anion exchange layer); and
(v) mosaic ion exchange films (which have certain domains that may be separated with an isolator of cation-exchange groups and also domains with anion-exchange groups).

On the other hand, a classification based on the constituent materials allows grouping such films as:

(i) perfluorocarbonated,
(ii) composed of hydrocarbons or partially halogenated hydrocarbons, and
(iii) composite films of inorganic ion exchanger and organic polymer (e.g., hybrids).

Moreover, in recent years the use polymers directly obtained from nature (such as alginate and chitosan) has been broadly extended in the fabrication of such films.[129]

In this thesis work only the first two types of films have been employed: Nafion (a perfluorocarbon film), and films made of Sulfonated poly(aryl)sulfones (hydrocarbon films).

1.5.1.1. Nafion

As ionomer membranes appeared, its development through the improvement of its robustness in order to be applied in the development of polymer electrolyte fuel-cell technology garnered significant research interest. A variety of proton exchange membranes (PEM) with enhanced stability, proton conductivity, and processability appeared. And, to date, perfluoronated sulfonic acid polymers have experienced the most widespread use in commercial applications.[132, 133] A classic example of this type is, indeed, Nafion.[134]

Nafion is a well-known and commonly used ionomer membrane produced by DuPont company, and is nowadays one of the most employed commercial ion exchange polymeric membranes involved in a variety of applications.[135] The main applications concern their use in fuel cells, electrochemical devices, chlor-alkali production, metal-ion recovery, water electrolysis, plating, surface treatment of metals, batteries, sensors, Donnan dialysis cells, drug release, gas drying or humidifaction, and superacid catalysis for the production of fine chemicals.[136] This wide range of applications comes up due the exceptional properties of this polymer, which can be summarized as follows:

- it is highly conductive to cations;
- it is highly stable to chemical attack (according to DuPont, only alkali metalscan degrade Nafion under normal temperatures and pressures);
- the Teflon backbone interlaced with the ionic sulfonic groups gives Nafion a high operating temperature, e.g. up to 190 °C, however, in membrane form, this is not possible due to the loss of water and mechanical strength;
- it has hight mechanical stability;
- it is a superacid catalyst: the combination of fluorinated backbone, sulfonic acid groups, and the stabilizing effect of the polymer matrix make Nafion a very strong acid, with pKa ~ -6;[137] and
- it is selectively and highly permeable to water.

These exceptional properties are determined, in last instance by its chemical structure, which consists of a polytetrafluoroethylene (PTFE) backbone and regularly spaced long perfluorovinyl ether pendant side chains ended by a sulfonic group, responsible of its IEC. See **Figure 1.19**.

Nafion can be produced as both a powder resin and a copolymer, and it has various chemical configurations and thus several chemical names in the IUPAC system. The molecular weight of the polymer is uncertain due to differences in processing and in solution morphology, what gives to the material a high variability of possible elemental unit conformations, as shown in

Figure 1.19 (left). Instead of its molecular weight (which has been estimated at 10^5–10^6 Da),[135, 136] instead of using it, the equivalent weight (EW) and material thickness are used to describe most commercially available membranes. The EW is defined as the weight of Nafion (the number of grams of dry Nafion) per mole of sulfonic acid groups when the material is in the acid form.[135] For example, Nafion-117 (the one used in this thesis work) represents 1100 g EW + 0.007 inch in thickness. Conventional ion-exchange properties are usually described in terms of its IEC which is the multiplicative inverse or reciprocal of the equivalent weight. IEC = 1000/EW.[135]

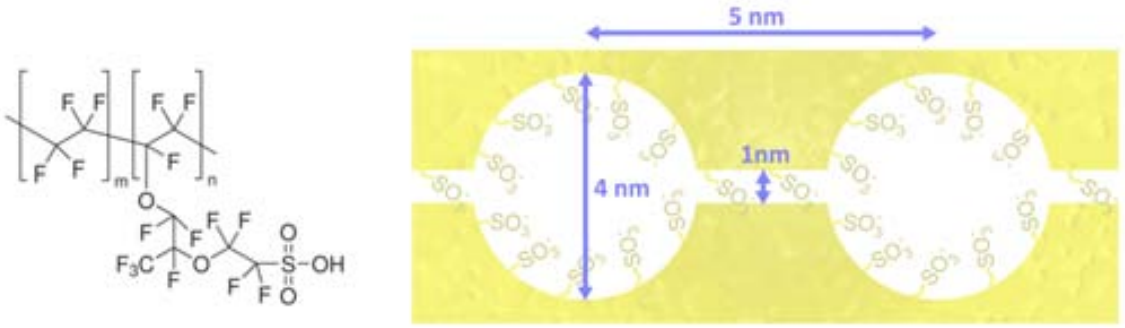

Figure 1.19. Polymeric structure of the elemental unit of Nafion (left) and Gierke's cluster structure and network model for the interactions between polymer and water in Nafion (right).

Because of the absence of chemical cross-linking between polymer chains there is phase segregation into hydrophilic and hydrophobic domains. Despite there have been several models under debate[138-144] (i.e. Fujimura's core-shell model, Dreyfus' local-order model, Haubold's sandwich-like model, Gebel's rodlike model, Litt's lamellar model and Kreuer's film-like morphology), the pioneering cluster-network model proposed by Gierke *et al.*[145] is frequently reported in the literature. According to this cluster-channel network model of Nafion (**Figure 1.19**), the polymer chains form reverse micelles in which sulfonic groups are lined in the wall encapsulating water cavities. This model, in fact, has lasted for many years as a conceptual basis in order to rationalize the properties of Nafion membranes, especially in what concerns to ion and water transport and ion permselectivity.[146] Based on small-angle X-ray scattering (SAXS) and wide-angle X-ray (WAXS) studies and several assumptions, it estimates clusters of diameters around 40 Å of sulfonic-ended perfluoroalkyl ether groups organized as inverse micelles and arranged on a lattice. These water clusters are linked with narrow channels (of about 10 Å in size), which have been experimentally confirmed by electrolithography of the Nafion membrane.[147]

Despite the fact that this cluster-network model has been the most widely referenced model in the history of perfluorosulfonate ionomers, it was never meant to be a definitive description of

the real morphology of Nafion. In this sense, even the same authors recognized that further experimental work would be required to completely define the nature of ionic clustering in these ionomers. Certainly, while the majority of morphological information about Nafion has been originated from SAXS and WAXS diffraction experiments, this polymer yields very little characteristic detail in the dimensions probed by these methods.[135, 136] Thus, nowadays there is quite an agreement regarding the inaccuracy of this model as it was based on the limited structure property information that was available at the time. Therefore the pursuit for a universally accepted model still goes on.

In any case, it is noteworthy that due to the presence of extremely hydrophobic and extremely hydrophilic domains Nafion does not present a static morphology in water. In this sense, and based on the results of this scattering analysis of Nafion over a wide range of water contents, combined with energetic considerations, Gebel *et al.* proposed a water channel model as a conceptual description for the swelling and dissolution process shown schematically in **Figure 1.20**.[135, 148]

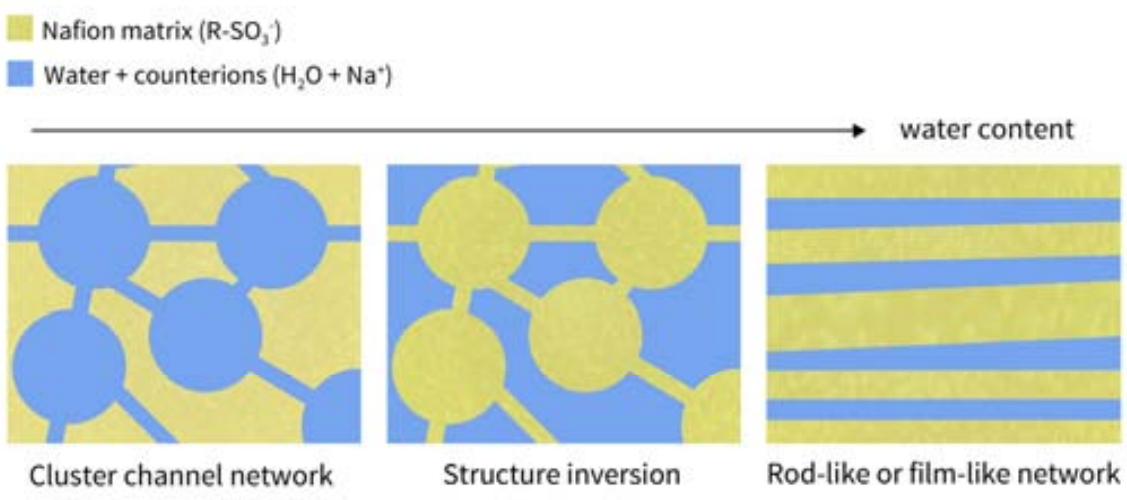

Figure 1.20. Conceptual model for the morphological reorganization of the ionic domains in Nafion as the dry membrane is swollen with water to complete dissolution.

In Gebel's qualitative model, the dry membrane is considered to contain isolated and spherical ionic clusters with diameters of about 1.5 nm and a center-to-center separation distance of about 2.7 nm. With the absorption of water, the clusters swell to hold pools of water surrounded by ionic groups at the polymer-water interface in order to minimize the interfacial energy. As the water content increases (between 0.3 and 0.5), structural reorganization occurs to keep the specific surface area constant, and the onset of percolation is achieved by connecting cylinders of water between the swollen, spherical clusters. At values greater than

0.5, an inversion of the structure occurs such that the structure resembles a connected network of rods. Finally, as the membrane "dissolves" into solution, the lamellar or film structures (based on Litt's and on Kreuer's model describing Nafion as multilayer structure where the ionic domains are defined as hydrophilic layers separated by thin hydrophobic PTFE-like domains) appear.[143, 144]

Thanks to these models, subsequent studies seemed to reveal a nanoscale arrangement that could explain the excellent transport properties of the material.[149, 150]

Accordingly, it is not only important but also necessary to understand the nature of such material, since it is clear that the study, tuning and application of these materials for its optimum performance requires a detailed knowledge of their chemical microstructure and nanoscale morphology. Through the collective information acquired among these years from the detailed works of many research groups and institutions, a broader understanding of this material has emerged. But much more seem to be yet to learn. That is in fact the great challenge for Nafion materials in which the possible chemical variations are rather limited. And, of course, all of these objectives must be achieved while trying to maintain a cost as lower as possible. Because even if Nafion is still considered the benchmark material against which most results are compared, their high cost and the absence of pores are still drawbacks to overcome. Thus, research is now focused on the obtainment new homogeneous cation exchange membranes. And, in fact, there are a wide number of alternative polymeric membranes (including nonfluorinated types) aimed to compete with Nafion.

1.5.1.2. Poly(arylsulfones)

Poly(arylsulfones) are a broad class of amorphous high glass transition temperature polymers with high mechanical, thermal, and chemical resistances. This family includes, among others, the poly(etherarylsulfones) which are engineering plastics with high performance that are attracting much interest as high-temperature resistant materials. Their applications stem from their excellent hydrolytic, thermal and dimensional stability over a wide range of temperature, in addition to good mechanical properties.[151, 152]

Some of the typical poly(etherarylsulfones) are presented in **Figure 1.21**: polysulfone (PSU), polyphenylsulfone (PPSU), polyethersulfone (PES) and polyetehersulfone with Cardo group (PES-C). All of these poly(etherarylsulfones) are aromatic polysulfones containing an ether link in the backbone, but they differ in the nature of aliphatic carbon situated between the two p-phenolate rings (tackled in green).

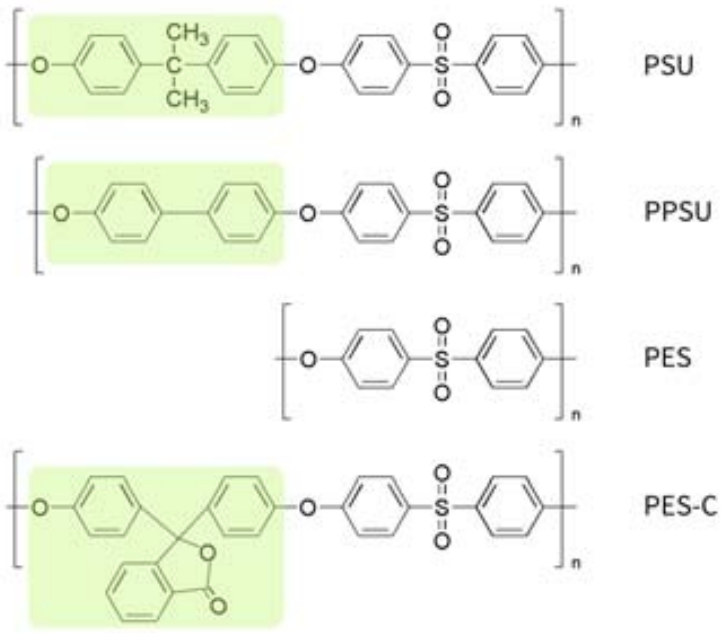

Figure 1.21. Chemical structures of different poly(etherarylsulfones) units: polysulfone (PSU), polyphenylsulfone (PPSU), polyethersulfone (PES) and polyetehersulfone with Cardo group (PES-C).

Their key features can be summarized as follows:

- temperature-independent properties,
- good dimensional stability,
- high stiffness,
- high mechanical strength,
- excellent hydrolysis resistance,
- high strength,
- transparent (yellowish),
- can be sterilized by superheated steam, resistant to hot water,
- good chemical resistance.

Thanks to these main properties they offer a profile that – in comparison to other engineering plastics- predestines these materials for a very broad applications spectrum that is still growing reaching from the automotive industry to the water treatment.

In the membrane field, they are widely used in the manufacture of asymmetric membranes (either in flat or hollow fiber shapes) with different and controllable pore sizes in the active (skin) layer.[153, 154] They are usually applied as ultrafiltration membranes in different industries, for the separation of solvent and small solutes as bacteria, viruses, or soluble macromolecules (synthetic or natural polymers).[155-158]

Their high hydrophobic character leads to an easy deposition of macromolecular solutes, with hydrophobic regions and to a bad wetting of the pores and low water flux through the membrane pores.[159] Therefore increasing the membrane hydrophilicity is a good way to improve the membrane resistance to solvent alteration and to fouling, and to give to the membrane new functions (such is ion transport) as well. In this sense, different strategies can be followed, such as addition of hydrophilic polymers to the membrane materials dope,[160, 161] immobilization of polymers with hydrophilic segments by photopolymerization[162] or adsorption[163] and chemical modification with ion exchange groups.[153, 159, 164]

Moreover, since these polymers are mainly used in ion transport technologies and in water treatment as membranes, their modification in order to introduce ion exchange positions has been widely explored. The modification of poly(arylsulfones) with sulfonic groups is a well-known strategy, widely used in polymers such as poly(etheretherketone)[88] or polysulfones.[165] Yet, the presence of these groups is known to highly increase the hydrophilicity of the polymer (maybe excessively), which can hinder the preparation of membranes with the required properties. For example, sulfonated poly(etheretherketone) has already proved to be a very suitable matrix for IMS of various Polymer Stabilized Metal Nanoparticles (PSMNPs)[88] but it cannot be used for the preparation of membranes by phase inversion technique (see Section 1.5.1). Due to its high hydrophilicity and its quite low mechanical stability, SPEEK yields to the obtainment of a gel instead of a solid flexible film. For this reason, a compromise needs to be found for each type of application by balancing hydrophilicity and hydrophobicity.

To cope with these drawbacks, the election of the polymer is essential, since the development of nanocomposite membranes requires the use of polymers with good chemical, thermal, and mechanical stability, and these polymers also have to be easily fabricated in a suitable form for their further practical application. For this reason, polyphenylsulfone (PPSU) and polyetehersulfone with Cardo group (PES-C) are suitable candidates to this purpose.

Concretely, **poly(arylene ether sulfone) with a Cardo group** (PES-C) prepared by a synthetic route involving toluene, sulfolane and anhydrous potassium carbonate has a high glass transition temperature (T_g=260°C) and is freely soluble in many common polar organic solvents and it has been considered to be useful for high temperature-resistant ultrafiltered film materials.[166, 167]

PES-C (**Figure 1.21**) is a relatively newly developed engineering thermoplastic with improved hydrophilicity caused by introducing bulky phenophthalein side groups into the polymer main chains. It is soluble in some aprotic polar solvents such us N,N-dimethylformaide (DMF) , N,N-

dimethylacefamide, dimethyl sulfoxide (DMSO), and N-methylpyrolidone (NMP).[167, 168] Furthermore, because of this Cardo group, the hydrophilicity of the polymer suits perfectly to proceed with a phase inversion methodology for membrane formation, and, moreover, it can be easily modified by various chemical reactions, and thus, more applications in membrane separation process can be found.

Contrary to the other better-known poly(arylsulfones) and maybe because this is a relatively new polymer, PES-C has not received much attention and not many papers can be found in the literature regarding its utilization. Nevertheless, few works concerning its modification can be found in literature. For example, Wang *et al*., Gao *et al*., Ren *et al*., and Huang *et al*. have reported the preparation of blends of the polymer with different polymers or modifiers, tuning the properties of the final membrane, improving its applications.[169-172] The sulfonation procedure was used by Blanco *et al*., Li *et al*. and Jia *et al*. to provide with ion exchange positions the polymer backbone.[153, 159, 173-175] This modification will be further discussed in Chapter 3, as it has been one of the main parts of this thesis work.

On the other hand**, polyphenylsulfone (PPSU)** (**Figure 1.21**) is an attractive polymeric material because of its high mechanical, thermal, and chemical resistances.This combination of chemical and physical properties, such as high hydrolytic, thermal (T_g = 230 ºC) and oxidation stabilities and low inflammability, comes together with a low cost and an easy processability.[176, 177] Up to now, several modifications of such polymer have been reported, such as the formation of block copolymers, obtainment blends with phosphonated PPSU, mixed sulfonated/phosphonated PPSU,[178] and mixed sulfonic acid/$SiPh(OH)_2$ PPSU,[179] sulfonation of a PPSU for reverse osmosis application,[180] and obtainment of pervaporation membranes,[181] ultrafiltration membranes,[174] dialysis membranes, nanofiltration membranes, among other applications. Again, one of the most popular modification methods is the postsulfonation. As mentioned before, polyphenylsulfone (PPSU) suit perfectly for its chemical modification (in order to introduce functional groups to further proceed with the ion exchange step of the nanoparticle synthesis) while maintaining their hydrophobic character. Due the presence of ta C-C bond between aryl units it possess a high hydrophobic character and high chemical stability. In this sense, PPSU have been postsulfonated using concentrated sulfuric acid at different temperatures and in different solvents,[182] sulfur trioxide in dichloromethane (CH_2Cl_2),[183] trimethylsilylchlorosulfonate (Me_3SiSO_3Cl) in CH_2Cl_2,[183] chlorosulfonic acid in CH_2Cl_2, oleum in chloroform ($CHCl_3$)[184] and sulfur trioxide-triethyl phosphate complex.[185]

However, the process is not so simple, as it was proved during the development of this thesis work (Chapter 3).

1.5.2. Polyurethane foams

Polyurethanes are a broad class of materials with different properties employed in a wide range of applications.[186] They were first developed in 1937 by Otto Bayer and his co-workers at I.G. Farben in Leverkusen, Germany through the reaction between diisocyanates and polyols.[187] These new class of polymers had some advantages over existing plastics made by polymerizing olefins, or by polycondensation. Early work focused on the production of fibres and flexible foams of polyurethanes to be applied as aircraft coating during World War II.[188] Polyisocyanates became commercially available in 1952 what made possible the production of flexible polyurethane in 1954 using toluene diisocyanate and polyester polyols. With the appearance of cheaper, easier to handle and more water resistant precursors such as polyether polyols (introduced in 1956 by DuPont) and polyalkylene glycols (by BASF and Dow Chemical in 1957), polyurethanes and became more popular. In 1960 more than 45 000 metric tons of flexible polyurethane foams were produced.

When the obtainment of the polymer was optimized, it was time to search for innovative processes in order to give to the material different shapes and properties. In 1969, Bayer exhibited a car entirely made of plastic in Düsseldorf (Germany) with parts manufactured using a new process called Reaction Injection Molding (RIM) in which the reactants were mixed and then injected into a mold. The addition of fillers (milled glass, mica, and processed mineral fibres) gave rise to reinforced RIM, which provided improvements in stiffness and thermal stability while reducing the thermal expansion.

Nowadays polyurethanes include polymers containing a significant number of urethane groups, regardless of the composition of the rest of the molecule. For instance, typical polyurethane may contain, in addition to urethane groups, aliphatic and aromatic hydrocarbon, ester, ether, amide, and urea groups. This wide range of polymer conformations bestow on a great versatility. In this regard, their applications include diverse types of foams (soft and rigid), coatings, adhesives, sealants, and elastomers.[189]

In fact, Polyurethane foams (PUFs) represent ca. 80 % of the total polyurethane market.[190] Moreover, PUFs exhibit high stability against chemical degradation, high mechanical durability, ease of separation from a solution, and they are also one of the most cost-effective polymers available, what makes them really suitable for practical low-cost applications.

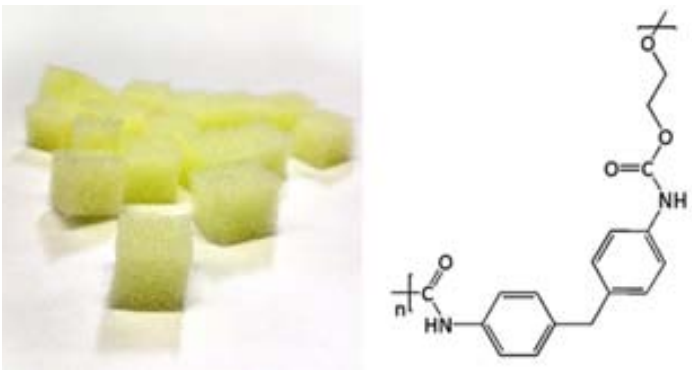

Figure 1.22. Image of Polyurethane foams cubes and the chemical structure of the elemental unit of polyurethane.

Regarding the synthesis, PUFs are obtained by adding a small amount of water during the polymerization process. Water molecule reacts with an isocyanate molecule first forming an unstable carbamic acid, which then decomposes into carbon dioxide and an amine. The amine reacts with more isocyanate to give a substituted urea, which is not very soluble in the reaction mixture and tends to form separate "hard segment" phases consisting mostly of polyurea. The concentration and organization of these polyurea phases allows tunning the properties of the final PUF. [190]

Although this polymer does not possess ion exchange positions it has been considered as a suitable material for the development of nanocomposite water filters. Due its low cost and favourable shape, its modification was studied by the present work, as it will be detailed in Chapter 3.

1.5.3. Textile fiber polymers

Fibers have been extensively used for thousand years, and nowadays still are of the greatest importance in our world. Clothes, high-performance fibers and non-woven materials suppose wide panoply of opportunities where textile industry finds its major market.

A textile is a flexible woven material consisting of a network of natural or artificial fibers often referred to as thread or yarn. Textiles are formed by weaving, knitting, crocheting, knotting, or pressing fibers together.[191] Understanding the chemical structure of these fibers shaping the network is crucial to an appreciation of their intrinsic final properties. And this chemical structure depends in last instance on how the material is processed.

Common textile fibers used in global fashion today include: natural fibers made of animal ohair or fur (polypeptide fibers such as silk or wool) or cellulosic fibers (such as cotton or bamboo) and synthetic fibers made of mineral-based fibers (such as asbestos or glass) or of synthetic polymers (such as polyester, nylon or acrylic).

They can be obtained by several synthetic methods that use naturally-occurring polymers (e.g. cellulose acetate), as well as by synthetic methods that use polymer-based materials, or even minerals such as metals to make foils and wires.

Regarding the final structure of the fibers, it can be explained by two-phase models, with phases being the crystalline and the non-crystalline material, as the ones shown in **Figure 1.23**. Although the fringed micelle model (shown in **Figure 1.23-a**) is maybe the oldest one, it still enjoys of considerable popularity when applied to unoriented polymers. However, most of the industrial fibers produced nowadays are highly oriented, and their structure is mostly characterized by the fringed fibril model (shown in **Figure 1.23-b**) where fibrils (clusters with diameters between 100 -1000 Å of partially aligned molecules) are oriented and linked due to weak forces. Yet, these two models have been often criticised because some chain bending and folding are in the surface of the crystal. Hence, a more accurate modified model (shown in **Figure 1.23-c**) was proposed for semicrystalline polymers. Finally, for highly orientated polymers (such as polyester) Peterlin model was proposed (**Figure 1.23-d**) taking into account that the orientation in the noncrystalline zones depends on the manufacturing process.[191]

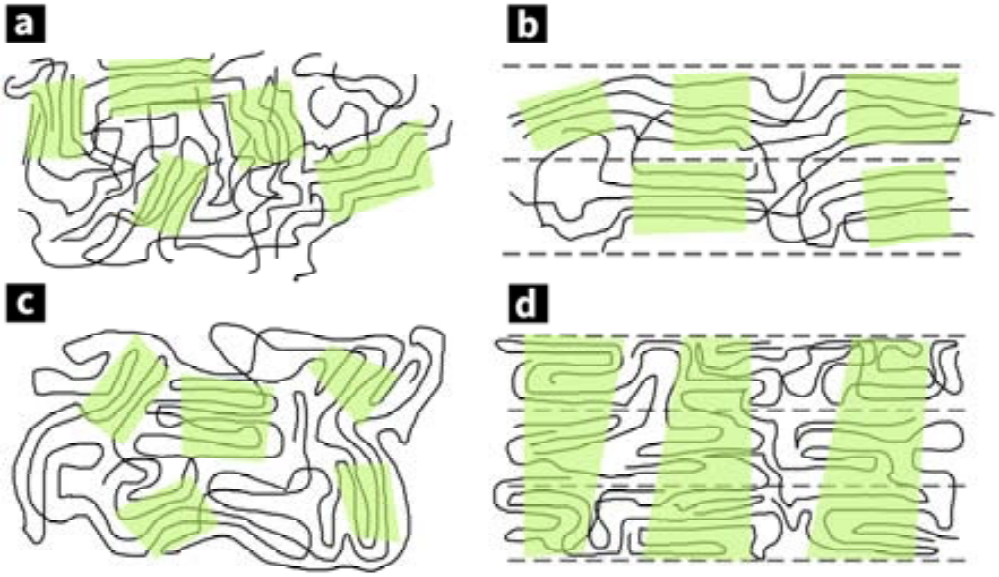

Figure 1.23. (a) Fringed micelle model, with crystallite regions shaded in green, (b) fringed fibril model, (c) modified fringed micelle model, and (d) Peterlin model.

During the present work, wool was first chosen as a suitable matrix for testing the possibility of applying the IMS procedure in textile fibers. But it was eventually discarded due to its instability, complexity and swelling properties. Hence, during the development of the present work only cellulosic and synthetic fibers have been used, and they are detailed in Figure **1.24** and briefly explained below.

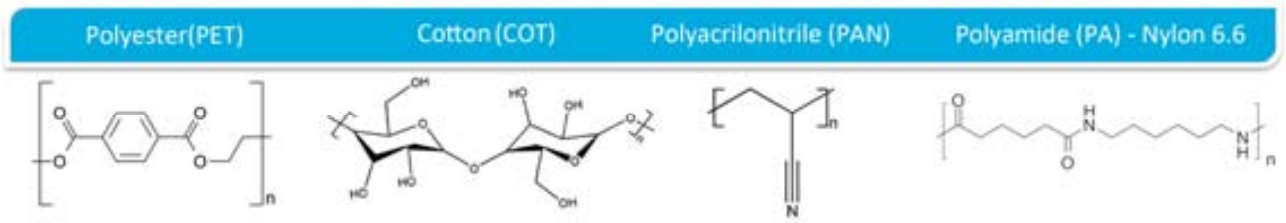

Figure 1.24. Different textile fibers with their elemental unit structure used during this thesis work.

- **Polyester** is a category of polymers which contain an ester functional group in their main chain, and although there are many types of polyesters, the term "polyester" as a specific material is most commonly referred to polyethyleneterephthalate (PET) with a low molecular weight ($15{\cdot}10^3$ - $25{\cdot}10^3$ g/mol). PET is a thermoplastic (T_g ~ 69 ºC) polymer used in synthetic fibers, beverage, food and other liquid containers; thermoforming applications and engineering resins often in combination with glass fiber.[191]
- **Cotton** (COT) is a soft, fluffy staple fibre that grows in a boll, or protective capsule, around the seeds of cotton plants of the genus *Gossypium*. Although it is mainly formed by cellulose (after scouring and bleaching, cotton is almost 99 % cellulose) its chemical composition also includes water, protoplasm and pectins, waxes and fatty substances and mineral salts.[191] Cellulose has a molecular weight of $1{\cdot}10^3$ g/mol, and it is difficult to dissolve without grading (cleaving bonds and reducing its molecular weight).

Cotton is not thermoplastic and, therefore, it has no glass transition temperature and remains flexible even at very low temperatures. At elevated temperatures, cotton decomposes instead of melting.

- **Polyacrylonitrile** (PAN) is a synthetic, semicrystalline organic polymer obtained by polyaddition reaction of monomers of acrylonitrile.[192] It is a versatile polymer used to produce large variety of products including ultrafiltration membranes, hollow fibers for reverse osmosis and fibers for textiles. Usually and in order to allow dying, commercial textile fibers are functionalized with sulfonic or sulfate groups ($R\text{-}SO_3^-$ or $R\text{-}SO_4^-$) using small amounts of other vinyl comonomers. PAN has properties involving low density, thermal stability (T_g ~ 85 ºC), high strength and modulus of elasticity. These unique properties have made PAN an essential polymer in high tech.[193]
- **Polyamide** (PA) can occur both naturally (proteins such as wool and silk) and artificially (made through step-growth polymerization or solid-phase synthesis, examples being nylons, aramids, and sodium poly(aspartate)). Synthetic polyamides are commonly used in textiles, automotives, carpet and sportswear due to their extreme durability and strength.[194] According

to the composition of their main chain, polyamides are classified as aliphatic (as is the case of Nylon-6,6, with a total amount of 12 carbon atoms in its elemental unit structure), polyphthalamides (with a semiaromatic main chain) and aramides (aromatic). Concretely, Nylon-6,6 is obtained by the polymeric condensation of an ammine and a carboxylic acid both containing 6 carbona toms. Fibers end with either a carboxylic group (R-COO-) or an ammine (R-NH_2). It possess high mechanical strength, great rigidity, and although it presents good stability under heat its glass transition temperature is not really high ($T_g \sim 55$ ºC).[194]

1.6. Polymer-metal nanocomposites

Up to now, it should come clear that with all the matrices, nanoobjects and synthetic methods described, the myriad of existing possibilities is certainly wide, allowing to cover a great range of practical applications, as described in **Figure 1.25** (see Section 1.8).

Nevertheless, the obtainment of high quality nanocomposites able to satisfy not only the industrial requirements, but also those regarding the aforementioned principles of Green Chemistry (see Section 1.1) is a crucial issue.

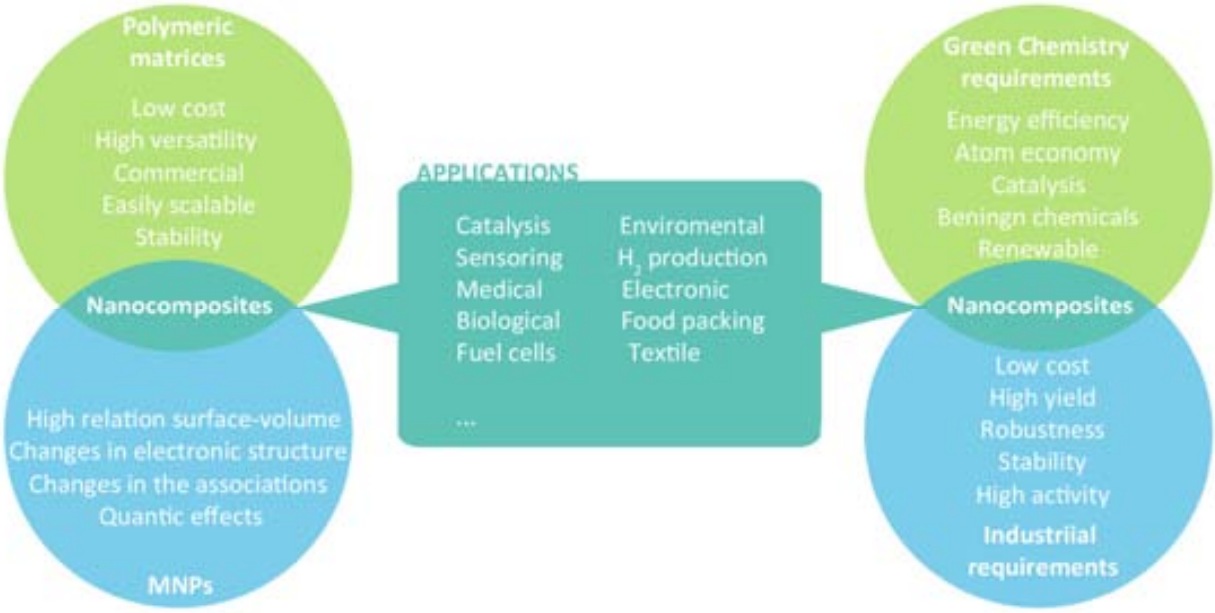

Figure 1.25. Nanocomposite materials: properties, requirements and applicability.

Therefore, and in order to focus the subject of study of the present work, it is imperative to assess the current state of art of the field. Thus, this section is mostly focused on a brief review of the literature regarding the inclusion of MNPs in the different said polymeric matrices and in each specific lack of knowledge or need.

1.6.1. Nanocomposite films

The preparation of many MNPs in films has been reported over the last few years.[120, 195-198] Typical synthetic procedures as the ones described in Section 1.3.2 can be applied for its obtainment. Ideally nanoparticles should be well dispersed on the support surface and highly active in their applications; and, what is more, the modification of the films by inclusion of these active MNPs should not affect the separation or mass transport properties of the film when used as a membrane.

1.6.1.1. Nafion nanocomposites

Thanks to Nafion morphology, a brilliant idea came up: the use of hydrated Nafion clusters as a reactive vessels (or templates) for the synthesis of other materials, such as metals. So, several numbers of studies were prompted in order to use these cavities as a template for NPs synthesis for the obtainment of AlNPs, PtNPs, AgNPs or PbSNPs (see **Table 1.1**). Most of the publications regarding this subject based the MNPs formation in the model cluster network of such matrix (Section 1.5.1.1)

Table 1.1. Data regarding NPs synthesis in Nafion.

Nanoparticle type	NPs diameter (nm)	Reacting agent	Location	Reference
CdS	2-4	H_2S	Uniform distribution	199
Pt	2.5	Heat treatment	Uniform distribution	200
CdS	2.9	Thioacetamide	Uniform distribution	201
TiO_2	3.7 ± 0.5	Boiling H_2O	Uniform distribution	202
CdS	4.1	Na_2S	Surface	201
Pd	5 ± 1	$NaBH_4$	Uniform distribution	203
PbS	6.3 ± 1	Na_2S	Uniform distribution	204
CdS	6.5 ± 1.2	Na_2S	Uniform distribution	204
ZnO	8	Ethanol/NaOH	Uniform distribution	205
Ag	9 ± 2	Formamide	Uniform distribution	206
Ag_2S	10.5 ± 2.2	Na_2S	Uniform distribution	207
Ag	13.0 ± 3.4	$NaBH_4$	Uniform distribution	207
Ag	13.4 ± 2.2	$NaBH_4$	Uniform distribution	208
Ag	15 ± 3	$NaBH_4$	Surface	209
Ag	15 ± 4	$NaBH_4$	Surface	208
CdS	ca. 1000	H_2S	Uniform distribution	210

For example, Rollins *et al.* obtained AgNPs with diameters about 13 nm by reduction with $NaBH_4$ (0.66 M) of Ag^+ immobilized in the matrix and stated that the final MNPs were embedded in the structural cavities of Nafion.[207] Similarly, Ya-Ping Sun *et al.* studied the formation of AgNPs obtained by reduction with $NaBH_4$ (0.2 M) of Ag^+ immobilized in the matrix after immersion of the membrane in different concentrations of $AgNO_3$ (from 0.001 to 0.1 M) for

different times (from 1 to 30 min), but they did not found significant changes neither in the mean diameter of the AgNPs (about 13 nm) nor in the distribution.[208]

However, as showed in **Table 1.1**, the obtained NPs usually have diameters above the cluster's size of the proposed cluster-channel network model, and its distribution (sometimes appearing as a homogenous distribution, others as a superficial one) seems not to reveal the cluster network proposed.

These odd results have been sometimes rationalized in terms of additional hydration of ionic clusters or to polymer chain reorganization due to the incorporation of NPs. In addition to the NPs size disagreement, NPs location is not always consistent with a simple template procedure. As a rule of thumb, it is generally accepted that anionic reagents (i.e. BH_4^-, S_2^-) are repelled due to Donnan exclusion effect (DEE)[106] and NPs are formed on the surface of the polymer whereas neutral reagents (ie. thioacetamide, formamide) or gases can freely diffuse through the matrix.[201, 211] This is why some authors, while studying MNPs formation in Nafion membranes, claim that all the disparities are indicating that the role played by the cluster-channel structure of Nafion-117 membrane in the formation of nanoparticles has been oversimplified.[206, 209]

1.6.1.2. Poly(arylsulfones) nanocomposites

Although inclusion of MNPs in poly(arylsulfones) has been broadly studied for polymers such as polyetheretherketone,[212] polyethersulfone[162] and polysulfones,[213] their obtainment in PES-C and PPSU is still a new subject under investigation. In the case of PPSU membranes, some examples can be found in literature, regarding the inclusion of ZnONPs,[214] TiO_2[215] or polyhedral oligosilsesquioxanes.[177]

However, for SPES-C membranes, the inclusion of MNPs results to be a completely new matter of study.

1.6.2. Nanocomposite polyurethane foams

Up to now, very few studies can be found focused on the development of nanocomposite polyurethane matrices.[216-224] These publications demonstrated that the incorporation of nano-objects (i.e. metal nanoparticles, carbon nanotubes) could significantly improve the mechanical or thermal properties of polyurethane materials and their further applicability. For example, Chou *et al*.[219] found that the thermal and mechanical properties and biostability were significantly improved in polyurethane containing AgNPs in the range of 4 to 7 nm. Furthermore, Deka *et al.*[220] stated that dispersed AgNPs in such matrices significantly improved the mechanical properties like tensile strength, impact resistance and Shore A hardness

without affecting the flexibility and elongation at break value of the pristine polymer. In a similar way, Dolomova *et al.*[225] stated that the addition of modified multi-walled carbon nanotubes yielded to a large improvement in both morphology and mechanical properties of the nano-reinforced PUF. Among these previous works, those undertaking the incorporation metal nanoparticles were focused on the obtainment of AgNPs in PUFs either by *in-situ* or *ex-situ* approaches.[218, 221-223]

Nevertheless, controlling the total metal load in the final nanocomposite and determining the leakage of these nanoparticles to the media is sometimes a pending issue.

1.6.3. Nanocomposite textile fibers

Textiles for specific applications have to satisfy consumer's growing demands such as wearing and economic aspects. So, it is desirable not only to improve the material properties but also to provide it with new features thus the new textile material could perform several functions. In general terms, textile fibers are vulnerable to microbial attack because of their hydrophilic porous structure and moisture transport characteristics and also because textiles are a good media and suitable nutrient source for generating and propagating of microorganisms.[226-228] Thus, the use of antibacterial agents to prevent or retard the growth of bacteria is becoming a standard finishing for textile goods. In this sense, Ye *et al.*[226] reported the obtainment of chitosan-based core-shell particles, with chitosan as the shell and a soft polymer as the core, as a novel antibacterial coating for cotton. Berendjchi *et al.*,[229] also reported the modification of cotton fibers, but this time by its modification with CuNPs in order to provide the material with hydrophobic and antibacterial properties. By their side, Sójka-Ledakowicz *et al.*[230] modified polyester, cotton, hydroxyethylcellulose and polyethylene glycol with ZnO and TiO_2 nanoparticles in order to develop nano-structural textiles with barrier properties, protecting against UV radiation and bacterial growth.

Nevertheless, few studies have focused they attention on the obtainment of AgNPs in textile fibers such the ones used in this work.

1.7. Nanocomposite characterisation techniques

Characterization techniques play a crucial role in the development of new materials and applications, due to the need to know their physicochemical characteristics. Fortunately nowadays many techniques allow us to further our understanding and description of the properties of these new materials, optimize their synthesis conditions and establish their best scopes of application.

Herewith I will present the techniques used in the course of this thesis, which have allowed a thorough characterization of the different materials developed in it.

When synthesizing and/or modifying polymeric materials, it is extremely important to determine the outcome of possible changes of their **chemical structure**, since the final structure will determine the final properties of the polymer matrix.
In this regard, spectroscopic methods (based on the excitation of the surface of the material by particle radiation and subsequent detection and identification of the associated emissions) provide extensive information of the atoms, bonds or functional groups present in the material. Nuclear Magnetic Resonance Spectroscopy (NMR) and Fourier Transform Infrared Attenuated Reflectance spectroscopic (FTIR-ATR) methods are the spectroscopic methods, intended for chemical characterization, employed in the development of this thesis.

- **Nuclear Magnetic resonance** (NMR) is a technique based on the absorption of electromagnetic radiation (in the range of radio frequencies) by the atomic nuclei (with nonzero magnetic moment) subjected to an external magnetic field. Each core environment determines the exact frequency of this absorption and, for this reason; it is generally used for the elucidation of molecular structures, although it can also be used with quantitative purposes in some cases.[231] Among the different possibilities, ^{13}C-NMR and ^{1}H-NMR are the most common methods used, and, as it will be explained in Chapter 3, they offered great information about the chemical structure of SPES-C polymer.
- **Infrared spectroscopy** (IR) is a highly reliable method to characterize, identify, and in few cases quantify a variety of substances.[231] When a molecule absorbs infrared radiation, the intermolecular vibration (with frequency equal to that of the incident radiation) increases in intensity. This generates signals whose frequency corresponds to the vibration of a specific bond, what is very useful for determining molecular structures. Moreover, by the sampling technique of Attenuated Total Reflectance (ATR) the analysis of solid and liquid samples has been facilitated in recent years, as it makes the sample preparation prior to analysis unnecessary. When radiation enters a transmitter ATR crystal with high refractive index, it allows a total internal reflection, thus generating a wave on the surface of the crystal. This wave extends through the sample (in intimate contact with the crystal), and registers the IR spectrum of the analyte.

In order to adjust the final applications of polymer matrices and nanocomposites obtained it is essential to know very well both their morphology and behaviour. It is therefore imperative to consider all the options offered by the different characterization techniques in the nanoscale to obtain a global picture as real as possible. Below the main **nanocomposite characterization techniques** are briefly explained.

- **Inductively Coupled Plasma Atomic Emission Spectroscopy** (ICP-AES) allows the multi-elemental analysis of a sample in aqueous solution from the singular electromagnetic radiation that the different elements emit when they are excited by high temperature plasma. The sample is aspirated into the nebulizer that turns into a fine aerosol which is transported directly into the plasma, where it interacts with electrons and charged ions, dissociates and gives to the formation of free atoms that, when losing electrons, recombine in the plasma. In this manner, radiation with a wavelength characteristic of the element involved is emitted, which is transmitted through the optical system to the detector CID (Charge Injection detector), where the UV and Vis region is captured.[231]
- **Inductively Coupled Plasma Mass Spectroscopy** (ICP-MS) allows multi-element analysis far more sensitive than ICP-AES by using a mass spectrometer which acts as a method of separation and detection, reaching detection and quantification concentrations in the order of ppb.[231]
- **Scanning Electron Microscopy** (SEM) is a type of microscopy uses a focused electron beam onto the sample to disclose specific details of its surface (topography) from the detection and amplification of the secondary electrons and rejected primary electrons emitted as a result of the interaction with the sample. The electron beam scans the sample while a cathode tube collects the emitted electrons allowing digitalizing the image.[232, 233] In this technique the sample pre-treatment plays an important role for two reasons. On one hand, because in order to observe the surface of non-conductive materials (the case of the polymeric matrices that will be presented in this work), it is indispensable to have a metal coating (usually Au, Au/Pd, etc.) of about 10 nm thick which avoids the accumulation of charges. Furthermore, when the cross-section view is required, usually it is necessary to freeze the sample with liquid N_2 and proceed either with a breaking for fracture or with a cutting with microtome, as outlined in **Figure 1.26**.

On the other hand, since when synthesizing nanoparticles stabilized in polymeric matrices, determining the shape, the distribution and the size of these become essential, several **nanoparticle characterization techniques** have to be applied.

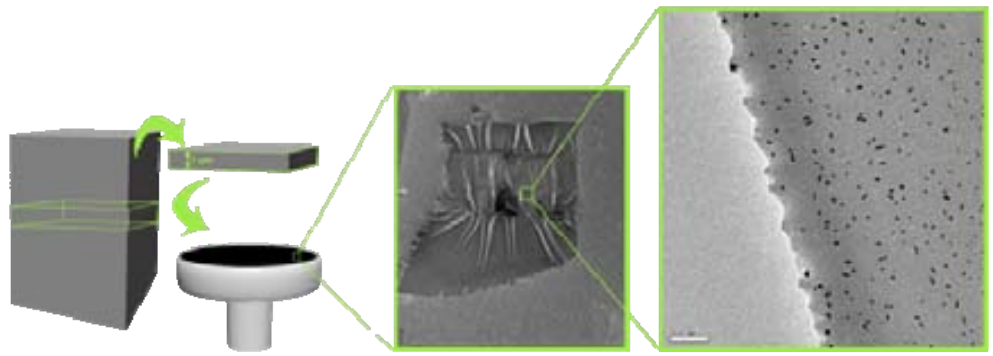

Figure 1.26. Scheme of the preparation of a semifilm cross section for SEM analysis.

- **Transmission Electron Microscopy** (TEM) is based on the generation of a punctual electron beam (as much as possible) from a thin film of tungsten subjected to a high potential difference. The generated electron beam is focused and accelerated by a number of electromagnetic lenses so as it passes through the sample interacting with it. Normally, the sample is bombarded with an electron source 100-200 keV and the image is generated from the elastic and inelastic scattering of electrons that traverse. This technique operates with magnifications between 100X and 106X and allows resolutions up to 0.5 Å.[232] It requires to work under high vacuum conditions and with an ultrathin sample since the electron beam has to be able to pass through. Depending on the solubility properties of the different polymer matrices, different methods of sample preparation must be considered. If the polymer matrix is soluble in a volatile organic solvent (e.g. DMF, CHCl3, THF), it is possible to prepare suspensions MNPs or "inks" (solutions of 5% in mass) in a suitable organic solvent which can then be deposited on a TEM grid to proceed with their microscopic characterization. In contrast, if the matrix is not soluble (such as Nafion), the sample preparation is more complicated because it requires cutting ultrathin films (thickness of about 1 μm or less) of the nanocomposite material to be deposited on the grid TEM and then, if necessary, coating it with a thin carbon film (for the sample to be conductive). The procedure is analogous to that described in **Figure 1.26** but this time cutting the sample with an ultra-microtome.
- **Diameter measurement methodologies**. In recent years there have appeared a variety of techniques in order to achieve automatic measurement and accurate assessment of the size and frequency (size distribution) of the nanoparticles. But when dealing with nanoparticles with diameters in the range of 10 nm (or lower) these techniques fail. A good option is to proceed with the analysis of the TEM and SEM images obtained. Although there are a huge variety of software to do so (Pebbles, ImageJ, Gatan Digital Micrograph, Image Pro plus, and so on) in practice, the quality of the images is often low, due to high ratio signal-noise and the low contrast, making its processing a difficult task to accomplish. That is why the quantitative

analysis of TEM images is often carried out through manual measurements of large number of nanoparticles.

In this work, the size distribution of the MNPs prepared has been obtained by direct observation of TEM images and with the construction of the corresponding histograms. In each case, for each prepared nanocomposite, at least 200 nanoparticles were measured and data obtained were fitted to a 3 parameter Gaussian curve (eq. (1-22)).

$$y = a \cdot \exp\left[-0.5 \cdot \left(\frac{(x - x_0)^2}{\sigma}\right)\right] \quad (1\text{-}22)$$

Where: x_0 is the mean diameter (the most common),

σ is the standard deviation of all measurements, and

a is a real constant defined as shown in eq. (1-23).

$$a = \frac{1}{\sigma \cdot \sqrt{2\pi}} \quad (1\text{-}23)$$

1.8. Nanocomposite Applications

As aforementioned, stabilization of MNPs in polymeric matrices has gained interest in the past years. Since the structural organization and properties of these nanocomposites do not only depend on the chemical structure of its individual components (nanoparticles and polymer), but also on the synergy between them, their application areas (compared with each individual component of the nanocomposite) increase, covering new industrial challenges. Thus, since polymer-metal nanocomposites (PMNCs) allow the capability to stabilize MNPs while providing unique applications of the final nanocomposite, they applications are wide and varied.[86, 90, 212, 234, 235]

In this sense, the use of nanomaterials to assemble architectures of defined size, composition and orientation allows researchers to utilize the particular electrical, optical, catalytic and magnetic properties of those materials for the creation of functional materials, devices, and systems through control of matter on the nanometer scale and the exploitation of novel phenomena and properties at that scale. Since these materials cover a wide field of practical applications, to achieve these goals, it is necessary to use multidisciplinary approaches with inputs from physicists, biologists, chemists, and engineers.

Although during this thesis work only applications in wastewater treatment have been considered, I think that it is essential to include a brief explanation of the other main applications such as fuel cell or sensors in to understand the state-of-the-art of the research. Furthermore, as in some of these applications, membrane processes are used, thus, in order to further understand the role of the nanocomposite in such applications, some concepts in membranes and membrane processes have to be d3etailed and considered.

1.8.1. Membranes and membrane processes

Theoretically, a membrane can be defined as a permeable or semi-permeable phase, traditionally in the form of a thin film, which can be made from a variety of materials ranging from inorganic solids to different types of polymers. The main role of the membrane during a separation process is to control the exchange of materials between two adjacent fluid phases, as shown in **Figure 1.27**. [127]

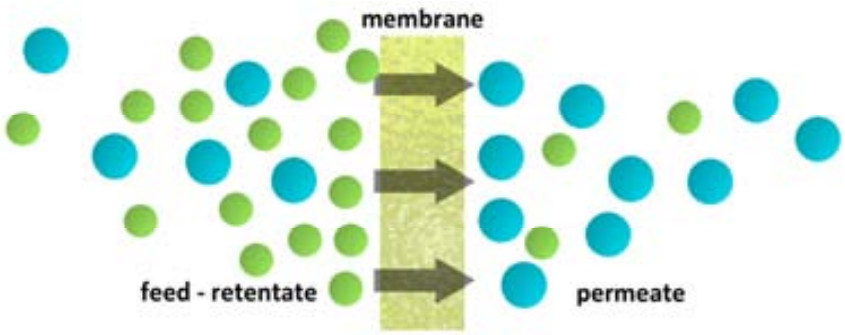

Figure 1.27. Schematic representation of the basic membrane separation principle.

In a general view, some of the main advantages of membrane separation processes, over the more conventional counterparts (adsorption, absorption, distillation, etc.), are:

(i) the separation occurs in a continuous way,
(ii) they are energy savings,
(iii) the processes are easily combinable with other separation processes,
(iv) the scaling of the process is simple,
(v) membrane properties are tunable and adjustable,
(vi) it is no necessary to add additives, and
(vii) there is reduction in the initial capital investment required.

Nevertheless, these are general virtues but they are no generally shared for all membrane separation processes. Thus, there are cases in which the energy required to carry out the separation is a major obstacle for its industrial application (e.g. electrodialysis). Other

processes involve necessarily the addition of additives to improve the performance of the separation process or to prevent fouling, which may impair the separation properties of these membranes. Consequently, each membrane separation process should be designed based on the final application and the properties of the membrane itself.

As it can be observed in **Figure 1.27**, membrane acts as a barrier, which separates different species. Therefore, the membrane action results in a feed (the retentate), which is dwindled from some of its original components, and another fluid stream (the permeate) which is concentrated in these components. This separation is usually controlled by transport processes across the membrane, which is the result of a driving force typically associated with a gradient of concentration, pressure, temperature, electric potential, etc.

In fact, the ability of the membrane to separate is determined by two main parameters, its permeability and its selectivity. The permeability is defined as the flux (molar or volumetric flow per unit membrane area) through the membrane scaled with respect to the membrane thickness and driving force (concentration gradient, pressure difference, …) . When membrane thickness is unknown, the permeance (which is defined as the flux through the membrane scaled with respect to driving force) is used instead of the permeability. The other important parameter is the membrane selectivity, which refers to the ability of the membrane to separate two given species and which is typically defined as the ratio of the individual permeabilities for the two species to separate.[109, 127, 236]

Membranes can be classified by whether the thin permselective layer is porous or dense, and by the type of material (organic, polymeric, inorganic, metallic, etc.) the membrane film is made of. The choice of a porous or a dense thin layer depends on the desired separation process, operating temperature and driving force used for the separation; the choice of material depends on the desired permeance and selectivity, and on thermal and mechanical stability requirements. And, as a rule of thumb, an extra requirement has to be taken in mind: the thin film has also to be stable under the catalytic reaction conditions. For porous membranes, the size pore would be determined by the molecular size of the species to be separated, and the related membrane process. **Figure 1.28** indicates the molecular size of species typically separated by these different processes.[237]

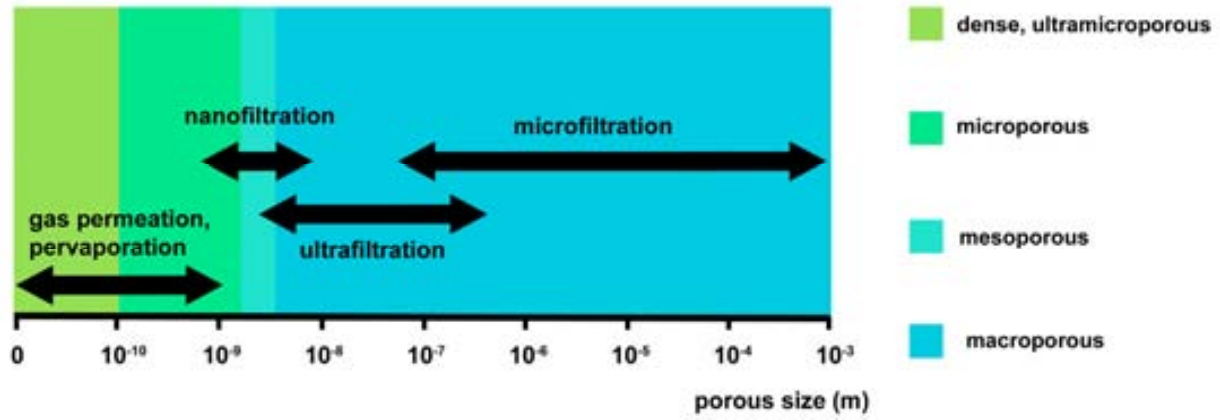

Figure 1.28. Classification of membrane processes in different types of porous membranes

Concretely, and thanks to the great versatility of polymer conformations, polymeric membranes offer added flexibility over their conventional counterparts. The accurate selection of the polymer molecular configuration and the control of its morphology would lead to the most appropriate membrane for a desired application. It is important to note, that membranes can be manufactured in a wide range of geometries, depending on the material they are made of, and which include flat, tubular, and multi-tubular, hollow-fiber, and spiral-wound films. The final choice of membrane type depends on parameters such as the productivity, the separation selectivity, the film life time, its mechanical and chemical integrity at the operating conditions, its cost, and, especially in the final application.

1.8.2. Fuell cells

As global fossil fuel resources are depleting, power generation from renewable sources has been growing rapidly in recent years. Scientists have started to search and find for new alternatives of renewable energies to overcome energy crisis in the near future. In this sense, Fuel cells offer nowadays the possibility of environmentally benign power. As devices for direct conversion of the chemical energy of a fuel into electricity by electrochemical reactions, they are among the key enabling technologies for the transition to a hydrogen based economy.[238] Although at present the major commercial markets are in residential applications and public or private transportation, the variety of possible applications for fuel cell technology ranges from portable/micro power and transportation through to stationary power for buildings and distributed generation, applications that will be in large numbers worldwide.[239, 240]

Among the several types of developed configurations proton exchange membrane fuel cells (PEMFCs) have been recognized as a potential future power source[241] and are being developed

for transport applications as well as for stationary fuel cell applications and portable fuel cell applications. **Figure 1.29** presents a schematic representation of a PEMFC. Hydrogen or hydrogen-containing gases are adsorbed at the anode (usually with a Pt catalyst), where dissociate and lose their electrons with the resulting formation of protons, which pass through the selective membrane under the action of a chemical potential gradient. At the cathode, the protons interact with oxygen to give water molecules.

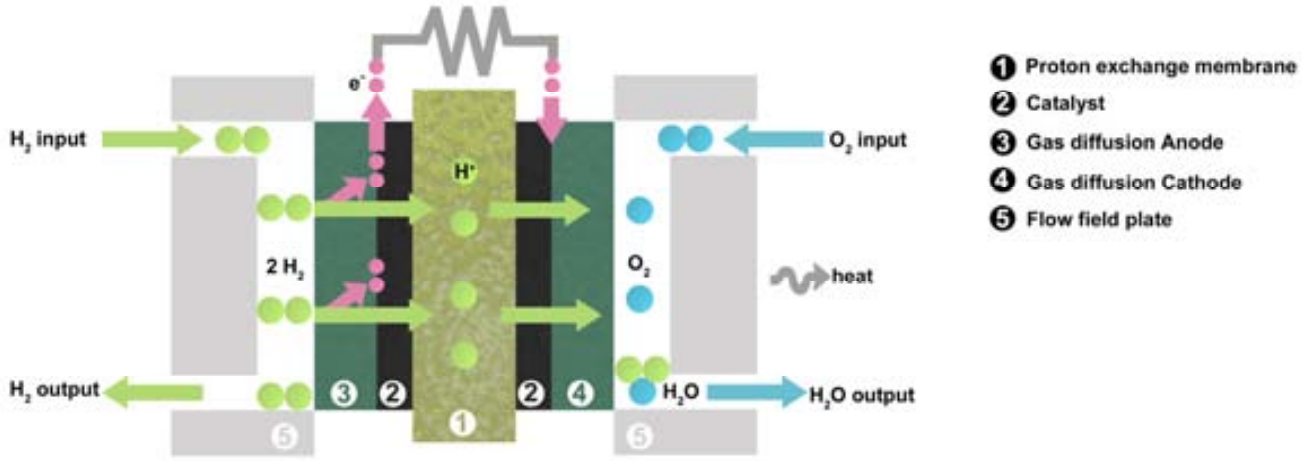

Figure 1.29. Schema of a PEMFC.

In such configurations, the PEM has important role since it should has a good ability to transport protons from anode to cathode compartment and must be able to prevent the transfer of other materials such as substrate or oxygen from anode and cathode chambers. Although their promising applications due to their advantages related as a high power density, simplicity of operation, high energy conversion efficiency and low harmful emissions, several efforts have still to be done in order to create a commercially available PEMFC.

In this sense, it is imperative to overcome the barrier of high catalyst cost caused by the exclusive use of platinum and platinum-based catalysts in the fuel-cell electrodes.[242, 243] Thus, although platinum is used in both the anode and the cathode of the fuel cell, many efforts are focused on developing alternative oxygen reduction catalysts for the cathode.[238, 244, 245]

On the other hand, there are still some shortcomings regarding proton exchange membrane (PEM) used in this type of fuel cells. Although Nafion is a common PEM, several problems still exist and are strongly hindering the commercialization of fuel cells. In this sense, drawbacks such as their high cost, limited operation temperature, oxygen leakage from cathode to anode, substrate loss, cation transport and accumulation rather than protons and biofouling have to be considered. Due to these disadvantages, researchers in the world are working to fabricate a new kind of PEM to overcome these disadvantages and induce better performance than Nafion

membrane as well.[244] Under this context, MNPs immobilized in a PEM can improve separation performance by generating preferential permeation paths while they can prevent from permeation of undesired species as well as they can increase thermal, and mechanical properties.[246-248] In this sense, Yang *et al*. developed a new method for membrane electrode assemblies fabrication by using different reduction agents to prepare Pt/Bacterial cellulose catalyst layer through liquid phase chemical deoxidization method. When tested in a fuel cell testing system they found that the catalyst layer showed high electrocatalytic activity, and that the matrix proton conductivity could be improved by doping with proton acid or inorganic acid on the membrane. As a result, the current density was increased.[35]

Another example of the use of such nanocomposites in fuel cells applications is the one recently reported by Rahimnejad *et al*.[248] Due to the unique and promising properties of Fe_3O_4 nanoparticles (magnetic, conductive, easy to be synthesized, and catalytic), they modified polyethersulfone (PES) membranes with different amounts of ferromagnetic MNPs by dissolving the polymer in an appropriate solvent (NMP) at 70 ºC with the produced ferric oxide nanoparticles (5 wt%, 10 wt%, 15 wt% and 20 wt% of PES). They compared the efficiency of a microbiological fuel cell (with *Saccharomyces cerevisiae* with glucose) with the modified membranes and with typical commercial Nafion membrane, and found that membrane with 15 wt% of Fe_3O_4 nanoparticles produced maximum current and power, and that it was a 29% more amount of power than what had been achieved with Nafion.

1.8.3. Amperometric sensors

In general terms, a chemical sensor is an analytical device that transforms chemical information, ranging from the concentration of a specific sample component to total composition analysis, into an analytically useful signal. The chemical information, mentioned above, may originate from a chemical reaction of the analyte or from a physical property of the system investigated. Chemical sensors contain two basic functional units:

- a transducer part capable of transforming the energy carrying the chemical information about the sample into a useful analytical signal, and
- a receptor part, based either on physical, chemical or biochemical principles.

Some sensors may include a separator which is, for example, a membrane.

They can be used for the detection and quantification of both organic and inorganic substances in several fields such as clinical, biomedical and environmental. Since the main requirements for a good sensor are: good sensitivity, selectivity, high response speed, long-live, and a low consumption of both analyte and power as well as the low cost of massive production for

industrial applications, they are often designed to operate under well-defined conditions for specified analytes in certain sample types.[249]

Amperometric devices are based on the application of an external potential leading to the electronic transfer between the working electrode and the species in solution. Since the current passing through an electrochemical cell containing the electro-active species is proportional to the analyte concentration, the measurement of this current allows for the quantitative determination of many analytes at trace levels. For this quantification, the main requirement is that the analyte could be oxidized or reduced electrochemically onto the electrodes surface. However, the main drawback of amperometric sensors is their limited selectivity and a relatively long response time. In this sense, the modification of these sensors with polymer stabilised metal nanoparticles (PSMNPs) may provide advantages such as the enhancement of both the rate of mass transfer inside the nanocomposite film (the actual sensing element of the sensor) and in the electrocatalytic activity due to a far higher specific surface area of nanocatalyst in comparison with that of the bulk material.

Under this approach, recent publications in our group[86, 87, 212] describe the modification of graphite-epoxy composite electrodes (GECE)[250] with Pt- and PdNPs of various types (both monometallic and polymetallic). For such modification, first MNPs are generated by Intermatrix Synthesis (see Section 1.4) in a sulfonated polyether–ether ketone (SPEEK) film; afterwards solutions of the nanocomposite membrane in an appropriate solvent are prepared in order to obtain the corresponding PSMNPs-inks, which are drop-by-drop deposited on the surface of GECE followed by air-drying at room temperature to form a film (**Figure 1.30**).

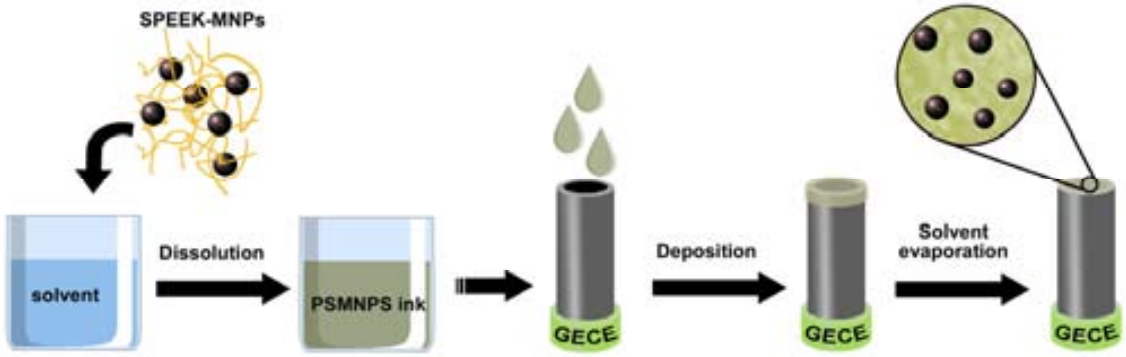

Figure 1.30. Schematic diagram of supramolecular construction of glucose biosensor based on SPEEK-Pt@Cu-PSMNP nanocomposite.

By this procedure it was possible to prepare GECE ampertometric sensors modified with core-shell MNPs (Pt@Cu, Pd@Cu, Pt@Co, Pd@Co, Pt@Ni, Pd@Ni, and Pd@CoNi)[a] stabilized in SPEEK

[a] X@Y corresponds to a core-shell NP with a shell made of X and a core of Y.

films for the detection of H_2O_2.[8] The results showed that the sensitivity of sensors toward the analyte under study increased in the following order:

For PSMNPs with ferromagnetic core:

Pd@Co > Pd@Ni > Pt@Ni > Pt@Co > Pt@Co-Ni

For PSMNPs with diamagnetic core:

Pd@Cu > Pd > Pt@Cu > Pt > Cu

As a main conclusion, they found that MNPs with Pd shell had the highest sensitivity, what could be explained by the higher catalytic activity of Pd in H_2O_2 decomposition than Pt-PSMNPs under the same experimental conditions.

1.8.4. Water treatment

There are about 780 million people in the world (it is to say, more than one-tenth of the world population) and mostly in developing countries, which have no access to clean and potable water[251] and a further more than 3.4 million people which die each year from water, sanitation, and hygiene-related causes.[252] Therefore, the importance of potable water for people in some countries dictates the need for the development of innovative technologies and materials for the production of safe potable water. This type of application can be a perfect niche for the nanomaterials here mentioned. However, it is necessary to develop ecologically-safe nanomaterials that prevent the post-contamination of the used samples.[253] Functionalized polymers containing MNPs are currently acquiring a prominent role as NPs stabilizers and for their excellent performance. It is true, but ion-exchange materials and membrane processes are already widely used for various water treatment actions, mainly to eliminate undesired or toxic ionic impurities including hardness ions, iron, heavy metals, and others. But stabilization and immobilization of MNPs in such membrane matrices is very promising since by this approach, two complementary water treatment steps could be performed with a single material and the safety of the nanocomposites could be increased.

1.8.4.1. Catalytic degradation of toxic compounds in water

Recently many works are focused on the degradation of toxic compounds in water with MNPs. Among those, various studies have been reported on the groundwater remediation through degradation of toxic chlorinated organic compounds (COCs) with Fe^0-based bimetallic NPs (Fe/Ni, Fe/Pd).[254-258]

For instance, Wu *et al.* reported the preparation and application of cellulose acetate (CA) supported iron and Pd/Fe nanoparticles obtained by the microemulsion methodology (see Section 1.3.2) for the dechlorination of trichloroethylene (TCE) from water.[259] They found that,

compared with the CA-supported FeNPs, the dechlorination rate was significantly increased by the second modifying metal, Pd, and that the membrane-supported Pd/Fe nanoparticles formed in microemulsion had superior performance compared to those formed in solution.

Another example is the one reported by Bhattacharyya *et al*., who studied the use of immobilized Pd modified bimetallic nanoparticles in the treatment of chlorinated aromatics such as polychlorinated Biphenyls (PCBs). In this reaction, the role of Pd is to collect H_2 generated from the iron corrosion reaction and decompose it into atomic H*, which can be utilized to replace the chlorine in PCBs).[260] The evaluation of the PCBs decomposition was evaluated by two different configurations: i) Pd nanoparticles immobilized in polypyrrole membranes using external H_2 supply,and ii) Fe/Pd bimetallic nanoparticles in polyacrylate-polyvinylidene fluoride microfiltration membranes without external H_2 supply. The results showed that the bimetallic nanoparticles exhibited higher reactivity in terms of kinetics for the dechlorination, what they explain by the in-situ H_2 generation at the Fe/Pd interface, which could minimize the hydrogen transfer resistance to the Pd surface. On the contrary, for the pure Pd (with Pd/polypyrrole) system, H_2 needs to be dissolved in the aqueous phase and then transferred to the Pd surface by diffusion, lowing the reaction rate. Moreover, when comparing their work with those procedures where MNPs were not stabilized,[254, 255, 257] Bhattacharyya *et al*. found that particle size could be controlled by varying the ratio of PAA and metal ions.

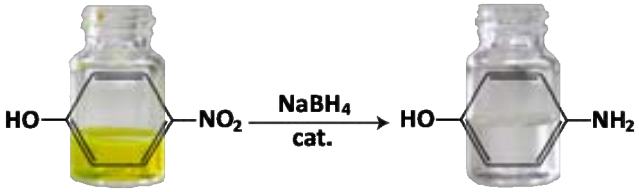

Figure 1.31. Catalytic reduction of 4-np to 4-ap.

Many other groups focused their efforts on the elimination of nitroaromatic compounds in water, which is usually tested by a model catalytic reaction involving the conversion of 4-nitrophenol (4-np) to 4-aminophenol (4-ap).[261]

For instance, Pal *et al*. [262] and Esumi *et al*. [263] were pioneers in identifying this reaction as a suitable reaction for testing the catalytic activity of free or immobilized nanoparticles. Since the reduction of 4-np with $NaBH_4$ does not proceed in the absence of catalyst, but it rapidly occurs in the presence of a metallic catalyst it is a perfect test for the nanocomposites here developed. Due to the change in the colour occurred by the conversion of 4-np (which is yellow and presents a maximum of Absorbance between 390-400 nm, depending on the pH) to 4-ap the reaction can be easily monitored by the disappearance of the 4-np pick by UV–Vis spectrophotometry. Since when performing the reaction the reductant is usually added in

excess, it is possible to consider that the reaction follows a *pseudo* first order kinetics (with respect to the initial reagent). So that, considering the Lambert-Beer equation, the variation of the absorbance is directly proportional to the apparent rate constant of the reaction (k_{app}), as follows:

$$\ln\left(\frac{|C(t)|}{|C_0|}\right) = -k_{app}t \approx \ln\left(\frac{|Abs^{\lambda}(t)|}{|Abs_0^{\lambda}|}\right) = -k_{app}t \qquad (1\text{-}24)$$

Where: $C(t)$ is the concentration of the specie at certain time,

C_0 is the initial concentration of the specie,

t states for time,

$Abs^{\lambda}(t)$ is the absorbance of the specie at certain time and wavelength,

Abs^{λ}_0 is the initial absorbance of the specie,

k_{app} is the apparent rate constant of the reaction.

In a typical procedure, Ouyang *et al*., developed hollow fibers modified with AuNPs obtained by a layer by layer approach[264] (which consist in exposing a substrate surface alternately to solutions of cationic and anionic polymers to create a multilayer film able to immobilize the MNPs). They applied the final nanocomposites in flow conditions using a reactive solution with a ratio of 50:1 of $NaBH_4$:4-np and found that the immobilized nanoparticles were highly active, although their activity declined over time, presumably because of catalyst fouling. In this sense they stated the need of improving catalyst stability.[265]

More recently, Emin *et al*. applied hollow fibers prepared by photografting polymerization and Intermatrix Synthesis of PdNPs to the same reaction (20:1 ratio of reactives) and found that flux conditions were extremely influent in the catalytic behaviour of the catalytic material, since when by decreasing the flow, the p-nitrophenol concentration decreased in the permeate until quasi-total conversion.[162]

In any case, this reaction appears to be a good option to test the catalytic activity in the elimination of nitroaromatic compounds in water of different nanocomposites, either in flux or batch conditions. This is why during the development of this work all of the nanocomposites developed have been tested using this reaction as a model reaction in different conditions, as will be explained in Chapter 3.

1.8.4.2. Bactericidal and anti-biofouling applications

Among the currently known nanomaterials, AgNPs have unique antimicrobial properties.[266, 267] As soon as in the ancient Greece, Hippocrates (460 BC - 370 BC), the father of the modern Medicine, already wrote that silver had beneficial healing and prophylactic properties. Phoenicians, Persians, Romans and Egyptians also used silver in one or another form to preserve food, wine and water and this was likewise practiced in the XXth century through World War II.[268]

Silver was widely used as a biomedical compound in hospitals before the appearance of antibiotics. In the early 1800s, surgical wounds were closed with silver sutures, and it also became a common practice to administrate aqueous $AgNO_3$ drops to new-born's eyes in order to treat the transmission of *Neisseria Gonorrhoea* from infected mothers to children.[269] It was also at the end of that century, when some scientists started to systematically study the bactericidal effect of some metals (the so-called oligodynamic effect) and, thanks to the great number of studies in the subject, it was later found that among all the metals with antimicrobial properties, silver has the highest effectiveness and the least toxicity to animal cells.[270] During the 1900s, people used to introduce silver dollars in milk bottles to prolong the freshness of milk; silver compounds were successfully used to prevent infection in World War I together with the use of surgical silver sutures. By 1940 there were approximately 50 different silver compounds on the market being used to treat every known infectious disease in many configurations including shavings, foils, sutures, solutions (e.g., silver nitrate, oxide, bromide, chloride, and iodide) and colloids providing fine particles (introduced in 1924).[270] The widespread use of silver went out of fashion with the appearance and spread of modern antibiotics. However, with the discovery of antibiotics, antibiotic-resistant strains also emerged and, therefore, a renewed interest in using silver in the treatment of burns to improve skin regeneration: Ag-containing hydrocolloids dressings are nowadays used to treat diabetic foot ulcers due to their regenerative effect and $AgNO_3$ has also long been used as cauterization agent to stop epistaxis or to stop the growth of post-traumatic granulomas.[271] Even today, at the beginning of the second decade of XXIth century, the broad-spectrum antimicrobial properties of silver encourage its use in biomedical applications, water and air purification, food production, cosmetics, clothing, and numerous household products development.

Nevertheless, the mechanisms behind the activity of silver on bacteria are not yet fully elucidated, but the three most common mechanisms of toxicity proposed to date are the ones depicted in **Figure 1.32**.

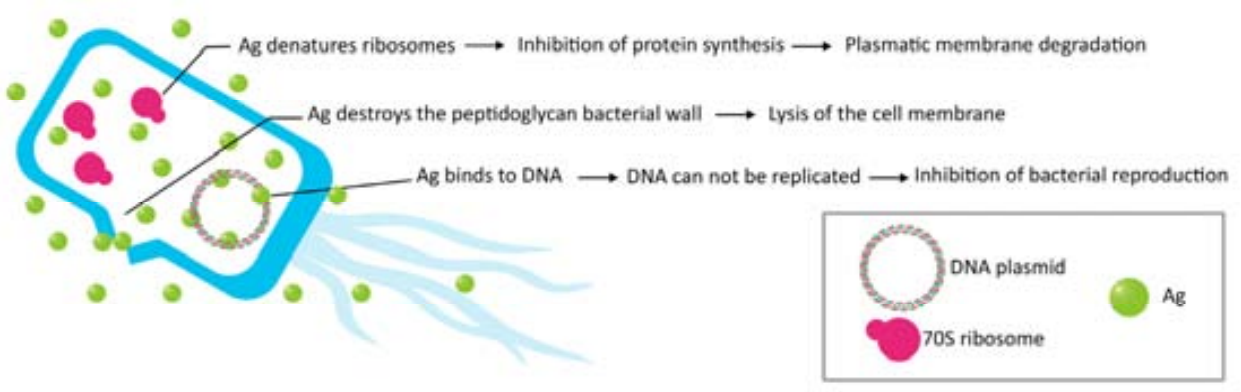

Figure 1.32. Mechanisms for the antibacterial activity of silver. Similar images have been published in bibliography.[271-273]

Generally it is widely accepted that the main antibacterial effect of AgNPs or AgNPs-based materials is due to its partial oxidation and release of silver ions (Ag^+).[274, 275] After this oxidation occurs, the following actions can happen either simultaneously or separately:

(1) uptake of free Ag^+ followed by disruption of ATP production and DNA replication;[276]

(2) AgNPs and Ag^+ interaction with bacterial proteins, disrupting protein synthesis;[277]

(3) AgNPs directly damage cell membranes, interacting with the peptidoglycan wall cell and the plasmatic membrane causing cell lysis.[278]

Besides, disregarding the exact mechanism of interaction, several works have stated that AgNPs may increase the cell membrane permeability and, subsequently, penetrate inside cells to induce any one or the entire cascade of effects just described.[279, 280] Thus, although it is not yet possible to confirm a single mechanism for the antibacterial action of silver, multifaceted antibacterial activity seems to be the key to the low bacterial resistance rates observed. The explanation for this low resistance can be understood due to the fact that bacterial mortality does not depends on the presence of one determinate molecule or chemical compound, what hugely hinders the adaptation of the microorganism, it is to say, avoiding the appearance of resistant strains.

Since the importance of potable water for people in some countries dictates the need for the development of innovative technologies and improved disinfection methods for the production of safe potable water, this type of application can be a perfect niche for nanomaterials containing AgNPs. The use of metal nanocomposites can play an important role in water disinfection, since compared to other strategies nowadays being employed (such as the use of chemical agents, physical treatments or mechanical ones) it does not require additional chemical reagents and can be employed under mild conditions.

Moreover, the use of these nanocomposites can also help to solve one of the major operational problems associated with membrane technology: the biofouling. With the coating of polymeric membranes with AgNPs, the accumulation of microorganism and their further multiplication in the material is impeded, thus the operational properties are maintained.

However, it is necessary to develop ecologically-safe nanomaterials that prevent the post-contamination of the used samples.[281] Again, functionalized polymers are currently acquiring a prominent role as NPs stabilizers for their excellent performance.

Accordingly, in this present work, the modification of several polymeric materials (such as PUFs and films) with AgNPs for disinfection and control of the biofouling have been studied, as it will be explained in Chapter 3.

1.9. References

1. Astruc, D.; Lu, F.; Aranzaes, J. R., Nanoparticles as recyclable catalysts: The frontier between homogeneous and heterogeneous catalysis. *Angew. Chem. Int. Edit.* **2005,** *44* (48), 7852-7872.
2. Allen, D. T.; Shonnard, D. R., Sustainability in chemical engineering education: Identifying a core body of knowledge. *AIChE Journal* **2012,** *58* (8), 2296-2302.
3. Mirkin, C. A., The beginning of a small revolution. *small* **2005,** *1* (1), 14-16.
4. Rothenberg, G., Introduction. In *Catalysis*, Wiley-VCH Verlag GmbH & Co. KGaA: 2008; pp 1-38.
5. Janssen, M.; Muller, C.; Vogt, D., Recent advances in the recycling of homogeneous catalysts using membrane separation. *Green Chemistry* **2011,** *13* (9), 2247-2257.
6. Anastas, P. T.; Warner, J., *Green Chemistry: Theory and Practice*. OXFORD University Press (NC): 2000.
7. Meurig Thomas, J.; Raja, R., Designing catalysts for clean technology, green chemistry, and sustainable development. *Annu. Rev. Mater. Res.* **2005,** *35*, 315-350.
8. Muraviev, D. N.; Ruiz, P.; Munoz, M.; Macanas, J., Novel strategies for preparation and characterization of functional polymer-metal nanocomposites for electrochemical applications. *Pure Appl. Chem.* **2008,** *80* (11), 2425-2437.
9. Drexler, K. E., *Engines of Creation*. Bantam Doubleday Dell Publishing Group Inc: New York, US, 1988; p 298.
10. Hassan, M. H. A., Small Things and Big Changes in the Developing World. *Science* **2005,** *309* (5731), 65-66.
11. Roduner, E., Size matters: why nanomaterials are different. *Chem Soc Rev* **2006,** *35* (7), 583-92.
12. Henderson, J., The analysis of ancient glasses part II: Luxury Roman and early medieval glasses. *JOM* **1996,** *48* (2), 62-64.
13. Boyle, S. J. R., *The Sceptical Chymist*. BiblioLife: US, 1661; p 244.
14. Hirsch, R., *Seizing the Light: A Social History of Photography*. 2nd ed.; McGraw-Hill Education - Europe: London/US, 2009; p 496.
15. Fitzpatrick, J. A. J.; Inouye, Y.; Manley, S.; Moerner, W. E., From "There's Plenty of Room at the Bottom" to Seeing What is Actually There. *ChemPhysChem* **2014**.

16. Taniguchi, N. In *On the Basic Concept of 'NanoTechnology*, International Conference on Production Engineering, Part II, Japan Society of Precision Engineering, Tokyo, Japan, Tokyo, Japan, 1974; p 3.
17. Binnig, G.; Rohrer, H., Scanning tunneling microscopy. *IBM J. Res. Dev.* **1986,** *30* (4), 355-369.
18. Rana, S.; Kalaichelvan, P. T., Ecotoxicity of Nanoparticles. *ISRN Toxicology* **2013,** *2013*, 11.
19. Bottero, J. Y.; Rose, J.; Wiesner, M. R., Nanotechnologies: tools for sustainability in a new wave of water treatment processes. *Integr Environ Assess Manag* **2006,** *2* (4), 391-5.
20. Hillie, T.; Hlophe, M., Nanotechnology and the challenge of clean water. *Nat Nano* **2007,** *2* (11), 663-664.
21. Ju-Nam, Y.; Lead, J. R., Manufactured nanoparticles: an overview of their chemistry, interactions and potential environmental implications. *Sci Total Environ* **2008,** *400* (1-3), 396-414.
22. Narayan, R., Use of nanomaterials in water purification. *Materials Today* **2010,** *13* (6), 44-46.
23. Theron, J.; Walker, J. A.; Cloete, T. E., Nanotechnology and water treatment: Applications and emerging opportunities. *CRC Cr. Rev. Microbiol.* **2008,** *34* (1), 43-69.
24. Astruc, D., Transition-metal Nanoparticles in Catalysis: From Historical Background to the State-of-the Art. In *Nanoparticles and Catalysis*, Wiley-VCH Verlag GmbH & Co. KGaA: 2008; pp 1-48.
25. Bönnemann, H.; Nagabhushana, K. S.; Richards, R. M., Colloidal Nanoparticles Stabilized by Surfactants or Organo-Aluminum Derivatives: Preparation and Use as Catalyst Precursors. In *Nanoparticles and Catalysis*, Wiley-VCH Verlag GmbH & Co. KGaA: 2008; pp 49-91.
26. Huang, T.; Xu, X.-H. N., Synthesis and characterization of tunable rainbow colored colloidal silver nanoparticles using single-nanoparticle plasmonic microscopy and spectroscopy. *Journal of Materials Chemistry* **2010,** *20* (44), 9867-9876.
27. Panyam, J.; Labhasetwar, V., Biodegradable nanoparticles for drug and gene delivery to cells and tissue. *Adv Drug Deliv Rev* **2003,** *55* (3), 329-47.
28. Metallic Nanoparticles. In *Handbook of Metal Physics*, John, A. B., Ed. Elsevier: 2008; Vol. Volume 5, p iii.
29. Hayashi, Y.; Inoue, M.; Takizawa, H.; Suganuma, K., Nanoparticle Fabrication. In *Nanopackaging*, Morris, J. E., Ed. Springer US: 2008; pp 109-120.
30. Campelo, J. M.; Luna, D.; Luque, R.; Marinas, J. M.; Romero, A. A., Sustainable Preparation of Supported Metal Nanoparticles and Their Applications in Catalysis. *Chemsuschem* **2009,** *2* (1), 18-45.
31. Pineda, A.; Balu, A. M.; Campelo, J. M.; Romero, A. A.; Carmona, D.; Balas, F.; Santamaria, J.; Luque, R., A Dry Milling Approach for the Synthesis of Highly Active Nanoparticles Supported on Porous Materials. *Chemsuschem* **2011,** *4* (11), 1561-1565.
32. Barau, A.; Budarin, V.; Caragheorgheopol, A.; Luque, R.; Macquarrie, D.; Prelle, A.; Teodorescu, V.; Zaharescu, M., A Simple and Efficient Route to Active and Dispersed Silica Supported Palladium Nanoparticles. *Catal Lett* **2008,** *124* (3-4), 204-214.
33. Haruta, M.; Tsubota, S.; Kobayashi, T.; Kageyama, H.; Genet, M. J.; Delmon, B., Low-Temperature Oxidation of CO over Gold Supported on TiO2, α-Fe2O3, and Co3O4. *Journal of Catalysis* **1993,** *144* (1), 175-192.
34. Iojoiu, E.; Walmsley, J.; Raeder, H.; Bredesen, R.; Miachon, S.; Dalmon, J., Comparison of different support types for the preparation of nanostructured catalytic membranes. *Review in Advanced Material Science* **2003,** *5*, 160-165.

35. Yang, J.; Sun, D.; Li, J.; Yang, X.; Yu, J.; Hao, Q.; Liu, W.; Liu, J.; Zou, Z.; Gu, J., In situ deposition of platinum nanoparticles on bacterial cellulose membranes and evaluation of PEM fuel cell performance. *Electrochimica Acta* **2009,** *54* (26), 6300-6305.
36. Chen, X.; Zhu, H.-Y.; Zhao, J.-C.; Zheng, Z.-F.; Gao, X.-P., Visible-Light-Driven Oxidation of Organic Contaminants in Air with Gold Nanoparticle Catalysts on Oxide Supports. *Angewandte Chemie* **2008,** *120* (29), 5433-5436.
37. Zhang, Y.; Erkey, C., Preparation of supported metallic nanoparticles using supercritical fluids: A review. *The Journal of Supercritical Fluids* **2006,** *38* (2), 252-267.
38. Yong, C.; Gan, L., Microemulsion Polymerizations and Reactions. In *Polymer Particles*, Okubo, M., Ed. Springer Berlin Heidelberg: 2005; Vol. 175, pp 257-298.
39. Cushing, B. L.; Kolesnichenko, V. L.; O'Connor, C. J., Recent advances in the liquid-phase syntheses of inorganic nanoparticles. *Chem Rev* **2004,** *104* (9), 3893-946.
40. Eriksson, S.; Nylén, U.; Rojas, S.; Boutonnet, M., Preparation of catalysts from microemulsions and their applications in heterogeneous catalysis. *Applied Catalysis A: General* **2004,** *265* (2), 207-219.
41. Korchev, A. S.; Bozack, M. J.; Slaten, B. L.; Mills, G., Polymer-Initiated Photogeneration of Silver Nanoparticles in SPEEK/PVA Films: Direct Metal Photopatterning. *J. Am. Chem. Soc.* **2003,** *126* (1), 10-11.
42. Scaiano, J. C.; Billone, P.; Gonzalez, C. M.; Marett, L.; Marin, M. L.; McGilvray, K. L.; Yuan, N., Photochemical routes to silver and gold nanoparticles. *Pure Appl. Chem.* **2009,** *81* (4), 635-647.
43. Nakaso, K.; Han, B.; Ahn, K. H.; Choi, M.; Okuyama, K., Synthesis of non-agglomerated nanoparticles by an electrospray assisted chemical vapor deposition (ES-CVD) method. *Journal of Aerosol Science* **2003,** *34* (7), 869-881.
44. Xia, W.; Schlüter, O. F. K.; Liang, C.; van den Berg, M. W. E.; Guraya, M.; Muhler, M., The synthesis of structured Pd/C hydrogenation catalysts by the chemical vapor deposition of Pd(allyl)Cp onto functionalized carbon nanotubes anchored to vapor grown carbon microfibers. *Catal. Today* **2005,** *102–103* (0), 34-39.
45. Turkevich, J.; Stevenson, P. C.; Hillier, J., A study of the nucleation and growth processes in the synthesis of colloidal gold. *Discussions of the Faraday Society* **1951,** *11* (0), 55-75.
46. Frens, G., Particle size and sol stability in metal colloids. *Kolloid-Z.u.Z.Polymere* **1972,** *250* (7), 736-741.
47. Spagnoli, D.; Banfield, J. F.; Parker, S. C., Free Energy Change of Aggregation of Nanoparticles. *The Journal of Physical Chemistry C* **2008,** *112* (38), 14731-14736.
48. Rozenberg, B. A.; Tenne, R., Polymer-assisted fabrication of nanoparticles and nanocomposites. *Progress in Polymer Science* **2008,** *33* (1), 40-112.
49. Imre, Á.; Beke, D. L.; Gontier-Moya, E.; Szabó, I. A.; Gillet, E., Surface Ostwald ripening of Pd nanoparticles on the MgO (100) surface. *Appl Phys A* **2000,** *71* (1), 19-22.
50. Simonsen, S. B.; Chorkendorff, I.; Dahl, S.; Skoglundh, M.; Sehested, J.; Helveg, S., Direct Observations of Oxygen-induced Platinum Nanoparticle Ripening Studied by In Situ TEM. *J. Am. Chem. Soc.* **2010,** *132* (23), 7968-7975.
51. Bernard, B. K.; Osheroff, M. R.; Hofman, A.; Mennear, J. H., Toxicology and carcinogenesis studies of dietary titanium dioxide□coated mica in male and female Fischer 344 rats. *Journal of Toxicology and Environmental Health* **1989,** *28* (4), 415-426.
52. Borm, P. J. A.; Berube, D., A tale of opportunities, uncertainties, and risks. *Nano Today* **2008,** *3* (1–2), 56-59.
53. Chen, X.; Schluesener, H. J., Nanosilver: a nanoproduct in medical application. *Toxicol Lett* **2008,** *176* (1), 1-12.
54. Chen, J. L.; Fayerweather, W. E., Epidemiologic study of workers exposed to titanium dioxide. *Journal of Occupational and Environmental Medicine* **1988,** *30* (12), 937-942.

55. Li, Q.; Mahendra, S.; Lyon, D. Y.; Brunet, L.; Liga, M. V.; Li, D.; Alvarez, P. J. J., Antimicrobial nanomaterials for water disinfection and microbial control: Potential applications and implications. *Water Research* **2008,** *42* (18), 4591-4602.
56. Hansen, S. F.; Baun, A., When enough is enough. *Nat Nano* **2012,** *7* (7), 409-411.
57. Levard, C.; Hotze, E. M.; Lowry, G. V.; Brown, G. E., Environmental Transformations of Silver Nanoparticles: Impact on Stability and Toxicity. *Environmental Science & Technology* **2012,** *46* (13), 6900-6914.
58. Abbott, L. C.; Maynard, A. D., Exposure Assessment Approaches for Engineered Nanomaterials. *Risk Analysis* **2010,** *30* (11), 1634-1644.
59. Ju-Nam, Y.; Lead, J. R., Manufactured nanoparticles: An overview of their chemistry, interactions and potential environmental implications. *Science of the Total Environment* **2008,** *400* (1–3), 396-414.
60. Maynard, A. D., Nanotechnology: The Next Big Thing, or Much Ado about Nothing? *Annals of Occupational Hygiene* **2007,** *51* (1), 1-12.
61. Tiede, K.; Hassellöv, M.; Breitbarth, E.; Chaudhry, Q.; Boxall, A., Considerations for environmental fate and ecotoxicity testing to support environmental risk assessments for engineered nanoparticles. *Journal of Chromatography A* **2009,** *1216* (3), 503-509.
62. Simonet, B. M.; Valcárcel, M., Monitoring nanoparticles in the environment. *Analytical and bioanalytical chemistry* **2009,** *393* (1), 17-21.
63. Pal, S.; Tak, Y. K.; Song, J. M., Does the Antibacterial Activity of Silver Nanoparticles Depend on the Shape of the Nanoparticle? A Study of the Gram-Negative Bacterium Escherichia coli. *Applied and environmental microbiology* **2007,** *73* (6), 1712-1720.
64. *Nanoscale Materials in Chemistry*. John Wiley and Sons Ltd: Chicester, GB, 2004.
65. Pomogailo, A. D.; Kestel'man, V. N., *Metallopolymer nanocomposites*. Springer-Verlag Berlin and Heidelberg GmbH & Co. KG: Berlin/DE, 2005.
66. *Metal-Polymer Nanocomposites*. John Wiley and Sons Ltd: New York/US, 2004.
67. Niu, Z.; Li, Y., Removal and Utilization of Capping Agents in Nanocatalysis. *Chem. Mater.* **2013,** *26* (1), 72-83.
68. Jeon, S.-H.; Xu, P.; Zhang, B.; Mack, N. H.; Tsai, H.; Chiang, L. Y.; Wang, H.-L., Polymer-assisted preparation of metal nanoparticles with controlled size and morphology. *Journal of Materials Chemistry* **2011,** *21* (8), 2550-2554.
69. Luckham, P. F., Manipulating forces between surfaces: applications in colloid science and biophysics. *Adv. Colloid Interfac.* **2004,** *111* (1–2), 29-47.
70. Kamat, P. V., Photophysical, Photochemical and Photocatalytic Aspects of Metal Nanoparticles. *The Journal of Physical Chemistry B* **2002,** *106* (32), 7729-7744.
71. Hamaker, H. C., The London—van der Waals attraction between spherical particles. *Physica* **1937,** *4* (10), 1058-1072.
72. Adamczyk, Z., Particle adsorption and deposition: role of electrostatic interactions. *Adv. Colloid Interfac.* **2003,** *100–102* (0), 267-347.
73. de Gennes, P. G., Polymers at an interface; a simplified view. *Adv. Colloid Interfac.* **1987,** *27* (3–4), 189-209.
74. Visser, J., The concept of negative hamaker coefficients. 1. history and present status. *Adv. Colloid Interfac.* **1981,** *15* (2), 157-169.
75. Macanás, J.; Ruiz, P.; Alonso, A.; Muñoz, M.; Muraviev, D. N., Ion Exchange-Assisted Synthesis of Polymer Stabilized Metal Nanoparticles. In *Ion Exchange and Solvent Extraction*, Sengupta, A. K., Ed. CRC Press: 2011; pp 1-44.
76. Miachon, S.; Dalmon, J.-A., Catalysis in Membrane Reactors: What About the Catalyst? *Topics in Catalysis* **2004,** *29* (1-2), 59-65.

77. Kumar, R.; Pandey, A. K.; Tyagi, A. K.; Dey, G. K.; Ramagiri, S. V.; Bellare, J. R.; Goswami, A., In situ formation of stable gold nanoparticles in polymer inclusion membranes. *J. Colloid. Interf. Sci.* **2009,** *337* (2), 523-530.
78. Ruiz, P.; Munoz, M.; Macanas, J.; Turta, C.; Prodius, D.; Muraviev, D. N., Intermatrix synthesis of polymer stabilized inorganic nanocatalyst with maximum accessibility for reactants. *Dalton T.* **2010,** *39* (7), 1751-1757.
79. Zhang, Z.; Shao, C.; Zou, P.; Zhang, P.; Zhang, M.; Mu, J.; Guo, Z.; Li, X.; Wang, C.; Liu, Y., In situ assembly of well-dispersed gold nanoparticles on electrospun silica nanotubes for catalytic reduction of 4-nitrophenol. *Chem. Commun.* **2011,** *47* (13), 3906-3908.
80. Chou, K.-S.; Lai, Y.-S., Effect of polyvinyl pyrrolidone molecular weights on the formation of nanosized silver colloids. *Materials Chemistry and Physics* **2004,** *83* (1), 82-88.
81. Ayyad, O.; Muñoz-Rojas, D.; Oró-Solé, J.; Gómez-Romero, P., From silver nanoparticles to nanostructures through matrix chemistry. *J. Nanopart. Res.* **2010,** *12* (1), 337-345.
82. Walter, P.; Welcomme, E.; Hallégot, P.; Zaluzec, N. J.; Deeb, C.; Castaing, J.; Veyssière, P.; Bréniaux, R.; Lévêque, J.-L.; Tsoucaris, G., Early Use of PbS Nanotechnology for an Ancient Hair Dyeing Formula. *Nano Lett.* **2006,** *6* (10), 2215-2219.
83. *Encyclopédie, ou dictionnaire raisonné des sciences, des arts et des métiers*. Paris, France, 1759.
84. Mirguet, C.; Fredrickx§, P.; Sciau, P.; Colomban, P., Origin of the self-organisation of Cu°/Ag° nanoparticles in ancient lustre pottery. A TEM study. *Phase Transitions* **2008,** *81* (2-3), 253-266.
85. Mills, G. F.; Dickinson, B. N., Oxygen Removal from Water by Ammine Exchange Resins. *Industrial & Engineering Chemistry* **1949,** *41* (12), 2842-2844.
86. Muraviev, D. N.; Macanas, J.; Farre, M.; Munoz, M.; Alegret, S., Novel routes for inter-matrix synthesis and characterization of polymer stabilized metal nanoparticles for molecular recognition devices. *Sensor. Actuat. B-Chem.* **2006,** *118* (1-2), 408-417.
87. Macanás, J.; Farre, M.; Munoz, M.; Alegret, S.; Muraviev, D. N., Preparation and characterization of polymer-stabilized metal nanoparticles for sensor applications. *Phys. Status Solidi A* **2006,** *203* (6), 1194-1200.
88. Ruiz, P.; Macanas, J.; Munoz, M.; Muraviev, D., Intermatrix synthesis: easy technique permitting preparation of polymer-stabilized nanoparticles with desired composition and structure. *Nanoscale Res. Lett.* **2011,** *6* (1), 343.
89. Muraviev, D. N.; Macanas, J.; Parrondo, J.; Munoz, M.; Alonso, A.; Alegret, S.; Ortueta, M.; Mijangos, F., Cation-exchange membrane as nanoreactor: Intermatrix synthesis of platinum-copper core-shell nanoparticles. *React. Funct. Polym.* **2007,** *67* (12), 1612-1621.
90. Ruiz, P.; Muñoz, M.; Macanás, J.; Muraviev, D. N., Intermatrix synthesis of polymer-stabilized PGM@Cu core–shell nanoparticles with enhanced electrocatalytic properties. *Reactive and Functional Polymers* **2011,** *71* (8), 916-924.
91. Park, J.-I.; Kim, M. G.; Jun, Y.-w.; Lee, J. S.; Lee, W.-r.; Cheon, J., Characterization of Superparamagnetic "Core−Shell" Nanoparticles and Monitoring Their Anisotropic Phase Transition to Ferromagnetic "Solid Solution" Nanoalloys. *J. Am. Chem. Soc.* **2004,** *126* (29), 9072-9078.
92. Alonso, A.; Macanas, J.; Shafir, A.; Munoz, M.; Vallribera, A.; Prodius, D.; Melnic, S.; Turta, C.; Muraviev, D. N., Donnan-exclusion-driven distribution of catalytic ferromagnetic nanoparticles synthesized in polymeric fibers. *Dalton T.* **2010,** *39* (10), 2579-2586.
93. Alonso, A.; Vigues, N.; Munoz-Berbel, X.; Macanas, J.; Munoz, M.; Mas, J.; Muraviev, D. N., Environmentally-safe bimetallic Ag@Co magnetic nanocomposites with antimicrobial activity. *Chemical Communications* **2011,** *47* (37), 10464-10466.

94. Alonso, A.; Muñoz-Berbel, X.; Vigués, N.; Macanás, J.; Muñoz, M.; Mas, J.; Muraviev, D. N., Characterization of Fibrous Polymer Silver/Cobalt Nanocomposite with Enhanced Bactericide Activity. *Langmuir* **2011,** *28* (1), 783-790.
95. Alonso, A.; Muñoz-Berbel, X.; Vigués, N.; Rodríguez-Rodríguez, R.; Macanás, J.; Muñoz, M.; Mas, J.; Muraviev, D. N., Superparamagnetic Ag@Co-Nanocomposites on Granulated Cation Exchange Polymeric Matrices with Enhanced Antibacterial Activity for the Environmentally Safe Purification of Water. *Advanced Functional Materials* **2013,** *23* (19), 2450-2458.
96. Alonso, A.; Shafir, A.; Macanás, J.; Vallribera, A.; Muñoz, M.; Muraviev, D. N., Recyclable polymer-stabilized nanocatalysts with enhanced accessibility for reactants. *Catal. Today* **2012,** *193* (1), 200-206.
97. Bastos-Arrieta, J.; Shafir, A.; Alonso, A.; Muñoz, M.; Macanás, J.; Muraviev, D. N., Donnan exclusion driven intermatrix synthesis of reusable polymer stabilized palladium nanocatalysts. *Catal. Today* **2012,** *193* (1), 207-212.
98. Alonso, A.; Munoz-Berbel, X.; Vigues, N.; Rodriguez-Rodriguez, R.; Macanas, J.; Mas, J.; Munoz, M.; Muraviev, D. N., Intermatrix synthesis of monometallic and magnetic metal/metal oxide nanoparticles with bactericidal activity on anionic exchange polymers. *RSC Advances* **2012,** *2* (11), 4596-4599.
99. George, S. C.; Thomas, S., Transport phenomena through polymeric systems. *Progress in Polymer Science* **2001,** *26* (6), 985-1017.
100. Levine, I. N., *Physical chemistry*. McGraw-Hill: Michigan, US, 2008.
101. Kammerer, J.; Carle, R.; Kammerer, D. R., Adsorption and ion exchange: basic principles and their application in food processing. *J Agric Food Chem* **2011,** *59* (1), 22-42.
102. Teorell, T., An Attempt to Formulate a Quantitative Theory of Membrane Permeability. *Experimental Biology and Medicine* **1935,** *33* (2), 282-285.
103. Meyer, K. H.; Sievers, J. F., La perméabilité des membranes. II. Essais avec des membranes sélectives artificielles. *Helvetica Chimica Acta* **1936,** *19* (1), 665-677.
104. Sarkar, S.; SenGupta, A. K.; Prakash, P., The Donnan Membrane Principle: Opportunities for Sustainable Engineered Processes and Materials. *Environmental Science & Technology* **2010,** *44* (4), 1161-1166.
105. Yeo, R. S., Ion Clustering and Proton Transport in Nafion Membranes and Its Applications as Solid Polymer Electrolyte. *Journal of The Electrochemical Society* **1983,** *130* (3), 533-538.
106. Donnan, F. G., Theory of membrane equilibria and membrane potentials in the presence of non-dialysing electrolytes. A contribution to physical-chemical physiology. *J. Membrane Sci.* **1995,** *100* (1), 45-55.
107. Alonso, A.; Macanás, J.; Shafir, A.; Muñoz, M.; Vallribera, A.; Prodius, D.; Melnic, S.; Turta, C.; Muraviev, D. N., Donnan-exclusion-driven distribution of catalytic ferromagnetic nanoparticles synthesized in polymeric fibers. *Dalton T.* **2010,** *39* (10), 2579-2586.
108. Sanchez Marcano, J. G.; Tsotsis, T. T., Modelling of Membrane Reactors: Catalytic Membrane Reactors. In *Catalytic Membranes and Membrane Reactors*, Wiley-VCH Verlag GmbH & Co. KGaA: 2004; pp 169-200.
109. Gallucci, F.; Basile, A.; Hai, F. I., Introduction – A Review of Membrane Reactors. In *Membranes for Membrane Reactors*, John Wiley & Sons, Ltd: 2011; pp 1-61.
110. Ozdemir, S. S.; Buonomenna, M. G.; Drioli, E., Catalytic polymeric membranes: Preparation and application. *Applied Catalysis a-General* **2006,** *307* (2), 167-183.
111. Merkel, T. C.; Bondar, V.; Nagai, K.; Freeman, B. D.; Yampolskii, Y. P., Gas Sorption, Diffusion, and Permeation in Poly(2,2-bis(trifluoromethyl)-4,5-difluoro-1,3-dioxole-co-tetrafluoroethylene). *Macromolecules* **1999,** *32* (25), 8427-8440.
112. McCaig, M. S.; Seo, E. D.; Paul, D. R., Effects of bromine substitution on the physical and gas transport properties of five series of glassy polymers. *Polymer* **1999,** *40* (12), 3367-3382.

113. Pixton, M. R.; Paul, D. R., Gas Transport Properties of Polyarylates: Substituent Size and Symmetry Effects. *Macromolecules* **1995,** *28* (24), 8277-8286.
114. Jian, Z.; Xiaohuai, H., The gas permeation property in trimethylsilyl-substituted PPO and triphenylsilyl-substituted PPO. *J. Membrane Sci.* **1994,** *97* (0), 275-282.
115. Hicke, H.-G.; Lehmann, I.; Malsch, G.; Ulbricht, M.; Becker, M., Preparation and characterization of a novel solvent-resistant and autoclavable polymer membrane. *J. Membrane Sci.* **2002,** *198* (2), 187-196.
116. Bhanushali, D.; Kloos, S.; Bhattacharyya, D., Solute transport in solvent-resistant nanofiltration membranes for non-aqueous systems: experimental results and the role of solute–solvent coupling. *J. Membrane Sci.* **2002,** *208* (1–2), 343-359.
117. Hickner, M. A.; Ghassemi, H.; Kim, Y. S.; Einsla, B. R.; McGrath, J. E., Alternative polymer systems for proton exchange membranes (PEMs). *Chem Rev* **2004,** *104* (10), 4587-611.
118. Vanherck, K.; Vandezande, P.; Aldea, S. O.; Vankelecom, I. F. J., Cross-linked polyimide membranes for solvent resistant nanofiltration in aprotic solvents. *J. Membrane Sci.* **2008,** *320* (1–2), 468-476.
119. Baker, R. W., Membranes and Modules. In *Membrane Technology and Applications*, John Wiley & Sons, Ltd: 2004; pp 89-160.
120. Buonomenna, M. G.; Choi, S. H.; Drioli, E., Catalysis in polymeric membrane reactors: the membrane role. *Asia-Pac. J Chem. Eng.* **2010,** *5* (1), 26-34.
121. Young, T.-H.; Cheng, L.-P.; Lin, D.-J.; Fane, L.; Chuang, W.-Y., Mechanisms of PVDF membrane formation by immersion-precipitation in soft (1-octanol) and harsh (water) nonsolvents. *Polymer* **1999,** *40* (19), 5315-5323.
122. Jeong, B.-H.; Hoek, E. M. V.; Yan, Y.; Subramani, A.; Huang, X.; Hurwitz, G.; Ghosh, A. K.; Jawor, A., Interfacial polymerization of thin film nanocomposites: A new concept for reverse osmosis membranes. *J. Membrane Sci.* **2007,** *294* (1–2), 1-7.
123. Castellari, C.; Ottani, S., Preparation of reverse osmosis membranes. A numerical analysis of asymmetric membrane formation by solvent evaporation from cellulose acetate casting solutions. *J. Membrane Sci.* **1981,** *9* (1–2), 29-41.
124. Ulbricht, M.; Belfort, G., Surface modification of ultrafiltration membranes by low temperature plasma II. Graft polymerization onto polyacrylonitrile and polysulfone. *J. Membrane Sci.* **1996,** *111* (2), 193-215.
125. Bouyer, D.; Faur, C.; Pochat, C., Procédés d'élaboration de membranes par séparation de phases. *Techniques de l'ingénieur Opérations unitaires : techniques séparatives sur membranes* **2011,** *base documentaire : TIB331DUO* (ref. article : j2799).
126. Loeb, S., The Loeb-Sourirajan Membrane: How It Came About. In *Synthetic Membranes*, AMERICAN CHEMICAL SOCIETY: 1981; Vol. 153, pp 1-9.
127. Mulder, M., *Basic principles of membrane technology*. Kluwer Academic: Dordrecht etc., 1996; Vol. 2, p 564.
128. Kesting, R., The four tiers of structure in integrally skinned phase inversion membranes and their relevance to the various separation regimes. *J. Appl. Polym. Sci.* **1990,** *41* (11□12), 2739-2752.
129. Sata, T., *Ion Exchange Membranes: Preparation, Characterization, Modification and Application*. Royal Society of Chemistry: Cambridge, UK, 2004.
130. Lu, G. Q.; Diniz da Costa, J. C.; Duke, M.; Giessler, S.; Socolow, R.; Williams, R. H.; Kreutz, T., Inorganic membranes for hydrogen production and purification: A critical review and perspective. *J. Colloid. Interf. Sci.* **2007,** *314* (2), 589-603.
131. McLeary, E. E.; Jansen, J. C.; Kapteijn, F., Zeolite based films, membranes and membrane reactors: Progress and prospects. *Microporous and Mesoporous Materials* **2006,** *90* (1–3), 198-220.

132. Halpert, G.; Surampudi, S.; Shen, D.; Huang, C. K.; Narayanan, S.; Vamos, E.; Perrone, D., Status of the development of rechargeable lithium cells. *J. Power Sources* **1994,** *47* (3), 287-294.
133. Chu, Y.-H.; Shul, Y. G.; Choi, W. C.; Woo, S. I.; Han, H.-S., Evaluation of the Nafion effect on the activity of Pt–Ru electrocatalysts for the electro-oxidation of methanol. *J. Power Sources* **2003,** *118* (1–2), 334-341.
134. Gargas, D. J.; Bussian, D. A.; Buratto, S. K., Investigation of the connectivity of hydrophilic domains in Nafion using electrochemical pore-directed nanolithography. *Nano Lett* **2005,** *5* (11), 2184-7.
135. Mauritz, K. A.; Moore, R. B., State of understanding of nafion. *Chem Rev* **2004,** *104* (10), 4535-85.
136. Heitner-Wirguin, C., Recent advances in perfluorinated ionomer membranes: structure, properties and applications. *J. Membrane Sci.* **1996,** *120* (1), 1-33.
137. Schuster, M.; Schuster, M. I. M. F. A. K. K. D. M. J., *Proton and Water Transport in Nano-separated Polymer Membranes*. Germany: Max-Planck-Institut für Festkörperforschung, n.d.: 2005.
138. Fujimura, M.; Hashimoto, T.; Kawai, H., Small-angle x-ray scattering study of perfluorinated ionomer membranes. 2. Models for ionic scattering maximum. *Macromolecules* **1982,** *15* (1), 136-144.
139. Dreyfus, B.; Gebel, G.; Aldebert, P.; Pineri, M.; Escoubes, M.; Thomas, M., Distribution of the « micelles » in hydrated perfluorinated ionomer membranes from SANS experiments. *J. Phys. France* **1990,** *51* (12), 1341-1354.
140. Gebel, G.; Lambard, J., Small-Angle Scattering Study of Water-Swollen Perfluorinated Ionomer Membranes. *Macromolecules* **1997,** *30* (25), 7914-7920.
141. Haubold, H. G.; Vad, T.; Jungbluth, H.; Hiller, P., Nano structure of NAFION: a SAXS study. *Electrochimica Acta* **2001,** *46* (10–11), 1559-1563.
142. Rubatat, L.; Rollet, A. L.; Gebel, G.; Diat, O., Evidence of Elongated Polymeric Aggregates in Nafion. *Macromolecules* **2002,** *35* (10), 4050-4055.
143. Litt, M. H., A Reevaluation of Nation Morphology. *American Chemical Society Polymer Preprints* **1997,** *38*.
144. Kreuer, K.-D.; Portale, G., A Critical Revision of the Nano-Morphology of Proton Conducting Ionomers and Polyelectrolytes for Fuel Cell Applications. *Advanced Functional Materials* **2013,** *23* (43), 5390-5397.
145. Gierke, T. D.; Munn, G. E.; Wilson, F. C., Morphology of Perfluorosulfonated Membrane Products. In *Perfluorinated Ionomer Membranes*, AMERICAN CHEMICAL SOCIETY: 1982; Vol. 180, pp 195-216.
146. *Perfluorinated Ionomer Membranes*. AMERICAN CHEMICAL SOCIETY: 1982; Vol. 180, p 516.
147. Chou, J.; McFarland, E. W.; Metiu, H., Electrolithographic Investigations of the Hydrophilic Channels in Nafion Membranes. *The Journal of Physical Chemistry B* **2005,** *109* (8), 3252-3256.
148. Gebel, G., Structural evolution of water swollen perfluorosulfonated ionomers from dry membrane to solution. *Polymer* **2000,** *41* (15), 5829-5838.
149. Diat, O.; Gebel, G., Fuel cells: Proton channels. *Nat Mater* **2008,** *7* (1), 13-14.
150. Schmidt-Rohr, K.; Chen, Q., Parallel cylindrical water nanochannels in Nafion fuel-cell membranes. *Nat Mater* **2008,** *7* (1), 75-83.
151. Johnson, R. N.; Farnham, A. G.; Clendinning, R. A.; Hale, W. F.; Merriam, C. N., Poly(aryl ethers) by nucleophilic aromatic substitution. I. Synthesis and properties. *Journal of Polymer Science Part A-1: Polymer Chemistry* **1967,** *5* (9), 2375-2398.
152. Rose, J., Preparation and properties of poly (arylene ether sulphones). *Polymer* **1974,** *15* (7), 456-465.

153. Jia, L.; Xu, X. F.; Zhang, H. J.; Xu, J. P., Permeation of nitrogen and water vapor through sulfonated polyetherethersulfone membrane. *J. Polym. Sci. Pol. Phys.* **1997,** *35* (13), 2133-2140.
154. van Zyl, A. J.; Kerres, J. A.; Cui, W.; Junginger, M., Application of new sulfonated ionomer membranes in the separation of pentene and pentane by facilitated transport. *J. Membrane Sci.* **1997,** *137* (1–2), 173-185.
155. Staude, E.; Breitbach, L., Polysulfones and their derivatives: Materials for membranes for different separation operations. *J. Appl. Polym. Sci.* **1991,** *43* (3), 559-566.
156. Chung, T. S.; Loh, K.-C.; Tay, H. L., Development of polysulfone membranes for bacteria immobilization to remove phenol. *J. Appl. Polym. Sci.* **1998,** *70* (13), 2585-2594.
157. Pouliot, Y.; Wijers, M. C.; Gauthier, S. F.; Nadeau, L., Fractionation of whey protein hydrolysates using charged UF/NF membranes. *J. Membrane Sci.* **1999,** *158* (1–2), 105-114.
158. Xu, Y.; Lebrun, R. E.; Gallo, P.-J.; Blond, P., Treatment of Textile Dye Plant Effluent by Nanofiltration Membrane. *Separation Science and Technology* **1999,** *34* (13), 2501-2519.
159. Blanco, J. F.; Nguyen, Q. T.; Schaetzel, P., Sulfonation of polysulfones: Suitability of the sulfonated materials for asymmetric membrane preparation. *J. Appl. Polym. Sci.* **2002,** *84* (13), 2461-2473.
160. Machado, P. S. T.; Habert, A. C.; Borges, C. P., Membrane formation mechanism based on precipitation kinetics and membrane morphology: flat and hollow fiber polysulfone membranes. *J. Membrane Sci.* **1999,** *155* (2), 171-183.
161. Boom, R. M.; Wienk, I. M.; van den Boomgaard, T.; Smolders, C. A., Microstructures in phase inversion membranes. Part 2. The role of a polymeric additive. *J. Membrane Sci.* **1992,** *73* (2–3), 277-292.
162. Emin, C.; Remigy, J.-C.; Lahitte, J.-F., Influence of UV grafting conditions and gel formation on the loading and stabilization of palladium nanoparticles in photografted polyethersulfone membrane for catalytic reactions. *J. Membrane Sci.* **2014,** *455* (0), 55-63.
163. Ulbricht, M.; Riedel, M.; Marx, U., Novel photochemical surface functionalization of polysulfone ultrafiltration membranes for covalent immobilization of biomolecules. *J. Membrane Sci.* **1996,** *120* (2), 239-259.
164. Di Vona, M. L.; Sgreccia, E.; Tamilvanan, M.; Khadhraoui, M.; Chassigneux, C.; Knauth, P., High ionic exchange capacity polyphenylsulfone (SPPSU) and polyethersulfone (SPES) cross-linked by annealing treatment: Thermal stability, hydration level and mechanical properties. *J. Membrane Sci.* **2010,** *354* (1–2), 134-141.
165. Noshay, A.; Robeson, L. M., Sulfonated polysulfone. *J. Appl. Polym. Sci.* **1976,** *20* (7), 1885-1903.
166. Liu, W.; Chen, T.; Xu, J., Gas permeation behavior of phenolphthalein based heat-resistant polymers PEK-C and PES-C. *J. Membrane Sci.* **1990,** *53* (3), 203-213.
167. Fan, G.; Jin, X.; Zhou, E.; Liu, K., Synthesis and characterization of (phenolphthalein/4, 4′-thiodiphenol) pes copolymers. *Eur. Polym. J.* **1998,** *34* (2), 277-282.
168. Zheng, S.; Guo, Q.; Mi, Y., Miscibility and phase behavior in blends of phenolphthalein poly (ether sulfone) and poly (hydroxyether of bisphenol A). *Polymer* **2003,** *44* (3), 867-876.
169. Wang, M.; Wu, L.-G.; Mo, J.-X.; Gao, C.-J., The preparation and characterization of novel charged polyacrylonitrile/PES-C blend membranes used for ultrafiltration. *J. Membrane Sci.* **2006,** *274* (1), 200-208.
170. Huang, D.; Yang, Y.; Li, B., Mechanical and structural characteristics of phenolphthalein poly (ether sulfone)/ultra□high molecular weight polyethylene blends. *Die Angewandte makromolekulare Chemie* **1997,** *251* (1), 73-80.
171. Gao, Q. J.; Wang, Y. X.; Xu, L.; Wang, Z. T.; Wei, G. Q., Proton-exchange Sulfonated Poly(ether ether ketone)/Sulfonated Phenolphthalein Poly(ether sulfone) Blend Membranes in DMFCs. *Chinese. J. Chem. Eng.* **2009,** *17* (6), 934-941.

172. Ren, Z.; Liu, W.; Hou, Y.; Zhu, Y.; Chang, L.; Ma, D., Comparative Thermogravimetric Studies of Poly (ether-ketone/sulfone) Imides and Their Parent Polymers: I. Poly (ether-ketone/sulfone) ethylimide. *Journal of thermal analysis and calorimetry* **2001,** *63* (1), 153-160.
173. Blanco, J. F.; Sublet, J.; Nguyen, Q. T.; Schaetzel, P., Formation and morphology studies of different polysulfones-based membranes made by wet phase inversion process. *J. Membrane Sci.* **2006,** *283* (1-2), 27-37.
174. Blanco, J. F.; Nguyen, Q. T.; Schaetzel, P., Novel hydrophilic membrane materials: sulfonated polyethersulfone Cardo. *J. Membrane Sci.* **2001,** *186* (2), 267-279.
175. Li, L.; Wang, Y. X., Quaternized polyethersulfone Cardo anion exchange membranes for direct methanol alkaline fuel cells. *J. Membrane Sci.* **2005,** *262* (1-2), 1-4.
176. Di Vona, M. L.; Luchetti, L.; Spera, G. P.; Sgreccia, E.; Knauth, P., Synthetic strategies for the preparation of proton-conducting hybrid polymers based on PEEK and PPSU for PEM fuel cells. *Comptes Rendus Chimie* **2008,** *11* (9), 1074-1081.
177. Hartmann-Thompson, C.; Merrington, A.; Carver, P. I.; Keeley, D. L.; Rousseau, J. L.; Hucul, D.; Bruza, K. J.; Thomas, L. S.; Keinath, S. E.; Nowak, R. M., Proto-conducting polyhedral oligosilsesquioxane nanoadditives for sulfonated polyphenylsulfone hydrogen fuel cell proton exchange membranes. *J. Appl. Polym. Sci.* **2008,** *110* (2), 958-974.
178. Parcero, E.; Herrera, R.; Nunes, S. P., Phosphonated and sulfonated polyhphenylsulfone membranes for fuel cell application. *J. Membrane Sci.* **2006,** *285* (1), 206-213.
179. Di Vona, M. L.; D'Epifanio, A.; Marani, D.; Trombetta, M.; Traversa, E.; Licoccia, S., SPEEK/PPSU-based organic–inorganic membranes: proton conducting electrolytes in anhydrous and wet environments. *J. Membrane Sci.* **2006,** *279* (1–2), 186-191.
180. Brousse, C.; Chapurlat, R.; Quentin, J. P., New membranes for reverse osmosis I. Characteristics of the base polymer: sulphonated polysulphones. *Desalination* **1976,** *18* (2), 137-153.
181. Tang, Y.; Widjojo, N.; Shi, G. M.; Chung, T.-S.; Weber, M.; Maletzko, C., Development of flat-sheet membranes for C1–C4 alcohols dehydration via pervaporation from sulfonated polyphenylsulfone (sPPSU). *J. Membrane Sci.* **2012,** *415–416* (0), 686-695.
182. Xing, D.; Kerres, J., Improved performance of sulfonated polyarylene ethers for proton exchange membrane fuel cells. *Polym. Advan. Technol.* **2006,** *17* (7□8), 591-597.
183. Dyck, A.; Fritsch, D.; Nunes, S., Proton□conductive membranes of sulfonated polyphenylsulfone. *J. Appl. Polym. Sci.* **2002,** *86* (11), 2820-2827.
184. Srithong, S.; Jiraratananon, R.; Hansupalak, N., A simple postsulfonation of poly (arylene ether sulfone) Radel® R. *J. Appl. Polym. Sci.* **2011,** *119* (2), 973-976.
185. Sun, H.; Venkatasubramanian, N.; Houtz, M.; Mark, J.; Tan, S.; Arnold, F.; Lee, C. Y., Molecular composites by incorporation of a rod-like polymer into a functionalized high-performance polymer, and their conversion into microcellular foams. *Colloid and Polymer Science* **2004,** *282* (5), 502-510.
186. Mark, J. E., *Physical properties of polymers handbook*. AIP Press: Michigan, US, 1996.
187. Bayer, O., Das Di-Isocyanat-Polyadditionsverfahren (Polyurethane). *Angewandte Chemie* **1947,** *59* (9), 257-272.
188. Seymour, R. B.; Kauffman, G. B., Polyurethanes: A class of modern versatile materials. *Journal of Chemical Education* **1992,** *69* (11), 909.
189. Saunders, J. H.; Frisch, K. C., *Polyurethanes: chemistry and technology*. Interscience Publishers: 1962.
190. Uhlig, K. K., *Discovering Polyurethanes*. Hanser-Gardner Publications: 1999.
191. Warner, S. B., *Fiber science*. Prentice Hall PTR: Michigan, US, 1995.
192. Gupta, A. K.; Paliwal, D. K.; Bajaj, P., Melting behavior of acrylonitrile polymers. *J. Appl. Polym. Sci.* **1998,** *70* (13), 2703-2709.

193. Serkov, A. T.; Radishevskii, M. B., Status and prospects for production of carbon fibres based on polyacrylonitrile. *Fibre Chem* **2008,** *40* (1), 24-31.
194. Palmer, R. J., Polyamides, Plastics. In *Encyclopedia of Polymer Science and Technology*, John Wiley & Sons, Inc.: 2002.
195. Dalmon, J.-A.; Cruz-López, A.; Farrusseng, D.; Guilhaume, N.; Iojoiu, E.; Jalibert, J.-C.; Miachon, S.; Mirodatos, C.; Pantazidis, A.; Rebeilleau-Dassonneville, M.; Schuurman, Y.; van Veen, A. C., Oxidation in catalytic membrane reactors. *Applied Catalysis A: General* **2007,** *325* (2), 198-204.
196. Vankelecom, I. F. J.; Jacobs, P. A., Dense organic catalytic membranes for fine chemical synthesis. *Catal. Today* **2000,** *56* (1–3), 147-157.
197. Fritsch, D.; Randjelovic, I.; Keil, F., Application of a forced-flow catalytic membrane reactor for the dimerisation of isobutene. *Catal. Today* **2004,** *98* (1–2), 295-308.
198. Brandao, L.; Fritsch, D.; Mendes, A. M.; Madeira, L. M., Propylene hydrogenation in a continuous polymeric catalytic membrane reactor. *Ind. Eng. Chem. Res.* **2007,** *46* (16), 5278-5285.
199. Smotkin, E. S.; Brown, R. M.; Rabenberg, L. K.; Salomon, K.; Bard, A. J.; Campion, A.; Fox, M. A.; Mallouk, T. E.; Webber, S. E.; White, J. M., Ultrasmall particles of cadmium selenide and cadmium sulfide formed in Nafion by an ion-dilution technique. *The Journal of Physical Chemistry* **1990,** *94* (19), 7543-7549.
200. Zhang, Y.; Kang, D.; Saquing, C.; Aindow, M.; Erkey, C., Supported platinum nanoparticles by supercritical deposition. *Ind. Eng. Chem. Res.* **2005,** *44* (11), 4161-4164.
201. Wang, S.; Liu, P.; Wang, X.; Fu, X., Homogeneously Distributed CdS Nanoparticles in Nafion Membranes: Preparation, Characterization, and Photocatalytic Properties. *Langmuir* **2005,** *21* (25), 11969-11973.
202. Liu, P.; Bandara, J.; Lin, Y.; Elgin, D.; Allard, L. F.; Sun, Y.-P., Formation of Nanocrystalline Titanium Dioxide in Perfluorinated Ionomer Membrane. *Langmuir* **2002,** *18* (26), 10398-10401.
203. Bertoncello, P.; Peruffo, M.; Unwin, P. R., Formation and evaluation of electrochemically-active ultra-thin palladium-Nafion nanocomposite films. *Chemical Communications* **2007,** (16), 1597-1599.
204. Rollins, H. W.; Whiteside, T.; Shafer, G. J.; Ma, J.-J.; Tu, M.-H.; Liu, J.-T.; DesMarteau, D. D.; Sun, Y.-P., Nanoscale metal sulfides in perfluorinated ionomer membranes. *Journal of Materials Chemistry* **2000,** *10* (9), 2081-2084.
205. Wang, J.; Liu, P.; Wang, S.; Han, W.; Wang, X.; Fu, X., Nanocrystalline zinc oxide in perfluorinated ionomer membranes: Preparation, characterization, and photocatalytic properties. *Journal of Molecular Catalysis A: Chemical* **2007,** *273* (1–2), 21-25.
206. Kumar, R.; Pandey, A. K.; Das, S.; Dhara, S.; Misra, N. L.; Shukla, R.; Tyagi, A. K.; Ramagiri, S. V.; Bellare, J. R.; Goswami, A., Galvanic reactions involving silver nanoparticles embedded in cation-exchange membrane. *Chemical Communications* **2010,** *46* (34), 6371-6373.
207. Rollins, H. W.; Lin, F.; Johnson, J.; Ma, J.-J.; Liu, J.-T.; Tu, M.-H.; DesMarteau, D. D.; Sun, Y.-P., Nanoscale Cavities for Nanoparticles in Perfluorinated Ionomer Membranes. *Langmuir* **2000,** *16* (21), 8031-8036.
208. Sun, Y.-P.; Atorngitjawat, P.; Lin, Y.; Liu, P.; Pathak, P.; Bandara, J.; Elgin, D.; Zhang, M., Nanoscale cavities in ionomer membrane for the formation of nanoparticles. *J. Membrane Sci.* **2004,** *245* (1–2), 211-217.
209. Sachdeva, A.; Sodaye, S.; Pandey, A. K.; Goswami, A., Formation of Silver Nanoparticles in Poly(perfluorosulfonic) Acid Membrane. *Analytical Chemistry* **2006,** *78* (20), 7169-7174.
210. Krishnan, M.; White, J. R.; Fox, M. A.; Bard, A. J., Integrated chemical systems: photocatalysis at semiconductors incorporated into polymer (Nafion)/mediator systems. *J. Am. Chem. Soc.* **1983,** *105* (23), 7002-7003.

211. Sode, A.; Ingle, N. J. C.; McCormick, M.; Bizzotto, D.; Gyenge, E.; Ye, S.; Knights, S.; Wilkinson, D. P., Controlling the deposition of Pt nanoparticles within the surface region of Nafion. *J. Membrane Sci.* **2011,** *376* (1–2), 162-169.
212. Macanás, J.; Parrondo, J.; Munoz, M.; Alegret, S.; Mijangos, F.; Muraviev, D. N., Preparation and characterisation of metal-polymer nanocomposite membranes for electrochemical applications. *Phys. Status Solidi A* **2007,** *204* (6), 1699-1705.
213. Zodrow, K.; Brunet, L.; Mahendra, S.; Li, D.; Zhang, A.; Li, Q.; Alvarez, P. J., Polysulfone ultrafiltration membranes impregnated with silver nanoparticles show improved biofouling resistance and virus removal. *Water Research* **2009,** *43* (3), 715-723.
214. Alsalhy, Q. F.; Ali, J. M.; Abbas, A. A.; Rashed, A.; Bruggen, B. V. d.; Balta, S., Enhancement of poly(phenyl sulfone) membranes with ZnO nanoparticles. *Desalination and Water Treatment* **2013,** *51* (31-33), 6070-6081.
215. Teli, S. B.; Molina, S.; Sotto, A.; Calvo, E. G. a.; Abajob, J. d., Fouling Resistant Polysulfone–PANI/TiO2 Ultrafiltration Nanocomposite Membranes. *Ind. Eng. Chem. Res.* **2013,** *52* (27), 9470-9479.
216. Madaleno, L.; Pyrz, R.; Crosky, A.; Jensen, L. R.; Rauhe, J. C. M.; Dolomanova, V.; de Barros Timmons, A. M. M. V.; Cruz Pinto, J. J.; Norman, J., Processing and characterization of polyurethane nanocomposite foam reinforced with montmorillonite–carbon nanotube hybrids. *Composites Part A: Applied Science and Manufacturing* **2013,** *44* (0), 1-7.
217. Han, J. G.; Xiang, Y. Q.; Zhu, Y., New Antibacterial Composites: Waterborne Polyurethane/Gold Nanocomposites Synthesized Via Self-Emulsifying Method. *J Inorg Organomet Polym* **2013**, 1-8.
218. Apyari, V.; Volkov, P.; Dmitrienko, S., Synthesis and optical properties of polyurethane foam modified with silver nanoparticles. *Advances in Natural Sciences: Nanoscience and Nanotechnology* **2012,** *3* (1), 015001.
219. Chou, C.-W.; Hsu, S.-h.; Chang, H.; Tseng, S.-M.; Lin, H.-R., Enhanced thermal and mechanical properties and biostability of polyurethane containing silver nanoparticles. *Polymer Degradation and Stability* **2006,** *91* (5), 1017-1024.
220. Deka, H.; Karak, N.; Kalita, R. D.; Buragohain, A. K., Bio-based thermostable, biodegradable and biocompatible hyperbranched polyurethane/Ag nanocomposites with antimicrobial activity. *Polymer Degradation and Stability* **2010,** *95* (9), 1509-1517.
221. Jain, P.; Pradeep, T., Potential of silver nanoparticle-coated polyurethane foam as an antibacterial water filter. *Biotechnol Bioeng* **2005,** *90* (1), 59-63.
222. Mulongo, G.; Mbabazi, J.; Nnamuyomba, P.; Hak-Chol, S., Water Bactericidal Properties of Nanosilver-Polyurethane Composites. *Nanoscience and Nanotechnology* **2011,** *1* (2), 40-42.
223. Phong, N. T. P.; Thanh, N. V. K.; Phuong, P. H. In *Fabrication of antibacterial water filter by coating silver nanoparticles on flexible polyurethane foams*, Journal of Physics: Conference Series, IOP Publishing: 2009; p 012079.
224. MacKay, W. Antimicrobial foam and method of manufacture. 2010.
225. Dolomanova, V.; Rauhe, J. C. M.; Jensen, L. R.; Pyrz, R.; Timmons, A. B., Mechanical properties and morphology of nano-reinforced rigid PU foam. *Journal of Cellular Plastics* **2011,** *47* (1), 81-93.
226. Ye, W.; Leung, M. F.; Xin, J.; Kwong, T. L.; Lee, D. K. L.; Li, P., Novel core-shell particles with poly (< i> n</i>-butyl acrylate) cores and chitosan shells as an antibacterial coating for textiles. *Polymer* **2005,** *46* (23), 10538-10543.
227. Sojka-Ledakowicz, J.; Lewartowska, J.; Kudzin, M.; Jesionowski, T.; Siwińska-Stefańska, K.; Krysztafkiewicz, A., Modification of textile materials with micro-and nano-structural metal oxides. *Fibres & Textiles in Eastern Europe* **2008**.
228. Sepahi Rad, P.; Montazer, M.; Karim Rahimi, M., Simultaneous antimicrobial and dyeing of wool: a facial method. *J. Appl. Polym. Sci.* **2011,** *122* (2), 1405-1411.

229. Berendjchi, A.; Khajavi, R.; Yazdanshenas, M. E., Fabrication of superhydrophobic and antibacterial surface on cotton fabric by doped silica-based sols with nanoparticles of copper. *Nanoscale Res. Lett.* **2011,** *6* (1), 594.
230. Sójka-Ledakowicz, J.; Olczyk, J.; Sielski, J., Synthesis of zinc oxide in an emulsion system and its deposition on PES nonwoven fabrics. *Fibres & Textiles in Eastern Europe* **2011,** *19* (2), 85.
231. Skoog, D. A.; Holler, F. J.; Nieman, T. A., *Principles of instrumental analysis*. Saunders College Pub.: 1998.
232. Egerton, R., *Physical Principles of Electron Microscopy: An Introduction to TEM, SEM, and AEM*. Springer: 2006.
233. Zhou, W.; Wang, Z. L., *Scanning Microscopy for Nanotechnology: Techniques and Applications*. Springer: 2007.
234. Erkey, C., Preparation of metallic supported nanoparticles and films using supercritical fluid deposition. *The Journal of Supercritical Fluids* **2009,** *47* (3), 517-522.
235. Han, J.; Liu, Y.; Guo, R., Reactive template method to synthesize gold nanoparticles with controllable size and morphology supported on shells of polymer hollow microspheres and their application for aerobic alcohol oxidation in water. *Advanced Functional Materials* **2009,** *19* (7), 1112-1117.
236. Sanchez Marcano, J. G.; Tsotsis, T. T., Modelling of Membrane Reactors: Modelling of Pervaporation Membrane Reactors / Modelling of Membrane Bioreactors. In *Catalytic Membranes and Membrane Reactors*, Wiley-VCH Verlag GmbH & Co. KGaA: 2004; pp 200-222.
237. Koros, W.; Ma, Y.; Shimidzu, T., Terminology for membranes and membrane processes (IUPAC Recommendations 1996). *J. Membrane Sci.* **1996,** *120* (2), 149-159.
238. Bashyam, R.; Zelenay, P., A class of non-precious metal composite catalysts for fuel cells. *Nature* **2006,** *443* (7107), 63-66.
239. Carpenter, I.; Edwards, N.; Ellis, S.; Frost, J.; Golunski, S. E.; Van Keulen, N.; Petch, M.; Pignon, J., On-board hydrogen generation for PEM fuel cells in automotive applications. **1999**.
240. Faur Ghenciu, A., Review of fuel processing catalysts for hydrogen production in PEM fuel cell systems. *Current Opinion in Solid State and Materials Science* **2002,** *6* (5), 389-399.
241. Steele, B. C. H.; Heinzel, A., Materials for fuel-cell technologies. *Nature* **2001,** *414* (6861), 345-352.
242. Semelsberger, T. A.; Borup, R. L., Fuel effects on start-up energy and efficiency for automotive PEM fuel cell systems. *Int. J. Hydrogen Energ.* **2005,** *30* (4), 425-435.
243. Berger, D. J., Fuel Cells and Precious-Metal Catalysts. *Science* **1999,** *286* (5437), 49.
244. Liu, H.; Logan, B. E., Electricity Generation Using an Air-Cathode Single Chamber Microbial Fuel Cell in the Presence and Absence of a Proton Exchange Membrane. *Environmental Science & Technology* **2004,** *38* (14), 4040-4046.
245. Chang, C. H.; Yuen, T. S.; Nagao, Y.; Yugami, H., Electrocatalytic activity of iridium oxide nanoparticles coated on carbon for oxygen reduction as cathode catalyst in polymer electrolyte fuel cell. *J. Power Sources* **2010,** *195* (18), 5938-5941.
246. Jadav, G. L.; Singh, P. S., Synthesis of novel silica-polyamide nanocomposite membrane with enhanced properties. *J. Membrane Sci.* **2009,** *328* (1–2), 257-267.
247. Taurozzi, J. S.; Arul, H.; Bosak, V. Z.; Burban, A. F.; Voice, T. C.; Bruening, M. L.; Tarabara, V. V., Effect of filler incorporation route on the properties of polysulfone-silver nanocomposite membranes of different porosities. *J. Membrane Sci.* **2008,** *325* (1), 58-68.
248. Rahimnejad, M.; Ghasemi, M.; Najafpour, G. D.; Ismail, M.; Mohammad, A. W.; Ghoreyshi, A. A.; Hassan, S. H. A., Synthesis, characterization and application studies of self-made

Fe3O4/PES nanocomposite membranes in microbial fuel cell. *Electrochimica Acta* **2012,** *85* (0), 700-706.
249. Adam, H.; Stanisław, G.; Folke, I., Chemical sensors definitions and classification. *Pure Appl. Chem* **1991,** *63*, 1274-1250.
250. Cespedes, F.; Martinez-Fabregas, E.; Alegret, S., New materials for electrochemical sensing I. Rigid conducting composites. *Trends in Analytical Chemistry* **1996,** *15* (7), 296-304.
251. Progress on Drinking-Water and Sanitation: 2012 Update. UNICEF and World Health Organization: United States of America, 2012.
252. Safer Water, Better Health: Costs, benefits, and sustainability of interventions to protect and promote health. World Health Organization: Spain, 2008.
253. Charnley, M.; Textor, M.; Acikgoz, C., Designed polymer structures with antifouling–antimicrobial properties. *Reactive and Functional Polymers* **2011,** *71* (3), 329-334.
254. Schrick, B.; Blough, J. L.; Jones, A. D.; Mallouk, T. E., Hydrodechlorination of Trichloroethylene to Hydrocarbons Using Bimetallic Nickel−Iron Nanoparticles. *Chem. Mater.* **2002,** *14* (12), 5140-5147.
255. Zhang, W.-x.; Wang, C.-B.; Lien, H.-L., Treatment of chlorinated organic contaminants with nanoscale bimetallic particles. *Catal. Today* **1998,** *40* (4), 387-395.
256. Lowry, G. V.; Johnson, K. M., Congener-Specific Dechlorination of Dissolved PCBs by Microscale and Nanoscale Zerovalent Iron in a Water/Methanol Solution. *Environmental Science & Technology* **2004,** *38* (19), 5208-5216.
257. Feng, J.; Lim, T.-T., Pathways and kinetics of carbon tetrachloride and chloroform reductions by nano-scale Fe and Fe/Ni particles: comparison with commercial micro-scale Fe and Zn. *Chemosphere* **2005,** *59* (9), 1267-1277.
258. Xu, J.; Bhattacharyya, D., Membrane-based bimetallic nanoparticles for environmental remediation: Synthesis and reactive properties. *Environ. Prog.* **2005,** *24* (4), 358-366.
259. Wu, L.; Ritchie, S. M. C., Enhanced dechlorination of trichloroethylene by membrane-supported Pd-coated iron nanoparticles. *Environ. Prog.* **2008,** *27* (2), 218-224.
260. Venkatachalam, K.; Arzuaga, X.; Chopra, N.; Gavalas, V. G.; Xu, J.; Bhattacharyya, D.; Hennig, B.; Bachas, L. G., Reductive dechlorination of 3, 3′, 4, 4′-tetrachlorobiphenyl (PCB77) using palladium or palladium/iron nanoparticles and assessment of the reduction in toxic potency in vascular endothelial cells. *Journal of hazardous materials* **2008,** *159* (2), 483-491.
261. Herves, P.; Pérez-Lorenzo, M.; Liz-Marzán, L. M.; Dzubiella, J.; Lu, Y.; Ballauff, M., Catalysis by metallic nanoparticles in aqueous solution: model reactions. *Chemical Society Reviews* **2012,** *41* (17), 5577-5587.
262. Pradhan, N.; Pal, A.; Pal, T., Silver nanoparticle catalyzed reduction of aromatic nitro compounds. *Colloids and Surfaces A: Physicochemical and Engineering Aspects* **2002,** *196* (2), 247-257.
263. Esumi, K.; Isono, R.; Yoshimura, T., Preparation of PAMAM-and PPI-metal (silver, platinum, and palladium) nanocomposites and their catalytic activities for reduction of 4-nitrophenol. *Langmuir* **2004,** *20* (1), 237-243.
264. Decher, G., Fuzzy Nanoassemblies: Toward Layered Polymeric Multicomposites. *Science* **1997,** *277* (5330), 1232-1237.
265. Lu, O.; Dotzauer, D. M.; Hogg, S. R.; Macanas, J.; Lahitte, J.-F.; Bruening, M. L., Catalytic hollow fiber membranes prepared using layer-by-layer adsorption of polyelectrolytes and metal nanoparticles. *Catal. Today* **2010,** *156* (3-4), 100-106.
266. Liau, S. Y.; Read, D. C.; Pugh, W. J.; Furr, J. R.; Russell, A. D., Interaction of silver nitrate with readily identifiable groups: relationship to the antibacterialaction of silver ions. *Letters in Applied Microbiology* **1997,** *25* (4), 279-283.

267. Gupta, A.; Silver, S., Molecular Genetics: Silver as a biocide: Will resistance become a problem? *Nat Biotech* **1998,** *16* (10), 888-888.
268. Chernousova, S.; Epple, M., Silver as Antibacterial Agent: Ion, Nanoparticle, and Metal. *Angewandte Chemie International Edition* **2013,** *52* (6), 1636-1653.
269. Silvestry-Rodriguez, N.; Sicairos-Ruelas, E. E.; Gerba, C. P.; Bright, K. R., Silver as a disinfectant. *Rev Environ Contam Toxicol* **2007,** *191*, 23-45.
270. Alexander, J. W., History of the medical use of silver. *Surgical infections* **2009,** *10* (3), 289-292.
271. Chaloupka, K.; Malam, Y.; Seifalian, A. M., Nanosilver as a new generation of nanoproduct in biomedical applications. *Trends in biotechnology* **2010,** *28* (11), 580-588.
272. Marambio-Jones, C.; Hoek, E., A review of the antibacterial effects of silver nanomaterials and potential implications for human health and the environment. *J. Nanopart. Res.* **2010,** *12* (5), 1531-1551.
273. Damm, C.; Münstedt, H., Kinetic aspects of the silver ion release from antimicrobial polyamide/silver nanocomposites. *Appl Phys A* **2008,** *91* (3), 479-486.
274. Morones, J. R.; Elechiguerra, J. L.; Camacho, A.; Holt, K.; Kouri, J. B.; Ramírez, J. T.; Yacaman, M. J., The bactericidal effect of silver nanoparticles. *Nanotechnology* **2005,** *16* (10), 2346-2353.
275. Hwang, E. T.; Lee, J. H.; Chae, Y. J.; Kim, Y. S.; Kim, B. C.; Sang, B.-I.; Gu, M. B., Analysis of the Toxic Mode of Action of Silver Nanoparticles Using Stress-Specific Bioluminescent Bacteria. *small* **2008,** *4* (6), 746-750.
276. Yang, H.-L.; Lin, J. C.-T.; Huang, C., Application of nanosilver surface modification to RO membrane and spacer for mitigating biofouling in seawater desalination. *Water Research* **2009,** *43* (15), 3777-3786.
277. Siddhartha, S.; Tanmay, B.; Arnab, R.; Gajendra, S.; Ramachandrarao, P.; Debabrata, D., Characterization of enhanced antibacterial effects of novel silver nanoparticles. *Nanotechnology* **2007,** *18* (22), 225103.
278. Jung, W. K.; Koo, H. C.; Kim, K. W.; Shin, S.; Kim, S. H.; Park, Y. H., Antibacterial activity and mechanism of action of the silver ion in Staphylococcus aureus and Escherichia coli. *Appl Environ Microbiol* **2008,** *74* (7), 2171-8.
279. Lok, C. N.; Ho, C. M.; Chen, R.; He, Q. Y.; Yu, W. Y.; Sun, H.; Tam, P. K.; Chiu, J. F.; Che, C. M., Proteomic analysis of the mode of antibacterial action of silver nanoparticles. *J Proteome Res* **2006,** *5* (4), 916-24.
280. Choi, O.; Deng, K. K.; Kim, N.-J.; Ross Jr, L.; Surampalli, R. Y.; Hu, Z., The inhibitory effects of silver nanoparticles, silver ions, and silver chloride colloids on microbial growth. *Water Research* **2008,** *42* (12), 3066-3074.
281. Murthy, P. K.; Murali Mohan, Y.; Varaprasad, K.; Sreedhar, B.; Mohana Raju, K., First successful design of semi-IPN hydrogel–silver nanocomposites: A facile approach for antibacterial application. *J. Colloid. Interf. Sci.* **2008,** *318* (2), 217-224.

> *Some people never go crazy. What truly horrible lives they must lead.*
> (C. Bukowski)

2 OBJECTIVES

The main aim of this PhD thesis is the **obtainment and study of new systems for dual-purpose wastewater treatment purposes *via* the development of polymer-metal nanocomposites (PMNCs) with biocide and/or catalytic activity**. To do so, several considerations have to be taken into account. First, as the final application dictates some of the main requirements for the NC final characteristics several properties such as the chemical stability, the MNPs type, and the ease of recovery, among others, were envisaged. Second, the synthesis procedure was considered in order to choose the more suited matrices for MNPs obtainment. Finally, the choice of the matrices included as well other needs, for instance, that the matrix type had to be stable, easy to obtain and, if possible, of low cost have also been considered. Having this in mind, and considering the discussion of **Chapter 1**, the major scientific and technical objectives of this PhD Thesis are:

1. **The obtainment of PMNCs in several matrices of interest by Intermatrix Synthesis.**
   The first and principal objective of the present work lies precisely in the obtainment of PMNCs in several polymeric matrices, such as films (able to be applied in membrane processes), foams (to be applied as water filters) and, as a preliminary test, textile fibers. Considering the afore-stated main requirements of the polymeric matrix (see Section1.4.2),

different approaches have been proposed; such are the obtainment of new ion-exchange films, the use of commercial ion-exchange films (i.e. Nafion 117) and the adequacy of non-ionogenic polymeric foams. Concretely, for the modification of non-ionogenic polymers, direct sulfonation is proposed as a suitable reaction allowing the obtaining of ion-exchange polymeric films by the simple phase inversion procedure. In fact, the specific objectives of such modification are the preparation of different films by changing some of the reaction parameters, the study of the effect of the content of polymer in the casting solutions in regards of the morphology of films, and the evaluation of the effect of membrane thickness.

Once the targeted polymeric matrices would be attained, the next objective is to synthesize and characterize PdNPs and AgNPs in the developed polymeric films and to compare the results with their commercial analogue (Nafion 117); to synthesize and characterize AgNPs in non-ionogenic polyurethane foams; and to evaluate the obtainment of AgNPs in textile fibers and the study of the effect of the glass transition temperature during the synthesis.

2. **The physico-chemical characterization of the parent matrices and of the obtained PMNCs and the correlation between properties and structure.**

   Since knowing their physico-chemical characteristics is essential in the development of new materials and applications, the characterization of all of the materials in this work is proposed as another main objective. Moreover, the study and possible correlation of the effect of the different physico-chemical properties of the parent matrices and nanocomposites should be assessed. In this sense, it is proposed to study, for each single polymer, the ion exchange properties, the morphology and the water uptake of the parent matrix and correlate it with the MNPs load, distribution and mean size.

3. **The application of the developed PMNCs in wastewater treatments.**

   Finally, the application of the PMNCs at lab-scale is proposed as the last but not least part of the study. On one hand, it is planed to evaluate the catalytic properties of the PMNCs developed in the catalytic reduction of *p*-nitrophenol to *p*-aminophenol by $NaBH_4$ (a reaction commonly used as a reference of catalytic effectivity). To do so, the study of the systems in both batch and in flow conditions is envisaged in order to assess the performance, the possibility of reuse and effect of the flow conditions in the catalytic activity of the developed materials.

   On the other hand, and only for some of those materials containing AgNPs (polymeric films and polyurethane foams) the additional objective of evaluating their biocidal effects and stability (in terms of Ag released to the media) would be undertaken.

During times of universal deceit,
telling the truth becomes a revolutionary act.
(G. Orwell)

3 RESULTS AND DISCUSSION

Taking into account the growing need for environmentally-friendly processes and products, high-effective treatments and reusable systems, this work is focused on the development of polymer-metal nanocomposites (PMNCs) with biocidal and/or catalytic activity. Concretely, it is mainly focused on the synthesis of silver and palladium nanoparticles (AgNPs and PdNPs, respectively) obtained by the Intermatrix Synthesis (IMS) technique in several polymeric matrices, such as films, foams and textile fibers. Although this synthetic methodology takes advantage of the ion exchange capacity of the polymeric matrix, as a novelty, during the development of this thesis it has been successfully applied to other counterfoils without functional groups (as it will be shown in this chapter).

In fact, during this chapter I will pay special attention to the obtainment, adequacy and characterization of the different studied polymeric matrices. Particularly, in the case of polymeric films the modification of polymers and the obtainment of an adequate morphology will be reported and fully explained. For polyurethane foams (PUFs), its chemical modification and adequacy will be also assessed in regards to the applicability of the IMS procedure. For textile fibers, the effect of the glass transition temperature of each polymer during the synthesis of metal nanoparticles (MNPs) will be evaluated.

Finally, the availability of the PMNCs here developed to be used as innovative dual-purpose water treatments will be evaluated by two methods:

(1) The catalytic reduction of nitroaromatic compounds in water, and

(2) The disinfection of aqueous media.

Moreover, and in regards to the final application, the leakage of MNPs from the matrix has also been evaluated.

Most of the results that I will present here have already been (or are going to be) published as journal articles or as chapters in books. In this sense, the publications that are part of the present thesis are listed below in chronological order of publication and are collected in Appendix A and Appendix B:

i. *Polymer-stabilized palladium nanoparticles for catalytic membranes: ad hoc polymer fabrication*.
   Nanoscale Research Letters (**2011**), 6, 406.
   B. Domènech, M. Muñoz, D.N. Muraviev, J. Macanás.

ii. *Catalytic membranes with palladium nanoparticles: From tailored polymer to catalytic applications*.
   Catalysis Today (**2012**), 193, 1, 158-164.
   B. Domènech, M. Muñoz, D.N. Muraviev, J. Macanás.

iii. *Nanocomposite Membranes with Pd and Ag Nanoparticles. A New Material for Catalytic Membranes Development*.
   Procedia Engineering (**2012**), 44, 1264-1267.
   B. Domènech, M. Muñoz, D.N. Muraviev, J. Macanás.

iv. *Bifunctional Polymer-Metal Nanocomposite Ion Exchange Materials*.
   Ion Exchange Technologies (**2012**), Ayben Kilislioğlu (Ed.), ISBN: 978-953-51-0836-8, InTech.
   B. Domènech, J. Bastos-Arrieta, A. Alonso, J. Macanás, M. Muñoz, D. N. Muraviev.

v. *Development of novel catalytically active polymer-metal-nanocomposites based on activated foams and textile fibers.*
   Nanoscale Research Letters (**2013**), 8, 238.
   B. Domènech, K. Ziegler, F. Carrillo, M. Muñoz, D.N. Muraviev, J. Macanás.

vi. *Polymer-Metal Nanocomposites Containing Dual-Function Metal Nanoparticles: Ion-Exchange Materials Modified With Catalytically-Active and Bactericide Silver Nanoparticles.*
   Solvent Extraction and Ion Exchange (**2013**), (*In press*)
   B. Domènech, M. Muñoz, D.N. Muraviev, N. Vigués, J. Mas, J. Macanás.

vii. *Nanocomposite materials for catalytic membranes development.*
Nanocomposites: Synthesis, Characterization and Applications (**2013**), Xiaoying Wang (Ed.), ISBN: 978-1-62948-227-9, Nova Science Publishers, Inc.
B. Domènech, M. Muñoz, D.N. Muraviev, J. Macanás.

viii. *Polymer-Silver Nanocomposites as Antibacterial materials*.
Volume 1: Microbial pathogens and strategies for combating them science, technology and education (**2013**), A. Méndez-Vilas (Ed.), ISBN Volume 1: 978-84-939843-9-7, FORMATEX Research Center.
B. Domènech, M. Muñoz, D.N. Muraviev, J. Macanás.

ix. *Uncommon patterns in Nafion films loaded with silver nanoparticles.*
Chemical Communications **(2014**), (*In press*)
B. Domènech, M. Muñoz, D.N. Muraviev, J. Macanás.

x. *Reusable polyurethane foams containing silver nanoparticles for dual-purpose water treatment*.
Polymers for advanced technologies. (*submitted*)
B. Domènech, K. Ziegler, M. Muñoz, D.N. Muraviev, N. Vigués, J. Mas, J. Macanás.

Besides, it is important to mention that some results concerning the obtainment of sulfonated polyethersulfone with Cardo group (SPES-C) porous films (and their characterization and further application as catalytic membrane reactors) have not yet been prepared for paper submission, because they have been recently obtained during a three-month stage in the *Laboratoire de Génie Chimique* (*Université Paul Sabatier*, *Centre National de la Recherche Scientifique*, Toulouse, France) under the supervision of Prof. J.-F. Lahitte and Prof. J.-C. Remigy. But due to the complementary aspect provided by this study in regards to the present work, their inclusion in this chapter has been considered essential.

Moreover, some studies regarding the sulfonation of polyphenylsulfone (PPSU) (Section 3.1.1.1) have also been included as a guideline for further research within our research group despite the odd results obtained.

Accordingly, during this chapter I will present the results organized in three main sections regarding the used polymeric matrices (section 3.1.), the synthesis and characterization of PdNPs and AgNPs (Section 3.2.) and the final applications of the Nanocomposites (NCs) obtained either as catalytic or biocidal materials (Section 3.3).

3.1 Synthesis, adequacy and characterization of the polymeric Matrices

As discussed in Chapter 1, many materials can be used as supports for the IMS.[1-3] In all cases, when using the IMS technique it is important to take into account both the polymer properties and the final application of the nanocomposite, since both dictate the requirements of the parent matrix (inside which the MNPs will be synthesized). Having this in mind, in this section the results regarding the obtainment of ion exchange polymeric films and the adequacy polymeric foams in order to then successfully apply the IMS methodology will be described and fully discussed. Precisely, all the polymers employed in this work are showed in **Figure 3.1**.

As it can be observed in **Figure 3.1**, in some cases, the original polymeric matrix does not contain any ion exchange groups (polyetehersulfone with cardo group, polyphenylsulfone, textile fibers and polyurethane foams (PUFs)). Hence, in those cases, a modification of the matrix before (for films and PUFs) or during (for textile fibers) the IMS was tested in order to successfully apply the ion exchange step involved in the MNPs synthetic procedure (see Section 1.5 of the present work).

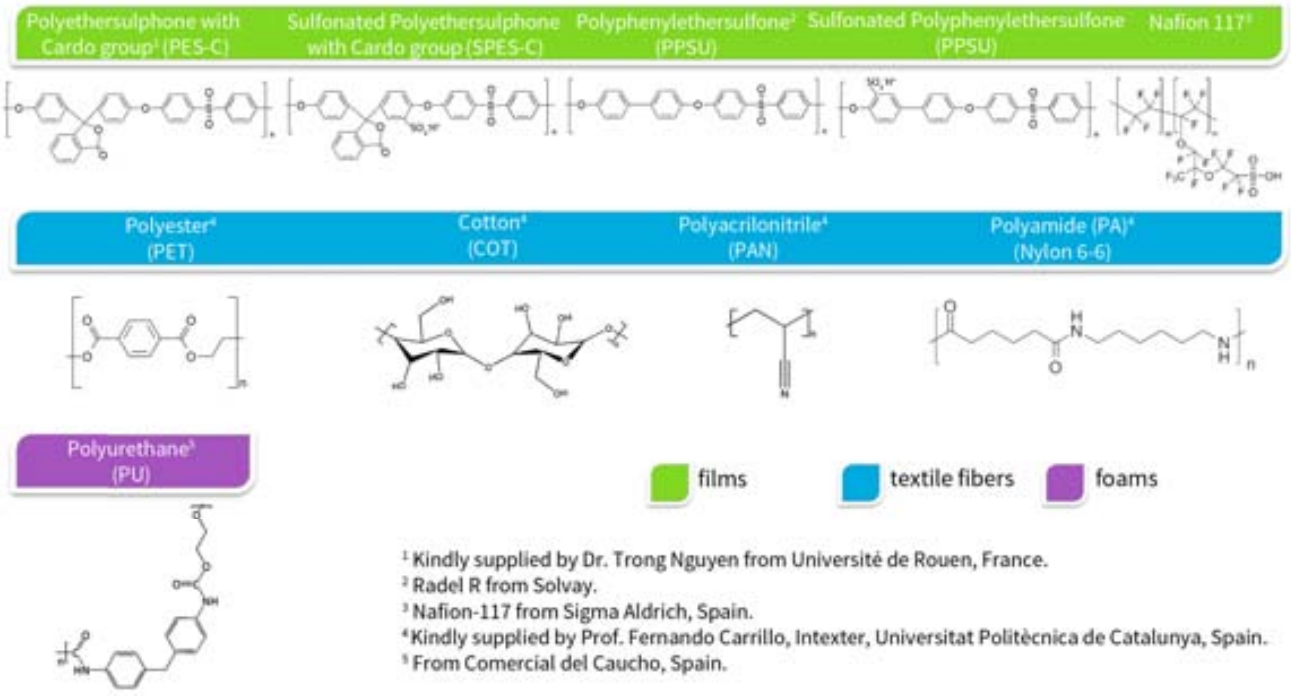

Figure 3.1. Polymeric matrices employed in this work.

In the case of polyphenylsulfone (PPSU) and polyethersulfone (PES-C) the followed strategy was to provide the polymers with ion exchange positions by their the modification before film formation. In this regard, although several modifications can be assessed, the post-sulfonation

was chosen, since it has been previously reported as a suitable and relatively simple methodology.[4-7]

In the case of Polyurethane foams (PUFs), the followed strategy has been the modification of the commercial matrix with chemical reagents while trying not to alter the morphology of the matrix itself, it is to say, maintaining the foam shape. Since polyurethane has functional groups able to be chemically attacked (such the carbamate group), their modification *via* acid or basic treatments seemed to be a good option in order to generate ion exchange positions able to bind metal ion precursors.

Finally, for textile fibers the followed strategy has been the study of the effect of the temperature during the MNPs synthesis. These results will be presented in Section 3.2.3 of this chapter.

Therefore, this section will be mainly focused on the obtainment and characterization of polymeric films (starting from the sulfonation of the polymers to the final morphology of the films obtained) and on the evaluation of the effect of different treatments to the chemical structure of the polyurethane foams. Further description of the polymers, of their modification and on their implications on the IMS procedure and on nanoparticle size and distribution will be discussed later in this chapter.

3.1.1. Synthesis and characterization of polymeric films

As mentioned in Chapter 1, the modification of poly(arylsulfones) with sulfonic groups is a well known strategy, widely used in polymers such as poly(etheretherketone)[8] or polysulfones.[5, 9] Since the presence of these groups is known to increase the hydrophilicity of the polymer (hindering in some cases the preparation of films with the required properties) the sulfonation procedure have to be fully studied and optimized for each particular polymer.

3.1.1.1. Sulfonated and non sulfonated PPSU

Polyphenylsulfone (PPSU) was chosen as a suitable polymer for the development of ion-exchange films by wet-phase inversion (see Section 1.5.1 of Chapter 1) due to its high hydrophobic character and high chemical stability (see Section 1.5.1.2 of Chapter 1). Regarding its modification, several post-sulfonations of PPSU can be found in literature. For example by using concentrated sulfuric acid at different temperatures and in different solvents,[10, 11] sulfur trioxide in dichloromethane (CH_2Cl_2),[12] trimethylsilylchlorosulfonate (Me_3SiSO_3Cl) in CH_2Cl_2,[12]

chlorosulfonic acid in CH_2Cl_2,oleum in chloroform ($CHCl_3$)[13] and sulfur trioxide-triethyl phosphate complex.[14]

During the development of this work two of the aforementioned sulfonation routes were applied under different conditions, as depicted in **Figure 3.2**.

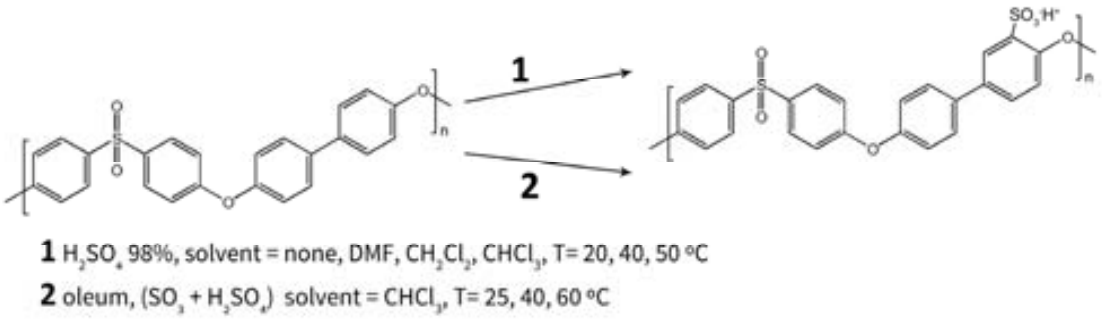

Figure 3.2. PPSU sulfonation routes.

The first route (an easy and inexpensive procedure) was carried out following a procedure similar to those published elsewhere.[6, 15, 16]
All the conditions and results of these sulfonations are summarized in **Table 3.1**.

In a typical run, the polymer powder was dried at 90 °C for 24 h prior to use. In a first attempt, PPSU was dissolved (20 g/L) in concentrated sulphuric acid and mixed at constant temperature (50 °C). After 120 h, the reaction medium was precipitated in an ice-water bath under strong stirring to obtain the SPPSU in its acid form. Despite what it was expected, the polymer did not precipitate in a solid form, what indicated a high sulfonation degree of the polymer, what made it soluble in an aqueous medium. For this reason, the procedure was repeated changing some of the conditions (bath temperature, ratio PPSU / H_2SO_4, time and solvent), in order to diminish the sulfonation degree. Nevertheless, none of the sulfonations procedures allowed recovering the polymer from the reaction media.
This is why in a last attempt, the heating of the reaction mixture was removed and the time decreased to less than 1 h. This procedure finally allowed recovering the final polymer from the reaction medium. But it was not sulfonated (as it was determined by its inability to further form MNPs by the IMS procedure).

Table 3.1. Summary of the PPSU sulfonations using route 1 depicted in **Figure 3.2**.

solvent	[PPSU] (g/L H_2SO_4)	time (h)	T (ºC)	RESULT
none	20	120	50	soluble
none	50	72	50	soluble
none	20	24	50	soluble
DMF	20	5	50	soluble
DMF	20	3	50	soluble
CH_2Cl_2	20	3	40	soluble
$CHCl_3$	20	0.75	20	Not sulfonated
$CHCl_3$	20	0.75	20	Not sulfonated

Since this first route did not seem to allow the obtainment of a suitably sulfonated polymer, the second route was tested, as it has been described in the literature as a more effective and controlled sulfonation. To do so, a procedure similar to those published elsewhere[13] was followed. A three necked round bottomed flask equipped with a mechanical stirrer was used to dissolve 4 g of oven-dried PPSU in 50 mL of chloroform ($CHCl_3$) at room temperature while stirring. A dropping funnel was used for drop-wise addition of a dispersion of 3 mL of 65% oleum and 30 mL of chloroform into the agitated flask over a period of 20 min. The reaction was then stirred at that temperature for 20 min and stopped by adding a sufficient quantity of methanol to cover the precipitate formed in the reaction flask. Finally the reaction medium was precipitated in an ice-water bath under strong stirring to obtain the SPPSU in its acid form. Once again, the polymer was not functionalized by this route, so harder conditions were applied (higher reaction time and higher temperature) giving the same unexpected result. The conditions and results of these two sulfonations are summarized in **Table 3.2**.

These odd results are, in fact, difficult to explain. What seems clear is that sulfonation routes are not as reproducible as needed and that the process is not so simple. In this sense, uncontrolled variables (such as air humidity, ambient temperature and so on) and the lack in a good control in the temperature could have played an important role in the reaction. In this sense, as none of the sulfonations seemed to work, films could not be prepared and this part of

the project could not be finished. Nevertheless, the inclusion of these results in the present work has been considered relevant enough because they could be profitable for further investigations within our research group.

Table 3.2. Summary of the PPSU sulfonations using route 2 depicted in **Figure 3.2**.

solvent	[PPSU] (g/mL oleum)	time (h)	T (ºC)	RESULT
$CHCl_3$	2	addition = 0.5 reaction = 0.25	25	Not sulfonated
$CHCl_3$	1.33	addition = 0.5 reaction = 0.5	40	Not sulfonated

3.1.1.2. Sulfonated and non sulfonated PES-C

During the development of this work, Polyethersulfone with Cardo group (PES-C) was chosen as a suitable matrix due to their highly hydrophobic character, conferred by the presence of a very hydrophobic group in its skeleton (a five-member lactone ring of a phenolphthalein moiety) (see **Figure 3.1**).[4, 17]

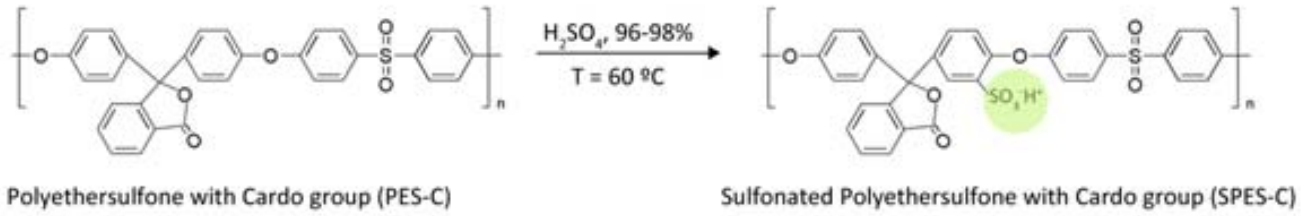

Figure 3.3. Sulfonation reaction of PES-C.

Sulfonation of PES-C was carried out following a procedure similar to those published elsewhere.[4, 5, 7] The polymer powder was dried at 70 ºC for 48 h prior to use. Then, it was dissolved (~10 % w/v) in concentrated sulphuric acid and mixed at constant temperature (60 ºC). After several hours (between 4 and 6 h, as specified in **Table 3.3**), the reaction medium was precipitated in an ice-water bath under strong stirring to obtain the SPES-C in its acid form. Afterward, it was neutralized (to reach pH ~ 7), filtered, washed with deionized water, and dried at 70 ºC (polymer in Na form).

Table 3.3. Characteristics of the three sulfonations of PES-C polymer.

LOT	Reaction time (h)*	Weight PES-C (g)	H_2SO_4	Volume H_2SO_4 (mL)	Ratio weight / volume (%)	Yield** (%)
SPES-C-1[18]	4.9	20.0100	98 %	185	10.8	81.4
SPES-C-2[19, 20]	6.3	20.0000	98 %	167	12.0	76.0
SPES-C-3***	3.6	30.0010	96 %	275	10.9	81.3

* Time measured between the first addition of polymer to the sulphuric acid and the last drop of the mixture precipitated in the coagulation bath.
** Yield was calculated versus the sulfonated polymer in its sodic form.
*** All the experiments involving this polymer were performed in the *Laboratoire de Génie Chimique,* Toulouse, France.

As it is shown in **Table 3.3**, during the development of this thesis three different reaction times were tested in order to obtain a different modification extent in the final polymer. *A priori*, modifications of the reaction time should lead to a different sulfonation of the final polymer, since the higher the time the polymer remains in the sulphuric acid, the higher the final sulfonation degree to be expected. In all the cases, the yield of the reaction was higher than 75 %. Conversely, it is known that an excess of sulfonation yields to a polymer highly hydrophilic (soluble in water)[21] which can not be recovered from the coagulation bath. Thus, although in this point further confirmation of the sulfonation extent is imperative, these high values of reaction performance seemed to testify for the suitability of the reaction.

In order to check the final **polymeric structure** and the degree of sulfonation after the reaction, FTIR-ATR and NMR techniques were applied to the polymer obtained. First, the FTIR-ATR[a] spectra of PES-C and SPES-C-1 shown in **Figure 3.4** were used to monitor the effectiveness of sulfonation procedure.

As it is clearly seen, a part from the CO_2 peak found at 2400 cm^{-1}, the spectra only differ by one single peak around 1030 cm^{-1} assigned to the symmetric stretching of S = O which appears due to the introduction of-SO_3H groups in the polymer chains. Moreover, these analyses also confirm that the remaining structure of the polymer was not degraded after the sulfonation.

[a] FTIR-ATR spectra were recorded with a IR Tensor 27, Bruker with Specac Golden Gate (ATR), from the *Servei d'Anàlisi Química* of UAB.

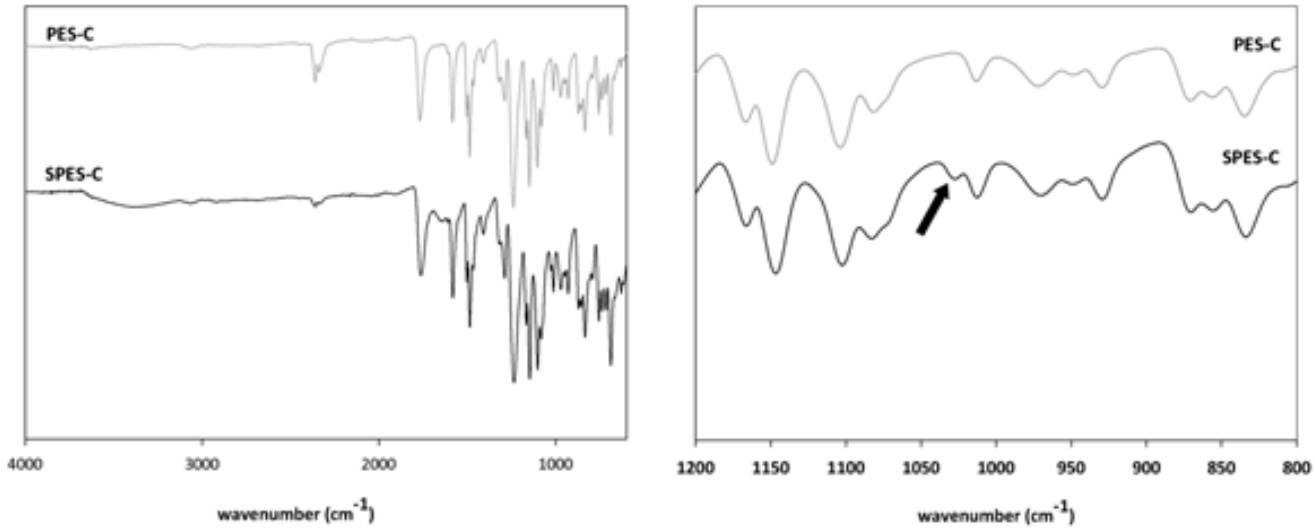

Figure 3.4. FTIR-ATR spectra of PES-C and SPES-C.

Nevertheless, a deeper look through the final polymeric structure is needed to elucidate the position where the $-SO_3H$ is introduced in the elemental unit of the polymeric structure. That is why ^{1}H-NMR and ^{13}C-NMR were recorded.

Figure 3.5 shows the ^{1}H-NMRs[a] of both polymers, PES-C and SPES-C (lot SPES-C-1) and their assigned bands. To assign the different peaks COSY spectra (coupling H) and NOESY (proximity of H), were also used. In the case of SPES-C (Na^+) the allocation of the bands was done based on reviewed literature.[15, 17] Comparing both spectra the appearance of a small peak at 7.0 ppm can be clearly seen, confirming the polymer sulfonation in the *orto* position with respect to the Cardo group. However, it is important to note that probably not all monomeric units of polymer would be sulfonated, nor in the same way, so it was not possible to determine the degree of sulfonation from these spectra.

Regarding the ^{13}C-NMR[b] spectrum of the SPES-C (lot SPES-C-1) in its sodium form (**Figure 3.6.**), the allocation of the bands was determined coinciding with the literature[17] and with the edited HSQC (CH coupling) .

[a] For performing the NMR spectra solutions of the different polymers were prepared in deuterated DMSO (1% by weight for samples for ^{13}C-NMR and 0.1% by weight for samples for ^{1}H-NMR) and were analysed with a DPX-360 AVANCE360 Bruker spectrometer from *Servei de Ressonància Magnètica Nuclear* of UAB.

[b] For performing the NMR spectra solutions of the different polymers were prepared in deuterated DMSO (1% by weight for samples for ^{13}C-NMR and 0.1% by weight for samples for ^{1}H-NMR) and were analysed with a DPX-360 AVANCE360 Bruker spectrometer from *Servei de Ressonància Magnètica Nuclear* of UAB.

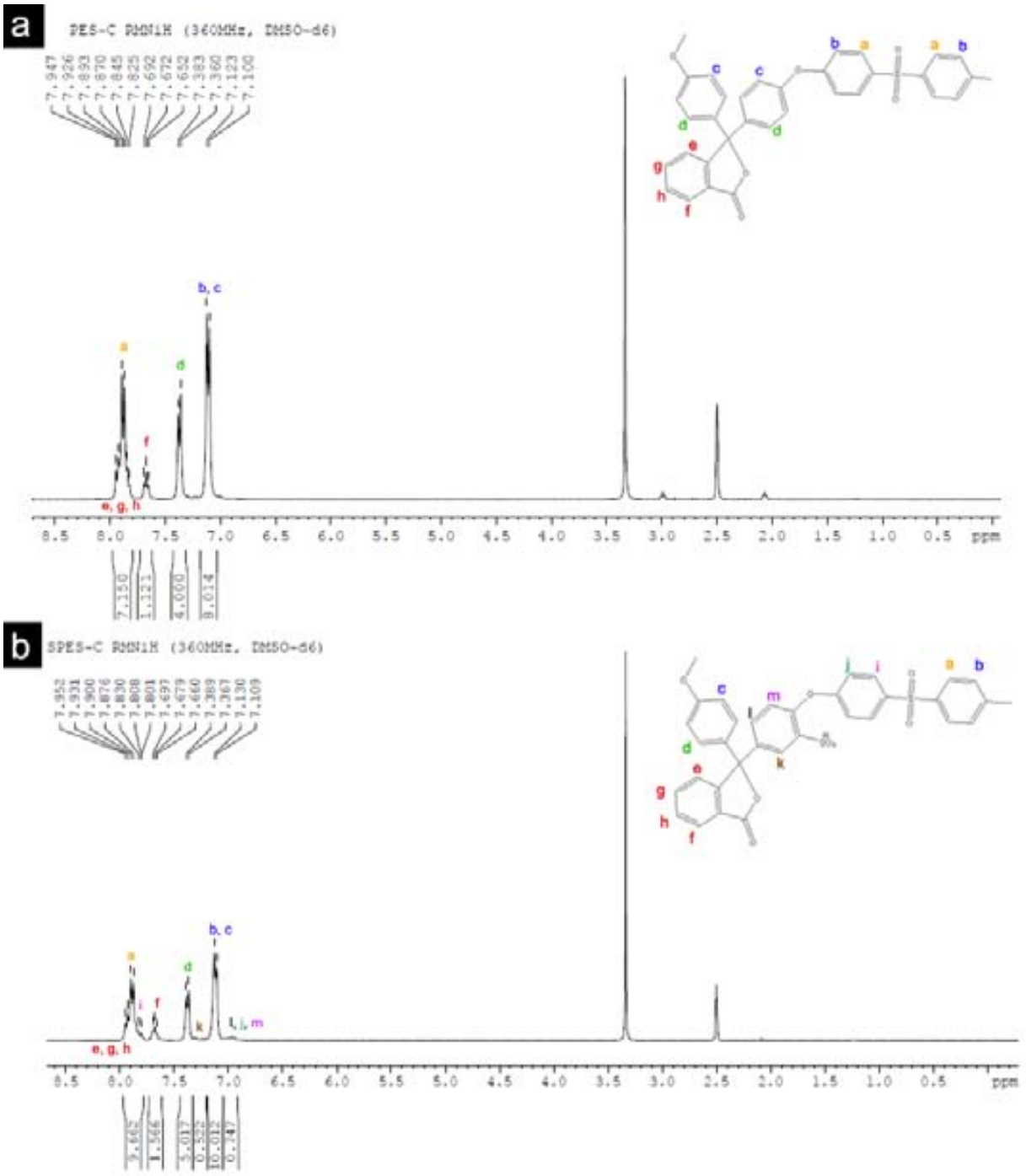

Figure 3.5. ^{1}H-NMR spectra with the corresponding peaks for (a) PES-C and (b) SPES-C (Na^{+}).

From all the spectra here showed it is possible to affirm that, since the peaks are preserved after sulfonation, the polymer was not substantially degraded. Moreover, taking into account that the spectra match the consulted literature, it is possible to conclude that the sulfonation process was satisfactory. In addition, it can be concluded that, due to the lack of variation between the spectra of PES-C and SPES-C, the degree of sulfonation achieved was low, so,

many of the PES-C chains were not sulfonated. Perhaps this is the reason why the integration had not been achieved according to the total number of H in the ^{1}H-NMR spectrum of SPES-C.

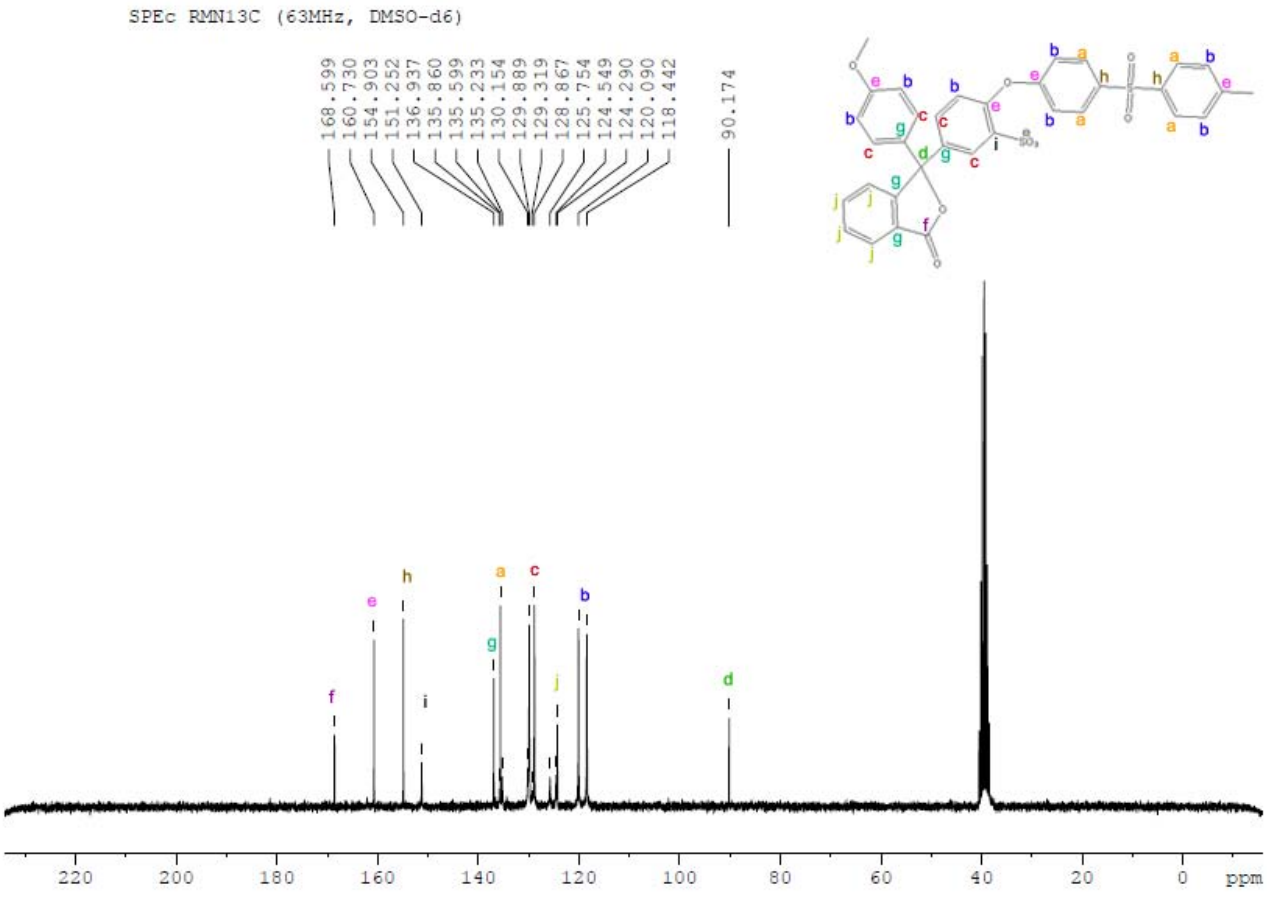

Figure 3.6. ^{13}C-NMR spectra with the corresponding peaks for SPES-C (Na^{+}).

Once the chemical structure of the sulfonated polymer was elucidated, and its stability in regards to such modification was confirmed, different types of **SPES-C films** were prepared by wet phase inversion methodology (see Section 1.5.1 of the present work).

In a typical procedure, the clean and dry polymer was dissolved in N-Methylpyrrolidone (NMP) to prepare a 20 or 25 % wt. (the so-called collodion). Once the collodion was homogeneous, it was casted in a glass with a calibrated casting knife. After casting, the glass was immersed in a water coagulation bath in order to proceed with the coagulation step of the phase inversion methodology by the addition of a non-solvent to the binary mixture. Films where subsequently stored in water to prevent their drying or any possible change in morphology (for instance, pore could collapse).

Table 3.4. Characteristics of each film preparation procedure for each lot of SPES-C.

Polymer LOT	% SPES-C	% PES-C	% NMP	Casting knife (μm)	Film nomenclature
SPES-C-1[18]	25	0	75	25	**SPES-C-1**
SPES-C-2[19, 20]	5	20	75	25	**BM**
SPES-C-3	25	0	75	250	**SPES-C-3-25a**
	25	0	75	300	**SPES-C-3-25b**
	20	0	80	250	**SPES-C-3-20a**
	20	0	80	300	**SPES-C-3-20b**

Different film types were obtained by this procedure from each lot of sulfonated polymer as specified in **Table 3.4.** In order to further compare them and to assert the reproducibility of the film obtainment, at least 4 different castings per film preparation procedure were prepared.

- From the lot SPES-C-1 only one type of films were prepared by dissolving a certain amount of polymer in NMP (enough to obtain a solution in 25% in total weight), and casting it with a casting knife of 25 μm of thickness.
- In the case of SPES-C-2, the binary mixture SPES-C-2 – NMP resulted to be more soluble in water than in the case of SPES-C-1, and films precipitated in a gel form that could not be recovered from the coagulation bath. Probably, as a result of increasing the reaction time during the sulfonation (from 4.9 to 6.3 h), a more sulfonated polymer was obtained, what resulted in an increase of its hydrophilicity, hinderingfilm preparation. For this reason, a certain amount of the non-sulfonated polymer (PES-C) (enough to obtain a ratio between polymers of PES-C:SPES-C of 4:1) was added to the collodion. By adding non-sulfonated polymer to the mixture, the hydrophilicity of the collodion decreased and allowed film formation in water. In order to facilitate the reading of the present work, from now on these films will be named as Blend Membranes (BMs), as they are made from a blend of polymers.
- Finally, in the case of SPES-C-3 a similar procedure as the one applied for SPES-C-1 was used, but this time the effect of the total amount of polymer and of the thickness of the casted film was evaluated, as specified in **Table 3.4**.

A visual inspection of the obtained films is shown in **Figure 3.7**. As observed, and although SPES-C-3 films seemed to posses the best mechanical strength (probably due to the increase of

the thickness), films prepared with SPES-C-1 and SPES-C-3 were quite similar showing a yellow tone and a rubbery aspect. Aversely, BMs (films prepared with the mixture SPES-C-2 and PES-C) appeared bright, white and more fragile (with an aspect between polystyrene and cellophane). Accordingly, it seemed clear that changes in the sulfonation parameters and in film preparation could have played a central role in the final film morphology, and, therefore, in the final applicability of the materials prepared.

Figure 3.7. Images of the membranes obtained with each lot of polymer.

The **characterization of the final morphology** of the films was expected to provide a wider image of the characteristics of the films obtained. On one hand, the characterization of the surface by **Scanning Electron Microscope** (SEM)[a] analysis provided information about the structure or defects present in the samples. On the other hand, from the SEM images of the cross section it was possible to determine the porosity of the films prepared.

Figure 3.8 shows the images obtained for SPES-C-1 films and as it can be seen, films precipitated in a dense form as observed from: (i) the absence of porosity, and (ii) the absence of significant surface defects. On the other hand, **Figure 3.9** shows the BMs SEM images where it is possible to observe: (i) the presence of porosity in the form of macrovoids, (ii) the existence of defects on the surface, and (iii) the presence of two clearly different surfaces.

[a] Images presented were obtained with Hitachi S-70 and Hitachi LTD microscopes from the *Servei de Microscòpia* from UAB .

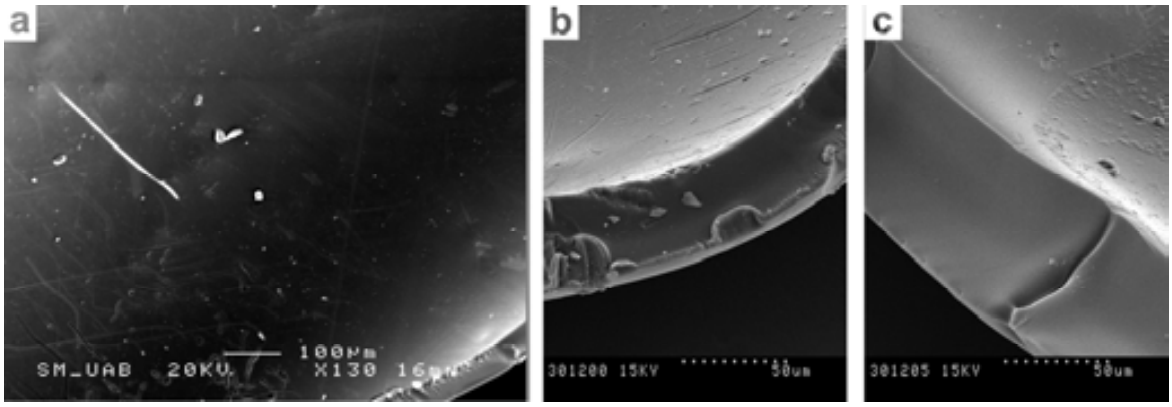

Figure 3.8. SEM images of SPES-C-1 films (a) surface, (b) cross-section, (c) cross-section at a higher magnification.

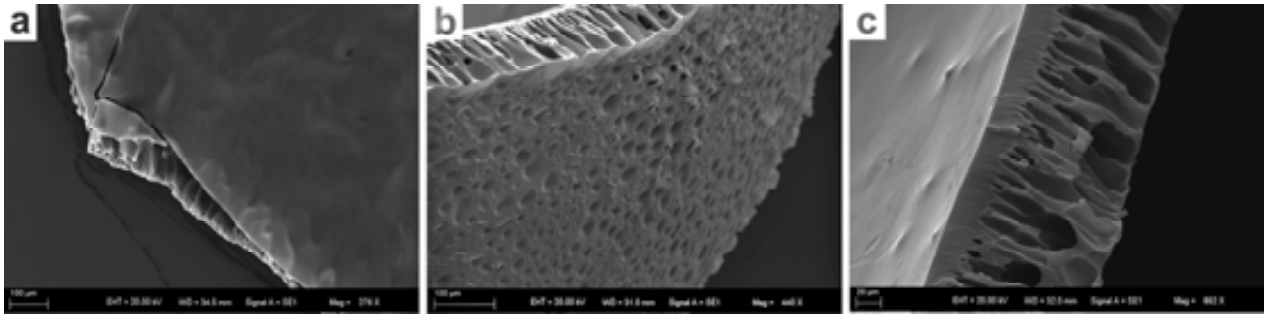

Figure 3.9. SEM images of BMs films (a) surface, (b) opposite surface, (c) BM cross-section.

The remarkable presence of two distinct parts in BMs (porous and dense) can be explained by the precipitation procedure, which was carried out onto a glass, thus, the polymer on the top of the glass (in direct contact with water) precipitates all at once when immersed in the coagulation bath, generating the so-called skin of the membrane; while for the polymer just above the glass it takes longer to come into full contact with water, allowing time for the water to generate the pores.[19, 20]

Comparing both types of films (SPES-C-1 and BMs), morphological differences may be explained by the difference in the hydrophilicity of the two types of casting solutions. When adding PES-C to the mixture, the hydrophobicity of the final collodion increases, although there are still some highly hydrophilic parts (due to the sulfonated polymer). Thus, pores are generated during the precipitation step because the different capacity to repulse water molecules of the same casted solution.[19] Therefore, it is possible to state that varying the composition of the casting solution films with different morphology can be obtained, what could lead to different final applications.

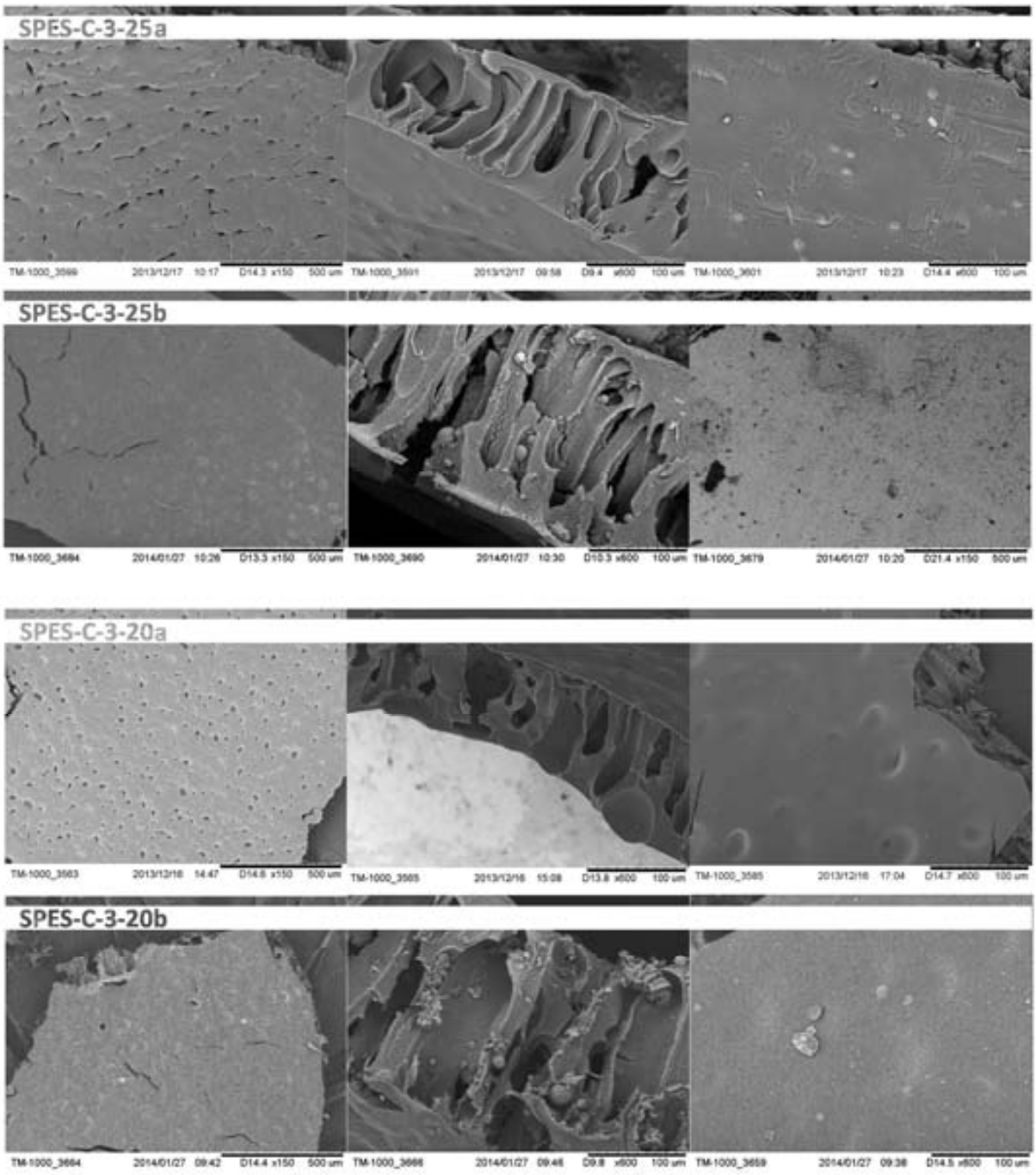

Figure 3.10. SEM images of SPES-C-3 films. From left to right (a) film surface, (b) cross-section, (c) film opposite surface.

Figure 3.10 shows the SEM[a] images obtained for SPES-C-3. For the four types of films prepared, some general features can be observed: (i) the presence of porosity in the form of macrovoids, (ii) the existence of defects on the surface, and (iii) the presence of two different surfaces.

[a] Images obtained with a Hitachi TM-1000 Tabletop Microscope from *Laboratire de Génie Chimique*, Université Paul Sabatier (Toulouse).

Since the polymer had been sulfonated during a shorter period of time (3.6 h), this morphology is quite unexpected. When decreasing the reaction time, less sulfonic groups should be able to be introduced in the polymer chains, thus less hydrophilic character should be expected in the resulting polymer, what would lead to a uniform precipitation all at once, in the form of a dense film (similar as the one observed for SPES-C-1 films). Instead, an asymmetric structure appeared what could, in fact, be the result of a highly sulfonated polymer.
Nevertheless, this hypothesis should be confirmed by a further characterization of the sulfonated polymer obtained.
Comparing SPES-C-3 films between them, it is noteworthy that thicker membranes (SPES-C-3-25b and SPES-C20b) seem to contain fewer holes in their surface that thinner ones, what could represent in last instance an increased mechanical strength and a decrease in the water permeability.

Nevertheless, it seems clear that each sulfonation has led to a different sulfonation extent and, therefore, to different films, with great differences in their morphology. Thus, it is reasonable to expect changes in their behaviour in terms of swelling properties (Matrix Water Uptake), and in their ion exchange properties. In order to determine the extent of these changes, **Matrix Water Uptake** (MWU, g H_2O/g wet film) was determined by a simple procedure: membrane samples stored in water were weighed (W_w), then dried in the oven for 48 h at 80 °C, and weighed again (W_d). MWU was calculated by using equation (3-1):

$$MWU = \frac{w_w - w_d}{w_w} \cdot 100 \qquad (3\text{-}1)$$

Where: W_w stands for the wet weight,
W_d is to the dry weight.

To calculate the MWU, three replicates per film and three films for the SPES-C-1 and SPES-C-3 (it is to say, nine samples per lot), and four for the BMs where analysed (twelve samples).

The final **Ion Exchange capacity** (IEC, equivalents of ion exchangeable positions *per* gram of dry membrane) of the membranes prepared was calculated by Indirect Acid – Base titration.[18] To calculate the IEC, three replicates per film and two films per lot were analysed (meaning 6 samples per lot). From the results obtained, the commonly used sulfonation degree (SD), which

corresponds to the molar ratio of sulfonated units to the total basic units, was calculated by equation (3-2):

$$SD = \frac{IEC \cdot M_{PES\text{-}C} \cdot 10^{-3}}{1 - IEC \cdot 102 \cdot 10^{-3}} \qquad (3\text{-}2)$$

Where: *IEC* is the ion exchange capacity obtained from the acid-base titration,

$M_{PES\text{-}C}$ was 532 g/mol,

102 (expressed in g/mol) is the molar mass variation (considering both the sulfonation and the conversion from H to Na form).

Table 3.5 presents the average values of the MWU, the SD and the IEC obtained for each type of film together with its uncertainty (95 %) and taking into account the dry weight of the film. In all of the cases, results showed no significant differences between samples of the same lot (proved by one-way analysis of variance, 95%), so a mean for film type could be given. For films made of SPES-C-3, since all films with the same amount of polymer were statistically equal (no matter the thickness), values presented are grouped regarding the amount of polymer in the collodion solution.

Table 3.5. IEC, SD and MWU values for SPES-C based films. Errors are expressed with the corresponding uncertainty (95 %).

Membrane type	IEC (meq/ g)	SD	MWU (%)
SPES-C-1	0.48 ± 0.12	0.27 ± 0.02	73.2 ± 0.5
BM	0.26 ± 0.02	0.13 ± 0.02	79.3 ± 0.4
SPES-C-3-25	2.07 ± 0.04	1.40 ± 0.03	77.6 ± 0.5
SPES-C-3-20	1.52 ± 0.06	0.95 ± 0.04	81.9 ± 0.6

From the MWU values, in general it is possible to state that films have a high capacity of water retention, meaning that the polymer is able to locate great amount of water between chains. This fact makes the films prepared really suitable for the Intermatrix Synthesis procedure, since all the reactions are performed in aqueous media, and both metallic ions and reducing agent should be able to properly diffuse into the matrix.

Taking a close look to the obtained values, small differences are observed. The most different value corresponds to films prepared with SPES-C-1 polymer (MWU of c.a. 73 %). In this case, it can be clearly seen that films could retain a lower content in water. This difference is possibly due to the change in porosity of the films prepared, as observed in SEM images showed before. Due to the absence of porosity in the films, the diffusion of water molecules into the interior of the polymer matrix is hindered, and consequently, the film is not able to swell as much as the others.

Regarding the IEC of the prepared films, the first thing that comes up is the high variability between lots. For films prepared with SPES-C-1 polymer and for BMs, values are below 0.5 meq/g, whereas for films prepared with SPES-C-3, values are above 1 meq/g.

Therefore, the hypothesis of the high sulfonation extent of SPES-C-3 polymer is confirmed. That is, in fact, an odd and unexpected result, since when decreasing the sulfonation reaction time, lower IEC should be obtained. Once again, the poor reproducibility of the reaction appears to be clear, since the lack of control of temperature during the synthesis and other non-controlled experimental variables (such as air humidity, external temperature and so on) could probably have played a crucial role.

Comparing SPES-C-1 films with BMs, values obtained for the IEC are not fully consistent. Films prepared with a 75% of the non-sulfonated polymer show half the IEC (0.26 meq/g) of films prepared only with sulfonated polymer (0.48 meq/g). In principle, a lower value of IEC for BMs should be expected. Due to the number of replicates and the low confidence interval found, an experimental error was discarded. It is noteworthy that, as stated before, the polymer used for BMs preparation (SPES-C-2) was highly sulfonated, what could probably lead to a higher IEC. Moreover, since BMs present pores in their structure, a higher number of ion exchangeable groups would be accessible. This fact means that during the Acid-Base titration, the exchange between H^+ and Na^+ species can be hindered in SPES-C-1 films due to their dense nature. Thus, the obtained IEC value for the films prepared should be considered just as indicative of the practical IEC.[19]

Comparing films obtained with SPES-C-3, it is possible to correlate the increase of amount of polymer in the collodion (20 or 25%) with the increase IEC: when decreasing the amount of polymer in the collodion, the ion exchange capacity diminishes in the same extent, what testifies for the reproducibility of the film preparation. Hence, by controlling the amount of

polymer in the casting mixture, it is possible to exert some control on the final ion exchange properties of the film.

Summing up, it is noteworthy that all these results prove that the sulfonation of PES-C can be achieved under mild reaction conditions corresponding to reasonable reaction temperature and time (at 60°C, in less than 6 h) just by using concentrated H_2SO_4. This procedure appears to be far simpler than, for instance, the polymer modification by the metalation route,[22] although it has been proved that the sulfonation extent appears to be irreproducible between different sulfonations, so the obtained samples should be fully characterized after preparation.

Moreover, it can also be concluded that from the different sulfonated polymers obtained, it is possible to prepare different kinds of films, with some tuneable physico-chemical properties (such as the matrix water uptake or their ion exchange capacity) since they are strongly affected by film morphology, which in turn, depends on the polymer nature and on the preparation method. Although from the first sulfonation (SPES-C-1) pure sulfonated polyethersulfone with Cardo group films resulted to be dense, what hinders their applicability in flux conditions, by changing the sulfonation conditions or adding non-sulfonated polymer to the collodion it was possible to provide certain porosity to the film.

So as to envisage the final application feasibility, it was possible to determine **membrane hydraulic permeability** of SPES-C-3 film. Hydraulic permeability (L_p) was tested in an Amicon® cell at 18 °C with pressures ranging from 0 to 1 bars. Measures of the flux where taken when increasing the pressure of the feed on the cell and also when decreasing it in order to determine a possible compaction. All fluxes were calculated with respect to the surface area of the film tested (with diameter of 40 mm). For all the cases, two different pieces of film were tested by measuring the flux trough the film (expressed in L/h·m^2) when variing the pressure applied. The values of permeability obtained were corrected to 20 °C by following equation (3-3):

$$L_p^{20} = \frac{L_p^T \cdot \mu_T}{\mu_{20}} = \frac{L_p^T}{e^{\left(6.435-\frac{1885}{T}\right)}} \qquad (3\text{-}3)$$

Where: L_p^{20} is the permeability at 20 ºC,

L_p^T is the permeability at certain temperature,

μ_{20} is the viscosity of the water at 20 ºC,

μ_T is the viscosity of the water at certain temperature,

T is the temperature.

Results of water permeability are shown in **Table 3.6**. As it can be observed form the uncertainty of the values, there is quite a variation between samples of the same membrane, but in all of the cases, the permeabilities found remained in the same order of magnitude. Comparing membranes with a thickness of ~200 μm with membranes with a thickness of ~300 μm, the permeability decreased when increasing the thickness; but it remained in the same order of magnitude.

Taking a closer look to the results, films with 25% of SPES-C were in the range of 10-100 L/h•m^2•bar, whereas films with 20 % of SPES-C showed a hydraulic permeability one order of magnitude higher (in the range of 1000 L/h•m^2•bar). This fact means that films with a lower content of polymer allow working at higher fluxes, maybe because they contain more holes, or maybe because their pores are bigger. On the other hand, when working with films with 25 % of polymer, the velocity at which the feed passes through the film is lower.

Table 3.6. Hydraulic permeability of SPES-C-3 films. Results are given with their corresponding uncertainty (95 %).

	Increasing P	Decreasing P
Membrane type	L_p^{20} (L/h•m^2•bar)	L_p^{20} (L/h•m^2•bar)
SPES-C-3-25a	284 ± 17	275 ± 20
SPES-C-3-25b	28 ± 1	29 ± 2
SPES-C-3-20a	3624 ± 200	4156 ± 300
SPES-C-3-20b	2543 ± 300	2565 ± 200

Measures of the flux where also taken when decreasing the pressure of the feed on the cell in order to determine a possible compaction of the film. Except in the case of SPES-C-20a, for all of the samples the permeability remained almost constant. Therefore it was possible to conclude that no compaction was observed, what seemed to state for the adequacy of the films prepared for flux applications. For SPES-C-20a, the hydraulic permeability obtained when decreasing the pressure resulted to be higher than when increasing the pressure. This can be explained because of a wider of the pores of the film occurred due to forcing a flux through the matrix.

Since these films have a lower content in polymer than any of the others, what make them physically less resistant this increase in the permeability is not unexpected.

Nevertheless, it is important to mention that when applying pressures above ~1.5 bar, films broke. It is to say, films prepared were not strong enough to force higher fluxes to pass through them. This fact will limit the operational conditions during their performance as catalytic membranes in flow conditions (see Section 3.3.1.1).

3.1.2. Nafion films

The use of existing functionalized polymers for the development of the PMNCs of the present work was also evaluated by taking advantage of commercial Nafion 117 films. As discussed during Chapter 1, Nafion is known for its cation exchange properties as well as for its thermal and chemical stability.[23] It has been extensively used for a variety of applications, [23] and it is still the benchmark material against which most results are compared.[23, 24]

Nafion 117 films were obtained from Sigma Aldrich (Spain), and parameters such as membrane thickness (~1.8 mm) and IEC (1.1 meq/g) were considered as predefined by the supplier.

In order to remove any possible impurity, commercial films were washed twice with bidistilled water in an ultrasonic bath for 30 min, then kept under stirring for 24 h in an aqueous oxidizing solution (10% of concentrated H_2SO_4 and 10% of commercial H_2O_2), and afterwards, washed again with boiling bidistilled water for several hours. Washed films were kept at 4 ºC.

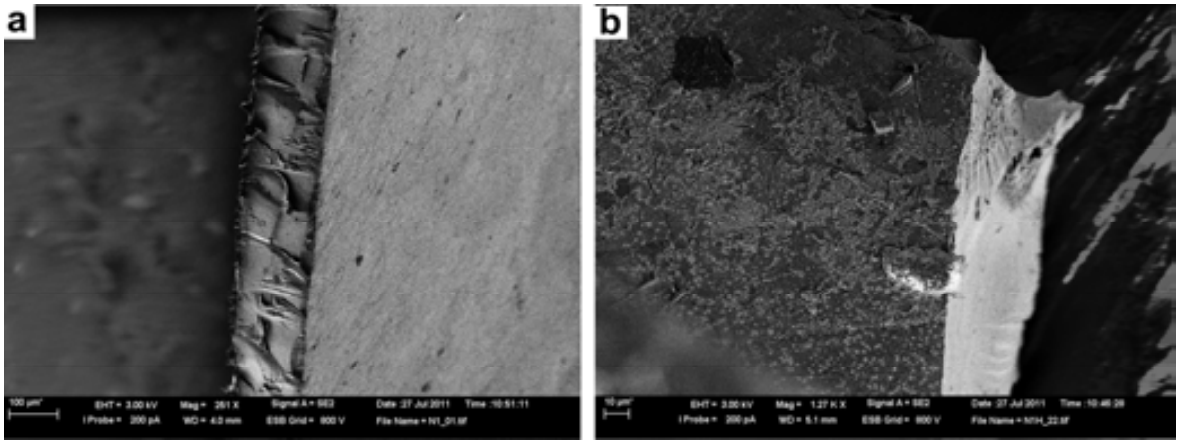

Figure 3.11. SEM images of Nafion sample (a) cross-section and (b) surface.

MWU of the washed samples was determined analogously as for SPES-C films (see Section 3.1.1.2), and it was found to be 40 ± 6 %. Compared to the values obtained for SPES-C films, this value appears to be a lower value, but it can be clearly explained due to the hydrophobic

skeleton of the Nafion and to its dense morphology, as observed from the SEM[a] images shown above.

3.1.3. Adequacy and characterization of polyurethane foams

During the development of this work, polyurethane foams (PUFs) received from *Comercial del Caucho,* Spain, and were treated as follows: either cubes (1 cm^3) or disks (3 cm diameter, 1 cm width, ca. 7 cm^3) were cut and squeezed in acetone for 1 h to open their pores and to remove any chemical compound used for sanitization, washed with deionized water and dried at room temperature. Similar procedures were found in literature.[25]

As it can be seen in **Figure 3.1** the polymeric structure of PUFs does not contain any ion exchange group, so some treatments were investigated in order to activate the material and provide it with ion exchangeable positions able to bind metal ions during the IMS procedure.[26] Thus, acid or basic treatments were chosen and applied after the afore-mentioned washing step, as showed in **Figure 3.12**.

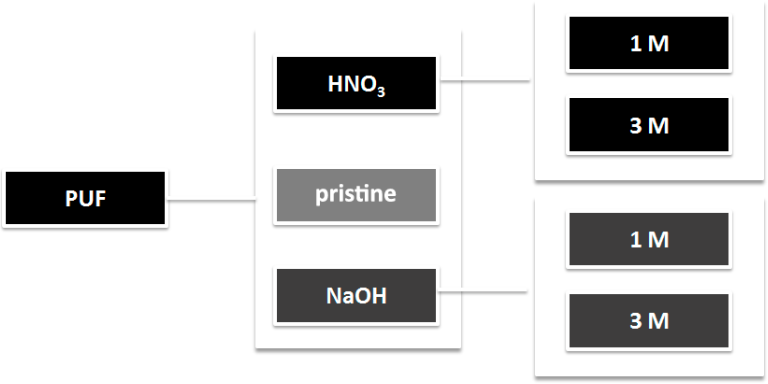

Figure 3.12. Treatments applied to PUFs: Acid, No treatment (pristine) and Basic.

In order to determine the possible effect of the treatments in the **chemical structure** of the PUFs, FTIR-ATR[b] spectra of all of the differently treated samples were recorded (**Figure 3.13**). The spectrum of PUF without treatment (Blank) showed the distinctive polyurethrane (PU) bands the broad peak at 3,270 cm^{-1} is characteristic of the υ(N-H), the peaks at 1,690 and 1,520 cm^{-1} are typical for υ(C=O) (urethane band) and δ(NH) with υ(CO-N) (amide II).[27]

[a] Images obtained with Zeiss Merlin microscopes from the *Servei de Microscòpia* from UAB.
[b] FTIR-ATR spectra were recorded with an IR Tensor 27, Bruker with Specac Golden Gate (ATR), from the *Servei d'Anàlisi Química* of UAB.

Surprisingly, no differences between all the spectra were observed, and therefore, no chemical modification was achieved after any treatment, what stated for the chemical stability of the matrix, but also for the inability to modify it by soft treatments.

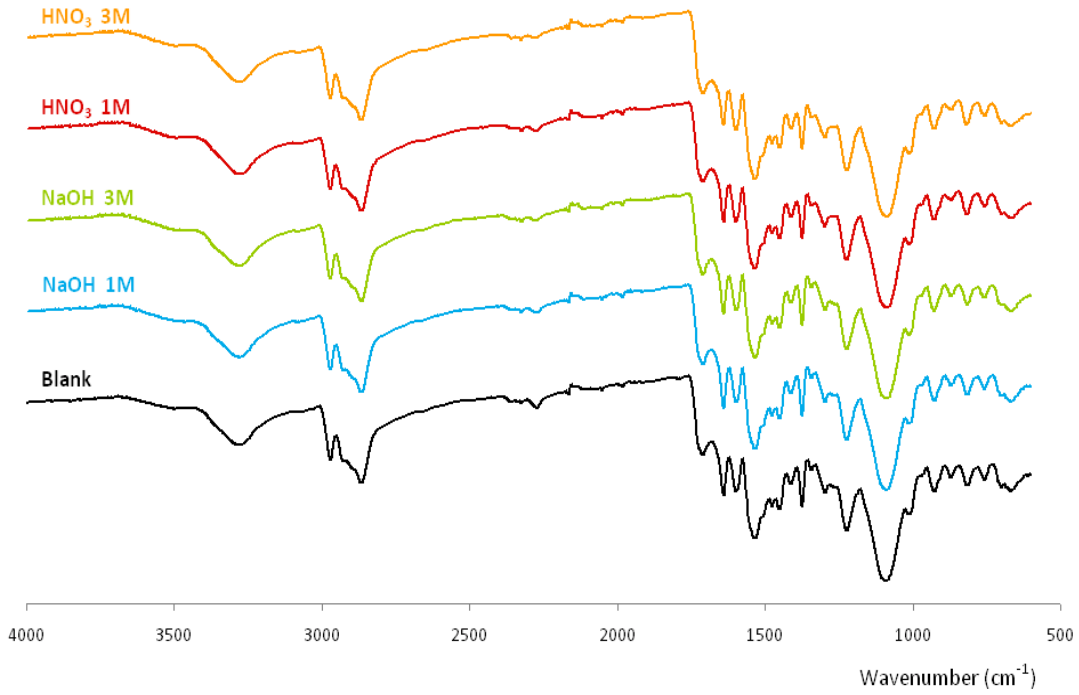

Figure 3.13. FTIR-ATR of PUFs after each treatment. The Blank corresponds to the clean PUF without any treatment.

Anyhow, even if no chemical modification of the polymeric structure was observed by FTIR-ATR, it was considered essential to calculate the **IEC** of the material. For determining the concentration of the functional groups able to bind or coordinate metal ions before and after the treatment of the matrix, two titration methods were applied:[26, 28]

1. For determining cation exchange groups, 1 cm^3 of PUF was immersed in 100 mL of NaOH 0.1 M and shaken at room temperature for 48 h, time enough to ensure a complete neutralization of the acidic groups. Then, an aliquot of 10 mL was titrated with standardized HCl 0.1 M (three replicates).
2. For determining anion exchange groups, a similar procedure was used, but by immersing the sample in 100 mL of HCl 0.1 M and using standardized NaOH 0.1 M to titrate the three aliquots of 10 mL.

The results obtained are presented in **Table 3.7**.

Table 3.7. IEC for PUFs.

Pretreatment	IEC (meq/ g)	
	Acid groups	Basic groups
Blank	0.65	0.62
NaOH 1 M	0.32	0.61
NaOH 3 M	0.57	0.61
HNO_3 1 M	0.66	0.71
HNO_3 3 M	0.61	0.57

Uncertainty in all of the cases was <1%.

As it can be seen, and in general terms, almost no differences between IEC values were observed. In addition, in most of the cases, IEC values were slightly lower than for the untreated foam. Just for the treatment using HNO_3 1M, and comparing the results obtained with the blank (without previous treatment), IEC values were slightly higher for both acidic and basic groups. But, this increase was so small that the IEC value can be considered constant. Note that there was an odd value for the acidic IEC of the NaOH 1 M treatment, which did not follow any clear or reasonable trend. Hence, this result was attributed to an experimental error. In any case, these results apparently indicated that the neither an acid nor basic treatment did not significantly affect the generation of ion exchange functional groups, confirming the FTIR-ATR results above mentioned.

Besides, the ability to absorb water (**MWU**) was calculated for the PUFs without treatment by following the procedure above-mentioned (equation 4-1), and it was found to be 96.3 ± 1.0 % (g H_2O/g dry PUF).

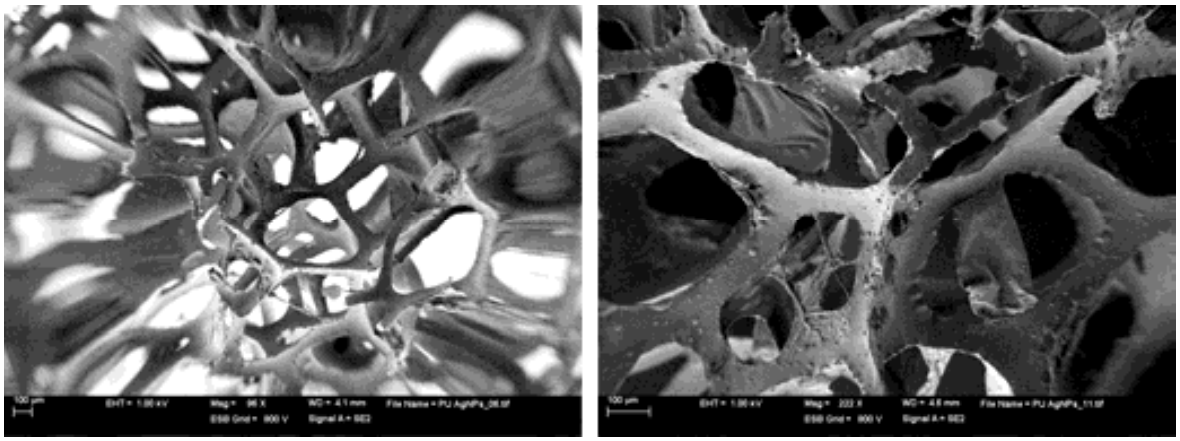

Figure 3.14. Typical SEM images of the physical structure of the PUFs.

This result indicates a good retention of water, close to 100% of the weight of the foam. This can be explained because of the internal structure of the foam, which can be illustrated by the **SEM**[a] images presented in **Figure 3.14.** The morphology of such matrices showed a large open porous structure, allowing and facilitating the entrance and therefore high retention of water.

3.1.4. Textile fibers

Typical textile fibers such as Polyester (PET, ISO 105-F04), Cotton (COT, ISO 105-F02), Polyamide (PA, Nylon 6.6, type 200, DuPont) and Polyacrylonitrile (PAN, type 75, DuPont) from woven fabrics and kindly supplied by Prof. Fernando Carrillo, from INTEXTER, *Universitat Politècnica de Catalunya* (UPC) were washed with bidistilled water before being used. Some photographies of pieces of 1 cm^2 of the fibers used during this work are presented in **Figure 3.15**.

Since the objective of this work was to evaluate the feasibility of applying the IMS to the neat fibers, no further modification or pre-treatments was carried out before use.

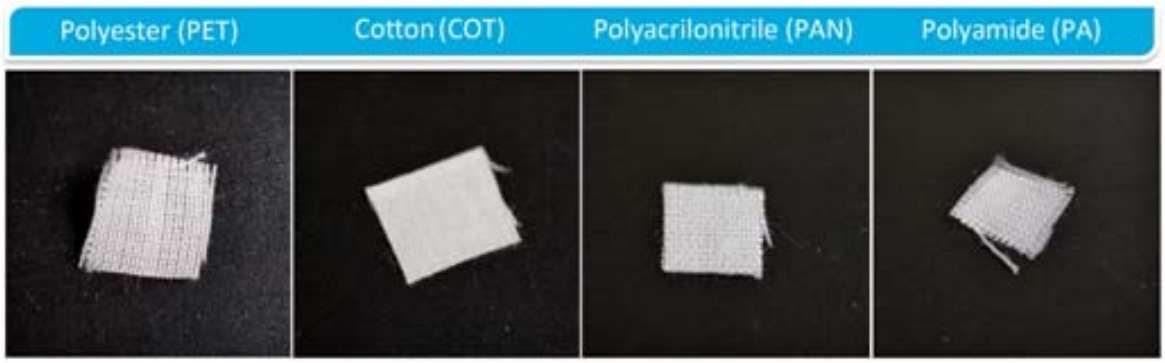

Figure 3.15. Images of the textile fibers used during this work.

Hence, as it has been showed in the present section, several polymeric matrices were used during the development of this work, some of them being expressly modified in order to successfully further apply the Intermatrix Synthesis, others used as received. The main implications of the specific characteristics of each matrix in the development of nanocomposites (NCs) containing metal nanoparticles (MNPs) will be discussed in next section.

[a] Images presented were obtained with Zeiss Merlin microscope from the *Servei de Microscòpia* from UAB.

3.2 Synthesis and characterization of Nanocomposites containing Polymer Stabilized Metal Nanoparticles

As mentioned in Chapter 1 the development of materials obtained by the inclusion of MNPs in polymeric matrices has drawn a great technical and scientific interest being nowadays widely applied in several fields such as catalysis of various organic reactions,[29, 30] water treatment,[31] and in fuel cells[32, 33] just to name a few. Nevertheless, for surface applications (catalysis, biocide) the contact between the reactive specie and the treated media is required and has to be as suitable as possible. In this regard, it is necessary to control the final distribution and sizes of the MNPs in the support in order to provide the best scenario for enhancing the performance of these materials. The control can be provided by both, the choice of an adequate matrix (point already developed in Section 3.1) and the synthetic procedure applied for the obtainment of MNPs. Up to now, the use of the Intermatrix Synthesis (see Section 1.4) has showed the possibility to obtain superficial homogenous and highly stabilized MNPs in several ion-exchange resin beads and in sulfonated polyetheretherketone films.[1, 34, 35] For this reason, this synthetic procedure seems to suit perfectly with the needs required for the nanocomposites of the present work.

In this thesis work, once each polymeric matrix was obtained, modified (if necessary) and fully characterized, the synthesis of MNPs was the next step to evaluate. Hence, the Intermatrix Synthesis (IMS) technique was applied (Section 1.4) to the different polymeric matrices (see **Figure 3.1**) in order to obtain Polymer Stabilized Metal Nanoparticles (PSMNPs) in each matrix. Two metals were used for the obtainment of MNPs: silver and palladium. Depending on the metal, the final application of each nanocomposite varies, as it will be explained in Section 3.3.

In this section a full description of synthetic methodology employed and the characterization of the different nanocomposites obtained will be given.

3.2.1. Synthesis and characterization of Nanocomposite polymeric films

3.2.1.1. Synthesis and characterization of PdNPs in polymeric films

To carry out the synthesis of PdNPs in polymeric films by the IMS technique, first, a piece of film measuring 1 cm^2 was equilibrated during 24 h in 25 mL of a solution of $[Pd(NH_3)_4]Cl_2$ so as to load the ionogenic groups of the polymer with the metal precursor. To assure an excess of Pd^{2+} in the loading solution and to force the ion exchange process in each matrix, the weight of each sample as well as its IEC were considered: either the IEC value from the Acid–Base titration for SPES-C-1 and BMs films (see **Table 3.5**) or the value offered by the commercial supplier for

Nafion (1.1 meq/g). Hence, SPES-C-1 and BMs were loaded with a 1 mM solution of $[Pd(NH_3)_4]Cl_2 \cdot H_2O$ and Nafion samples with 10 mM. For SPES-C-3 films the load was performed before knowing the real IEC of the films, and it was calculated considering IEC ≦ 1 meq/g, therefore they were loaded with a 0.3 mM solution of $[Pd(NH_3)_4]Cl_2 \cdot H_2O$ .This step is reported in equation (3-4). Afterwards, the immobilized ions underwent a chemical reduction by using a $NaBH_4$ 0.5 M solution. (see equation (3-5)).[18-20]

$$2R\text{-}SO_3^-Na^+ + [Pd(NH_3)_4]^{2+} \rightleftharpoons (R\text{-}SO_3^-)_2[Pd(NH_3)_4]^{2+} + 2\ Na^+ \quad (3\text{-}4)$$

$$(R\text{-}SO_3^-)_2[Pd(NH_3)_4]^{2+} + 2\ NaBH_4 + 6H_2O \rightarrow 2R\text{-}SO_3^-Na^+ + 7H_2 + 2B(OH)_3 + 4NH_3 + Pd^0 \quad (3\text{-}5)$$

Note from equation (3-5) that after the reduction of Pd^{II} to Pd^0 the sulfonic groups of the matrix are regenerated, making possible to proceed with a second load of the metal in the matrix. This means that, if desired, applying a second loading-reduction cycle could increase the final metal content. This last approach was, in fact, tested for BMs, in which due to the low IEC values obtained (see **Table 3.5**), low palladium content was expected, what could hinder the fnal performance of the films when applied as catalysts.

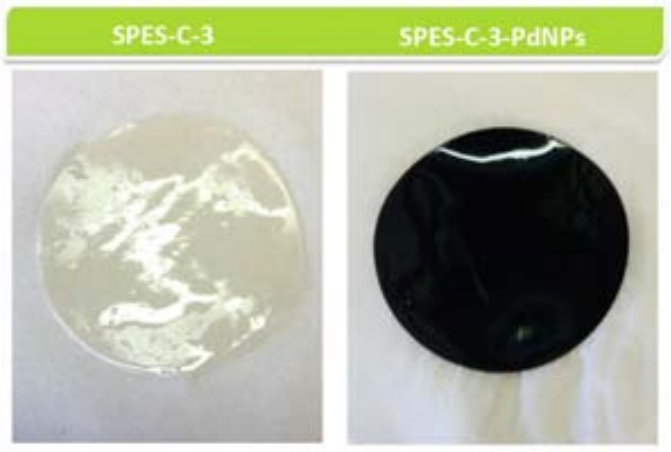

Figure 3.16. SPES-C film without (left) and with (right) PdNPs.

After applying IMS, a visual inspection confirmed the load of the PdNPs. As shown in **Figure 3.16** for SPEs-C-3 films, it could be observed a change in the colour of the membranes from white to black what stated for a successful loading of the membranes with Pd.

Therefore, SEM and TEM images and elemental analysis by ICP-AES and ICP-MS were carried out in order to afford a more quantitative picture of the polymer modification by inclusion of PdNPs.

In this sense, the **palladium content** in the nanocomposites was determined by analysing three replicates per film, from three different films of SPES-C-1 (by ICP-AES[a]) and for BMs (by ICP-MS[b]). It is to say, 9 different pieces of the nanocomposite-films were analysed for each matrix type. For commercial Nafion the Pd content was determined by analysing by ICP-MS two replicates per film from three different films (it is to say, 6 samples). Finally for SPES-C-3 nanocomposites, two replicates per film and two pieces of different films per film type (it is to say, 4 samples per film type) were analysed by ICP-MS. The results are shown in **Table 3.8**.

Table 3.8. Pd content and loading efficiency for the different prepared nanocomposites (uncertainty 95%). Pd content values of the films with the corresponding standard deviation.

matrix	Pd loads	Pd content (meq/g)	Loading efficiency
SPES-C-1	1	0.31 ± 0.02	70.5 ± 0.1
BM	1	0.08 ± 0.01	30.8 ± 0.1
BM	2	0.16 ± 0.01	61.5 ± 0.1
Nafion	1	0.53 ± 0.04	48.2 ± 0.1
SPES-C-3-20a	1	0.38 ± 0.01	25.0 ± 0.7
SPES-C-3-20b	1	0.36 ± 0.01	23.4 ± 0.6
SPES-C-3-25a	1	0.40 ± 0.01	19.2 ± 0.6
SPES-C-3-25b	1	0.37 ± 0.01	17.8 ± 0.5

Firstly, and similarly to other studied parameters, it is important to point out the low value of the measure deviations, what testified for the high homogeneity of nanocomposite batches, probably due to the IMS methodology as well as to the homogeneity of samples.

Secondly, comparing the loadings for SPES-C-1 membranes and BMs, in that case the ratio closely approached 4:1, which is the theoretical relation for the respective IECs having in mind that BMs included only a 25% of pure SPES-C-2 in their composition. Despite the fact that IEC values obtained by titration were not in agreement with this relation, from a practical point of view it has been demonstrated that the modification of the sulfonated polymer concentration directly affected the final Pd content. Hence, it seems reasonable to state that it is possible to control the content of the nanoparticles in the matrix by controlling the sulfonation degree of

[a] Spectrometer Iris Intrepid II XSP, Thermo Electron Co from the *Grup de Tècniques de Separació* of UAB was used. Prior to the analysis, it was necessary a digestion of the sample in *aqua regia* (HCl: HNO_3 3:1), dilution and filtration through 0.22 µm Millipore filter of the samples. The equipment calibration was performed using certified standard solutions (JT Baker). In all cases the measurement of the error was less than 2%.

[b] Spectrometer ICP-MS, Agilent 7500 was used. Prior to the analysis, it was necessary a digestion of the sample *aqua regia* (HCl: HNO_3 3:1), dilution and filtration through 0.22 µm Millipore filter of the samples. In all cases the measurement error was less than 2%. Analyses were carried out in *LEITAT Technological Center*, Terrassa, Spain.

the matrix. In my personal opinion, the chemical analysis of the loaded ions is more confident than the IEC determination, or, at least, more practical (from the point of view of the development of NC materials)

Besides, by applying a second loading cycle to BMs it was possible to exactly duplicate the metal content (from 0.08 to 0.16 meq/g) which in fact shows another possibility to tune the metal composition in this kind of polymer–metal nanocomposites. For Nafion nanocomposites the load was higher than for SPES-C-1 and BMs, as expected from the IEC value offered by the supplier (1.1 meq/g).

Finally, for SPES-C-3 films, loads of around 0.4 meq/g were obtained, what confirmed the higher IEC obtained for this polymer (in comparison with SPES-C-1 and SPES-C-2). Moreover, comparing SPES-C-3 films between them it is possible to state that the load depended on the % of polymer, and on the thickness (significant differences between values were proved by one-way analysis of variance, 95%). In this regard, two main conclusions can be drawn. On one hand, it is possible to state that that the higher the amount of polymer, and therefore ion exchange positions, the higher the load of PdNPs. On the other hand, the higher the thickness, the lower the load obtained per gram of dry film. This can be explained because by increasing the thickness of the film increases the pathway by which the ion must diffuse, so that it will takes longer to load the deeper areas of the film than the superficial ones. Besides, it is noteworthy that due to the DEE, penetration of the ions in the matrix could be, maybe not absolutely impeded but hindered.

Table 3.8 also shows the loading efficiency percentage, which corresponds to the ratio of the amount of metal loaded in each sample in relation to the IEC parameter. A value of 100% would indicate that all the available sulfonic groups in the membrane were charged with metal. Notice that two loading–reduction cycles on BMs only reached about 60% of the theoretical maximal loading, whereas about a 50% efficiency was obtained for Nafion in a single cycle. Thus, it is reasonable to take into account that the nature of the polymeric backbone does play a significant role in the loading–reduction cycles. For SPES-C-3 films, and in comparison to the other films, loading efficiencies found were extremely low (around 20). Since, based on the results and on the number of replicates done, it seems that there is no experimental error in the IEC values obtained by Acid-Base titration, a possible explanation for these low values may be the lowest concentration of the loading solution. As commented before, SPES-C-3 films were loaded with less concentrated solutions (0.3 mM). Therefore, there were fewer Pd^{2+}ions

available in order to shift the equilibrium (see equation (3-4)), thus, less Pd^{2+} ionscould be immobilized in the matrix.

Samples were also characterized by **TEM**[a] in order to evaluate NPs size and shape. In the case of SPES-C-1 and BMs, images of the inks prepared by dissolving a small amount of the nanocomposite in DMF were taken, as showed in **Figure 3.17**.

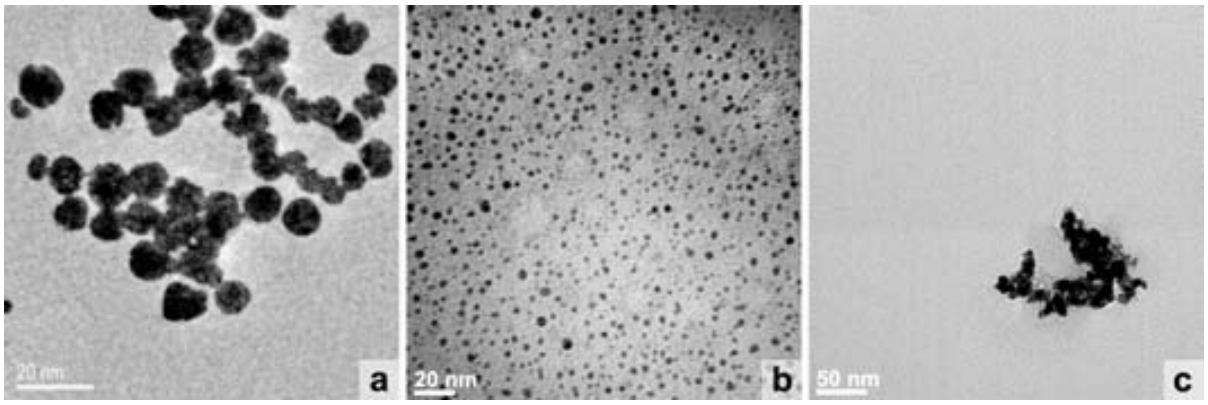

Figure 3.17. TEM images of inks prepared with (a) SPES-C-1 film with 1 load of PdNPs, (b) BM with 1 load of PdNPs, (c) BM with 2 loads of PdNPs.

In the case of Nafion, as it was not possible to dissolve the matrix in organic solvents in order to prepare the corresponding ink, it was necessary to cut thin slices of the membrane with an ultra-microtome[b]. This sample-preparation methodology allowed obtainment a real image of the PdNPs distribution in the matrix so it was also applied to SPES-C-3 films. TEM images of PdNPs in Nafion and SPES-C-3 films are presented in **Figure3.18** and in **Figure3.17**, respectively.

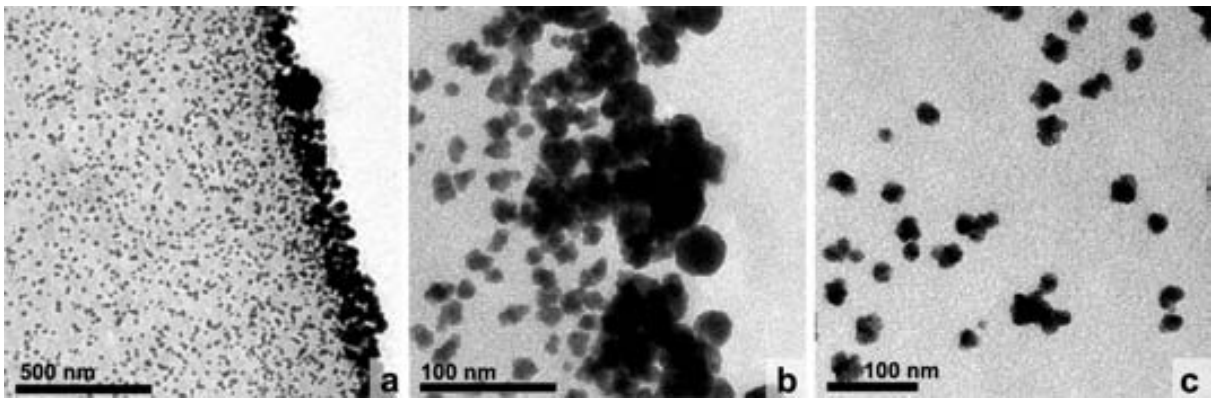

Figure 3.18. TEM images of Nafion-PdNPs (a) cross section, (b) surface PdNPs, (c) inner PdNPs.

[a] Images taken with JEOL JEM-2011, Jeol LTD and JEOL JEM-1400 microscopes from *Servei de Microscòpia* from UAB.
[b] Leica EM UC6 with a 35° diamond knife, Diatome.

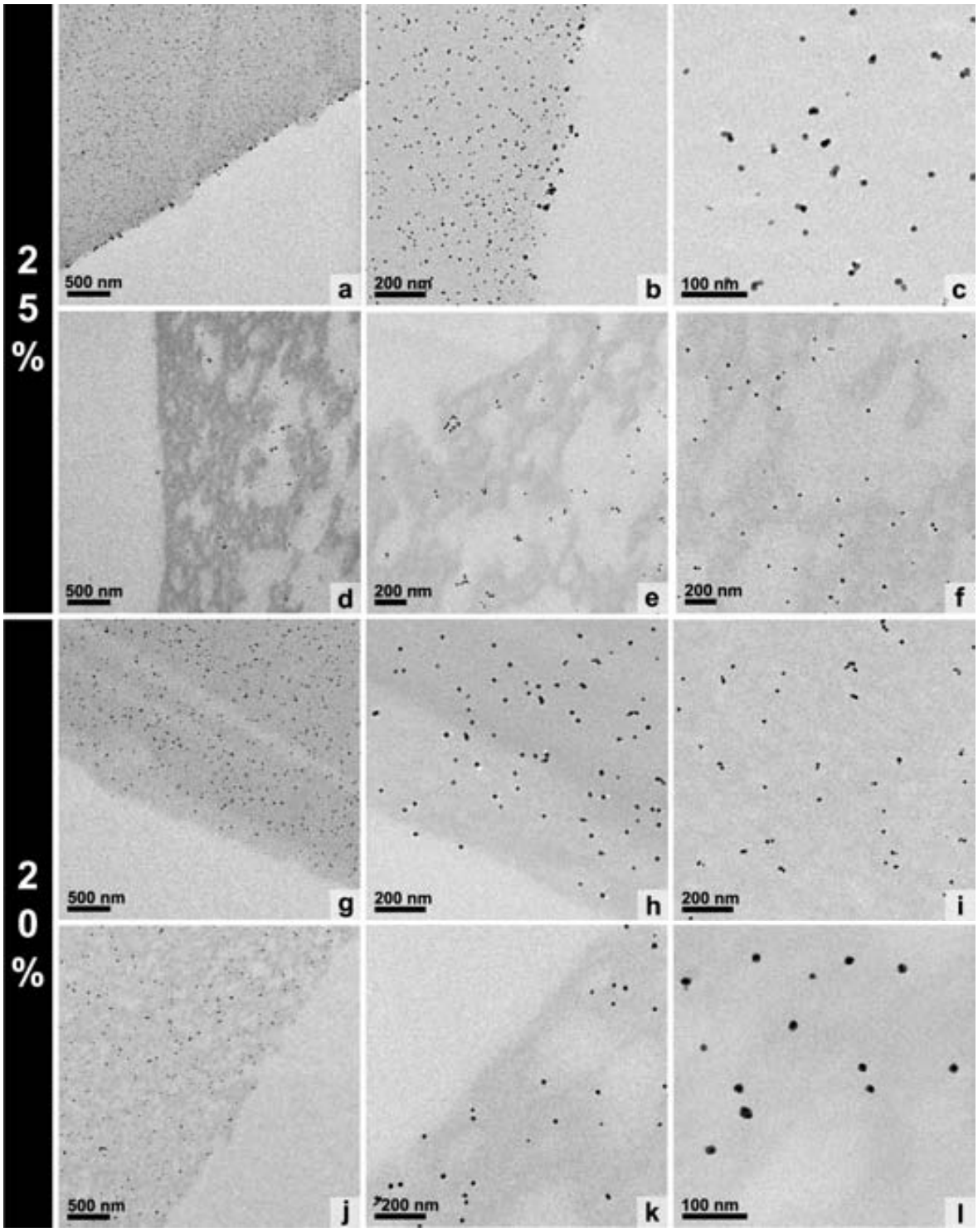

Figure 3.19. TEM images of the cross section of SPES-C-3-PdNPs (a-c) SPES-C-3-25-a PdNPs, (d-f) SPES-C-3-25-b PdNPs, (g-i) SPES-C-3-20-a PdNPs, (j-k) SPES-C-3-20-b PdNPs.

Let me discuss the difference found for the aforementioned samples. As it can be seen, in the case of SPES-C-1 and BMs with one load (**Figure 3.17** (a) and (b)), non-aggregated spherical nanoparticles were formed, so it was possible to calculate the corresponding size distribution histograms, whereas in the case of the membrane with two loads of Pd (**Figure 3.17** (c)),

aggregates were obtained, whose formation can be attributed either to the preparation procedure or due to the change in the mobility of the PdNPS in the second load, when the solid particles came together via random aggregation processes. The characteristic parameters of the obtained histograms are shown in **Table 3.9**.

Taking into account the cross-sectional images for Nafion films (**Figure 3.18**) aggregated nanoparticles close to the matrix edge and spherical ones all over the matrix and far from the edge were obtained. In this case this distribution can be considered as quite in agreement with the Donnan exclusion effect (DEE) (see Section 1.4.3). Since, although some penetration inside the matrix was observed, a great amount of PdNPs was located on the surface. This is, in fact, in agreement with the previous works of our group,[36, 37] in which either for fibers and resin beds, a superficial distribution of MNPs were always obtained, and suppose, in fact, a favourable for surface applications (catalytic and bactericidal). In this case, it was only possible to calculate the size distribution histogram for the inland PdNPs (see **Table 3.9**).

On the other hand, for SPES-C-3 films (**Figure 3.19**), PdNPs grew uniformly all over the matrix, thanks to film porosity, which allowed the entrance of the ions inside the matrix, leading to such NPs distribution. Furthermore, no agglomerates were found (not even in the surface), and it was possible to calculate the size distribution histograms (see **Table 3.9**).

Table 3.9. Characteristic parameters of MNPs size distribution histograms for Pd containing samples (1 metal loading).

matrix	$Ø_m$ (nm)	σ (nm)	N_p
SPES-C-1	**6.5**	0.1	222
BM	**3.3**	0.1	530
Nafion	**13.4**	0.1	311
SPES-C-3-20a	**13.5**	0.3	261
SPES-C-3-20b	**13.2**	0.3	212
SPES-C-3-25a	**9.0**	0.1	255
SPES-C-3-25b	**11.5**	0.2	233

$Ø_m$ = MNP most frequent diameter, σ = standard deviation, and N_p = counted NPs

Comparing BMs and SPES-C-1 PdNPs size distributions, PdNPs obtained in BMs had a smaller mean diameter than those obtained in SPES-C membranes and in Nafion (almost the half and a

fourth respectively). This can be explained by the hypothesis that the growth of MNP is influenced by the spatial distribution of the sulfonic groups available, as it is illustrated in **Figure 3.20**. In the case of SPES-C films, there are more available sulfonic groups (and closer to each other) than in BMs (since the film contains non-sulfonated polymer) so that during the formation and growth of PdNPs, the crystallization nuclei can interact to each other leading to the formation of larger PdNPs. It is to say, the Pd^{2+} ions from the sulfonic groups can interact, during the growing step and the PdNPs produced initially fuse together leading to larger PdNPs. Oppositely, when the sulfonic groups are further apart (the case of BM), the PdNPs can grow only from a limited source of Pd^{2+} ions, those which are close in the space. Accordingly, small PdNPs are formed farther apart.

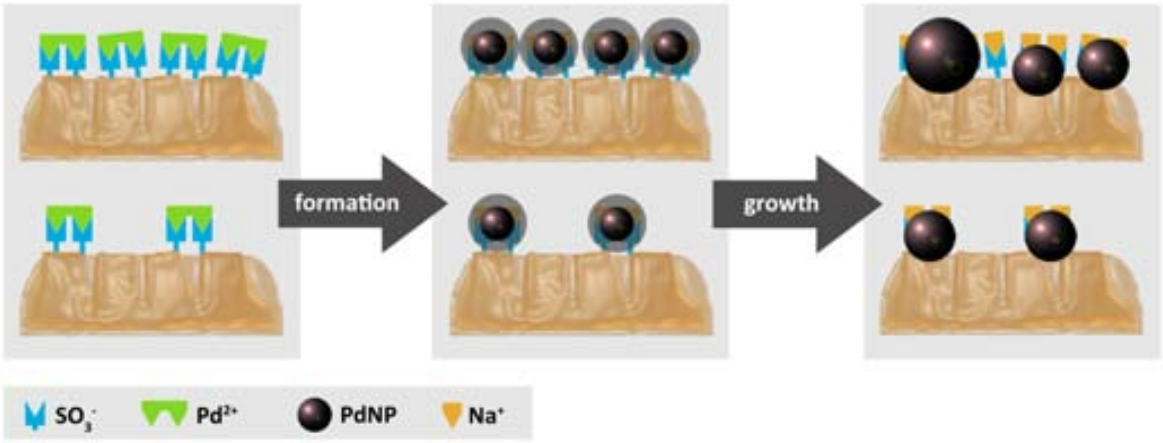

Figure 3.20. Scheme of how the distribution of the sulfonic groups in the membrane affects the size of the PdNPs obtained by the IMS technique.

This hypothesis also works when when comparing the diameters of PdNPs obtained in Nafion or SPES-C-3 films with the rest of the matrices. The higher the IEC, the higher the diameters obtained. Yet, when comparing between them the results obtained for PdNPs in SPES-C-3 films the hypothesis appears to be not fully consistent. Diameters of NPs obtained in films prepared with 25% of polymer (SPES-C-3-25) are smaller than the ones observed for NPs obtained in films with 20% of polymer (SPES-C-3-20), what contradicts the prediction. In these cases the matrix porosity might also have affected the PdNPs formation. Although porosity is a difficult to measure parameter, permeability data (**Table 3.6**) pointed that SPES-C-3-20 had a higher hydraulic permeability than SPES-C-25 films, therefore, probably a higher porosity. This means that aqueous solutions are able to easily penetrate in SPES-C-20 films than in SPES-C-3-25 films, making that much ions reach the sulfonic groups available.

Summing up and regarding the obtained results, it is possible to state that PdNPs-nanocomposites in polymeric films can be prepared. PdNPs can be easily obtained by IMS in the four different films (SPES-C dense films, BMs, Nafion and SPES-C porous films). Small non-aggregated PdNPs were obtained in all of the matrices, except in BMs with 2 loads. Moreover, it has been showed that the influence of the film morphology and of the IEC played a crucial role in PdNPs formation, allowing tuning the size and final distribution of the NPs in the matrix. In this sense, from the results obtained of the cross-section of NC-samples, PdNPs formation seems not only to be controlled by the Donnan Exclusion Effect (DEE) (see Section 1.4.3), since PdNPs were found all over the matrix.

3.2.1.2. Synthesis and characterization of AgNPs in polymeric films

Similarly to what was done for the obtainment of PdNPs, the synthesis of AgNPs in polymeric films was carried out by the IMS technique. However, this synthesis was limited to Nafion and SPES-C-1 and BMs films.

Regarding the experimental procedure, a piece of the polymeric film measuring 1 cm^2 was equilibrated during 24h in 25 mL of a solution of $AgNO_3$ so as to load the ionogenic groups of the polymer with the metal precursor. The concentration of $AgNO_3$ in the loading solutions was 5 fold the IEC of each matrix, in order to assure an excess of the metal ion during the loading step of the film. This step is reported in equation (3-6). Afterwards, immobilized ions underwent a chemical reduction by using a $NaBH_4$ 0.5 M solution, giving as a result the metal nanoparticles (see equation (3-7)).[38]

$$R\text{-}SO_3^-Na^+ + Ag^+ \rightleftharpoons (R\text{-}SO_3^-)Ag^+ + Na^+ \quad (3\text{-}6)$$

$$(R\text{-}SO_3^-)Ag^+ + NaBH_4 + 3H_2O \rightarrow R\text{-}SO_3^-Na^+ + 7/2H_2 + B(OH)_3 + Ag^0 \quad (3\text{-}7)$$

Again, a simple visual inspection of the samples allowed concluding that membranes contained metal due to their darkening after the IMS. Some images were observed, though. In the case of BMs, the film was grey, what seemed to indicate that, probably, the metal content would be also low, compared to the other matrices, which were black.

Thanks to TEM images and elemental analysis by ICP-MS a more quantitative picture of the polymer modification was drawn.

The **content of AgNPs** in the nanocomposites was determined by analysing two replicates per nanocomposite by ICP-MS[a]. The results are shown in **Table 3.10.**

Table 3.10. Ag content values of the membranes with the corresponding standard deviations.

matrix	Ag content (meq/g)
SPES-C-1	0.14 ± 0.03
BM	0.03 ± 0.01
Nafion	0.48 ± 0.01

As happened in the case of the PdNPs in membranes, Nafion membranes were able to load more metal than SPES-C-1 ones, and even more than in the case of BMs, due to the higher IEC of Nafion (*versus* the other films). Note that, when comparing the loading of metal obtained for Nafion and SPES-C-1 nanocomposites (**Table 3.11**) it is possible to affirm that it was almost equal, no matter the metal, even if this ratio is far beyond the IEC differences. This suggests that ion access to functional groups must be hindered for the case of SPES-C-1 films. What seems reasonable due to the dense morphology observed for SPES-C-1 films (**Figure 3.8**). On the other hand, comparing the load of each metal for Nafion and SPES-C-1 films separately, the ratio Pd:Ag was found to be always higher than 1 (concretely in μeq/cm^2, 1.4 ± 0.4 for SPES-C-1 and 1.2 ± 0.7 for Nafion). The different ion mobility and, particularly, the different charge of ions (Ag^+ and $[Pd(NH_3)_4]^{2+}$) might be the reasons for such differences.

Table 3.11. Comparison between Nafion and SPES-C membranes with loadings of silver and palladium. Errors are expressed with the corresponding standard deviation.

ratio	μeq/cm^2
Ag Nafion: SPES-C	19 ± 6
Pd Nafion: SPES-C	18 ± 3

Once the metal content in each nanocomposite film was elucidated, TEM[b] images of the corresponding cross-sections were obtained in order to evaluate the **size, the shape and the**

[a] Spectrometer ICP-MS, Agilent 7500 was used. Prior to the analysis, it was necessary a digestion of the sample in HNO_3, dilution and filtration through 0.22 μm Millipore filter of the samples. In all cases the measurement error was less than 2%. Analyses were carried out in *LEITAT Technological Center*, Terrassa, Spain.

[b] Images were taken with JEOL JEM-2011, Jeol LTD and JEOL JEM-1400 microscopes from the *Servei de Microscòpia* from UAB.

distribution of the AgNPs obtained (**Figure 3.21**). In all of the cases, small non-aggregated spherical AgNPs were found but some differences were observed between the nanocomposites depending on the film type. As it can be clearly seen in **Figure 3.21**, the occurrence of AgNPs in BMs was really low, what was in agreement with the ICP-MS results. SPES-C-1 and BMs samples showed mainly a superficial distribution of AgNPs together with little penetration through the film (~4.7 μm for SPES-C-1 and in the porous in BMs) (see **Figure 3.21** (a) and (b)). Again, such distribution near the surface of the stabilizing polymer is in agreement with the DEE of ion exchange matrices.

On the other hand, TEM images for Nafion nanocomposites portrayed plenty of AgNPs in the bulk, but in a particular arrangement. Focusing the attention on the image presented for Nafion-nanocomposites (**Figure3.21 (c)**), uncommon patterns in the form of aligned AgNPs were found. Due to the exceptional nature of these patterns, I have decided to dedicate a whole section of the present work to their explanation, in order facilitate the reading (Section 3.2.1.4).[39]

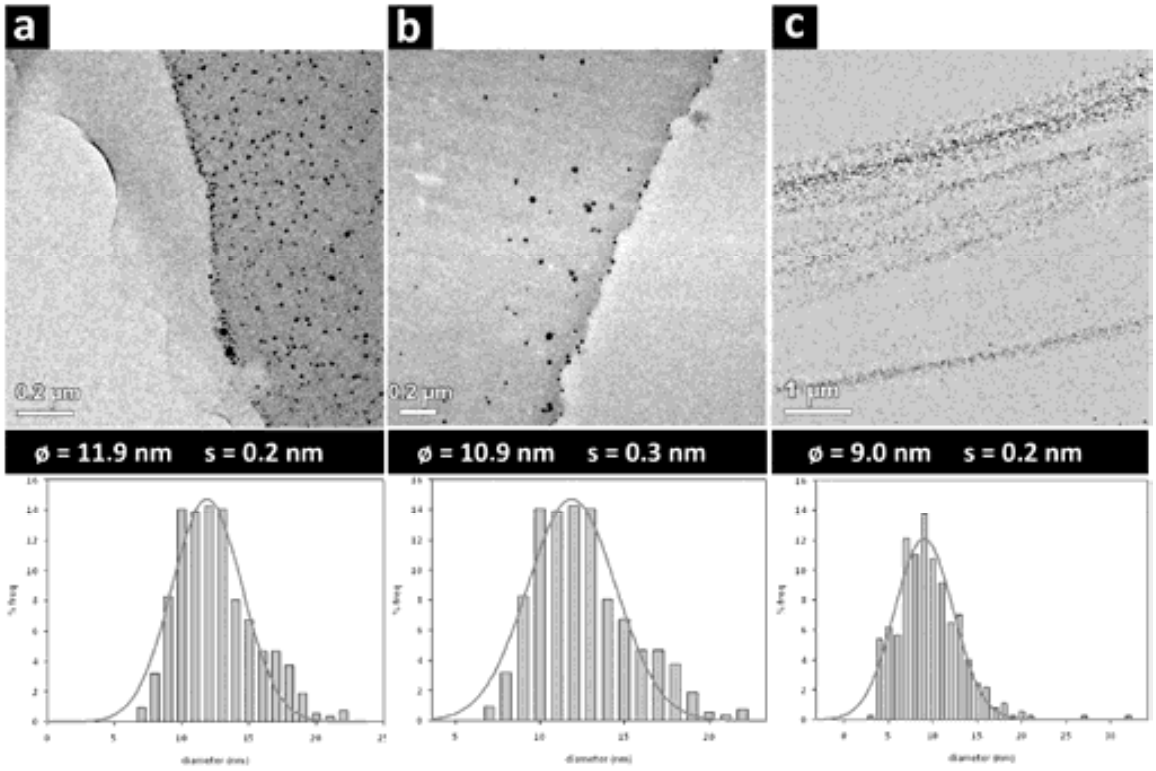

Figure 3.21. Typical HR-TEM images for the cross-section of AgNPs containing samples and the corresponding size distribution histograms for nanocomposites made of (a) SPES-C-1, (b) BM, (c) Nafion.

The results regarding the AgNPs size distribution are also shown in **Figure 3.21.** Results proved that it was possible to obtain small AgNPs, even smaller than those found previously by different approaches.[38, 40-45] This size distribution might provide a higher surface/volume ratio for surface phenomena, such as catalysis.

As in the case of the obtainment of PdNPs in polymeric films, it is possible to state that AgNPs-nanocomposites in polymeric films could also be prepared by IMS in the three different films (SPES-C dense films, BMs and Nafion). The loading of metal was found to be lower than for Pd-NCs, and the ratio Pd:Ag was found to be constant for Nafion and SPES-C-1, what seems to state for the reproducibility of the synthetic methodology employed and of the films used. Small non-aggregated AgNPs were obtained in all of the matrices and, in the case of Nafion films, uncommon patterns were obtained.

3.2.1.3. Stability of the AgNPs in polymeric films

The final objective of the synthesized nanocomposites is their use in water treatment (as biocides and catalysts), so the evaluation of the metal leakage to the media was considered to be an important parameter to fully characterize them. This feature was studied just for AgNPs containing NCs and samples were treated either by immersion in warm water or by the use of ultrasounds in aqueous media, as specified in **Table 3.12**. In all cases, samples of 1 cm^2 were deposited in a vessel with 10 mL of the appropriated solution and placed for different times in the corresponding bath: an ultrasonic cleaner (Branson 1200, 20W), a thermostatic bath (Grant W6, Grant Inst.) or an incubator (Aquatron Infors AG, shaker incubator). As ultrasounds can heat the solution, temperature variation in the ultrasonic bath was also monitored during the experiment. It is worth to note that BMs were discarded, due to the low content in AgNPs observed in BMs, these nanocomposites and to the lack in their practical use in the final applications.[38]

Table 3.12. Experimental conditions of the stability characterization.

Experiment	Sample	Temperature (ºC)	Solution composition	Duration (h)
Ultrasonic bath	SPES-C-1 /Nafion	20-40	Deionised water	2
Thermostatic bath	Nafion	37	Deionised water	135
Cultivation conditions	Nafion	37	$1 \cdot 10^6$ CFU *E.coli* (aq)	24

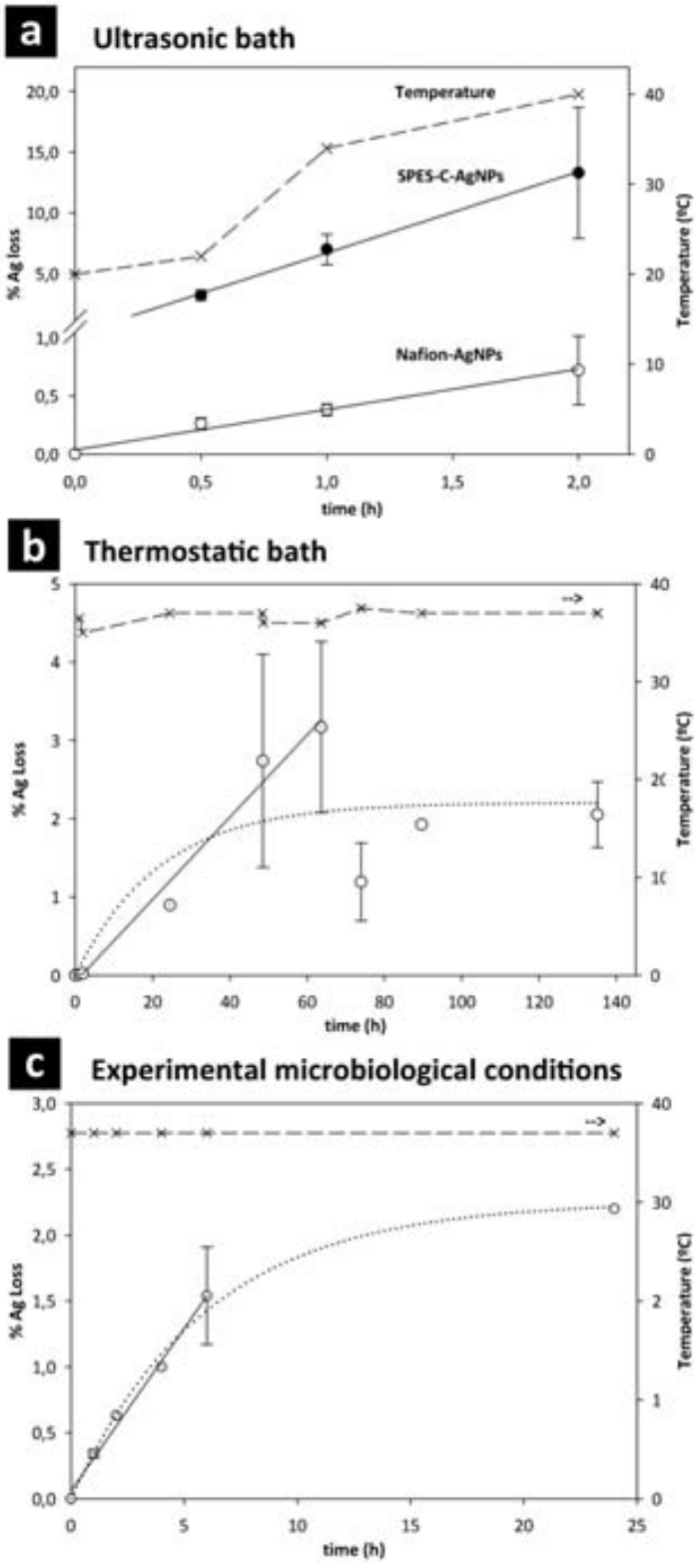

Figure 3.22. Ag release in different aging experiments: (a) Nafion and SPES-C-1 nanocomposites in ultrasounds bath, (b) Nafion nanocomposite in thermostatic bath at 37 ºC and (c) Nafion nanocomposite at cultivation conditions.

After each experiment, the silver content in both solutions ($n_{Ag,\ solution}$) and films ($n_{Ag,\ film}$) was analysed by ICP-MS (es previously described) so as to determine the total release percentage (*%R*). Note that film samples were digested as aforementioned. Typically, 2 replicates per time and sample were analysed. Equation (3-8) was used to calculate *% R:*

$$\%R = 100 \cdot \frac{n_{Ag,\ solution}}{\left(n_{Ag,\ solution} + n_{Ag,\ membrane}\right)} \quad (3\text{-}8)$$

Where:

$n_{Ag,\ solution}$ was the silver content in the solution, and $n_{Ag,\ film}$ was the silver content remaining in the film.

From the obtained results, it was possible to calculate the rate of loss (expressed in % Ag/h) for each nanocomposite after different aging conditions. Data are plotted in **Figure 3.22** and the initial slopes of the curves are summarized in **Table 3.13**. Some of the curves are only lineal for short times and then % AgNPs loss became almost constant, reaching a plateau as it has been reported by other authors.[46]

Taking a close look at the results, it appears that a higher NPs leakage was observed for ultrasonic treatment as one can expect *a priori* since this treatment promotes AgNPs vibration and at the same time it increases the solution temperature. It is particularly interesting to note that the loss was very linear with time under such conditions. It is also noteworthy that the loss rate was relatively high for SPES-C-1 nanocomposites (6.7 ± 0.2), what might be explained considering the superficial distribution of AgNPs obtained in SPES-C membranes, which are less stabilized by the polymeric matrix than inner nanoparticles obtained in Nafion.

SPES-C-1 results resulted to be, in fact, in agreement to that obtained by Cao *et al.* for similar membranes made of polyethersulfone/sulfonated polyethersulfone[46] but for a longer time: up to a 20% of silver release for 120 h in physiological saline solution and up to 5% in distilled water. Accordingly, the ultrasound treatment effectively acts as an accelerating aging treatment for films. Conversely, the rate of Ag loss for Nafion was much lower and, in light of these results, Nafion was chosen as a model matrix to evaluate the stability behaviour of the AgNPs under different experimental conditions. In the case of the thermostatic bath and cultivation conditions the silver loss was very low and a plateau can be observed in the plotted data (**Figure 3.22** (b) and (c)). This loss was never higher than the 5% after 135 h in the thermostatic bath even, considering the significant divergence of some of the replicates.

Table 3.13. Rate of AgNPs loss in the different treatments.

NC-film	rate of loss (%Ag/h)*		
	ultrasonic bath	thermostatic bath	cultivation conditions
SPES-C-1	6.7 ± 0.2	-	-
Nafion	0.4 ± 0.1	0.053 ± 0.004**	0.23 ± 0.01**

* Typical error values are expressed as slope standard deviation.
** Maximal loss at 2-3 %.

I would like to remark that experimental cultivation conditions were expected to be more aggressive since there is a direct contact with the microorganisms in the medium. As mentioned above, similar effect had been observed for silver release in physiological saline solution that was also 4-fold higher than in distillate water.[46]

Taking into account this low release rate for Nafion nanocomposites, the film is expected to be effective for a long time, conserving the bactericidal and catalytic properties of AgNPs.

3.2.1.4. Unexpected patterns in Nafion films

As mentioned before (Section 3.2.1.2), unexpectedly, the synthesis of AgNPs inside Nafion 117 was found to produce NPs organization, following a regular pattern in the form of aligned AgNPs. In order to evaluate such patterns and discern their formation, TEM[a] images of ultrathin slices of the samples were also obtained after applying the ultrasonic treatment described for the evaluation of the stability of the prepared nanocomposites (**Table 3.12**). Results are presented in **Figure 3.23**.[39]

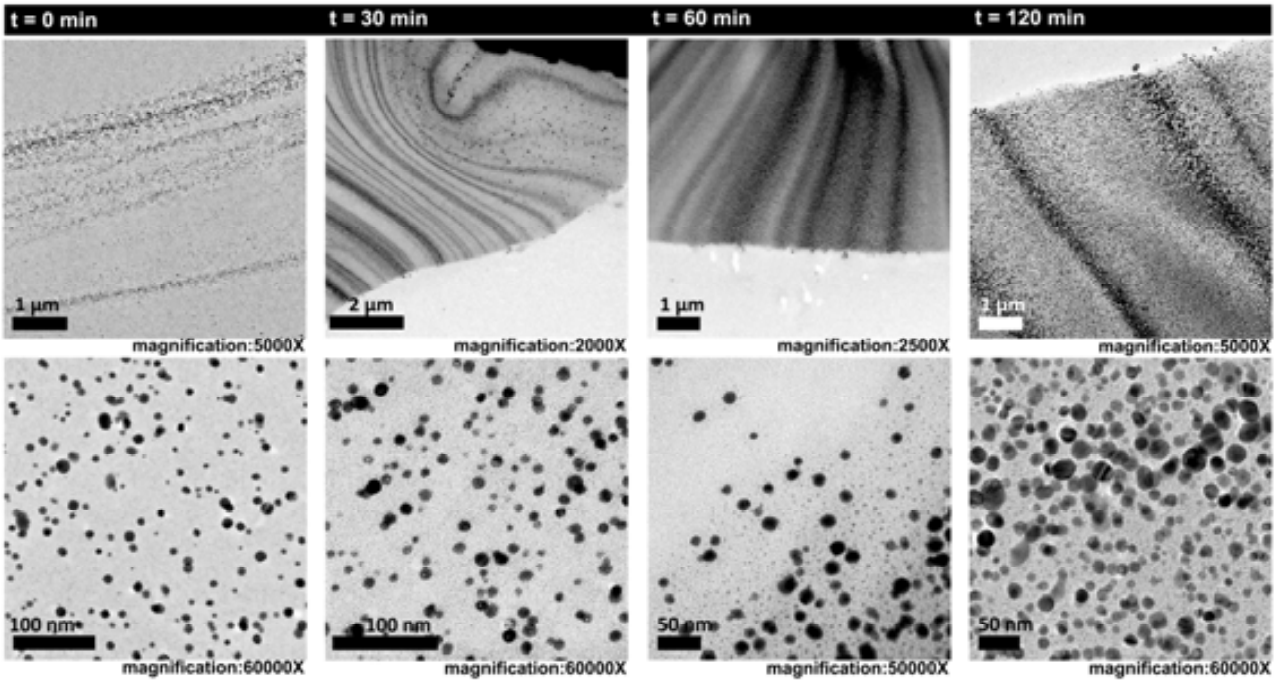

Figure 3.23. Patterns observed for TEM images of Nafion samples containing AgNPs treated by ultrasounds at different times.

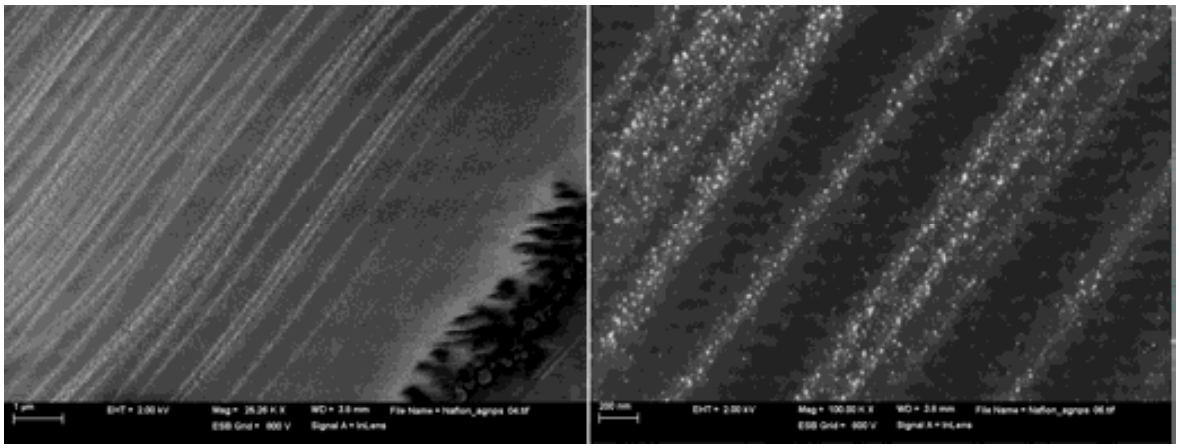

Figure 3.24. Patterns observed for FE-SEM images of Nafion samples containing AgNPs.

[a] Images taken with JEOL JEM-2011, Jeol LTD and JEOL JEM-1400 microscopes from *Servei de Microscòpia* from UAB.

As it can be clearly seen, the presence of adjacent but not aggregated AgNPs in almost parallels stripes was confirmed. In a further attempt to discard any artifact, different samples prepared by the same way were also analyzed by high-resolution SEM[a], giving the same result (**Figure 3.24**).

By a thorough analysis of TEM images it came clear that after the ultrasonic treatment, stripes got coarser and more separated. Moreover, by measuring up to 600 AgNPs per sample and fitting the obtained data to a 3 parameter Gaussian curve (eq. (1-22)) the mean diameter was found and it also came clear that the average diameter of AgNPs varied linearly with time (**Figure 3.25**).

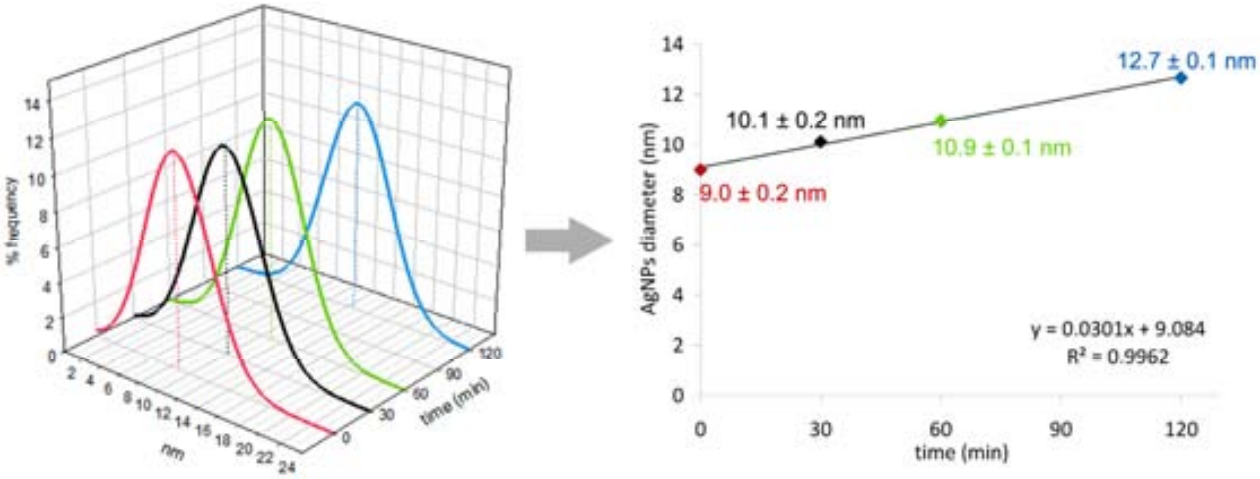

Figure 3.25. Evolution of the distribution of nanoparticles diameter due to the duration of the ultrasounds treatment.

Up to now, and to the best of my knowledge, this sort of images has never been published before for Nafion nanocomposites. Though, these patterns occurring during materials deposition have been demonstrated experimentally for more than a century ago and are known as Liesegang rings (LRs) or bands.[47, 48] LRs form when a soluble reactant (typically an ion) diffuses from the periphery of a medium (often a gel) uniformly filled with a second soluble reactant (typically another ion) to produce an insoluble substance. In this case, the gel medium would be the Nafion film loaded with Ag^+ whilst BH_4^- would be the reactant that diffuses through.

In order to discern why such nanostructures were obtained, several factors, most of them being before discussed in Chapter 1 were taken into account:

[a] Images obtained with Zeiss Merlin microscopes from the *Servei de Microscòpia* from UAB.

i) Nafion structure;
ii) membrane hydration and membrane pre-treatment;
iii) reducing agent diffusion;
iv) Ag^+ mobility and
v) ultrasound effect.

As mentioned during Chapter 1, there is quite a controversy regarding Nafion structure because there have been several models under debate (i.e. Fujimura's core-shell model, Dreyfus' local-order model, Haubold's sandwich-like model, Rubatat's rod-like model and Litt's lamellar model).[49-55] But the pioneering cluster-network model proposed by Gierke *et al.*[56] is frequently reported in the literature as the single one for rationalizing Nafion properties, and MNPs formation.[56] But when obtainment nanocomposites of embedded MNPs in Nafion, this model results to be oversimplified since, as commented during Chapter 1, very often the sizes of the formed NPs are much larger than the size of water clusters and NPs location is not always consistent with a simple template procedure (see **Table 1.1**).[57-61] Therefore, under the new insight offered by the results here presented, since the stripes are quite parallel instead of circular, the development of such LR-like bands would be more in agreement with Litt's and Kreuer's models[55] (see section 1.5.1.1) than with Gierke's model[56]. These models describe Nafion as a multilayer structure where the ionic domains are defined as hydrophilic micelle layers separated by thin hydrophobic PTFE-like lamellar crystallites.[24] Swelling on the microscopic level should occur by having water incorporating between the lamellae, thereby pushing them farther apart what is a convenient and simple explanation for the swelling behaviour of Nafion as well as for the observed bands.

Second, Moore and Martin[62] found that Nafion pre-treatment is crucial to define the polymer morphology since it rules the hydration state of the polymer and hydration controls the ions extent of penetration into the polymer. Water uptake measurements found in literature showed that boiling in water clearly enhanced the ability of Nafion to absorb water when compared to the vacuum dried and as-received samples. Therefore, the pretreatment applied to Nafion before AgNPs synthesis, could have enhanced the MWU (which was found to be 67 ± 6 g of water per 100 g of dry polymer).[19, 38, 39]

Third, it has been demonstrated by Pintauro *et al*.[63] that the afore-mentioned Donnan exclusion effect (DEE) explanation is also oversimplified. They realized that anion transport through Nafion (previously boiled in water for 30 min) occurred efficiently for NaCl and the movement of Cl^- was thought to occur by co-ions moving together as a neutral particle, thus reducing the

DEE. In this sense, Na^+ and BH_4^- could act similarly to Na^+ and Cl^-, entering together into a fully hydrated region of the Nafion, while single BH_4^- ions may experience limited transport. As a result, the feasibility of BH_4^- to reduce metal ion precursors deep past the film surface might be hindered and the nucleation and growth of NPs occurs near this surface. Conversely, Na^+ BH_4^- pairs can diffuse in a larger extent.[64] As well, it is important to consider that the decomposition of BH_4^- produces H_2 molecules, which can diffuse freely through the membrane providing an additional autocatalytic reduction of Ag^+ without any electrostatic repulsion.

Besides, it is worth to mention that Ag is one of the most attractive metal for nanomaterials synthesis and many different nanostructures have already been reported (i.e nanowires, nanoparticles, nanocubes).[65, 66] This myriad of nanostructures testifies for Ag ability to undergo shape transformations by dissolution-precipitation processes even though the mechanisms are not fully understood.[67, 68]The mobility of Ag^+ might play a crucial role since this cation possess a very high self-diffusion coefficient ($1.61x10^{-6}$ cm^2s^{-1}) in Nafion 117,[69] which provides it with a higher mobility when compared with other cations (i.e. Na^+, K^+, Ca^{2+}). Then, it is not surprising that Ag^+ ions are often associated with the formation of LR as their mobility aids in generating alternate regions of high and low concentration of the solid phase.

Finally, it is well-known that ultrasounds offer a very attractive and fast method for the synthesis of metal NPs. Combining ultrasounds with classical Ostwald ripening[70, 71] (see Section 1.3.2.1) it is feasible that bigger nanocrystals grow at the expense of smaller ones that get dissolved, so, the growth of stripes can be a result of and induced dissolution-precipitation process.

It is worth mention that, the AgNPs average diameter found for the original samples (without being treated by ultrasounds) was ~9.0 nm which is in close agreement with the water cavity size for a Nafion membrane extrapolated from data plotted in reference,[58] considering the content of water of 67 ± 6 g of water per 100 g of dry polymer.[72, 73]

As a conclusion it is possible to state that the simple concept of synthesizing NPs by using Nafion's cavities ends up to be a much complex scenario that can give rise to uncommon patterned nanostructures as those shown here. But, even if the observed patterns have never been reported before for Nafion nanocomposites, their existence is in agreement with the general knowledge regarding reaction-diffusion mechanisms and reinforces the idea of hydrophilic-hydrophobic lamellar domains in Nafion. Accordingly, the embedment of AgNPs can be regarded as a sort of nanometric staining agent because the incorporation of NPs in the matrix can reveal the true morphology of the ionic channels of the film.

3.2.2. Synthesis and characterization of Nanocomposite Polyurethane foams

As it has been said before, polyurethanes are a broad class of materials with different properties employed in a wide range of applications,[74] representing PUFs ca. 80 % of the total polyurethane market.[75] Moreover, PUFs exhibit high mechanical durability, ease of separation from a solution, and they are one of the most cost-effective available polymers, making them really suitable for practical low-cost applications.[76] Moreover, as it has been commented in Section 1.5.2 they also exhibit high stability against chemical degradation.

Quite surprisingly very few studies had been focused on the development of nanocomposite polyurethane matrices[77-85] and, although these publications demonstrated that the incorporation of nano-objects could significantly improve the mechanical or thermal properties of polyurethane materials and their further applicability,[79-84] controlling the total metal load in the final nanocomposite was sometimes a pending issue. Therefore, this section is mainly focused on the obtainment, optimizing and understanding of AgNPs formation in PUFs.

3.2.2.1. Synthesis and characterization of AgNPs in Polyurethane foams

Even if the chemical structure of PUFs seemed not to change after applying acid or basic treatments (see Section 3.1.3), it was considered necessary to further study the possibility of loading such different matrices with AgNPs by IMS. Although the IMS methodology takes advantage of an ion-exchange process, it was considered that the generation of coordination bonds between species might also result in the immobilization of the ionic species in the polymeric matrix. Therefore, the synthesis of AgNPs in the polymeric matrices by the IMS methodology (see eq. (3-6) and (3-7) consisted of two steps: (1) loading of the material with the metal ions ($AgNO_3$ 0.4 M solution) and (2) reduction of metal ions (by using $NaBH_4$ 0.5 M solution) to build zero-valent MNPs up.

As expected, after applying the IMS technique, a darkening of the matrices was observed, indicative of the metal loading, what was a substancial improvement of the IMS use as it had never been applied to matrices without ionogenic groups.

A quantitative value of **metal loading** was obtained by ICP-MS[a] analyses and results are shown in **Table 3.14**, and as it can be seen, the total metal amount in the nanocomposites was found to be in the range from 12 to 22 mg Ag/g matrix depending on the sample treatment, which has finally been found to play an important role in the metal loading capacity. Even if the chemical

[a] Spectrometer ICP-MS, Agilent 7500 was used. Prior to the analysis, it was necessary a digestion of the sample in HNO_3, dilution and filtration through 0.22 µm Millipore filter of the samples. In all cases the measurement error was less than 2%. Analyses were carried out in *LEITAT Technological Center*, Terrassa, Spain.

characterization was very similar for all the samples, and the use of such treatments did not affect the chemical composition of PUFs as new functional groups were not detected by Infrared Spectroscopy, [26] they do have some effect on the total metal load.

Compared to pristine PUFs (17mg/g), an acid treatment caused a lower metal retention (around 13 mg/g) whilst PUFs immersed in alkaline solutions were able to incorporate a higher metal amount (about 20 mg/g). In other words, pre-treatments provide a way for tuning the total metal content in nanocomposite.

Table 3.14. Ag content in cubic samples. All values are presented with their corresponding standard deviation of two replicates.

Pre-treatment	HNO_3 1M	HNO_3 3M	pristine	NaOH 1M	NaOH 3M
Total metal load (mg Ag/g matrix)	12.7±0.2	13.4±1.5	16.7±1.4	19.6±1.0	20.0±1.3

The observed loading differences can be attributed to the possible coordination of Ag^+ ions with lone electron pairs of nitrogen atoms of the polymeric structure: when an acid pre-treatment is applied, the nitrogen atom of the carbamate group is mostly protonated and the formation of coordination bonds between the nitrogen and the Ag^+ is hindered. Therefore, less Ag^+ ions remain immobilized in the matrix and less AgNPs can be formed. Conversely, by a basic pre-treatment the number of binding positions is maximized. The same idea of coordination bonds was reported by Jain *et al*.[82] However, they incorporated *ex-situ* fabricated AgNPs into PUFs and their reasoning considered the formation of coordination bonds between the nitrogen lone pairs and the pre-formed AgNPs. Hence, it seems that the chemical structure of PUF plays an important role in both the formation and stabilization of the AgNPs.

To investigate the **size, morphology and nanoparticles location** of nanocomposites, TEM[a] images of the cross-section were carried out. **Figure 3.26** clearly shows that AgNPs were well dispersed in the matrix, without any clear agglomeration and that a narrow size distribution of the nanoparticles was observed, although the average diameter was not the same for all the samples. In addition, nanocomposites showed far larger AgNPs on the surface while smaller ones were observed inside the matrix, as is shown on the right column of **Figure 3.24** for the nanocomposites made of pristine PUF. The size of inner particles was in the range of 6 to 10 nm.

[a] Images taken with JEOL JEM-2011, Jeol LTD and JEOL JEM-1400 microscopes from the *Servei de Microscòpia* from UAB.

Still, acid or basic treatments seem not to dramatically affect the size and distribution of the AgNPs since there is not any well-defined correlation between the treatments applied and the average diameter.

From the results obtained up to this point, it is possible to say that, despite what has always been stated,[8, 86] the IMS methodology does not necessarily require the presence of ion-exchange positions in the stabilizing matrix, as it has been successfully applied to the synthesis of AgNPs with diameters below 10 nm in PUF and no agglomeration of NPs was found. By using the IMS approach, the total metal content was up to ten-fold higher than the previously reported values corresponding to similar systems where *ex-situ* formed AgNPs were incorporated to PUF.[80, 82, 84] Moreover, comparing with other synthetic methods[87] IMS does not require any stabilizer other than the polymeric matrix itself and it is possible to tune easily the AgNPs loading in the nanocomposites by applying simple chemical treatments to the matrix.

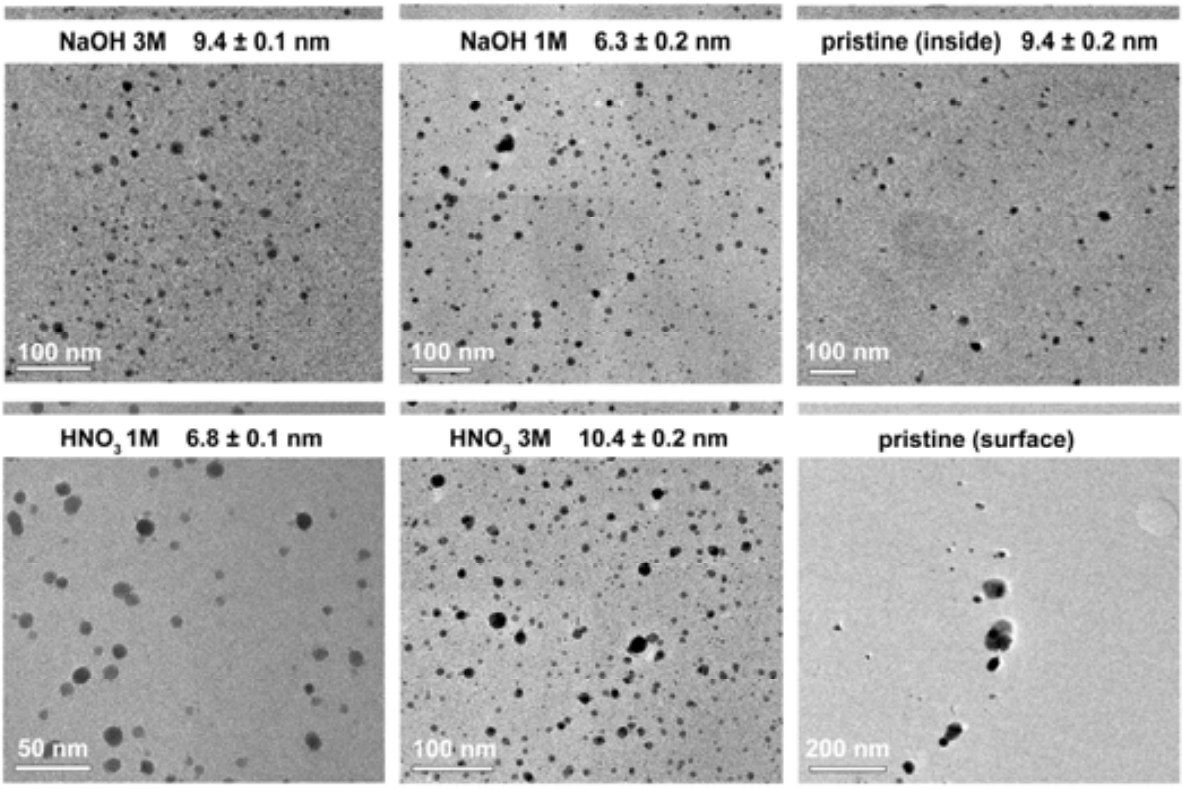

Figure 3.26. TEM images of the PUF-NCs cross-section and AgNPs diameter average.

3.2.2.2. Stability of the AgNPs in PUFs

Since one of the most serious concerns associated with the production and final uses of MNPs in real-life applications deals with the possibility of their uncontrollable release to the medium

under treatment, the evaluation of the AgNPs loss to the media was considered to be an important parameter to fully characterize them. Thus, nanocomposite samples were treated either by long-term immersion in warm water or by ultrasounds, as specified in **Table 3.15**. Two replicates of cubic samples of 1 cm^3 were deposited in a vessel with 10 mL of distilled water and placed for different times in the corresponding bath: an ultrasonic cleaner (Branson 1200) or an incubator (Aquatron Infors AG, shaker incubator). As ultrasounds can heat the solution, temperature variation in the ultrasonic bath was also monitored during the experiment. As in the case of nanocomposite films, after each experiment, the silver content in both solutions ($n_{Ag,\ solution}$) and films ($n_{Ag,\ matrix}$) was analysed by ICP-MS[a] so as to determine the release percentage (*R%*). (See equation (3-8)).

Table 3.15. Experimental conditions of the nanocomposites stability characterization.

Experiment	T (ºC)	Solution composition	Duration (h)
Ultrasonic bath	19-43	Deionised water	3
Thermostatic stirred bath	37	Deionised water	24

This study was limited to those treatments that involved the highest concentrations of reactants (e.g. HNO_3 3M and NaOH 3M) and results were compared with the pristine PUF nanocomposites. As it can be observed in **Figure 3.27**, after 3h under aging conditions provided by sonication, the total Ag release calculated by equation (3-8) did not exceed the 0.2% for any of the nanocomposites. On the other hand, after immersing the samples for 24h at 37 ºC, the amount of lost Ag was higher but it never exceeded 1% of the total amount of metal in the nanocomposites. It is significant that the basic pre-treatment (NaOH 3M) allowed a better preservation of the nanoparticles inside the polymeric matrix for both aging treatments (ultrasonic or thermostatic bath with agitation). Again, this higher stability is in agreement with the Ag^+ coordination due to nitrogen atom lone electron pair, which can retain ionic species as well as AgNPs as suggested previously. Accordingly, one may think that the basic treatment would be preferable for a final application since it allowed a higher loading of AgNPs and provided a stronger stabilization, even if all the obtained release values were very low. Nevertheless, in terms of simplicity, the nanocomposites prepared with pristine PUF are more

[a] Spectrometer ICP-MS, Agilent 7500 was used. Prior to the analysis, it was necessary a digestion of the sample in HNO_3, dilution and filtration through 0.22 µm Millipore filter of the samples. In all cases the measurement error was less than 2%. Analyses were carried out in *LEITAT Technological Center*, Terrassa, Spain.

advantageous as they can be prepared without difficulty and without any unnecessary previous step.

Besides, the influence of the ultrasounds aging treatment on AgNPs size and size distribution was also considered and **Table 3.16** reports the AgNPs average diameters measured (obtained by measuring more than 300 NPs *per* sample and fitting data obtained to a 3 parameter Gaussian curve (eq. (1-22)) from TEM[a] images of the different samples after different periods of time together with the original values (0 h).

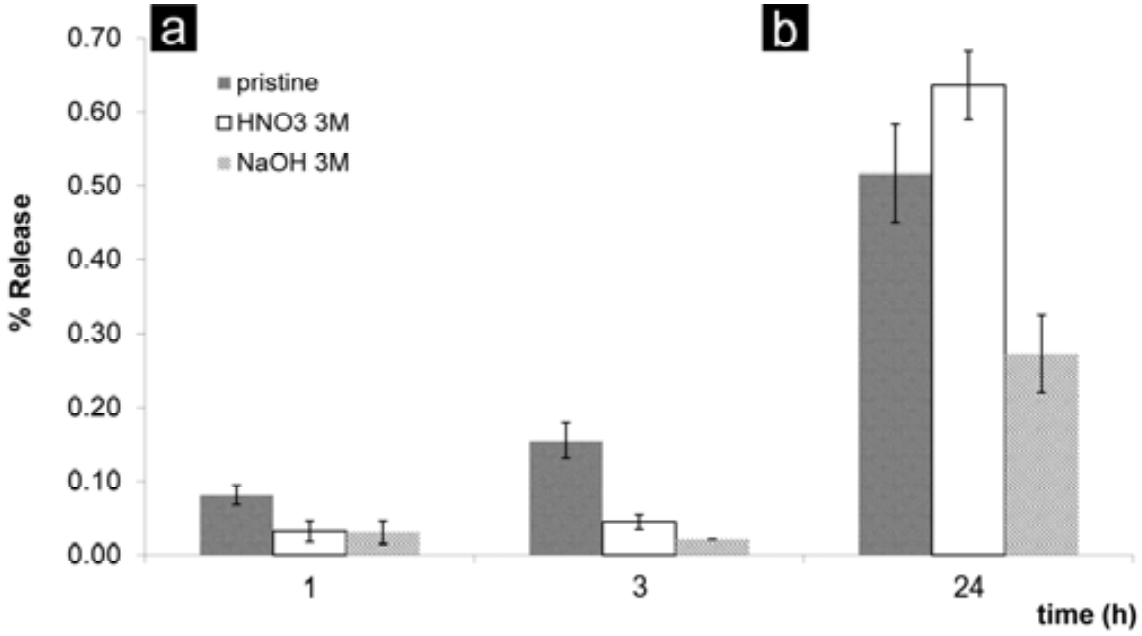

Figure 3.27. Ag release (a) after 1 and 3 h in the ultrasonic bath, and (b) after 24h at 37 ºC, 160 rpm. Results are presented with the corresponding standard deviation.

The experimental results evidenced that after ultrasonic treatment, the AgNPs average diameter slightly diminished from 6-10 nm to 4-6 nm except for one of the samples which tendency was not consistent (HNO_3 3M). The diameter shrinkage was achieved in 1 h and no further diminution was observed for a longer period (3 h). Note that samples that originally contained AgNPs of about 6 nm did not dramatically change their size whereas bigger particles (> 6 nm) became smaller.

The size change can be attributed to the loss of the larger unstable AgNPs to the medium, so that only those AgNPs that were better stabilized (the smaller ones, mainly found in the inner

[a] Images taken with JEOL JEM-2011, Jeol LTD and JEOL JEM-1400 microscopes from *Servei de Microscòpia* from UAB.

part of the nanocomposite) remained. Therefore, the use of ultrasounds can be understood as an interesting post-treatment for the synthesized nanocomposites, useful to remove the unstable AgNPs as well as to reduce the average diameter of AgNPs what would result in a greater catalytic surface and, accordingly, in a substantially improved reactivity. Such post-treatment will somehow guarantee that the amount of AgNPs lost to the reacting media will be minimized. Notice that these advantages can be afforded without an important reduction in the amount of immobilised silver since the AgNPs losses were extremely low (< 0.2 %).

Table 3.16. AgNPs average diameters (nm) before and after ultrasounds treatment with the corresponding standard deviation.

Sample	0 h	1 h	3 h
pristine	9.4 ± 0.2	5.2 ± 0.1	4.70 ± 0.03
HNO_3 1M	6.8 ± 0.1	6.1 ± 0.4	6.4 ± 0.3
HNO_3 3M	10.4 ± 0.2	5.4 ± 0.1	8.4 ± 0.2
NaOH 1M	6.3 ± 0.2	5.0 ± 0.3	6.4 ± 0.1
NaOH 3M	9.4 ± 0.1	4.9 ± 0.4	4.3 ± 0.3

3.2.3. Synthesis and characterization of Nanocomposite Textile fibers

It is now time to discuss the results found for the use of textile fibers as polymeric materials for the fabrication of nanocomposites. One of the reasons which has motivated this study is the potential obtainment of textile products with enhanced functionalities able to satisfy not only the final costumer needs, yet the manufacturer economic aspects, but also the growing ecological concerns. For instance, it is widely acknowledged that some textile fibers are vulnerable to microbial attack reducing their performance.[88-91] Hence, the treatment of these textiles with several antimicrobiological agents is an issue of great interest. Under this regard, the modification of textile fibers with AgNPs seems to be a good option for such purposes.

During the development of the present work only some cellulosic and synthetic fibers have been used. Although the results that I will present here are quite preliminar and a more detailed study will be still necessary in order to further optimize such new materials, they suppose a good basis for a further development.

The synthesis of AgNPs in the textile fibers was realised by the IMS methodology (depicted in equations (3-6) and (3-7)) by the loading of the material with the metal ions ($AgNO_3$ 0.4 M

solution) and (2) reduction of metal ions to zero-valent MNPs through reaction (by using $NaBH_4$ 0.5M solution). Once again, although equations depict a pure ion exchange mechanism, the generation of coordination bonds between species may also result in the immobilization of the ionic species in the polymeric matrix.

The entry of metal ions into the matrix could be significantly affected by the synthetic conditions. In this case, temperature can be a crucial parameter, since it can affect the structural organization of the polymer fibers thus making the matrix temporarily more accessible to metal ions by opening their structure. This approach is, in fact, not so different from the traditional dying of clothes and fabrics, which is also carried out at high temperatures.[92] After the synthesis, the fibers revert back to their closely packed state thus trapping the MNPs within the polymer structure. For these reasons, different synthetic temperatures (25°C, 40°C, and 80°C) were applied to each polymer in order to evaluate the final metal content and the distribution of the AgNPs in the matrices.

As aforementioned (Section 1.5.1 of the Introduction), each polymer has its own glass transition Temperature (T_g), and it is an important parameter to be taken into account. In **Table 3.17** the different polymers with their corresponding T_g are presented. After applying the IMS procedure a visual inspection of the samples showed a darkening of the fibers, what confirmed the presence of metal after the IMS step. Anyhow, in some cases, the darkening was soft, predicting a low metal content. In this case, characterization of the samples by TEM images and elemental analysis by ICP-MS[a] afforded a more quantitative picture of the polymer modification.

Table 3.17. Glass transition temperature of the different polymers employed.

Polymer	Abbreviation	T_g (°C)
Polyacrylonitrile	**PAN**	85
Polyamide	**PA**	55
Cotton	**COT**	-
Polyester	**PET**	69

[a] Spectrometer ICP-MS, Agilent 7500 was used. Prior to the analysis, it was necessary a digestion of the sample in HNO_3, dilution and filtration through 0.22 µm Millipore filter of the samples. In all cases the measurement error was less than 2%. Analyses were carried out in *LEITAT Technological Center*, Terrassa, Spain.

The **content of AgNPs** in the nanocomposites was determined by analysing two replicates per textile fiber and temperature by ICP-MS. **Figure 3.28** shows the amount of AgNPs loaded in each of the polymer at the 3 different working temperatures.[26]

As it can be clearly observed, PET fibers barely allow the fabrication of NPs what can be explained by different reasons. PET is quite hydrophobic, and it does not usually contain ionic moieties that could serve as binding groups for Ag^+. Furthermore, its structure is densely packed and it is highly affected by thermal history what means that its mechanical and elastic properties change after a thermal treatment. All these factors can hinder the immobilization of Ag^+ and, therefore, reducing the final AgNPs loading.

For COT fibers, because of its high hydrophobicity, which boosts ion precursors diffusion, high metal content was found, but remained almost constant at 25 and 40 ºC. Due to the high error associated to the value at 80 ºC, no general conclusion can be drawn. From this value, nevertheless, since this polymer has no glass transition temperature and remains flexible even at very low temperatures, it would not be odd that the metal content remained constant for all the tested temperatures of synthesis.

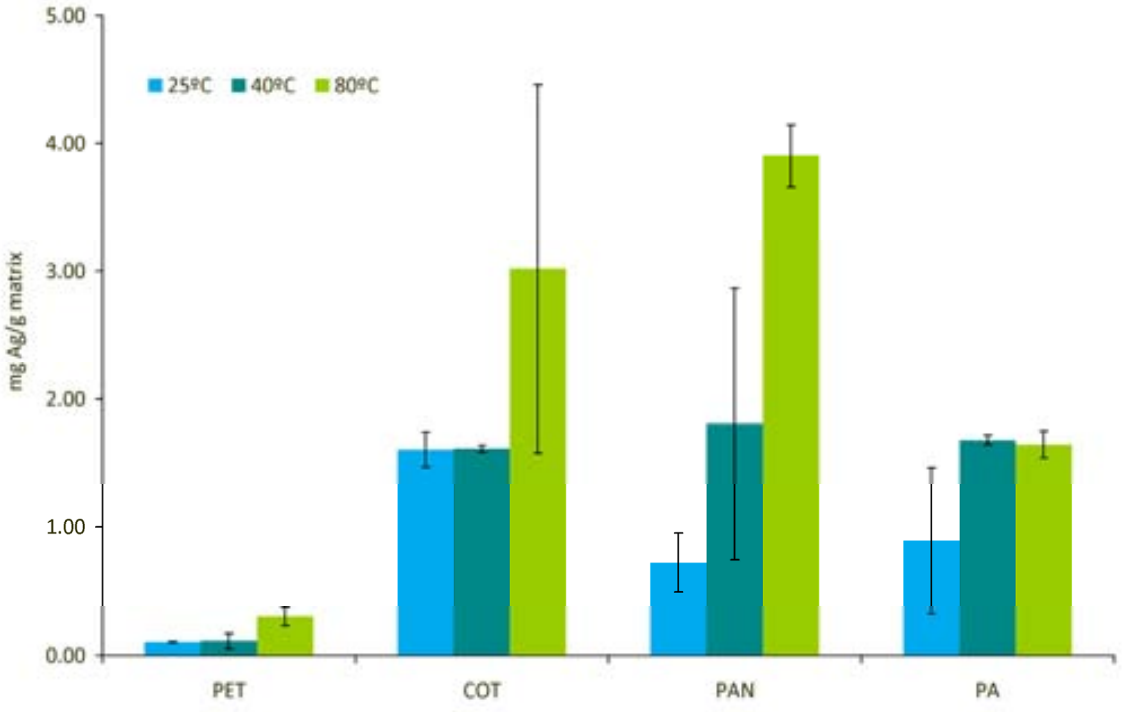

Figure 3.28. Results of the ICP-MS analysis of the Ag content.

More interesting results were found for the remaining polymers (PAN and PA). A general trend was observed: the closer the temperature to the T_g, the higher the loading.

For PA fibers obtained at 40°C and 80°C, the metal content remained almost constant whereas in the case of PAN fibers, the metal content raised with the increase of the working temperature. In both cases, that can be explained because rising the temperature to the glass transition point of each polymer (T_g PAN = 85°C whereas T_g PA = 55°C) increases the macromolecular mobility of the glassy amorphous phase, enhancing the accessibility of the polymer matrix. This change is more noticeable for PAN fibers than for PA fibers due to the higher thermosensitivity of the mesomorphic PAN fibers[93] at temperatures around T_g in comparison with the more stable and high crystalline structure of the PA fibers. Basically, PAN fibers are strongly influenced by temperature because their structural organization is intermediate between amorphous and crystalline phases, whereas the strong intermolecular hydrogen bonds through the amide groups in PA fibers configure a more stable semi-crystalline structure which hinders the ion diffusion.

TEM[a] **images** of the cross-section of the nanocomposites are shown in **Figure 3.29**. The MNPs average diameter was determined by counting between 200-300 MNPs per sample (except for PET for which only 30-40 NPs could be counted), and data was fitted to a 3 parameter Gaussian curve (eq. (1-22)). The results are presented in **Table 3.18**, with their corresponding standard deviation.

Table 3.18. AgNPs average diameters (nm) in textile fibers with the corresponding standard deviation.

Sample	25 ºC	40 ºC	80 ºC
COT	2.9 ± 0.1	4.6 ± 0.3	5.8 ± 0.3
PET	5.7 ± 0.1	4.7 ± 0.3	5.2 ± 0.5
PA	4.5 ± 0.1	9.9 ± 0.7	10.3 ± 0.4
PAN	4.2 ± 0.2	6.9 ± 0.2	6.7 ± 0.3

In all cases, small non-aggregated AgNPs (with diameters between 3 – 10 nm) were obtained and they were mostly located on the surface. In general terms, it is possible to state that the higher the temperature of synthesis, the biggest the AgNPs formed. This can be explained similarly as the effect of the ultrasounds treatment before observed in Nafion with AgNPs. Combining temperature with classical Ostwald ripening (see Section 1.3.2.1) it is feasible that bigger nanocrystals grow at the expense of smaller ones that get dissolved during the synthesis.

[a] Images taken with JEOL JEM-2011, Jeol LTD and JEOL JEM-1400 microscopes from *Servei de Microscòpia* from UAB.

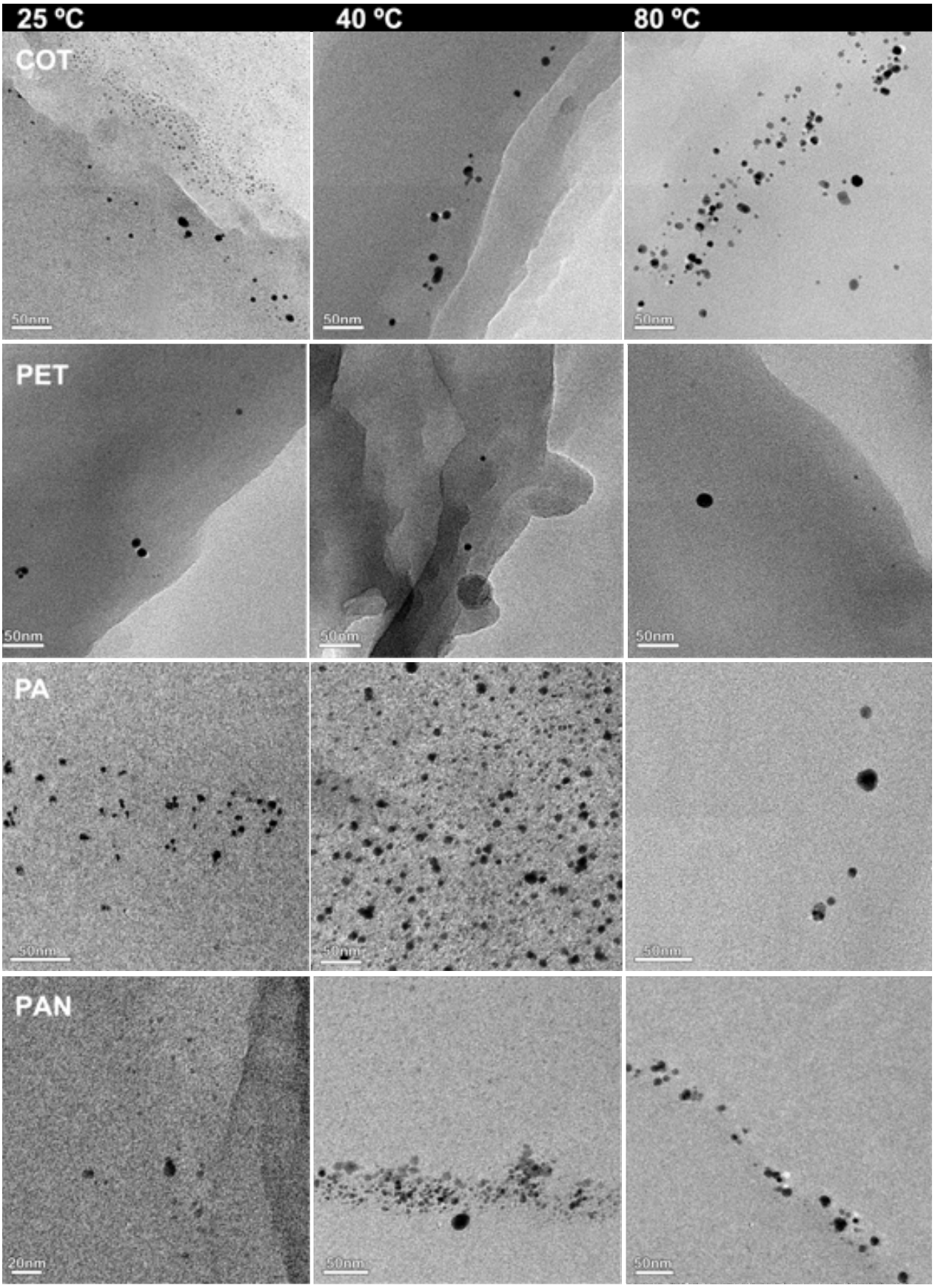

Figure 3.29. TEM images of the cross-section of textile fibers with AgNPs obtained at different temperatures.

Therefore it is possible to state that AgNPs could be obtained in different common textile fibers by the IMS approach, although such matrices do not contain ion-exchange positions. By using a similar approach as the one used typically for dyeing textiles and clothes, such is applying relatively high temperatures; a new approach to modification of such matrices has been successfully tested. Moreover, both, the metal load and the MNPs mean diameter could be tuned by working at different temperatures. Nevertheless, further studies should be necessary in order to increase the total metal load in some of the targeted textiles.

3.2.4. Comparison of the NCs developed

In order to present a whole picture of the results obtained up to now, in **Table 3.19** there is shown a summary of the main characteristics of the load of MNPs in each matrix. As it can be observed, MNPs could be obtained in all of the tested matrices, and, therefore, the targeted PMNCs could be obtained.

The total metal loading strongly depended on the matrix employed. Moreover, IEC has proved to play a crucial role on the final loading, although it has been shown to be not an essential characteristic to successfully load the matrices. In this sense, the absence of ion-exchange positions on the polymer was not an impediment to successfully apply the IMS (as results obtained with PUFs demonstrate). Therefore, from now on, when applying the IMS, the possibility of generate coordination bonds -between the matrix and either the ions or MNPs- will have to be considered.

On the other hand, MNPs distribution was strongly influenced by not only the nature of the matrix, but also by the nature of the metal ion immobilized. For example, in the case of Nafion films, the load of PdNPs resulted in aggregates on the surface (in agreement with the DEE predicted distribution) and small non-aggregated inner particles. Whereas, the load of AgNPs resulted in the appearance of aligned NPs.

Finally, from all the results here presented, it comes clear that Nafion films allowed loading the highest amount of metal (either Pd or Ag), although MNPs obtained were bigger than the ones obtained in the other matrices. Nevertheless, considering the other matrices, SPES-C-3 films and PUFs also allowed loading a high amount of MNPs (around 20 mg/g), with slightly small diameters. Moreover, considering the low cost of these matrices and their porous morphology, such developed NCs seem to be far more attractive in regards to their possible final application.

Table 3.19. Summary of the loading with MNPs of the polymeric matrices.

	matrix	Metal load (mg_{metal}/g_{matrix})	$Ø_m$ (nm)	MNPs distribution
Pd	**SPES-C-1**	16.6	6	-
	BM	4.3	3	-
	Nafion	28.1	13	Aggregates on the surface, small MNPs all over the matrix.
	SPES-C-3	20.0	9-13	All over the matrix.
Ag	**SPES-C-1**	14.9	12	Surface.
	BMs	2.5	11	Surface.
	Nafion	51.8	9	All over the matrix, in lines.
	PUFs	12.7 – 20.0	6 – 10	All over the matrix.
	Textile fibers	0.3 – 3.9	3 - 10	Surface.

3.3. Nanocomposite applications

As shown in Chapter 1, metal-polymer nanocomposites may cover a wide field of practical applications because they combine the properties of both, MNPs and polymers.[94] Such combination allows not only to handle a great number of industrial and everyday challenges but also to accomplish with some of the principles established by the Green Chemistry philosophy (**Figure 1.1**).

In regards to the materials developed in the present work, some wastewater treatment applications, mainly focused on the catalytic and bactericidal decontamination of water, were tested.

On the one hand, since palladium is probably one of the most versatile metals for catalytic reactions, particularly those involving C-C bond formation (e.g. Heck, and Suzuki) and hydrogenation,[95-98] the preparation of supported metallic nanoparticles on different supports has been extensively investigated.[87] Concerning the current work, all the prepared palladium-nanocomposites (PdNCs) were tested in catalytic applications. Precisely, they were tested as catalysts in the elimination of nitroaromatic compounds of water by following the reduction of *p*-nitrophenol (4-ap) to *p*-aminophenol (4-ap) in basic media, which is a typical reaction to evaluate the catalytic performance of nanoparticles and nanocomposites.[95]

On the other hand, it is known that silver and silver-based compounds exhibit a strong toxicity towards a wide range of bacterial strains including *Escherichia coli*. Thanks to this broad-spectrum of antimicrobial properties, most of the recent applications of metallic silver nanocompites (AgNCs) have been related to biological/medical areas.[96] This is why the use of

the materials such as the here developed can play an important role in water disinfection, since compared to other strategies being used nowadays (such as the use of chemical agents, physical treatments or mechanical ones) their activity does not require additional chemical reagents and can be employed under mild conditions. Thus, during the present work the obtained AgNCs from PUFs and polymeric films were tested in regards to their antimicrobial activity versus *Escherichia coli*.

Therefore, the results presented in this Section and their subsequent discussion will cover both applications and will be organized concerning their use as catalysts or as bactericidal agents.

3.3.1. Catalytic reduction of nitroaromatic compounds in water

The reduction of aqueous 4-nitrophenol (4-np) to 4-aminophenol (4-ap) by $NaBH_4$ was used to evaluate the catalytic performance of nanocomposites as the reaction does not proceed in the absence of catalyst, but it rapidly occurs in the presence of MNPs (usually Pd) and can be easily monitored by UV–Vis spectrophotometry (λ=390-400 nm).[95] The reaction was assumed to follow *pseudo*-first order kinetics due to the high excess of reducing agent used and, accordingly, an apparent constant rate (kapp) could be calculated by equation (1-24).

Initially, the catalytic evaluation was performed in batch conditions, by adding a piece of any of the developed NCs to the reaction vessel (containing the afore-mentioned reactants) under stirring. The carefully mixed solution was homogeneous and only small samples were taken periodically, analysed and then returned to the vessel in order to keep the reaction volume almost constant. Later, the catalytic evaluation was also performed in continuous flow conditions for those samples that could be used in flux conditions, such as PUFs and SPES-C-3 films.

In order to help the reader, the main characteristics of each experiment (volumes, concentrations and so on) will be detailed for each type of tested NC.

3.3.1.1. Palladium-nanocomposite polymeric films

To carry out the catalytic experiments in **batch conditions**, a given amount of $NaBH_4$ was added to 5 mL of 4-np solution (5 mM) to achieve a $NaBH_4$ concentration of 50 mM, and a final ratio $NaBH_4$:4-np = 100:1. Then, a piece of nanocomposite (1 cm^2) was added to the vessel.[a]

Two different blanks per film type were tested (Blank 1 with 4-np and 1cm^2 of bare film and Blank 2 with 4-np and $NaBH_4$) and they did not show significant absorption, even after 10 h of reaction time.[18, 19] Conversely, when testing the different samples a decrease in the absorption was noticed due to the conversion of 4-np to 4-ap (**Figure 3.30**).

[a] The process was monitored by a Pharmacia LKB Novaspec II spectrometer (λ = 390 nm).

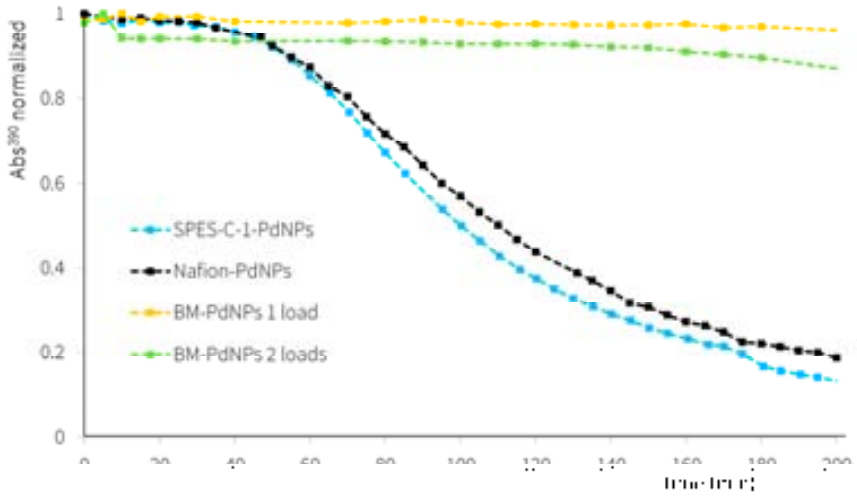

Figure 3.30. Catalytic performance of PdNPs-SPES-C-1 (red), PdNPs-BMs with one load (blue), PdNPs-BMs with 2 loads (green) and PdNPs-Nafion (black).

However, in the best of the cases, an induction period of at least 1 h was needed to start de reaction. After this induction period the reaction followed a *pseudo*-first order velocity equation, so it was possible to linearize the data to obtain the k_{app} velocity constant.[97] This induction time can be explained since Pd is a classical H_2 - storage metal[98] and H_2 evolved from the decomposition of $NaBH_4$ can be loaded inside PdNPs, competing with the catalytic reaction.[99] Once the absorption of H_2 has reached a saturation value (after the induction/activation period) the catalytic reaction prevails and the reaction rate follows pseudo-first order kinetics at high extend. This situation is very compatible with the experimental results. In fact, taking into account the well-known and fully accepted Langmuir-Hinshelwood mechanism for the reduction of 4-np to 4-ap,[95] there is a first step during the reaction that involves the loading of the catalytic nanoparticles with hydride (H^-). **Figure 3.31** illustrates the aforementioned mechanism.

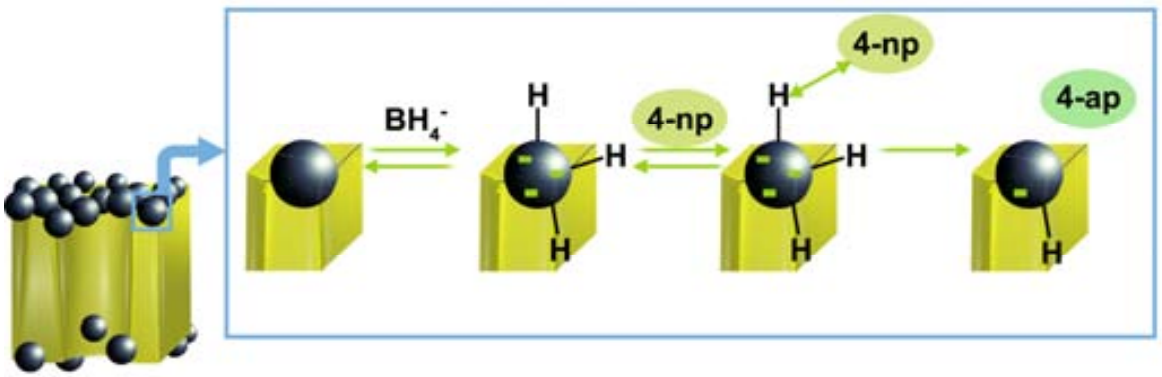

Figure 3.31. Langmuir-Hinselwood mechanism for the reduction of 4-np to 4-ap with $NaBH_4$.

As it can be observed in **Figure 3.30**, four different nanocomposite samples were tested and the results showed that:

(i) SPES-C-1 nanocomposite films offered the best catalytic performance (k_{app} = 0,0132 s^{-1}), allowing to reduce almost 90% of 4-np in less than 5 h reaction time;

(ii) Nafion nanocomposite also gave a good catalytic performance (k_{app} = 0,0123 s^{-1}) and allowed to reduce until 80% of 4-np;

(iii) for BMs samples with 1 load of PdNPs the reaction was really slow (k_{app} = 0,0009 s^{-1}) and only occurred with a 10% of efficiency, and with 2 loads, although it worked faster (k_{app} = 0,0028 s^{-1}) it was possible to reduce 4-np to 40% but only with 6 h of reaction time.

Although Nafion and SPES-C-1 nanocomposites seemed to have a similar catalytic performance, their efficiencies cannot be compared directly because it is important to take into account the different Pd loaded in each film (see Section 3.2.1.1). By comparing the normalized efficiency (k_{app} /mmol Pd) it is clearly seen that with the same Pd content, Nafion had a really low catalytic performance (see **Table 3.20**). This can be explained because PdNPs grew in the surface of the Nafion forming aggregates, so that the superficial catalytic area diminished, giving fewer available catalytic sites.

Table 3.20. Normalized catalytic efficiency (k_{app}/$mmol_{Pd}$) per type of PdNC. Results are expressed with their corresponding standard deviation.

Matrix	k_{app} (s^{-1}·$mmol_{Pd}^{-1}$)
SPES-C-1	18 ± 3
Nafion	1.2 ± 0.6

Because of the great catalytic efficiency of SPES-C-1 nanocomposite films, the possibility to reuse nanocomposite catalytic membranes was also evaluated. **Figure 3.32** shows the decrease of the normalized absorbance *versus* time for four consecutive runs, where it can be clearly seen the decrease of the reaction rate and the increase of the activation time. This fact could be explained by the poisoning of the catalyst due to the generation of by-products of the 4-np reduction, which could interfere with the catalyst surface,[100] or (and most probably) by a stronger competition between hydrogen absorption and catalytic reactions, after the initial discharge in the first cycle. It must be pointed out that the loss of catalytic activity cannot be explained by the leaching of PdNPs from the matrix to the aqueous solution since the

absorbance of reacting solutions did not keep decreasing after the catalytic membrane was removed, even when stored overnight.

It is worth mentioning that the difference between the first run and second run, was much higher than that corresponding to the third and fourth. This fact may suggest that after few runs, the catalytic efficiency could be preserved, although at a lower value when compared with the first run. However, this point requires a stricter experimental confirmation.

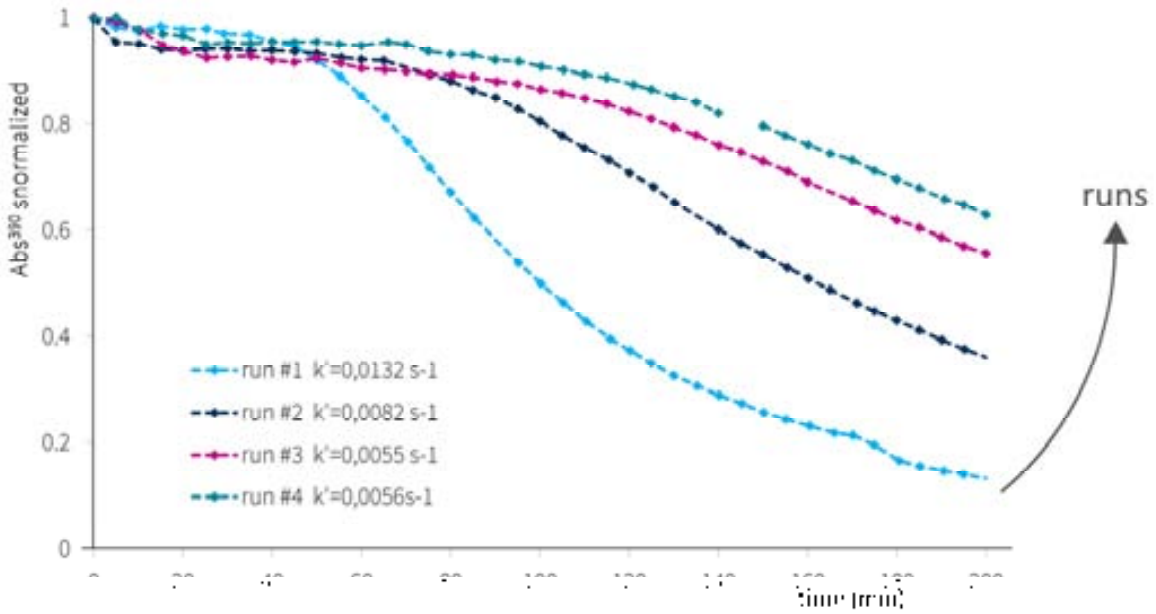

Figure 3.32. Catalytic performance of PdNPs-SPES-C-1 films in four consecutive runs.

Anyway, what is has been clearly shown is that PdNCs obtained in polymeric films exhibited catalytic activity although an induction time was needed before the reaction happened at high extent. Moreover, the efficiency was not directly related to the Pd load, since for the same load of PdNPs, SPES-C-1 nanocomposites showed the better catalytic efficiency and Nafion the worst, what is explained by the distribution of the catalytic nanoparticles in the surface of each matrix.

In view of these results and taking into account that SPES-C-3 films showed porosity offering the possibility to be applied in flow conditions, SPES-C-3-PdNPs were tested as **flow-through catalytic membrane reactors**. To do so, some experiments were carried out with a disk of 40 mm of diameter of the nanocomposite placed in an Amicon® cell connected to a peristaltic pump that forced the test solution (4-np 1 mM and $NaBH_4$ 20 mM, it is to say a final ratio

$NaBH_4$:4-np = 20:1) to pass through the nanocomposite. The peristaltic pump always operated at the same velocity, so i) the change in the flow between experiments is determined by the membrane type, and ii) no change in the flux was expected during the experiment. Nevertheless, flux was measured during all the experiment in order to assure its stability.

All experiments were done with recirculation of the treated solution, in a total volume of 40 mL using an experimental set-up as the one showed in **Figure 3.33**. Measures were taken in continuous, it is to say, the permeate was analysed after a single pass.

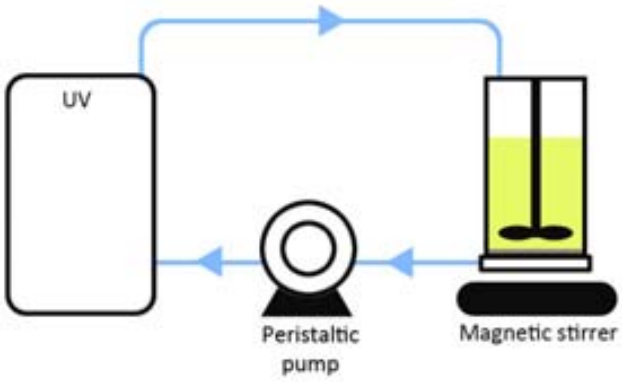

Figure 3.33. Experimental set-up for the catalytic activity evaluation in flow conditions.

For a given residence time (determined by the flow through the membrane), the concentration was followed as a function of the time[a]. The results that I will present here were plotted as the % conversion of 4-np in the permeate a function of time (see equation (3- 9)). For all of the NCs two different samples were tested, and, for both, the result was almost equal. Hence, only the results of one of them will be presented.

$$\%\,\text{Conversion} = 100 \cdot \left[\left(\text{Abs}^{\lambda}(0) - \text{Abs}^{\lambda}(t) \right) / \text{Abs}^{\lambda}(0) \right] \qquad (3\text{-}9)$$

Where: $Abs^{\lambda}(0)$ is the initial Absorbance,

$Abs^{\lambda}(t)$ is the measured Absorbance.

Before starting with the discussion of the results obtained, just recall that samples labelled as *20* or *25* correspond to 20 % or 25 % of polymer in the collodion. And *a* or *b* stand for the film thickness: ~200 μm or ~300 μm.

[a] The process was monitored by a spectrometer Uvilight, XTD5, λ = 400 nm.

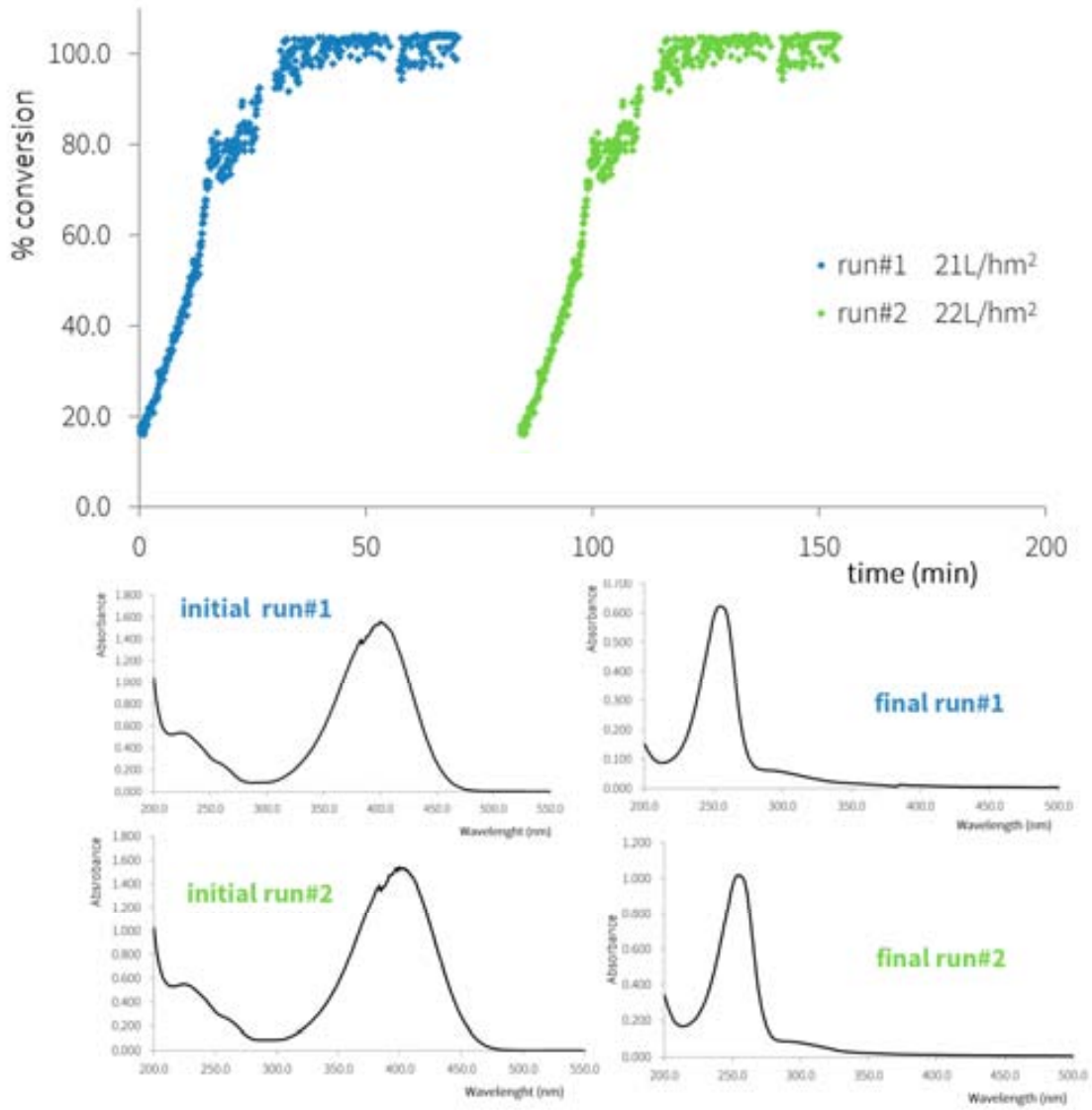

Figure 3.34. Results obtained for the two consecutive cycles with the SPES-C-3-25a-PdNPs (25 % in polymer, ~200 μm of thickness) in the catalytic conversion of 4-np to 4-ap.

First experiments were performed with NC obtained in films of thickness of ca. ~200 μm (SPES-C-·-25a and SPES-C-20a), but the process was difficult to monitor and to control. Due to the low mechanical strength, NC-films broke very often and the flux through them could not be controlled. Anyhow, the results obtained for the samples of SPES-C-3-25a-PdNPs are shown in **Figure 3.34**. In this case, two consecutive cycles (run#1 in blue, run#2 in green) with the same piece of NC were performed, with fluxes of about 20 L/hm^2. At the beginning of the experiment low conversions were obtained (ca. 20 %) but no induction time was found before the reaction started. Moreover, after ~40 min of reaction a conversion up to 100 % was obtained. In order to assure that 4-np (with a maximum of absorbance at 400 nm) was completely converted to 4-ap (with a maximum of absorbance at 297 nm), samples of the reacting solution were taken before

and after the experiment, and screenings of the absorbance were performed in such samples. These are also presented in **Figure 3.34** (below).

These results pointed out that high conversion could be obtained working at low fluxes and that the nanocomposites prepared could be reused maintaining their catalytic efficiency.

Similar experiments were performed for SPES-C-3-20b-PdNPs films, and due to the increasing of the film thickness (ca. 300 μm), it was easier to exert some control on the flux and NC-films did not break. **Figure 3.35** presents the results for two consecutive cycles for one of them cycles (run#1 in blue, run#2 in green). As observed, SPES-C-3-20b-PdNPs films showed a similar behaviour in the catalytic reduction of 4-np as if there were applied in batch conditions. This can be explained because of the high flux at which these films operate (about 180 L/hm^2) and because of the presence of some imperfections as small holes, what makes them unsuitable for flow condition applications (see **Figure 3.10**).

In any case, by analysing the resulting solution at the end of each cycle by UV-Vis spectrometry (200 to 600 nm) it was possible to state that almost all the 4-np were consumed during the reaction.

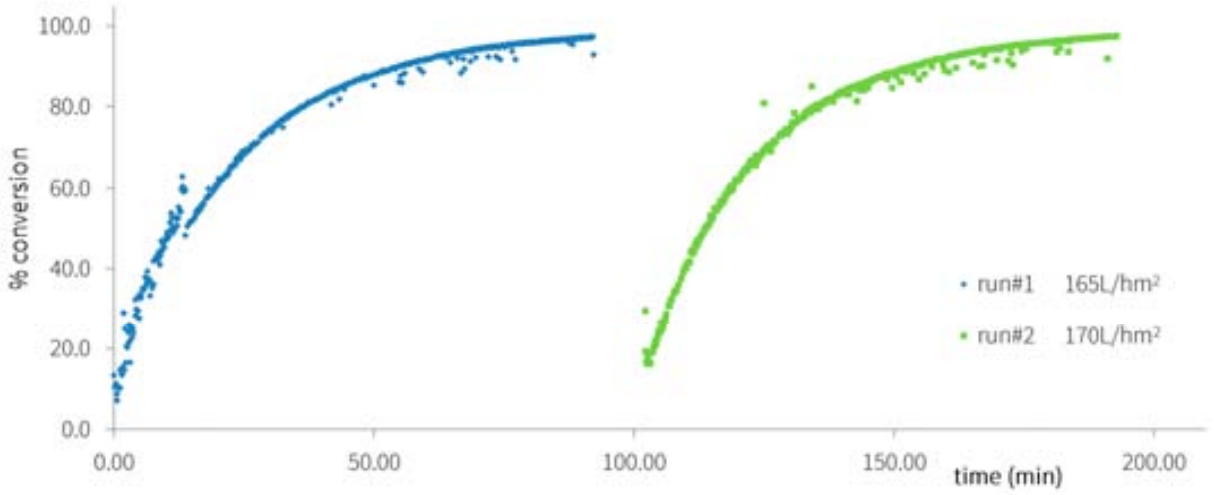

Figure 3.35. Results obtained for the two consecutive cycles with the SPES-C-3-20b-PdNPs (20 % in polymer, ~300 μm of thickness) in the catalytic conversion of 4-np to 4-ap.

Finally, results of three consecutive cycles (run#1 in blue, run#2 in green, run#3 in orange) of one sample of SPES-C-3-25b-PdNPs are presented in **Figure 3.36**.

As it can be clearly seen, SPES-C-3-25b-PdNPs showed a great conversion (up to 100%) in the reduction of 4-np, when evaluated up to 3 cycles. Once again, by analysing the resulting

solution at the end of each cycle by UV-Vis spectrometry (200 to 600 nm) it was possible to state that all the 4-np was consumed during the reaction. In comparison to SPES-C-3-20b-PdNPs, the high conversions obtained for these NC-films can be attributed to the low fluxes at which they can operate (about 17 L/hm^2). Nevertheless, comparing these results with those of SPES-C-25a-PdNPs (**Figure 3.34**) that showed worst catalytic performance even when working at similar fluxes, it is clear that some improvement was attained by the use SPES-C-25b-PdNPs. These last NC-films offered, in fact, a higher mechanical strength, and the absence of holes in the surface. This absence means the only way for the reactants to go through the film is by passing through its pores, which are full of catalytically active PdNPs (as observed in TEM images presented in **Figure 3.17**).

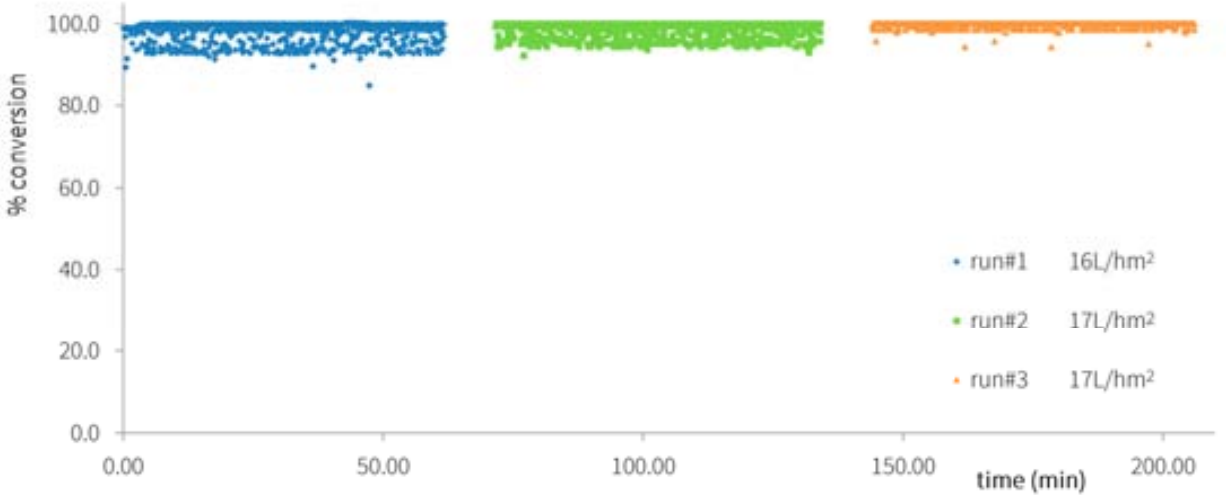

Figure 3.36. Results obtained for the two consecutive cycles with the SPES-C-3-25b-PdNPs (25 % in polymer, ~300 μm of thickness) in the catalytic conversion of 4-np to 4-ap.

Taking into account the good results obtained for SPES-C-3-25b-PdNPs, it was considered important to evaluate the effect of the flux in the kinetic of the reaction. Hence, different fluxes were tested and results showed that at fluxes between 16-30 L/hm^2, conversions of 100 % could be obtained (what suppose an improvement if we compare with results obtained by NC-materials developed by other authors[101]), but when increasing the fluxes up to 40 L/hm^2, nanocomposites showed lower catalytic activity, although conversions of 100% could be obtained after 15 min. It is important to mention that in these experiments at high fluxes, controlling the flux through the membranes was critic and difficult because each piece of membrane had a different behaviour no matter what the velocity of the peristaltic pump. This situation suggests that SPES-C-3-25b-PdNPs can only be correctly applied at fluxes below 40 L/hm^2.

Therefore, it has been proved that the inclusion of PdNPs in polymeric films such as the ones here presented offered great possibilities concerning their applicability as catalytic materials. On the one hand, when applied in batch conditions, it has been shown that the effect of the distribution of PdNPs, it is to say, their availability to the reactants, played has a crucial role. On the other hand, when films were applied in flow conditions, conversions up to 100 % in three consecutive cycles (~60 min of operability by cycle) could be obtained even when working at lower ratios of $NaBH_4$:4-np. Thus it is possible to state that probably the leakage of PdNPs from the NC to the media was very low (or even inexistent), hence the NCs developed could be applied as reusable catalytic materials.

3.3.1.2. Silver-nanocomposite polymeric films

Even if silver is not usually thought as a typical catalytic metal in comparison to classical Pd or Pt, it has also been used for catalytic purposes.[102, 103] Hence, it seemed reasonable to test the Ag-NCs materials developed as catalysers for the decontamination of water. Therefore, the reduction of aqueous 4-nitrophenol (4-np) to 4-aminophenol (4-ap) by $NaBH_4$ was also used to evaluate the catalytic performance of Ag-NCs in batch conditions. Analogously as for PdNCs, to carry out the catalytic experiments, a given amount of $NaBH_4$ was added to 5 mL of 4-np solution (5 mM) to achieve a $NaBH_4$ concentration of 50 mM ($NaBH_4$:4-np = 100:1). After mixing, a piece of nanocomposite (1 cm^2) was added to the stirred vessel and the solution was sampled periodically.[a]

Data plotted in **Figure 3.37** show a high catalytic activity for Nafion and SPES-C-1 nanocomposites with AgNPs whereas almost no effect for the blank experiments. It is important to note that, in both nanocomposites, a certain induction time was observed before the reaction started as it was observed for PdNPs.[18, 19] For Pd, it was suggested that H_2 evolved from the decomposition of $NaBH_4$ can be loaded inside PdNPs competing with the catalytic reaction,[95] but for the case of silver this situation has not been already reported in the literature.

From these experiments it came that SPES-C-1 nanocomposites offered the best catalytic performance as they were able to halve the concentration of 4-np in 30 minutes and reduce it more than 90 % in less than 1 h. Conversely, Nafion nanocomposites were still in the induction period after 1 h and a reduction of 80 % was only achieved after 2 h. These differences were in

[a] The process was monitored by a Pharmacia LKB Novaspec II spectrometer (λ = 390 nm).

agreement with the most favourable location of the catalytic material[104] in the matrix: for SPES-C-1, AgNPs were mainly formed in the surface, whereas in the case of Nafion nanocomposites AgNPs were also found inside the matrix, reducing the overall number of catalytic sites.[38]

For a better comparison, the normalized catalytic efficiency (k_{app}/mmol$_{Ag}$) were calculated, considering a *pseudo* first order reaction (equation (1-24)). The calculated normalized k_{app} were: 72 and 3.51 s^{-1}·$mmol^{-1}$, for SPES-C-1 and Nafion respectively, so about 20-fold higher for SPES-C-1. After these positives results, the opportunity to reuse the catalytic materials was also evaluated and positive results are also shown in **Figure 3.37**. Similarly to what was concluded for PdNPs,[18] it was definitively possible to reuse the catalytic supports maintaining good catalytic efficiencies although a progressive decrease of the reaction rate occurs (results shown in **Table 3.21**). Equally, the activation time after each cycle was maintained or even enlarged.

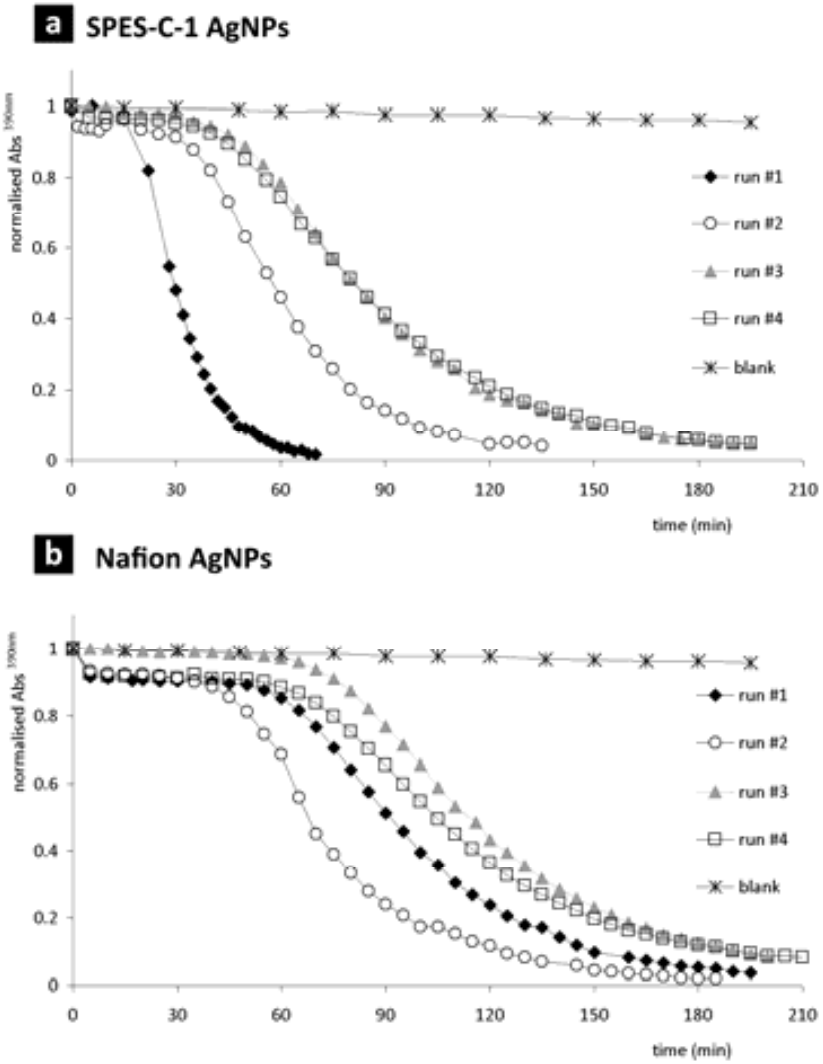

Figure 3.37. Catalytic evaluation of nanocomposite samples with AgNPs in successive catalytic cycles (a) SPES-C with AgNPs and (b) Nafion with AgNPs. Blank experiments were carried out without any nanocomposite.

As a first explanation, one can relate the catalytic efficiency loss and the silver release but, since the silver loss was proven to be low (see Section 3.2.1.3), the weaker performance after successive cycles could be attributed to the poisoning of the catalyst due to the generation of by-products of the 4-np reduction that can interfere with the catalyst surface and that has been previously reported.[100]

Table 3.21. Normalized k_{app} values for the catalytic reduction of 4-np by SPES-C-1 and Nafion nanocomposites (uncertainties correspond to standard deviation). The ratios between each run and the first run are presented in brackets.

	Normalized k_{app} ($s^{-1}mmol^{-1}$) ($k/k_{\#1}$)*			
	run #1	**run #2**	**run #3**	**run #4**
SPES-C-1-AgNPs	71.8 ± 0.4 (1)	32.6 ± 0.5 (0.45)	20.5 ± 0.3 (0.29)	19.3 ± 0.2 (0.27)
Nafion-AgNPs	3.5 ± 0.1 (1)	3.1 ± 0.1 (0.88)	2.5 ± 0.1 (0.71)	2.3 ± 0.1 (0.66)
$k_{SPES-C}:k_{Nafion}$	20.5 ± 0.3	10.6 ± 0.2	8.2 ± 0.1	8.3 ± 0.1

* Numbers in brackets correspond to the ratio between the k_{app} of each cycle and the original value for the first experiment ($k_{app,\#1}$) for both nanocomposites.

Anyhow, it was not possible to discard the loss of the catalytic material, which once in the media cannot be recovered for the following catalytic cycle. The last hypothesis is in agreement with the experimental results: (i) AgNPs were mostly located nearby to the membrane surface for SPES-C-1, which explains its higher catalytic activity even if the metal loading was lower than that of Nafion; (ii) AgNPs were less retained by SPES-C-1 matrix as it has been proved by the treatment with ultrasounds (see Section 3.2.1.3). Therefore, the performance decrease was much more important for SPES-C-1 nanocomposites than for Nafion ones, since more abundant and less retained AgNPs escaped from the SPES-C-1 matrix. To visualize this conclusion, **Table 3.21** also includes the ratio between the normalized k_{app} of each cycle and the original value for the first experiment ($k_{app,\#1}$) for both nanocomposites. After 4 cycles, only about a 30% of the initial reaction rate remained for SPES-C-1 whereas for Nafion the value is close to 70%.

Comparing the normalized catalytic efficiencies obtained with these AgNCs with the ones obtained for the same films loaded with PdNPs, an increase of the reaction rate (up to 3-fold higher) can be clearly observed. On the other hand, SPES-C-1 nanocomposites performed better but the reaction rate was clearly reduced after successive cycles. Finally, Nafion

nanocomposites performance was less efficient but more stable, maybe due to the higher stability of the AgNPs, which have been shown to grow all over the matrix.

3.3.1.3. Silver-nanocomposite polyurethane foams

The catalytic performance of PUFs containing AgNPs was also evaluated by using the reduction of 4-np to 4-ap by $NaBH_4$, in batch and in flow conditions.

First studies in **batch conditions** were performed with a piece of nanocomposite (1 cm^3) immersed in a stirred vessel of 50 mL solution containing 4-np (0.5 mM) and $NaBH_4$ (500 mM), it is to say with a ratio $NaBH_4$:4-np = 1000:1.[a] As it happened for NC-films, only PUFs containing AgNPs exhibited catalytic activity when evaluated in batch tests (**Figure 3.38**), although as it has been always found in these kind of experiments, and induction time is required before the reaction starts.

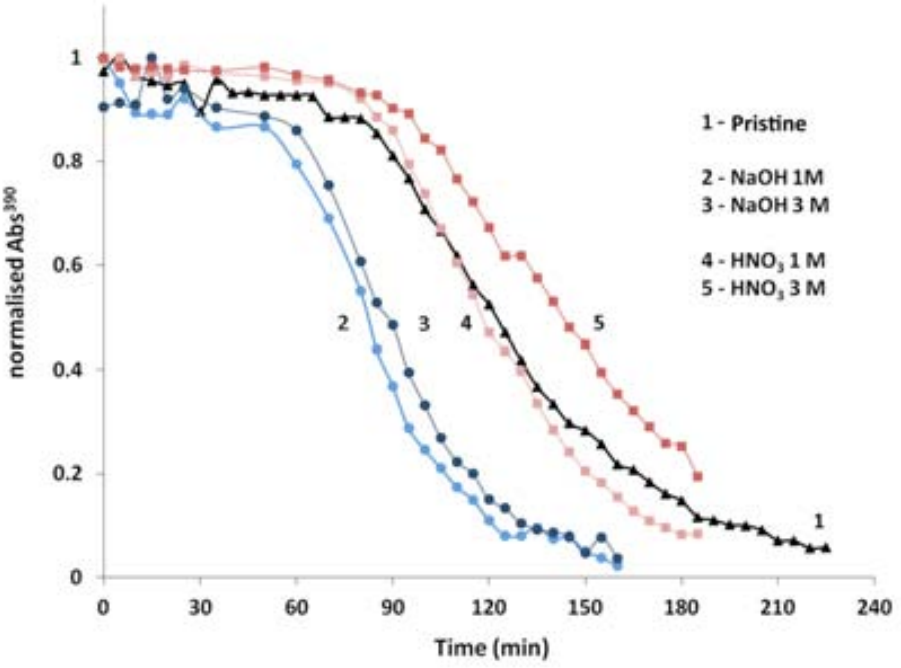

Figure 3.38. Catalytic evaluation of PUFs-AgNPs.

In this case, normalized reaction rate values (**Table 3.22**) expressed by mg of the catalytic metal increased for the PUFs with basic treatments. However, in PUFs with HNO_3 treatments, even if their metal content was lower (c.a. 40% less), the normalized catalytic activity remained almost constant. This fact can be explained because of the smaller AgNPs diameters obtained with the treatments (**Figure 3.26**) which implies a higher catalytic area for the same amount of metal.

[a] The process was monitored by a Pharmacia LKB Novaspec II spectrometer (λ = 390 nm).

Table 3.22. Normalized Reaction rates (k_{app}) obtained for each PUF-NC. 1 replicate.

Treatment	k_{app} ($s^{-1} \cdot mg_{Ag}^{-1}$)
Pristine	0.05
NaOH 1 M	0.10
NaOH 3 M	0.10
HNO_3 1 M	0.12
HNO_3 3 M	0.06

Since the batch tests confirmed that the reduction of a nitroaromatic compounds in water could be easily performed by the PUFs-AgNPs in batch conditions, next step was focused on their applicability in **catalytic flow conditions**. To do so, experiments were carried out as it is described in **Figure 3.39**: a disk-shaped nanocomposite sample was placed in a filter holder connected to a peristaltic pump that forced the test solution (4-np 0.5 mM and $NaBH_4$ 500 mM) to pass though the nanocomposite at different flow rates: 0.4, 1.7, 4,1 and 6.8 $mL \cdot min^{-1}$. Samples were used for up to 3 cycles of catalysis to evaluate their possible reuse.

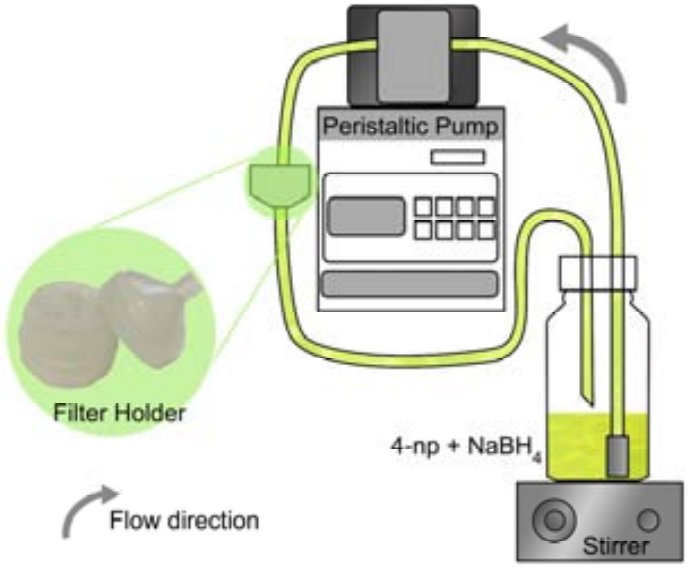

Figure 3.39. Experimental set-up for the catalytic experiments in flow conditions.

Since the nanocomposite used for these catalytic experiments had to be placed in the circular filter holder showed in **Figure 3.39**, disk-shaped foams were cut out and nanocomposites were prepared as usual. The total metal load was evaluated by ICP-MS and results were in close agreement with the ones obtained for cubic samples (showed in **Table 3.14**), proving the high reproducibility of the IMS technique (see **Table 3.23**).

Table 3.23. Ag content in disk PUFs samples. All values are presented with their corresponding standard deviation of two replicates.

Pre-treatment	HNO_3 1M	HNO_3 3M	pristine	NaOH 1M	NaOH 3M
Total metal load (mg Ag/g matrix)	11.0±0.1	10.9±0.3	15.6±3.3	21.2±1.7	21.2±5.4

The catalytic activity of all the nanocomposites made of different PUF (pristine, NaOH 1M, NaOH 3M, HNO_3 1M and HNO_3 3M) was first evaluated at a constant flow rate (1.7 mL·min^{-1}) and the corresponding results are shown in **Figure 3.40** (a). Plotted data of normalized absorbance at 390 nm (at which the maximum absorbance of 4-np was produced) indicated that the catalytic performance was very similar for all the nanocomposites disregarding the endured treatment. This situation was quite controversial since, *a priori*, one might expect that those nanocomposites with higher silver content (NaOH 1M or NaOH 3M) would have performed better. However, as no significant differences were found for the different samples it is possible to assume that all of them exceed a minimal amount of catalyst that ensured the catalytic reaction at that flow rate.

Likewise, from a practical point of view, one can reason that those nanocomposites prepared with PUFs that undergone an acid treatment could be preferable as the amount of precious metal is the lowest (ca. 11 mg/g) and the catalytic efficiency was the same. Anyhow, in terms of simplicity, the nanocomposites prepared with pristine PUF are more advantageous as they can be prepared without difficulty and without any unnecessary step.

Consequently, once the effect of the treatment was discarded, the impact of the flow conditions was evaluated by using exclusively those nanocomposites made of pristine PUF (without any treatment except for the acetone rinsing). Results presented in **Figure 3.40** (b) show the variation of the normalised absorbance for experiments carried out at different flow conditions: 0.4, 1.7, 4.1 and 6.8 mL·min^{-1}. In this case, there was a remarkable effect: the higher the flow, the fastest the reaction, albeit the trend was not linear. This result is, in fact, in contradiction with the ones obtained for SPES-C-3-PdNPs, where it was found that at higher flow conditions, the reaction was slower. For PUFs-NCs, since there is a high excess of reactant ($NaBH_4$:4-np = 1000:1), at higher flow conditions, a higher amount of reactants flow through the

nanocomposite for the same period of time and, therefore, the conversion of reactants to products is faster. For SPEs-C-3-NCs, because that excess is smaller ($NaBH_4$:4-np = 20:1), there is only a certain fraction of reactants that can react when passing through the catalytic material.

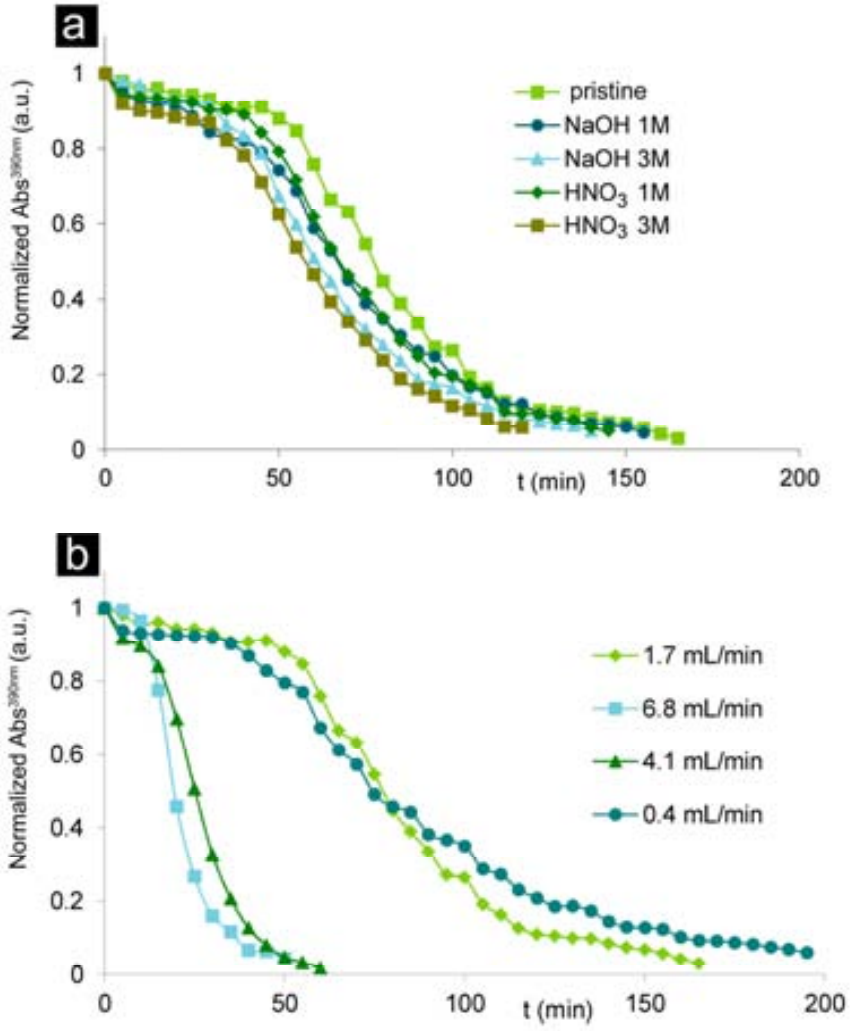

Figure 3.40. Catalytic evaluation of the nanocomposites (a) with different pre-treatments and (b) at different flow conditions for the nanocomposite made of pristine PUF.

Additionally, in order to verify the good results regarding AgNPs stability (proved in Section 3.2.2.2) the synthesized new materials were evaluated in different consecutive catalytic runs. Results presented in **Figure 3.41** correspond to the 4-np reduction by $NaBH_4$ performed with nanocomposites made of pristine PUF for 3 consecutive catalytic runs and at different flow conditions. As it can be clearly seen, the effect of the flow conditions in each run remained the

same as before and it is noteworthy that almost no variation in the reaction rates between runs was observed. The single experiment that was not perfectly consistent was that performed at 1.7 mL·min^{-1}, what can be attributed to experimental errors.

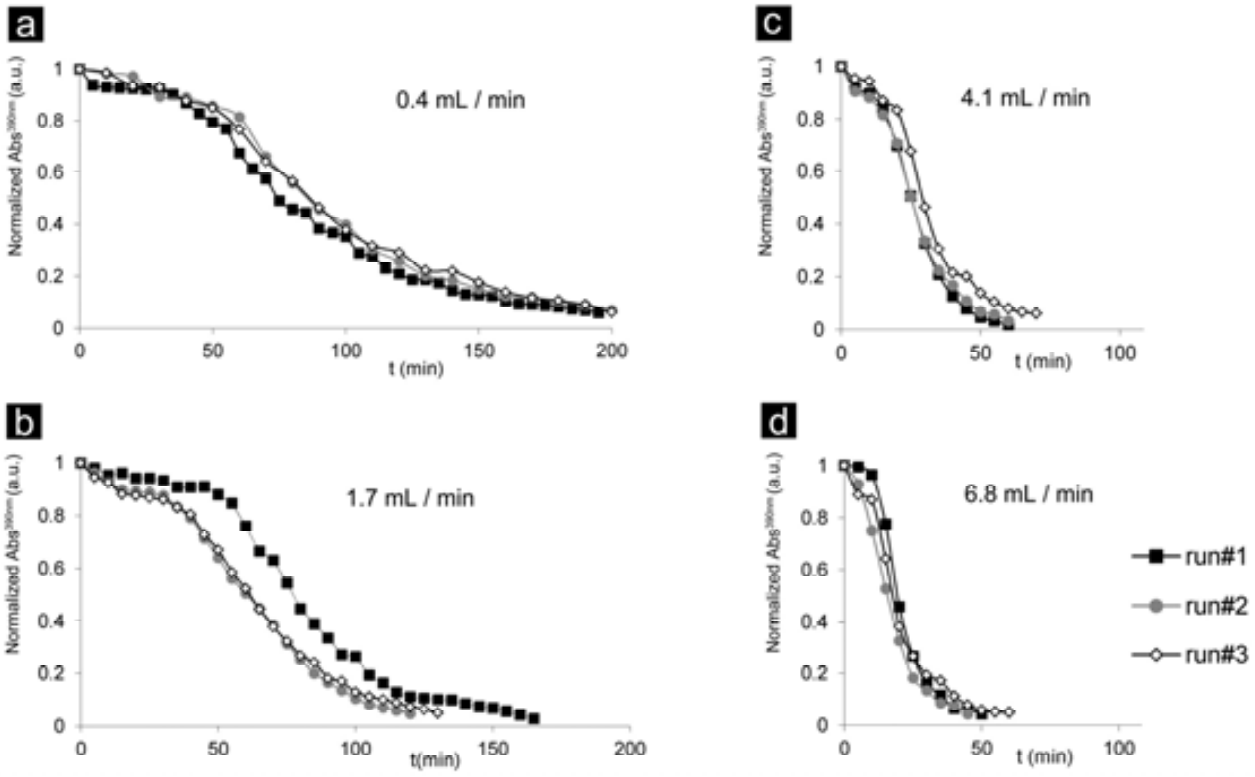

Figure 3.41. Comparison between catalytic cycles in different flow conditions of the nanocomposite made of pristine PUF. ■run#1, ● run#2, ◇ run#3.

So, the developed NCs exhibited durable catalytic activity when evaluating the reduction of nitroaromatic compounds in water. By changing the flow conditions, the catalytic efficiency could be improved: the higher the flow, the higher the reaction rate. This trend was confirmed even after 3 consecutive catalytic cycles, showing that there were almost no losses in the catalytic efficiency after each cycle, what testifies the great suitability of the synthetic technique and of the matrix itself.

Moreover, as main conclusion of this part, the durable catalytic efficiency together with the low loss of the AgNPs to the media seemed to confirm the suitability of the material for catalytic purposes.

3.3.1.4. Silver-nanocomposite textile fibers

For some of the textile-NCs developed, and just as a preliminary prove of concept, the catalytic performance of modified textile was also evaluated by using the same catalytic reduction of 4-np to 4-ap by $NaBH_4$. In a typical run, a piece of nanocomposite (1 cm^2) was added to a stirred vessel of 50 mL containing 4-np (0.5 mM) and $NaBH_4$ (500 mM).[a]

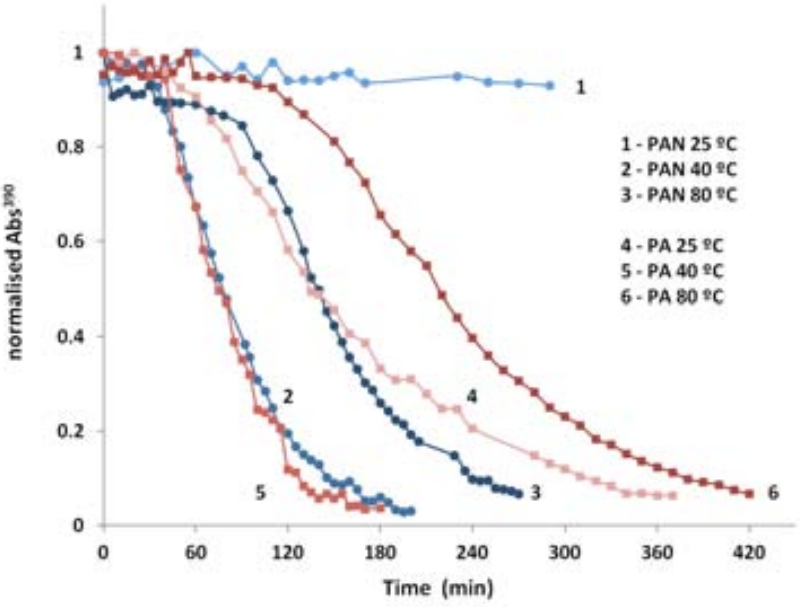

Figure 3.42. Catalytic evaluation of textiles-AgNPs.

As usually, only textile fibers containing AgNPs exhibited catalytic activity when evaluated in batch tests and compared with fabrics without AgNPs (**Figure 3.42**). The only nanocomposite without catalytic activity was PAN (25°C), which also contained the lowest amount of AgNPs (see **Figure 3.28**). That fact might be the most probable cause for such failure. Normalized reaction rate values (**Table 3.24**) fibers (except PAN prepared at 25°C) exhibited the following trend: and increase of the temperature during the synthesis of AgNPs promoted a decrease in the reaction rate. For PAN fibers, this can be clearly explained by TEM images: at a higher temperature, some of the AgNPs were formed inside the matrix and, therefore, they might not be accessible to the reagents.

From these results, it comes that catalytic efficiency not only depends on the metal loading but also on the MNPs' diameter and their spatial distribution. Moreover, these results prove that the fictionalization of typical textile fibers by the inclusion of AgNPs can lead in useful functional materials.

[a] The process was monitored by a Pharmacia LKB Novaspec II spectrometer (λ = 390 nm).

Table 3.24. Normalized reaction rates (k_{app}) obtained for each NC-textiles.

	PAN			PA		
T (°C)	25°C	40°C	80°C	25°C	40°C	80°C
k_{app} (s^{-1}·mg_{Ag}^{-1})	-	0.47	0.13	0.49	0.40	0.31

3.3.1.5. Comparison of the Catalytic performance of the NCs developed

In order to summarize and to facilitate the final comparison of the performance of all the NCs developed when applied in the catalytic reduction of 4-np, **Table 3.25** presents the main results obtained for the first run with each material.

Table 3.25. Main parameters in the catalytic reduction of 4-np for all of the tested NCs (one cycle).

	matrix	Ratio $NaBH_4$:4np	% maximum conversion	k_{app} (s^{-1}·mg_{metal}^{-1})	Induction time (min)
Pd	**SPES-C-1**	100	90	0.17	50
	BM	100	10	X	X
	Nafion	100	90	0.01	50
	SPES-C-3-25a*	20	**100**	-	**0**
	SPES-C-3-20a	20	0	X	X
	SPES-C-3-25b*	20	**100**	X	**0**
	SPES-C-3-20b***	20	**100**	-	**0**
Ag	**SPES-C-1**	100	**100**	**0.67**	20
	Nafion	100	**100**	0.03	60
	PUF-Blank	1000	**100**	0.05	60
	PUF-NaOH 1 M	1000	**100**	0.10	50
	PUF-NaOH 3 M	1000	**100**	0.10	50
	PUF-HNO_3 1 M	1000	**100**	0.12	50
	PUF-HNO_3 3 M	1000	**100**	0.06	50
	PUF-Blank***	1000	**100**	-	10
	PAN 25°C	1000	0	X	X
	PAN 40°C	1000	95	**0.47**	40
	PAN 80°C	1000	90	0.13	100
	PA 25°C	1000	90	**0.49**	60
	PA 40°C	1000	95	**0.40**	40
	PA 80°C	1000	90	0.31	130

* Flux ~0.42 mL·min^{-1}; **Flux ~ 3.7 mL·min^{-1}; *** Flux ~ 6.8 mL·min^{-1}; *X* The parameter could no be obtained; - Not calculated. Best results are highlighted in green.

Note that both batch experiments and flux are included, and that the apparent constat rates are normalized by the catalyst amount (in mg).

As it can be clearly seen, SPES-C-3-25b films loaded with PdNPs offered the best catalytic performance when applied in flux conditions. Moreover, although the flux through the membrane was low (lower than for PUFs-AgNPs and than for SPES-C-3-20b-PdNPs), no activation time was needed so as the reaction started, and conversions of 100 % could be obtained immediately even working with an extremely low ratio $NaBH_4$:4-np (20:1).

Therefore, SPES-C-3-25b films loaded with PdNPs (developed during the last period of this thesis in *Laboratorie de Gènie Chimique*, Toulouse, France) can be considered as the best catalytic nanomaterials obtained during the present work, although some improvements have still to be done (specially regarding their operational flux).

On the other hand, it is also remarkable the high stability of AgNPs-PUFs, that allowed maintaining the catalytic efficiency even after several catalytic runs.

Finally, although the experiments with textile fibers-NCs are preliminary, it is important to note the high reaction rate values obtained for some of the samples, what suggest that such materials could be useful in some catalytic applications.

3.3.2. Bactericidal and anti-biofouling applications

Although the antibacterial mechanism of AgNPs (see Section 1.8.4.2) is still not completely understood, it is thought to be caused by the interaction of metallic silver and Ag^+ ions with different cell targets such as cellular membrane.[105] Considering this well-known bactericidal activity of AgNPs,[41] some of the synthetized nanocomposites containing AgNPs were evaluated in order to determine their bactericidal activity. The experimental procedure is summarized in **Figure 3.43**.

First, to determinate the bactericidal properties of the as-prepared AgNCs and bare matrices, a sample (1cm^2 for films and 1 cm^3 for PUFs) of material was immersed in 20 mL of bacterial suspension of *Escherichia coli*[a] and maintained at 37 °C with gentle agitation (300 rpm). The

[a] *Escherichia coli* (CGSC 5073 K12) was grown overnight in Luria-Bertani medium (LB) at 37 ºC. An aliquot of 20 mL of culture was centrifuged for 10 min at 10000 x g (Eppendorf 5804R) centrifuge. The supernatant liquid was removed and the pellet was suspended again in 10 mL of phosphate buffer saline (PBS) at pH 7.4. The bacterial suspension

microorganisms decay in just phosphate buffered saline (PBS) solution was also evaluated. Periodically, 100 µL of each suspension were collected at different times and counted using plating and incubation on Luria-Bertani (LB). All the manipulations were performed under sterile conditions. (**Figure 3.43** (a))

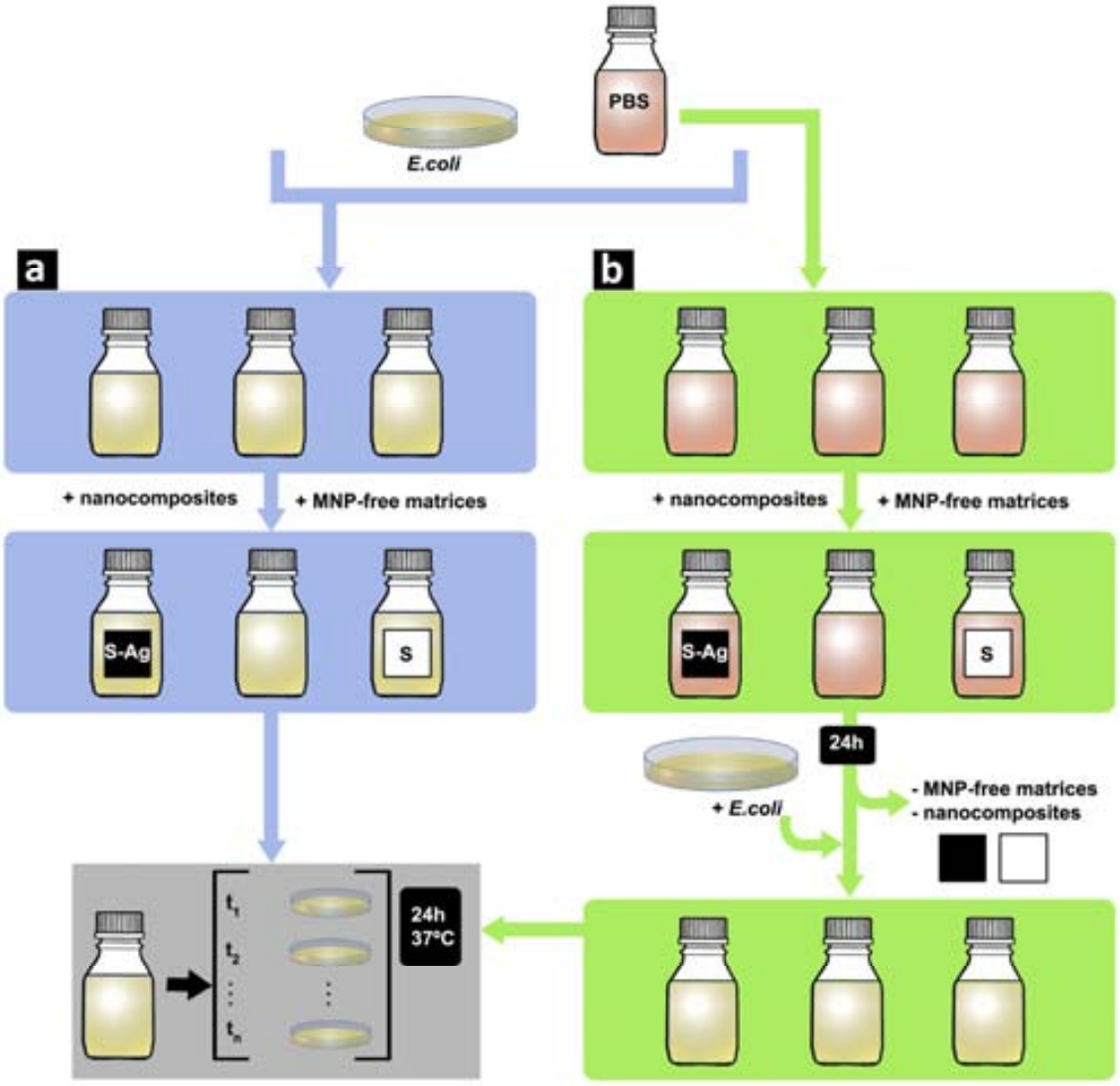

Figure 3.43. Experimental procedure to determine the bactericidal activity of (a) the NC samples, and (b) the Ag released to the media.

Second, in order to evaluate the possible effect of the AgNPs or Ag^+ ions released to the media during the experiments, a piece (1 cm^2 for films and 1 cm^3 for PUFs) of each sample (with or without AgNPs) was immersed in 20 mL of PBS and maintained for 24h at 37 °C with gentle

was then serially diluted down to $1{\cdot}10^7$ colony forming units (CFU) per mL for PUFs and down to $1{\cdot}10^3$ CFU/mL for films. The initial concentration was measured by plating on LB agar.

agitation (300 rpm). After this time, samples were removed, and an *E. coli* pellet was suspended again in the solution. Aliquots of 100 µL were collected at different times and viable microorganisms were counted after cultivation on LB medium. (**Figure 3.43** (b)).

Finally, with the purpose of evaluating the possible adsorption of microorganisms onto the samples during the experiments, some samples used in the microbiological experiments were stained using the Live/Dead Invitrogen Kit BacLight (Invitrogen) by following the protocol detailed by the supplier.[a]

3.3.2.1. Silver-nanocomposite polymeric films

Based on the contact-killing mechanism already observed in previous works[2, 104] nanocomposite samples with a similar area were exposed to the cultivation medium. Samples without AgNPs were also evaluated in order to discriminate any possible effect of the polymeric matrices, such as adsorption of the microorganisms in the matrix. **Figure 3.44** (a) shows the percentage of bacterial viability during the time of the experiment. In all cases, the percentage of cell viability decreased with time.

As it can be seen, both Nafion and SPES-C-1 samples containing AgNPs were able to kill the 100% of bacteria in about 2 h. Comparing these results with the decay of microorganisms in the experiments with film samples without AgNPs, it is possible to observe that cell viability also decayed but at a much-reduced rate. The possibility of *E. coli* adsorption in the matrix was evaluated by fluorescence microscope, and any adsorption was not found in the evaluated samples. Thus the decay in the cell viability in the experiments with MNPs-free samples can principally be attributed to the lack of nutrients in the media.

The effect of the silver loss was evaluated in a different manner: samples containing AgNPs were immersed in PBS solutions and removed after 24 h. Any Ag^+ or leached AgNPs would have remained in this solution. The solutions were then tested as cultivation media after the re-suspension of an *E. coli* pellet and the cell viability over time wasplotted in **Figure 3.44** (b).

From the obtained results, it is possible to conclude that after 24 h at 37 ºC and under gentle agitation, nanocomposite films released some silver to the medium silver (either AgNPs or Ag^+) enough to kill all the microorganisms in 1 h (Nafion) or 3 h (SPES-C-1). This result can be judged in several ways. On the one hand, since Nafion nanocomposites were able to kill all microorganisms in less than 2 h, and that the percentage of silver loss in 2 h (under

[a] Images were acquired with a Zeiss AXIO Imager A1 microscope using a 470 nm laser and suitable filter sets, from *Department de Genètica i Microbiologia* from UAB.

experimental microbiological conditions) was found to be less than the 0.5 % (see Section 3.2.1.3)of the total AgNPs immobilised in the matrix (much lower than the loss due to 24 h of agitation), it seems reasonable to conclude that microorganisms decay in the presence of nanocomposites is not only attributable to the leaching of AgNPs to the media, *ergo* the as-prepared nanocomposites should kill bacteria by a contact mechanism.

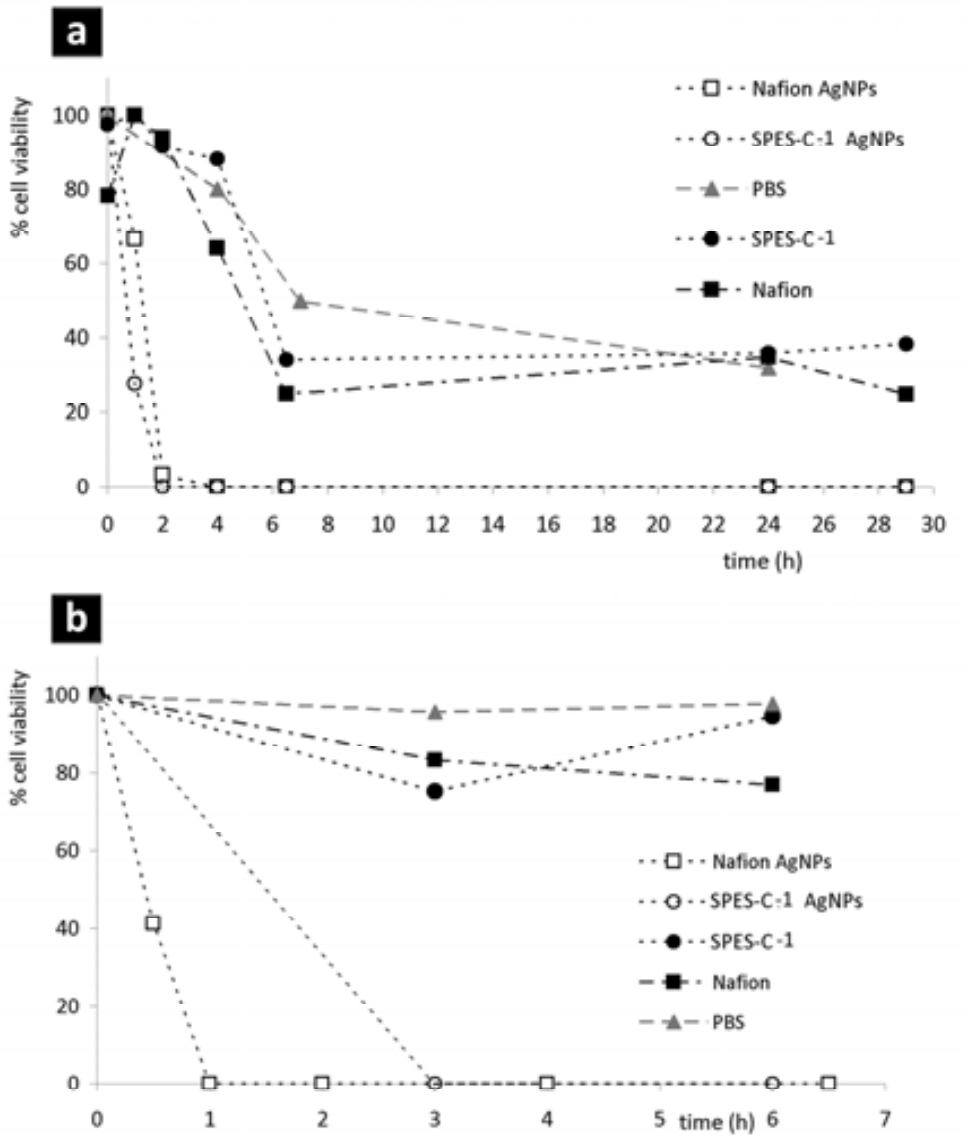

Figure 3.44. a) Bactericidal activity of the different nanocomposites, MNPs-free polymers and PBS solution, b) bactericidal activity of released AgNPs to the media. Initial dose: 10^3 CFU/mL in PBS.

On the other hand, since the amount of silver release to the medium after 24 h of agitation was able to completely disinfect the solution, these nanocomposites can be regarded as silver reservoirs able to provide a residual disinfection effect comparable to that of residual chlorine

which takes place when chlorine or hipochlorous acid are use for water treatment. Thus, thanks to this remaining antibacterial effect the few remaining bacteria cannot rapidly multiply as the reagent is not completely exhausted. Moreover, such a system is preferable instead of strong oxidising agents because they can severely damage membranes as well as they eliminate the biofouling.

3.3.2.2. Silver-nanocomposite polyurethane foams

Up to now, there have been few but encouraging attempts to prepare AgNPs-containing antimicrobial materials based on PUFs.[82-84] Taking into account the previous promising results obtained by other authors using the same polymeric matrix, the catalytic nanocomposite filters were also evaluated as bactericidal filters, envisaging a dual-purpose filter for advanced water treatment.

Following the same procedure described before, cubic samples (1 cm^3) of AgNPs-containing nanocomposite made of pristine PUF were exposed to the cultivation medium. Samples without AgNPs were also evaluated to ascertain any possible effect of the polymeric matrix, such as adsorption of the microorganisms on the matrix. Besides, the antibacterial properties of released silver were also estimated by using a water solution where nanocomposites were immersed for 24 h.

In **Figure 3.45**, where the cell viability percentage is plotted versus time, it is possible to see that the cell population is not affected by the presence of pristine PUF without AgNPs. Even if small variations in the number of cells can be observed, they can be attributed to experimental error of CFU counting or to cell adsorption onto the polymeric matrix. As expected, the percentage of cell viability strongly decreased with time for those samples with AgNPs . In fact, nanocomposite samples (AgNPs-PUF) were able to kill the 100% of bacteria in less than 6.5 h.

Again, the evaluation of the bactericidal efficiency of silver species (AgNPs or Ag^+) was carried out and showed that, the Ag released from the sample (after 24h in 20 mL of a PBS solution under gentle agitation at 37 ºC) was enough to kill all the microorganisms in a short period as 2 h. This means that once the solution is not in contact with the nanocomposite (either because it is missing, deactivated, or exhausted), a remaining mortality rate would be still active, providing a residual disinfection effect prolonging the possible use of the nanocomposite filter.

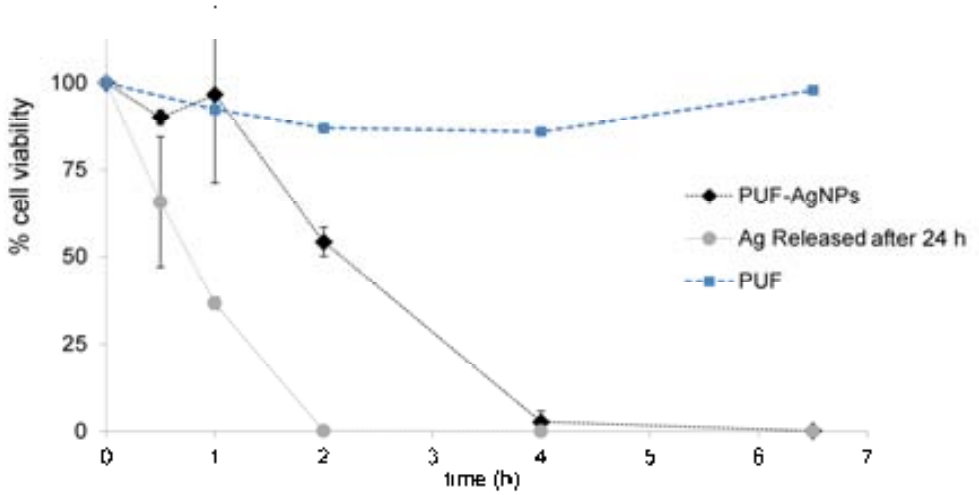

Figure 3.45. Cell viability *vs.* time. Initial dose: 10^7 CFU/mL in PBS.

3.3.2.3. Comparison of the bactericidal performance of the developed NCs

In order to summarize and to facilitate the final comparison of the performance of all the NCs developed when applied in disinfection of water, **Table 3.26** presents the main obtained results, including the estimation of the mortality, expressed as the number of CFU deactivated per second in a single milliliter of the treated solution ($CFU \cdot mL^{-1} \cdot s^{-1}$).

Among the NCs tested, PUF-AgNPs, for whose the calculated value was ca 1000 $CFU \cdot mL^{-1} \cdot s^{-1}$, exhibited the best performance. Although in previous publications focused on the antibacterial application of AgNPs-PUF nanocomposites[82-84] this rate was not explicated, it was possible to calculate it and to state that the nanocomposites here-developed showed a mortality rate 3-6 fold higher. For instance, from the data reported by Phong *et al.*, the calculated mortality rate that attains the highest value was about just 300 $CFU \cdot mL^{-1} \cdot s^{-1}$.[84] This increase in the bactericidal activity could be first accredited to the higher load of AgNPs found in the nanocomposites obtained by the IMS procedure. However, when comparing the results here presented with other Ag-nanocomposites prepared by the same synthetic methodology, (polymeric films (Section 3.3.2.1), resin beads and fibers)[104] the mortality rate of the AgNPs-PUF appeared to be up to 2 orders of magnitude higher. This exceptional result states not only for the synthetic methodology, but also for the suitable usefulness of the polymeric matrix employed.

Table 3.26. Main results in the cell viability studies.

matrix	initial CFU/mL	NC mortality rate CFU/mL·s	*time (h) required for total disinfection*	
			NC	*Ag released after 24h*
SPES-C-1	10^3	1	2	3
Nafion	10^3	1	2	1
PUF	10^7	1014	<6.5	2

Moreover, from the results obtained with the Ag released from the sample (after 24h in 20 mL of a PBS solution under gentle agitation at 37 ºC) a second conclusion can be drawn: the metal amount released to the media (either AgNPs or Ag^+) was enough to kill all the microorganisms in a short period as 2 h. This means that once the solution is not in contact with the nanocomposite (either because it is missing, deactivated, or exhausted), a remaining mortality rate of about 2500 $CFU \cdot mL^{-1} \cdot s^{-1}$ is still active. Hence, these nanocomposites can be considered as Ag reservoirs with a remaining antibacterial effect and, consequently, they can provide a residual disinfection effect prolonging the possible use of the nanocomposite filter.

3.4. References

1. Alonso, A.; Muñoz-Berbel, X.; Vigués, N.; Rodríguez-Rodríguez, R.; Macanás, J.; Muñoz, M.; Mas, J.; Muraviev, D. N., Superparamagnetic Ag@Co-Nanocomposites on Granulated Cation Exchange Polymeric Matrices with Enhanced Antibacterial Activity for the Environmentally Safe Purification of Water. *Advanced Functional Materials* **2013,** *23* (19), 2450-2458.
2. Alonso, A.; Muñoz-Berbel, X.; Vigués, N.; Macanás, J.; Muñoz, M.; Mas, J.; Muraviev, D. N., Characterization of Fibrous Polymer Silver/Cobalt Nanocomposite with Enhanced Bactericide Activity. *Langmuir* **2011,** *28* (1), 783-790.
3. Ruiz, P.; Macanas, J.; Munoz, M.; Muraviev, D., Intermatrix synthesis: easy technique permitting preparation of polymer-stabilized nanoparticles with desired composition and structure. *Nanoscale Res. Lett.* **2011,** *6* (1), 343.
4. Blanco, J. F.; Nguyen, Q. T.; Schaetzel, P., Novel hydrophilic membrane materials: sulfonated polyethersulfone Cardo. *J. Membrane Sci.* **2001,** *186* (2), 267-279.
5. Blanco, J. F.; Nguyen, Q. T.; Schaetzel, P., Sulfonation of polysulfones: Suitability of the sulfonated materials for asymmetric membrane preparation. *J. Appl. Polym. Sci.* **2002,** *84* (13), 2461-2473.
6. Di Vona, M. L.; Luchetti, L.; Spera, G. P.; Sgreccia, E.; Knauth, P., Synthetic strategies for the preparation of proton-conducting hybrid polymers based on PEEK and PPSU for PEM fuel cells. *Comptes Rendus Chimie* **2008,** *11* (9), 1074-1081.

7. Jia, L.; Xu, X. F.; Zhang, H. J.; Xu, J. P., Permeation of nitrogen and water vapor through sulfonated polyetherethersulfone membrane. *J. Polym. Sci. Pol. Phys.* **1997,** *35* (13), 2133-2140.
8. Macanás, J.; Ruiz, P.; Alonso, A.; Muñoz, M.; Muraviev, D. N., Ion Exchange-Assisted Synthesis of Polymer Stabilized Metal Nanoparticles. In *Ion Exchange and Solvent Extraction*, Sengupta, A. K., Ed. CRC Press: 2011; pp 1-44.
9. Noshay, A.; Robeson, L. M., Sulfonated polysulfone. *J. Appl. Polym. Sci.* **1976,** *20* (7), 1885-1903.
10. Xing, D.; Kerres, J., Improved performance of sulfonated polyarylene ethers for proton exchange membrane fuel cells. *Polym. Advan. Technol.* **2006,** *17* (7□8), 591-597.
11. Di Vona, M. L.; D'Epifanio, A.; Marani, D.; Trombetta, M.; Traversa, E.; Licoccia, S., SPEEK/PPSU-based organic–inorganic membranes: proton conducting electrolytes in anhydrous and wet environments. *J. Membrane Sci.* **2006,** *279* (1–2), 186-191.
12. Dyck, A.; Fritsch, D.; Nunes, S., Proton-conductive membranes of sulfonated polyphenylsulfone. *J. Appl. Polym. Sci.* **2002,** *86* (11), 2820-2827.
13. Srithong, S.; Jiraratananon, R.; Hansupalak, N., A simple postsulfonation of poly (arylene ether sulfone) Radel® R. *J. Appl. Polym. Sci.* **2011,** *119* (2), 973-976.
14. Sun, H.; Venkatasubramanian, N.; Houtz, M.; Mark, J.; Tan, S.; Arnold, F.; Lee, C. Y., Molecular composites by incorporation of a rod-like polymer into a functionalized high-performance polymer, and their conversion into microcellular foams. *Colloid and Polymer Science* **2004,** *282* (5), 502-510.
15. Di Vona, M. L.; Sgreccia, E.; Tamilvanan, M.; Khadhraoui, M.; Chassigneux, C.; Knauth, P., High ionic exchange capacity polyphenylsulfone (SPPSU) and polyethersulfone (SPES) cross-linked by annealing treatment: Thermal stability, hydration level and mechanical properties. *J. Membrane Sci.* **2010,** *354* (1–2), 134-141.
16. Xing, D.; Kerres, J., Improved performance of sulfonated polyarylene ethers for proton exchange membrane fuel cells. *Polym. Advan. Technol.* **2006,** *17* (7-8), 591-597.
17. Gao, Q. J.; Wang, Y. X.; Xu, L.; Wang, Z. T.; Wei, G. Q., Proton-exchange Sulfonated Poly(ether ether ketone)/Sulfonated Phenolphthalein Poly(ether sulfone) Blend Membranes in DMFCs. *Chinese. J. Chem. Eng.* **2009,** *17* (6), 934-941.
18. Domènech, B.; Munoz, M.; Muraviev, D. N.; Macanas, J., Polymer-stabilized palladium nanoparticles for catalytic membranes: ad hoc polymer fabrication. *Nanoscale Res. Lett.* **2011,** *6* (406), 5.
19. Domènech, B.; Muñoz, M.; Muraviev, D. N.; Macanás, J., Catalytic membranes with palladium nanoparticles: From tailored polymer to catalytic applications. *Catal. Today* **2012,** *193* (1), 158-164.
20. Domènech, B.; Muñoz, M.; Muraviev, D. N.; Macanás, J., Nanocomposite Membranes with Pd and Ag Nanoparticles. A New Material for Catalytic Membranes Development. *Procedia Engineering* **2012,** *44* (0), 1264-1267.
21. Li, L.; Wang, Y. X., Sulfonated polyethersulfone Cardo membranes for direct methanol fuel cell. *J. Membrane Sci.* **2005,** *246* (2), 167-172.
22. Kerres, J.; Ullrich, A.; Hein, M., Preparation and characterization of novel basic polysulfone polymers. *J. Polym. Sci. Pol. Chem.* **2001,** *39* (17), 2874-2888.
23. Heitner-Wirguin, C., Recent advances in perfluorinated ionomer membranes: structure, properties and applications. *J. Membrane Sci.* **1996,** *120* (1), 1-33.
24. Mauritz, K. A.; Moore, R. B., State of understanding of nafion. *Chem Rev* **2004,** *104* (10), 4535-85.
25. Hasany, S. M.; Saeed, M. M.; Ahmed, M., Sorption of traces of silver ions onto polyurethane foam from acidic solution. *Talanta* **2001,** *54* (1), 89-98.

26. Domènech, B.; Ziegler, K.; Macanas, J.; Carrillo, F.; Munoz, M.; Muraviev, D., Development of novel catalytically active polymer-metal-nanocomposites based on activated foams and textile fibers. *Nanoscale Res. Lett.* **2013,** *8* (1), 238.
27. Pretsch, E.; Bühlmann, P.; Affolter, C.; Pretsch, E.; Bhuhlmann, P.; Affolter, C., *Structure determination of organic compounds*. Springer: 2000.
28. López-Mesas, M.; Navarrete, E. R.; Carrillo, F.; Palet, C., Bioseparation of Pb (II) and Cd (II) from aqueous solution using cork waste biomass. Modeling and optimization of the parameters of the biosorption step. *Chemical Engineering Journal* **2011,** *174* (1), 9-17.
29. Louis, C., Gold Nanoparticles: Recent Advances in CO Oxidation. In *Nanoparticles and Catalysis*, Wiley-VCH Verlag GmbH & Co. KGaA: 2008; pp 475-503.
30. Bhattacharjee, S.; Dotzauer, D. M.; Bruening, M. L., Selectivity as a Function of Nanoparticle Size in the Catalytic Hydrogenation of Unsaturated Alcohols. *J. Am. Chem. Soc.* **2009,** *131* (10), 3601-3610.
31. Bhattacharyya, D.; Xu, J.; Bachas, L.; Meyer, D.; Tee, Y., Bimetallic nanoparticles: Membrane-based synthesis for applications to PCB and TCE dechlorination. *Abstr. Pap. Am. Chem. S.* **2005,** *229*, 168-IEC.
32. Yang, J.; Sun, D.; Li, J.; Yang, X.; Yu, J.; Hao, Q.; Liu, W.; Liu, J.; Zou, Z.; Gu, J., In situ deposition of platinum nanoparticles on bacterial cellulose membranes and evaluation of PEM fuel cell performance. *Electrochimica Acta* **2009,** *54* (26), 6300-6305.
33. Berger, D. J., Fuel Cells and Precious-Metal Catalysts. *Science* **1999,** *286* (5437), 49.
34. Ruiz, P.; Munoz, M.; Macanas, J.; Muraviev, D. N., Intermatrix Synthesis of Polymer-Copper Nanocomposites with Tunable Parameters by Using Copper Comproportionation Reaction. *Chem. Mater.* **2010,** *22* (24), 6616-6623.
35. Ruiz, P.; Munoz, M.; Macanas, J.; Turta, C.; Prodius, D.; Muraviev, D. N., Intermatrix synthesis of polymer stabilized inorganic nanocatalyst with maximum accessibility for reactants. *Dalton T.* **2010,** *39* (7), 1751-1757.
36. Alonso, A.; Macanas, J.; Shafir, A.; Munoz, M.; Vallribera, A.; Prodius, D.; Melnic, S.; Turta, C.; Muraviev, D. N., Donnan-exclusion-driven distribution of catalytic ferromagnetic nanoparticles synthesized in polymeric fibers. *Dalton T.* **2010,** *39* (10), 2579-2586.
37. Bastos-Arrieta, J.; Shafir, A.; Alonso, A.; Muñoz, M.; Macanás, J.; Muraviev, D. N., Donnan exclusion driven intermatrix synthesis of reusable polymer stabilized palladium nanocatalysts. *Catal. Today* **2012,** *193* (1), 207-212.
38. Domènech, B.; Vigués, N.; Mas, J.; Muñoz, M.; Muraviev, D. N.; Macanás, J., Polymer-Metal Nanocomposites Containing Dual-Function Metal Nanoparticles: Ion-Exchange Materials Modified With Catalytically-Active and Bactericide Silver Nanoparticles. *Solvent Extraction and Ion Exchange* **2013**.
39. Domènech, B.; Muñoz, M.; Muraviev, D.; Macanás, J., Uncommon patterns in Nafion films loaded with sil-ver nanoparticles. *Chemical Communications* **2014**.
40. Zodrow, K.; Brunet, L.; Mahendra, S.; Li, D.; Zhang, A.; Li, Q.; Alvarez, P. J., Polysulfone ultrafiltration membranes impregnated with silver nanoparticles show improved biofouling resistance and virus removal. *Water Research* **2009,** *43* (3), 715-723.
41. Panáček, A.; Kvítek, L.; Prucek, R.; Kolář, M.; Večeřová, R.; Pizúrová, N.; Sharma, V. K.; Nevěčná, T. j.; Zbořil, R., Silver Colloid Nanoparticles: Synthesis, Characterization, and Their Antibacterial Activity. *The Journal of Physical Chemistry B* **2006,** *110* (33), 16248-16253.
42. Choi, O.; Deng, K. K.; Kim, N.-J.; Ross Jr, L.; Surampalli, R. Y.; Hu, Z., The inhibitory effects of silver nanoparticles, silver ions, and silver chloride colloids on microbial growth. *Water Research* **2008,** *42* (12), 3066-3074.

43. Taurozzi, J. S.; Arul, H.; Bosak, V. Z.; Burban, A. F.; Voice, T. C.; Bruening, M. L.; Tarabara, V. V., Effect of filler incorporation route on the properties of polysulfone-silver nanocomposite membranes of different porosities. *J. Membrane Sci.* **2008,** *325* (1), 58-68.
44. Lee, S. Y.; Kim, H. J.; Patel, R.; Im, S. J.; Kim, J. H.; Min, B. R., Silver nanoparticles immobilized on thin film composite polyamide membrane: characterization, nanofiltration, antifouling properties. *Polym. Advan. Technol.* **2007,** *18* (7), 562-568.
45. Yang, H.-L.; Lin, J. C.-T.; Huang, C., Application of nanosilver surface modification to RO membrane and spacer for mitigating biofouling in seawater desalination. *Water Research* **2009,** *43* (15), 3777-3786.
46. Cao, X.; Tang, M.; Liu, F.; Nie, Y.; Zhao, C., Immobilization of silver nanoparticles onto sulfonated polyethersulfone membranes as antibacterial materials. *Colloids and Surfaces B: Biointerfaces* **2010,** *81* (2), 555-562.
47. Schleußner, C., Diffusionsvorgänge in Gelatine. *Kolloid-Zeitschrift* **1922,** *31* (6), 347-352.
48. Henisch, H. K., *Crystals in gels and Liesegang rings*. Cambridge University Press: 2005.
49. Fujimura, M.; Hashimoto, T.; Kawai, H., Small-angle x-ray scattering study of perfluorinated ionomer membranes. 2. Models for ionic scattering maximum. *Macromolecules* **1982,** *15* (1), 136-144.
50. Dreyfus, B.; Gebel, G.; Aldebert, P.; Pineri, M.; Escoubes, M.; Thomas, M., Distribution of the « micelles » in hydrated perfluorinated ionomer membranes from SANS experiments. *J. Phys. France* **1990,** *51* (12), 1341-1354.
51. Gebel, G., Structural evolution of water swollen perfluorosulfonated ionomers from dry membrane to solution. *Polymer* **2000,** *41* (15), 5829-5838.
52. Gebel, G.; Lambard, J., Small-Angle Scattering Study of Water-Swollen Perfluorinated Ionomer Membranes. *Macromolecules* **1997,** *30* (25), 7914-7920.
53. Rubatat, L.; Rollet, A. L.; Gebel, G.; Diat, O., Evidence of Elongated Polymeric Aggregates in Nafion. *Macromolecules* **2002,** *35* (10), 4050-4055.
54. Litt, M. H., A Reevaluation of Nation Morphology. *American Chemical Society Polymer Preprints* **1997,** *38*.
55. Kreuer, K.-D.; Portale, G., A Critical Revision of the Nano-Morphology of Proton Conducting Ionomers and Polyelectrolytes for Fuel Cell Applications. *Advanced Functional Materials* **2013,** *23* (43), 5390-5397.
56. Gierke, T. D.; Munn, G. E.; Wilson, F. C., Morphology of Perfluorosulfonated Membrane Products. In *Perfluorinated Ionomer Membranes*, AMERICAN CHEMICAL SOCIETY: 1982; Vol. 180, pp 195-216.
57. Bertoncello, P.; Peruffo, M.; Unwin, P. R., Formation and evaluation of electrochemically-active ultra-thin palladium-Nafion nanocomposite films. *Chemical Communications* **2007,** (16), 1597-1599.
58. Smotkin, E. S.; Brown, R. M.; Rabenberg, L. K.; Salomon, K.; Bard, A. J.; Campion, A.; Fox, M. A.; Mallouk, T. E.; Webber, S. E.; White, J. M., Ultrasmall particles of cadmium selenide and cadmium sulfide formed in Nafion by an ion-dilution technique. *The Journal of Physical Chemistry* **1990,** *94* (19), 7543-7549.
59. Zhang, Y.; Kang, D.; Saquing, C.; Aindow, M.; Erkey, C., Supported platinum nanoparticles by supercritical deposition. *Ind. Eng. Chem. Res.* **2005,** *44* (11), 4161-4164.
60. Liu, P.; Bandara, J.; Lin, Y.; Elgin, D.; Allard, L. F.; Sun, Y.-P., Formation of Nanocrystalline Titanium Dioxide in Perfluorinated Ionomer Membrane. *Langmuir* **2002,** *18* (26), 10398-10401.
61. Sun, Y.-P.; Atorngitjawat, P.; Lin, Y.; Liu, P.; Pathak, P.; Bandara, J.; Elgin, D.; Zhang, M., Nanoscale cavities in ionomer membrane for the formation of nanoparticles. *J. Membrane Sci.* **2004,** *245* (1–2), 211-217.

62. Moore, R.; Martin, C., Chemical and morphological properties of solution-cast perfluorosulfonate ionomers. *Macromolecules* **1988,** *21* (5), 1334-1339.
63. Pintauro, P. N.; Bennion, D. N., Mass transport of electrolytes in membranes. 1. Development of mathematical transport model. *Industrial & engineering chemistry fundamentals* **1984,** *23* (2), 230-234.
64. Sode, A.; Ingle, N. J. C.; McCormick, M.; Bizzotto, D.; Gyenge, E.; Ye, S.; Knights, S.; Wilkinson, D. P., Controlling the deposition of Pt nanoparticles within the surface region of Nafion. *J. Membrane Sci.* **2011,** *376* (1–2), 162-169.
65. Sun, Y.; Xia, Y., Shape-controlled synthesis of gold and silver nanoparticles. *Science* **2002,** *298* (5601), 2176-2179.
66. Ahamad, N.; Prezgot, D.; Ianoul, A., Patterning silver nanocubes in monolayers using phase separated lipids as templates. *J. Nanopart. Res.* **2012,** *14* (2), 1-10.
67. Sun, Y.; Mayers, B.; Herricks, T.; Xia, Y., Polyol synthesis of uniform silver nanowires: a plausible growth mechanism and the supporting evidence. *Nano Lett.* **2003,** *3* (7), 955-960.
68. Wiley, B.; Sun, Y.; Mayers, B.; Xia, Y., Shape-Controlled Synthesis of Metal Nanostructures: The Case of Silver. *Chemistry-A European Journal* **2005,** *11* (2), 454-463.
69. Sachdeva, A.; Sodaye, S.; Pandey, A. K.; Goswami, A., Formation of Silver Nanoparticles in Poly(perfluorosulfonic) Acid Membrane. *Analytical Chemistry* **2006,** *78* (20), 7169-7174.
70. Imre, Á.; Beke, D. L.; Gontier-Moya, E.; Szabó, I. A.; Gillet, E., Surface Ostwald ripening of Pd nanoparticles on the MgO (100) surface. *Appl Phys A* **2000,** *71* (1), 19-22.
71. Houk, L. R.; Challa, S. R.; Grayson, B.; Fanson, P.; Datye, A. K., The Definition of "Critical Radius" for a Collection of Nanoparticles Undergoing Ostwald Ripening. *Langmuir* **2009,** *25* (19), 11225-11227.
72. Wang, J.; Liu, P.; Wang, S.; Han, W.; Wang, X.; Fu, X., Nanocrystalline zinc oxide in perfluorinated ionomer membranes: Preparation, characterization, and photocatalytic properties. *Journal of Molecular Catalysis A: Chemical* **2007,** *273* (1–2), 21-25.
73. Wang, S. M.; Liu, P.; Wang, X. X.; Fu, X. Z., Homogeneously distributed CdS nanoparticles in Nafion membranes: Preparation, characterization, and photocatalytic properties. *Langmuir* **2005,** *21* (25), 11969-11973.
74. Mark, J. E., *Physical properties of polymers handbook*. AIP Press: Michigan, US, 1996.
75. Uhlig, K. K., *Discovering Polyurethanes*. Hanser-Gardner Publications: 1999.
76. Kroschwitz, J. I.; Seidel, A., *Kirk-Othmer Encyclopedia of Chemical Technology*. John Wiley and Sons: 1999.
77. Madaleno, L.; Pyrz, R.; Crosky, A.; Jensen, L. R.; Rauhe, J. C. M.; Dolomanova, V.; de Barros Timmons, A. M. M. V.; Cruz Pinto, J. J.; Norman, J., Processing and characterization of polyurethane nanocomposite foam reinforced with montmorillonite–carbon nanotube hybrids. *Composites Part A: Applied Science and Manufacturing* **2013,** *44* (0), 1-7.
78. Han, J. G.; Xiang, Y. Q.; Zhu, Y., New Antibacterial Composites: Waterborne Polyurethane/Gold Nanocomposites Synthesized Via Self-Emulsifying Method. *J Inorg Organomet Polym* **2013**, 1-8.
79. Apyari, V.; Volkov, P.; Dmitrienko, S., Synthesis and optical properties of polyurethane foam modified with silver nanoparticles. *Advances in Natural Sciences: Nanoscience and Nanotechnology* **2012,** *3* (1), 015001.
80. Chou, C.-W.; Hsu, S.-h.; Chang, H.; Tseng, S.-M.; Lin, H.-R., Enhanced thermal and mechanical properties and biostability of polyurethane containing silver nanoparticles. *Polymer Degradation and Stability* **2006,** *91* (5), 1017-1024.
81. Deka, H.; Karak, N.; Kalita, R. D.; Buragohain, A. K., Bio-based thermostable, biodegradable and biocompatible hyperbranched polyurethane/Ag nanocomposites with antimicrobial activity. *Polymer Degradation and Stability* **2010,** *95* (9), 1509-1517.

82. Jain, P.; Pradeep, T., Potential of silver nanoparticle-coated polyurethane foam as an antibacterial water filter. *Biotechnol Bioeng* **2005,** *90* (1), 59-63.
83. Mulongo, G.; Mbabazi, J.; Nnamuyomba, P.; Hak-Chol, S., Water Bactericidal Properties of Nanosilver-Polyurethane Composites. *Nanoscience and Nanotechnology* **2011,** *1* (2), 40-42.
84. Phong, N. T. P.; Thanh, N. V. K.; Phuong, P. H. In *Fabrication of antibacterial water filter by coating silver nanoparticles on flexible polyurethane foams*, Journal of Physics: Conference Series, IOP Publishing: 2009; p 012079.
85. MacKay, W. Antimicrobial foam and method of manufacture. 2010.
86. Domènech, B.; Bastos-Arrieta, J.; Alonso, A.; Muñoz, M.; Muraviev, D. N.; Macanás, J., *Bifunctional Polymer-Metal Nanocomposite Ion Exchange Materials*. 1 ed.; Iva Lipovic: Reijeka, 2012; p 35-72.
87. Campelo, J. M.; Luna, D.; Luque, R.; Marinas, J. M.; Romero, A. A., Sustainable Preparation of Supported Metal Nanoparticles and Their Applications in Catalysis. *Chemsuschem* **2009,** *2* (1), 18-45.
88. Ye, W.; Leung, M. F.; Xin, J.; Kwong, T. L.; Lee, D. K. L.; Li, P., Novel core-shell particles with poly (< i> n</i>-butyl acrylate) cores and chitosan shells as an antibacterial coating for textiles. *Polymer* **2005,** *46* (23), 10538-10543.
89. Sójka-Ledakowicz, J.; Olczyk, J.; Sielski, J., Synthesis of zinc oxide in an emulsion system and its deposition on PES nonwoven fabrics. *Fibres & Textiles in Eastern Europe* **2011,** *19* (2), 85.
90. Sojka-Ledakowicz, J.; Lewartowska, J.; Kudzin, M.; Jesionowski, T.; Siwińska-Stefańska, K.; Krysztafkiewicz, A., Modification of textile materials with micro-and nano-structural metal oxides. *Fibres & Textiles in Eastern Europe* **2008**.
91. Sepahi Rad, P.; Montazer, M.; Karim Rahimi, M., Simultaneous antimicrobial and dyeing of wool: a facial method. *J. Appl. Polym. Sci.* **2011,** *122* (2), 1405-1411.
92. Yoon, N. S.; Lim, Y. J.; Tahara, M.; Takagishi, T., Mechanical and dyeing properties of wool and cotton fabrics treated with low temperature plasma and enzymes. *Textile research journal* **1996,** *66* (5), 329-336.
93. Kalashnik, A., The role of different factors in creation of the structure of stabilized acrylic fibres. *Fibre Chem* **2002,** *34* (1), 10-17.
94. *Metal-Polymer Nanocomposites*. John Wiley and Sons Ltd: New York/US, 2004.
95. Herves, P.; Pérez-Lorenzo, M.; Liz-Marzán, L. M.; Dzubiella, J.; Lu, Y.; Ballauff, M., Catalysis by metallic nanoparticles in aqueous solution: model reactions. *Chemical Society Reviews* **2012,** *41* (17), 5577-5587.
96. Jose Ruben, M.; Jose Luis, E.; Alejandra, C.; Katherine, H.; Juan, B. K.; Jose Tapia, R.; Miguel Jose, Y., The bactericidal effect of silver nanoparticles. *Nanotechnology* **2005,** *16* (10), 2346.
97. Astruc, D.; Lu, F.; Aranzaes, J. R., Nanoparticles as recyclable catalysts: The frontier between homogeneous and heterogeneous catalysis. *Angew. Chem. Int. Edit.* **2005,** *44* (48), 7852-7872.
98. Schlapbach, L.; Zuttel, A., Hydrogen-storage materials for mobile applications. *Nature* **2001,** *414* (6861), 353-358.
99. Vogel, W.; He, W.; Huang, Q. H.; Zou, Z. Q.; Zhang, X. G.; Yang, H., Palladium nanoparticles "breathe" hydrogen; a surgical view with X-ray diffraction. *Int. J. Hydrogen Energ.* **2010,** *35* (16), 8609-8620.
100. Macanás, J.; Ouyang, L.; Bruening, M. L.; Munoz, M.; Remigy, J. C.; Lahitte, J. F., Development of polymeric hollow fiber membranes containing catalytic metal nanoparticles. *Catal. Today* **2010,** *156* (3-4), 181-186.

101. Emin, C.; Remigy, J.-C.; Lahitte, J.-F., Influence of UV grafting conditions and gel formation on the loading and stabilization of palladium nanoparticles in photografted polyethersulfone membrane for catalytic reactions. *J. Membrane Sci.* **2014,** *455* (0), 55-63.
102. Signori, A. M.; Santos, K. d. O.; Eising, R.; Albuquerque, B. L.; Giacomelli, F. C.; Domingos, J. B., Formation of catalytic silver nanoparticles supported on branched polyethyleneimine derivatives. *Langmuir* **2010,** *26* (22), 17772-17779.
103. Nguyen, R.-V.; Yao, X.-Q.; Bohle, D. S.; Li, C.-J., Gold-and silver-catalyzed highly regioselective addition of active methylenes to dienes, triene, and cyclic enol ethers. *Organic letters* **2005,** *7* (4), 673-675.
104. Alonso, A.; Vigues, N.; Munoz-Berbel, X.; Macanas, J.; Munoz, M.; Mas, J.; Muraviev, D. N., Environmentally-safe bimetallic Ag@Co magnetic nanocomposites with antimicrobial activity. *Chemical Communications* **2011,** *47* (37), 10464-10466.
105. Jung, W. K.; Koo, H. C.; Kim, K. W.; Shin, S.; Kim, S. H.; Park, Y. H., Antibacterial activity and mechanism of action of the silver ion in Staphylococcus aureus and Escherichia coli. *Appl Environ Microbiol* **2008,** *74* (7), 2171-8.

Learn what is to be taken seriously and laugh at the rest.
(H.Hesse)

4 CONCLUSIONS

In the present work I have introduced and further discussed the results achieved during the development of my PhD thesis, focused on the obtainment and the study of new materials for wastewater treatment purposes *via* the development of polymer-metal nanocomposites (PMNCs) with biocidal and/or catalytic activity. To do so, I have divided the whole content in three main areas:

i) the obtainment and/or modification and deep characterization of the polymeric matrices,
ii) the synthesis of metal nanoparticles (MNPs) in the polymeric matrices *via* the Intermatrix Synthesis (IMS) procedure and the characterization of the corresponding nanocomposites, and
iii) the application of the developed PMNCs as catalysts and/or as biocides.

Hence, in this Chapter I will present those conclusions that have been derived from each part, and which have allowed me to draw a general conclusion of the work done.

As main conclusion it is possible to state that the principal objective of this thesis has been attained since **the obtainment and study of new systems for dual-purpose wastewater**

treatment purposes *via* the development of polymer-metal nanocomposites (PMNCs) with biocide and/or catalytic activity, has been successfully achieved by the Intermatrix Synthesis Procedure (IMS).

Considering that part of the work has been specially focused on the correct choice of the polymeric matrices (in regards to their shape, stability, low cost, an son on) and on their adequacy to the final application and to the synthetic methodology employed, some of the experimental results regarding the **obtainment and adequacy of the polymeric matrices** in regards to the IMS have to be considered. In fact, this part of the work has allowed concluding that:

[1] In regards to the sulfonation of polyphenylsulfone (PPSU) and taking into account that after 10 different attempts, none of the routes leaded to a successful sulfonation, I conclude that such modification can not be performed under the experimental conditions tested. In this sense, and although two sulfonation routes based on literature were applied, uncontrolled variables (such as air humidity, ambient temperature and so on) and the lack in a good control in the temperature could have played an important role in the reaction.

[2] The feasibility of the sulfonation of polyethersulfone with Cardo group (PES-C) was successfully attained under mild reaction conditions. By changing some of the reaction parameters (reaction time, mostly), three different SPES-C polymers (SPES-C-1, SPES-2 and SPES-C-3) with different physico-chemical properties were obtained.

[3] Given that the degree of sulfonation could not be perfectly controlled, it is also possible to conclude that the sulfonation reaction is irreproducible. Again, uncontrolled variables (such as air humidity, ambient temperature and so on) and the lack in a good control in the temperature could have played an important role in the reaction. That means that the obtained polymer needs to be fully characterized before use.

[4] It has been confirmed that it is possible to obtain SPES-C films by wet phase inversion. However, each different polymer leaded to different film morphology: films made of SPES-C-1 appeared to be dense, films made with a blend of SPES-C-2 and PES-C (Blend membranes, BM) were porous and films made of SPES-C-3 were also porous.

[5] The experimental results regarding the characterization of films ratify that film morphology strongly affects the physico-chemical properties of the film, such as the matrix water uptake (MWU), hydraulic permeability (L_p) or their ion exchange capacity (IEC).

[6] For the study comprising the modification of Polyurethane foams (PUFs) the results provided that the chemical structure of the matrix can not be altered in order to generate ion-exchange positions by applying mild treatments (NaOH 1M, NaOH 3M, HNO_3 1M or HNO_3 3M). Therefore, and as suggested by literature, the chemical stability of PUFs is confirmed. In addition, after determining the IEC (either possible cation or anion exchange groups present in the matrix), in general terms, almost no differences between IEC values were observed.

Once some of the polymeric matrices have been shown to be appropriate for the central purpose of the thesis, in regards to the results showed, the *a priori* idea of evaluating the possibility to **obtain MNPs in the targeted by IMS** has led to conclude that:

[7] The IMS can be successfully applied to all of the targeted polymeric matrices in order to obtain either PdNPs or AgNPs.

[8] Either PdNPs or AgNPs (diameters between 3-13 nm) can be obtained by IMS in SPES-C-1 films, BMs, Nafion and SPES-C-3 films.

[9] The loading of the metal was found to be strongly influenced by the IEC of the matrix. In this sense, and in general, it is possible to state that: the higher the IEC, the higher the load. However the exception was found for SPES-C-3 films, in which although the IEC was found to be higher than for Nafion films, the load was lower.

[10] The mean size of the MNPs is strongly influenced by the IEC of the matrix, especially for PdNPs: the higher the IEC, the biggest the MNPs obtained.

[11] The *a priori* idea that sequential MNPs loads can be performed has been successfully proved, since, by applying a second IMS step, it has been possible to double the load of Pd in BMs. But, aggregates were obtained, whose formation can be attributed either to the

preparation procedure or due to the change in the mobility of the PdNPS in the second load, when the solid particles came together via random aggregation processes.

[12] In all of the matrices tested, and comparing the load between Pd and Ag, the obtained results showed a higher load of Pd. The different ion mobility and, particularly, the different charge of ions (Ag^+ and $[Pd(NH_3)_4]^{2+}$) might be the reasons for such differences. Moreover, the ratio Pd:Ag was found to be constant, what seems to state for the reproducibility of the synthetic methodology employed and of the films used.

[13] It has also been verified that both, the metal and the matrix, strongly influence the final MNPs distribution. Although MNPs were usually found to grow mostly on the surface (what is in agreement with the Donnan exclusion effect, DEE), in some cases small well-dispersed and non-aggregated MNPs could be found in the inner part of the matrices.

[14] Furthermore, considering the uncommon patterns found in Nafion films loaded with AgNPs, the embedment of AgNPs can be considered as a sort of nanometric staining agent because the incorporation of NPs in the matrix can reveal the true morphology of the ionic channels of the film.

[15] The knowledge basis concerning the suitability of MNPs stabilization by polymers has also been proved. In this sense, and taking into account that the studies under extreme aging conditions, such us sonication, showed that the release of Ag to the medium was less than 5 % (for SPEs-C-1 and Nafion films, even after 135 h) and 0.2 % for PUFs, the embedment of AgNPs *via* the IMS procedure in the targeted polymeric matrices can be considered as a suitable stabilization procedure.

[16] Despite what it has traditionally been stated, AgNPs can be obtained in a non-ionic matrix such PUFs by the IMS methodology. Small non-aggregated AgNPs (diameters between 6-10 nm) all over the matrix.

[17] Besides, the total metal loading of the prepared PUFs-nanocomposites as well as the nanoparticle size can be tuned by applying simple acid or basic treatments to the polymeric matrix. The observed loading differences can be attributed to the possible coordination of Ag^+ ions with lone electron pairs of nitrogen atoms of the polymeric structure: when an acid treatment is applied, the nitrogen atom of the carbamate group is

mostly protonated and the formation of coordination bonds between the nitrogen and the Ag^+ is hindered. Therefore, less Ag^+ ions remain immobilized in the matrix and less AgNPs can be formed.

[18] As suggested from the previous conclusions, AgNPs with diameters between 3-10 nm can be also obtained in non-ionic matrices such as the tested textile fibers.

[19] The characterization of the textile fibers-NCs confirmed that by working at different temperatures of synthesis, the metal load and the mean AgNPs diameter can be tuned: the higher the temperature, the higher the load and the bigger the MNPs.

As a last resort and given that the development of these new materials become meaningless without a future clear application, from a practical point of view and considering the **applicability of the obtained NCs**, it can be concluded that:

[20] The different PMNCs developed can be successfully applied as catalysts in the catalytic reduction of *p*-nitrophenol (4-np) to *p*-aminophenol (4-ap) by $NaBH_4$ in different conditions, except for Polyacrilonitrile with AgNPs obtained at 25 ºC, which also contained the lowest amount of MNPs of all of the obtained NCs of the present work.

[21] SPES-C-3 films loaded with PdNPs offer the best catalytic performance when applied in flux conditions. Moreover, although the flux through the membrane was low (lower than for PUFs-AgNPs) no activation time was needed so as the reaction started, and conversions of 100 % could be obtained immediately even working with an extremely low ratio $NaBH_4$:4-np (20:1). Therefore, these films-NCs can be considered as the best catalytic nanomaterials obtained during the present work, although some improvements have still to be done (especially regarding their operational flux).

[22] The AgNPs-PUFs can be considered as suitable reusable catalysts, thanks to the high stability of the obtained AgNPs and considering the catalytic efficiency found after several runs

[23] Although the experiments with textile fibers-NCs are preliminary, it is noteworthy that due to the high reaction rate values obtained for some of the samples, such materials could be useful in some catalytic applications.

[24] It can also be stated that all of the tested AgNPs-NCs (SPES-S-1, Nafion and PUFs) can be successfully applied as biocides in aqueous media, using suspensions of *Escherichia coli*.

[25] The bactericidal experiments showed that, under the conditions tested, it is possible to wipe out all of the microorganisms in quite short times with Ag-containing polymeric matrices, without adsorption of the microorganisms on the surface of the, deactivating it.

[26] Although there was some release of AgNPs to the media that affected the cell viability, as the silver content found on media was very low, it is possible to conclude that the effect in the cell viability is mostly due to the interaction with metal nanocomposites. Nonetheless, from the obtained results it is not possible to entirely ignore the bactericidal effect of released silver. However this would not be a crucial problem for a practical application if we consider the nanocomposites as antifouling catalytic supports that act as silver reservoirs providing a residual disinfection effect.

[27] It is possible state that the targeted stable dual-function reusable polymer-metal nanocomposites has been achieved by using available polymers that can be used for high effective and low-cost new water treatments.

Ergo, as final remarks of the work here presented and in order to sum up the different conclusions to better-draw a whole idea of the scope of this work, it can be stated that:

- **The Sulfonation of PES-C polymer *via* mild conditions has been possible, and has allowed the obtainment of different polymeric films with a wide range of physico-chemical properties and morphologies, leading to different final applications.**
  Nevertheless, in general it is possible to state that the adequacy of polymeric matrices *via* chemical modification to further apply the IMS procedure has resulted to be more complex than expected. On one hand, sulfonation procedures tested were difficult to control, hindering the obtainment of all the deserved polymers. On the other, modification of highly chemical stable matrices such as polyurethane foams *via* mild conditions has not been possible. From this point it comes clear that chemical modification of matrices should be

further studied for each specific case, in order to establish the best synthetic conditions, it is to say, find those variables which may affect a suitable way such modifications.

- **The obtainment of MNPs of Pd and Ag has been possible *via* the IMS procedure, regardless of the presence of ionogenic groups in the matrix.**

  In general, small non-aggregated MNPs could be obtained in all of the matrices tested, although the load, size and distribution were significantly affected for the matrix properties. Moreover, as it has been proved by the uncommon patterns found in Nafion films loaded with AgNPs, matrix intrinsic properties, the DEE, adsorption processes, existence of coordination bonds, occurrence of dissolution-precipitation processes, the matrix hydration and ion mobility have to be considered in order to fully understand MNPs formation.

- Finally, **it has been possible to achieve the targeted stable dual-function reusable polymer-metal nanocomposites that can be used for high effective and low-cost new water treatments.** Almost all the NCs tested were able to successfully catalyse the conversion of 4-np to 4-ap. Moreover, all the NCs tested in bactericide studies were able to successfully disinfect water in few hours.

  In my humble opinion, materials such as PUFs–AgNPs could be successfully applied as water disinfection filters, although further studies would be necessary to better-stabilize the AgNPs in the foam. On the other hand, the obtainment of NC-SPES-C-3 films could open a new window through their use in water treatment, because they would allow the combination of reaction and separation processes in a single step. Further studies regarding the inclusion of AgNPs, the control of the porosity (and therefore, of their permeability characteristics) and the study of MNPs stability in the matrix would probably lead to the development of new useful NC-membranes.

ANNEX A

A1. Catalysis Today (**2012**), 193, 1, 158-164.

A2. Procedia Engineering (**2012**), 44, 1264-1267.

A3. Ion Exchange Technologies (**2012**), InTech.

A4. Nanoscale Research Letters (**2013**), 8, 238.

A5. Solvent Extraction and Ion Exchange (**2013**), (In press)

A6. Nanocomposites: Synthesis, Characterization and Applications (**2013**), Nova Science Publishers, Inc.

A7. Microbial pathogens and strategies for combating them science, technology and education (**2013**), FORMATEX Research Center.

Catalysis Today 193 (2012) 158–164

Contents lists available at SciVerse ScienceDirect

Catalysis Today

journal homepage: www.elsevier.com/locate/cattod

Catalytic membranes with palladium nanoparticles: From tailored polymer to catalytic applications

B. Domènech[a], M. Muñoz[a], D.N. Muraviev[a], J. Macanás[b,*]

[a] Chemistry Department, Universitat Autònoma de Barcelona, UAB, 08193 Bellaterra, Barcelona, Spain
[b] Department of Chemical Engineering, Universitat Politècnica de Catalunya, UPC, C/Colom, 1, 08222 Terrassa, Barcelona, Spain

ARTICLE INFO

Article history:
Received 16 September 2011
Received in revised form 9 January 2012
Accepted 24 February 2012
Available online 23 March 2012

Keywords:
Metal nanoparticles
Nanocomposite
Polyethersulphone Cardo
Catalytic membrane
Intermatrix synthesis
Palladium

ABSTRACT

A new polymer–metal nanocomposite containing catalytic metal nanoparticles and useful for the preparation of catalytic membranes was developed. Pd^0 nanoparticles were grown by intermatrix synthesis methodology on polymeric membranes made of either sulfonated and non sulfonated polyethersulphone with Cardo group or Nafion. The synthesized polymer, the developed membranes and the corresponding nanocomposites were characterized by chemical and microscopic techniques and their catalytic efficiency was tested following a model reaction: the reduction of *p*-nitrophenol to *p*-aminophenol.

1. Introduction

Today, the development of catalytic membranes (CMs) and derived processes is still a challenge although they are known for more than three decades [1]. The range of application of CMs is very wide going from the petrochemical industry (*e.g.* for steam reforming of methane [2]) and the water treatment field (*e.g.* for nitrate removal [3]) to the more sophisticated catalytic amperometric sensors development [4–6].

In general terms, CMs consist in a membrane that controls the transfer of chemical compounds (either reagents or products) and a catalyst in charge of the conversion of reactants to products [7]. The immobilization of a heterogeneous catalyst in a CM allows the achievement of several general aspects of Green catalysis such as the easy separation of the catalyst of the reaction medium and the possibility to reuse the catalytic species without a loss in the catalytic efficiency [8].

Most of the industrially used CMs are ceramic or metallic and, for that reason, can withstand high temperatures and/or pressures and high concentrations of corrosive products. Unfortunately, their main disadvantages are their high cost and fragility [9]. These drawbacks can be overcome by the use of polymeric membranes [10]. The main advantage of this family of CMs is the great variety of existing polymers that can be used for membrane design [9]. The accurate selection of the polymer molecular configuration and the control of its morphology would lead to the most appropriate membrane for a desired application. Moreover, polymeric organic membranes are usually less expensive than their abovementioned ceramic or metallic counterparts [9,10].

Still, the main issue of these materials (excepting polydimethylsiloxane, Nafion, polyimides and some others [11–13]) is that organic membranes have to be employed at mild conditions to avoid polymer degradation, so in order to be used as CMs, it is necessary to have very efficient catalysts.

In this context, it is demonstrated nowadays that metal nanoparticles (MNPs) of transition metals are suitable materials to perform catalysis in moderate conditions of temperature and pressure [14,15], reaching high selectivity and efficiency [16]. This fact is due their unusual electronic properties related to their size and the large percentage of surface atoms [17]. However, the main drawback of MNPs is their low stability in the absence of stabilizing agents. Thus, due to their high tendency to aggregate, for most practical applications, catalytic MNPs must be immobilized on solid supports to (i) prevent the uncontrolled growth and (ii) prevent their aggregation [18].

As a result, the encapsulation of MNPs inside polymeric matrices can be considered as a win–win strategy to cope with the drawbacks of both polymeric materials and MNPs [19]. This approach has already proved to be an efficient methodology as it yields to

* Corresponding author at: Department of Chemical Engineering, UPC, C/Colom, 1, 08222 Terrassa, Spain. Tel.: +34 937398239.
E-mail address: jorge.macanas@upc.edu (J. Macanás).

0920-5861/$ – see front matter © 2012 Elsevier B.V. All rights reserved.
doi:10.1016/j.cattod.2012.02.049

useful materials for process intensification through the combination of catalysis and membrane process within the same nanocomposite, which may destroy and separate pollutants in a single step [20–22].

One practical possibility to prepare such nanocomposite materials is by intermatrix synthesis (IMS) [23,24] a technique based in the immobilization of MNPs precursors (metal ions or complexes) in a polymeric matrix followed by a chemical or electrochemical reduction that provides the desired MNPs [25]. It is noteworthy to remark that, for a successful IMS, polymers have to be functionalized in the sense of having ionogenic groups (*e.g.* sulfonic or carboxylic) in their molecular skeleton. A possible option is to use existing functionalized polymers (*e.g.* Nafion [26]) although it somehow limits the applicability of the technique to the commercially available membranes since some parameters such as membrane thickness are predefined by the supplier. On the contrary, it is feasible to synthesize *ad hoc* polymers suitable for both the IMS and the final application as CMs [27].

Regarding this last option it is important to take into account that an excess of ionic groups could cause the dissolution of the polymeric material in water. As a solution, our approach is the sulfonation of a polymer with a very hydrophobic group so as to reduce the hydrophilicity of the final polymer. The selected polymer is the polyethersulphone with Cardo group (PES-C) [28,29] which bears a five-member lactone ring and whose sulfonation can be done in a simple way [30].

In this article we report the use of Nafion and sulfonated PES-C (SPES-C), the optimization of the ratio of the sulfonated polymer to prepare porous membranes for IMS of PdMNPs and their final application in catalysis following the reduction of *p*-nitrophenol (4-np) to *p*-aminophenol (4-ap) with $NaBH_4$ [20].

2. Materials and methods

2.1. Materials

Commercial PES-C was kindly supplied by Dr. Trong Nguyen from Université de Rouen, France. Nafion 117 was used as received from Sigma Aldrich. H_2SO_4, HCl, HNO_3, *N*-methyl-2-pyrrolidone (NMP), and *N*,*N*-dimethyl-formamide (DMF) were all from Panreac, S.A., Castellar del Vallès, Spain). 4-np, NaCl, NaOH, $NaBH_4$, and $[Pd(NH_3)_4]Cl_2{\cdot}H_2O$ were purchased from Aldrich, Munich, Germany.

2.2. Nafion pretreatment

Commercial Nafion 117 membranes (see Fig. 1) were washed twice with bidistilled water in an ultrasonic bath for 30 min. Then they were kept under stirring for 24 h in an aqueous oxidizing solution (10% of concentrated H_2SO_4 and 10% of commercial H_2O_2) to remove impurities. Afterwards, samples were washed again with bidistilled water and kept in the fridge at 4 °C.

2.3. Sulfonation of PES-C polymer

Sulfonation of PES-C was carried out following a procedure similar to those published elsewhere [27,28,31]: the polymer powder was dried at 70 °C for 48 h prior to use. Then, it was dissolved in concentrated H_2SO_4 (ratio 11%, w/v) and mixed at constant temperature (60 °C). After about 5 h, the reaction medium was precipitated in a cold-water bath under strong stirring to obtain the SPES-C in its acid form. Fig. 1 presents the chemical structure of the obtained polymer.

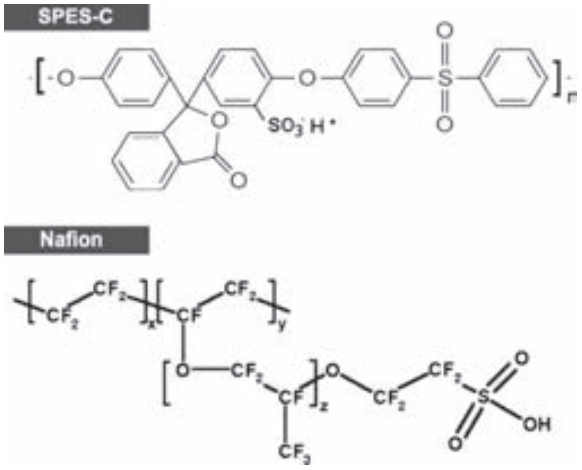

Fig. 1. Structural units of sulfonated polyethersulphone with Cardo group (SPES-C) and Nafion.

Afterwards, the polymer was neutralized with NaOH 1 M solution, filtered, washed with deionized water, and dried at 70 °C. The obtained polymer was in its sodium salt form.

2.4. Membrane casting

Two types of membranes were prepared by wet phase inversion method by using polymer solutions in NMP (25 wt.%). For the preparation of the pure SPES-C membranes, 4.30 g of the sulfonated polymer were dissolved in 12.4 mL of NMP. For the preparation of membranes containing both sulfonated and bare polymer (blend membranes, BMs), 5.00 g of SPES-C were dissolved in 14.5 mL of NMP and then 4.02 g of the solution were mixed with 4.00 g of PES-C in NMP (up to the volume necessary to obtain a 25 wt.% solution).

After casting, membranes were stored in deionized water until their use in catalysis or their characterization. The time of storage ranged from 1 week to 6 months.

2.5. Synthesis of Pd-NPs

The synthesis of Pd-NPs inside the membranes was carried out by a three-steps procedure (see below Eqs. (1) and (2))[5], consisting in the loading of sulfonic groups with $[Pd(NH_3)_4]^{2+}$ ions and their subsequent chemical reduction inside polymeric matrix by using $NaBH_4$ 0.1 M solution:

$$2\text{R-SO}_3\text{Na} + [Pd(NH_3)_4]^{2+} \leftrightarrow (\text{R-SO}_3)_2[Pd(NH_3)_4] + 2Na^+ \quad (1)$$

$$(\text{R-SO}_3)_2[Pd(NH_3)_4] + 2NaBH_4 + 6H_2O \rightarrow 2\text{R-SO}_3\text{Na} + 7H_2 + 2B(OH)_3 + 4NH_3 + Pd^0 \quad (2)$$

To assure an excess of Pd^{2+} in the loading solution and to force the ion exchange process in each matrix, the weight of each sample as well as its IEC were considered (concretely, the value from the acid–base titration). Hence, SPES-C and BMs were loaded with a 1×10^{-3} M solution of $[Pd(NH_3)_4]^{2+}$, whereas Nafion samples were loaded with a more concentrated solution (1×10^{-2} M).

As it can be seen in Eq. (2), after the reduction and formation of Pd-NPs the sulfonic groups are regenerated, thus it is possible to proceed with a second load of the metal to reach the metal content in the membrane. This possibility has already been tested in previous publications [32,33].

Membranes containing Pd-NPs were stored in the same conditions of non-modified membranes.

2.6. Membrane and nanocomposite characterization

Several physico-chemical parameters (*i.e.* metal content, water absorption...) were evaluated in order to provide an adequate characterization of the developed membranes and derived nanocomposites.

Membrane ion-exchange capacity (IEC, meq/g of dry membrane) was determined by indirect titration [27] for synthesized membranes whereas for Nafion 117, the considered IEC was that given by the commercial supplier (IEC_{Nafion} = 1.1 meq/g).

Membrane water uptake (MWU) was determined by a simple procedure: membrane samples were stored in water for 48 h and weighed (W_w), then dried in the oven for 48 h at 80 °C and weighed again (W_d). MWU was calculated according to Eq. (3):

$$\%\,\mathrm{MWU} = \left[\frac{(W_w - W_d)}{W_w}\right] \times 100 \quad (3)$$

To determine the amount of Pd loaded in the nanocomposites, they were immersed in aqua regia (3:1, $HCl:HNO_3$) for 24 h, and this solution was then diluted and analyzed by inductively coupled plasma atomic emission spectroscopy (ICP-AES) (Intrepid II XSP, Thermo Elemental) and by inductively coupled plasma mass spectrometry (ICP-MS) (Agilent 7500).

Several samples (from 3 to 12) were analyzed for each parameter and an ANOVA analysis was performed with the obtained data so as to give an accurate mean value.

2.7. Microscopic characterization

For the microscopic characterization, scanning electron microscope (SEM) images of bare and loaded membranes were taken using a HITACHI S-750, Hitachi LTD SEM and a Zeiss Merlin, Carl Zeiss High Resolution SEM, both installed in Servei de Microscòpia, UAB. For bare membranes characterization, a thin layer of sputtered gold was coated on the surface before imaging. For cross-sectional images, the membrane was fractured in liquid nitrogen before gold coating.

With the aim of characterizing the size and structure of Pd-NPs transmission electron microscopy (TEM) was carried out by using a JEOL JEM-2011 microscope (Jeol LTD, Tokyo, Japan). SPES-C and BMs samples were first dissolved in DMF to get a sort of ink. An ink drop was then deposited onto a Cu TEM-grid, followed by solvent evaporation at room temperature. Being insoluble in most solvents, Nafion samples were cut with a microtome to obtain thin slides to be deposited onto a Cu TEM-grid.

2.8. Catalytic properties evaluation

The reduction of aqueous 4-np to 4-ap by $NaBH_4$ was used as a model reaction to evaluate the catalytic performance of modified membranes [34,35]. In a typical run, 45 mL of a $NaBH_4$ 55.0 mM solution were mixed with 5 mL of a 4-np 5.0 mM solution. After mixing, a piece of nanocomposite (1 cm^2) was added to the vessel. The process was monitored by a Pharmacia LKB Novaspec II spectrometer (λ = 390 nm) by sampling 3 mL from the vessel. After each lecture, sample aliquots were returned to the reaction recipient.

Due to the high excess of $NaBH_4$ (100:1 ratio), this reaction can be considered to follow pseudo-first order kinetics so it is possible to calculate the apparent constant rate for the reaction (k_{app}) from the linearization of the absorbance (Abs) data (see Eqs. (4) and (5)).

$$-\frac{d[\text{4-np}]}{dt} = k \times [\text{4-np}] \times [BH_4^-] \cong k_{app} \times [\text{4-np}] \quad (4)$$

$$\ln\left(\frac{\mathrm{Abs}}{\mathrm{Abs}_0}\right) = \ln\left(\frac{|[\text{4-np}]|}{|[\text{4-np}]_0|}\right) = -k_{app} \times t \quad (5)$$

3. Results and discussion

3.1. Membrane characterization

The successful sulfonation of PES-C at mild conditions can be confirmed regarding the quantitative determination of the IEC presented in Table 1. These values also confirm that by changing the ratio of the sulfonated polymer in the membranes it is possible to modify the IEC of the membranes so as to adapt them to the final application and loading of Pd-NPs. However, the obtained values do not agree with expected results since the BMs, having a 25% of sulfonated polymer, exhibit an IEC of about the half of the pure sulfonated polymer membranes. This odd result can be explained considering that the penetration of aqueous solutions in both membranes is quite different as it is shown below (being BMs much more porous than SPES-C membranes, see Fig. 2) and the exchange between H^+ and Na^+ spices can be hindered in SPES-C membranes due to their dense nature. Thus, the obtained IEC value for SPES-C should be considered as indicative of the practical IEC although the potential IEC would be probably higher if a thinner membrane was obtained.

Similarly, the MWU seems to be also affected by the morphology of the membrane samples. The measured values of MWU for SPES-C, BMs and Nafion were found to be 73.2 ± 0.5%, 79.3 ± 0.4% and 40 ± 2% respectively. The slight but significant increase in MWU for BMs should be also ascribed to their more porous structure (Fig. 2) that can retain more water as a result of capillary forces. The lower value of Nafion water uptake is clearly due to the hydrophobic skeleton of the polymer (see Fig. 1). After loading the membranes with Pd-NPs the values changed to 76.1 ± 1.0%, 79.6 ± 0.5% and 40 ± 6%, respectively, showing that in non-perflourinated membranes the presence of MNPs modifies either the hydrophilicity or the morphology of the matrices. On the one hand, it has been reported that the presence of Pd can increase the hydrophilicity of membranes by presenting a higher affinity for water molecules [36]. On the other hand, the presence of NPs can provoke an increase in membrane porosity as it was previously reported for nanocomposites made of sulfonated polyetheretherketone [5]. An increase in porosity would imply a higher membrane surface and, hence, a higher accessibility of water molecules that can be retained inside the matrix.

It is worth to note that even if MWU values are not negligible (70–80%) they are far lower than those that could cause membrane dissolution.

3.2. Nanocomposite characterization

When synthesizing the nanocomposites, for all the tested polymers it is possible to observe at first sight a change in the membrane color from white to black. This event qualitatively confirms a successful loading of the membranes with Pd^0. SEM and TEM images and elemental analysis by ICP-AES and ICP-MS afford a more quantitative picture of the material modification.

The content of Pd-NPs in the nanocomposites was determined by analyzing three replicates per membrane foil, and three

Table 1
IEC values of the SPES-C and BMs determined by titration (uncertainty 95%).

Matrix	IEC (meq/g)
SPES-C	0.44 ± 0.02
BMs	0.26 ± 0.02

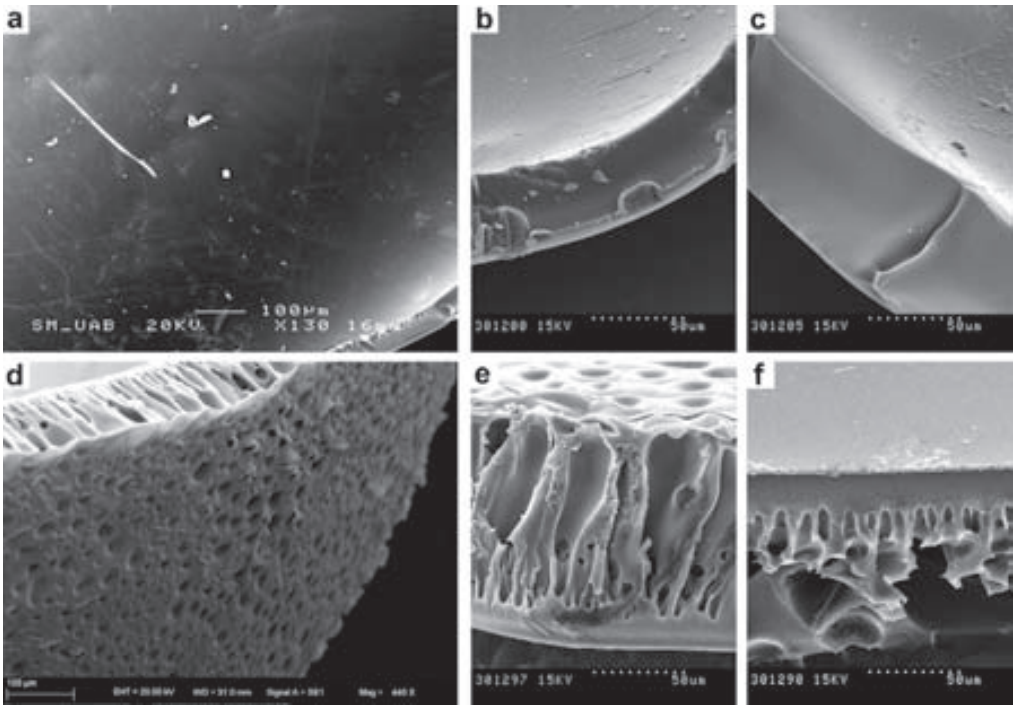

Fig. 2. SEM images of (a) SPES-C membrane surface, (b) unloaded SPES-C cross-section, (c) Pd-SPES-nanocomposite cross-section, (d) BM surface, (e) unloaded BM cross-section and (f) Pd-BM nanocomposite cross-section.

membranes foils for SPES-C batch. For commercial Nafion, Pd content was determined by analyzing two replicates per membrane from three different membrane portions (from a single Nafion sheet). The obtained results are shown in Table 2.

Firstly, it is important to point out that all measure deviations are very low disregarding the matrix nature what testifies for the high homogeneity of nanocomposite batches, probably due to the IMS methodology as well as to the homogeneity of samples. Secondly, comparing the loadings for SPES-C membranes and BMs, in this case the ratio closely approaches 4:1, which is the theoretical relation for the respective IECs having in mind that BMs included only a 25% of pure SPES-C in their composition. Despite the fact that IEC values obtained by titration are not in agreement with this relation, from a practical point of view it has been demonstrated that the modification of the sulfonated polymer concentration directly affects the final Pd content.

On the other hand, by applying a second loading cycle to BMs it is possible to exactly duplicate the metal content (from 0.08 to 0.16 meq/g) which in fact shows another possibility to tune the metal composition in this kind of polymer–metal nanocomposites.

Table 2 shows the loading efficiency percentage, which corresponds to the ratio of the amount of metal loaded in each sample in relation to the IEC parameter. A value of 100% would indicate that all the available sulfonic groups in the membrane were charged with metal. Notice that two loading–reduction cycles on BMs only reach about 60% of the theoretical maximal loading, whereas about a 50% efficiency is obtained for Nafion in a single cycle. Thus, it is reasonable to take into account that the nature of the polymeric backbone does play a significant role in the loading–reduction cycles.

Table 2
Pd content and loading efficiency for the different prepared nanocomposites (uncertainty 95%).

Matrix	Pd loads	Pd content (meq/g)	Loading efficiency (%)
SPES-C	1	0.31 ± 0.02	70.5 ± 0.1
BMs	1	0.08 ± 0.01	30.8 ± 0.1
BMs	2	0.16 ± 0.01	61.5 ± 0.1
Nafion	1	0.53 ± 0.04	48.2 ± 0.1

About the membranes morphology, Fig. 2 shows SEM images of loaded and unloaded SPES-C and BMs, clearly unveiling the different morphology of both materials. Unexpectedly, in the case of SPES-C membranes there is a noticeable absence of porosity and surface defects whereas finger-like porous are clearly perceived for BMs samples. Moreover, BMs show two very distinct parts: a more porous layer and a dense one. This particular pore distribution comes with the membrane casting method (immersion precipitation) as the polymer next to the casting support (a glass plate), takes longer to come into full contact with water, so water has enough time to create numerous pathways which later turn into pores [37]. The final morphology is that of an asymmetric membrane [38].

Regarding the dense morphology of SPES-C membranes, one expects to find asymmetric membranes by wet phase inversion method and dense membranes by solvent evaporation approach [39]. However, since none of the commonly applied porogen agents (such as LiCl or polyvinylpirrolidone) has been used in membrane manufacture, the absence of pores is not so unexpected and have been previously reported in the literature [29,30].

As stated before, the structural difference between BMs and SPES-C membranes also helps to explain the results of MWU (Section 3.1). The difference in porosity between the two types of membranes can be explained by the increase in the hydrophobicity provided by the non-sulfonated polymer in the BMs. In relation to that, it is expectable that a range of porosity could be obtained by modifying the SPES-C percentage in BMs. As a result, and under the hypothesis that MWU and IEC are affected by the membrane morphology, a range of these parameters might also be tuneable.

Table 3
Characteristic parameters of MNPs distribution histograms for Pd loaded samples (1 loading).

Matrix	$Ø_m$ (nm)	σ (nm)	R	Np
SPES-C	6.5	0.1	0.994	222
BMs	3.3	0.1	0.993	530
Nafion	13.4	0.1	0.978	311

$Ø_m$ = MNP most frequent diameter, σ = standard deviation, and Np = counted NPs.

Images c and d from Fig. 2 show that the presence of Pd-NPs does not significantly affect the microporous structure of the membrane.

Besides, Fig. 3 shows the cross-section and the surface of a Pd-Nafion nanocomposites after a single loading-reduction cycle. Similarly to SPES-C, Nafion membranes are dense and do not show any surface defect. High-resolution SEM images of Nafion nanocomposites surface (Fig. 4) make it possible to perceive the Pd-NPs surface distribution mainly due to the higher metal content and the higher performance of the Zeiss Merlin SEM.

With the aim of better characterize the Pd-NPs samples, they were also analyzed by TEM (Figs. 5 and 6) in order to evaluate nanoparticles size, shape and distribution. For some DMF soluble nanocomposites (SPES-C membranes and BMs with a single Pd load) non-aggregated spherical MNPs were realized (Fig. 5a and b). Hence, it was possible to measure the particle size and represent the corresponding size distribution histograms that were fitted to a Gaussian curve and which characteristics parameters are reported in Table 3.

In the case of Nafion, since it is not possible to dissolve it in organic solvents, it was necessary to cut thin slices of the membrane with a microtome. This methodology allows us to obtain a real image of the Pd-NPs distribution in the membranes. As it can be seen in Fig. 6 we obtained aggregated nanoparticles close to the membrane edge and spherical and quite isolated ones far from the edge. Then, it was only possible to calculate the size distribution histogram for the inland Pd-NPs (see Table 3). Notice that higher average diameters are found for Pd-NPs grown in Nafion matrix (about 13 nm) that approximately coincide with those observed by high resolution SEM (Fig. 4). Size differences are also observed between SPES-C and BMs. Here, the difference in Pd-NPs size might be explained by a different spatial distribution of the SO_3^- groups in the membranes: the higher the density of SO_3^- groups, the higher the chance for particles to interact and grow.

Surprisingly, the images of BMs with two loads of Pd (Fig. 5c) show MNPs aggregates. Since there is a compulsory sample preparation procedure (dissolution in DMF) required to allow the deposition of the nanocomposite material onto the TEM grid, it is not possible to discern if aggregates are already present in the solid material before dissolution or MNPs aggregate as a consequence of an excessive concentration [40].

3.3. Catalytic properties evaluation

Palladium is probably the most versatile metal in promoting or catalyzing reactions; particularly those involving C—C bond formation (*e.g.* Suzuki, Heck and Sonogashira) [41,42]. Consequently is not difficult to find suitable test reactions to characterize a catalytic material containing Pd. For this study we have chosen a simple reaction mainly because of its easy monitoring even though it is better catalyzed by Au [34,35]: the catalytic reduction of 4-np with $NaBH_4$. The reaction does not proceed in the absence of catalyst yet it rapidly occurs in the presence of Pd-NPs [27] and the disappearance of 4-np can be easily monitored by UV–Vis spectrophotometry (λ = 390 nm).

Two different blanks per membrane type were tested (Blank 1 with 4-np and 1 cm^2 of unloaded membrane; and Blank 2 with 4-np and $NaBH_4$ but without nanocomposites, nor membrane) and they did not show any significant absorption change, even after 10 h. When testing the different samples, a decrease in the absorption is noticed due to the conversion of 4-np to 4-ap (Fig. 7), but in the best of the cases, an induction period of 1 h is needed to start de reaction. We have suggested that H_2 evolved from the decomposition of $NaBH_4$ can be loaded inside Pd-NPs (as Pd is a classical H_2 storage metal), competing with the catalytic reaction. Once the absorption

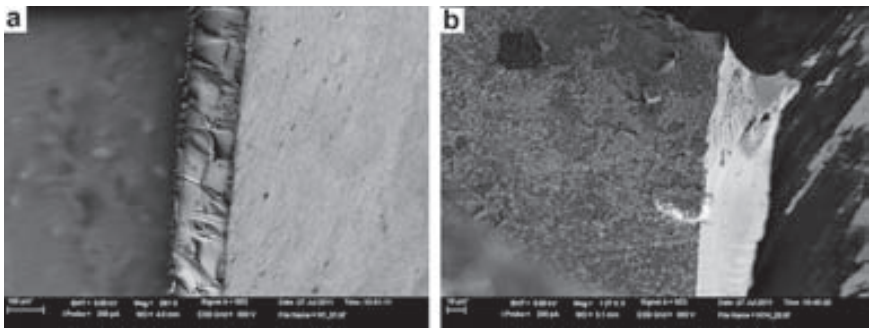

Fig. 3. SEM images of Nafion sample with Pd-NPs (a) cross-section and (b) nanocomposites surface.

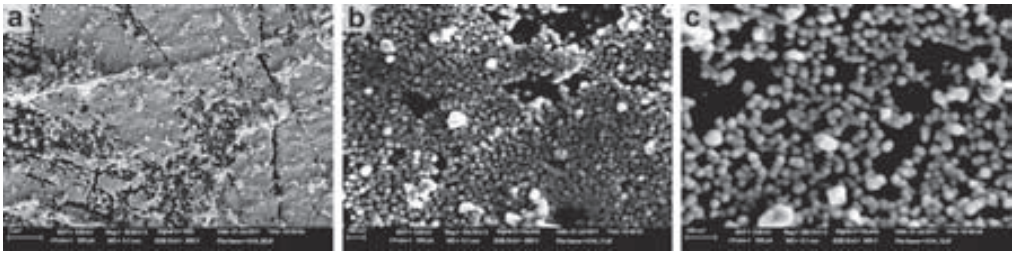

Fig. 4. High-resolution SEM images of Nafion nanocomposites surface at different magnifications (a) 30,000×, (b) 154,760×, and (c) 265,740×.

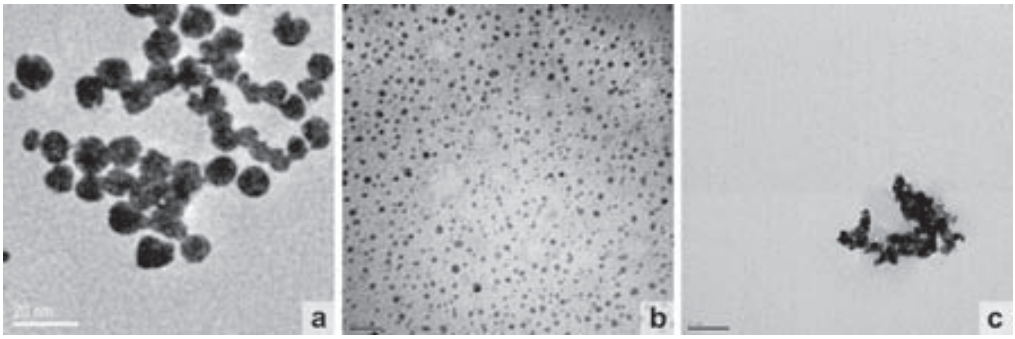

Fig. 5. TEM images of inks prepared with (a) SPES-C membrane with 1 load of Pd-NPs, (b) BM with 1 load of Pd-NPs, (c) BM with 2 loads of Pd-NPs.

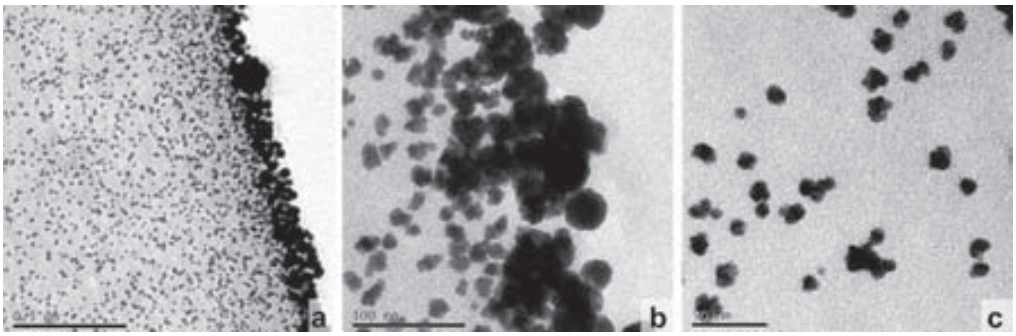

Fig. 6. TEM images of Nafion sliced samples (a) edge (b) edge at higher magnification and (c) inland Pd-NPs.

of H_2 has reached a saturation value the catalytic reaction prevails [27].

After the induction period the reaction follows a pseudo first order kinetics, so it is possible to linearize the data and obtain a k_{app} velocity constant. SPES-C nanocomposite membranes offer the best catalytic performance ($k_{app} = 0.0132\ s^{-1}$), and they are able to reduce almost 90% of 4-np in less than 5 h. Nafion nanocomposites also show a good catalytic performance ($k_{app} = 0.0123\ s^{-1}$) and allow to reduce about 80% of 4-np. On the contrary, BMs samples perform very poorly either with a single loading of Pd-NPs ($k_{app} = 0.0009\ s^{-1}$) or two ($k_{app} = 0.0028\ s^{-1}$), being the last one slightly better and reaching up to 40% of conversion but only after 6 h.

Taking into account the different Pd content of each membrane, it is possible to compare the normalized efficiency for each type of membrane (Fig. 8). The normalized efficiency corresponds to the k_{app} value divided by the exact amount of Pd in each sample. This parameter is quite useful for comparing. For instance, a first glance to Fig. 7 might suggest that Nafion and SPES-C nanocomposites share a similar catalytic performance but when comparing the normalized efficiency it is evidently seen that Nafion has a worse catalytic efficiency that any of the others nanocomposites. This can be explained because Pd-NPs in the surface of the Nafion grow forming aggregates, so that the catalytic surface diminishes, and there are fewer catalytic sites available. Thus, the distribution of Pd-NPs in Nafion matrix can be stated as unfavorable for its application in CMs. It is possible to find a similar explanation to BMs with 1 or 2 Pd loadings: despite the Pd content doubles; nanoobjects are aggregated as TEM images (Fig. 5c) clearly show.

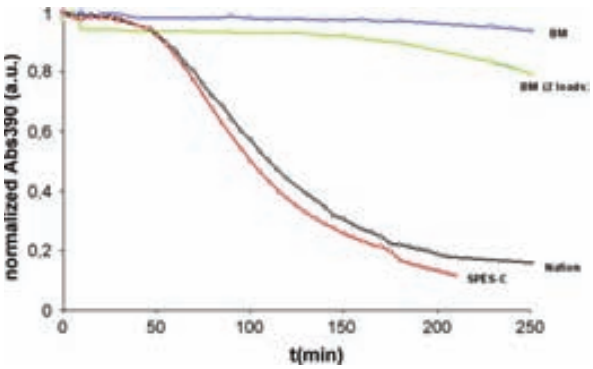

Fig. 7. Catalytic performance of different nanocomposites containing Pd.

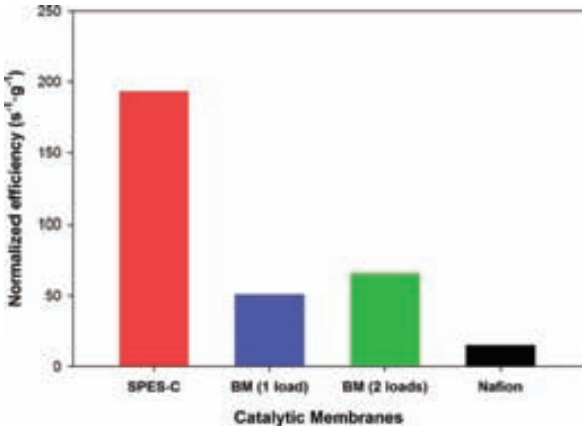

Fig. 8. Catalytic efficiency (k_{app}/μg Pd) of different nanocomposites.

4. Conclusions

The synthesis of Pd-NPs in different polymeric matrices was successfully achieved. Some of the physico-chemical properties (such as the membrane water uptake) of the obtained nanocomposites were affected by the membranes morphology, which in turn, depends on the polymer nature and the preparation method. Although pure sulfonated polyethersulfone with Cardo group membranes are dense, it is possible to provide certain membrane porosity by changing the polymer blend composition.

Regarding the nanoobjects, small Pd^0 nanoparticles (with an average diameter between 3 and 7 nm) were obtained in the prepared membranes and they did not show significant aggregation, at least for nanocomposites that undergo a single loading–reduction cycle. It is proposed that the change in the MNPs size is related to the IEC of the material.

Particularly, Nafion nanocomposites show a clear segregation of nanoparticles, being the membrane edge the region more densely charged. In this case larger nanoparticles are obtained (diameter about 13 nm) and two different distributions were observed.

All the obtained nanocomposite materials exhibit catalytic activity although an induction time is needed before reaction happens at high extent and the efficiency of catalysis (regarding the amount of immobilized Pd) clearly changes depending on the matrix. Thus, for the same load of Pd-NPs, SPES-C nanocomposites show the best catalytic efficiency and Nafion the worst.

Acknowledgments

We thank ACC1O for VALTEC09-02-0058 grant within the "Programa Operatiu de Catalunya" (FEDER). Prof. Trong Nguyen is acknowledged for supplying the polythersulfone Cardo. We really appreciate the efforts of A. Conesa and B. Guerrero regarding ICP analysis. Special thanks are given to Servei de Microscòpia from Universitat Autònoma de Barcelona and to the ICCMR 10 Organizing Committee.

References

[1] M-B. Hagg, Separation and Purification Methods 27 (1) (1998) 51–168.
[2] T. Tsuru, K. Yamaguchi, T. Yoshioka, M. Asaeda, AIChE Journal 50 (11) (2004) 2794–2805.
[3] K. Daub, G. Emig, M.-J. Chollier, M. Callant, R. Dittmeyer, Chemical Engineering Science 54 (1999) 1577–1582.
[4] W. Cha, M.R. Anderson, F. Zhang, M.E. Meyerhoff, Biosensensors and Bioelectronics 24 (8) (2009) 2441–2446.
[5] D.N. Muraviev, J. Macanás, M. Farre, M. Munoz, S. Alegret, Sensors and Actuators B – Chemical 118 (1–2) (2006) 408–417.
[6] B. Prieto-Simón, J. Macanás, M. Muñoz, E. Fábregas, Talanta 71 (5) (2007) 2102–2107.
[7] J.G. Sánchez-Marcano, Th.T. Tsotsis, Catalytic Membranes and Membrane Reactors, Wiley-VCH, 2002, pp. 133–168.
[8] G. Rothenberg, Catalysis: Concepts and Green Applications, Wiley-VCH, 2008, pp. 1–38.
[9] R.W. Baker, Membrane Technology and Applications, John Wiley & Sons, Ltd., 2004, pp. 89–160.
[10] M.G. Buonomenna, S.H. Choi, E. Drioli, Asia-Pacific Journal of Chemical Engineering 5 (1) (2010) 26–34.
[11] I.F.J. Vankelecom, P.A. Jacobs, Catalysis Today 56 (2000) 147–157.
[12] P.P. Knops-Gerrits, I.F.J. Vankelecom, E. Beatse, P.A. Jacobs, Catalysis Today 35 (1996) 63–70.
[13] D. Fritsch, I. Randjelovic, F. Keil, Catalysis Today 98 (2004) 295–300.
[14] B. Roldan Cuenya, Thin Solid Films 518 (2010) 3127–3150.
[15] R. Narayanan, Molecules 15 (2010) 2124–2138.
[16] D. Astruc, F. Lu, J.R. Aranzaes, Angewandte Chemie – International Edition 44 (48) (2005) 7852–7872.
[17] G. Schmid, Nanoparticles, from Theory to Application, Wiley-VCH, 2004, pp. 1–3.
[18] S. Kidambi, M.L. Bruening, Chemistry of Materials 17 (2) (2005) 301–307.
[19] J. Macanás, P. Ruiz, A. Alonso, M. Muñoz, D.N. Muraviev, Ion exchange-assisted synthesis of polymer stabilized metal nanoparticles Ion Exchange and Solvent Extraction. A Series of Advances, vol. 20, CRC Press, 2011, pp. 1–44.
[20] D.M. Dotzauer, S. Bhattacharjee, Y. Wen, M.L. Bruening, Langmuir 25 (3) (2009) 1865–1871.
[21] J. Macanás, L. Ouyang, M.L. Bruening, M. Muñoz, J.C. Remigy, J.F. Lahitte, Catalysis Today 156 (3–4) (2010) 181–186.
[22] L. Ouyang, D.M. Dotzauer, S.R. Hogg, J. Macanaïs, J-F. Lahitte, M.L. Bruening, Catalysis Today 156 (3–4) (2010) 100–106.
[23] D.N. Muraviev, J. Macanás, M.J. Esplandiu, M. Farre, M. Muñoz, S. Alegret, Physica Status Solidi (a) – Applications and Materials Science 204 (6) (2007) 1686–1692.
[24] D.N. Muraviev, P. Ruiz, M. Muñoz, J. Macanás, Pure and Applied Chemistry 80 (11) (2008) 2425–2437.
[25] P. Ruiz, M. Muñoz, J. Macanás, D.N. Muraviev, Reactive & Functional Polymers 71 (8) (2011) 916–924.
[26] A. Sachdeva, S. Sodaye, A.K. Pandey, A. Goswami, Analytical Chemistry 78 (20) (2006) 7169–7174.
[27] B. Domenech, M. Muñoz, D.N. Muraviev, J. Macanás, Nanoscale Research Letters 6 (2011) 406.
[28] J.F. Blanco, Q.T. Nguyen, P. Schaetzel, Journal of Membrane Science 186 (2) (2001) 267–279.
[29] J.F. Blanco, J. Sublet, Q.T. Nguyen, P. Schaetzel, Journal of Membrane Science 283 (1–2) (2006) 27–37.
[30] J.F. Blanco, Q.T. Nguyen, P. Schaetzel, Journal of Applied Polymer Science 84 (13) (2002) 2461–2473.
[31] L. Jia, X.F. Xu, H.J. Zhang, J.P. Xu, Journal of Polymer Science Part B – Polymer Physics 35 (13) (1997) 2133–2140.
[32] A. Alonso, N. Vigués, X. Muñoz-Berbel, J. Macanás, M. Muñoz, J. Mas, D.N. Muraviev, Chemical Communications 47 (2011) 10464–10466.
[33] A. Alonso, J. Macanaïs, A. Shafir, M. Muñoz, A. Vallribera, D. Prodius, S. Melnic, C. Turta, D.N. Muraviev, Dalton Transactions 39 (10) (2010) 2579–2586.
[34] D.M. Dotzauer, J. Dai, L. Sun, M.L. Bruening, Nano Letters 6 (10) (2006) 2268–2272.
[35] Y. Xia, Z. Shi, Y. Lu, Polymer 51 (2010) 1328–1335.
[36] A.H. Tian, J.Y. Kim, J.Y. Shi, K. Kim, K. Lee, Journal of Power Sources 167 (2) (2007) 302–308.
[37] M. Mulder, Basic Principles of Membarne Technology, Kluwer Academic, 1996, pp. 1–564.
[38] C. Barth, M.C. Gonçalves, A.T.N. Pires, J. Roeder, B.A. Wolf, Journal of Membrane Science 169 (2000) 287–299.
[39] C. Klaysom, B.P. Ladewig, G.Q.M. Lu, L. Wang, Journal of Membrane Science 368 (2011) 48–53.
[40] C.M. Sorensen, Aerosol Science and Technology 45 (7) (2011) 765–779.
[41] A. Suzuki, Pure Applied Chemistry 63 (1991) 419–422.
[42] J.M. Campelo, D. Luna, R. Luque, J.M. Marinas, A.A. Romero, ChemSusChem 2 (1) (2009) 18–45.

Available online at www.sciencedirect.com

SciVerse ScienceDirect

Procedia Engineering 44 (2012) 1264 – 1267

Procedia Engineering

Euromembrane Conference 2012

[P2.041]

Nanocomposite membranes with Pd and Ag nanoparticles. A new material for catalytic membranes development

B. Domènech*[1], M. Muñoz[1], D.N. Muraviev[1], J. Macanás[2]

[1]*Universitat Autònoma de Barcelona, Spain,* [2]*Universitat Politècnica de Catalunya, Spain*

The development of Catalytic Membranes (CMs) is a topic of great importance due to their wide range of applications in various fields such as petrochemical processes, water treatment, the development of new sensors and biosensors and some others[1-3].

In general terms, CMs consist of a membrane that controls the transfer of chemical compounds (either reagents or products) and a catalyst providing the conversion of reactants to products [4]. The immobilization of a heterogeneous catalyst in a CM allows for the easy separation of the catalyst of the reaction medium and the possibility to reuse the catalytic species without any loss in the catalytic efficiency [5].

Although CMs employed in industrial processes are usually metallic o ceramic, nowadays the polymeric membranes start to attract more and more attention because of the fragility and high cost of the formers [6]. However polymeric matrices have to work under mild conditions (close to ambient temperatures and / or pressures and in a media without corrosive products) to avoid their degradation, and as a consequence very efficient catalysts have to be designed to work with. With the raise of the nanotechnology this drawback has found a great solution: the use of transition Metal Nanoparticles (MNPs) as effective and selective catalysts [7].

In this sense, inclusion of MNPs in polymeric matrices has been a good innovation to this field. However, it is imperative to choose an appropriate polymeric matrix suitable for both synthesis of MNPs and the practical application of CMs.

Intermatrix synthesis (IMS) [8], a technique based on the immobilization of MNPs precursors (metal ions or complexes) in a polymeric matrix followed by their chemical or electrochemical reduction, provides the production of the desired nanocomposite materials. But for a successful IMS, the polymers must contain ionogenic groups (e.g. sulfonic) in their molecular skeleton. Regarding this request, two possible options have been considered:

(i) The use of an existing functionalized polymer although it somehow limits the applicability of the technique to the commercially available membranes since some parameters such as membrane thickness are predefined by the supplier. We have selected commercial Nafion 117 for this approach.

(ii) Synthesize ad hoc polymers suitable for both the IMS and the final application as CMs, taking into account that an excess of ionic groups could cause the dissolution of the polymeric material in water. As a solution, our approach is the sulfonation of a polymer with a very hydrophobic group so as to reduce the hydrophilicity of the final polymer. The selected polymer for this approach is Polyethersulphone with Cardo group (PES-C) which bears a five-member lactone ring and whose sulfonation can be done in a simple way. [9]

In this work we report the development of three types of catalytic nanocomposite membranes made of pure sulfonated PES-C (SPES-C), a blend of sulfonated and non sulfonated PES-C

1877-7058 © 2012 Published by Elsevier Ltd.
doi:10.1016/j.proeng.2012.08.749

and, finally, commercial Nafion membranes. All the membranes and nanocomposites were physical and chemically characterized.

In all the matrices, small non-aggregated Ag- or Pd-NPs (diameters between 3-13 nm) were obtained by IMS, what demonstrates the applicability of this technique to obtain MNPs in polymeric matrices.

The catalytic activity of the nanocomposites was studied by monitoring a model catalytic reaction: the reduction of p-nitrophenol to p-aminophenol in aqueous media. Although an induction time is necessary to start the reaction, nanocomposites of SPES-C and Nafion exhibit a good catalytic activity (better for Ag nanocomposites than for Pd ones), whereas blend membranes do not show it, probably due to of the low loading of MNPs.

In our opinion, some of the developed materials are suitable to operate in flow conditions with promising results.

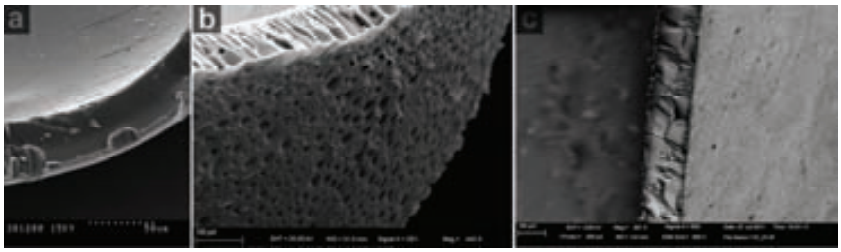

Figure 1. SEM cross section images of (a) SPES-C membrane and (b) SPES-C/PES-C membrane and (c) Nafion membrane.

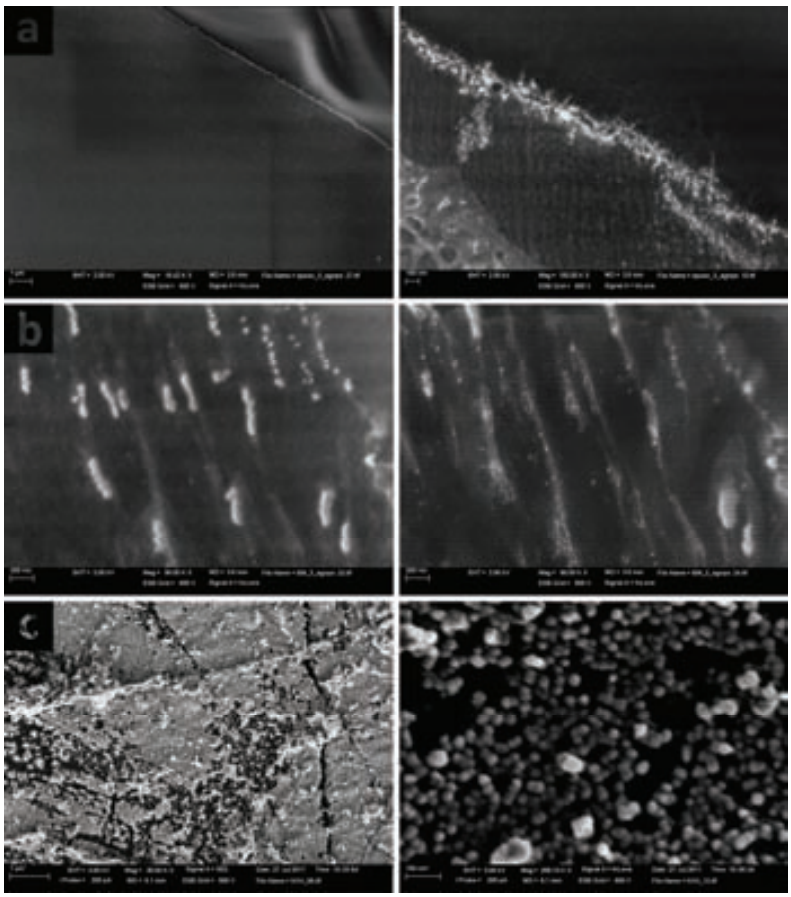

Figure 2: High Resolution FE-SEM images of (a) semifilm of SPES-C membrane with Ag-NPs, (b) semifilm of SPES-C/PES-C membrane with Ag-NPs and (c) Nafion surface membrane with Pd-NPs.

[1] T. Tsuru, K. Yamaguchi, T. Yoshioka, M. Asaeda, AIChE Journal 50 (11) (2004) 2794–2805.

[2] K. Daub, G. Emig, M.-J. Chollier, M. Callant, R. Dittmeyer, Chemical Engineering

Science 54 (1999) 1577–1582.

[3] D.N. Muraviev, J. Macanás, M. Farre, M. Munoz, S. Alegret, Sensors and Actuators B – Chemical 118 (1–2) (2006) 408–417.

[4] J.G. Sánchez-Marcano, Th.T. Tsotsis, Catalytic Membranes and Membrane Reactors,Wiley-VCH, 2002.

[5] G. Rothenberg, Catalysis: Concepts and Green ApplicationsIntroduction in Catalysis, Wiley-VCH, 2008.

[6] R.W. Baker, Membranes and modules, in: Membrane Technology and Applications, John Wiley & Sons, Ltd., 2004, pp. 89–160.

[7] D. Astruc, F. Lu, J.R. Aranzaes, Angewandte Chemie – International Edition 44

(48) (2005) 7852–7872.

[8] J. Macanás, P. Ruiz, A. Alonso, M. Muñoz, D.N. Muraviev, Ion exchange-assisted synthesis of polymer stabilized metal nanoparticles, In: Ion Exchange and Solvent Extraction. A Series of Advances, vol. 20, A. SenGupta, Ed.CRC Press, 2011, pp. 1–44.

[9] J.F. Blanco, J. Sublet, Q.T. Nguyen, P. Schaetzel. Journal of Membrane Science.

2006, 283 (1-2), 27-37

Keywords: Nanocomposite, Catalytic membrane, Nanoparticles, Intermatrix Synthesis

Chapter 3

Bifunctional Polymer-Metal Nanocomposite Ion Exchange Materials

Berta Domènech, Julio Bastos-Arrieta, Amanda Alonso, Jorge Macanás, Maria Muñoz and Dmitri N. Muraviev

Additional information is available at the end of the chapter

http://dx.doi.org/10.5772/51579

1. Introduction

The unusual electrical, optical, magnetic, and chemical properties of metal colloids (better known in nowadays as metal nanoparticles, MNPs) have attracted increasing interest of scientists and technologists during the last decade. In fact, although Nanoscience and Nanotechnology are quite recent disciplines, there have already been a high number of publications that discuss these topics. [1-11] What is more, there are quite new high impact peer-reviewed journals especially devoted to these research fields and there is also a particular subject category "Nanoscience & Nanotechnology" in the Journal Citation Reports from Thomson Reuters.

MNPs can be obtained by various synthetic routes, such as electrochemical methods, decomposition of organometallic precursors, reduction of metal salts in the presence of suitable (monomeric or polymeric) stabilizers, or vapour deposition methods. Sometimes, the presence of stabilizers is required to prevent the agglomeration of nanoclusters by providing a steric and/or electrostatic barrier between particles and, in addition, the stabilizers play a crucial role in controlling both the size and shape of nanoparticles.

In this sense, the development of polymer-stabilized MNPs (PSMNPs) is considered to be one of the most promising solutions to the MNPs stability problem. For this reason, the incorporation of MNPs into polymeric matrices has drawn a great deal of attention within the last decade as polymer-metal nanocomposites have already demonstrated unusual and valuable properties in many practical applications.

The modification of commercially available ion exchange resins and the development of suitable polymeric membranes with metal nanoparticles (MNPs) having certain functionality, such as for example, biocide or catalytic activity has proved to be a theme of

great interest. The main advantage of the nanocomposite ion exchange materials is the location of metal nanoparticles near the surface of the polymer what substantially enhances the efficiency of their biocide and catalytic application.

1.1. Metal nanoparticles

The most commonly accepted definition for a nanomaterial is "a material that has a structure in which at least one of its phases has a nanometer size in at least one dimension." [12] Regarding this definition, it is possible to classify nanoobjects in three groups:

i. 1D nanometer-size objects (e.g., thin films)
ii. 2D nanometer-size objects (e.g., nanowires, nanorods and nanotubes)
iii. 3D nanometer-size objects (e.g. nanoparticles and/or nanoclusters)

Such materials include porous materials (with porous sizes in the nanometer range), polycrystalline materials (with nanometer-sized crystallites), materials with surface protrusions separated by nanometric distances, or nanometer-sized metallic clusters. Among all of these materials, metal nanoparticles (MNPs) have attracted increasing interest of scientists and technologists during the last decade, due to their unique electrical, optical, magnetic, and chemical properties.

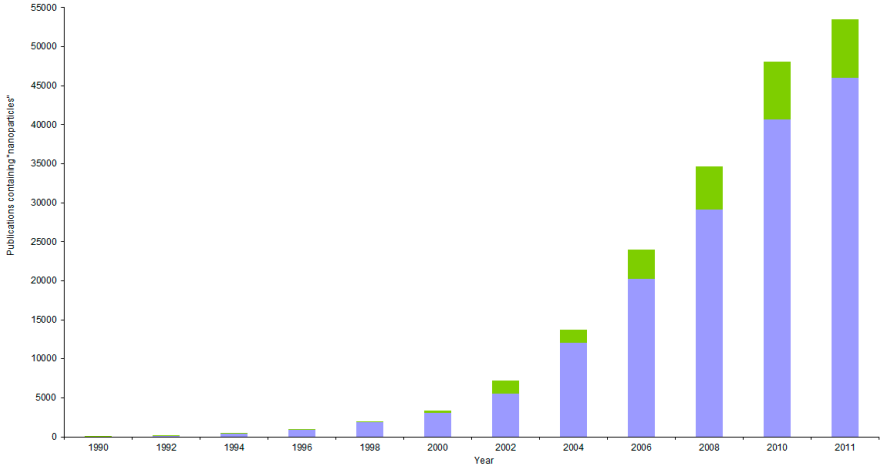

Figure 1. Bibliographic analysis based on the search of "nanoparticles" in Scifinder Scholar. Blue represents scientific publications (e.g. books, articles, reviews) and green represents patents.

Within the last two decades a new focus has been initiated to control and to better understand the nanometer-size objects due to the appearance of a new interdisciplinary field, which is known now as Nanoscience and Nanotechnology. This has stimulated a new wave of intensive and more detailed studies of MNPs and various nanocomposites on their base. Figure 1 shows the tendency in publication about this issue, where it is shown that the

number of publications has increased exponentially due to their wide applications in different fields such as Medicine, Chemistry, and Physics and so on. Moreover, not only scientific publications have been growing in the last decades but also a huge number of patents have been issued in the last decade.

The main goal of Nanoscience and Nanotechnology is the creation of useful/functional materials, devices and systems through the control of matter on the nanometer length scale and exploitation of novel phenomena and properties (physical, chemical and biological) at that scale. To achieve such goal it is necessary to use a multidisciplinary approach: inputs from physicists, biologists, chemists and engineers are required for the advancement of the understanding in the preparation, application and impact of new nanotechnologies.

1.2. General properties

Because of the decrease in the scale of the materials, their behaviour changes in a remarkable form. In fact, the reduction of the bulk materials to a nanometric size induces size-dependant effects resultant from:

i. An increase of the ratio surface-volume, what gives to an increase in the total surface area and in the fraction of the entities (e.g. atoms) in the surface of the material, as shown Figure 2.
ii. Changes in the electronic structure of the entities forming the nanoparticles and in the nanoparticles as whole.
iii. Changes in the associations (e.g. interatomic distances) of the entities forming the nanoparticle and presence of defects.
iv. Confinement and quantic effects (due to the confinement of the charge carriers in a particle of size comparable to the wavelength of the electron).

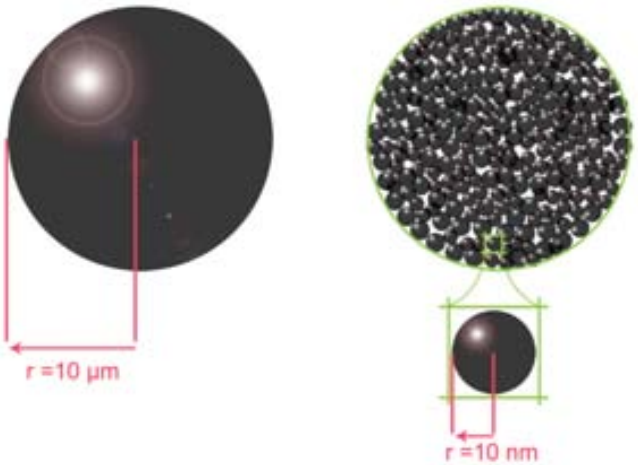

Figure 2. Schematic representation of the change in the ratio surface/volume between a bulk microsphere and the same microsphere composed by NPs.

This can be illustrated, for example, by the dependence of gold melting point on the size of gold nanoparticles, or by suspensions of Ag nanoparticles with sizes ranging from 40 to 100 nm which show different colours. [13] In addition, there are physical phenomena that do not exist in materials with larger grain sizes, as the general quantum-size effect for optical transitions in semiconductor nanocrystals which occurs in very small nanoparticles (<10 nm) due to the quantum confinement effects inherent in particles of that size.

Is due to all of these new properties that, indeed, research centred on nanoscopic materials have a large field of application which extends from the semiconductor industry, where the ability to produce nanometer-scale features leads to faster and less expensive transistors [6], to biotechnology, where luminescent nanoparticles are extremely interesting as bioprobes. [14] Some other particular examples are catalyst for fuel cells [15] or electrocatalysts used in sensing devices with enhanced properties. But, as a rule of thumb, nanoparticles, due to the large percentage of surface atoms [12, 16], have already made a major impact on the field of surface science, as Catalysis or Biocide treatment.

1.3. MNPs Preparation: Stability challenges and stabilization mechanisms

In general there are two routes for the preparation of MNPs (see Figure 3):-Down and Bottom-Up. The top-down methods are those that reduce the macroscopic particles to the nanoscale. This route is not very suitable to prepare uniform particles of very small sizes. In contrast, with the bottom-up methods it is possible to obtain uniform particles (usually of different shapes and structures). These routes start from atoms that can be added (either in solution or gas phase) to form larger particles.

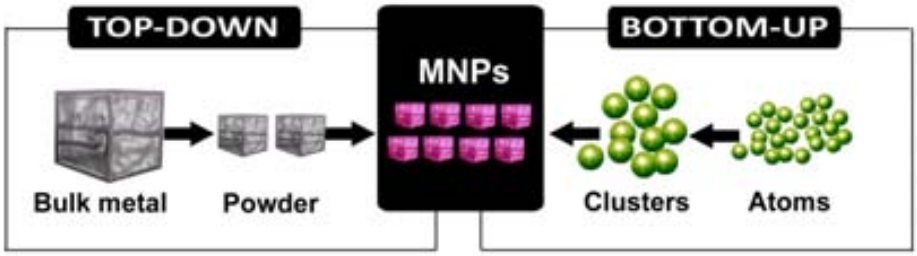

Figure 3. Scheme of Top-Down and Bottom-Up approaches to the synthesis of MNPs.

Overall, a good method to classify the different methods of synthesis of MNPs is by Physical, Physicochemical and Chemical routes (See Figure 4). [13] Many synthetic pathways can be used but the chemical ones are generally cheaper and do not require equipment or instruments as specific as in the case of physical methods the physical methods.

However, the main drawback which still limits the wide application of MNPs is their insufficient stability dealing with their high tendency to self-aggregate. [17] MNPs are so reactive that when they touch each other, they surfaces fuse, what results in a loss of the nanometric size and in their special properties. These features of nanoparticles, in part

determined by the conditions of synthesis, create enormous difficulties in their fabrication and application. [18]

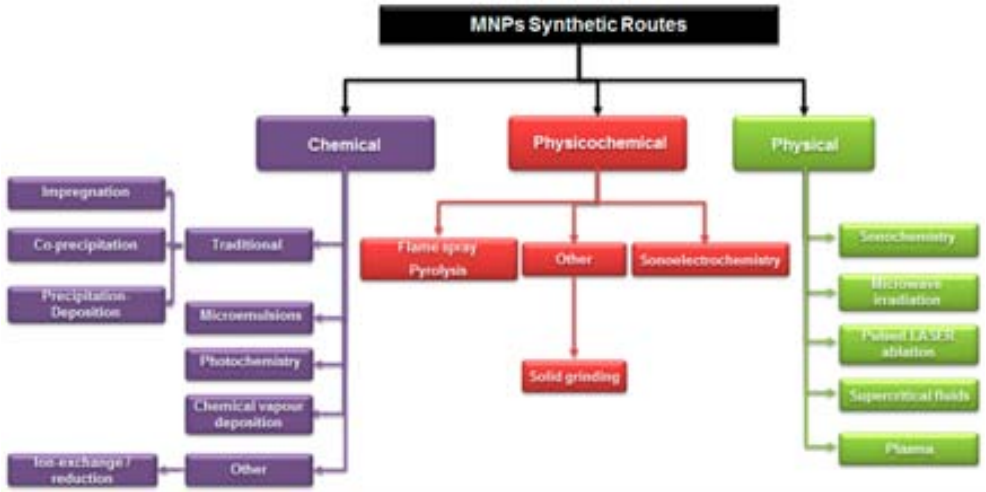

Figure 4. Physical, Physicochemical and Chemical routes for the preparation of MNPs.

It is noteworthy that NPs can aggregate not only as a result of a further manipulation but also during their growth. A typical mechanism of aggregation is the Ostwald ripening which is a growth mechanism where small particles dissolve, and are consumed by larger particles. [19] So, the average nanoparticle size increases with time, the particle concentration decreases and their solubility diminishes.

Therefore, the stabilization of MNPs is specifically required to:

i. prevent their uncontrollable growth
ii. prevent particle aggregation
iii. control their final shape and size
iv. allow particle solubility in various solvents
v. terminate the particle growth reaction

The successful synthesis of nanoparticles usually involves three steps: nucleation, growth, and termination by a capping agent or ligand (or stabilizing agent) through colloidal forces.[20] These colloidal forces can be classified in three main types as follows: Van der Waals interactions, electrical double-layer interactions, and steric interactions. In addition, hydrophobic and solvation forces may be important. [21]

Some of the mechanisms regarding the stabilization forces have been thoroughly revised in the literature.[13, 22]

Specially the use polymer-assisted fabrication of inorganic nanoparticles is probably one of the most efficient and universal ways to overcome the stability problem of MNPs and to save their properties. Metal nanoparticles synthesized by this approach exhibit long-time

stability against aggregation and oxidation while nanoparticles prepared in the absence of polymers are prone to quick aggregation and oxidation.[18, 23]

In this sense, stabilization of MNPs can be done by different strategies. In the ex-situ synthesis, NPs are dispersed after their synthesis in a solid or liquid medium by using different mechanochemical approaches. The problem is that in these cases, the success of the stabilization is limited by the possibility of re-aggregation of the MNPs along the time. On the opposite hand, by the in-situ synthesis, MNPs are grown directly in the stabilizer medium yielding a material that can be directly used for a foreseen purpose. For this reason, in-situ approaches are getting much attention, because of their technological advantages (Figure 5).

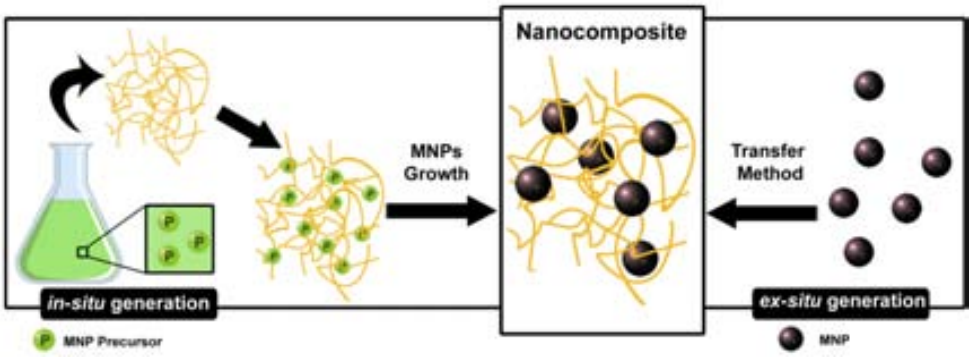

Figure 5. Schematic comparison between in-situ and ex-situ methodologies.

Despite the methodology employed, it is of crucial importance to understand the processes occurring in polymer interactions with nanoparticles. In this regard, the mechanism of MNP stabilization with polymers can be explained by two approaches which run simultaneously in the system and influence one another: the substantial increase of viscosity of the immobilizing media (the polymer matrix), and the decrease of the energy of particle-particle interaction in PSMNP systems versus non-stabilized MNP dispersions. [24]

In the first approach, the substantial increase of viscosity of the immobilizing media (the polymer matrix), the Coagulation velocity depends on factors as the range of attraction forces, Brownian motion velocity, concentration of colloidal solution, presence of electrolytes… As follows from the Smoluchowsky equation [25], the rate constant of particle coagulation, k_c, is inversely proportional to the viscosity of the media, η, (here k stands for the Boltzman constant, and T is the temperature):

$$k_c = \frac{8kT}{\eta} \tag{1}$$

The second approach is the decrease of the energy of particle-particle interaction in PSMNP systems versus non-stabilized MNP dispersions. The potential energy of attraction U_r between two spherical particles of radius r and minimum distance l_o between their surfaces can be given by the following equation:

$$U_r \approx \frac{Ar}{12\, l_o} \text{ at } r >> l_o \quad (2)$$

where A is the effective Hamaker's constant with dimensions of energy. The value of A is known to be close to *kT* for polymer particles (e.g 6.3×10^{-20}J for polystyrene), while for the metal dispersions it is far higher (40×10^{-20} J for silver). [24]

2. Inter-Matrix synthesis in ion exchange matrices

The ion-exchange synthesis of Metal Nanoparticles (MNPs) refers to a group of methods which can be generally classified as Inter-Matrix Synthesis (IMS) technique. The main feature of IMS is the dual function of the matrix, which allows the stabilization of the MNPs to prevent their uncontrollable growth and aggregation and provides a medium for the synthesis.

It is noteworthy that IMS was essentially the first method employed by the humans to incorporate nanoparticles inside inorganic materials. In this sense, one of the oldest nanocomposite materials found is the "Lycurgus cup" which dates back to the late 4th century B.C.[26] and it is made of a sort of glass that changes its colours depending on the incident light: in reflected light the glass turns green, but when the light is shone directly through it, it turns red due to the presence of small amount of Ag-Au-MNPs with the diameter of approximately 70 nm. It is remarkable that Greco-Roman techniques have been used up to modern times: related recipes were described by Arabian authors during the medieval period [27], during the Renaissance as practical application of alchemical knowledge[28], and by modern chemists, from the Encyclopedie of Diderot and d'Alembert [29] through to the present day.

Another example is the "lustre pottery"[30] employed at the same time in Asian an European countries by a simple two-step procedure:

1. the immobilization of metal cations (MNP precursors) inside the ceramic matrix.
2. the reduction of metal ions to the zero-valent state with carbon monoxide leading to the formation of MNPs.

Examples of this ceramics are showed in Figure 6.

Although, as it has been shown above, humanity had used the properties of the nanoscale materials for a long time, the fundamentals of the scientific Nanoscience and Nanotechnology studies did not appear since the middle of the XIXth. As an example, in 1949 the first communication of the IMS is published by Mills and Dickinson.[31] In this pioneered publication it is described the preparation of the anionic resin containing Cu-MNP ("colloid copper") and the use of this nanocomposite material for the removal of oxygen from water due to its interaction with copper MNPs. Since that, a great number of researchers focused their efforts to the development of a new class of ion-exchange materials, combining ion-exchange and redox properties (known also as "redoxites" or "electron-ion exchangers").

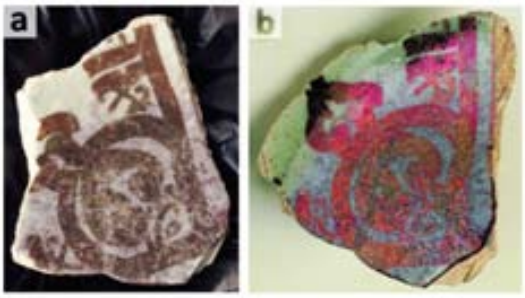

Figure 6. Lustre Pottery. Fatimid-sherds excavated from Fustât; (a) the sample and (b) sample with an orientation that corresponds to the diffraction angle and lustre shining is observed.

2.1. General principles

This section describes the principles of the IMS in ionic exchange matrices. This technique takes advantatges of the in-situ approach (above mentioned), and has a wide range of application because of the multiple metal-polymer existing possibilities. In this sense, even if the number of polymers is reduced to those with ion exchange capacities, the multiple possibilities remain and a different number of polymer-nanocomposites can be obtained. Figure 7 shows the multiple possibilities of the IMS methodology.

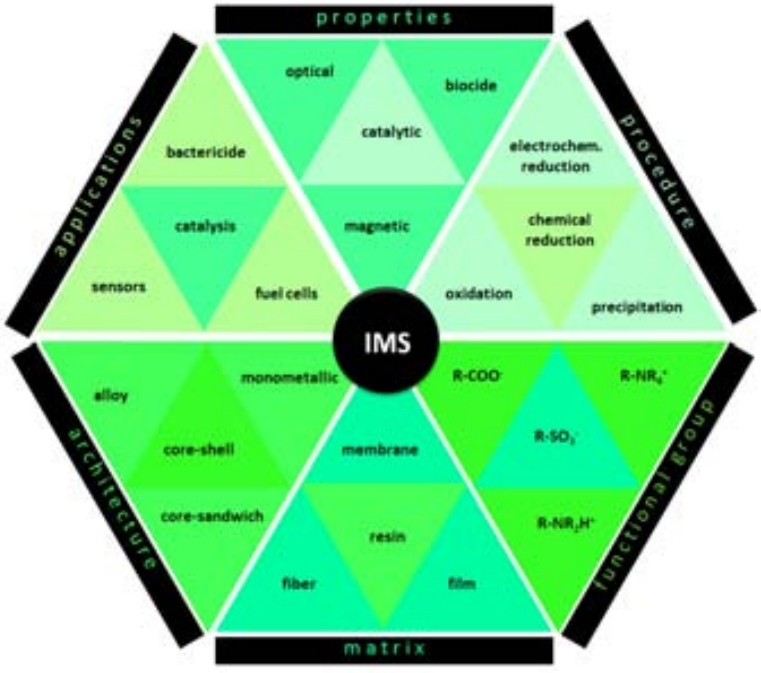

Figure 7. Scheme of the multiple possibilities of Ion-Matrix Synthesis.

The general principles of IMS, valid for any kind of polymer matrix and type of nanoparticle, are based on:

1. The nanoreactor effect: the confinement of the particles by the polymer molecules which allows limiting the size and the particle size distribution; and,
2. The barrier effect: the polymer molecules locally isolate the formation of each single NP preventing the contact between their surfaces and therefore their aggregation.

These guidelines are only achievable if NPs precursors can properly be immobilized in the polymeric matrix. In this sense, Ion Exchange matrices are the perfect template to retain the ionic species, either metal cations, anions or any kind of coordination compound.

To illustrate this approach, two anion charged groups as sulfonic group (SO_3^-) can efficiently interact with the metal cation (M_1^{2+}) which afterwards can undergo a chemical reaction (precipitation, reduction, etc.) which finally will yield to the formation of the MNP.

The same can be done for an anion exchange matrix bearing a functional group such as a quaternary ammonium ($-NR_4^+$), capable to immobilize metal complexes (i.e. $[CoCl_4]^{2-}$)or other anions (i.e. BH_4^-).

Figure 8 illustrate the two main consecutive stages which rule the IMS technique: (i) the immobilization of the metal ion or complex (in a Cation Exchange Matrix, CEM) or immobilization of the reductant (in an Anion Exchange Matrix, AEM) and (ii) the reduction of the metal ion inside the matrix.

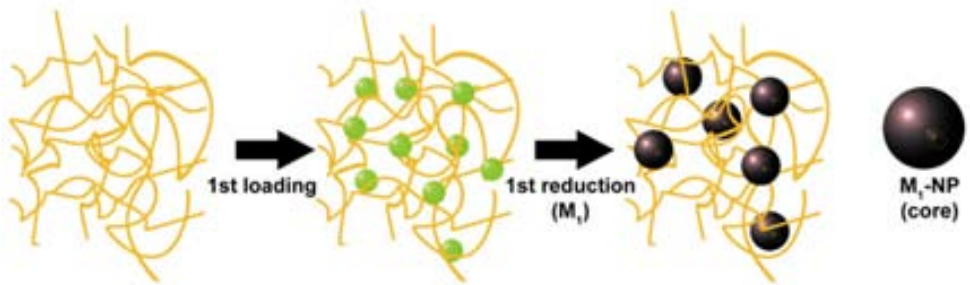

Figure 8. Monometallic MNPs preparation inside a polymeric ion-exchange matrix by IMS. Green spheres represent the M_1^{2+} cation, and the black ones the MNPs obtained after the reduction.

These two stages may be described by the following equations (equations 3-4 and 5-6) considering the presence of strong acid groups ($2R\text{-}SO_3^-$) in the CEMs and the presence of strong basic groups ($R\text{-}R_3N^+$) in the AEMs. M_1 represents a divalent metal and R the organic radical.

For CEMs:

$$2\left(R-SO_3^-Na^+\right) + M_1^{2+} \leftrightarrow \left(R-SO_3^-\right)_2 M_1^{2+} + 2\,Na^+ \quad (3)$$

$$\left(R-SO_3^-\right)_2 M_1^{2+} + 2\,NaBH_4 + 6H_2O \rightarrow 2\left(R-SO_3^-Na^+\right) + 7H_2 + 2B(OH)_3 + M_1^0 \quad (4)$$

For AEMs:

$$R-\left(R_3N\right)^+ Cl^- + NaBH_4 \leftrightarrow R-\left(R_3N\right)^+ BH_4^- + NaCl \quad (5)$$

$$2\left(R-\left(R_3N\right)^+ BH_4^-\right) + \left[M_1\right]^{2+} Cl_2 + 6H_2O \rightarrow 2\left(R-\left(R_3N\right)^+ Cl^-\right) + 7H_2 + 2B(OH)_3 + M_1^0 \quad (6)$$

A deeper look in the second stage reveals that the MNPs formation (equations 4 and 6) is, indeed, a combination of an ion-exchange reaction and a reduction reaction, accordingly the reduction of the metal ions to the zero-valent metal takes place in the solution boundary, close to the ion exchange groups:

For CEMs:

$$\left(R-SO_3^-\right)_2 M_1^{2+} + 2\,Na^+ \leftrightarrow 2\left(R-SO_3^-Na^+\right) + M_1^{2+} \quad (7)$$

$$M_1^{2+} + 2\,BH_4^- + 6H_2O \rightarrow 7H_2 + 2B(OH)_3 + M_1^0 \quad (8)$$

For AEMs:

$$R-\left(R_3N\right)^+ BH_4^- + Cl^- \leftrightarrow R-\left(R_3N\right)^+ Cl^- + BH_4^- \quad (9)$$

$$M_1^{2+} + 2\,BH_4^- + 6H_2O \rightarrow 7H_2 + 2B(OH)_3 + M_1^0 \quad (10)$$

Additionally, as it can be seen from equations 7 and 9 in both cases the matrix is regenerated after the second stage of the IMS, so it is possible to apply consecutive IMS cycles to increase the total loaded metal [32] or to obtain bimetallic nanoparticles (core-shell, alloys or core-sandwich).

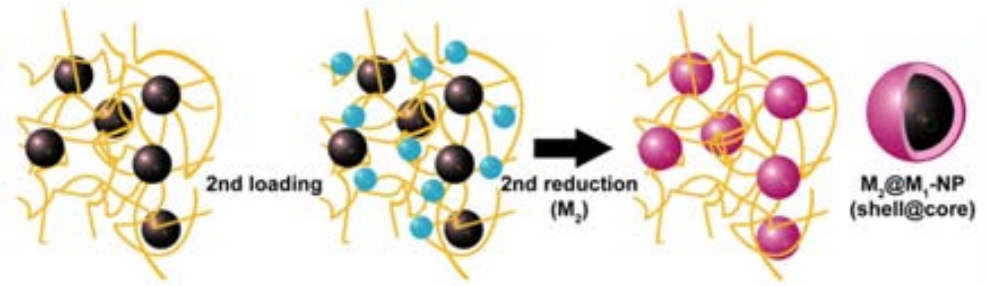

Figure 9. Bimetallic core-shell MNPs preparation. Black spheres represent the MNPs obtained after he first loaing-reduction cycle, blue spheres the M_2^{2+} cations and the pink ones are the final core-shell MNPs.

In Figure 9, there is an schematic representation for the preparation of core-shell NPs by coating the monometallic MNPs obtained after the first cycle with a secondary functional metal shell. As follows, the formation of core-shell MNPs (M_1-M_2, represented as $M_2@M_1$ where M_2 is the coating and M_1 is the core) allows modification of charge and functionality, improves the stability or combines the properties of both metals to make their future applications more efficient. The final activity of the nanocomposite is determined by the properties of the shell metal, although in some cases the properties of the metal core may add an additional advantage to the final nanocomposite (e.g. magnetic core).

To better understand the procedure shown in Figure 9, let us consider the reactions corresponding to the IMS of PSMNPs inside the parent polymeric matrix after the first loading-reduction cycle for example in the CEM:

$$2\left(R-SO_3^-Na^+\right) + M_1^0 + M_2^{2+} \leftrightarrow \left(R-SO_3^-\right)_2 M_2^{2+} + M_1^0 + 2\,Na^+ \tag{11}$$

$$\left(R-SO_3^-\right)_2 M_2^{2+} + M_1^0 + 2NaBH_4 + 6H_2O \rightarrow 2\left(R-SO_3^-Na^+\right) + \\ + 7H_2 + 2B(OH)_3 + M_2@M_1 \tag{12}$$

According to some authors [33], the second metal ion can act as an oxidizing agent towards the core-metal (M_1^0) resulting in the oxidation of the first metal by the following transmetallation reaction:

$$M_2^{2+} + 2M_1^0 \rightarrow M_1^{2+} + M_2^0@M_1^0 \tag{13}$$

As it can be seen, in the general IMS procedure described before, there are always two species bearing the same charge: the matrix and the reducing agent (in CEMs) or the metal ion (in AEMs). This means that there is an electrostatic repulsion between the matrix and one of the species mentioned that impede the penetration inside the polymeric matrix, referred to as Donnan-exclusion effect [34, 35].

The Donnan-exclusion effect is based on the exclusion (inability to deeply penetrate inside the polymer) of co-ions when the sign of their charge coincides with that of the polymer

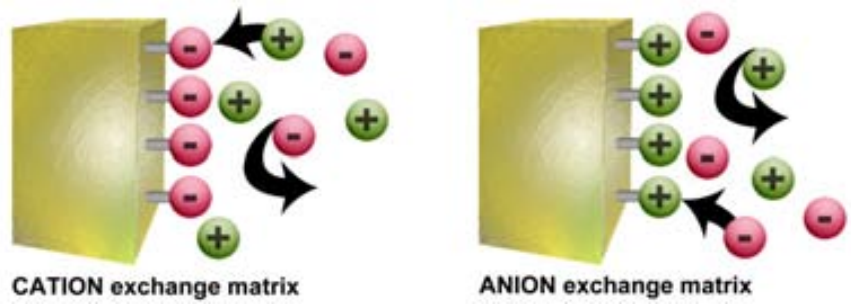

Figure 10. Donnan Exclusion Effect.

functional groups. Consequently, ion penetration inside the matrix is balanced by the sum of two driving forces acting in opposite directions: the gradient of the ion concentration and the Donnan-effect itself. The result of these two driving forces is the formation of the MNPs mainly near the surface of the polymer matrix (see Figure 10).

Regarding the final application of the nanocomposite, this is a really suitable distribution, since MNPs remain maximally accessible for substrates of interest such as chemical reagents or bacteria.

2.2. Requirements for parent polymers

Many materials which contain functional groups can be used as supports for the IMS disregarding their form or shape: granulated form, fibrous or membranes. In all cases, when using the IMS technique it is important to take into account both the polymer properties and the final application of the nanocomposite since as both points dictate certain necessary requirements to the parent matrix (inside which the MNPs must be synthesized).

For example, when using a nanocomposite for making a sensor or a biosensor to be applied in aqueous solutions, the polymer must be insoluble in water. But, at the same time, the polymer has to provide sufficient permeability towards the analyte under study (ions or molecules). Besides, the polymer must either slightly swell in water or at least be hydrophilic to enhance both the sensor and the response rate.

Similarly, the solubility of the nanocomposite in some organic solvents allows for the preparation of homogeneous Polymer Stabilized MNPs solutions (PSMNPs “inks”) that can be deposited onto the desired surfaces (e.g. electrodes) to modify their properties. This solubility would also allow the characterization via microscopic analysis, electrochemical techniques and others.[36]

The main requirements for a polymer to be used as a matrix for the IMS technique are the following:

- The polymer must be chemically compatible with the MNPs surface.
- The polymer must bear functional groups which would act as nanoreactors.
- Appropriate distances between the coordinating centers to insure the hopping of charge carriers.
- Sufficient flexibility of the polymer chain segments to facilitate movements of ionic carriers.
- Appropriate swelling ratio of the matrix.
- Adequate hydrophilicity.

In polymer functional matrices, ionic transport occurs in a highly amorphous, viscoelastic (solid) state. In this sense, the most intensively studied polymers are based on poly(oxa alkanes), poly(aza alkanes), or poly(thia alkanes).

In general, it is possible to state that functional groups define the chemical properties of the polymer matrix, by bearing on the surface a negative or positive charge. Due to this fact

different dissociation properties of group lead to strong and weak exchangers (which are named similar to that of strong and weak electrolytes). Based on these functional groups, classification of Ion Exchange matrices involves four main groups:

1. Cation exchangers (with anionic functionalities and positively charged mobile ions)
    a. strong acid exchangers (e.g., containing sulfonic acid groups or the corresponding salts)
    b. weak acid exchangers (e.g., containing carboxylic acid groups or the corresponding salts)
2. Anion exchangers (with cationic functionalities)
    a. strong base exchangers (e.g., containing quaternary ammonium groups)
    b. weak base exchangers (e.g., containing amine groups)

The Ion exchange capacity (IEC) is the main feature of ion exchange materials. Taking into account that an ion exchanger can be considered as a "reservoir" containing exchangeable counterions, the counterion content in a given amount of material is defined essentially by the amount of fixed charges which must be compensated by the counterions, and thus is essentially constant.

Above all mentioned polymer matrices, this chapter is mainly focused in the use of cross-linked polymers in the form of resins and in commercial or tailored polymeric membranes.

2.2.1. Resin beads

As IMS is based on the feasibility of the polymeric support used, which must contain ionic functional groups, one of the typical matrices that accomplish this requirement are Ion-exchange resins, also known as granulated polymers.[34, 37]

Ion-exchange resins are commercial products commonly available and their shape and size allow these materials to be easily and quantitatively recovered by simple filtration or decantation. Ion exchange resins are usually used in water treatment processes (e.g. water softening) but have many other applications in chemical production. For instance, several common applications include immobilization of biological an inorganic catalysts, extraction procedures, metal recovery and separation and acid-base catalysis.[38, 39]

The first effort to obtain more stable synthetic resins for ion exchange reactions is attributed to B.A. Adams and E.L. Holmes, who in 1935 published the condensation polymerization of methanal (formaldehyde) with phenol or polysubstituted benzene compounds to give reversible exchange resins. [40] Based on the same concept Adams and Holmes quickly developed anion exchange resins, obtained by the condensation between methanal and phenylamines giving directly a copolymer matrix bearing weak basic secondary amine groups, that in presence of strong acid solutions result in acid amine salts (anion exchangers). Although nowadays the polymerization mechanism is entirely different, based on the so called addition or vinyl polymerization (first applied by D'Alelio in 1944) commercial ion exchange resins production uses the same principles as their predecessors, and the two kind of resin explained before are still the most commonly used resins.[41]

Regarding their chemical composition, most ion-exchange resins are based on cross-linked polystyrene- divinylbenzene (DVB) copolymers bearing ion-exchanging functional groups. Besides, from the morphological point of view, the following types can be considered:

- Gel type: resins with a macroscopic homogeneous and elastic framework which contains the solvent employed in its synthesis. What characterizes the resin is the presence of channels (instead of pores) in the matrix, with a size depending on the proportion of DVB employed in the synthesis. Is the size of these channels what determines the size of the specie, ion or molecule allowed to pass though it and the velocity and diffusion.
- Macroporous type: resins with a higher cross-linking level than gel type. Inside their structure macropores and micropores coexist as a result of the elimination of the solvent, what gives to these kinds of resins a high inner surface area. In this sense, it is necessary a high amount of DVB to maintain the resin structure. The high level of porosity affect to the swelling properties, making the inner structure heterogeneous, thus their behaviour in to polar solvents or to nonpolar solvents solvents is really different. As advantages it is important to say that they are easily sulfonated and they are really resistant.
- Isoporous type: Their structure is modified during their synthesis, thus polymers with a relative uniform pore size are obtained. These resins present a low sensibility to the fouling, have a higher capacity, high regenerating effectiveness and low production costs.
- Film type resins: They are an special type of ion exchangers that consist in an exchange material in a film shape deposited above an inert support. These resins present quick kinetics and allow working in high pressure conditions (i.e. chromatography).

Considering the feasibility of this matrix type for the synthesis of MNPs, it is noteworthy to mention that they lead to obtain a stable support for the embedded MNPs, are insoluble in water and offer different types of functionalities (e.g. sulfonic, carboxylic, quaternary ammonium), as well as different distributions of functional groups. Some common important parameters, from chemical and physical points of view, are listed in the following table (Table 1).

Chemical Parameters	Physical Parameters
Polymer structure, Ion conductivity	Grading
Functional group type	Particle Size
Ion Exchange Capacity	Pore size and morphology
pH working range	Form
Chemical stability	Density
Water absorption (swelling)	Shipping weight

Table 1. Common important parameters in Ion Exchange Resins.

From those parameters listed in Table 1, the functional groups nature is one of the key ones since it defines the chemical properties and applicability of ion-exchange resins and, what is crucial for IMS, the sign of the matrix charge (either positive or negative). Moreover, the

different dissociation properties of the functional groups leads to the distinction between strong and weak exchangers, which have to be considered separately since they have a remarkably different chemical behaviour. In this sense, in Figure 11 are shown some typical resin beads with their polymeric structure formula.

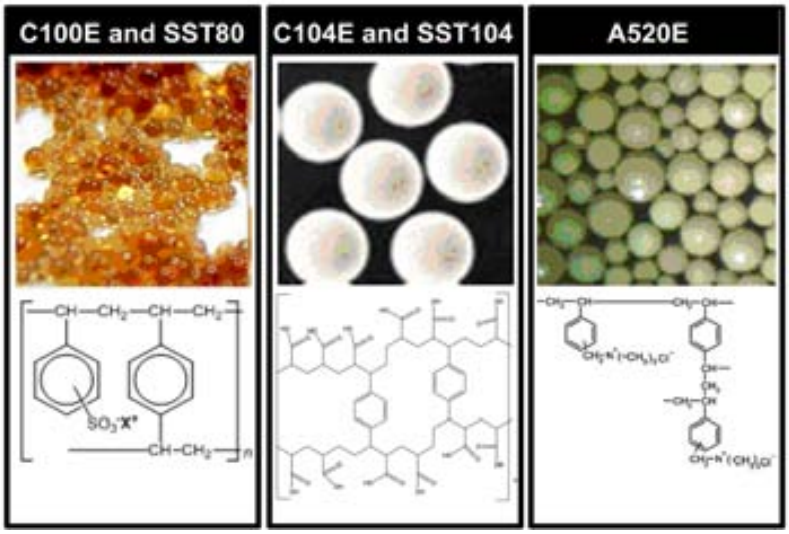

Figure 11. Physical and chemical features of some ion exchange resins.

Another very important parameter to be taken into account is porosity, which affects some bulk properties of the resins, and which have important consequences on their catalytic applications through direct influence on swelling capacity, equilibration rate, and selectivity. In this sense, swelling is an important to be taken account on resin behaviour, because depending on the nature of the ion-exchange resin, this interaction with the solvent may lead to a volume increase (swelling volume) up to 800% and a decrease around 90% of the cross-linking percentage, Hence, gel-type resins are generally preferred over macroporous ones due to enhanced mass transfer inside the polymer beads, resulting in good active-sites accessibility to all soluble reactants.

2.2.2. Membranes

The separation of substances by membranes has been (and still is) essential in the industry development and in the human life. Among various separation membranes, the ion exchange membranes, membranes with ionic groups permeable to electrolytes in an aqueous solution, are widely used in different fields: dialysis, solid polymer electrolyte of batteries, analytical chemistry, etc.

In its origins, the ion exchange membrane was developed from two different sources: the finding of ion exchange phenomena in soil and biological phenomena in cell membranes. In 1939 many researchers focused to the establishment of the basis of the studies on

electrochemical ion exchange membrane. For example, in 1939 K.H. Meyer, J.F. Sievers and T. Teorell obtained the first artificial charged membrane with the aim of developing a theory of membrane potential; in 1949 Sollner published a paper concerning bi-ionic potential (a measure of permselectivity between ions with the same charge through the membrane); etc. But it is not until 1950, with the work of M.R.J. Wyllie, W. Juda and M.R.C. McRae, when the first ion exchange membranes synthesis is published.

After these works, studies on ion exchange membranes, their synthetic methods, modifications, theorical explanations and applications in industry became very active. But what really made the researchers focus in the development of this kind of membrane is that the charged groups of the membrane act as a fixed carrier for various ionic materials and provide new applications of the membrane.[42, 43] (See Table 2).

Characteristcs	Application	Example
Ion conductivity	Electrodialysis	Separation between electrolyte and non-electrolyte
	Separator for electrolysis	Synthesis of H_2O_2
	Diffusion Dialysis	Acid or alkali recovery from waste
	Neutralization Dialysis	Desalination of water
	Donnan Dialysis	Recovery of precious metals
	Up-hill transport	Separation and recovery of ions
	Piezodialysis	Desalination
	Thermo-dialysis	Desalination
	Battery	Concentration cell
	Fuel cell	H_2-O_2
	Actuator	Catheter for medical use
Hydrophilicity	Pervaporation	Dehydration of water miscible organic solvents
	Dehumidification	Dehumidification of air
	Sensors	Gas sensor
Fixed Carrier (Ion exchange groups)	Facilitated transport	Separation of sugars
	Modified Electrodes	-

Table 2. Principal applications of Ion Exchange membranes

Though ion exchange membranes can be used in many fields, most are used in electrochemical processes such as electrodialysis, separation of electrolytes and solid polymer electrolytes for fuel cells (which really boosted the development of these membranes).

The properties required basically depend on their final application, but generally they can be summarized as:

1. low electrical resistance,
2. high transport number of counterions,
3. low diffusion coefficient of salt,
4. low osmotic water and low electroosmotic water,
5. permselectivity for specific ions with the same charge,
6. antiorganic properties,
7. mechanical strength,
8. dimensional stability,
9. high chemical stability and durability,
10. low cost.

Ion Exchange membranes can be classified in various ways: by their structure and microstructure, by their functionality, materials, etc. But maybe one of the simplest classifications is the morphology which, in first instance, will determine their preparation methodology. In this sense, it is possible to classify ion exchange membranes in two main types: Heterogeneous and Homogeneous membranes.[43]

In an initial stage of membrane development, heterogeneous ion exchange membranes were actively developed by blending finely powdered ion- exchange materials and a binder. In a general procedure, cation or anion exchange resins are homogenously blended and heated with a thermoplastic polymer (i.e. polyethylene, polypropylene, etc.) and the mixture is formed as a membrane by pressing or heating.

Although these types of membranes are easily prepared and have a great mechanical strength, their electrochemical properties are lower than the ones of homogenous ones in which the fixed charged groups are evenly distributed over the entire membrane polymer matrix. This homogeneity in the homogeneous membranes structure is due to the fact that they can be produced, e.g. by polymerization or polycondensation of functional monomers such as phenylsulfonic acid with formaldehyde, or by functionalizing a polymer such as polysulfone dissolved in an appropriate solvent.

But the completely homogeneous and the macroscopically heterogeneous ion-exchange membranes are extreme structures. Most ion-exchange membranes show a certain degree of heterogeneity on the microscopic scale. Thus, other properties may be considered to classify them. In this regard, according to the distribution and species of the fixed charge (ion exchange groups) it is possible to difference between:

i. cation exchange membranes (with anionic charged groups)

ii. anion exchange membranes (with cationic charged groups)
iii. amphoteric ion exchange membranes (with both cation and anion exchange groups at random throughout the membrane
iv. bipolar exchange membranes (bilayer membranes composed by a cation exchange membrane layer and an anion exchange membrane layer)
v. mosaic ion exchange membranes (which have certain domains that may be separated with an isolator of cation-exchange groups and also domains with anion-exchange groups).

On the other hand, a classification based on the constituent materials allows grouping such membranes as:

1. membranes composed of hydrocarbons or partially halogenated hydrocarbons
2. perfluorocarbon membranes
3. inorganic membranes
4. composite membranes of inorganic ion exchanger and organic polymer (e.g., hybrids).

Nowadays, one of the most employed commercial ion exchange membranes is Nafion, a cation exchange homogenous perfluorinated membrane. It is an excellent proton conductor: it has excellent chemical stability, high ionic conductivity, good mechanical strength, good thermal stability, etc. ideal for performance in fuel cells. The main drawback of these membranes and of those containing Fluor in their structure (i.e. Selemion) are their high cost and, specially, the absence of pores that limits their application to the transport of ions in solution or vapour (pervaporation). Thus, the search of new homogeneous cation exchange membranes has been focussing much of efforts. In these sense, sulfonated polymers open a new window to the ion exchange membranes field. Some typical sulfonated polymers are shown in Figure 12.

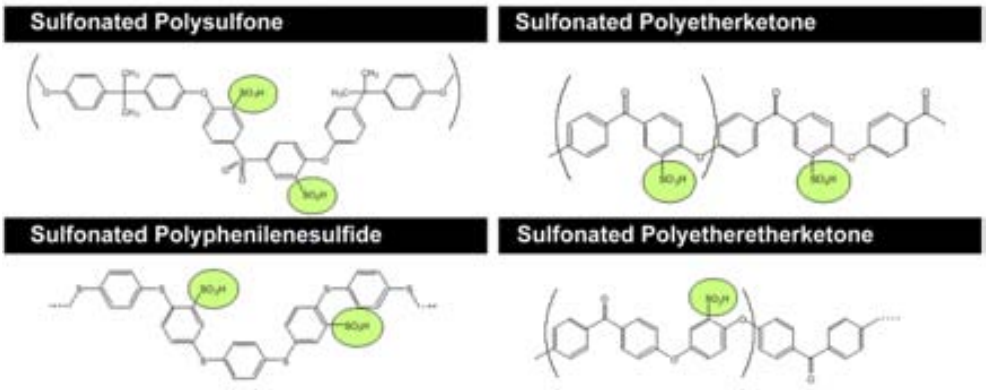

Figure 12. Typical Sulfonated polymers.

One of the polymers that fulfils the properties to be casted as an ion exchange membrane is sulfonated poly(ether-ether ketone) (SPEEK) which is nowadays attracting great interest regarding the fabrication of membranes for fuel cells, due to its thermoplastic properties, its high chemical strength, its high stability towards oxidation and its low cost.[44, 45]

However, regarding this last option it is important to take into account that an excess of ionic groups (in this case, sulfonic groups) could cause the dissolution of the polymeric material in water since an increase of the ionic groups in the polymer directly increases the hydrophilicity of the material.

To cope with this limitation, one good option is the sulfonation of a polymer with a very hydrophobic group so as to reduce the hydrophilicity of the final polymer, the polyethersulphone with Cardo group (PES-C) [46-48] which bears a five-member lactone ring and whose sulfonation can be done in a simple way. Among all the stability properties mentioned, this polymer can be casted by wet phase inversion methodology to obtain porous membranes be applied in filtration. By controlling the ratio of sulfonic groups in the polymer, different porosity can be obtained.

3. Environmental and safety concerns

Perception and knowledge are important parts of public understanding of nanotechnology. They can be influential, for an achievable benefit obtained and the possible risks and hazard which it could imply.

The use of engineered nanoparticles (ENPs) in the environment, as a consequence of the development of nanotechnology, is a serious case of worldwide concern. However, a few studies have already demonstrated the toxic effects of nanoparticles on various organisms, including mammals. Nanotechnology is still in a discovery phase in which novel materials are first synthesized in small scale in order to identify new properties and further applications.

Therefore, detail understanding of their sources, release interaction with environment, and possible risk assessment would provide a basis for safer use of ENPs with minimal or no hazardous impact on environment

In order to do that, future directions such as the inclusion of regulatory and knowledge gaps within the risk identification framework should be designed and applied.

Thus, the evaluation of potential health impact as well as an enhanced design of the production of higher performance nanomaterials is mandatory; as well as defining criteria that distinguish between technologies and products more or less likely to present a health risk to avoid inappropriate and possibly deleterious sweeping conclusions regarding potential impact.

It is required to study their release, uptake, and mode of toxicity in the organisms. Furthermore, to understand the long-term effect of ENPs on the ecosystem, substantial information is required regarding their persistence and bioaccumulation.

3.1. Safe polymer-metal nanocomposites

A massive industrial production of nanomaterials in the near future may result in the appearance of both NPs and the waste generated during their production in various

environments, yielding the possibility that humans could be exposed to these NPs through inhalation, dermal contact or ingestion and absorption through the digestive tract. Nowadays, there is claim for more restrictive legislation that would allow a better protection for both human beings and the global environment.

In this sense, for a comprehensive knowledge of properties of these materials (both physical and chemical), it is important to find standards and control materials to work with as reference models (such those from the British Standards Institute and International Standards Organisation).[49]

An investigation into nanomaterials toxicity involves: a determination of the inherent toxicity of the material, their interaction with living cells and the effect of exposure time.[50] It should be noted that the doses or exposure concentrations used for in vitro and in vivo toxicological studies are most often extraordinarily high in comparison with possible accidental human exposure.[51, 52]

Consequently, more research is needed before generalized statements can be made regarding NPs ecotoxicology.

Unfortunately, only few initiatives in this direction have been started so far. For instance, the German Federal Ministry for Education and Research, together with industry, has established the research programme NanoCare. This programme has a budget of €7.6 million and aims to assess and communicate new scientific knowledge of the effects of NPs on health and the environment.[53]

Scientists and technologists in this area have to deal with NPs presence in the environment but very often they do not have the appropriate tools and analytical methods for NPs detection and quantification to guarantee a satisfactory detection.[4]

Thus, it is of vital relevance to dedicate those efforts towards this direction, as we have not yet invented a so-called "Geiger counter" for NPs.

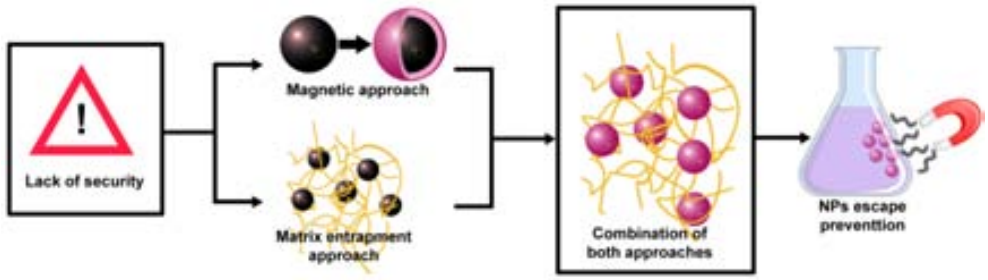

Figure 13. Schema describing the concepts involved in the design of safe polymer-metal nanocomposites.

As a consequence, the prevention of NPs escape into the environment is currently most likely the best approach that can be considered. In this regard, a possible solution appeared

through the development of this project, which describes the results obtained by developing environmentally safe polymer–metal nanocomposite materials exhibiting magnetic properties. These materials prevent NPs escape by profiting of the embedding of NPs into organic matrices and the use of magnetism. [54] As a result, NPs reduce their mobility and, in case of leakage, NPs could be easily recovered by using simple magnetic traps.[13, 55-57]

4. Characterization of Polymer-Stabilized Nanoparticles (PSMNPs)

One of the main features for the development of polymer stabilized metal nanoparticles (PSMNPs) and nanocomposites is their detailed characterization. Specific techniques have to be applied in order to better understand the parameters affecting their synthesis, explain their properties and to adequate them to their final application.

In this sense, several techniques can be used, involving techniques for the chemical characterization and the typical techniques applied in Material Science to determine the MNPs composition, size and shape and their distribution into the matrix as well as the nanocomposite morphology and their special properties (such as magnetism, biocidal, electrocatalytic and catalytic activity among others). These parameters can be studied by using some of the techniques explained in this chapter (or by a combination of some) which include:

- Scanning Electron Microscopy (SEM)
- Transmission Electron Microscopy (TEM)
- Atomic Force Microscopy (AFM)
- Nuclear Magnetic Resonance (NMR)
- X-Rays Diffraction (XRD)
- Impedance Spectroscopy (IS)
- X-rays Photoelectron Spectroscopy (XPS)
- X-Rays Energy Dispersion Spectroscopy (EDS)
- Infrared-Attenuated Total Refraction (IR-ATR)
- Inductively Coupled Plasma Atomic Emission Spectrometry (ICP-AES)
- and many others.

4.1. Characterization of MNPs

When synthesizing PSMNPs the first parameter to determine is the metal content of the polymer-metal nanocomposite.

The composition of MNPs (even that of a single nanoparticle) can be determined by High Resolution TEM or SEM analysis coupled with EDS techniques. The microscopic techniques allow for the selection of the nanoobject(s) whereas the EDS provides the composition analysis. These methods usually gives qualitative or semi-quantitative results which can be useful to have an estimation of the composition differences in a sole sample. An example of this analysis is showed in in Figure 14, where a crossed-section resin bead sample is shown, prepared as described afterwards.

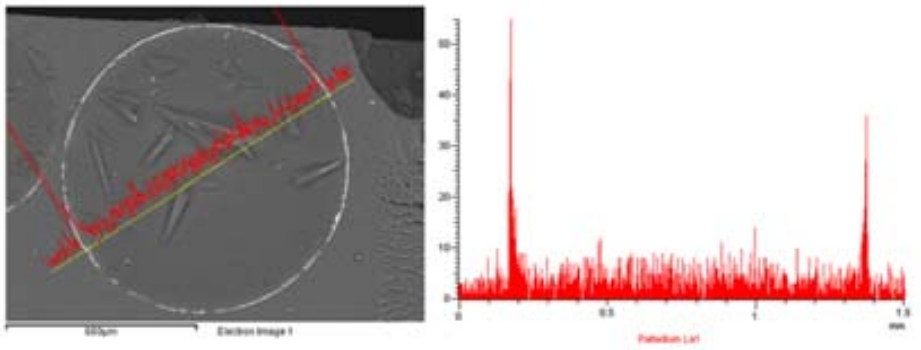

Figure 14. SEM image of an Ion Exchange resin with PdNPs and the corresponding EDS analysis.

If a quantitative analysis is required, the total metal content in the matrix can be determined by using and ICP coupled to an Atomic Emission Spectrometer (for metal concentrations between 0.1 to 500 ppb, depending on the metal) or coupled to a Mass Spectrometer (for metal concentrations between 0.1 to 10 ppb, depending on the metal)[58] to analyse the solution obtained after the treatment of a known amount of the nanocomposite with aqua regia to completely dissolve the MNPs and degrade the polymeric matrix.

The size and the shape of the MNPs obtained are important parameters allowing determining the nanocomposite characteristics. Further development of Nanotechnology needs a better understanding of nanomaterial properties and implies a better characterization of the above parameters, which are evaluated as a rule by using TEM technique.

In this sense, depending on the solubility properties of the polymeric matrices different sample preparation methodologies have to be considered. If the polymeric matrix is soluble in a volatile organic solvent (e.g. DMF, $CHCl_3$, THF) it is possible to prepare MNPs suspensions or "inks" (5% mass solutions) in adequate organic solvents which can be deposited onto a TEM grid to perform the microscopic characterization. On the contrary, if the MNPs are stabilized in a non-soluble matrix (e.g. Nafion), the preparation of the sample is more difficult (although allows us to determine the distribution of the MNPs in the matrix), since it requires to cut thin or ultrathin slices (thickness about 1μm or less) of the nanocomposite material and deposit them onto a TEM grid. An example of this procedure and the final image obtained is showed in Figure 15.

Unfortunately, in practice, in many instances the quality of TEM images appear to be quite low due to the high noise and low contrast, making their processing a challenging task to accomplish. Also, the quantitative treatment of TEM images is often carried out by manual measurements of high number of nanoparticles, a task that is highly subjective and time consuming. During the last years, several computer imaging particle analysis software tools have been conceived to achieve a more accurate assessment of the size and frequency (size distribution) of nanoparticles.

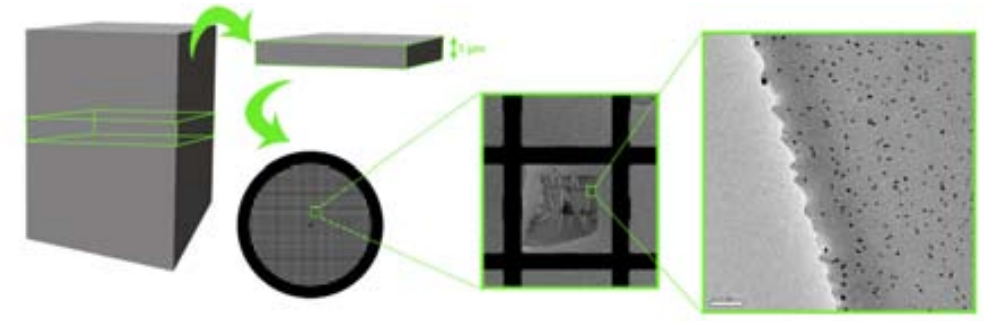

Figure 15. Sample preparation of cross-sectioned with microtome of a sulfonated polyetehersulphone (SPES-C) membrane with AgNPs and the corresponding TEM image obtained.

Through the image analysis of TEM micrographs (either manually or automatically) it is possible to make size distribution histograms from the sample data as the one shown in Figure 16. The obtained data can be used fitted to a 3-parameter Gaussian curve (14) where *a* is the height of Gaussian peak, d_m is the position of the center of the peak (corresponding to the most frequent diameter), and σ is the standard deviation.

$$y=a\cdot\exp\left[-0.5\cdot\left(\frac{d-d_m}{\sigma}\right)^2\right] \tag{14}$$

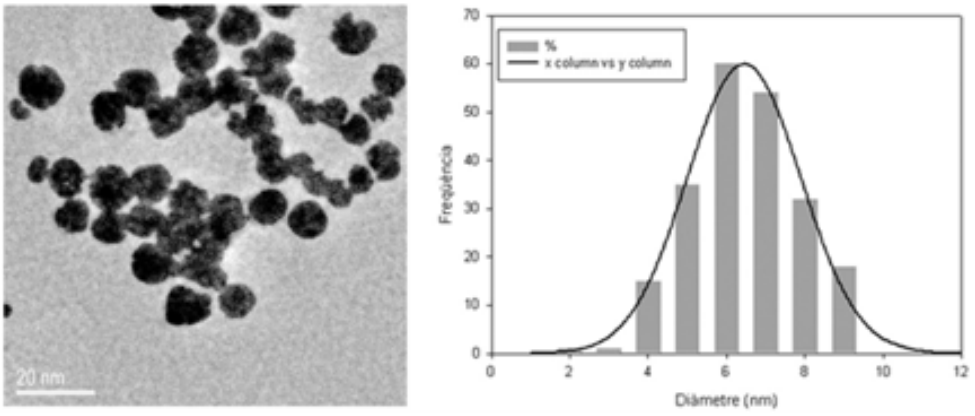

Figure 16. TEM image of an ink of PdNPs obtained in a SPES-C membrane with the corresponding histogram adjusted by a 3 parameter Gaussian curve.

4.2. Metal–polymer nanocomposite morphology

The loading of MNPs in the polymeric matrix may cause important changes in the polymer morphology. For this reason, a characterization of the matrix previous and after the stabilization of the MNPs on it is required.

In this sense and among other techniques, SEM has been established as a referent in the field of the surface characterization. Because polymeric matrices usually are not conductive, in some cases (in matrices without MNPs or with a low content of MNPs) it is imperative to prepare the sample for the study, by a sputter coating with gold, carbon or palladium layers of about 50Å of thickness.

For membranes and films, cross-section images can be obtained by cutting the samples under liquid N_2. For resin nanocomposites, it is necessary to embed the material in an epoxy resin to cut it transversally with a microtome, as shown in Figure 17.

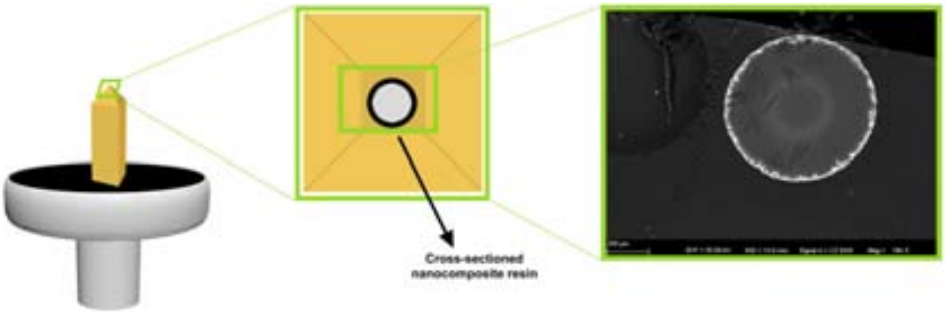

Figure 17. Sample preparation of a resin bead for SEM characterization.

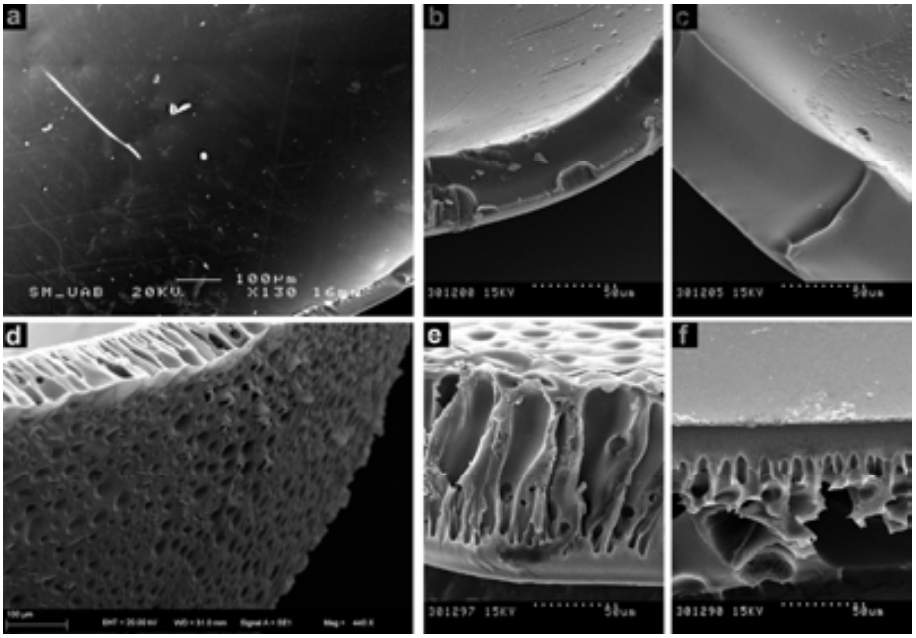

Figure 18. SEM images of (a) SPES-C membrane surface, (b) bare SPES-C membrane, (c) SPES-C membrane with PdNPs, (d) Blend membrane surface, (e) bare Blend membrane and (f) Blend membrane with PdNPs.[32]

Figure 18 shows SEM images of bare and coated SPES-C and Blend membranes (prepared with sulfonated and non sulfonated Polyethersulphone). Whereas in the case of SPES-C membranes there is an absence of porosity and surface defects in the case of Blend membranes it can be observed a finger structure porosity, and the existence of defects on the surface. In both cases, the load with PdNPs do not affect the final structure of the membrane.

The difference in porosity between the two types of membranes can be explained by an increase in the hidrofobicity of the final polymer: adding PES-C polymer increases the capacity of repulsion of H_2O molecules thus, when preparing the membranes by wet phase inversion method by immersion in a non-solvent such as water, pores are generated during the precipitation of the membrane.

In this way, changing the ratio of PES-C / SPES-C in the final polymer blend membranes with different morphology and, therefore, different final application can be obtained.

4.3. Magnetic properties

The metallic nanoparticles have larger magnetization compared to metal oxides, which is interesting for many applications. But metallic magnetic nanoparticles are not air stable, and are easily oxidized, resulting in changes or loss in their magnetization properties.

Thus, IMS of magnetic NPs open a new range of research. Lack of stability of this kind of nanoparticles finds a counterpart by their stabilization on a polymeric matrix.

Magnetic properties of metallic nanoparticles are dependent on the oxidative state of the NPs components. Therefore, the true knowledge of the degree of nanoparticle oxidation is necessary for the forecasting of magnetic characteristics of the obtained samples. This is not easy, but techniques such as XANES (X-Ray Absorption Near Edge Structure) may do it achievable by interaction of the atom core with the source of energy. By comparison with previously placed and analyzed patterns, information about chemical bonding and oxidative states is obtained. Figure 19 shows XANES analysis of nanocomposites containing either Ag or Ag@Co MNPs (with a superparamagnetic Co^0-core) on sulfonic resin. Standard elements spectra were linearly combined and fitted with the sample in order to determine the oxidative state of each element in the sample. The linear combination results are also included (normalized) inset. Ag@Co NPs in sulfonated matrices showed an average Co spectrum similar to that recorded by the Co^0 standard. In fact, linear combination fitting results confirmed that all the Co present in that sample was Co^0.

Furthermore, to characterize magnetic behavior SQUID (Superconducting Quantum Interference Device) magnetization curves are obtained. In order to do that, sample is placed in a changing magnetic field over at room temperature. Magnetization loops are registered through the overall process.

In general, ferromagnetic species have normally evident hysteresis curves. However, superparamagnetic materials (frequently, ferromagnetic materials at nanometer scale) shows a lack of hysteresis but high magnetic saturation. Figure 20 presents SQUID

magnetization curves for Pd@Co MNPs supported on a sulfonic (C100E) and carboxylic(C104E) cation exchange resin.

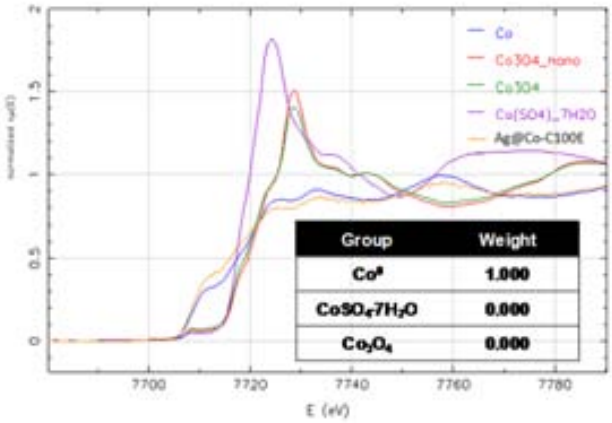

Figure 19. XANES spectra of Ag in comparison with Ag standards for Ag@Co-C100E sample (blue line in the graphic) and the linear combination fitting among all of the compounds analyzed is also shown in a fitting range from -20 to 30 eV. Ag^0 (red) and $AgNO_3$ (green) are standards.

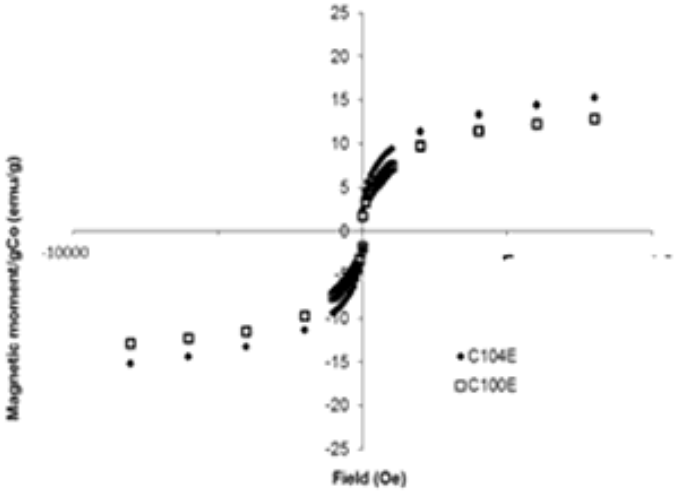

Figure 20. SQUID Magnetic curves obtained of Pd@Co-NPs stabilized in C100E and C104E supports

5. Applications

The use of nanomaterials to assemble architectures of defined size, composition and orientation allows researchers to utilize the particular electrical, optical, catalytic and magnetic properties of those materials for:

- the creation of functional materials, devices, and systems through control the matter on the nanometer scale and,
- the exploitation of novel phenomena and properties at that scale.

To achieve these goals, it is necessary to use multidisciplinary approaches; inputs from physicists, biologists, chemists, and engineers[59-61] are required to advance our understanding of nanomaterials.[62] In fact, NPs properties are already used for developing new products[63, 64] such as paints, where they serve to break down odour substances, on surgical instruments in order to keep them sterile, in highly effective sun creams, slow release pharmaceuticals and many others.[50, 65-67] Bench-marketing studies on main current industries[53, 68] revealed that market opportunities that are illustrated in Figure 21.

As it is clearly shown, most of these market opportunities are involved in the development of new materials. Moreover, among the applied NPs, metal nanoparticles and metal oxide nanoparticles are of the most importance. However, because of the aforementioned toxicity and stability concerns have driven the research to develop nanomaterials with higher levels of safety. In this sense, here two different examples of safe and stable nanocomposites applications are discussed: their use for organic catalysis or for water disinfection.

Figure 21. Possible marketable applications of nanocomposites in different fields.

5.1. Bactericidal activity of MNPs

Among the currently known nanomaterials, it is well-known that AgNPs have unique antimicrobial properties.[69] Textiles, keyboards, wound dressings, and biomedical devices now contain AgNPs that continuously release a low level of Ag ions to provide protection against bacteria. Even if Ag has been known to be a bactericidal element for at least 1200 years, considering the unusual properties of nanometric scale materials, largely different from those of their bulk counterparts[70], it is not surprising that AgNPs have been found significantly more efficient than Ag^+ ions in mediating their antimicrobial activities.[71-75] All in all, the exact antibacterial action of AgNPs is still under debate.

Conversely, in many countries the microbial contamination of potable water sources poses a major threat to public health and the emergence of microorganisms resistant to multiple antimicrobial agents increases the demand for improved disinfection methods.[76] The importance of potable water for people in some countries dictates the need for the development of innovative technologies and materials for the production of safe potable water. This type of application can be a perfect niche for nanomaterials containing AgNPs. However, it is necessary to develop ecologically-safe nanomaterials that prevent the post-contamination of the used samples.[77] In this sense and as it has been already stated, functionalized polymers are currently acquiring a prominent role as NPs stabilizers for their excellent performance.[78, 79]

It is worthy to note here that ion-exchange materials are already widely used for various water treatment processes, mainly to eliminate undesired or toxic ionic impurities including hardness ions, iron, heavy metals, and others. The stabilization and immobilization of Ag-NPs in such matrices is very promising since using this approach, two complementary water treatment steps could be performed with a single material and the safety of the nanocomposites could be increased.

In our research group, the surface modification of ion-exchange materials used for traditional water treatment has been undertaken and promising results have been patented.[80] Such modification included the incorporation of either Ag or Ag@Co NPs.

As an example of the obtained results, Table 3 shows the synthetic conditions and the corresponding compositions of some nanocomposites of this family, probing the feasibility of the synthesis of both pure and core-shell nanoparticles.

To evaluate the efficiency of these nanocomposites for disinfection procedures, an increasing amount of nanocomposites beads was added to individual wells containing 10^5 CFU/mL of *E. coli* suspension in LB medium. After overnight incubation, bacterial proliferation was evaluated by measuring the optical density of each well at 550 nm (this wavelength is indicative of bacterial proliferation). The bactericidal activity of the Ag, Co and Ag@Co nanocomposites (in all the polymeric granulated matrices studied) was determined and raw materials were used as control (results are shown in Figure 22).

As it was expected, Ag and Ag@Co NPs containing sulfonated granulted materials increased their activity due to the presence NPs, but the enhancement was slightly higher for modified Ag@Co NPs. Anyhow, this proof of concept demonstrates the rightness of the approach.

Matrix	IEC / meq·g^{-1}	NPs	[Ag^{+}]/M	[Co^{2+}]/M	$mmol_{Ag}$/meq	$mmol_{Co}$/meq
C100E	2.3	Ag	0.01	--	0.064	--
(-SO_3^-)		Ag@Co	0.01	0.01	0.069	0.061
C104E	6.0	Ag	0.01	--	0.010	--
(-COO^-)		Ag@Co	0.01	0.01	0.010	0.017

Table 3. Metal content in granulated nanocomposites containing Ag- or Ag@Co-NPs and, analyzed by ICP-MS.

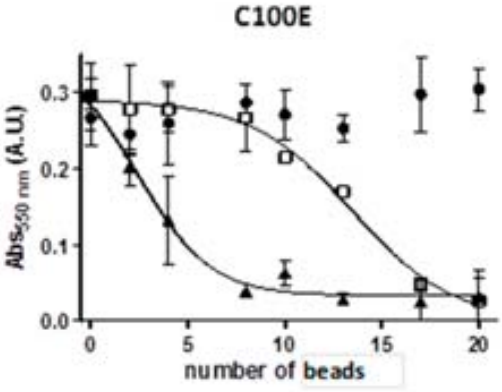

Figure 22. Variation of the absorbance at 550 nm with the number of polymer beads for (●) the raw material, (□) Ag- and, (▲) Ag@Co-nanocomposites (3 replicates).

5.2. Nanocatalysts for organic synthesis

Nanoparticles are increasingly used in catalysis, where the large surface area per unit volume of the catalyst may enhance reactions. This enhanced reactivity significantly reduces the quantity of catalytic materials required to carry out the reactions. Particular industries, including the oil and the automobile ones, are interested in this area for the use of NPs in catalytic converters.[81] As a prove of their industrial potentiality, many big companies, including BASF, Johnson Matthey and 3M, have interests in developing commercial applications for AuNPs catalysts.

In the last decade, heterogeneous catalysts have attracted much interest because of their general advantages that have been boosted thanks to the use of nanomaterials.[82, 83] One crucial property for catalysts is their recovery and, in this sense, magnetic nanocatalysts present some outstanding advantages because they can be conveniently recovered by using an external magnetic field.[84]

On the one hand, Platinum Group Metals (PGMs) are well-known as highly selective catalysts and are widely used in organic synthesis, chemical industry and other areas like dehalogenation, hydrodechlorination, carbonylation or oxidation.[85-87] Concerning the potential applications, Pd, Pt, Rh, and Au-NPs have proven to be very versatile as they are

efficient and selective catalysts for several types of catalytic reactions, including olefin hydrogenation and C-C coupling such as Heck, Suzuki and Sonogashira reactions.[88-90] Among them, Pd-catalyzed cross-coupling has emerged as an effective synthetic methodology that is employed in both academic and industrial sectors.[91] Despite such progress, a number of challenges still remain unknown, including the dilucidation of highly efficient and selective catalysts able to react with multiple reactive C-H or N-H bonds.

On the other hand, several types of magnetic materials have been used, including magnetite, hematite, maghemite, wüstite.[92] Magnetic aggregation and their need for functionalization do still hinder the application of magnetic NPs in industry. Thus, searching for more suitable magnetic materials to overcome these restrictions is still a challenge for realizing practical catalytic applications. Yet, for catalytic purposes, magnetic NPs surface is often chemically functionalized with molecular catalytic complexes because of the poor catalytic properties of the bare Fe oxides or other catalytic materials (*e.g.*, Co).[93, 94]

Therefore, and taking into account, the demonstrated efficiency of PGMs and the advantages of magnetic nanoparticles, it has been possible to apply develop Pd@Co-based nanocomposites for a typical C-C coupling reaction: the Suzuki reaction.[95] The preparation of such catalyses has only been possible thanks to the characteristics of IMS procedure, which allows the combination of a magnetic nanocore (made of Co) with the catalytic activity of a shell (Pd). The resulting material can be separated by simple filtration methods and, moreover, NPs can be re-covered and re-used by their retention under a magnetic field (Figure 23).[96]

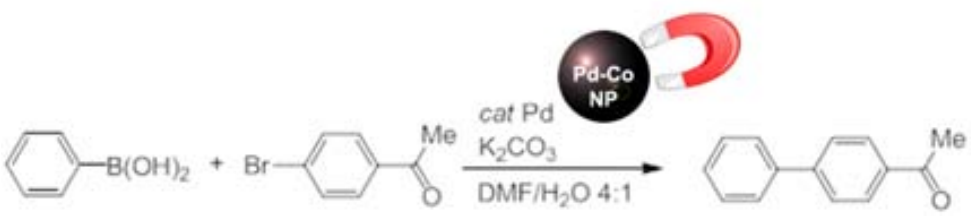

Figure 23. Suzuki reaction by using Pd or Pd@Co nanocomposites with optimized conditions.

Previous results with Pd@Co-NPs incorporated to fibrous materials showed the feasibility of this approach.[37] Differently, as it can be seen in Table 4, the catalytic efficiency of granulated polymers (containing either sulfonic or carboxylic groups) was very scarce, very likely due to the low metal immobilization achieved. However, two interesting results can be withdrawn: a substantial increase of the reaction yield was obtained when using the nanocomposite samples with higher Pd-content and the reaction yield could increase for consecutive runs.

Even if low conversions where achieved, this results are not discouraging since granulated polymeric matrices are still interesting for industrial applications because of their mechanical properties. Their high mechanical resistance leads to obtain higher reproducibility in synthesis as well as easier manipulation. Moreover, granulated polymer

industry is big enough to pay attention on it. Further research is needed to successfully increase the amount of immobilised metals what, very probably will provide better catalytic nanocomposites.

Samples		Metal Content		Yield (%)		
Matrix	**MNPS**	**Pd (mg/gNC)**	**Co (mg/gNC)**	**#0**	**#1**	**#2**
C100E	**Pd**	57	-	44	-	-
	Pd	30	50	8.6	-	-
C104E	**Pd@Co**	47	48	9.8	8.4	-
	Pd@Co	30	7,6	4	**26**	28

Table 4. Suzuki reaction yields (in %) for the Pd- and Pd@Co-nanocomposites

6. Conclusions

The conclusions derived from the results presented in this chapter can be briefly formulated as follows:

1. The ion-exchange assisted Intermatrix Synthesis (IMS) technique represents one of the most promising techniques that allows for the production of a large variety of polymer–metal nanocomposites of practical importance for different fields of modern science and technology.

   The attractiveness of this technique is basically determined by its relative simplicity in comparison with other methods used for production of nanocomposite materials and also by its flexibility and the possibility of tuning the specific properties of the final nanocomposites to meet the requirements of their final applications. IMS technique gives a unique possibility of production of nanocomposites containing MNPs of various composition and structure (for example, monometallic, bimetallic or polymetallic MNPs with core-shell, core-sandwich and even more complex structures) for the applications of interest.

2. The spectrum of polymers applicable for IMS of PSMNPs is quite wide and includes various functionalized polymers, i.e. those bearing functional groups in the form of granules, fibers or membranes, which are capable to bind either metal or reducer ions prior to the metal reduction inside the polymer matrix (IMS of PSMNPs).

   The dissociated ionogenic functional groups of the polymer bearing positive or negative charges provide a possibility to couple IMS technique with Donnan exclusion effect. In case of polymers with negatively charged groups the IMS technique consists of the metal loading stage followed by metal reduction inside the polymer. When polymer bears positively charged groups the IMS procedure starts with the reducer loading followed by the simultaneous metal loading-reduction stage.

3. It has been shown that the use of, for example, anionic reducing agents (e.g., borohydride) for the synthesis of PSMNPs by using IMS coupled with Donnan effect in both cation exchange and anion exchange matrices results in their formation mainly near the surface of the polymer. This type of MNP distribution is favorable for many practical applications of polymer–metal nanocomposites such as reagent-free water disinfection, catalysis and some others.
4. The general properties of polymer-metal nanocomposite are not determined only by the properties of the MNPs. The formation of MNPs within the polymer matrices may strongly modify the polymer morphology, for example due to the appearance of nanoporosity in gel-type polymers, which enhances the rate of mass transfer inside the nanocomposites as well as some other structural parameters of great importance in their practical applications.
   The polymer matrix also serves as the MNPs stabilizing media preventing their aggregation and release to the medium under treatment. The functional properties of the nanocomposites (e.g., catalytic or bactericide) are mainly determined by the properties of MNPs immobilized inside the matrix.
5. The repetitive metal-loading-reduction (in case of cation exchangers) or reducer-loading-metal-reduction (in case of anion exchangers) permits to synthesize MNPs of core-shell or even more complex structure provided with additional functional properties.
   For example, the IMS of core shell PSMNPs consisting of superparamagnetic cores coated with functional shells having for example, catalytic or bactericide properties provides the polymer–metal nanocomposites with additional advantages. In the case of catalytic applications, the nanocomposite can be easily recovered from the reaction mixture and reused. In water treatment applications, the magnetic nature of MNPs permits for preventing their uncontrollable escape into the treated water by using simple magnetic traps.
6. Finally, the last and the most important in our opinion conclusion concern the general strategy in the development of novel nanocomposite materials. This strategy has to be focused not only on the desired properties of material, which is dictated by its further practical applications, but also on the material safety in both environmental and human health senses. The last point seems to be of particular importance for the further development of Nanoscience and Nanotechnology.

Author details

Berta Domènech, Julio Bastos-Arrieta, Amanda Alonso, Maria Muñoz
and Dmitri N. Muraviev
Analytical Chemistry Division, Chemistry Department, Autonomous University of Barcelona, Barcelona, Spain

Jorge Macanás
Department of Chemical Engineering, Universitat Politècnica de Catalunya, Barcelona, Spain

7. References

[1] Ajayan, P.M., Schadler, L.S. and Braun, P.V., *Nanocomposite Science and Technology*. 2003: Wiley-Vch.

[2] *Metallic Nanoparticles*, in *Handbook of Metal Physics*, A.B. John, Editor. 2008, Elsevier. p. iii.

[3] Campelo, J.M., Luna, D., Luque, R., Marinas, J.M. and Romero, A.A., *Sustainable Preparation of Supported Metal Nanoparticles and Their Applications in Catalysis.* ChemSusChem, 2009. 2(1): p. 18-45.

[4] Giannazzo, F., Eyben, P., Baranowski, J., Camassel, J. and Lanyi, S., *Advanced materials nanocharacterization.* Nanoscale Research Letters, 2011. 6(1): p. 107.

[5] Hassan, M.H.A., *Small Things and Big Changes in the Developing World.* Science, 2005. 309(5731): p. 65-66.

[6] Wang, F.-C., Zhang, W.E., Yang, C.H., Yang, M.J., Bennett, B.R., Wilson, R.A. and Stone, D.R., *A tunneling field-effect transistor with 25 nm metallurgical channel length.* Applied Physics Letters, 1997. 70(22): p. 3005-3007.

[7] Davis Paul, H., Morrisey Cody, P., Tuley Sean, M.V. and Bingham Chris, I., *Synthesis and Stabilization of Colloidal Gold Nanoparticle Suspensions for SERS*, in *Nanoparticles: Synthesis, Stabilization, Passivation, and Functionalization*. 2008, American Chemical Society. p. 16-30.

[8] *Nanoparticles: Synthesis, Stabilization, Passivation, and Functionalization, Copyright, Foreword*, in *Nanoparticles: Synthesis, Stabilization, Passivation, and Functionalization*. 2008, American Chemical Society. p. i-v.

[9] Nagarajan, R., *Nanoparticles: Building Blocks for Nanotechnology*, in *Nanoparticles: Synthesis, Stabilization, Passivation, and Functionalization*. 2008, American Chemical Society. p. 2-14.

[10] Li, Q., El Khoury Jouliana, M., Zhou, X., Urbas, A., Qu, L. and Dai, L., *Synthesis of Thiol Surfactant with Tunable Length as a Stabilizer of Gold Nanoparticles*, in *Nanoparticles: Synthesis, Stabilization, Passivation, and Functionalization*. 2008, American Chemical Society. p. 41-54.

[11] Gaponik, N., Eychmüller, A., Schmid, G., Talapin, D.V. and Shevchenko, E.V., *Organization of Nanoparticles*, in *Nanoparticles*. 2010, Wiley-VCH Verlag GmbH & Co. KGaA. p. 311-370.

[12] Astruc, D., *Transition-metal Nanoparticles in Catalysis: From Historical Background to the State-of-the Art*, in *Nanoparticles and Catalysis*. 2008, Wiley-VCH Verlag GmbH & Co. KGaA. p. 1-48.

[13] Jorge, M., Patricia, R., Amanda, A., María, M. and Dmitri, M., *Ion Exchange-Assisted Synthesis of Polymer Stabilized Metal Nanoparticles*, in *Ion Exchange and Solvent Extraction*. 2011, CRC Press. p. 1-44.

[14] Gerion, D., Parak, W.J., Williams, S.C., Zanchet, D., Micheel, C.M. and Alivisatos, A.P., *Sorting Fluorescent Nanocrystals with DNA.* Journal of the American Chemical Society, 2002. 124(24): p. 7070-7074.

[15] Zhao, X., Yin, M., Ma, L., Liang, L., Liu, C., Liao, J., Lu, T. and Xing, W., *Recent advances in catalysts for direct methanol fuel cells.* Energy & Environmental Science, 2011. 4(8): p. 2736-2753.

[16] Astruc, D., Lu, F. and Aranzaes, J.R., *Nanoparticles as Recyclable Catalysts: The Frontier between Homogeneous and Heterogeneous Catalysis.* Angewandte Chemie International Edition, 2005. 44(48): p. 7852-7872.
[17] Spagnoli, D., Banfield, J.F. and Parker, S.C., *Free Energy Change of Aggregation of Nanoparticles.* The Journal of Physical Chemistry C, 2008. 112(38): p. 14731-14736.
[18] Rozenberg, B.A. and Tenne, R., *Polymer-assisted fabrication of nanoparticles and nanocomposites.* Progress in Polymer Science, 2008. 33(1): p. 40-112.
[19] Imre, Á., Beke, D.L., Gontier-Moya, E., Szabó, I.A. and Gillet, E., *Surface Ostwald ripening of Pd nanoparticles on the MgO (100) surface.* Applied Physics A: Materials Science & Processing, 2000. 71(1): p. 19-22.
[20] Carotenuto, G., Nicolais, L., Martorana, B. and Perlo, P., *Metal-Polymer Nanocomposite Synthesis: Novel ex situ and in situ Approaches*, in *Metal–Polymer Nanocomposites*. 2005, John Wiley & Sons, Inc. p. 155-181.
[21] Luckham, P.F., *Manipulating forces between surfaces: applications in colloid science and biophysics.* Advances in Colloid and Interface Science, 2004. 111(1–2): p. 29-47.
[22] Kamat, P.V., *Photophysical, Photochemical and Photocatalytic Aspects of Metal Nanoparticles.* The Journal of Physical Chemistry B, 2002. 106(32): p. 7729-7744.
[23] Jeon, S.-H., Xu, P., Zhang, B., Mack, N.H., Tsai, H., Chiang, L.Y. and Wang, H.-L., *Polymer-assisted preparation of metal nanoparticles with controlled size and morphology.* Journal of Materials Chemistry, 2011. 21(8): p. 2550-2554.
[24] Visser, J., *The concept of negative hamaker coefficients. 1. history and present status.* Advances in Colloid and Interface Science, 1981. 15(2): p. 157-169.
[25] Pomogailo, A. and Kestelman, V.N., *Metallopolymer nanocomposites*. Springer series in materials science, 81. 2005, New York.
[26] Henderson, J., *The analysis of ancient glasses part II: Luxury Roman and early medieval glasses.* JOM Journal of the Minerals, Metals and Materials Society, 1996. 48(2): p. 62-64.
[27] Walter, P., Welcomme, E., Hallégot, P., Zaluzec, N.J., Deeb, C., Castaing, J., Veyssière, P., Bréniaux, R., Lévêque, J.-L. and Tsoucaris, G., *Early Use of PbS Nanotechnology for an Ancient Hair Dyeing Formula.* Nano Letters, 2006. 6(10): p. 2215-2219.
[28] Meurdrac, M. and Jacques, J., *La chymie charitable et facile en faveur des dames : 1666*. 1999, Paris: CNRS.
[29] Diderot, D.D.A., M., *Encyclopédie ou Dictionnaire raisonné des sciences, des arts et des métiers*. 1751: Tome troisième: Paris.
[30] Mirguet, C., Fredrickx§, P., Sciau, P. and Colomban, P., *Origin of the self-organisation of Cu°/Ag° nanoparticles in ancient lustre pottery. A TEM study.* Phase Transitions, 2008. 81(2-3): p. 253-266.
[31] Mills, G.F., *Ammine Exchange Resins.* Ind. Eng. Chem, 1949. 41(12).
[32] Domènech, B., Muñoz, M., Muraviev, D.N. and Macanás, J., *Catalytic membranes with palladium nanoparticles: From tailored polymer to catalytic applications.* Catalysis Today, (0).
[33] Park, J.-I., Kim, M.G., Jun, Y.-w., Lee, J.S., Lee, W.-r. and Cheon, J., *Characterization of Superparamagnetic "Core–Shell" Nanoparticles and Monitoring Their Anisotropic Phase Transition to Ferromagnetic "Solid Solution" Nanoalloys.* Journal of the American Chemical Society, 2004. 126(29): p. 9072-9078.

[34] Bastos-Arrieta, J., Shafir, A., Alonso, A., Muñoz, M., Macanás, J. and Muraviev, D.N., *Donnan exclusion driven intermatrix synthesis of reusable polymer stabilized palladium nanocatalysts.* Catalysis Today, (0).

[35] Alonso, A., Macanas, J., Shafir, A., Munoz, M., Vallribera, A., Prodius, D., Melnic, S., Turta, C. and Muraviev, D.N., *Donnan-exclusion-driven distribution of catalytic ferromagnetic nanoparticles synthesized in polymeric fibers.* Dalton Transactions, 2010. 39(10): p. 2579-2586.

[36] Muraviev, D.N., Macanás, J., Farre, M., Muñoz, M. and Alegret, S., *Novel routes for inter-matrix synthesis and characterization of polymer stabilized metal nanoparticles for molecular recognition devices.* Sensors and Actuators B: Chemical, 2006. 118(1–2): p. 408-417.

[37] Alonso, A., Shafir, A., Macanás, J., Vallribera, A., Muñoz, M. and Muraviev, D.N., *Recyclable polymer-stabilized nanocatalysts with enhanced accessibility for reactants.* Catalysis Today, (0).

[38] Barbaro, P. and Liguori, F., *Ion Exchange Resins: Catalyst Recovery and Recycle.* Chemical Reviews, 2008. 109(2): p. 515-529.

[39] Harland, C.E. and Grimshaw, R.W., *Ion exchange : theory and practice*. 1994, Cambridge: Royal Society of Chemistry.

[40] Myers, R.J., Eastes, J.W. and Myers, F.J., *Synthetic Resins as Exchange Adsorbents.* Industrial & Engineering Chemistry, 1941. 33(6): p. 697-706.

[41] Abrams, I.M. and Millar, J.R., *A history of the origin and development of macroporous ion-exchange resins.* Reactive and Functional Polymers, 1997. 35(1–2): p. 7-22.

[42] Xu, T., *Ion exchange membranes: State of their development and perspective.* Journal of Membrane Science, 2005. 263(1–2): p. 1-29.

[43] Sata, T., *Ion Exchange Membranes: Preparation, Characterization, Modification and Application*. 2004, Cambridge: The Royal Society of Chemistry 2004.

[44] Huang, R.Y.M., Shao, P., Burns, C.M. and Feng, X., *Sulfonation of poly(ether ether ketone)(PEEK): Kinetic study and characterization.* Journal of Applied Polymer Science, 2001. 82(11): p. 2651-2660.

[45] Xing, P., Robertson, G.P., Guiver, M.D., Mikhailenko, S.D., Wang, K. and Kaliaguine, S., *Synthesis and characterization of sulfonated poly(ether ether ketone) for proton exchange membranes.* Journal of Membrane Science, 2004. 229(1–2): p. 95-106.

[46] Domènech, B., Muñoz, M., Muraviev, D.N. and Macanás, J., *Polymer-stabilized palladium nanoparticles for catalytic membranes: ad hoc polymer fabrication.* Nanoscale Research Letters, 2011. 6(406).

[47] Blanco, J.F., Nguyen, Q.T. and Schaetzel, P., *Novel hydrophilic membrane materials: sulfonated polyethersulfone Cardo.* Journal of Membrane Science, 2001. 186(2): p. 267-279.

[48] Blanco, J.-F., Sublet, J., Nguyen, Q.T. and Schaetzel, P., *Formation and morphology studies of different polysulfones-based membranes made by wet phase inversion process.* Journal of Membrane Science, 2006. 283(1–2): p. 27-37.

[49] Maynard, R.L. and Howard, C.V., *Particulate Matter: Properties and Effects upon Health*. 1999, Oxford: Bios Scientific Publishers.

[50] Bottero, J.-Y., Rose, J. and Wiesner, M.R., *Nanotechnologies: Tools for Sustainability in a New Wave of Water Treatment Processes.* Integrated Environmental Assessment and Management, 2006. 2(4): p. 391-395.

[51] Borm, P.J.A. and Berube, D., *A tale of opportunities, uncertainties, and risks.* Nano Today, 2008. 3(1–2): p. 56-59.
[52] Abbott, L.C. and Maynard, A.D., *Exposure Assessment Approaches for Engineered Nanomaterials.* Risk Analysis, 2010. 30(11): p. 1634-1644.
[53] Schulenburg M., N.s.t., big effects Opportunities and risks., *Nanoparticles – small things, big effects Opportunities and risks.* . 2008, Bonn: Bundesministerium für Bildung und Forschung (BMBF) / Federal Ministry of
[54] n and Research.
[55] Vatta, L.L., Sanderson, R.D. and Koch, K.R., *Magnetic nanoparticles: Properties and*
[56] *applications.* Pure Appl. Chem., 2006. 78(9).
[57] Talapatra, S., Ganesan, P.G., Kim, T., Vajtai, R., Huang, M., Shima, M., Ramanath, G., Srivastava, D., Deevi, S.C. and Ajayan, P.M., *Irradiation-Induced Magnetism in Carbon Nanostructures.* Physical Review Letters, 2005. 95(9): p. 097201.
[58] Hyeon, T., *Chemical synthesis of magnetic nanoparticles.* Chemical Communications, 2003(8): p. 927-934.
[59] Ding, Y., Hu, Y., Zhang, L., Chen, Y. and Jiang, X., *Synthesis and Magnetic Properties of Biocompatible Hybrid Hollow Spheres.* Biomacromolecules, 2006. 7(6): p. 1766-1772.
[60] Bower, N.W., *Principles of Instrumental Analysis. 4th edition (Skoog, D. A.; Leary, J. J.).* Journal of Chemical Education, 1992. 69(8): p. A224.
[61] Schmid, G., *Conclusions and Perspectives*, in *Nanoparticles*. 2010, Wiley-VCH Verlag GmbH & Co. KGaA. p. 513-515.
[62] Fendler, J.H. and Tian, Y., *Nanoparticles and Nanostructured Films: Current Accomplishments and Future Prospects*, in *Nanoparticles and Nanostructured Films*. 2007, Wiley-VCH Verlag GmbH. p. 429-461.
[63] Plieth, W.J., *Electrochemical properties of small clusters of metal atoms and their role in the surface enhanced Raman scattering.* The Journal of Physical Chemistry, 1982. 86(16): p. 3166-3170.
[64] Weller, H., *Clusters and Colloids: From Theory to Applications. Edited by G. Schmid, VCH, Weinheim 1994, 555 pp., hardcover, DM 248.00, ISBN 3–527–29043–5.* Advanced Materials, 1995. 7(1): p. 94-94.
[65] Milev, A.S., Kannangara, G.S.K., Wilson, M.A., Sydney, U.o.W., College of Science, T., Environment, School of Science, F. and Horticulture, *Nanotechnology*.
[66] Lane, N., *Nanotechnologies meet market realities.* Chem Eng News 2002: p. 17.
[67] Hillie, T. and Hlophe, M., *Nanotechnology and the challenge of clean water.* Nat Nano, 2007. 2(11): p. 663-664.
[68] Ju-Nam, Y. and Lead, J.R., *Manufactured nanoparticles: An overview of their chemistry, interactions and potential environmental implications.* Science of The Total Environment, 2008. 400(1–3): p. 396-414.
[69] Narayan, R., *Use of nanomaterials in water purification.* Materials Today, 2010. 13(6): p. 44-46.
[70] Theron, J., Walker, J.A. and Cloete, T.E., *Nanotechnology and Water Treatment: Applications and Emerging Opportunities.* Critical Reviews in Microbiology, 2008. 34(1): p. 43-69.

[71] Li, W.R., Xie, X.B., Shi, Q.S., Zeng, H.Y., Ou-Yang, Y.S. and Chen, Y.B., *Antibacterial activity and mechanism of silver nanoparticles on Escherichia coli.* Applied microbiology and biotechnology, 2010. 85(4): p. 1115-1122.

[72] Kelly, K.L., Coronado, E., Zhao, L.L. and Schatz, G.C., *The Optical Properties of Metal Nanoparticles: The Influence of Size, Shape, and Dielectric Environment.* The Journal of Physical Chemistry B, 2002. 107(3): p. 668-677.

[73] Kumar, R., Howdle, S. and Münstedt, H., *Polyamide/silver antimicrobials: Effect of filler types on the silver ion release.* Journal of Biomedical Materials Research Part B: Applied Biomaterials, 2005. 75B(2): p. 311-319.

[74] De Gusseme, B., Sintubin, L., Baert, L., Thibo, E., Hennebel, T., Vermeulen, G., Uyttendaele, M., Verstraete, W. and Boon, N., *Biogenic Silver for Disinfection of Water Contaminated with Viruses.* Applied and Environmental Microbiology, 2010. 76(4): p. 1082-1087.

[75] Dibrov, P., Dzioba, J., Gosink, K.K. and Häse, C.C., *Chemiosmotic Mechanism of Antimicrobial Activity of Ag+ in Vibrio cholerae.* Antimicrobial Agents and Chemotherapy, 2002. 46(8): p. 2668-2670.

[76] Lok, C.-N., Ho, C.-M., Chen, R., He, Q.-Y., Yu, W.-Y., Sun, H., Tam, P.K.-H., Chiu, J.-F. and Che, C.-M., *Proteomic Analysis of the Mode of Antibacterial Action of Silver Nanoparticles.* Journal of Proteome Research, 2006. 5(4): p. 916-924.

[77] Silvestry-Rodriguez, N., Bright, K.R., Slack, D.C., Uhlmann, D.R. and Gerba, C.P., *Silver as a Residual Disinfectant To Prevent Biofilm Formation in Water Distribution Systems.* Applied and Environmental Microbiology, 2008. 74(5): p. 1639-1641.

[78] Ruparelia, J.P., Chatterjee, A.K., Duttagupta, S.P. and Mukherji, S., *Strain specificity in antimicrobial activity of silver and copper nanoparticles.* Acta Biomaterialia, 2008. 4(3): p. 707-716.

[79] Charnley, M., Textor, M. and Acikgoz, C., *Designed polymer structures with antifouling–antimicrobial properties.* Reactive and Functional Polymers, 2011. 71(3): p. 329-334.

[80] Murthy, P.S.K., Murali Mohan, Y., Varaprasad, K., Sreedhar, B. and Mohana Raju, K., *First successful design of semi-IPN hydrogel–silver nanocomposites: A facile approach for antibacterial application.* Journal of Colloid and Interface Science, 2008. 318(2): p. 217-224.

[81] Childs, W.R., Motala, M.J., Lee, K.J. and Nuzzo, R.G., *Masterless Soft Lithography: Patterning UV/Ozone−Induced Adhesion on Poly(dimethylsiloxane) Surfaces†.* Langmuir, 2005. 21(22): p. 10096-10105.

[82] D.N., M. 2010.

[83] Bonet, F., Grugeon, S., Herrera Urbina, R., Tekaia-Elhsissen, K. and Tarascon, J.M., *In situ deposition of silver and palladium nanoparticles prepared by the polyol process, and their performance as catalytic converters of automobile exhaust gases.* Solid State Sciences, 2002. 4(5): p. 665-670.

[84] Liu, G., Gu, H., Sun, Y., Long, J., Xu, Y. and Li, H., *Magnetically Recoverable Nanoparticles: Highly Efficient Catalysts for Asymmetric Transfer Hydrogenation of Aromatic Ketones in Aqueous Medium.* Advanced Synthesis & Catalysis, 2011. 353(8): p. 1317-1324.

[85] Kidambi, S., Dai, J., Li, J. and Bruening, M.L., *Selective Hydrogenation by Pd Nanoparticles Embedded in Polyelectrolyte Multilayers.* Journal of the American Chemical Society, 2004. 126(9): p. 2658-2659.

[86] Brock, S.L. and Senevirathne, K., *Recent developments in synthetic approaches to transition metal phosphide nanoparticles for magnetic and catalytic applications.* Journal of Solid State Chemistry, 2008. 181(7): p. 1552-1559.

[87] Wilson, O.M., Knecht, M.R., Garcia-Martinez, J.C. and Crooks, R.M., *Effect of Pd Nanoparticle Size on the Catalytic Hydrogenation of Allyl Alcohol.* Journal of the American Chemical Society, 2006. 128(14): p. 4510-4511.

[88] Umpierre, A.P., Machado, G., Fecher, G.H., Morais, J. and Dupont, J., *Selective Hydrogenation of 1,3-Butadiene to 1-Butene by Pd(0) Nanoparticles Embedded in Imidazolium Ionic Liquids.* Advanced Synthesis & Catalysis, 2005. 347(10): p. 1404-1412.

[89] Durand, J., Teuma, E. and Gómez, M., *An Overview of Palladium Nanocatalysts: Surface and Molecular Reactivity.* European Journal of Inorganic Chemistry, 2008. 2008(23): p. 3577-3586.

[90] Moreno-Mañas, M. and Pleixats, R., *Formation of Carbon−Carbon Bonds under Catalysis by Transition-Metal Nanoparticles.* Accounts of Chemical Research, 2003. 36(8): p. 638-643.

[91] Torborg, C. and Beller, M., *Recent Applications of Palladium-Catalyzed Coupling Reactions in the Pharmaceutical, Agrochemical, and Fine Chemical Industries.* Advanced Synthesis & Catalysis, 2009. 351(18): p. 3027-3043.

[92] Diéguez, M., Pàmies, O., Mata, Y., Teuma, E., Gómez, M., Ribaudo, F. and van Leeuwen, P.W.N.M., *Palladium Nanoparticles in Allylic Alkylations and Heck Reactions: The Molecular Nature of the Catalyst Studied in a Membrane Reactor.* Advanced Synthesis & Catalysis, 2008. 350(16): p. 2583-2598.

[93] Hoffmann, R., Imamura, A. and Hehre, W.J., *Benzynes, dehydroconjugated molecules, and the interaction of orbitals separated by a number of intervening sigma bonds.* Journal of the American Chemical Society, 1968. 90(6): p. 1499-1509.

[94] de Dios, A.S. and Díaz-García, M.E., *Multifunctional nanoparticles: Analytical prospects.* Analytica Chimica Acta, 2010. 666(1–2): p. 1-22.

[95] Hu, A., Yee, G.T. and Lin, W., *Magnetically Recoverable Chiral Catalysts Immobilized on Magnetite Nanoparticles for Asymmetric Hydrogenation of Aromatic Ketones.* Journal of the American Chemical Society, 2005. 127(36): p. 12486-12487.

[96] Gleeson, O., Tekoriute, R., Gun'ko, Y.K. and Connon, S.J., *The First Magnetic Nanoparticle-Supported Chiral DMAP Analogue: Highly Enantioselective Acylation and Excellent Recyclability.* Chemistry – A European Journal, 2009. 15(23): p. 5669-5673.

[97] M., P.C., S., K.M. and J., P., *Palladium Nanoparticles in Polymers: Catalyst for Alkene Hydrogenation, Carbon–Carbon Cross-Coupling Reactions, and Aerobic Alcohol Oxidation.* Synthesis, 2006.

[98] C., Z., D., X., W., J.-w. and X., H., *An efficient and recyclable ionic liquid-supported proline catalyzed Knoevenagel Condensation.* ISRN Organic Chemistry, 2011: p. 5.

Domènech et al. Nanoscale Research Letters 2013, 8:238
http://www.nanoscalereslett.com/content/8/1/238

Nanoscale Research Letters
a SpringerOpen Journal

NANO EXPRESS Open Access

Development of novel catalytically active polymer-metal-nanocomposites based on activated foams and textile fibers

Berta Domènech[1], Kharla K Ziegler[1], Fernando Carrillo[2,3], Maria Muñoz[1], Dimitri N Muraviev[1] and Jorge Macanás[2*]

Abstract

In this paper, we report the intermatrix synthesis of Ag nanoparticles in different polymeric matrices such as polyurethane foams and polyacrylonitrile or polyamide fibers. To apply this technique, the polymer must bear functional groups able to bind and retain the nanoparticle ion precursors while ions should diffuse through the matrix. Taking into account the nature of some of the chosen matrices, it was essential to try to activate the support material to obtain an acceptable value of ion exchange capacity. To evaluate the catalytic activity of the developed nanocomposites, a model catalytic reaction was carried out in batch experiments: the reduction of *p*-nitrophenol by sodium borohydride.

Keywords: Metal nanoparticles, Polyurethane foams, Polyacrylonitrile fibers, Polyamide fibers

Background

In the last decade, heterogeneous catalysts have attracted much interest because of their general advantages [1] that have been boosted thanks to the use of nanomaterials [2-4]. In fact, nanoparticles (NPs) are increasingly used in catalysis since their enhanced reactivity significantly reduces the quantity of catalytic material required to carry out reactions with a high turnover [1,2,5]. However, following the basic principles of nanosafety, the prevention of uncontrollable escape of these materials to the reaction media as well as the minimization of the probability of their appearance in the environment is becoming a crucial issue [3-6]. In this sense, the synthesis of polymer-metal nanocomposites (PMNCs) [1,7-10], obtained by the incorporation of metal nanoparticles (MNPs) in polymeric matrices, has demonstrated to be an attractive approach [5,8]. By stabilizing MNPs in a polymeric matrix, it is possible to prevent their escape to the reaction medium, thus providing an easy separation of the catalyst from the reaction mixture which, in turn, allows the possibility to reuse the catalytic species without losing efficiency.

One of the methodologies that allow obtaining these PMNCs in a feasible way is the so-called intermatrix synthesis (IMS) [8,11,12], based on the dual function of the matrix, which stabilizes the MNPs preventing their uncontrollable growth and aggregation and provides a medium for the synthesis. IMS proceeds by a simple two sequential steps: (a) the immobilization of metal cations (MNPs precursors) inside the matrix and (b) the reduction of metal ions to the zero-valent state leading to the formation of MNPs.

The main goal of this work is the development of advanced nanocomposite materials obtained by the incorporation of silver nanoparticles (AgNPs) in typical textile fibers (polyacrylonitrile, PAN, and polyamide, PA) and in polyurethane foams (PUFs). Yet, up to now, the IMS technique has been applied to polymers bearing ionogenic functional groups that retain the MNPs ion precursors [8,13,14]. Regarding this issue, and taking into account the nature of some of the polymeric matrices (e.g., PUF), it was considered essential to activate the support material to obtain an acceptable value of ion exchange capacity (IEC).

Finally, in order to evaluate the catalytic activity of the different developed PMNCs, a model catalytic reaction was carried out in batch experiments: the reduction of

* Correspondence: jorge.macanas@upc.edu
[2]Chemical Engineering Department, UPC, Universitat Politècnica de Catalunya, C/Colom, 1, 08222 Terrassa, Barcelona, Spain
Full list of author information is available at the end of the article

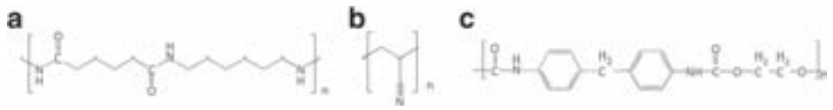

Figure 1 Structural units of the polymeric matrices (a) PA, (b) PAN, and (c) PUF.

p-nitrophenol (4-np) to *p*-aminophenol (4-ap) in the presence of $NaBH_4$ and metallic catalyst [15].

Methods

Materials

Commercial PUF was obtained from Comercial del Caucho (Daplasca, Sabadell, Spain), PA (Nylon 6.6, type 200, DuPont) and PAN fibers (type 75, DuPont) from woven fabrics were used (Figure 1). Organics and metal salts (acetone, 4-np, NaOH, HCl, $NaBH_4$, HNO_3, and $AgNO_3$) from Panreac Company (Castellar del Vallès, Barcelona, Spain) were used as received.

Pretreatment of the PUFs

The pretreatment of PUFs was investigated to activate the material. First, foams were washed with acetone and then with distilled water to eliminate the possible commercial treatments applied to the material. Different pretreatments were applied to 1 cm^3 of foam samples, which were immersed in 25 ml of the pretreatment reagent solution (1 M HNO_3, 3 M HNO_3, 1 M NaOH, and 3 M NaOH) for 2 h under agitation. Afterwards, the samples were washed several times with distilled water.

In order to determine the possible effect of the pretreatments in the chemical structure of the PUFs, attenuated total reflectance Fourier transform infrared (FTIR-ATR) spectra were recorded with a Perkin Elmer Spectrum GX spectrometer (Norwalk, CT, USA). Moreover, for determining the concentration of the functional groups before and after the pretreatment of the matrix, two titration methods were applied to calculate IEC (in meq/g) of the material [16]:

1. For determining cation exchange groups: 1 cm^3 of PUF was immersed in 100 ml of NaOH 0.1 M and shaked at room temperature for 48 h, time enough to ensure a complete neutralization of the acidic groups. Then, an aliquot of 10 ml was titrated with standardized HCl 0.1 M (3 replicates).
2. For determining anion exchange groups a similar procedure was used, but immersing the sample in 100 ml of HCl 0.1 M, and using standardized NaOH 0.1 M to titrate the 3 aliquots of 10ml.

Synthesis of AgNPs

The synthesis of AgNPs in the polymeric matrices by the IMS methodology consisted of the following: (1) loading of the material with the metal ions ($AgNO_3$ 0.4 M solution) and (2) reduction of metal ions to zero-

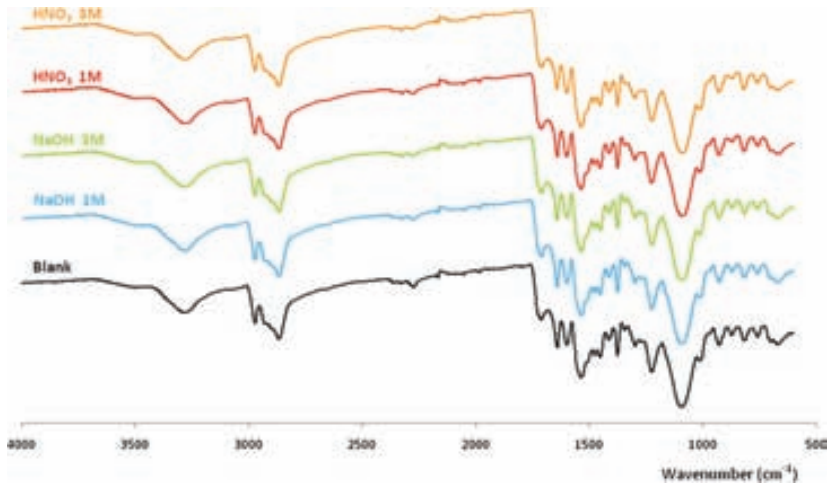

Figure 2 FTIR-ATR of PUFs before and after pretreatments.

Table 1 PUF IEC values

	IEC (meq/g)	
Treatment	Acid groups	Basic groups
Blank	0.65	0.62
NaOH 1M	0.32	0.61
NaOH 3M	0.57	0.61
HNO3 1M	0.66	0.71
HNO3 3M	0.61	0.57

IEC, ion exchange capacity. Uncertainty in all of the cases was <1%.

valent MNPs through reaction (by using $NaBH_4$ 0.5M solution). The reactions involved are as follows:

$$R - X^{-}Na^{+} + Ag^{+} \rightleftarrows (R - X^{-})Na^{+} + Ag^{+} \quad (1)$$

$$(R - X^{-})Ag^{+} + \ NaBH_4 + 3H_2O \rightarrow (R - X^{-})Na^{+} + 7/2\ H_2 + B(OH)_3 + Ag^{0} \quad (2)$$

Although equations depict a pure ion exchange mechanism, the generation of coordination bonds between species may also result in the immobilization of the ionic species in the polymeric matrix. In addition, the entry of metal ions into the matrix could be significantly affected by the synthetic conditions (i.e., temperature) which can affect the structural organization of the polymer matrices thus making the matrix temporarily accessible to the metal ions by opening their structure; after the synthesis, the fibers revert back to their closely packed state thus trapping the MNPs within the polymer structure. For the PUFs, the procedure described above was performed at room temperature; whereas in the case of the textile fibers, synthesis using different temperatures (25°C, 40°C, and 80°C) were applied.

Nanocomposite characterization

In order to determine the exact metal content in the prepared nanocomposites, samples of known weight were digested with concentrated HNO_3. The resulting solutions (two replicates) were diluted and analyzed by inductively coupled plasma mass spectrometry (ICP-MS).

With the aim of characterizing the size and structure of the obtained AgNPs, transmission electron microscopy (TEM) was performed by a JEOL JEM-2011 HR-TEM (JEOL Ltd., Tokyo, Japan). Before observation, the samples were deposited between two plastic sheets in an epoxy resin, and ultra-thin slices were obtained using an ultramicrotome.

Catalytic properties evaluation

The catalytic performance of nanocomposites was evaluated by using the reduction of 4-np to 4-ap by $NaBH_4$ as a model reaction, which was considered to follow a pseudo-first-order kinetics, and the apparent rate constant (k_{app}) was calculated. In a typical run, a piece of nanocomposite (1 cm^2 for textile fibers and 1 cm^3 for PUFs) was added to a vessel of 50 ml solution containing 4-np (0.5 mM) and $NaBH_4$ (500 mM). The process was monitored at 390 nm by a Pharmacia LKB Novaspec II spectrometer (Biochrom Ltd., Cambridge, UK).

Results and discussion

Characterization of the polyurethane foams and their pretreatments

PUF resulted to be a very stable material. The FTIR-ATR spectra of PUFs (Figure 2) show the distinctive polyurethrane (PU) bands [17]: the broad peak at 3,270 cm^{-1} is characteristic of the υ(N-H), the peaks at 1,690 and 1,520 cm^{-1} are typical for υ(C=O) (urethane band) and δ(NH) with υ(CO-N) (amide II). Surprisingly, no differences between spectra were observed. Thus, no chemical modification took place after any pretreatment.

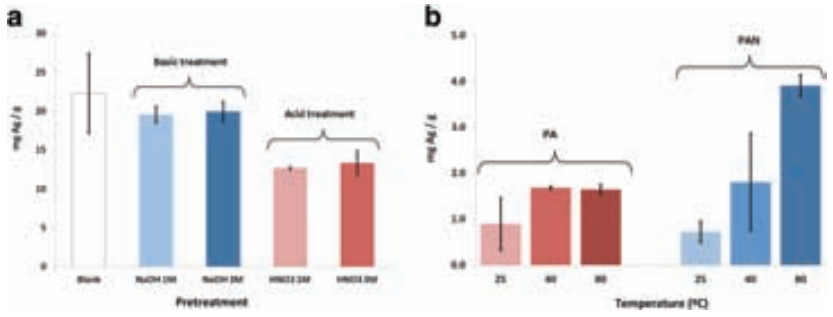

Figure 3 Results of the ICP-MS analysis of the Ag content in (a) PUFs and (b) PAN and PA fibers.

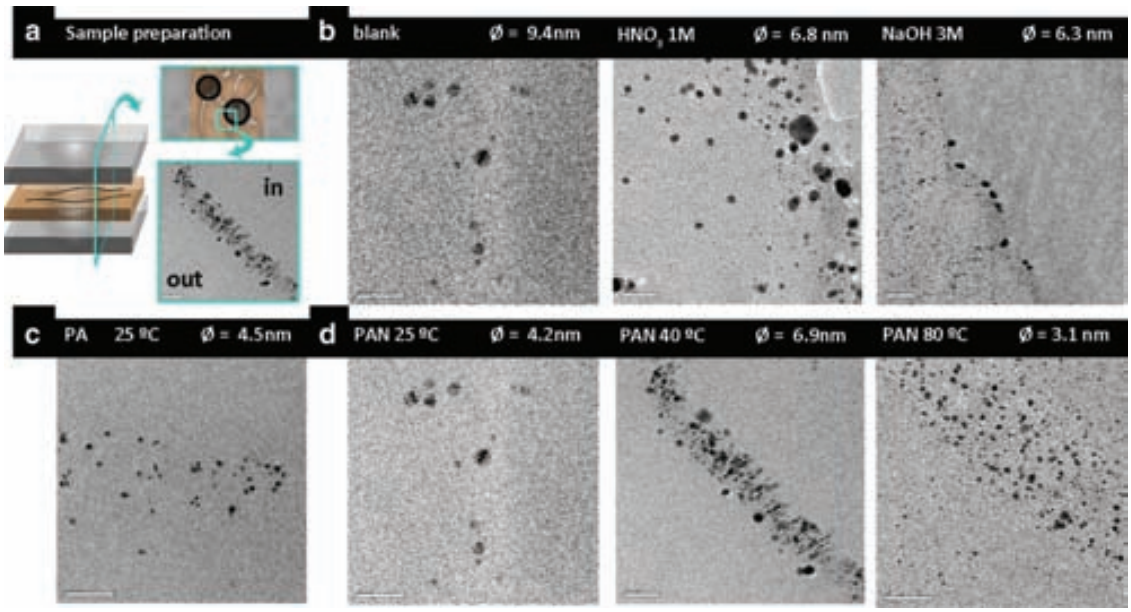

Figure 4 TEM images of some matrices. (**a**) Preparation of the ultra-thin films samples by cross-section for TEM analysis. TEM images obtained of (**b**) PUFs, (**c**) PA and (**d**) PAN fibers at different temperatures.

In addition, as seen in Table 1, similar values of IEC were obtained in all the cases, which also pointed out that a basic or acid pretreatment did not significantly affect the presence of ion-exchangeable positions.

Nanocomposites characterization

After applying the IMS technique, a darkening of the matrices was observed, indicative of the metal loading. The color for modified PUFs was similar, but clear differences in color intensity were detected for textile fibers: the higher the temperature, the darker the color.

For PUFs, the metal content did not increase after pretreatments. On the one hand, a basic pretreatment allowed loading of metal in a similar way compared to untreated foams, whereas acid treatments resulted in a lower metal concentration (Figure 3). *A priori*, both treatments were expected to increase the total metal loading due to the formation of ionogenic groups. However, since no new ionogenic groups were generated (as concluded from the FTIR-ATR and from the IEC values), the loading of the Ag^+ can be attributed to coordination with lone electron pairs of nitrogen atoms. Accordingly, the acid/basic treatments just 'tune' the possibility of coordination bonds to happen (depending on the isoelectric point of the matrix).

Very differently, for PAN fibers, increasing the temperature of the synthesis provided a higher metal loading. For PA fibers obtained at 40°C and 80°C, the metal content remains almost constant. In both cases, this can

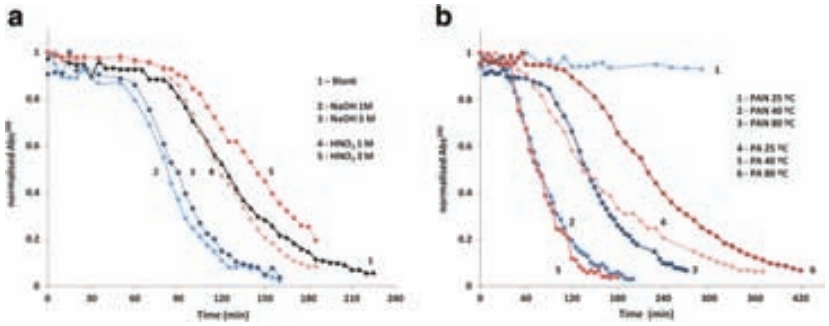

Figure 5 Catalytic evaluation of (a) PAN and PA nanocomposite fibers and (b) PUFs nanocomposites.

Table 2 Reaction rates (k_{app}) obtained for each nanocomposite

	Pretreatment / T (°C)	k_{app} ($s^{-1} \cdot mg_{Ag}^{-1}$)
PUFs	Blank	0.05
	NaOH 1M	0.10
	NaOH 3M	0.10
	HNO_3 1M	0.12
	HNO_3 3M	0.06
PAN	25°C	-
	40°C	0.47
	80°C	0.13
PA	25°C	0.49
	40°C	0.40
	80°C	0.31

be explained because rising the temperature to the glass transition point of each polymer ($T_{g\ PAN}$ = 85°C whereas $T_{g\ PA}$ = 55°C) increases the macromolecular mobility of the glassy amorphous phase, enhancing the accessibility of the polymer matrix. This change is more notable in PAN fibers than in PA fibers due to the higher thermosensitivity of the mesomorphic PAN fibers [18] at temperatures around T_g in comparison with the more stable and high crystalline structure of the PA fibers. Basically, PAN fibers are strongly influenced by temperature because their structural organization is intermediate between amorphous and crystalline phases, whereas the strong intermolecular hydrogen bonds through the amide groups in PA fibers configure a more stable semi-crystalline structure which hinders the ion diffusion.

TEM images of some matrices are shown in Figure 4. Nanocomposites based on untreated PUFs showed large AgNPs on the surface, while smaller ones were observed inside the matrix. By applying any pretreatment, smaller AgNPs are obtained. When comparing PA (25°C) and PAN (25°C), it was observed that there was a higher content of AgNPs for PA, but all the MNPs showed similar diameters. Yet, more MNPs were found for samples synthesized at higher temperatures, very probably because a higher diffusion of the AgNPs inside the matrix was achieved. The MNPs average diameter (Ø) was determined by counting between 200 and 300 MNPs per sample, representing the corresponding size distribution histograms that were fitted to a Gaussian curve of the three parameters [10].

Catalytic evaluation

Only PUFs and textile fibers containing AgNPs exhibited catalytic activity when evaluated in batch tests (Figure 5). The only nanocomposite without catalytic activity was PAN (25°C), which also contains the lowest amount of AgNPs. Reaction rate values (Table 2) increased for the PUFs with basic pretreatments. However, in PUFs with HNO_3 pretreatments, even if their metal content was lower (*c.a.* 40% less), the normalized catalytic activity remained almost constant. This fact can be explained because of the smaller AgNPs diameters obtained with the pretreatments which implies a higher catalytic area for the same amount of metal.

For textile fibers (except PAN prepared at 25°C), increasing the temperature of synthesis decreased the reaction rate. For PAN fibers, this can be clearly explained by TEM images: at a higher temperature, some of the AgNPs were formed inside the matrix and, therefore, they might not be accessible to the reagents.

Although almost all of the nanocomposites exhibited good catalytic activity for the reduction of 4-np, an induction time was needed for the reaction to proceed at high extent. This induction time has also been observed in other works for PdNPs [9,11,19,20], where it has usually been suggested that H_2 evolved from the decomposition of $NaBH_4$ can be loaded inside PdNPs competing with the catalytic reaction. Thus, once the absorption of H_2 has reached a saturation value, the catalytic reaction prevails. As far as we know, in the case of silver, this situation has not been already described but is very compatible with the experimental results. In fact, taking into account the well-known and fully accepted Langmuir-Hinshelwood mechanism for the reduction of 4-np to 4-ap [19], there is a first step during the reaction that involves

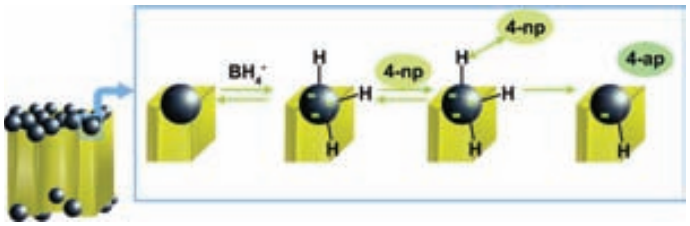

Figure 6 Langmuir-Hinselwood mechanism for the reduction of 4-np to 4-ap with $NaBH_4$.

the loading of the catalytic nanoparticles with hydride (H^-). Figure 6 illustrates the aforementioned mechanism.

Conclusions

The synthesis AgNPs in PUFs and textile fibers was successfully achieved: small nonaggregate MNPs were obtained in all of the matrices and mainly located on the surface. Neither acid nor basic pretreatments significantly affected the metal loading in PUFs. Instead, a tuning effect of the matrix after applying different pretreatments was observed, since the AgNPs distribution and size depended on the treatment. For textile fibers, the higher the temperature of synthesis, the higher the metal loading, very probably due to macromolecular chains mobility. In addition, for PAN fibers, the temperature significantly affected the spatial distribution of AgNPs due to the low values of the glass transition temperature. Almost all of the nanocomposites exhibited good catalytic activity for the reduction of 4-np, although an induction time was needed for the reaction to proceed at high extent. From these results, it comes that catalytic efficiency not only depends on the metal loading but also on the MNPs' diameter and their spatial distribution. Finally, these results prove that matrices not bearing ion-exchangeable groups can also be successfully used for nanocomposites synthesis by IMS.

Competing interests

The authors declare that they have no competing interests.

Authors' contributions

KZ carried out the experimental part concerning the polyurethane foams characterization, nanocomposite synthesis and characterization, and their catalytic evaluation. BD participated in the design and coordination of the study, carried out the experimental part concerning the textile fibers characterization, nanocomposite synthesis and characterization, catalytic evaluation, and wrote the main part of the manuscript. JM conceived the study and participated in its design and coordination. FC participated in the experimental design and interpretation of the textile fibers nanocomposites procedure and results. MM and DNM participated in the interpretation of the results. All authors read and approved the final manuscript.

Acknowledgments

We thank ACC1O for VALTEC09-02-0058 grant within the 'Programa Operatiu de Catalunya' (FEDER). Special thanks are given to Servei de Microscòpia from Universitat Autònoma de Barcelona.

Author details

[1]Department of Chemistry, Universitat Autònoma de Barcelona, UAB, 08193 Bellaterra, Barcelona, Spain. [2]Chemical Engineering Department, UPC, Universitat Politècnica de Catalunya, C/Colom, 1, 08222 Terrassa, Barcelona, Spain. [3]INTEXTER, Universitat Politècnica de Catalunya, UPC, C/Colom 15, 08222 Barcelona, Spain.

Received: 16 November 2012 Accepted: 12 April 2013
Published: 16 May 2013

References

1. Dioos BML, Vankelecom IFJ, Jacobs PA: **Aspects of immobilisation of catalysts on polymeric supports.** *Adv. Synth. Catal.* 2006, **348:**1413–1446.
2. Astruc D, Lu F, Ruiz Aranzaes J: **Nanoparticles as recyclable catalysts: the frontier between homogeneous and heterogeneous catalysis.** *Angew Chem Int Ed* 2005, **44:**7852–7872.
3. Schulenburg M: *Nanoparticles - small things, big effects.* Berlin: Bundesministerium für Bildung und Forschung (BMBF)/Federal Ministry of Education and Research; 2008.
4. Bhattacharjee S, Dotzauer DM, Bruening ML: **Selectivity as a function of nanoparticle size in the catalytic hydrogenation of unsaturated alcohols.** *J Am Chem Soc* 2009, **131:**3601–3610.
5. Campelo JM, Luna D, Luque R, Marinas JM, Romero AA: **Sustainable preparation of supported metal nanoparticles and their applications in catalysis.** *ChemSusChem* 2009, **2:**18–45.
6. Abbott LC, Maynard AD: **Exposure assessment approaches for engineered nanomaterials.** *Risk Anal* 2010, **30:**1634–1644.
7. Xu J, Bhattacharyya D: **Modeling of Fe/Pd nanoparticle-based functionalized membrane reactor for PCB dechlorination at room temperature.** *J Phys Chem C* 2008, **112:**9133–9144.
8. Muraviev DN, Macanás J, Farre M, Muñoz M, Alegret S: **Novel routes for inter-matrix synthesis and characterization of polymer stabilized metal nanoparticles for molecular recognition devices.** *Sensor Actuat B-Chem* 2006, **118:**408–417.
9. Domènech B, Muñoz M, Muraviev DN, Macanás J: **Polymer-stabilized palladium nanoparticles for catalytic membranes: *ad hoc* polymer fabrication.** *Nanoscale Res Lett* 2011, **6:**406.
10. Macanás J, Ouyang L, Bruening ML, Muñoz M, Remigy J-C, Lahitte J-F: **Development of polymeric hollow fiber membranes containing catalytic metal nanoparticles.** *Catalysis Today* 2010, **156:**181–186.
11. Domènech B, Muñoz M, Muraviev DN, Macanás J: **Catalytic membranes with palladium nanoparticles: from tailored polymer to catalytic applications.** *Catalysis Today* 2010, **193:**158–164.
12. Ruiz P, Macanás J, Muñoz M, Muraviev DN: **Intermatrix synthesis: easy technique permitting preparation of polymer-stabilized nanoparticles with desired composition and structure.** *Nanoscale Res Lett* 2011, **6:**343.
13. Alonso A, Muñoz-Berbel X, Vigués N, Macanás J, Muñoz M, Mas J, Muraviev DN: **Characterization of fibrous polymer silver/cobalt nanocomposite with enhanced bactericide activity.** *Langmuir* 2011, **28:**783–790.
14. Alonso A, Muñoz-Berbel X, Vigués N, Rodríguez-Rodríguez R, Macanás J, Mas J, Muñoz M, Muraviev DN: **Intermatrix synthesis of monometallic and magnetic metal/metal oxide nanoparticles with bactericidal activity on anionic exchange polymers.** *RSC Adv* 2012, **2:**4596–4599.
15. Dotzauer DM, Bhattacharjee S, Wen Y, Bruening ML: **Nanoparticle-containing membranes for the catalytic reduction of nitroaromatic compounds.** *Langmuir* 2009, **25:**1865–1871.
16. López-Mesas M, Navarrete ER, Carrillo F, Palet C: **Bioseparation of Pb(II) and Cd(II) from aqueous solution using cork waste biomass. Modeling and optimization of the parameters of the biosorption step.** *Chem Eng J* 2011, **174:**9–17.
17. Badertscher M, Bühlmann P, Pretsch E: *Structure Determination of Organic Compounds.* Heidelberg: Springer; 2009.
18. Kalashnik AT, Panichkina ON, Serkov AT, Budnitskii GA: **The structure of acrylic fibres.** *Fibre Chem* 2002, **34:**393–399.
19. Hervés P, Pérez-Lorenzo M, Liz-Marzán LM, Dzubiella J, Lubc Y, Ballauff M: **Catalysis by metallic nanoparticles in aqueous solution: model reactions.** *Chem Soc Rev* 2012, **41:**5577–5587.
20. Wunder S, Lu Y, Albrecht M, Ballauff M: **Catalytic activity of faceted gold nanoparticles studied by a model reaction: evidence for substrate-induced surface restructuring.** *ACS Catal* 2011, **1:**908–916.

doi:10.1186/1556-276X-8-238
Cite this article as: Domènech *et al.*: **Development of novel catalytically active polymer-metal-nanocomposites based on activated foams and textile fibers.** *Nanoscale Research Letters* 2013 **8**:238.

Solvent Extraction and Ion Exchange
Publication details, including instructions for authors and subscription information:
http://www.tandfonline.com/loi/lsei20

Polymer-Metal Nanocomposites Containing Dual-Function Metal Nanoparticles: Ion-Exchange Materials Modified With Catalytically-Active and Bactericide Silver Nanoparticles

Berta Domènech [a] , Núria Vigués [b] , Jordi Mas [b] , Maria Muñoz [a] , Dmitri N. Muraviev [a] & Jorge Macanás [c]

[a] Department of Chemistry , Universitat Autònoma de Barcelona, UAB , Bellaterra , Barcelona , 08193 , Spain

[b] Department of Genetics and Microbiology , Universitat Autònoma de Barcelona, UAB , Bellaterra , Barcelona , 08193 , Spain

[c] Department of Chemical Engineering , Universitat Politècnica de Catalunya, UPC-BarcelonaTech , C/Colom, 1, Terrassa , Barcelona , 08222 , Spain

Accepted author version posted online: 12 Sep 2013.Published online: 12 Sep 2013.

To cite this article: Solvent Extraction and Ion Exchange (2013): Polymer-Metal Nanocomposites Containing Dual-Function Metal Nanoparticles: Ion-Exchange Materials Modified With Catalytically-Active and Bactericide Silver Nanoparticles, Solvent Extraction and Ion Exchange, DOI: 10.1080/07366299.2013.839192

To link to this article: http://dx.doi.org/10.1080/07366299.2013.839192

Polymer-Metal Nanocomposites Containing Dual-Function Metal Nanoparticles: Ion-Exchange Materials Modified With Catalytically-Active and Bactericide Silver Nanoparticles

Berta Domènech1, Núria Vigués2, Jordi Mas2, Maria Muñoz1, Dmitri N. Muraviev1,*, Jorge Macanás3, *

[1]Department of Chemistry, Universitat Autònoma de Barcelona, UAB, 08193 Bellaterra, Barcelona, Spain

[2]Department of Genetics and Microbiology, Universitat Autònoma de Barcelona, UAB, 08193 Bellaterra, Barcelona, Spain

[3]Department of Chemical Engineering, Universitat Politècnica de Catalunya, UPC-BarcelonaTech, C/Colom, 1, 08222 Terrassa, Barcelona, Spain

* *corresponding author:* dimitri.muraviev@uab.cat, jorge.macanas@upc.edu

ABSTRACT

This work reports the results obtained by the development of two types of nanocomposite membranes containing metal nanoparticles prepared by applying the Intermatrix Synthesis technique for the synthesis of silver nanoparticles in the ion-exchange matrices of sulfonated polyethersulfone-Cardo and Nafion membranes. The stability (in terms of silver nanoparticles loss) of the polymer-metal nanocomposites was evaluated by using both ultrasonic and thermostatic baths and appeared to be appropriate for their practical applications. The dual-function nanocomposites were characterised in batch tests: i) by monitoring their catalytic activity in reaction of the reduction of p-nitrophenol to p-aminophenol and ii) by evaluating their antibacterial efficiency towards *E. coli*. The results of catalytic tests have shown that polymer-silver nanocomposites demonstrate remarkably better activity in comparison with their polymer-

palladium nanocomposite analogues. The same nanocomposites have been shown to permit the complete disinfection of *E. coli* containing water within a short period of time.

KEYWORDS

Ion-exchange materials, catalytic membranes, silver nanoparticles, nanocomposites, disinfection, wastewater treatment

1. INTRODUCTION

In recent years, the use of polymeric materials for the development of catalytic membranes has attracted much interest due to their main advantages related to low cost, simple scalability and a myriad of polymer configurations. However, most of these polymeric materials can only be employed under mild conditions due to their instability towards strong oxidizers (i.e. chlorine-based chemicals) and high temperatures (above 200-300 ºC). Nevertheless, thanks to the particular properties of nanomaterials such as high surface area to volume ratio, high activity and recyclability [1,2] new approaches in the development of organic membranes are being considered in order to cope with the aforementioned drawbacks. In this sense, nanocomposites prepared by immobilization of nanoparticles (NPs) in polymers have been broadly studied [1,3,4]. The main advantage of this synthetic approach is the prevention of NPs aggregation as the polymer chains minimise the probability of NPs contact and subsequently prevent their uncontrolled growth and aggregation [5, 6]. In this context, the polymer-metal nanocomposites are very suitable candidates to be used for the development of catalytic membrane reactors, which can be applied in various fields, including for instance, complex treatment of wastewaters.

An example of this approach is the use of nanocomposites for the removal of chlorinated compounds from water [7, 8] along with simultaneous elimination of microbiological contamination.

Additionally, the immobilization of silver NPs (AgNPs) in polymeric supports for antibacterial and biofouling prevention purposes can also improve the catalytic polymeric membrane performance [9-12]. Certainly, bulk silver, colloidal silver and AgNPs have been identified as a powerful alternative for water purification applications and have already been utilized for imparting biocidal properties to separation membranes, mainly to prevent biofouling formation [13-18]. Indeed, membrane biofouling causes a great number of operational problems due to the undesirable accumulation of microorganisms on the membrane surface [19]. That is why it is worth to develop nanocomposites that simultaneously provide catalytic degradation of pollutants, deactivation of pathogenic microorganisms and biofouling prevention [11,20].

There is a wide range of available approaches applicable for incorporation of different kinds of NPs in polymeric matrices and fabrication of polymer-metal nanocomposites with desired properties [1,9,10,21-23]. Among them, the Intermatrix Synthesis (IMS) is one of the most promising techniques as it has proved to be successfully applicable for the easy preparation of catalytically and electrocatalytically active nanocomposites containing zero-valent metal nanoparticles (MNPs) (e.g. Cu, Pd, Pt) by modifying several ion-exchange matrices in the form of porous membranes, polymeric films, resin beads, foams, fibres and hollow fibres [24-27]. The IMS procedure is characterized by the use of the ion exchange properties of the host polymeric matrix, which acts as a nanoreactor and serves for the synthesis of the dual-function MNPs [3].

In general terms, the IMS proceeds via a first ion-exchange step that allows the immobilization of metal ions, which undergo a subsequent chemical or electrochemical reduction [28]. Moreover, experimental conditions can be modified in order to tune and control the NPs location, shape, size and size distribution and proceed in the absence of organic solvents or additional capping agents [24,26].

Concerning stability, catalytic membranes or supports are often affected by aging that sometimes results in the loss of the catalyst to the media. In the case of applications for water treatment, this issue must be properly addressed as NPs human toxicity is under investigation [29]. In this sense, the IMS technique has a supplemental advantage, since the polymeric matrix provides an additional security level regarding NPs leakage.

In earlier works [27,30], we undertook the development of several catalytic ion-exchange membranes and catalytic supports containing PdNPs, which exhibited good catalytic activity. We are now investigating the fabrication of ion-exchange nanocomposites containing silver with the aim of providing a double functionality to the nanocomposites. In this study we have developed and characterized dual-function (catalytic and bactericidal) nanocomposites obtained by modification of two ion exchange matrices: sulfonated polyethersulfone with cardo group (SPES-C), and commercial Nafion-117 with AgNPs. Special attention has been drawn to membrane stability so as to determine the amount of AgNPs released and their biocidal effect.

2. EXPERIMENTAL SECTION

2.1. Materials

Commercial PES-C was kindly supplied by Dr. Trong Nguyen from Université de Rouen, France. HNO_3 (65% w/w) was purchased from Fisher Chemical, N-methyl-2-pyrrolidone (NMP) was purchased from Merck, whereas other reagents ($AgNO_3$, $NaBH_4$, 4-nitrophenol, solvents) were all from Panreac. For bacterial tests, *Escherichia coli* (CGSC 5073 K12), Luria-Bertani medium (LB) and phosphate buffered saline (PBS) from Life Technologies were used.

SPES-C was obtained by a simple sulfonation procedure described elsewhere [30,31,32]. The sulfonated polymer was dissolved (25% wt) in NMP and then precipitated in a water bath [31]. After casting, membranes were stored in deionised water until their use or characterization. The time of storage ranged from 1 week to 1 year.

Nafion-117 membranes (purchased from Sigma Aldrich) were chemically pre-treated in order to remove impurities or solvent residues [30]. All the Nafion samples were pre-treated in the same way as it is known that perfllourinated membranes physical structure and chemical properties might be changed depending upon the pre-treatment conditions [33].

For SPES-C membranes the ion exchange capacity (IEC) value was found to be 0.44 ± 0.02 meq/g dry membrane by an acid-base titration (three replicates, 95% confidence level) [31] whereas that for Nafion IEC (1.1 meq/g) was provided by the supplier. All the membrane

samples were equilibrated with a 0.1 M $NaNO_3$ solution for 24 hours before their use to ensure that all the ion-exchange groups turned to Na-form.

2.2. Synthesis of AgNPs.

The synthesis of MNPs in the membranes was carried out by a two-step procedure [27]. First, a piece of membrane measuring 1 cm^2 was equilibrated for 24h in 25 ml of a solution of $AgNO_3$ so as to load the ionogenic groups of the polymer with the metal precursor. The concentration of $AgNO_3$ in the loading solutions was 0.49 mM and 6.65 mM for SPES-C and Nafion, respectively, and corresponded to 5 fold the IEC of each matrix. This step is reported in **equation (1)**, where M^{n+} stands for Ag^+. Second, immobilized ions underwent a chemical reduction by using a $NaBH_4$ 0.5 M solution, giving as a result the metal nanoparticles (see **equation (2)**, where M^0 stands for Ag^0):

$$n\ (R\text{-}SO_3^-)Na^+ + M^{n+} \leftrightarrow (R\text{-}SO_3^-)_nM^{n+} + n\ Na^+ \quad \textbf{(1)}$$

$$(R\text{-}SO_3^-)_nM^{n+} + n\ NaBH_4 + 3n\ H_2O \rightarrow n\ (R\text{-}SO_3^-)Na^+ + (7n/2)H_2 + n\ B(OH)_3 + M^0 \quad \textbf{(2)}$$

After synthesis, membrane samples were rinsed twice with distilled water and stored in wet form.

2.3. Nanocomposite characterization

In order to determine the exact metal content in the prepared nanocomposites, samples of 1 cm^2 were digested with 1 mL of concentrated HNO_3 (65% w/w) overnight and then diluted 1:100 with distilled water. The resulting solutions (2 replicates) were appropriately diluted and analysed by Inductively Coupled Plasma Mass Spectrometry (ICP-MS, Agilent 7500).

High Resolution Transmission Electron Microscopy (HR-TEM) was performed by a Jeol JEM-2011 HR-TEM, and was used to establish the real distribution of the AgNPs in each matrix, as well as to evaluate the size and shape of the obtained MNPs. In this sense, by using an image processing software (Adobe Professional) it was possible to measure the NPs size and represent the corresponding size distribution histograms (in average, about 300 particles were measured for sample) that were fitted to a three parameter Gaussian curve [31]. Before observation with the High Resolution Transmission Electron Microscope (TEM), membrane samples were embedded in an epoxy resin and ultra-thin slices were obtained using an ultramicrotome (Leica EM UC6 with a 35° diamond knife, Diatome). Samples were deposited onto a TEM grid and then sputtered with carbon.

2.4. Nanocomposite stability characterization

In order to evaluate the stability of the nanocomposites obtained, samples were treated either by immersion in warm water or by ultrasounds, as specified in **Table 1**. In all cases, samples of 1 cm^2 were deposited in a vessel with 10 mL of the appropriated solution and placed for different times in the corresponding bath: an ultrasonic cleaner (Branson 1200, 20W), a thermostatic bath

(Grant W6, Grant Inst.) or an incubator (Aquatron Infors AG, shaker incubator). As ultrasounds can heat the solution, temperature variation in the ultrasonic bath was also monitored during the experiment.

After each experiment, the silver content in both solutions ($n_{Ag,\ solution}$) and membranes ($n_{Ag,\ membrane}$) was analysed by ICP-MS so as to determine the release percentage (R%). In the case of membranes, samples were digested as aforementioned. Typically, 2 replicates per time and sample were analysed. **Equation (3)** was used to calculate the Total release (%):

$$R\% = 100 \cdot n_{Ag,\ solution} / (n_{Ag,\ solution} + n_{Ag,\ membrane}) \quad \textbf{(3)}$$

2.5. Catalytic properties evaluation

The reduction of aqueous 4-nitrophenol (4-np) to 4-aminophenol (4-ap) by $NaBH_4$ was used to evaluate the catalytic performance of nanocomposites, as it is easy to monitor by a UV-vis spectrometer (Pharmacia LKB Novaspec II spectrometer, $\lambda = 390$ nm) [34, 35]. The reaction was assumed to follow pseudo-first order kinetics due to the high excess of reducing agent and, thus, an apparent constant rate (k_{app}) could be calculated by **equation (4)**, where Abs_t and Abs_0 respectively correspond to the solution absorbance at a defined time (t) and at the beginning of the experiment [30].

$$Ln\ (Abs_t / Abs_0) = -k_{app} \cdot t \quad (4)$$

To carry out the catalytic experiments, a given amount of $NaBH_4$ was added to 5 ml of 4-np solution (5 mM) to achieve a $NaBH_4$ concentration of 50 mM. After mixing, a piece of nanocomposite (1 cm^2) was added to the vessel and the solution was sampled periodically.

2.6. Characterization of the bactericidal properties

To determinate the bactericidal properties of the as-prepared nanocomposites and bare matrices, a sample (1cm^2) of material was immersed in 20 mL of bacterial suspension and maintained at 37°C with gentle agitation (300 rpm). The microorganisms decay in PBS solution was also evaluated. Periodically, 100 µL of each suspension were collected at different times and counted using plating and incubation on LB medium. All the manipulations were performed under sterile conditions.

In order to evaluate the possible effect of the AgNPs or Ag^+ ions released to the media by the nanocomposites during the experiments, a piece (of 1 cm^2) of each sample (with or without AgNPs) was immersed in 20 mL of PBS and maintained for 24h at 37 °C with gentle agitation (300 rpm). After this time, samples were removed, and an *E. coli* pellet was suspended again in the solution. Aliquots of 100 µL were collected at different times and viable microorganisms were counted after cultivation on LB medium.

Finally, with the purpose of evaluating the possible adsorption of microorganisms onto the samples during the experiments, the pieces of Nafion used in the microbiological experiments were stained using the Live/Dead Invitrogen Kit BacLight (Invitrogen) by following the protocol

detailed by the supplier. Images were acquired with a Zeiss AXIO Imager A1 microscope using a 470 nm laser and suitable filter sets.

3. RESULTS AND DISCUSSION

3.1. AgNPs characterization

After the IMS procedure, all the membrane samples turned dark, what testifies for the successful loading of the metal. A quantitative value of metal loading was obtained thanks to ICP-MS analyses and results are shown in **Table 2**, together with the palladium loading previously obtained for the same polymers [30].

As it can be observed, similar amount of metal ion equivalents were loaded in both ion-exchange matrices although the ratio Pd:Ag was always higher than 1 (concretely 1.4 ± 0.4 for SPES-C and 1.2 ± 0.7 for Nafion). The different ion mobility and, particularly, the different charge of ions (Ag^+ and $[Pd(NH_3)_4]^{2+}$) might be the reasons of such differences.

Regarding the important differences between the amount of metal loaded in both polymers (ratio Nafion:SPES-C) they almost coincide for the different metals (19 ± 6 for Ag and 18 ± 3 for Pd), even if this ratio is far beyond the IEC differences. This suggests that ion access to functional groups must be hindered for the case of SPES-C polymer.

Taking into account that, *a priori*, a high metal content in the nanocomposites is favoured for both catalytic and bactericidal purposes, Nafion seems to be a preferable matrix compared to SPES-C. However, the amount of nanocatalyst is not the only important parameter for the

applications discussed above since the accessibility of reagents to the nanocatalyst must be enabled [36]. In relation to this, **Figure 1** shows typical TEM images obtained from each nanocomposite. In all of the cases, small non-aggregated spherical AgNPs were obtained but some differences can be observed between the two polymers.

Although the amount of loaded AgNPs is lower for SPES-C, these samples show mainly a superficial distribution of AgNPs together with little penetration through the membrane (~4.7 μm) (see **Figure 1b**). Such distribution of AgNPs near the surface of the stabilizing polymer is favourable for catalytic and bactericidal applications [36].

On the other hand, TEM images for Nafion nanocomposites portray plenty of AgNPs in the bulk. Thus, in the case of Nafion, as AgNPs grow throughout the membrane, a higher load can be achieved.

The results regarding the AgNPs size distribution are also shown in **Figure 1c** and **Figure 1f**. Results proved that it was possible to obtain small AgNPs, even smaller than those found previously by different approaches [9,14-16,20,21]. This size distribution provides a higher surface/volume ratio for the catalysts. Only small differences in size were found for the different matrices as the AgNPs obtained in Nafion are slightly smaller (9.0 ± 0.2 nm) than those obtained in SPES-C (11.9 ± 0.2 nm).

3.2. Stability characterization

To determine the eventual loss of AgNPs from the matrices, samples underwent different aging treatments (see Table 1) and the amount of metal measured in solution was compared with the

remaining amount in the sample (see **equation (3)**). Accordingly, it was possible to calculate the rate of loss (expressed in % Ag/h) for each nanocomposite. Data are plotted in **Figure 2** and the initial slopes of the curves are summarized in **Table 3**. It is noteworthy that some of the curves are only lineal for short times and then % AgNPs loss becomes almost constant, reaching a plateau as it has been reported by other authors [9].

Taking a close look at the results, appears that a higher NPs leakage is observed for ultrasonic treatment as one can expect *a priori* since this treatment promotes AgNPs vibration and at the same time it increases the solution temperature. It is particularly interesting to note that the loss was very linear with time under such conditions. It is also noteworthy that the loss rate was exceptionally high for SPES-C nanocomposites (6.7 ± 0.2), wich might be explained with to the superficial distribution of AgNPs obtained in SPES-C membranes, which are less stabilized by the polymeric matrix than inner nanoparticles obtained in Nafion membranes.

This important loss (~17-fold higher compared with Nafion) made us discard the use of this polymer in the other aging experiments. The observed silver loss for SPES-C is in agreement to that obtained by Cao et al. for similar membranes made of polyethersulfone/sulfonated polyethersulfone [9] but for a longer time: up to a 20% of silver release for 120 h in physiological saline solution and up to 5% in distilled water. Accordingly, the ultrasound treatment effectively acts as an accelerating aging treatment for membranes. In light of these results, Nafion was chosen as a model matrix to evaluate the stability behaviour of the AgNPs under different experimental conditions. In the case of the thermostatic bath and cultivation conditions the silver loss was very low and a plateau can be observed in the plotted data (**Figure**

2b and 2c). This loss was never higher than the 5% after 135 h in the thermostatic bath even, considering the significant divergence of some of the replicates.

It is important to remark that experimental cultivation conditions were expected to be more aggressive, since there is a direct contact with the microorganisms in the medium. As mentioned above, similar effect has been observed for silver release in physiological saline solution that was also 4-fold higher than in distillate water [9]. In our case, a more detailed study will agree with the observed trend that limits the loss to about a 2% of the loaded metal, more in agreement with the results found by Zhu et al. for chitosan membranes [22].

Taking into account this low release rate for Nafion nanocomposites, the membrane is expected to be effective for a long time, thus conserving the bactericidal and catalytic properties of AgNPs.

3.4. Bactericidal studies

Considering the well-known bactericidal activity of AgNPs [14], nanocomposites containing AgNPs were evaluated in order to determine their bactericidal kinetic activity. Although the antibacterial mechanism of AgNPs is still not completely understood, it is thought to be caused by the interaction of metallic silver and Ag^{+} ions with different cell targets such as cellular membrane [37]. Based on the contact-killing mechanism already observed in previous works [25,38], nanocomposite samples with a similar area were exposed to the cultivation medium. Samples without AgNPs were also evaluated in order to discriminate any possible effect of the polymeric matrices, such as adsorption of the microorganisms in the matrix. **Figure 3a** shows the

percentage of bacterial viability during the time of the experiment. In all cases, the percentage of cell viability decreased with time.

As it can be seen, both nanocomposite samples were able to kill the 100% of bacteria in about 2 h. Comparing these results with the decay of microorganisms in the experiments with membrane samples without AgNPs, it is possible to observe that cell viability also decayed although at a much-reduced rate. The possibility of *E. coli* adsorption in the matrix was evaluated by fluorescence microscope, and adsorption was not found in any of the samples evaluated. Thus the decay in the cell viability in the experiments with MNPs-free samples can principally be attributed to the lack of nutrients in the media.

It has been suggested in the literature that bactericidal properties of AgNPs arise from the release of Ag^+ ions [10,39]. Hence, the effect of the silver lost was evaluated again in a different manner: samples containing AgNPs were immersed in PBS solutions and removed after 24 h. The solutions were then tested as cultivation media after the resuspension of an *E. coli* pellet (see Section 2). The cell viability over time curves are plotted in **Figure 3b**.

From the obtained results, it is possible to conclude that after 24 h at 37 ºC and under gentle agitation, nanocomposite membranes released to the media silver (either AgNPs or Ag^+) enough to kill all the microorganisms in 1 h (Nafion) or 3 h (SPES-C). This result can be judged in several ways. On the one hand, since Nafion nanocomposites were able to kill all microorganisms in less than 2 h, and that the percentage of silver loss in 2 h (under experimental microbiological conditions) is less than the 0.5% of the total AgNPs immobilised in the matrix (much lower than the loss due to 24 h of agitation), it seems reasonable to conclude that

microorganisms decay in the presence of nanocomposites is not only attributable to the leaching of AgNPs to the media, *ergo* the as-prepared nanocomposites should kill bacteria by a contact mechanism. On the other hand, since the amount of silver release to the media after 24 h of agitation was able to completely disinfect the solution, these nanocomposites can be regarded as silver reservoirs able to provide a residual disinfection effect comparable to that of residual chlorine which takes place when chlorine or hipochlorous acid are use for water treatment. Thus, thanks to this remaining antibacterial effect the few remaining bacteria cannot rapidly multiply because the reagent is not completely exhausted. Moreover, such a system is preferable to the use of strong oxidising agents because they can severely damage membranes and as well as biofouling [40].

3.3. Catalytic properties evaluation

In our previous studies [30], nanocomposites containing PdNPs exhibited catalytic activity when evaluated in batch tests whereas membranes without MNPs did not exhibit any catalytic activity. Even if silver is probably not thought as a typical catalytic metal in comparison to classical Pd or Pt, it has been also used for catalytic purposes [23,34] and the nanocomposites containing AgNPs developed in this work have proved the same performance but with an increased reaction rate. Indeed, data plotted in **Figure 4** show a high catalytic activity for Nafion and SPES-C nanocomposites whereas almost no effect for the blank experiments.

It is important to note that, in both nanocomposites, a certain induction time was observed before the reaction started. This delay has been also observed in other works for PdNPs [30,31]. It has always been suggested that H_2 evolved from the decomposition of $NaBH_4$ can be loaded inside

PdNPs competing with the catalytic reaction. Thus, once the absorption of H_2 has reached a saturation value the catalytic reaction prevails [35]. For the case of silver this situation has not been already described but is very compatible with the experimental results.

From these experiments it can be observed that SPES-C nanocomposites offer the best catalytic performance as they were able to halve the concentration of 4-np in 30 minutes and reduce it more than 90% in less than 1 h. Conversely, after 1 h Nafion nanocomposites where still in the induction period and a reduction of 80% was only achieved after 2 h. These differences are in agreement with the most favourable location of the catalytic material [38] in the matrix: for SPES-C, AgNPs were mainly formed in the surface, whereas in the case of Nafion nanocomposites, AgNPs were also found inside the matrix, reducing the overall number of catalytic sites. In addition, it can be observed in **Figure 4** that the delay for SPES-C containing AgNPs is considerable shorter than for Nafion what can also be due to the aforesaid surface location of AgNPs in SPES-C nanocomposites.

For a better comparison, the apparent velocity constants (k_{app}) were calculated, considering a pseudo first order reaction [35]. The calculated k_{app} were: 72 and 3.51 $s^{-1} \cdot mmol^{-1}$, for SPES-C and Nafion respectively, so about 20 times higher for SPES-C. After these positives results, the opportunity to reuse the catalytic materials was also evaluated and positive results are shown in **Figure 4**. Similarly to what was concluded in previous works for PdNPs [31], it is definitively possible to reuse the catalytic supports maintaining good catalytic efficiencies although a progressive decrease of the reaction rate occurs (results shown in **Table 4**). Equally, the activation time after each cycle was maintained or even enlarged.

As a first explanation, it is possible to establish a relationship between the catalytic efficiency loss and the silver release but, since the silver loss was proven to be low, the weaker performance after successive cycles can also be attributed to a possible poisoning of the catalyst due to the generation of by-products of the 4-np reduction that can interfere with the catalyst surface and that has been previously reported [27].

Anyhow, it is not possible to discard the loss of the catalytic material, which once in the media cannot be recovered for the following catalytic cycle. The last hypothesis is in agreement with the experimental results: (i) AgNPs are mostly located nearby to the membrane surface for SPES-C, which explains its higher catalytic activity even if the metal loading is lower than that of Nafion; (ii) AgNPs are less retained by SPES-C matrix as it has been proved by the treatment with ultrasounds. Therefore, the performance drop is much more important for SPES-C nanocomposites since more abundant and less retained AgNPs escape from the matrix. To visualize this conclusion, **Table 4** includes the ratio between the k_{app} of each cycle and the original value for the first experiment ($k_{app,\#1}$) for both nanocomposites. After 4 cycles, only about a 30% of the initial reaction rate remained for SPES-C whereas for Nafion the value is close to 70%.

4. CONCLUSIONS

In this work, the preparation of AgNPs inside SPES-C and Nafion membranes by using the ion exchange capacities by the IMS methodology was achieved. By this procedure, small non aggregated AgNPs (diameters between 9-12 nm) were obtained but dissimilar distribution was observed for the different matrices: for SPES-C membranes a lower loading was achieved but the

most of NPs were found on the surface and little diffusion to the inner of the membrane was observed. On the contrary, Nafion exhibited an opposite behaviour with most of the particles located throughout the matrix. This particular distribution provided clear differences in the nanocomposite stability and in the catalytic properties. Stability studies under extreme aging conditions, such us sonication, showed that the release of AgNPs to the medium was higher for SPES-C samples than for Nafion nanocomposites. For the later, results show that silver loss was less than %5 (even after 135 h), which confirmed the suitability of the IMS procedure to obtain polymer stabilized MNPs in this specific matrix.

When evaluating the catalytic properties of the nanocomposites prepared, and comparing the results with previous works with PdNPs, an increase of the reaction rate was observed. SPES-C nanocomposites performed better but the reaction rate was clearly reduced after successive cycles. Nafion nanocomposites performance was less efficient but more stable.

Regarding bactericidal experiments, it was possible to wipe out all of the microorganisms in less than 2 h with Ag-containing nanocomposites and the hypothesis of adsorption of the microorganisms in the samples was discarded. It is important to notice that, although there was some release of AgNPs to the media that affected the cell viability, as the silver content found on media was very low, it was possible to conclude that the effect in the cell viability was mostly due to the interaction with metal nanocomposites. Nonetheless, from the obtained results it was not possible to entirely ignore the bactericidal effect of released silver. However this would not be a crucial problem for a practical application if we consider the nanocomposites as antifouling catalytic supports that act as silver reservoirs.

Therefore, the targeted polymer-metal nanocomposites containing dual-function metal nanoparticles were successfully synthesised. Moreover, taking into account the improvement of the catalytic efficiency (compared to the corresponding PdNPs counterparts) and the bactericide effect observed, the nanocomposites here developed create a perfect niche for further industrial applications. Thanks to the use of AgNPs, instead of PdNPs, a reduction of the final cost and prevention of the biofouling problem always associated with membrane reactors can be achieved.

ACKNOWLEDGEMENTS

This work was supported by CTQ2009-14390-C02-02 from the Ministry of Science and Innovation of Spain (MCINN). Prof. Trong Nguyen is acknowledged for supplying the polythersulfone Cardo. Special thanks are given to Servei de Microscòpia from Universitat Autònoma de Barcelona.

REFERENCES

[1] Chaudhuri, R.G.; Paria, S. *Chem. Rev*., **2012**, *112*, 2373-2433.

[2] Hogg, S.R.; Muthu, S.; O'Callaghan, M.; Lahitte, J-F.; Bruening, M.L. *ACS Appl. Matter. Interfaces* **2012**, *4*, 1440-1448.

[3] Rozenberg, B.A.; Tenne, R. *Prog. Polym. Sci.,* **2008**, *33*, 40-112.

[4] Muraviev, D.N.; Pividory, M.I.; Montañez Soto, J.L.; Alegret, S. *Solvent Extr. Ion Exc*., **2006**, 25(5), .731-745

[5] Simonsen, S.B.; Chorkendorff, I.; Dahl, S.; Skoglundh, M.; Sehested, J.; Helveg, S. *J. Am. Chem. Soc*., **2010**, *132,* 7968-7975.

[6] Arar, Ö.; Wohlgemuth, J.; Hetzerb, B.; Franzreb, M. *Solvent Extr. Ion Exc*., **2012**, 30(4), 333-340.

[7] Xu, J; Bhattacharyya, D. *Ind. Eng. Chem. Res*., **2007**, *46*, 2348-2359.

[8] Meyer, D.E.; Wood, K.; Bachas, L.G.; Bhattacharyya, D. *Environmental Prog.*, **2004**, *23*, 232-242.

[9] Cao, X.; Tang, M.; Liu, F.; Nie, Y.; Zhao, C. *Colloids Surface B,* **2010**, *81,* 555-562.

[10] Zodrow, K.; Brunet, L.; Mahendra, S.; Li, D.; Zhang, A.; Li. Q.; Alvarez, P.J.J. *Water Res.,* **2009**, *43*, 715-723.

[11] Buonamena, M.G.; Choi, S.H.; Drioli, E. *Asia-Pac. J. Chem. Eng*. **2010**; *5*; 26-34.

[12] Yin, J.; Yang, Y; Hu, Z.; Deng, B. *J. Membrane Sci*, **2013**, *441*, 73-82.

[13] Chernousova, S.; Epple, M. *Angew. Che. Int. Ed.,* **2013**, *52*, 1636-1653.

[14] Panáček, A.; Kvítek, L.; Prucek, R.; Kolar, M.; Vecerova, R.; Pizúrova, N.; Sharma, V.K.; Nevecna, T.; Zboril, R. *J. Phys. Chem. B.*, **2006**, *110*, 16248-16253.

[15] Choi, O.; Deng, K.K.; Kim, N-J.; Ross Jr., L.; Surampalli, R.Y.; Hu, Z. *Water Res.,* **2008**, *42*, 3066-3074.

[16] Taurozzi, J.S.; Arul, H.; Bosak, V.Z.; Burban, A.F.; Voice, T.C.; Bruening, M.L.; Tarabara, V.V. *J. Membrane Sci.*, **2008**, *325*, 58-68.

[17] Morones, J.R.; Elechiguerra, J.L.; Camacho, A.; Holt, K.; Kouri, J.B.; Ramírez, J.T.; Yacaman, M.J. *Nanotechnology*, **2005**, *16*, 2346-2353.

[18] Tarabara, V.V. In: *Nanotechnology Applications for Clean Water*, Savage, N.; Diallo, M., Duncan, J., Street, A., Sustich, R., Eds.; William Andrew Publication, **2009**; p. 59-75.

[19] Baker, J.S.; Dudley, L.Y. *Desalination*, **1998**, *118*, 81-89.

[20] Lee, S.Y.; Kim, H.J.; Patel, R.; Im, S.J.; Kim, J.H.; Min, B.R. *Polym. Advan. Technol.,* **2007**, *18,* 562-568.

[21] Yang, H.-L.; Lin, J.C.-T; Huang, C. *Water Res.,* **2009**, *43*, 3777-3786.

[22] Zhu, X.; Bai, R.; Wee, K-H.; Liu, C.; Tang, S-L. *J. Membrane Sci.,* **2010**. *363,* 278-286.

[23] Dhar, J.; Patil, S. *ACS Appl. Matter. Interfaces* **2012**, *4*, 1803-1812.

[24] Ruiz, P.; Muñoz, M.; Macanás, J.; Muraviev, D.N. *Chem. Mater*., **2010**, *22*, 6616–6623.

[25] Alonso, A.; Muñoz-Berbel, X.; Vigués, N.; Macanás, J.; Muñoz, M.; Mas, J.; Muraviev, D.N. *Langmuir,* **2011**, *28*, 783-390.

[26] Ruiz, P.; Muñoz, M.; Macanás, J.; Turta, C.; Prodius, D.; Muraviev, D.N. *Dalton Trans*., **2010**, *39*, 1751-1757.

[27] Macanás, J.; Ouyang, L.; Bruening, M.L.; Muñoz, M.; Remigy, J-C.; Lahitte, J-F. *Catal Today*, **2010**, *156*, 181-186.

[28] Muraviev, D.N.; Macanás, J.; Farre, M.; Muñoz, M.; Alegret, S. *Sensor Actuat. B-Chem.*, **2006**, *118,* 408-417.

[29] Yang, X.; Gondikas, A.P.; Marinakos, S.M.; Auffan, M.; Liu, J.; Hsu-Kim, H.; Meyer, J.N. *Environ. Sci. Technol*., **2012**, *46*, 1119-1127.

[30] Domènech, B.; Muñoz, M.; Muraviev, D.N.; Macanás, J. *Catal. Today*, **2012**, *193*, 158-164.

[31] Domènech, B.; Muñoz, M.; Muraviev, D.N.; Macanás, J. *Nanoscale Res. Lett.*, **2011**, *6*, 406.

[32] Blanco, J.F.; Nguyen, Q.T.; Schaetzel, P. *J. Membrane Sci.*, **2001**, *186*, 267-279.

[33] Sachdeva, A.; Sodaye, S.; Pandey, A.K.; Goswami, A. *Anal. Chem*., **2006**, *78*, 7169-7174.

[34] Xiao, S.; Xu, W.; Ma, H.; Fang, X. *RSC Advances*, **2012**, *2*, 319-327.

[35] Herves, P.; Pérez-Lorenzo, M.; Liz-Marzán, L.M.; Dzubiella, J.; Lu, Y.; Ballauff, M. *Chem. Soc. Rev.,* **2012**, 41, 5577-5587.

[36] Domènech, B.; Bastos-Arrieta, J.; Alonso, A.; Macanás, J.; Muñoz, M.; Muraviev, D.N. Bifunctional Polymer-Metal Nanocomposite Ion Exchange Materials on *Ion Exchanhe Technologies*, **2012**. Prof. Ayben Kilislioglu (Ed.), ISBN: 978-953-51-0836-8.

[37] Jung, W.; Koo, H.; Kim, K.; Shin, S.; Kim, S.; Park, Y. *Appl. Environ. Microbiol*. **2008**, *74*, 2171-2178.

[38] Alonso, A., Vigués, N.; Muñoz-Berbel, X.; Macanás, J.; Muñoz, M. Mas, J.; Muraviev, D.N. *Chem. Commun.*, **2011**, *47*, 10464-10466.

[39] Pradeep T.; Anshup. *Thin Solid Films*, **2009**, *517*, 6441-6478.

[40] Ettori, A.; Gaudichet-Maurin, E.; Schrotter, J-C.; Aimar, P.; Causserand, C. *J. Membrane Sci.*, **2011**, *375*, 220–230.

1 **Table 1.** Experimental conditions of the stability characterization.

Experiment	**Temperature (ºC)**	**Solution composition**	**Duration (h)**
Ultrasonic bath	20-40	Deionised water	2
Thermostatic bath	37	Deionised water	135
Cultivation conditions	37	$1 \cdot 10^6$ cfu *E.coli* in deionised water	24

2

1 **Table 2**. Metal loading of the samples.

		Metal loading (meq·cm^{-2})	
		Ag	**Pd** [28]
Membrane	SPES-C*	0.31 ± 0.09	0.42 ± 0.05
	Nafion*	5.9 ± 0.8	7.30 ± 0.7
Ratio	Ratio Nafion:SPES-C**	19 ± 6	18 ± 3

2 * Error corresponds to standard deviation of, at least, 2 replicates.

3 ** Error was calculated by propagation of uncertainties.

4

Table 3. Rate of AgNPs loss in the different treatments.

Membrane	rate of loss (%Ag/h)*		
	ultrasonic bath	**thermostatic bath**	**cultivation conditions**
SPES-C	6.7 ± 0.2	-	-
Nafion	0.4 ± 0.1	0.053 ± 0.004**	0.23 ± 0.01**

* Typical error values are expressed as slope standard deviation.

** Maximal loss at 2-3 %.

Table 4. k_{app} values for the catalytic reduction of 4-np by SPES-C and Nafion nanocomposites (uncertainties correspond to standard deviation). The ratios between each run and the first run are presented in brackets.

Membrane	k_{app} ($s^{-1}mmol^{-1}$) ($k/k_{\#1}$)			
	run #1	run #2	run #3	run #4
SPES-C	71.8 ± 0.4 (1)	32.6 ± 0.5 (0.45)	20.5 ± 0.3 (0.29)	19.3 ± 0.2 (0.27)
Nafion	3.5 ± 0.1 (1)	3.1 ± 0.1 (0.88)	2.5 ± 0.1 (0.71)	2.3 ± 0.1 (0.66)
k_{SPES-C}:k_{Nafion}	20.5 ± 0.3	10.6 ± 0.2	8.2 ± 0.1	8.3 ± 0.1

Figure 1. Typical HR-TEM images for the cross-section of AgNPs containing samples and the corresponding size distribution histograms. (a) SPES-C edge, (b) SPES-C inside, (c) SPES-C histogram, d) Nafion edge, e) Nafion inside, f) Nafion histogram.

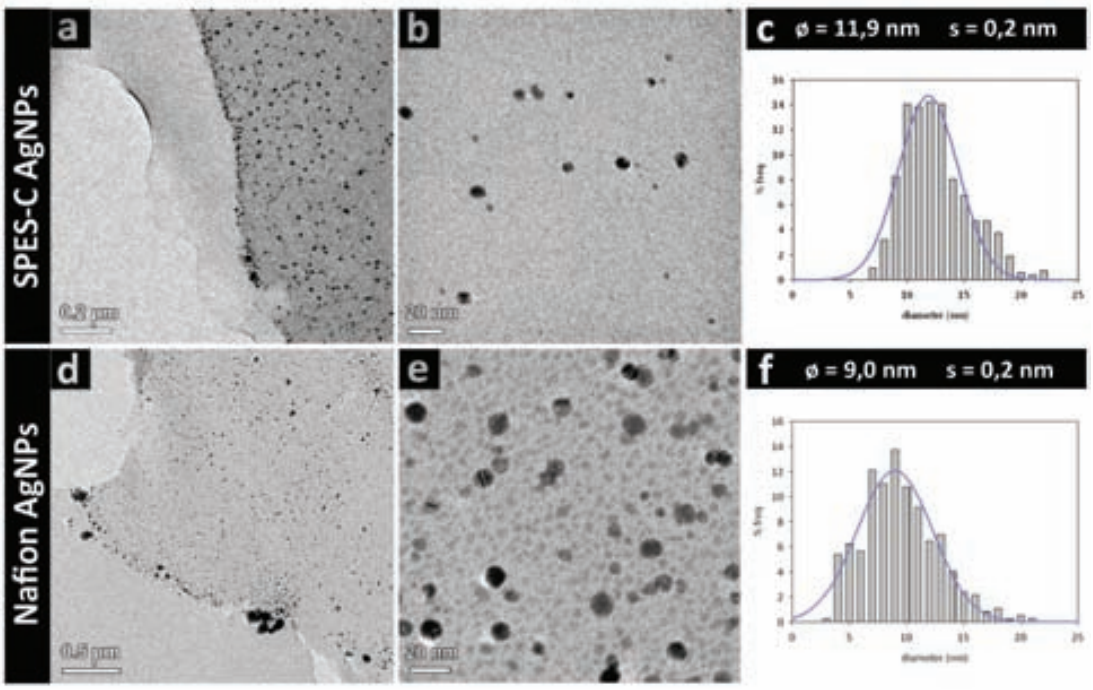

Figure 2. Ag release during different experiments: (a) Nafion and SPES-C nanocomposites in ultrasounds bath, (b) Nafion nanocomposite in thermostatic bath at 37 ºC and (c) Nafion nanocomposite at cultivation conditions.

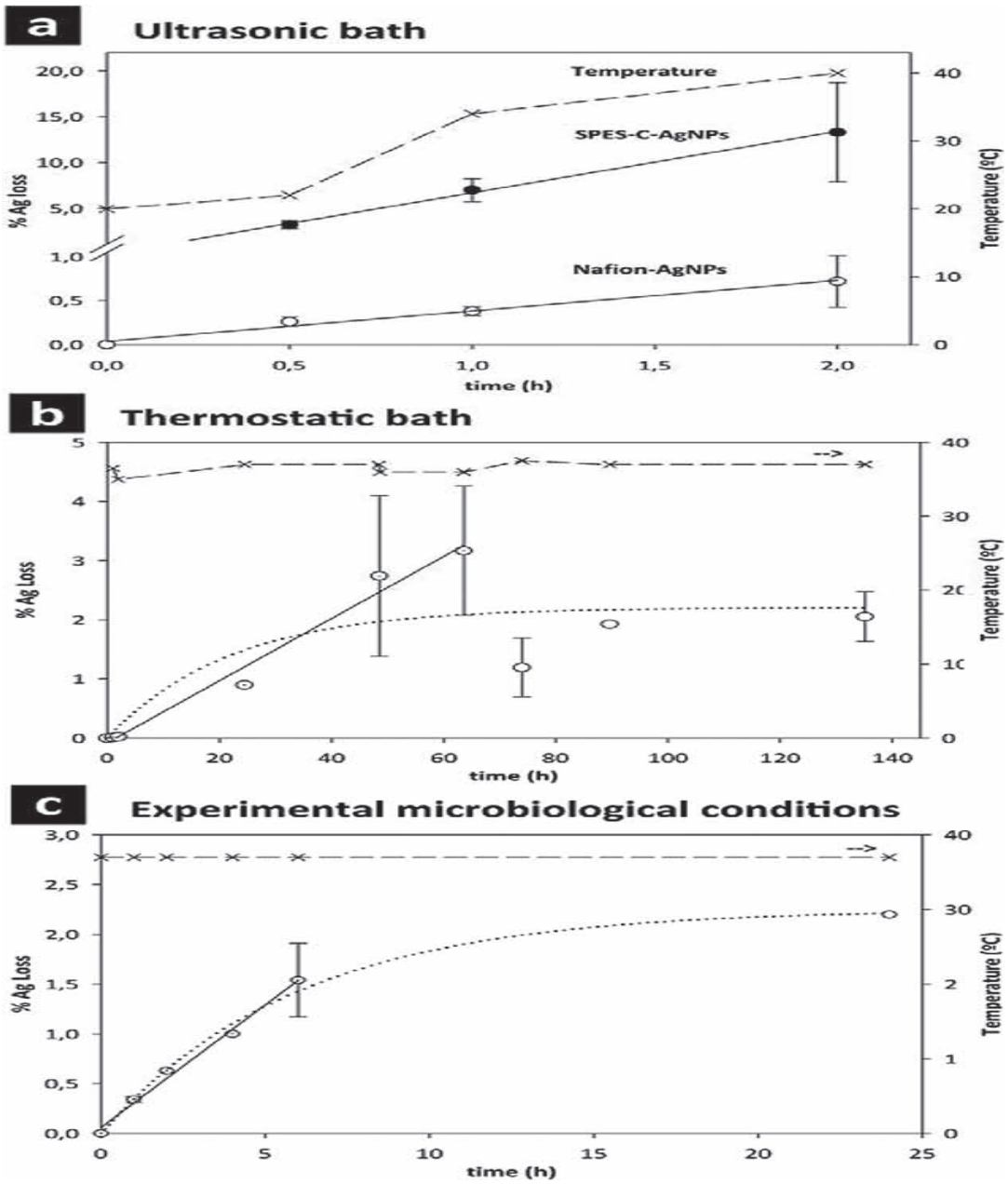

Figure 3. a) Bactericidal activity of the different nanocomposites, MNPs-free polymers and PBS solution, b) bactericidal activity of released AgNPs to the media.

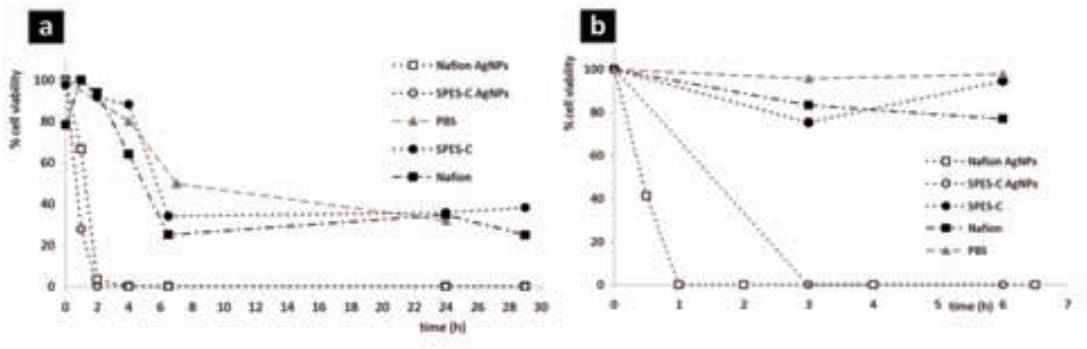

Figure 4. Catalytic evaluation of nanocomposite samples with AgNPs in successive catalytic cycles (a) SPES-C with AgNPs and (b) Nafion with AgNPs. Blank experiment were carried out without any nanocomposite.

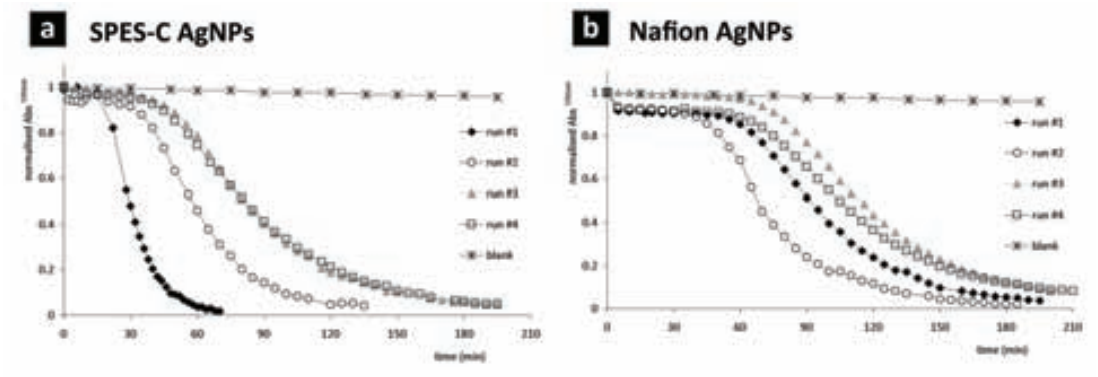

Chapter

NANOCOMPOSITE MATERIALS FOR CATALYTIC MEMBRANES DEVELOPMENT

Berta Domènech[1], **Maria Muñoz**[1], **Dmitri. N. Muraviev**[1] and **Jorge Macanás**[2,*]

[1] Department of Chemistry, Universitat Autònoma de Barcelona, UAB, 08193 Bellaterra, Barcelona, Spain

[2]Department of Chemical Engineering, UPC-BarcelonaTech, C/Colom, 1, 08222 Terrassa, Barcelona, Spain

ABSTRACT

Since the early 21th century, Catalysis has played a central role in chemistry and, with the recent rise of nanotechnology, the catalytic processes have made a giant leap forward, mainly due to the use of nanoparticles. Membranes loaded with catalytically active metal nanoparticles represent a bright example of properties combination as the related processes simultaneously profit from the advantages of Membrane Technology and from the high efficiency of these new catalysts.

Catalytic membranes were usually ceramic or metallic, materials that can withstand high temperatures and/or pressures and high concentrations of corrosive products. Unfortunately their main disadvantages were their high cost and fragility. These drawbacks can be coped by the use of polymeric membranes, which can be made from a myriad of polymers and, therefore, it is possible to exercise some control over the molecular configuration and the final morphology of the polymeric membrane. However, most of organic membranes can only be employed at mild conditions due to its instability towards strong oxidizers and high temperatures, so it is necessary to use very efficient catalysts at these mild conditions.

The use of nanocomposites for the development of polymeric catalytic membranes is a topic which has not been deeply discussed in the current bibliography although its increasing appearance. This chapter provides a wide overview of catalytic membranes focusing on those that are based in organic polymers containing nano-objects (mainly metallic nanoparticles). Production methods such as layer-by-layer deposition, and intermatrix synthesis are depicted. Some environmental possible applications of the nanocomposite catalytic membranes are also tackled.

Keywords: nanocomposites, nanoparticles, catalysis, membrane, intermatrix synthesis

INTRODUCTION

Catalysis and green chemistry

It is widely acknowledged that there is a growing need for more environmentally friendly processes and products. In the chemistry field, this eco-friendly thinking is the so-called green chemistry and consists on the use and development of chemicals and chemical processes in order to reduce or eliminate negative environmental impacts, involving reduced waste products, non-toxic components, and improved efficiency [1] Green chemistry not only deals with the minimization of the potential negative impacts of procedures, but must also be an additional objective itself for the optimization of processes and products.

There is a pressing need for cleaner fuels, free-solvent processes, one-step processes in the chemical, petrochemical and pharmaceutical industries, and industrial processes that minimize energy consumption, waste production, or the use of corrosive, explosive, volatile, and non-biodegradable materials [2]. All these needs can be achieved by the design of appropriate catalysts: low cost, environmentally friendly, with high efficiency and that allow an easy separation from the reaction media and reusable without incurring in a loss of the catalytic efficiency [1].

Up to now, homogenous catalysts [3] (in which the catalyst is generally a soluble metal complex in the same phase as the reactant) have been generally accepted for chemists. They have several advantages such as high selectivity and better yield because all the catalytic sites are accessible to reactants. However, the inherent difficulty of catalyst recovery from media creates economic and environmental barriers, narrowing its scope. To overcome these separation problems, the use of heterogeneous catalyst (usually a high-surface area solid with an active component either dispersed or attached) seems to be the best logical solution [6]. Nevertheless, they also present some disadvantages. On the one hand, although up to now several attempts have been made to increase the accessibility to all the active sites on solid supports (therefore, allowing rates and selectivities comparable to those obtained with homogeneous catalysts), only those sites on the surface are really available for catalysis, which decreases the overall reactivity of the catalyst system. On the other hand, the leaching of the active molecule/complex from the solid support is habitual, what again involves the need of trace metal separation from the final product.

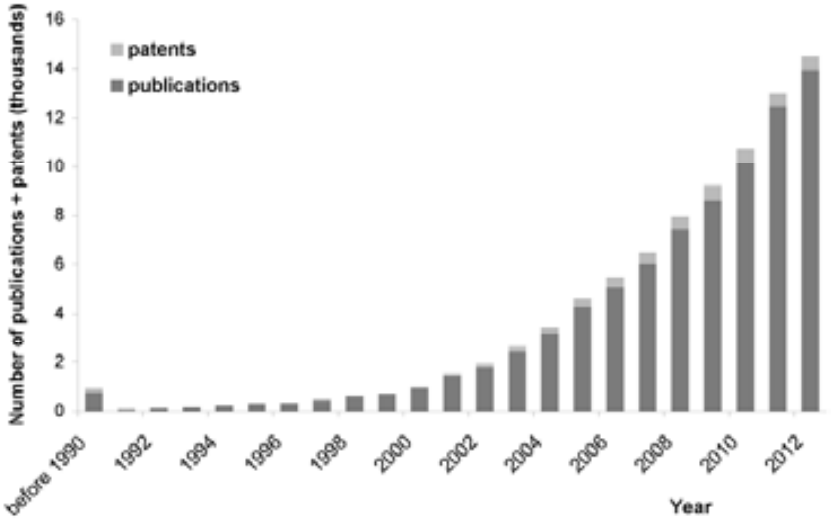

Fig. 1. Evolution of the number of publications in English (books, journal articles, reviews, editorials and patents) containing the words “catalysis” and “nanotechnology”. Source: Scifinder Scholar, CAS.

Hence, new research objectives for the development of catalysts that work at the interface between homogeneous and heterogeneous catalysis have to be considered. The considerable knowledge accumulated in homogeneous, heterogeneous, biphasic and supported catalysis will help in the design of those more efficient and careful with the environment catalytic systems [4-7].

As it can be seen in Fig. 1, the evolution of scientific publications dealing with engineered nanomaterials as catalysts is almost exponential testifying the enormous efforts that are devoted to this topic. For example, in 2011, over the 55,000 references of publications containing the word "nanoparticles", almost a fourth were referred to its application in catalysis.

Catalysis and Nanotechnology

The most commonly accepted definition for a nanomaterial is "a material that has a structure in which at least one of its phases has a nanometer size in at least one dimension" [8,9]. Regarding the 3D nanometer-size objects, it is possible to find porous materials, polycrystalline materials, materials with surface protrusions separated by nanometric distances, or nanometer-sized metallic clusters.

Compared to their bulk counterpart, the behaviour of the nanosized materials changes in a remarkable form due to size-dependant effects derivative from:

(i) an increase of the relation surface-volume,
(ii) changes in the electronic structure of the present species in the nanoparticles,
(iii) changes in the interatomic distances and presence of defects,
(iv) confinement and quantic effects (due to the confinement of the charge carriers in a particle of size comparable to the length wave of the electron).

Among all of these nano-objects, some of those being extensively used in catalysis are shown in Fig. 2:

- Polyhedral oligomeric silsesquioxanes (POSSs) that are widely used in both homogeneous and heterogeneous catalytic systems, as catalysts for alkene metathesis, polymerization, epoxidation and Diels-Alder reactions of enones [10].
- Zeolites are micro- and nano-porous aluminosilicate minerals commonly used as commercial adsorbents. They are widely used in industry for water purification, as catalysts [11], for the preparation of advanced materials and in nuclear reprocessing, to extract nitrogen from air, and in the production of laundry detergents.
- Metal-organic frameworks (MOFs) are crystalline compounds consisting of metal ions or clusters coordinated to rigid organic molecules to form one-, two-, or three-dimensional structures that can be porous. MOFs allow an easy post-reaction separation and recyclability and, in some cases, they also give highly enhanced catalyst stability. Additionally, they typically offer substrate-size selectivity [12].
- Polyoxometalate (POMs) are polyatomic ions, usually anions, which consist of three or more transition metal oxyanions linked together by shared oxygen atoms to form a large, closed 3D framework. Some potential applications have been reported, such as catalysis of dye bleaching by hydrogen [13].
- Carbon-based nano-catalysts, such as fullerenes, carbon nanotubes (CNTs) and graphene, have boosted their applications in catalysis of this element [14]. As an exemple, CNTs have been used mainly for important liquid-phase reactions (hydrogenation, hydroformylation) or gas-phase reactions (Fischer–Tropsch process, ammonia decomposition), for photocatalysis and for electrocatalysis (fuel-cell electrodes).
- Enzymes are proteins that exhibit high catalytic capability by accelerating reactions with striking efficiency and selectivity and being sterically and electronically complementary to the reactants in their rate-determining transition states [15].

- Dendrimeric structures are repetitively branched molecules, typically symmetric around the core, and often with a spherical three-dimensional morphology. Among other potential applications, they are suitable soluble supports for homogeneous transition metal complex catalysts [16].

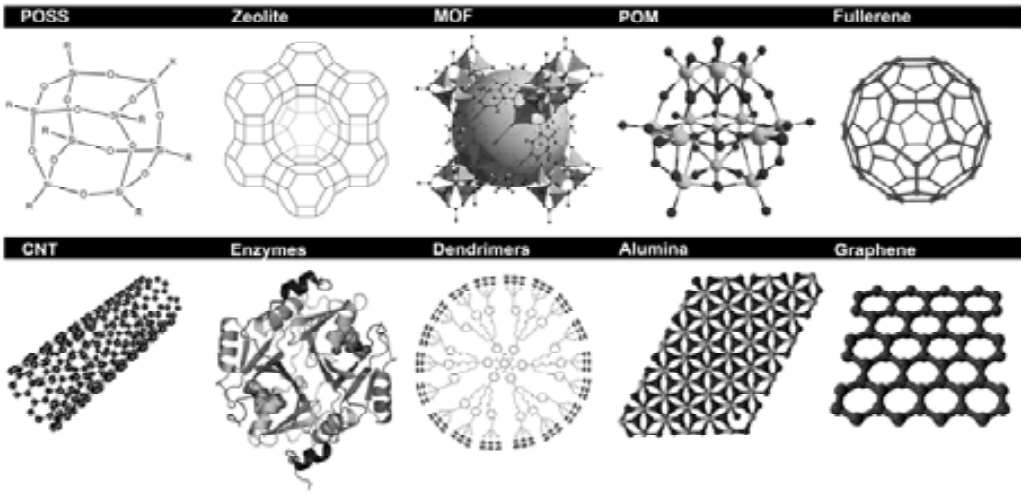

Fig. 2. Schematic representation of different nano-objects used in catalysis.

Anyhow, although there is a myriad of catalytic nano-objects, metal nanoparticles (MNPs) have already made the major impact on the fields of surface science and as catalysis [17], due to their large percentage of surface atoms. In fact, the use of MNPs in catalysis is not new; it already appeared in the 19th century. In photography, supported silver halides decomposed producing AgNPs with the incident of light (AgNPs were "the pixels" of the photographic image), whereas in the industry, PtNPs (known as Bredig's colloidal platinum) were used as a catalyst for the decomposition of hydrogen peroxide [18].

Just to understand the evolution of this topic, it is worth to know that the first pioneer catalytic applications date back from the mid-1900; in 1940 Nord reported the use of MNPs in the reduction of nitrobenzene [19]; in 1970 Parravano et al. reported the hydrogen-atom transfer between benzene and cyclohexane and oxygen-atom transfer between CO and CO_2 using nanoparticles [20] and in the 1970s, Bond and Sermon [21] and Hirai et al. [22] disclosed AuNP-catalyzed olefin hydrogenation. But, the real leap forward came with the studies in the oxidation of CO by O_2 at low temperature and catalysed by AuNPs, studied by Haruta et al. [23]. Thus, last decades supposed a big breakthrough for the development of novel catalytically active MNPs [7] and nanocatalysts have emerged to tackle the catalysis challenges, since the end of 1990 [24].

Nowadays, the real scientific challenge is still the development of well-defined catalysts, which may include either MNPs or any other nanomaterial as a support. These new catalysts should display high efficiency and selectivity, stability and easy recovery/recycling, so special efforts have to be done in order to synthesize specific-size and shape nanocatalysts, to control their morphology, to tailor their physical and chemical properties and to stabilize the catalytic specie in order to avoid its leakage or agglomeration.

The stabilization of MNPs is usually performed by covering them with a polymeric material or with reactive stabilizers that prevent the interaction between neighbouring MNPs. The disadvantage of such strategy is that, as a result of this protection, particles not always retain their original properties. Furthermore, the manipulation of particles involves certain risks of aggregation. Thus, a good strategy to achieve the immobilisation and stabilization of these MNPs in order to obtain a maximum catalytic performance is their inclusion in membranes. This inclusion has two main advantages: (i) particles grow where they should be

used, without further modification, manufacturing or processing in order to place them where necessary, and (ii) the membrane controls the transfer of chemical compounds (either reagents or products), what allows obtaining a highly effective catalyst combined with membrane processes in one single step [25].

Nanocomposite membranes obtained by the immobilization of catalytic MNPs in a membrane would allow the achievement of several general aspects of green catalysis such as the easy separation of the catalyst of the reaction medium and the possibility to reuse the catalytic specie without a loss in the catalytic efficiency [1].

CATALYTIC MEMBRANES

A Catalytic Membrane (CM) is a membrane reactor system with an integral coupling of a membrane separation process and a chemical reactor, coupled in a manner that a synergy is created between both units. Such combination involves several possibilities, making it a complex and exciting research field has attracted in recent years the attention of scientist and engineers from different disciplines [25-27].

IUPAC [28] defines a membrane reactor as device for simultaneously performing a reaction and a membrane-based separation in the same physical device. Therefore, the membrane not only plays the role of a separator but also takes place in the reaction itself, enhancing the process performance in terms of separation, selectivity and yield [29].

To understand the role of the membrane in such configurations, some concepts and basic definitions of membrane and membrane-based separation processes must be given in order to familiarize those readers who might be novel in the membrane field.

Principles of membrane separation processes

A membrane can be defined as a permeable or semi-permeable phase, traditionally in the form of a thin film, which can be made from a variety of materials ranging from inorganic solids to different types of polymers. The main role of the membrane during a separation process is to control the exchange of materials between two adjacent fluid phases [30].

Therefore, the membrane action results in a feed (the retentate), which is dwindled from some of its original components, and another fluid stream (the permeate), where these components are found in a higher concentration. This separation is usually controlled by transport processes across the membrane, which are the result of a driving force typically associated with a gradient of concentration, pressure, temperature, electric potential, etc.

The ability of the membrane to separate is determined by two main parameters, its permeability and its selectivity. The permeability is defined as the flux through the membrane normalized with respect to the membrane thickness and driving force. Selectivity refers to the ability of the membrane to separate two given species and it is typically defined as the ratio of the individual permeabilities [25,29,30].

In a general view, some of the main advantages of membrane separation processes, over the more conventional counterparts (adsorption, absorption, distillation, etc.), are:

- the separation occurs in a continuous way,
- they are energy savings,
- the processes are easily combinable with other separation processes,
- the scaling of the process is simple,
- membrane properties are tunable and adjustable,
- additives are not needed, and
- there is reduction in the initial capital investment required.

Nevertheless, these are general virtues but they are no generally shared for all membrane separation processes. Thus, there are cases in which the energy required to carry out the separation is a major obstacle for its industrial application (e.g. electrodialysis). Other processes involve some additives to improve the performance of the separation process or to prevent fouling, which may impair the separation properties of these membranes. Therefore, each membrane separation process should be designed based on the final application and the properties of the membrane itself.

Besides, membranes can be classified by whether the permselective layer is porous or dense, and by the type of material (organic, polymeric, inorganic, metallic, etc.) the membrane film is made of. The choice of a porous or a dense thin layer depends on the desired separation process, operating temperature and driving force used for the separation; the choice of material depends on the required permeance and selectivity, and on thermal and mechanical stability requirements. And, as a rule of thumb, an extra requirement has to be taken in mind: the thin film has also to be stable under the catalytic reaction conditions.

So, the selection of membrane type to be used as a CM depends on parameters such as the productivity, the separation selectivity, the membrane lifetime, its mechanical and chemical integrity at the operating conditions and, in particularly, its cost.

Catalytic membranes configurations

Different approaches can be envisaged in order to combine the reaction and the separation process in a membrane. In these configurations the separation capability of the membrane may improve the performance of a catalytic system [29,31]. Usually, three main generic configurations can be used being their main difference the specific role of the membrane in the process. Accordingly, if there is a selective product separation after reaction, an extractor membrane is conceived; if the membrane is itself the reaction zone where the different reactants coincide, we face to a membrane contactor; and when there is a selective reactant addition, we deal with distributor membranes. All these configurations are depicted in Fig. 3.

The extractor membrane type is the most commonly studied. In this case, the function of the membrane is to selectively extract one or some of the reaction products from the reactor. When an equilibrium-restricted reaction is carried out, the role of the membrane can force the reaction to proceed in a high extent by selectively remove one of the generated products. This mode is particularly well suited to favor conversion or selectivity [31].

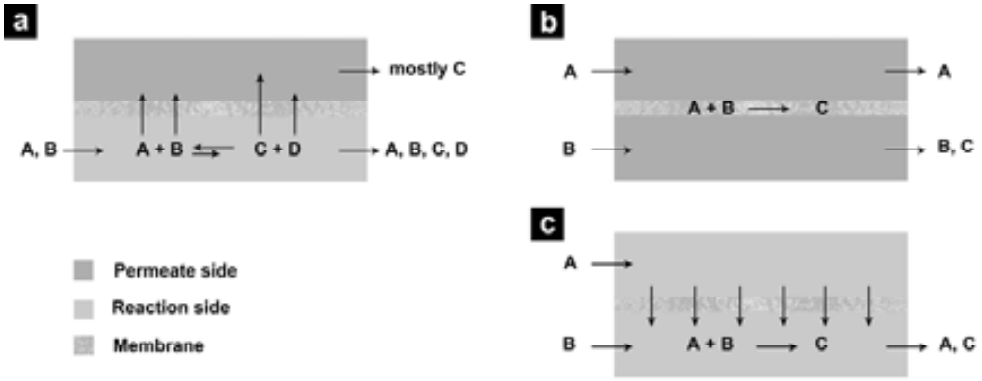

Fig. 3. Schematic catalytic membrane configurations: (a) extractor, (b) contactor and (c) distributor.

The contactor mode takes advantage of the geometry of a membrane, i.e. a permeable wall separating two media. When the membrane is also a support for a catalyst, it is therefore possible to separately feed the system with reactants (for instance a gas from one side and a liquid from the other) or to force a reactive mixture through the active wall. In this case, it is

possible to distinguish two main approaches. In a first approach, by using an interfacial contactor [32] it is possible to favor the contact between the catalyst and the reactant, which usually limits the performance of conventional reactors (e.g. gas in gas–liquid–solid processes, hydrophobic reactant with hydrophilic catalyst, etc.). In a second approach, using the membrane as a flow-through contactor, the residence time in the active pore of reactants and products is controlled by operating parameters (pressure drop across the membrane) and not only by diffusion, usually leading to a better control of activity or selectivity [31].

Finally, in a distributor mode, the membrane is used to control the addition of one of the reactants to the catalyst bed. In this approach, both perm-selective and non-permselective membranes can be used to feed one of the reactants. When compared to a conventional reactor, the distribution of one reactant through the membrane will modify the local reactant composition in the catalyst bed.

Membranes for catalytic membranes development

The use of membrane processes combined with catalytic processes in one single step has been boosted in recent years, and in part, it has been due to the discovery of new membrane materials, which have allowed tuning the final characteristics of the CM to the required conditions. Several efforts have been done to develop synthetic membrane that are more stable and controllable and can be subdivided into organic (polymeric) and inorganic (ceramic, metallic).

Inorganic Membranes

Inorganic membranes are commonly ceramic, carbon-made or metallic and they show wide tolerance to pH and high resistance to chemical degradation. They can operate at elevated temperatures, ranging from 300 to 800 ºC, even over 1000 ºC. But inorganic membranes usually present a high cost and fragility as main drawbacks.

- Metallic Membranes. The most conventional configuration of metallic membranes is in its dense form, and they have been extensively used for hydrogen separation from gas mixtures. In this field, palladium and its alloys are the dominant materials for the preparation of this kind of membranes [33] due to the high solubility and permeability to hydrogen in these materials. As palladium is scarce and expensive, supported thin metallic membranes have been recently fabricated by coating a thin layer of palladium on a ceramic support. Although this strategy seems to reduce material costs and improve resistance to mechanical strength, the surface poisoning becomes dramatically more significant [26,34].
- Ceramic Membranes. These membranes are commonly made of aluminium, titanium or silica oxides, what makes them chemically inert and stable at high temperatures. Ceramic microfiltration and ultrafiltration membranes resulted to be particularly suitable for food, biotechnology and pharmaceutical applications in which membranes require repeated steam sterilization and chemical cleaning [29]. Nevertheless, some disadvantages remain to be solved, such as its fragility and their extremely high sensitivity to temperature gradient leading to membrane cracking.
- Carbon Membranes. Carbon membrane materials are porous solids containing constricted apertures that approach the molecular dimensions of diffusing gas molecules. They are becoming important candidates in the new era of membrane technology for its application in gas separation due to their higher selectivity, permeability and stability in corrosive and high temperature operations. Carbon membranes can be produced by pyrolysis of a suitable polymeric precursor under controlled conditions, such as poly(vinylidene chloride), cellulose triacetate or polyacrylonitrile [35]. Even if the separation properties of

these carbon membranes are superior to those of other materials here mentioned, a significant drawback has been their vulnerability to adverse effects from water vapor exposure [36].

Polymeric membranes

Organic or polymeric membranes constitute the wider and most developed sort of membranes, from a standpoint of production volume and regarding its practical applications. The main reason that has led to this situation has to do with the versatility of available polymers and can be resumed as follows [29]:

- there is a possibility to exert control over the molecular configurations of polymers, which directly affect permeability and selectivity of the membranes,
- polymers can easily adopt different physical forms, and
- the large variety of existing polymers allows to choose those most interesting to design a particular membrane.

In Table 1 the main advantages and disadvantages of these types of membranes *versus* the inorganic ones, are presented.

Table 1. Advantages and disadvantages of inorganic *vs*. polymeric membranes [29].

Disadvantages	Advantages
Low-term stability at high temperatures	Low cost
Low resistance to high pressure drops	High membrane surface per module volume
Low resistance to harsh environments (chemical degradation, pH, etc.)	Simple scalability
Susceptibility to microbiological degradation	Ease of achieving high selectivities in large scale microporous membranes
Difficult cleaning after fouling	Generally, high permeability of membranes highly selective to hydrogen at medium temperatures

In the literature, several works are focused on the research of simultaneously higher permeability and selectivity by coupling chain stiffness with an increase of the interchain separation [37]. In other cases, some efforts have been done to create materials with significant chemical and thermal resistance [38].

New research is focused on the development of polymeric membranes that overcome the typical disadvantages of such membranes and, for instance, new solvent-resistant membranes have been developed [38].

Thanks to the great versatility of polymer conformations, polymeric catalytic membranes offer added flexibility over their conventional reactor counterparts. The accurate selection of the polymer molecular configuration and the control of its morphology would lead to the most appropriate membrane for a desired application. Moreover, polymeric organic membranes are usually less expensive than their ceramic or metallic counterparts [39,40].

Nonetheless, the main issue of these materials [40-42] has traditionally been that organic membranes have to be employed at mild conditions to avoid polymer degradation, so in order to be used as CMs, it is necessary to have very efficient catalysts, with a high performance at such conditions.

Polymeric membranes with metal nanoparticles

Manipulations of single nanoscopic objects are difficult to achieve and most of nano-sized metals are very instable: they aggregate because of their high surface free energy and

can be easily oxidized by air, moisture, SO_2, and so on [43]. In this sense, the embedding of nanoscopic metals into polymeric matrices represents a valid solution to the manipulation and stabilization problems since [44]:

- they can be an electrical and thermal insulator or conductor;
- may have a hydrophobic or hydrophilic nature;
- can be mechanically hard, plastic, or rubbery, etc.
- is the easiest and most convenient way for nanostructured metals stabilization, handling, and use.

It is of crucial importance take a deeper look into the interaction forces acting between nanoparticles in order to understand the role of the polymer as the most effective candidate for stabilizing MNPs preventing their aggregation and as solubilizing agents, providing a convenient tool for further manipulation and application. In a general view, there are three main types of colloidal forces [45]:

(i) The Van der Waals interaction between two spherical particles with diameters between 10-100 nm predicted for the Hamaker equation is positive, resulting in an attractive force between both particles.

(ii) The electrical double-layer interactions between charged ionic moieties, which are attracted to an oppositely charged interface and, in many cases, form a diffuse layer near the surface.

(iii) The steric interactions, due to the adsorption of a polymer in a surface.

The mechanism of MNP stabilization with polymers can be explained by two approaches which run simultaneously in the system and influence one another: the substantial increase of viscosity of the immobilizing media (the polymer matrix), and the decrease of the energy of particle-particle interaction in Polymer Stabilized MNPs (PSMNPs) systems versus non-stabilized MNP dispersions [46].

Regarding the possible routes for PSMNPs fabrication, they can be grouped by two different approaches, namely, *in-situ* [32] and *ex-situ* [47] techniques, schematized in Fig. 4.

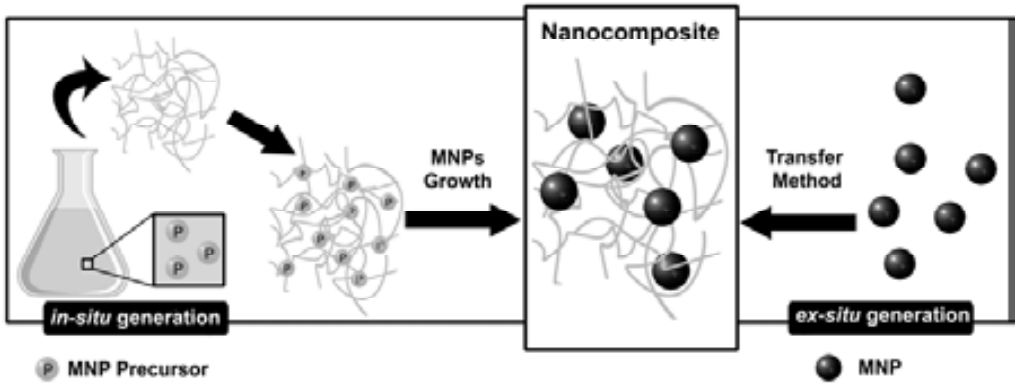

Fig. 4. Schematic comparison between *in-situ* and *ex-situ* methodologies.

In the *ex-situ* synthesis [47] MNPs are chemically synthesized, and their surface is passivated. Then, they are dispersed into a polymer solution or liquid monomer that is afterwards polymerized. This approach increases the compatibility of the particles with the polymer and simplifies their homogeneous dispersion inside the matrix. However, significant challenges are associated with blending polymers and nanoparticles and, in some cases, the success of the stabilization is limited by the possibility of re-aggregation of the MNPs along the time.

On the opposite hand, by the *in-situ* synthesis [32] the metal ions are introduced before or after polymerization and then metal ions in the polymer matrix are reduced chemically, thermally, or by UV irradiation. Hereby, MNPs are grown directly in the stabilizer medium

yielding a material that can be directly used for a foreseen purpose. *In-situ* approaches are getting much attention, because of their technological advantages [48-50] and they can be extended to the preparation of many metal–polymer nanocomposites. Thus, it is feasible to make useful materials for process intensification through the combination of catalysis and membrane process within the same nanocomposite, which, for instance, may destroy and separate pollutants in a single step [32,51,52].

INCORPORATION OF METAL NANOPARTICLES INTO MEMBRANES

Different specific routes for the inclusion of MNPs in membranes have been well developed over the last few years for a wide range of catalytic applications [40,42,53]. Since the advances in the techniques of synthesis are often the key to reach the desired nanocomposite polymeric membranes, it is of huge importance to bring readers up-to-date on recent advances in the field. In this sense, different strategies are considered such as the Layer by Layer approach, impregnation, chemical vapor deposition, deposition method and finally, the one developed by our research group, the Intermatrix Synthesis.

Impregnation

This methodology entails the "wetting" of the solid support with a solution containing either the metal precursor (by an *in-situ* approach) or with the preformed MNPs (in the *ex-situ* approach). The MNP precursor, which is normally a salt (e.g. metal nitrate, chloride), is dissolved in the minimum quantity of solvent and the resulting solution is then added to a porous support, filling its pores so that a thick paste is formed. The solvent is then removed in a rotary evaporator and the final solid is oven-dried and subsequently calcinated and reduced (if needed) before being tested as a catalyst [54].

By this procedure, Luo et al. [55] prepared TiO_2 nanoparticles in a polyethersulfone (PES) membrane by dipping the neat PES into a solution of TiO_2 NPs obtained by controlled hydrolysis of titanium tetraisopropoxide at acidic condition. They explain the self-assembly behavior of TiO_2 on the surface of polymer which contains -COOH, -SO_2OH, and sulfone groups by two different adsorption schemes:

(i) the TiO_2 bounding with oxygen atoms of these groups via coordination to Ti^{4+} cations, and
(ii) the formation of an hydrogen bond between the groups and the hydroxyl group of TiO_2 surface.

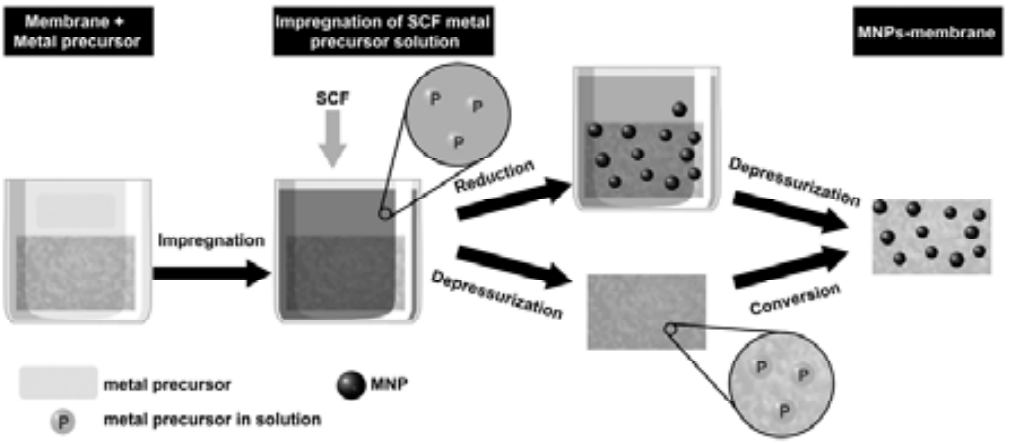

Fig. 5. Scheme of SCF use as solvent to synthesize supported nanoparticles via impregnation.

On the other hand, Zhang et al. [56] reported the *in-situ* formation of MNPs by impregnation of a polymeric support in a supercritical fluid (SCF) solution of the metal precursor (Fig. 5). Afterwards, the formation of the MNPs can proceed by three procedures:

(i) chemical reduction in the SCF with a reducing agent, such as hydrogen and an alcohol;
(ii) thermal reduction in the SCF; or
(iii) thermal decomposition in an inert atmosphere or chemical conversion with hydrogen or air after depressurization.

Thanks to the low surface tension of SCFs, a better penetration and wetting of pores than liquid solvents is obtained, and it is also possible to avoid the pore collapse (which can occur on certain structures such as organic and silica aerogels with liquid solvents).

Deposition

This methodology, initially developed by Haruta et al. [57], involves the dissolution of the metal precursor followed by pH adjustment (i.e. 5–10) so as to achieve a complete precipitation of the metal hydroxide (e.g. $Au(OH)_3$), which is deposited on the support surface. Afterwards, the hydroxide is calcinated and therefore reduced to the elemental gold.

Iojoiu et al. [58] reported the synthesis of different nanostructured catalytic membranes by platinum deposition (by evaporation-crystallisation or by ionic impregnation), and found that the chemical interactions between the platinum precursor an the surface species was a crucial parameter for the choice of the deposition method, since the intensity and location of those interactions would determine the amount and distribution of the final PtNPs. They stated that the anionic impregnation, largely controlled by chemical interactions, allowed a better dispersion of the MNPs in the support.

Another deposition approach is the one reported by Yang et al. [59] in which the *in-situ* deposition of PtNPs on a bacterial cellulose membrane (BCM) was performed in a 3D network structure of BCM through a liquid phase chemical deoxidization method. By this procedure they were able to obtain PtNPs on the membrane surface, what made the nanocomposite membrane obtained suitable for fuel cell applications.

Anyhow, although there are several approaches that can be suitable for a deposition method, usually, these methodologies lack in the control of the size and distribution of the final MNPs, and sometimes require the use an excess of external reducing agent (e.g. $NaBH_4$, H_2, hydrazine) to ensure the complete formation of the supported metal nanoparticle, that has to be removed after the reaction [47].

Layer by layer

This technique has been developed by a large number of research groups for the modification of flat surfaces. It lays on the idea of a simple layer-by-layer (LBL) method popularized by Decher [60], who exposed a substrate surface alternately to solutions of cationic and anionic polyelectrolytes to create a multilayer film [61,62].

By this procedure, films are formed by depositing alternating layers of oppositely charged materials with wash steps in between on almost any substrate that will support the adsorption of an initial layer of polymer. The resulting layers formed by polyelectrolytes of opposite charge are attracted to each other by electrostatic interactions, thus creating dense layers [63].

Although the growth of multilayer films of diverse substances by this approach is easy, the high sensitivity of the growth and properties of the multilayer films to chemical factors such as polyelectrolyte concentration and the presence of other electrolytes, pH, and hydrogen-bonding and covalent-bonding grouping has to be considered [62]. In this sense, some of the dependence can be related to the stability of the layers to rinsing steps, to the

surface charge of the successive component layers, and to the relationship between the polyelectrolyte structure and to the charge density.

Up to now, this approach has demonstrated bo be a simple way to immobilize highly accessible, well-separated nanoscopic components such as semiconductor nanoparticles and quantum dots [64], magnetic nanoparticles [65], enzymes [66] and metal nanoparticles [67].

In a general view, the immobilization of MNPs in a polymeric matrix by such procedure can be described as schematized in Fig. 6. Moreover, the *ex-situ* formation of nanoparticles in solution prior to their deposition permits tailoring the nanoparticle size and surface composition, but several efforts are still necessary to exercise a higher control over the amount of colloid deposited [68].

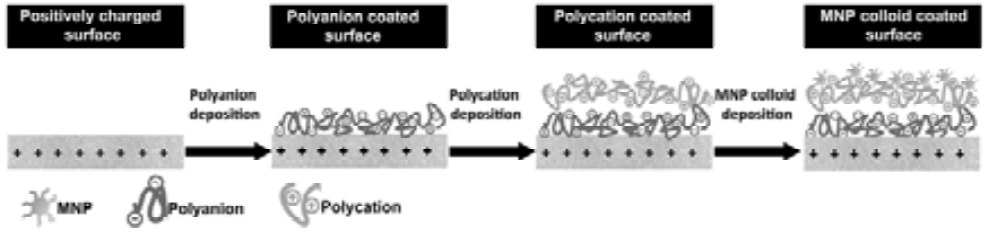

Fig. 6. Modification of a membrane by adsorption of two polyelectrolytes and MNPs (*ex-situ*).

Chemical vapor deposition

Chemical vapor deposition (CVD) is a promising route allowing the obtention of highly dispersed catalysts in a controlled and reproducible manner [69]. In a general run, this procedure involves the sublimation of metals and the posterior growth of the MNPs under high vacuum in the presence of an excess of stabilizing organic solvent (e.g. aromatic hydrocarbons, alkenes and tetrahydrofuran) and/or reducing agent (e.g. H_2) [47]. This methodology allows the preparation of MNPs on a wide range of organic and inorganic supports under very mild conditions (<50 ºC) to afford highly active heterogeneous catalysts [70], thereby avoiding the formation of large agglomerated nanoparticles from other protocols. The method is often limited by the vapor pressure of the precursor and mass-transfer-limited kinetics [47].

Intermatrix Synthesis

The Intermatrix Synthesis (IMS) [6] takes advantage of the abovementioned *in-situ* approach. The general principles of IMS, valid for any kind of polymer matrix and type of nanoparticle, are based on:

(i) the nanoreactor effect: the confinement of the particles by the polymer molecules which allows limiting the size and particle size distribution; and,
(ii) the barrier effect: the polymer molecules isolate the formation of each single NP preventing the contact between their surfaces and therefore their aggregation.

These guidelines are only achievable if NPs precursors can be properly immobilized in the polymeric matrix. In this sense, ion exchange matrices are the perfect plate to retain the ionic species, metal cations, anions or any kind of coordination compound.

Fig. 7 illustrates the two main consecutive stages that rule the IMS technique in a cation exchange membrane:

(i) the immobilization of the metal ion or complex, and
(ii) the reduction of the metal ion inside the matrix.

To illustrate this approach, two anion charged group as sulfonic group ($-SO_3^-$) can efficiently interact with the divalent metal cation (M_1^{2+}), which afterwards can undergo a chemical reaction (precipitation, reduction, etc.) and finally yield to the formation of the MNP.

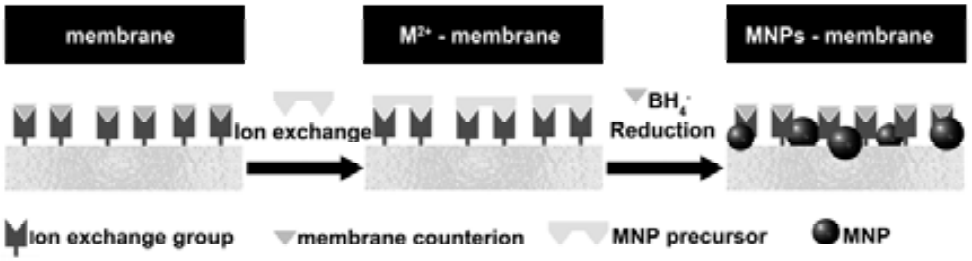

Fig. 7. Monometallic MNPs preparation inside a polymeric ion-exchange matrix by IMS.

A symmetrical procedure can be done for an anion exchange matrix bearing a functional group such as quaternary ammonium ($-NR_4^+$), capable to immobilize metal complexes (i.e. $[CoCl_4]^{2-}$) or other anions (i.e. BH_4^-).

For cation exchange matrices (CEM):

$$2(R\text{-}SO_3^-Na^+) + M_1^{2+} \leftrightarrow (R\text{-}SO_3^-)_2M_1^{2+} + 2\ Na^+ \quad (1)$$

$$(R\text{-}SO_3^-)_2\ M_1^{2+} + 2\ NaBH_4 + 6H_2O \rightarrow 2(R\text{-}SO_3\text{-}Na^+) + 7H_2 + 2B(OH)_3 + M_1^0 \quad (2)$$

For anion exchange matrices (AEM):

$$R\text{-}(R_3N)^+Cl^- + NaBH_4 \leftrightarrow R\text{-}(R_3N)^+BH_4^- + NaCl \quad (3)$$

$$2(R\text{-}(R_3N)^+BH_4^-) + [M_1]^{2+}Cl_2 + 6H_2O \rightarrow 2(R\text{-}(R_3N)^+Cl^-) + 7H_2 + 2B(OH)_3 + M_1^0 \quad (4)$$

As it can be seen from Fig. 7, the matrix is regenerated after the second stage of the IMS, so it is possible to apply consecutive IMS cycles. Previous works [53] reported the IMS of PdNPs in sulfonated polyethersulfone with Cardo group (SPES-C) membranes and in blend membranes made of sulfonated and non sulfonated polyethersulfone (PES-C/SPES-C). Blend membranes showed a low content in Pd, due to the low sulfonic positions available to proceed with the first step of the IMS synthesis. Thus, by applying a second IMS cycle the total metal load was doubled. In other works the obtaining of bimetallic nanoparticles has been reported, achieving structures such as core-shell, alloys or core-sandwich.

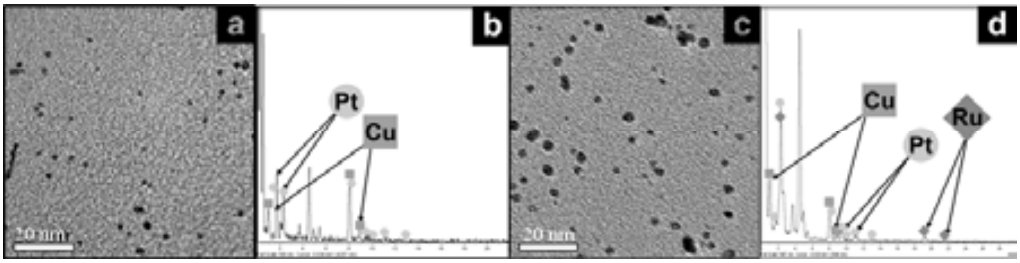

Fig. 8. TEM images and EDS spectra of core shell Pt@Cu- (a, b) and core sandwich Ru@Pt@Cu-PSMNPs(c, d). Adapted from Ruiz et al. [133].

For instance, Ruiz et al., reported the synthesis of bi-metallic core-shell Pt@Cu and tri-metallic core-sandwich Ru@Pt@Cu-PSNPs in sulfonated polyetheretherketone (SPEEK) obtained by two and three consecutive loading cycles respectively [71]. Results presented in Fig. 8 confirm the formation of these bi-metallic and tri-metallic structures showing TEM images and the corresponding EDS spectra of core-shell Pt@Cu (Fig. 8a, 8b) and core-

sandwich Ru@Pt@Cu-PSMNPs (Fig. 8c, 8d), what confirms the simplicity and versatility of IMS technique, which provides a wide range of of tuneable compositions and structures.

Note that in the general IMS procedure described before, there are always two species bearing the same charge: the matrix and the reducing agent (in CEM), the matrix and the metal ion or the matrix and the reducing agent (in AEM). This means that there is an electrostatic repulsion between the matrix and one of the species mentioned that impede the penetration inside the polymeric matrix, referred to as Donnan-exclusion effect [72]. Consequently, ion penetration inside the matrix is balanced by the sum of two driving forces acting in opposite directions: the gradient of the ion concentration and the Donnan-effect itself. The result of these two driving forces is the formation of the MNPs mainly near the surface of the polymer matrix, what makes it suitable for surface applications, since MNPs remain maximally accessible for substrates of interest such as chemical reagents. This can be noticed in Fig. 9 where AgNPs mainly grew on the surface of SPES-C membranes, although some penetration inside de matrix is also observed (less than 4 μm). For porous membranes, MNPs can grow inside the pores, as it is seen in Fig. 10 where AgNPs are also located inside the pores of the aforementioned PES-C/SPES-C blend membranes. This last distribution is more appropriate for the application of the material in catalytic flux conditions.

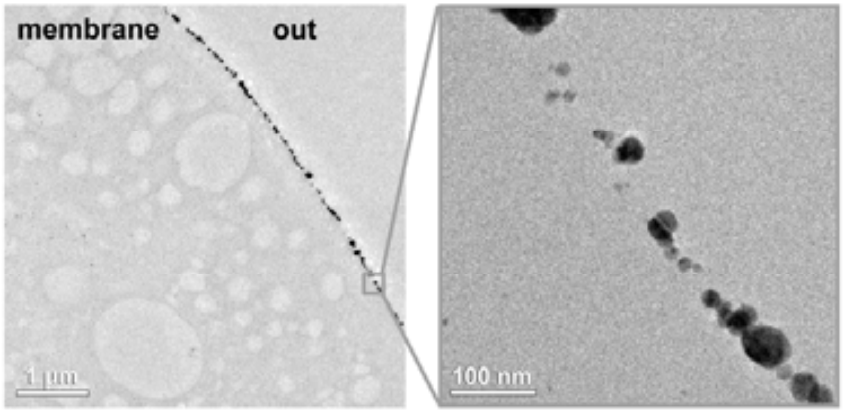

Fig. 9. TEM images of ultrathin slices of a polymeric dense membrane containing AgNPs.

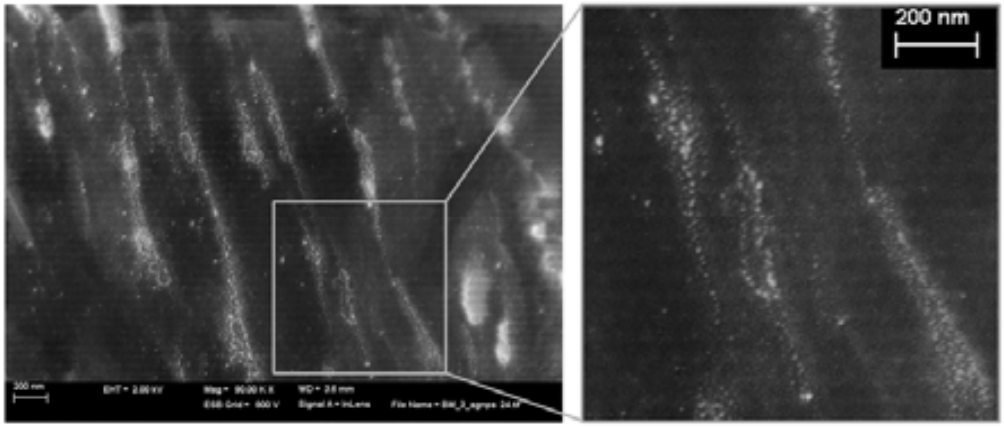

Fig. 10. Scanning Electron Microscopy Merlin images of a thin slice of a polymeric porous membrane (PES-C/SPES-C) containing AgNPs inside the pores.

EXAMPLES OF APPLICATION

Catalytic metal-polymer nanocomposite membranes cover a wide field of practical applications and some of them will be revised in this part of the chapter.

Water treatment

There are about 780 million people in the world who have no access to clean and potable water [73]. This situation dictates the need for the development of innovative technologies and materials for the production of safe potable water. This type of application can be a perfect niche for the nanomaterials here mentioned. However, it is necessary to develop ecologically-safe nanomaterials that prevent the post-contamination of the used samples [74].

Several studies have been focused on the deactivation of pathogenic waterborne microorganisms while other studies have reported groundwater remediation through the degradation of toxic chlorinated organic compounds (COCs) with iron-based bimetallic NPs (Fe/Ni, Fe/Pd) [75,76].

Wu et al. [77] reported the preparation and application of cellulose acetate (CA) supported iron and Pd/Fe nanoparticles obtained by the microemulsion methodology (previously described) for the dechlorination of trichloroethylene from water. They found that compared with the CA-supported FeNPs, the dechlorination rate was significantly increased by the second modifying metal, Pd, and that the membrane-supported Pd/Fe nanoparticles formed in microemulsion exhibited higher performance compared to those formed in solution.

Bachas et al. [78] studied the use of immobilized Pd modified bimetallic nanoparticles in the treatment of chlorinated aromatics such as polychlorinated biphenyls (PCBs). In this reaction, the role of Pd is to collect H_2 generated from the iron corrosion reaction and decompose it into atomic H*, which can be utilized to replace the chlorine in PCBs.

The evaluation of the PCBs decomposition was carried out by two different configurations:

(i) PdNPs immobilized in polypyrrole membranes using external H_2 supply, and
(ii) (Fe/Pd)NPs in polyacrylate-polyvinylidene fluoride microfiltration membranes without external H_2 supply.

Results showed that the bimetallic nanoparticles exhibited higher reactivity in terms of kinetics for the dechlorination, what they explained by the *in-situ* H_2 generation at the Fe/Pd interface, which could minimize the H_2 transfer resistance to the Pd surface. Whereas in the pure Pd (with Pd/polypyrrole) system, H_2 needed to be first dissolved in the aqueous phase and then transferred to the Pd surface by diffusion, lowing the reaction rate. On the other hand, when compared to those procedures in which MNPs are not stabilized, [75,76] Bachas et al. found that the particle size could be controlled by varying the ratio of polymer and metal ions, and that no metal was lost in polyacrylate membranes [79].

Other research groups have focused their investigation on the elimination of nitroaromatic compounds. Bruening et al., developed hollow fibres modified with AuNPs obtained by the aforesaid LBL approach and applied to the catalytic reduction of p-nitrophenol (4-np) with $NaBH_4$ [32,52]. Our research group performed the same reaction in a different approach: membranes of SPES-C and commercial Nafion containing PdNPs obtained by Intermatrix Synthesis were evaluated in batch tests. The results, presented in Fig. 11, showed a good performance of the membrane nanocomposites, which were able to degrade the 50% of the 4-np present in the solution in less than 100 min [49,53]. The possibility to reuse the nanocomposite catalytic membranes was also evaluated for four consecutive cycles [49] and it was observed that the catalytic material could be used on consecutive reductions, although a decrease of the reaction rate and an increase of the activation time after each cycle were observed, due to a stronger competition between hydrogen absorption and catalytic reactions,

after the initial discharge in the first cycle, and to the generation of by-products of the 4-np reduction, which can interfere with the catalyst surface [32].

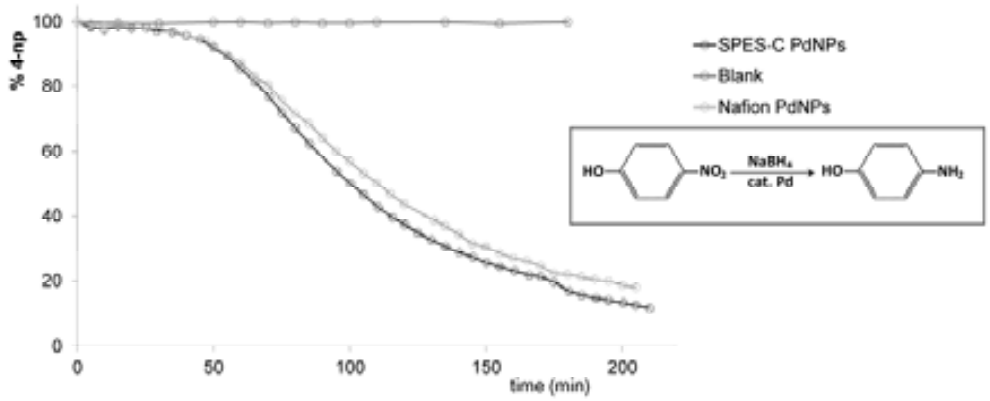

Fig. 11. Catalytic performance of different membrane nanocomposites containing Pd.

Fuel Cells

Fuel cells directly transform the chemical energy of a fuel into electricity by electrochemical reactions and are among the key enabling technologies for the transition to the said hydrogen based economy [80].

Fuel cells are a particular case of catalytic reactors. Among the several types of developed configurations, proton exchange membrane fuel cells (PEMFCs) have been recognized as a potential future power source [81] and are being developed for transport applications as well as for stationary fuel cell applications and portable fuel cell applications. Fig. 12 depicts a PEMFC: hydrogen is adsorbed at the anode (usually with a Pt catalyst), where it dissociates and loses their electrons with the resulting formation of protons, which should pass through a selective membrane under the action of a chemical potential gradient. Conversely, at the cathode, the protons interact with oxygen to produce water molecules.

In such configurations, the PEM has an important role since it should has a good ability to transport protons from anode to cathode compartment and must be able to prevent the transfer of other materials such as substrate or oxygen from anode and cathode chambers.

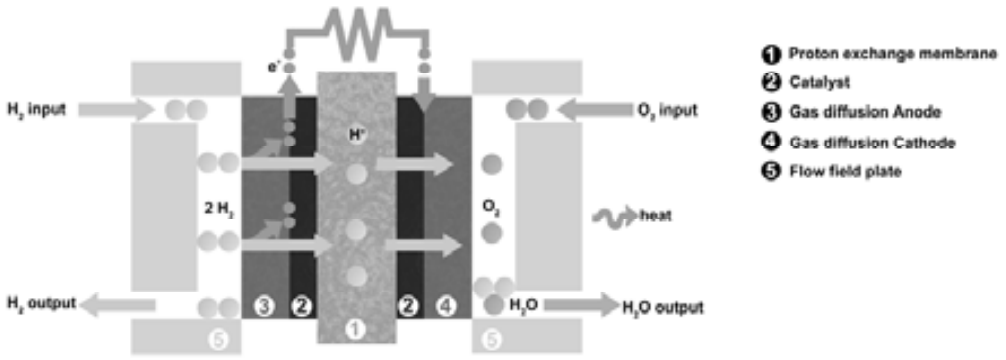

Fig. 12. Scheme of a PEMFC.

Although their promising applications due to their advantages related as a high power density, simplicity of operation, high-energy conversion efficiency and low harmful emissions, several efforts have still to be done in order to create a commercially available PEMFC. For instance, it is imperative to overcome the barrier of high catalyst cost caused by the exclusive use of platinum catalysts in the fuel-cell electrodes [82,83]. Many efforts are

focused on developing alternative oxygen reduction catalysts for the cathode [80,84] the use of MNPs deposited on porous materials in order to increase the specific surface area should lead to obtain an acceptable catalytic performance [85].

Even if Nafion is a common PEM material, several problems still exist and are strongly hindering the commercialization of such devices. Drawbacks as high cost, limited operation temperature, oxygen leakage from cathode to anode, substrate loss, cation transport rather than protons have to be considered. Due to these disadvantages, researchers in the world are working to fabricate a new kind of PEM to overcome these disadvantages and induce better performance than Nafion membrane as well [86]. Under this context, MNPs immobilized in a PEM can improve separation performance by generating preferential permeation paths while they can prevent from permeation of undesired species as well as they can increase thermal, and mechanical properties [87,88].

For example, Rahimnejad et al. [88] propose to take advantage of the unique and promising properties of magnetic Fe_3O_4 nanoparticles Rahimnejad et al. modified polyethersulfone (PES) membranes with different amounts of ferromagnetic MNPs by dissolving the polymer in an appropriate solvent (n-methylpyrrolidone) at 70 ºC with the produced ferric oxide nanoparticles (5 wt%, 10 wt%, 15 wt% and 20 wt% of PES). They compared the efficiency of a microbiological fuel cell (with *Saccharomyces cerevisiae* with glucose) with the modified membranes and with typical commercial Nafion membrane, and found that membrane with 15 wt% Fe_3O_4 nanoparticles produced maximum current and power, and that it was a 29% more amount of power than what had been achieved with Nafion.

Amperometric Sensors and biosensors

A chemical sensor is an analytical device that transforms chemical information into an analytically useful signal. This chemical information may originate from a chemical reaction of the analyte or from a physical property of the system investigated. They can be used for the detection and quantification of both organic and inorganic substances in several fields such as clinical, biomedical and environmental.

The main requirements for a worthy sensor are:

- good sensitivity, selectivity,
- high response speed,
- long-life,
- low consumption of both analyte and power, and
- low cost of massive production for industrial applications

Accordingly, they are often designed to operate under well defined conditions for specified analytes in certain sample types [89].

Some sensors may also include a separator that is, for example, a membrane.

This section is focused on the application of polymer-metal nanocomposites for design of amperometric sensors and biosensors which are based on the application of an external potential leading to the electronic transfer between the working electrode and the species in solution. Since the current passing through an electrochemical cell containing the electroactive species is proportional to the analyte concentration, the measurement of this current allows for the quantitative determination of many analytes at trace levels. For this quantification, the main requirement is that the analyte could be oxidized or reduced electrochemically onto the electrodes surface. However, the main drawback of amperometric sensors is their limited selectivity and a relatively long response time. That is why the modification of amperometric sensors with PSMNPs may provide advantages such as the enhancement of both the rate of mass transfer inside the nanocomposite membrane and the electrocatalytic activity due to the special properties of nanocatalysts in comparison to those of bulk material.

Under this approach, recent publications [90-92] describe the modification of graphite-epoxy composite electrodes (GECE) [93] with Pt- and PdNPs of various types. For such modification, MNPs were first generated by Intermatrix in a SPEEK membrane. Afterwards, solutions of the nanocomposite membrane in an appropriate solvent were prepared in order to obtain a sort of PSMNPs-ink that was drop-by-drop deposited on the surface of GECE. Finally, the solvent was evaporated at room temperature to yield a membrane. These steps are illustrated in Fig. 13.

This general procedure allowed for the manufacture of GECE amperometric sensors modified with core-shell MNPs (Pt@Cu, Pd@Cu, Pt@Co, Pd@Co, Pt@Ni, Pd@Ni, and Pd@CoNi) stabilized in SPEEK membranes, useful for the electrochemical detection of H_2O_2 [163]. The results showed that the sensitivity of sensors toward the analyte under study increased in the following order:

- PSMNPs with ferromagnetic core: Pd@Co > Pd@Ni > Pt@Ni > Pt@Co > Pt@Co-Ni
- PSMNPs with diamagnetic core: Pd@Cu > Pd > Pt@Cu > Pt > Cu

As a main conclusion, it was found that MNPs with Pd shell had the highest sensitivity, what could be explained by the higher catalytic activity of Pd in H_2O_2 decomposition than Pt-PSMNPs under the same experimental conditions.

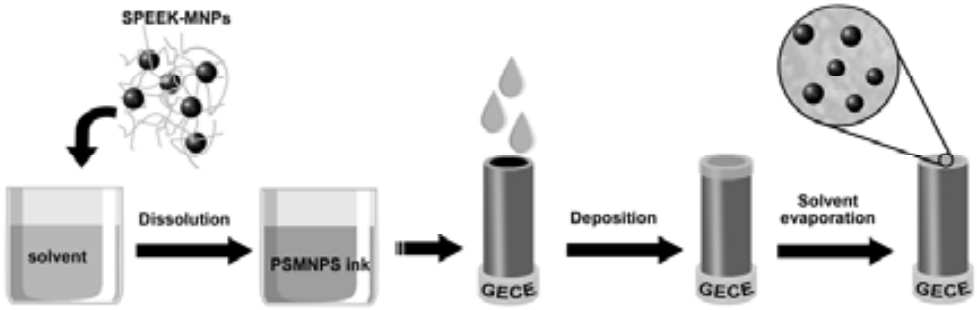

Fig. 13. Scheme of sensor modification by formation of a SPEEK-Pt@Cu-PSMNP nanocomposite.

These PSMNP-based nanocomposites can be also used for the enhancement of the biosensor performance by improving the electron-transfer ion the ampertometric biosensor (i.e. sensors containing enzymes). The introduction of PSMNPs can substantially improve the electron conductivity of the matrix and, therefore enhance the electron transfer from the enzyme molecule to the surface of the electrode [94].

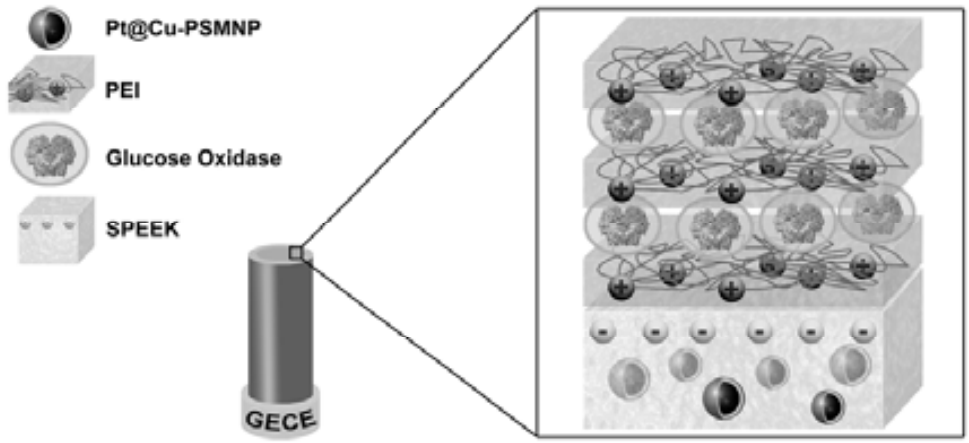

Fig. 14. Supramolecular construction of glucose biosensor based on SPEEK-Pt@Cu-PSMNP nanocomposite adapted from Muraviev et al. [163].

Therefore, in a similar way as the one explained above, glucose biosensors were prepared by using the LBL deposition technique. The GECE modified with SPEEK-Pt@Cu-PSMNPs membrane was sequentially treated with polyethylenimne (PEI) and glucose oxidase solutions. As a consequence, alternate monolayers were created as it is schematically shown in Fig. 14.

In this case, the use of LBL technique made it possible to accumulate a higher amount of the enzyme onto the biosensor membrane, which provided the desired increase of sensitivity. Authors found that the sensitivity of the biosensor strongly depended on the thickness of Pt-shell, similarly to what was revealed previously. It is to say, that the thickness of the catalytically active shell of MNPs could be used as an additional parameter for enhancing the biosensor performance [95].

With this approach, it was proved that MNPs immobilized on the SPEEK membrane surface fulfilled two functions: as mediators, and enhancing the electrical conductivity of the polymer-metal nanocomposite membrane.

CONCLUSION

To conclude, at the end of the last century and remarkably during the current 21st century, the concerns about the limited resources of planet together with the global economical crisis have put scientists in the avant-garde of technological development to look for and find scientific and technological solutions for the current challenges.

This chapter tries to contribute to this idea by giving a general overview of the assorted nanomaterials that can be combined with membranes to yield catalytic membranes of dissimilar nature. Such catalytic membranes might be use in several fields, from water treatment to sensor development, also including hot topics as fuel cells development. Maybe, they can also be useful for many other technical areas where their application has not been envisaged yet. The existing membrane configurations should be understood just as the basis for more complex systems to handle more complex problems.

The different sections of this chapter illustrate the wide-ranging advantages of nanomaterials, particularly metal nanoparticles, as well as they describe the existing fabrication methods able to make the required nanocomposites. In addition, the reasons why immobilizing metal nanoparticles in polymers is a win-win strategy have been presented and the potential synergies of this element combination into a catalytic membrane reactor have been reported.

Specific efforts have been done to properly describe the Intermatrix Synthesis procedure, which, as far as we understand, is one of the best approaches to successfully achieve the incorporation of metal nanoparticles into polymeric matrices (not only those bearing ion-exchange groups).

REFERENCES

1. Rothenberg, G. (2008). Introduction. In Catalysis, Wiley-VCH Verlag GmbH & Co. KGaA, pp 1-38.
2. Meurig Thomas, J., Raja, R. (2005). Designing catalysts for clean technology, green chemistry, and sustainable development. Annu. Rev. Mater. Res., 35, 315-350.
3. Beller, M., Renken, A., van Santen, R.A. (2012). Catalysis. From Principles to Applications. Wiley: Weinheim/DE.
4. Safari, J., Zarnegar, Z. (2013). Ni ion-containing immobilized ionic liquid on magnetic Fe_3O_4 nanoparticles: An effective catalyst for the Heck reaction. C. R. Chim. dx.doi.org/10.1016/j.crci.2013.03.018.
5. Chng, L.L., Erathodiyil, N., Ying, J.Y. (2013). Nanostructured Catalysts for Organic Transformations. Accounts Chem. Res. Article ASAP. DOI: 10.1021/ar300197s.
6. Domènech, B., Bastos-Arrieta, J., Alonso, A., Muñoz, M., Muraviev, D.N. et al. (2012). Bifunctional Polymer-Metal Nanocomposite Ion Exchange Materials. 1 ed.; Iva Lipovic: Reijeka, p 35-72.
7. Astruc, D., Lu, F., Aranzaes, J.R. (2005). Nanoparticles as recyclable catalysts: The frontier between homogeneous and heterogeneous catalysis. Angew. Chem. Int. Ed. 44, 7852-7872.
8. Hassan, M.H.A. (2005). Small Things and Big Changes in the Developing World. Science. 309, 65-66.
9. Schmid, G. (2005). General Introduction. In Nanoparticles, Wiley-VCH Verlag GmbH & Co. KGaA. pp 1-3.
10. Niu, M., Li, T., Xu, R., Gu, X., Yu, D., et al. (2013). Synthesis of PS-g-POSS hybrid graft copolymer by click coupling via ”graft onto” strategy. J. Appl. Polym. Sci. 129, 1833-1844.
11. Weitkamp, J., Weiß, U.; Ernst, S., (1995). New aspects and trends in zeolite catalysis. In Studies in Surface Science and Catalysis, H.K. Beyer, H. G. K. I. K.; Nagy, J. B., Eds. Elsevier: Vol. 94, pp 363-380.
12. Farrusseng, D., Aguado, S., Pinel, C. (2009). Metal-organic frameworks: opportunities for catalysis. Angew. Chem. Int. Ed. 48, 7502-13.
13. Gould, D.M., Griffith, W.P., Spiro, M. (2001). Polyoxometalate catalysis of dye bleaching by hydrogen peroxide. J. Mol. Catal. A-Chem. 175, 289-291.
14. Machado, B.F., Serp, P. (2012). Graphene-based materials for catalysis. Catal. Sci. Technol. 2, 54-75.
15. Wulff, G., Liu, J. (2011). Design of Biomimetic Catalysts by Molecular Imprinting in Synthetic Polymers: The Role of Transition State Stabilization. Accounts Chem. Res. 45, 239-247.
16. Gade, L.H. (2006). Dendrimer Catalysis. Springer: Berlin/DE.
17. Astruc, D. (2008). Transition-metal Nanoparticles in Catalysis: From Historical Background to the State-of-the Art. In Nanoparticles and Catalysis, Wiley-VCH Verlag GmbH & Co. KGaA. pp 1-48.
18. Bradley, J.S. (2007). The Chemistry of Transition Metal Colloids. In Clusters and Colloids, Wiley-VCH Verlag GmbH. pp 459-544.
19. Rampino, L.D., Nord, F.F. (1941). Applicability of palladium synthetic high polymer catalysts. J. Am. Chem. Soc. 63, 3208.
20. Cha, D.Y., Parravano, G. (1968). Catalytic oxygen transfer between CO and CO_2 on TiO_2. J. Catal. 11, 228-237.
21. Sermon, P. (1976). Gold: An uncommonly good catalyst. Gold Bull. 9, 129-131.
22. Hirai, H., Nakao, Y., Toshima, N. (1979). Preparation of Colloidal Transition Metals in Polymers by Reduction with Alcohols or Ethers. J. Macromol. Sci. A. 13, 727-750.

23. Haruta, M., Yamada, N., Kobayashi, T., Iijima, S. (1989). Gold catalysts prepared by coprecipitation for low-temperature oxidation of hydrogen and of carbon monoxide. J. Catal. 115, 301-309.
24. Thomas, J.M. (1988). Colloidal metals: past, present and future. Pure Appl. Chem. 60, 1517-1528.
25. Sanchez Marcano, J.G., Tsotsis, T.T. (2004). Modelling of Membrane Reactors: Catalytic Membrane Reactors. In Catalytic Membranes and Membrane Reactors, Wiley-VCH Verlag GmbH & Co. KGaA. pp 169-200.
26. Lin, Y.S. (2001). Microporous and dense inorganic membranes: current status and prospective. Sep. Purfi. Technol. 25, 39-55.
27. Lu, G.Q., Diniz da Costa, J.C., Duke, M., Giessler, S., Socolow, R., et al. (2007). Inorganic membranes for hydrogen production and purification: A critical review and perspective. J. Colloid. Interf. Sci. 314, 589-603.
28. Koros, W., Ma, Y., Shimidzu, T. (1996). Terminology for membranes and membrane processes (IUPAC Recommendations 1996). J. Membrane Sci. 120, 149-159.
29. Gallucci, F., Basile, A., Hai, F.I. (2011). Introduction – A Review of Membrane Reactors. In Membranes for Membrane Reactors, John Wiley & Sons, Ltd. pp 1-61.
30. Mulder, M. (1996). Basic principles of membrane technology. Kluwer Academic: Dordrecht etc. Vol. 2, p 564.
31. Mota, S., Miachon, S., Volta, J.C., Dalmon, J.A. (2001). Membrane reactor for selective oxidation of butane to maleic anhydride. Catal. Today. 67, 169-176.
32. Macanás, J., Ouyang, L., Bruening, M.L., Muñoz, M., Remigy, J.C., et al. (2010). Development of polymeric hollow fiber membranes containing catalytic metal nanoparticles. Catal. Today. 156, 181-186.
33. Shu, J., Grandjean, B.P.A., Neste, A.V., Kaliaguine, S. (1991). Catalytic palladium-based membrane reactors: A review. Can. J. Chem. Eng. 69, 1036-1060.
34. Adhikari, S., Fernando, S. (2006). Hydrogen Membrane Separation Techniques. Ind. Eng. Chem. Res. 45, 875-881.
35. Saufi, S.M., Ismail, A.F. (2004). Fabrication of carbon membranes for gas separation—a review. Carbon. 42, 241-259.
36. Jones, C.W., Koros, W.J. (1995). Carbon Composite Membranes: A Solution to Adverse Humidity Effects. Ind. Eng. Chem. Res. 34, 164-167.
37. McCaig, M.S., Seo, E.D., Paul, D.R. (1999). Effects of bromine substitution on the physical and gas transport properties of five series of glassy polymers. Polymer. 40, 3367-3382.
38. Hicke, H.-G., Lehmann, I., Malsch, G., Ulbricht, M., Becker, M. (2002). Preparation and characterization of a novel solvent-resistant and autoclavable polymer membrane. J. Membrane Sci. 198, 187-196.
39. Baker, R.W. (2004). Membranes and Modules. In Membrane Technology and Applications, John Wiley & Sons, Ltd. pp 89-160.
40. Buonomenna, M.G., Choi, S.H., Drioli, E. (2010). Catalysis in polymeric membrane reactors: the membrane role. Asia-Pac. J Chem. Eng. 5, 26-34.
41. Vankelecom, I.F.J. (2002). Polymeric membranes in catalytic reactors. Chem. Rev. 102, 3779-3810.
42. Fritsch, D., Randjelovic, I., Keil, F. (2004). Application of a forced-flow catalytic membrane reactor for the dimerisation of isobutene. Catal. Today. 98, 295-308.
43. Rozenberg, B.A., Tenne, R. (2008). Polymer-assisted fabrication of nanoparticles and nanocomposites. Prog. Polym. Sci. 33, 40-112.
44. Nicolais, L., Carotenuto, G. (2004). Metal-Polymer Nanocomposites. John Wiley and Sons Ltd: New York/US.
45. Luckham, P.F. (2004). Manipulating forces between surfaces: applications in colloid science and biophysics. Adv. Colloid Interfac. 111, 29-47.

46. Visser, J. (1981). The concept of negative hamaker coefficients. 1. history and present status. Adv. Colloid Interfac. 15, 157-169.
47. Campelo, J.M., Luna, D., Luque, R., Marinas, J.M., Romero, A.A. (2009). Sustainable Preparation of Supported Metal Nanoparticles and Their Applications in Catalysis. Chemsuschem. 2, 18-45.
48. Kumar, R., Pandey, A.K., Tyagi, A.K., Dey, G.K., Ramagiri, S.V., et al. (2009). In situ formation of stable gold nanoparticles in polymer inclusion membranes. J. Colloid. Interf. Sci. 337, 523-530.
49. Domènech, B., Muñoz, M., Muraviev, D.N., Macanás, J. (2011). Polymer-stabilized palladium nanoparticles for catalytic membranes: ad hoc polymer fabrication. Nanoscale Res. Lett. 6.
50. Ruiz, P., Muñoz, M., Macanás, J., Turta, C., Prodius, D., et al. (2010). Intermatrix synthesis of polymer stabilized inorganic nanocatalyst with maximum accessibility for reactants. Dalton T. 39, 1751-1757.
51. Dotzauer, D.A., Bhattacharjee, S., Wen, Y., Bruening, M.L. (2009) Nanoparticle-Containing Membranes for the Catalytic Reduction of Nitroaromatic Compounds. Langmuir. 25, 1865-1871.
52. Lu, O., Dotzauer, D.M., Hogg, S.R., Macanás, J., Lahitte, J.-F., et al. (2010). Catalytic hollow fiber membranes prepared using layer-by-layer adsorption of polyelectrolytes and metal nanoparticles. Catal. Today. 156, 100-106.
53. Domènech, B.; Muñoz, M.; Muraviev, D.N.; Macanás, J. (2012). Catalytic membranes with palladium nanoparticles: From tailored polymer to catalytic applications. Catal. Today. 193, 158-164.
54. Barau, A., Budarin, V., Caragheorgheopol, A., Luque, R., Macquarrie, D., et al. (2008). A Simple and Efficient Route to Active and Dispersed Silica Supported Palladium Nanoparticles. Catal Lett. 124, 204-214.
55. Luo, M.-L., Zhao, J.-Q., Tang, W.; Pu, C.-S. (2005). Hydrophilic modification of poly(ether sulfone) ultrafiltration membrane surface by self-assembly of TiO2 nanoparticles. App. Surf. Sci. 249, 76-84.
56. Zhang, Y., Erkey, C. (2006). Preparation of supported metallic nanoparticles using supercritical fluids: A review. J. Supercrit. Fluid. 38, 252-267.
57. Haruta, M., Tsubota, S., Kobayashi, T., Kageyama, H., Genet, M.J., et al. (1993). Low-Temperature Oxidation of CO over Gold Supported on TiO_2, α-Fe_2O_3, and Co_3O_4. J. Catal.. 144, 175-192.
58. Iojoiu, E., Walmsley, J., Raeder, H., Bredesen, R., Miachon, S., et al. (2003). Comparison of different support types for the preparation of nanostructured catalytic membranes. RAMS. 5, 160-165.
59. Yang, J., Sun, D., Li, J., Yang, X., Yu, J., et al. (2009). In situ deposition of platinum nanoparticles on bacterial cellulose membranes and evaluation of PEM fuel cell performance. Electrochim. Acta. 54, 6300-6305.
60. Decher, G. (1997). Fuzzy Nanoassemblies: Toward Layered Polymeric Multicomposites. Science. 277, 1232-1237.
61. Schmitt, J., Decher, G., Dressick, W.J., Brandow, S.L., Geer, R.E., et al. (1997). Metal nanoparticle/polymer superlattice films: Fabrication and control of layer structure. Adv. Mat. 9, 61-65.
62. Hicks, J.F. Seok-Shon, Y. Murray, R.W. (2002). Layer-by-Layer Growth of Polymer/Nanoparticle Films Containing Monolayer-Protected Gold Clusters. Langmuir. 18, 2288-2294.
63. Bruening, M.L., Dotzauer, D.M., Jain, P., Ouyang, L., Baker, G.L. (2008). Creation of functional membranes using polyelectrolyte multilayers and polymer brushes. Langmuir. 24, 7663-7673.

64. Sun, Y., Hao, E., Zhang, X., Yang, B., Shen, et al. (1997). Buildup of Composite Films Containing TiO2/PbS Nanoparticles and Polyelectrolytes Based on Electrostatic Interaction. Langmuir. 13, 5168-5174.
65. Mamedov, A., Ostrander, J., Aliev, F., Kotov, N.A. (2000). Stratified Assemblies of Magnetite Nanoparticles and Montmorillonite Prepared by the Layer-by-Layer Assembly. Langmuir. 16, 3941-3949.
66. Smuleac, V., Varma, R., Baruwati, B., Sikdar, S., Bhattacharyya, D. (2011). Nanostructured Membranes for Enzyme Catalysis and Green Synthesis of Nanoparticles. Chemsuschem. 4, 1773-1777.
67. Kidambi, S., Bruening, M.L. (2005). Multilayered polyelectrolyte films containing palladium nanoparticles: Synthesis, characterization, and application in selective hydrogenation. Chem. Mater. 17, 301-307.
68. Lee, D., Gemici, Z., Rubner, M.F., Cohen, R.E. (2007). Multilayers of Oppositely Charged SiO2 Nanoparticles: Effect of Surface Charge on Multilayer Assembly. Langmuir. 23, 8833-8837.
69. Serp, P., Kalck, P., Feurer, R. (2002). Chemical Vapor Deposition Methods for the Controlled Preparation of Supported Catalytic Materials. Chem. Rev. 102, 3085-3128.
70. Xia, W., Schlüter, O.F.K., Liang, C., van den Berg, M.W.E., Guraya, M., et al. (2005). The synthesis of structured Pd/C hydrogenation catalysts by the chemical vapor deposition of Pd(allyl)Cp onto functionalized carbon nanotubes anchored to vapor grown carbon microfibers. Catal. Today. 102–103, 34-39.
71. Ruiz, P., Macanás, J., Muñoz, M., Muraviev, D.N. (2011). Intermatrix synthesis: easy technique permitting preparation of polymer-stabilized nanoparticles with desired composition and structure. Nanoscale Res. Lett. 6, 343.
72. Alonso, A., Macanás, J., Shafir, A., Muñoz, M., Vallribera, A., et al. (2010). Donnan-exclusion-driven distribution of catalytic ferromagnetic nanoparticles synthesized in polymeric fibers. Dalton T. 39, 2579-2586.
73. Progress on Drinking-Water and Sanitation: 2012 Update. UNICEF and World Health Organization: United States of America.
74. Charnley, M., Textor, M., Acikgoz, C. (2011)). Designed polymer structures with antifouling–antimicrobial properties. React. Funct. Polym. 71, 329-334.
75. Zhang, W.-x., Wang, C.-B., Lien, H.-L. (1998). Treatment of chlorinated organic contaminants with nanoscale bimetallic particles. Catal. Today. 40 (4), 387-395.
76. Feng, J., Lim, T.-T. (2005). Pathways and kinetics of carbon tetrachloride and chloroform reductions by nano-scale Fe and Fe/Ni particles: comparison with commercial micro-scale Fe and Zn. Chemosphere. 59, 1267-1277.
77. Wu, L., Ritchie, S.M.C. (2008). Enhanced dechlorination of trichloroethylene by membrane-supported Pd-coated iron nanoparticles. Environ. Prog. 27, 218-224.
78. Venkatachalam, K., Arzuaga, X., Chopra, N., Gavalas, V.G., Xu, J., et al. (2008). Reductive dechlorination of 3,3',4,4'-tetrachlorobiphenyl (PCB77) using palladium or palladium/iron nanoparticles and assessment of the reduction in toxic potency in vascular endothelial cells. J. Hazard. Mater. 159, 483-91.
79. Xu, J., Bhattacharyya, D. (2005). Membrane-based bimetallic nanoparticles for environmental remediation: Synthesis and reactive properties. Environ. Prog. 24, 358-366.
80. Bashyam, R., Zelenay, P. (2006). A class of non-precious metal composite catalysts for fuel cells. Nature. 443, 63-66.
81. Steele, B.C.H., Heinzel, A. (2001). Materials for fuel-cell technologies. Nature. 414, 345-352.
82. Berger, D.J. (1999). Fuel Cells and Precious-Metal Catalysts. Science. 286, 49.
83. Semelsberger, T.A., Borup, R.L. (2005). Fuel effects on start-up energy and efficiency for automotive PEM fuel cell systems. Int. J. Hydrogen Energ. 30, 425-435.

84. Liu, Z., Gan, L.M., Hong, L., Chen, W., Lee, J.Y. (2005). Carbon-supported Pt nanoparticles as catalysts for proton exchange membrane fuel cells. J. Power Sources. 139, 73-78.
85. Bell, A.T. (2003). The Impact of Nanoscience on Heterogeneous Catalysis. Science. 299, 1688-1691.
86. Liu, H., Logan, B.E. (2004). Electricity Generation Using an Air-Cathode Single Chamber Microbial Fuel Cell in the Presence and Absence of a Proton Exchange Membrane. Environ. Sci. Technol. 38, 4040-4046.
87. Taurozzi, J.S., Arul, H., Bosak, V.Z., Burban, A.F., Voice, T.C., et al. (2008). Effect of filler incorporation route on the properties of polysulfone–silver nanocomposite membranes of different porosities. J. Membrane Sci. 325, 58-68.
88. Rahimnejad, M., Ghasemi, M., Najafpour, G.D., Ismail, M., Mohammad, A.W., et al. (2012). Synthesis, characterization and application studies of self-made Fe3O4/PES nanocomposite membranes in microbial fuel cell. Electrochim. Acta. 85, 700-706.
89. Adam, H., Stanisław, G., Folke, I. (1991). Chemical sensors definitions and classification. Pure Appl. Chem. 63, 1274-1250.
90. Muraviev, D.N., Macanás, J., Farre, M., Muñoz, M., Alegret, S. (2006). Novel routes for inter-matrix synthesis and characterization of polymer stabilized metal nanoparticles for molecular recognition devices. Sensor. Actuat. B-Chem. 118, 408-417.
91. Macanás, J., Farre, M., Muñoz, M., Alegret, S., Muraviev, D.N. (2006). Preparation and characterization of polymer-stabilized metal nanoparticles for sensor applications. Phys. Status Solidi A. 203, 1194-1200.
92. Macanás, J., Parrondo, J., Muñoz, M., Alegret, S., Mijangos, F., et al. (2007). Preparation and characterisation of metal-polymer nanocomposite membranes for electrochemical applications. Phys. Status Solidi A. 204, 1699-1705.
93. Céspedes, F., Martínez-Fàbregas, E., Alegret, S. (1996). New materials for electrochemical sensing I. Rigid conducting composites. Trends in Analytical Chemistry. 15, 296-304.
94. Habermüller, K., Mosbach, M., Schuhmann, W. (2000). Electron-transfer mechanisms in amperometric biosensors. Fresenius J. Anal. Chem+. 366, 560-568.
95. Muraviev, D.N., Ruiz, P., Muñoz, M., Macanás, J. (2008). Novel strategies for preparation and characterization of functional polymer-metal nanocomposites for electrochemical applications. Pure Appl. Chem. 80, 2425-2437.

Polymer-Silver Nanocomposites as Antibacterial materials

B. Domènech[1] , **M. Muñoz**[1], **D.N. Muraviev**[1] and **J. Macanás**[2,*]

[1]Analytical Chemistry Division, Department of Chemistry, Universitat Autònoma de Barcelona, UAB, 08193 Bellaterra, Barcelona, Spain

[2]Department of Chemical Engineering, Universitat Politècnica de Catalunya, UPC, C/Colom, 1, 08222 Terrassa, Barcelona, Spain

The antibacterial effect of silver has been used in a variety of commercially available products and medical devices for many years, either in its metallic or salt form. Nowadays, due to the knowledge acquired within the last decade in the field of Nanoscience and Nanotechnology, the use of silver nanoparticles (AgNPs) for medical and sanitary purposes has been thoroughly studied and dramatically increased. One of the major concerns dealing with the use of AgNPs in human health and disinfection is, in fact, its toxicity what dictates the need to use safe strategies for AgNPs applications. Nanocomposites are a good approach since the mobility of the nanoobjects is reduced whereas their activity remains. In this context, the Intermatrix Synthesis technique provides a novel route for both synthesis and immobilisation of AgNPs in commercially available ion-exchange matrices. This chapter reviews the state-of-the-art of the nanotechnological approach in bactericidal application of AgNPs from ancient to modern time focusing on the Intermatrix Synthesis.

Keywords: Nanoparticles; Antibacterial action; Toxicity; Silver; Intermatrix Synthesis

1. Introduction

Silver (Ag) has long been known to exhibit a strong toxicity towards a wide range of microorganisms. Thanks to these broad-spectrum antimicrobial properties, silver has been extensively used for biomedical applications and other environmental disinfection processes for centuries.[1-3] In fact, nowadays it is still used in several commercially-available products such as composites with undergo a slow silver release and which act as preservatives, or products containing silver thiosulfate complexes which are introduced in packaging plastics for long-lasting antibacterial protection of packed products. [3, 4]

Up to now, silver ions (Ag^+) have demonstrated to be useful and efficient for antibacterial purposes,[5] but, due to their unique properties, silver nanoparticles (AgNPs) represent a reasonable alternative for boosting the development of new bactericides. Because of their high surface area to volume ratio and their high active surface (with highly active facets), metal nanoparticles (MNPs) exhibit remarkable and outstanding properties, such as increased catalytic activity. Therefore, AgNPs could be more reactive and become more antimicrobiologically active than the bulk counterpart[6] and, with the rise of the Nanotechnology, a new control on the behaviour of silver metal can be achieved.[7] Applications such in clothing, respirators, household water filters, contraconceptives, antibacterial sprays, cosmetics, detergents, dietary supplements, cutting boards, shoes, cell phones, laptop keyboards, and children's toys are typical products currently in the market that exploit the antimicrobial properties of silver nanomaterials.[8]

But, even if the use of AgNPs seems to open a new window of possibilities in the development of new-age antibacterial agents, some environmental and health safety risks, sometimes referred as nanotoxicity[9-14] must be intensively considered. Accordingly, the use of nanomaterials has come under some scrutiny by both private and public institutions regarding in particular the possible hazards associated with NPs either deliberately or inadvertently produced.[15-21] In this context, it is clear that new and safe strategies for AgNPs applications must be applied. On one hand, since AgNPs toxicity is presumed to be size and shape-dependent[22], controlling these parameters has turned to be a crucial factor during their synthesis. On the other hand, controlling the escape of the nanoparticles to the media, thus, avoiding a possible exposure to the environment, can bring a second security level. Hence, the development of stabilized nanometer sized particles has been intensively pursued within this broad field.[19, 23-25]

The synthesis of MNPs may be carried out through various synthetic routes based either on bottom-up or top-down approaches, which have been summarized in recent publications.[19, 26-30] However, as it has been abovementioned, preventing their escape and controlling both their size and shape is decisive, so the presence of stabilizers is very often required.[31-33] As a result, the development of stabilized polymer-metal nanocomposites containing MNPs is considered to be one of the most promising solutions. The modification of commercially available ion-exchange resins, fibers and films and the development of suitable polymeric membranes with biocidal MNPs have been pursued by scientists and engineers. Under this context, the Intermatrix synthesis (IMS) based on the ion exchange synthesis of MNPs, provides a novel route of synthesis with the main feature of taking advantage of the dual function of the matrix that serves as both the medium for the synthesis of MNPs and as a stabilizer that prevents their uncontrollable growth, aggregation and escape to the media.[34, 35]

2. History of Silver as antibacterial agent

Humans have used silver metal for about 7,000 years in several applications such as the manufacture of jewellery, currency and religious objects, as well as for the fabrication of mirrors or even in photography. [36]
However, one of the most studied applications of silver is, very probably, as antibacterial material.
As soon as in the ancient Greece, Hippocrates (460 BC - 370 BC), the father of the modern Medicine, already wrote that silver had beneficial healing and prophylactic properties. Phoenicians, Persians, Romans and Egyptians also used silver in one or another form to preserve food, wine and water and this was likewise practiced in the XXth century through World War II.[36]

Regarding the use of silver as a biomedical compound it was widely used in hospitals as a bactericide before the appearance of antibiotics. In the early 1800s, surgical wounds were closed with silver sutures, and it also became a common practice to administrate aqueous $AgNO_3$ drops to new-born's eyes in order to treat the transmission of *Neisseria Gonorrhoea* from infected mothers to children.[37] It was also at the end of this century, when some scientists started to systematically study the bactericidal effect of some metals (the so-called *oligodynamic effect*) and, thanks to the great number of studies in the subject, it was later found that among all the metals with antimicrobial properties, silver has the highest effectiveness and the least toxicity to animal cells.[38]
During the 1900s, people used to introduce silver dollars in milk bottles to prolong the freshness of milk; silver compounds were successfully used to prevent infection in World War I together with the use of surgical silver sutures. By 1940 there were approximately fifty different silver compounds on the market being used to treat every known infectious disease in many configurations including shavings, foils, sutures, solutions (e.g., silver nitrate, oxide, bromide, chloride, and iodide) and colloids providing fine particles (introduced in 1924 [38]).
The widespread use of silver went out of fashion with the appearance and spread of modern antibiotics. However, with the discovery of antibiotics, antibiotic-resistant strains also emerged and, therefore, a renewed interest in using silver as an antibacterial agent. For instance, silver sulfadiazine creams have been long used in the widespread treatment of burns to improve skin regeneration; Ag-containing hydrocolloids dressings are nowadays used to treat diabetic foot ulcers due to their regenerative effect; and $AgNO_3$ has also long been used as cauterization agent to stop epistaxis or to stop the growth of post-traumatic granulomas.[7] Even today, at the beginning of the second decade of XXIth century, the broad-spectrum antimicrobial properties of silver encourage its use in biomedical applications, water and air purification, food production, cosmetics, clothing, and numerous household products development.
Besides, with the rise of the Nanotechnology, and as a result of reducing the scale of metals particles, new electrical, optical, magnetic, and chemical properties appear, so a new control on the behaviour of silver metal has been achieved. [30]

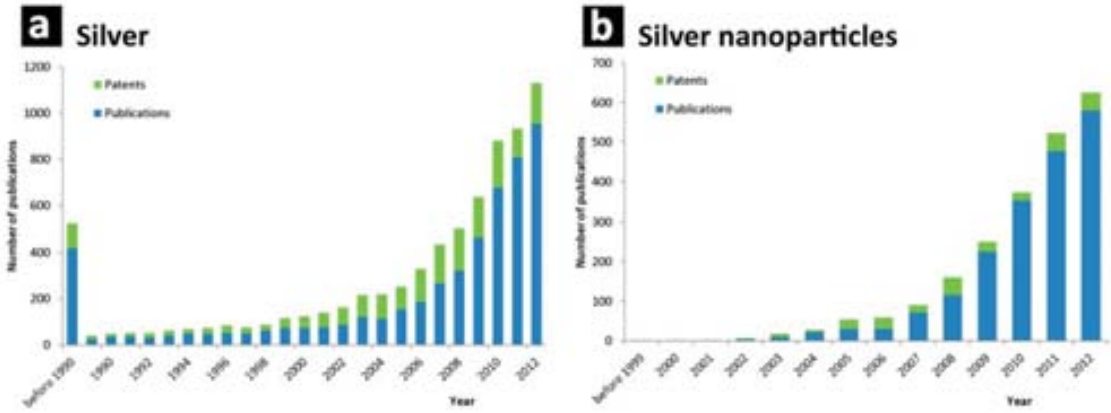

Fig. 1 Evolution of the number of publications in English (books, journal articles, reviews, editorials and patents) containing the words Bactericidal, Biocidal and Antibacterial and (a) Silver; or (b) Silver nanoparticles. Source: Scifinder.

As a result, the use of antibacterial silver nanoparticles (AgNPs) has attracted increasing interest of scientists and technologists during the last decades and their applications have been further extended and now silver is the engineered nanomaterial most commonly used in consumer products.[39] A clear growing trend in the production of both research articles and patents is shown in Figure 1. As it can be seen, this evolution is almost exponential testifying the enormous efforts that are devoted to this topic.

2.1. Current uses of Silver nanoparticles as antibacterial agent

Many different uses of silver are pondered nowadays. As it has been aforesaid, AgNPs are emerging as the next-generation antibacterial agent[11] getting-through antibiotics and disinfectants in coating of house-products or medical

devices. As well, the research in AgNPs applications for medical uses has been extremely active, and the obtained products allow to treat several infections and to design new infection-safe devices. Some of them are summarized in Figure 2.

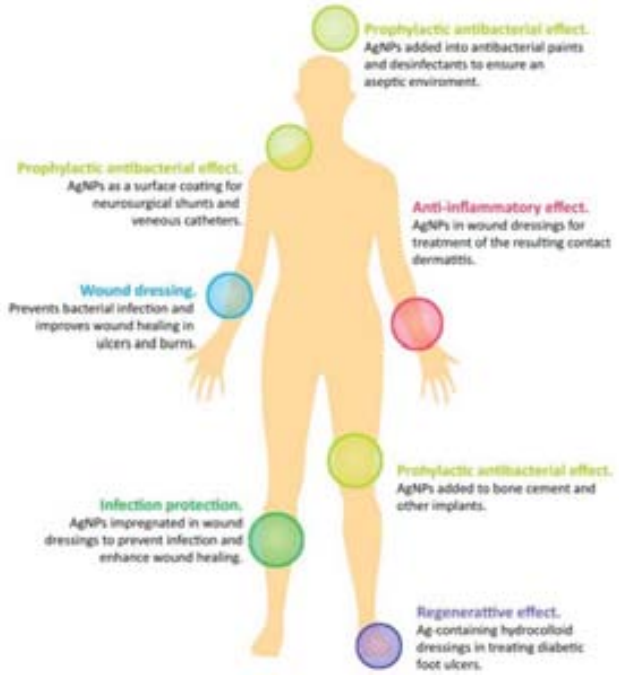

Fig. 2 Some uses of AgNPs in human health.

In this context, there is a wide variety of commercially available products being used clinically (Table 1). For instance, AgNPs-based wound dressings are already commercially available (e.g. Acticoat™)[40]; AgNPs are also used as coatings or additives applied to a variety of catheters such as cardiovascular implants and central venous catheters[41]; they are also added as antibacterial additive to poly(methylmethacrylate) (PMMA) in bone cement[42]; and can also be used in hand gels[43] and paints[44] as a prolonged antibacterial disinfectants.[45]

Table 1 Some commercially available medical products containing AgNPs.

Product	Company	Description	Clinical uses
Acticoat™	Smith & Nephew	AgNPs wound dressing	Prevents bacterial infection and improves wound healing for burns and ulcers.
Silverline®	Spiegelberg	Polyurethane ventricular catheter impregnated with AgNPs.	Neurosurgical drain hydrocephalus, and can also be adapted for use as shunts. Antibacterial AgNPs prevent catheter-associated infections.
SilvaSorb®	Medline Industries and AcryMed	Antibacterial products: hand gels, wound dressings, cavity filler	Wound dressings and cavity filler prevent bacterial infection. Hand gels used to disinfect skin in clinical and personal hygiene purposes.
ON-Q SilverSoaker™	I-Flow Corporation	Corporation AgNPs-coated catheter for drug delivery	Delivery of medication for pain management or for antibiotic treatment.
Actisorb® Plus 25	Systagenix	Dressings with AgNPs adsorbed in Carbon	Prevents bacterial infection and improves wound healing for burns

On the other hand, antimicrobial biocides are also typically added in small quantities in many other applications in order to prevent bacterial growth.[46] A paradigmatic use is the AgNPs combination with organic biocide compounds and inorganic active agents in order to obtain bacteriostatic water filters for household use[47] or for swimming pool algaecides[48], which are everyday more common in the market.[49]

In all of the variety of applications here mentioned, different forms of silver nanomaterials are found, such as metallic silver nanoparticles[50, 51], silver chloride particles[50], silver-impregnated zeolite powders and activated carbon materials[52], dendrimer–silver complexes and composites[53], polymer-silver nanoparticle composites[54], silver-titanium dioxide composite nanopowders[55], and silver nanoparticles coated onto polymers like polyurethane.[56, 57]
Although all of these forms of silver exhibit antimicrobial activity at some extent through the release of silver ions, it has been recently stated that AgNPs exert additional antimicrobial power compared with the bulk or ionic silver.[11]

3. How does antibacterial Silver work?

One may think that this question is irrelevant. Yet, researchers do not completely agree in this question despite the fact that it is well known that Ag^+ ions and Ag-based compounds are toxic to microorganisms, possess strong biocidal effects on at least 12 species of bacteria including multiresistant bacteria (Methicillin-resistant *Staphylococcus aureus*), as well as multidrug-resistant microorganisms (*Pseudomonas aeruginosa*), ampicillin-resistant bacteria (*Eschericha coli* O157: H7) and erythromycin-resistant bacteria (*Streptococcus pyogenes*).[58-60]
Nevertheless, despite the vast number of publications (already shown in Figure 1b) related to the antimicrobial effects of AgNPs, a relatively modest number of them are related to the mechanism by which silver nanomaterials interact with the microorganisms.

3.1. Antimicrobial silver mechanism

As aforesaid, the mechanisms behind the activity of silver on bacteria are not yet fully elucidated, but the three most common mechanisms of toxicity proposed to date are the ones depicted in Figure 3.

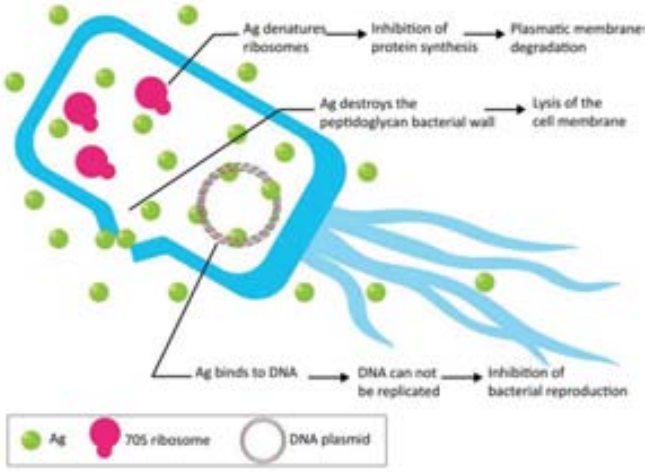

Fig. 3 Mechanisms for the antibacterial activity of silver. Similar images have been published in bibliography.[45, 57, 61]

Generally it is widely accepted that the main antibacterial effect of AgNPs or AgNPs-based materials is due to its partial oxidation and release of silver ions (Ag^+).[62, 63] After this oxidation occurs, the following actions can happen either simultaneously or separately:
(1) uptake of free Ag^+ followed by disruption of ATP production and DNA replication[64] ;
(2) AgNPs and Ag^+ interaction with bacterial proteins, disrupting protein synthesis[65] ;
(3) AgNPs directly damage cell membranes, interacting with the peptidoglycan wall cell and the plasmatic membrane causing cell lysis.[66]

Besides, disregarding the exact mechanism of interaction, several works have stated that AgNPs may increase the cell membrane permeability and, subsequently, penetrate inside cells to induce any one or the entire cascade of effects just described.[50, 67]

Thus, although it is not yet possible to confirm a single mechanism for the antibacterial action of silver, multifaceted antibacterial activity seems to be the key to low bacterial resistance rates observed. The explanation for this low resistance can be understood due to the fact that bacterial mortality does not depends on the presence of one determinate

molecule or chemical compound, what hugely hinders the adaptation of the microorganism, it is to say, avoiding the appearance of resistant strains.

3.2. Why do Silver Nanoparticles work better?

On this point it is necessarily to understand the reasons why nanometric silver has different properties than the ones shown by the bulk counterpart. This requires reviewing and understanding the singular properties of nanopartciles.
The most commonly accepted definition for a nanomaterial is "a material that has a structure in which at least one of its phases has a nanometer size in at least one dimension."[17]
With the decrease in the scale of bulk metals to the nanometric size, new properties do appear:

(i) an increase of the relation surface-volume, what gives to an increase in the total surface area and in the fraction of the species in the surface of the material;
(ii) changes in the electronic structure of the present species in the nanoparticles and in the same nanoparticles;
(iii) changes in the atoms bonding (e.g. interatomic distances) which provide the presence of defects;
(iv) confinement and quantic effects (due to the confinement of the charge carriers in a particle of size comparable to the lengthwave of the electrons).

Such nanomaterials might be found in a great number of conformations, such as porous materials (with particle sizes in the nanometer range), polycrystalline materials (with nanometer-sized crystallites), materials with surface protrusions separated by nanometric distances, or nanometer-sized metallic clusters.[68] Among all of these materials metal nanoparticles (MNPs) have attracted increasing interest of scientists and technologists during the last decade, due to their unique electrical, optical, magnetic, and chemical properties. Thus, ecotoxicology of NPs have been deeply studied, [58, 69] and it has been proved that their bactericide and toxic properties are highly correlated with their intrinsic properties, such the ones shown in Table 2.

Table 2 Toxicological effects due to physicochemical properties of nanomaterials.

Physicochemical properties	**Toxicological findings**
Size	Affects reactivity and permeability of cells and organs
Surface /volume ratio	Higher reactivity
Aggregation state	More pronounced cytotoxic effects
Surface Charge	Charged NPs present higher deposition degree

As a conclusion, AgNPs are therefore more reactive with its increased catalytic properties and become more antimicrobiologically active than the bulk counterpart. What is more, AgNPs are even more attractive because they are non-toxic to the human body at low concentrations and have a broader antibacterial action.[70]
Since particle size and distribution are the most important characteristics of nanoparticle systems, and taking into account that they determine the *in vivo* distribution, the biological fate and the toxicity,[71] it is a crucial issue to search for an accurate synthesis route that allows us controlling the aforementioned parameters.
Moreover it is also important to consider that the wide application of engineered NPs, their entry into the environment, and the study of their impact on the ecosystem are a growing concern in society because of the possible adverse effects.[16, 72, 73] Therefore, it is required to study their release, uptake, and mode of toxicity in the organisms. Furthermore, it is imperative to develop nanomaterials in which a controllable escape to the media could be acquired.

4. Synthesis of Silver nanoparticles

With the currently available technology, there are several synthetic routes for AgNPs preparation including electrochemical methods[74]: vapour deposition methods[75] and some miscellaneous procedures which include, for instance, the decomposition of organometallic precursors[76] or the reduction of metal salts in the presence of suitable (monomeric or polymeric) stabilizers.[77]

For some of the chemical methods, the presence of stabilizers is very often required to prevent the agglomeration of nanoclusters by providing a steric and/or electrostatic barrier between particles.[25] Moreover, in some cases, stabilizers might play a crucial role in controlling both the size and shape, and the final distribution of nanoparticles. In this sense, the development of polymer-metal nanocomposites containing MNPs is considered to be one of the most promising solutions to their inherent stability problem[25], and the incorporation of MNPs (including AgNPs) into polymeric matrices has drawn a great deal of attention within the last decade as the resulting materials show unusual and valuable properties in many practical applications.

Polymer-metal nanocomposites can be prepared by two different approaches, namely, *in-situ*[78] and *ex-situ*[28] techniques. By the *in-situ* approach, MNPs can be directly generated inside a polymer matrix by decomposition (e.g., thermolysis, photolysis, radiolysis, etc.) or by chemical reduction of a metallic precursor, conversely, by the *ex-situ* approach; NPs are first produced by soft-chemistry routes and then dispersed into polymeric matrices.

Up to now, *in-sit*u approaches have allowed the preparation of a variety of metal–polymer nanocomposites with highly controllable particle size, material morphology and other properties, thus are currently the focus of much attention and applications.[48] Among all of them, the Intermatrix Synthesis (IMS) approach provides a novel route of synthesis, allowing us to obtain a controlled location of MNPs near the surface of the polymer what substantially enhances their biocidal efficiency, avoid the NPs aggregation and control both, the size of the shape of the final MNPs.[34] The main advantages of this method are explained in detail in the following section.

4.1. Intermatrix Synthesis

The Intermatrix Synthesis (IMS) can be defined as a host-guest synthetic method that takes advantage of the ion exchange properties of some polymeric matrices. In this case, the binding of the ionic prrecursors to the functional groups available in the matrix can be understood as the first synthetic step. Afterwards, the immobilized ions undergo a chemical reaction (either a reduction, or an oxidation or either a precipitation) which yields to small non-aggregated nanoparticles.[35] Accordingly, the dual function of the matrix allows the stabilization of the MNPs to prevent their uncontrollable growth, escape and aggregation while providing a medium for the synthesis.

In a close regard, the general features of the IMS, valid for any kind of polymer matrix and any type of nanoparticle, are:

1.*the nanoreactor effect*: the confinement of the particles by the polymer molecules which allows limiting the size and particle size distribution; and,

2.*the barrier effect*: the polymer molecules locally isolate the formation of each single NP preventing the contact between the surfaces of neighbour particles and therefore avoiding their fusion.

These guidelines are only achievable if NPs precursors can be properly immobilized in the polymeric matrix. So, ion exchange matrices are the perfect template to retain ionic species, regardless if they are metal cations, anions or any kind of coordination compound.

To clarify this approach, Figure 4 illustrates how an anion charged group represented as $–X^-$ (e.g. sulfonic group, SO_3^-) can efficiently interact with a metal cation such as Ag^+ that then undergoes a chemical reduction which finally yields to the formation of the AgNP.

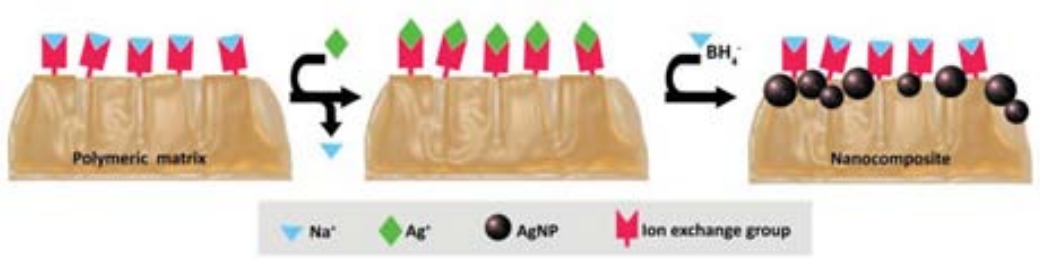

Fig. 4 MNPs preparation inside a polymeric ion-exchange matrix by IMS. Triangles represent the Na^+ ions, diamonds the Ag^+ ions and black spheres represent the AgNPs obtained after the reduction.

This procedure can be described by the following equations:

$$R\text{-}X^-Na^+ + Ag^+ \leftrightarrow R\text{-}X^-Ag^+ + Na^+ \quad (1)$$

$$R\text{-}X^-Ag^+ + NaBH_4 + 3H_2O \rightarrow R\text{-}X^-Na^+ + 7/2H_2 + B(OH)_3 + Ag^0 \quad (2)$$

As it can be seen, for this particular procedure there are always two species bearing the same charge: the functional groups of the matrix and the reducing agent (BH_4^-). This implying an electrostatic repulsion that impedes the penetration of the reducing agent inside the polymeric matrix, known as Donnan-exclusion effect[79]. As a result, ion penetration inside the matrix is balanced by the sum of two driving forces acting in opposite directions: the gradient of the ion concentration and the Donnan-effect itself. This fact forces the formation of the AgNPs mainly on the surface of the polymer matrix, making the final nanocomposite suitable for contact applications, as the ones mentioned above.[29] (Figure 5)

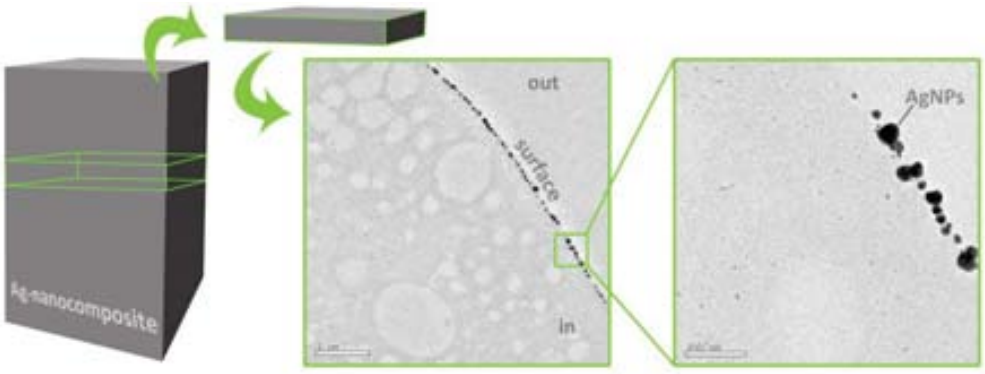

Fig. 5 Scheme of a Transmission Electron Microscopy image of a thin slice of a polymeric membrane (made of sulfonated polyethersulfone with cardo group) containg AgNPs nearly to the surface.

5. Example of application

By the IMS procedure, different nanocomposite materials with AgNPs have been obtained in fibers[80], polymeric resins, polymeric membranes[81, 82] and textile fibers, and that can be finally applied as disinfectants in several number of experimental configurations.

These disinfection applications are indeed of the greatest importance. In many countries the microbial contamination of potable water sources poses a major threat to public health and the emergence of microorganisms resistant to multiple antimicrobial agents increases the demand for improved disinfection methods. The importance of potable water for people in some countries dictates the need for the development of innovative technologies and materials. This type of application can be a perfect niche for nanomaterials containing AgNPs. It is worthy to note here that ion-exchange materials are already widely used for various water treatment processes, mainly to eliminate undesired or toxic ionic impurities including hardness ions, iron, heavy metals, and others. The main problem of such materials used in water treatment is that they are often affected by the contamination of bacteria, fungi and algae that grow up in their surface. In Figure 6 it is observed the growing of fungi and bacteria in one ion exchange resin bead after their use in a conventional domestic tap water treatment filter usually used for the removal of undesired metal ions (hardness ions, iron, heavy metal, etc.).

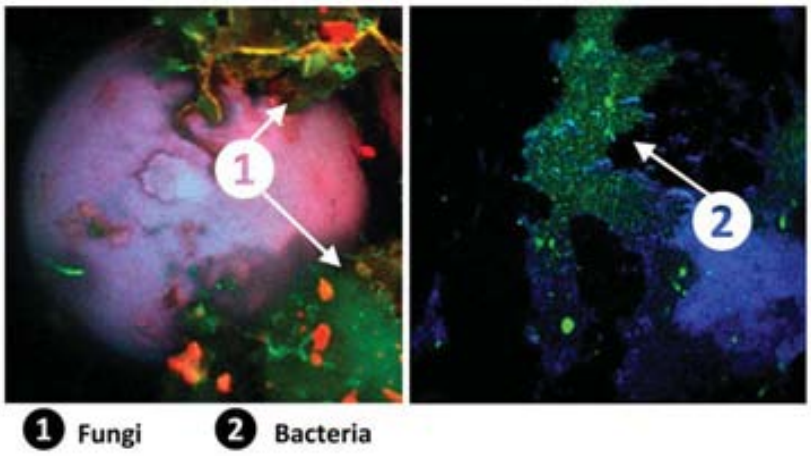

Fig. 6 Confocal microscope image of surface of carboxylic ion exchange resin after being used for the domestic water treatment.

The stabilization and immobilization of AgNPs in such matrices is thus a promising approach since two complementary water treatment processes could be performed with a single material while safety of the nanocomposites could be increased.[35]

That is why in our research group, the surface modification of ion-exchange materials used for traditional water treatment has been undertaken. As an example of the obtained results, Figure 7 shows the variation of cell viability

during time of *Escherichia coli* suspensions in contact with a membrane nanocomposite (with AgNPs) or with the same membrane without AgNPs.

To determinate the bactericidal properties of the as-prepared nanocomposites and the bare matrix, a sample of 1cm^2 of each material was immersed in 20 mL of bacterial suspension and maintained at 37°C with gentle agitation (300 rpm). Periodically, 100 µL of each suspension were collected at different times and counted using plating and incubation in petri dishes containing LB medium.

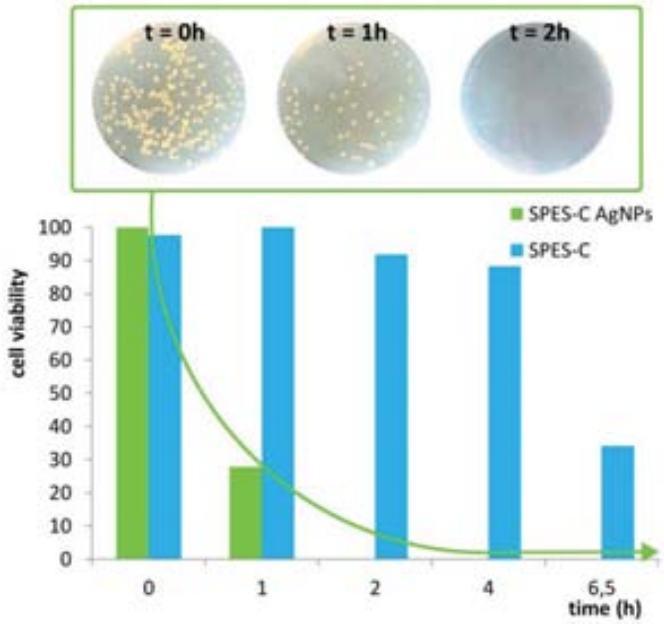

Fig. 7 Bactericidal activity of a SPES-C with AgNPs sample (in green) and of the MNPs-free polymer (in blue).

As it can be seen, the nanocomposite membrane is able to kill the 100% of bacteria in about 2 h, whereas for the unmodified polymer (without AgNPs), the cell viability remains almost constant during the first 4h. After this time, because of the lack of nutrients in the media, the cell viability decay a little, exactly at the same extent than for pure *Escherichia coli* suspensions.

6. What is next?

As it has been reported here, among the currently known nanomaterials, it is well-known that AgNPs have unique antimicrobial properties. Even if Ag has been known to be a bactericidal element for at least 1200 years, considering the unusual properties of nanometric scale materials (largely different from those of their bulk counterparts), it is not surprising that AgNPs have been found significantly more efficient than Ag^+ ions in mediating their antimicrobial activities. Textiles, keyboards, wound dressings, and biomedical devices now contain AgNPs that continuously release a low level of Ag ions to provide protection against bacteria.

All in all, the full potential of this technology has yet to be fully exploited, since the mechanisms underlying the biological properties of AgNPs are not still understood. Once the mechanisms of AgNPs release to the environment would have been completely mastered, it is to say, that the engineered NPs could not uncontrollably reach either water effluents or living beings, the use of Ag-containing nanomaterials will experience a breakthrough advance.

Taking into account the antimicrobial power of the Ag-nanocomposites, it is not unimaginable that these materials could be used in the near future for the development of artificial organs, engineered tissues or medical instruments.
In our humble opinion, the application of AgNPs is far to have reached its maximal potential in the environmental, medical or chemical fields.

Acknowledgements: We are sincerely grateful to all the authors cited throughout the text for making this publication possible. Part of this work was supported by Research Grant MAT2006-03745, 2006–2009 from the Ministry of Science and Technology of Spain. We also thank ACC1Ó for VALTEC 09-02-0057 Grant within "Programa Operatiu de Catalunya" (FEDER). A. Alonso and Servei de Microscopia de la UAB are acknowledged for providing confocal images. N. Vigués and J. Mas are acknowledged for their collaboration in the bactericidal activity experiments.

References

[1] Liau, S. Y.; Read, D. C.; Pugh, W. J.; Furr, J. R.; Russell, A. D., Interaction of silver nitrate with readily identifiable groups: relationship to the antibacterialaction of silver ions. *Letters in Applied Microbiology* 1997, *25* (4), 279-283.

[2] Nomiya, K.; Yoshizawa, A.; Tsukagoshi, K.; Kasuga, N. C.; Hirakawa, S.; Watanabe, J., Synthesis and structural characterization of silver(I), aluminium(III) and cobalt(II) complexes with 4-isopropyltropolone (hinokitiol) showing noteworthy biological activities. Action of silver(I)-oxygen bonding complexes on the antimicrobial activities. *Journal of Inorganic Biochemistry* 2004, *98* (1), 46-60.

[3] Gupta, A.; Silver, S., Molecular Genetics: Silver as a biocide: Will resistance become a problem? *Nat Biotech* 1998, *16* (10), 888-888.

[4] Jose Ruben, M.; Jose Luis, E.; Alejandra, C.; Katherine, H.; Juan, B. K.; Jose Tapia, R.; Miguel Jose, Y., The bactericidal effect of silver nanoparticles. *Nanotechnology* 2005, *16* (10), 2346.

[5] Brown, M. R. W.; Anderson, R. A., The bactericidal effect of silver ions on Pseudomonas aeruginosa. *Journal of Pharmacy and Pharmacology* 1968, *20* (S1), 1S-3S.

[6] Zodrow, K.; Brunet, L.; Mahendra, S.; Li, D.; Zhang, A.; Li, Q.; Alvarez, P. J. J., Polysulfone ultrafiltration membranes impregnated with silver nanoparticles show improved biofouling resistance and virus removal. *Water Research* 2009, *43* (3), 715-723.

[7] Chaloupka, K.; Malam, Y.; Seifalian, A. M., Nanosilver as a new generation of nanoproduct in biomedical applications. *Trends in biotechnology* 2010, *28* (11), 580-588.

[8] Marambio-Jones, C.; Hoek, E., A review of the antibacterial effects of silver nanomaterials and potential implications for human health and the environment. *J. Nanopart. Res.* 2010, *12* (5), 1531-1551.

[9] Bernard, B. K.; Osheroff, M. R.; Hofman, A.; Mennear, J. H., Toxicology and carcinogenesis studies of dietary titanium dioxide-coated mica in male and female Fischer 344 rats. *Journal of Toxicology and Environmental Health* 1989, *28* (4), 415-426.

[10] Borm, P. J. A.; Berube, D., A tale of opportunities, uncertainties, and risks. *Nano Today* 2008, *3* (1–2), 56-59.

[11] .Chen, X.; Schluesener, H. J., Nanosilver: a nanoproduct in medical application. *Toxicol Lett* 2008, *176* (1), 1-12.

[12] Chen, J. L.; Fayerweather, W. E., Epidemiologic study of workers exposed to titanium dioxide. *Journal of Occupational and Environmental Medicine* 1988, *30* (12), 937-942.

[13] Li, Q.; Mahendra, S.; Lyon, D. Y.; Brunet, L.; Liga, M. V.; Li, D.; Alvarez, P. J. J., Antimicrobial nanomaterials for water disinfection and microbial control: Potential applications and implications. *Water Research* 2008, *42* (18), 4591-4602.

[14] Hansen, S. F.; Baun, A., When enough is enough. *Nat Nano* 2012, *7* (7), 409-411.

[15] Levard, C.; Hotze, E. M.; Lowry, G. V.; Brown, G. E., Environmental Transformations of Silver Nanoparticles: Impact on Stability and Toxicity. *Environmental Science & Technology* 2012, *46* (13), 6900-6914.

[16] Abbott, L. C.; Maynard, A. D., Exposure Assessment Approaches for Engineered Nanomaterials. *Risk Analysis* 2010, *30* (11), 1634-1644.

[17] Hassan, M. H. A., Small Things and Big Changes in the Developing World. *Science* 2005, *309* (5731), 65-66.

[18] Ju-Nam, Y.; Lead, J. R., Manufactured nanoparticles: An overview of their chemistry, interactions and potential environmental implications. *Science of the Total Environment* 2008, *400* (1–3), 396-414.

[19] *Nanoscale Materials in Chemistry*. John Wiley and Sons Ltd: Chicester, GB, 2004.

[20] Maynard, A. D., Nanotechnology: The Next Big Thing, or Much Ado about Nothing? *Annals of Occupational Hygiene* 2007, *51* (1), 1-12.

[21] Theron, J.; Walker, J. A.; Cloete, T. E., Nanotechnology and water treatment: Applications and emerging opportunities. *CRC Cr. Rev. Microbiol.* 2008, *34* (1), 43-69.

[22] Pal, S.; Tak, Y. K.; Song, J. M., Does the Antibacterial Activity of Silver Nanoparticles Depend on the Shape of the Nanoparticle? A Study of the Gram-Negative Bacterium Escherichia coli. *Applied and environmental microbiology* 2007, *73* (6), 1712-1720.

[23] *Metal-Polymer Nanocomposites*. John Wiley and Sons Ltd: New York/US, 2004.

[24] Pomogailo, A. D.; Kestel'man, V. N., *Metallopolymer nanocomposites*. Springer-Verlag Berlin and Heidelberg GmbH & Co. KG: Berlin/DE, 2005.

[25] Rozenberg, B. A.; Tenne, R., Polymer-assisted fabrication of nanoparticles and nanocomposites. *Progress in Polymer Science* 2008, *33* (1), 40-112.

[26] Ajayan, P. M., Bulk Metal and Ceramics Nanocomposites. In *Nanocomposite Science and Technology*, Wiley-VCH Verlag GmbH & Co. KGaA: 2004; pp 1-75.

[27] *Springer Handbook of Nanotechnology*. Springer-Verlag Berlin and Heidelberg GmbH & Co. KG: Berlin/DE, 2004.

[28] Campelo, J. M.; Luna, D.; Luque, R.; Marinas, J. M.; Romero, A. A., Sustainable Preparation of Supported Metal Nanoparticles and Their Applications in Catalysis. *Chemsuschem* 2009, *2* (1), 18-45.

[29] Macanás, J.; Ruiz, P.; Alonso, A.; Muñoz, M.; Muraviev, D. N., Ion Exchange-Assisted Synthesis of Polymer Stabilized Metal Nanoparticles. In *Ion Exchange and Solvent Extraction*, Sengupta, A. K., Ed. CRC Press: 2011; pp 1-44.

[30] Schmid, G., General Introduction. In *Nanoparticles*, Wiley-VCH Verlag GmbH & Co. KGaA: 2005; pp 1-3.

[31] Houk, L. R.; Challa, S. R.; Grayson, B.; Fanson, P.; Datye, A. K., The Definition of "Critical Radius" for a Collection of Nanoparticles Undergoing Ostwald Ripening. *Langmuir* 2009, *25* (19), 11225-11227.

[32] Imre, Á.; Beke, D. L.; Gontier-Moya, E.; Szabó, I. A.; Gillet, E., Surface Ostwald ripening of Pd nanoparticles on the MgO (100) surface. *Appl Phys A* 2000, *71* (1), 19-22.

[33] Kidambi, S.; Bruening, M. L., Multilayered polyelectrolyte films containing palladium nanoparticles: Synthesis, characterization, and application in selective hydrogenation. *Chem. Mater.* 2005, *17* (2), 301-307.

[34] Muraviev, D. N.; Macanas, J.; Farre, M.; Munoz, M.; Alegret, S., Novel routes for inter-matrix synthesis and characterization of polymer stabilized metal nanoparticles for molecular recognition devices. *Sensor. Actuat. B-Chem.* 2006, *118* (1-2), 408-417.
[35] Domènech, B.; Bastos-Arrieta, J.; Alonso, A.; Muñoz, M.; Muraviev, D. N.; Macanás, J., *Bifunctional Polymer-Metal Nanocomposite Ion Exchange Materials" Ion Exchange technologies*. 1 ed.; Iva Lipovic: Reijeka, 2012; p 35-72.
[36] Chernousova, S.; Epple, M., Silver as Antibacterial Agent: Ion, Nanoparticle, and Metal. *Angewandte Chemie International Edition* 2013, *52* (6), 1636-1653.
[37] Silvestry-Rodriguez, N.; Sicairos-Ruelas, E. E.; Gerba, C. P.; Bright, K. R., Silver as a disinfectant. *Rev Environ Contam Toxicol* 2007, *191*, 23-45.
[38] Alexander, J. W., History of the medical use of silver. *Surg Infect* 2009, *10* (3), 289-92.
[39] Lem, K. W.; Choudhury, A.; Lakhani, A. A.; Kuyate, P.; Haw, J. R.; Lee, D. S.; Iqbal, Z.; Brumlik, C. J., Use of nanosilver in consumer products. *Recent Pat Nanotechnol* 2012, *6* (1), 60-72.
[40] Gravante, G.; Caruso, R.; Sorge, R.; Nicoli, F.; Gentile, P.; Cervelli, V., Nanocrystalline silver: a systematic review of randomized trials conducted on burned patients and an evidence-based assessment of potential advantages over older silver formulations. *Ann Plast Surg* 2009, *63* (2), 201-5.
[41] .Samuel, U.; Guggenbichler, J. P., Prevention of catheter-related infections: the potential of a new nano-silver impregnated catheter. *Int J Antimicrob Agents* 2004, *23* (1), S75-8.
[42] Alt, V.; Bechert, T.; Steinrucke, P.; Wagener, M.; Seidel, P.; Dingeldein, E.; Domann, E.; Schnettler, R., An in vitro assessment of the antibacterial properties and cytotoxicity of nanoparticulate silver bone cement. *Biomaterials* 2004, *25* (18), 4383-91.
[43] Jain, J.; Arora, S.; Rajwade, J. M.; Omray, P.; Khandelwal, S.; Paknikar, K. M., Silver nanoparticles in therapeutics: development of an antimicrobial gel formulation for topical use. *Mol Pharm* 2009, *6* (5), 1388-401.
[44] Kumar, A.; Vemula, P. K.; Ajayan, P. M.; John, G., Silver-nanoparticle-embedded antimicrobial paints based on vegetable oil. *Nat Mater* 2008, *7* (3), 236-241.
[45] Chaloupka, K.; Malam, Y.; Seifalian, A. M., Nanosilver as a new generation of nanoproduct in biomedical applications. *Trends Biotechnol.* 2010, *28* (Copyright (C) 2013 American Chemical Society (ACS). All Rights Reserved.), 580-588.
[46] Dallas, P.; Sharma, V. K.; Zboril, R., Silver polymeric nanocomposites as advanced antimicrobial agents: Classification, synthetic paths, applications, and perspectives. *Adv. Colloid Interfac.* 2011, *166* (1–2), 119-135.
[47] Sharma, V. K.; Yngard, R. A.; Lin, Y., Silver nanoparticles: Green synthesis and their antimicrobial activities. *Adv. Colloid Interface Sci.* 2009, *145* (Copyright (C) 2013 American Chemical Society (ACS). All Rights Reserved.), 83-96.
[48] Vestal, C. R.; Zhang, Z. J., Effects of surface coordination chemistry on the magnetic properties of MnFe(2)O(4) spinel ferrite nanoparticles. *J Am Chem Soc* 2003, *125* (32), 9828-33.
[49] Nowack, B.; Krug, H. F.; Height, M., 120 Years of Nanosilver History: Implications for Policy Makers. *Environmental Science & Technology* 2011, *45* (4), 1177-1183.
[50] Choi, O.; Deng, K. K.; Kim, N.-J.; Ross Jr, L.; Surampalli, R. Y.; Hu, Z., The inhibitory effects of silver nanoparticles, silver ions, and silver chloride colloids on microbial growth. *Water Research* 2008, *42* (12), 3066-3074.
[51] Chi, Z.; Liu, R.; Zhao, L.; Qin, P.; Pan, X.; Sun, F.; Hao, X., A new strategy to probe the genotoxicity of silver nanoparticles combined with cetylpyridine bromide. *Spectrochimica Acta Part A: Molecular and Biomolecular Spectroscopy* 2009, *72* (3), 577-581.
[52] Cowan, M.; Abshire, K.; Houk, S.; Evans, S., Antimicrobial efficacy of a silver-zeolite matrix coating on stainless steel. *J IND MICROBIOL BIOTECHNOL* 2003, *30* (2), 102-106.
[53] Zhang, Y.; Peng, H.; Huang, W.; Zhou, Y.; Zhang, X.; Yan, D., Hyperbranched Poly(amidoamine) as the Stabilizer and Reductant To Prepare Colloid Silver Nanoparticles in Situ and Their Antibacterial Activity. *The Journal of Physical Chemistry C* 2008, *112* (7), 2330-2336.
[54] Bajpai, S. K.; Mohan, Y. M.; Bajpai, M.; Tankhiwale, R.; Thomas, V., Synthesis of polymer stabilized silver and gold nanostructures. *J Nanosci Nanotechnol* 2007, *7* (9), 2994-3010.
[55] Xiong, Z.; Ma, J.; Ng, W. J.; Waite, T. D.; Zhao, X. S., Silver-modified mesoporous TiO2 photocatalyst for water purification. *Water Research* 2011, *45* (5), 2095-2103.
[56] Jain, P.; Pradeep, T., Potential of silver nanoparticle-coated polyurethane foam as an antibacterial water filter. *Biotechnology and Bioengineering* 2005, *90* (1), 59-63.
[57] Marambio-Jones, C.; Hoek, E. M. V., A review of the antibacterial effects of silver nanomaterials and potential implications for human health and the environment. *J. Nanopart. Res.* 2010, *12* (Copyright (C) 2013 American Chemical Society (ACS). All Rights Reserved.), 1531-1551.
[58] Lara, H. H.; Garza-Trevino, E. N.; Ixtepan-Turrent, L.; Singh, D. K., Silver nanoparticles are broad-spectrum bactericidal and virucidal compounds. *J. Nanobiotechnol.* 2011, *9* (Copyright (C) 2013 American Chemical Society (ACS). All Rights Reserved.), 30.
[59] Shahverdi, A. R.; Fakhimi, A.; Shahverdi, H. R.; Minaian, S., Synthesis and effect of silver nanoparticles on the antibacterial activity of different antibiotics against Staphylococcus aureus and Escherichia coli. *Nanomedicine* 2007, *3* (2), 168-71.
[60] Sondi, I.; Salopek-Sondi, B., Silver nanoparticles as antimicrobial agent: a case study on< i> E. coli</i> as a model for Gram-negative bacteria. *J. Colloid. Interf. Sci.* 2004, *275* (1), 177-182.
[61] Damm, C.; Münstedt, H., Kinetic aspects of the silver ion release from antimicrobial polyamide/silver nanocomposites. *Appl Phys A* 2008, *91* (3), 479-486.
[62] Morones, J. R.; Elechiguerra, J. L.; Camacho, A.; Holt, K.; Kouri, J. B.; Ramírez, J. T.; Yacaman, M. J., The bactericidal effect of silver nanoparticles. *Nanotechnology* 2005, *16* (10), 2346-2353.
[63] Hwang, E. T.; Lee, J. H.; Chae, Y. J.; Kim, Y. S.; Kim, B. C.; Sang, B.-I.; Gu, M. B., Analysis of the Toxic Mode of Action of Silver Nanoparticles Using Stress-Specific Bioluminescent Bacteria. *small* 2008, *4* (6), 746-750.

[64] Yang, H.-L.; Lin, J. C.-T.; Huang, C., Application of nanosilver surface modification to RO membrane and spacer for mitigating biofouling in seawater desalination. *Water Research* 2009, *43* (15), 3777-3786.
[65] Siddhartha, S.; Tanmay, B.; Arnab, R.; Gajendra, S.; Ramachandrarao, P.; Debabrata, D., Characterization of enhanced antibacterial effects of novel silver nanoparticles. *Nanotechnology* 2007, *18* (22), 225103.
[66] Jung, W. K.; Koo, H. C.; Kim, K. W.; Shin, S.; Kim, S. H.; Park, Y. H., Antibacterial activity and mechanism of action of the silver ion in Staphylococcus aureus and Escherichia coli. *Appl Environ Microbiol* 2008, *74* (7), 2171-8.
[67] Lok, C. N.; Ho, C. M.; Chen, R.; He, Q. Y.; Yu, W. Y.; Sun, H.; Tam, P. K.; Chiu, J. F.; Che, C. M., Proteomic analysis of the mode of antibacterial action of silver nanoparticles. *J Proteome Res* 2006, *5* (4), 916-24.
[68] Mirkin, C. A., The beginning of a small revolution. *small* 2005, *1* (1), 14-16.
[69] Seil, J. T.; Webster, T. J., Antimicrobial applications of nanotechnology: methods and literature. *Int. J. Nanomed.* 2012, *7* (Copyright (C) 2013 American Chemical Society (ACS). All Rights Reserved.), 2767-2781.
[70] Baker, C.; Pradhan, A.; Pakstis, L.; Pochan Darrin, J.; Shah, S. I., Synthesis and Antibacterial Properties of Silver Nanoparticles. *Journal of Nanoscience and Nanotechnology* 2005, *5* (2), 244-249.
[71] Panyam, J.; Labhasetwar, V., Biodegradable nanoparticles for drug and gene delivery to cells and tissue. *Adv Drug Deliv Rev* 2003, *55* (3), 329-47.
[72] Tiede, K.; Hassellöv, M.; Breitbarth, E.; Chaudhry, Q.; Boxall, A., Considerations for environmental fate and ecotoxicity testing to support environmental risk assessments for engineered nanoparticles. *Journal of Chromatography A* 2009, *1216* (3), 503-509.
[73] Simonet, B. M.; Valcárcel, M., Monitoring nanoparticles in the environment. *Analytical and bioanalytical chemistry* 2009, *393* (1), 17-21.
[74] Hirsch, T.; Zharnikov, M.; Shaporenko, A.; Stahl, J.; Weiss, D.; Wolfbeis, O. S.; Mirsky, V. M., Size-Controlled Electrochemical Synthesis of Metal Nanoparticles on Monomolecular Templates. *Angewandte Chemie International Edition* 2005, *44* (41), 6775-6778.
[75] Murakami, T. N.; Kijitori, Y.; Kawashima, N.; Miyasaka, T., Low temperature preparation of mesoporous TiO2 films for efficient dye-sensitized photoelectrode by chemical vapor deposition combined with UV light irradiation. *Journal of Photochemistry and Photobiology A: Chemistry* 2004, *164* (1–3), 187-191.
[76] Domènech, B.; Muñoz, M.; Muraviev, D. N.; Macanás, J., Catalytic membranes with palladium nanoparticles: From tailored polymer to catalytic applications. *Catal. Today* 2012, *193* (1), 158-164.
[77] Sidorov, S. N.; Bronstein, L. M.; Davankov, V. A.; Tsyurupa, M. P.; Solodovnikov, S. P.; Valetsky, P. M.; Wilder, E. A.; Spontak, R. J., Cobalt Nanoparticle Formation in the Pores of Hyper-Cross-Linked Polystyrene: Control of Nanoparticle Growth and Morphology. *Chem. Mater.* 1999, *11* (11), 3210-3215.
[78] Macanas, J.; Ouyang, L.; Bruening, M. L.; Munoz, M.; Remigy, J. C.; Lahitte, J. F., Development of polymeric hollow fiber membranes containing catalytic metal nanoparticles. *Catal. Today* 2010, *156* (3-4), 181-186.
[79] Alonso, A.; Macanas, J.; Shafir, A.; Munoz, M.; Vallribera, A.; Prodius, D.; Melnic, S.; Turta, C.; Muraviev, D. N., Donnan-exclusion-driven distribution of catalytic ferromagnetic nanoparticles synthesized in polymeric fibers. *Dalton T.* 2010, *39* (10), 2579-2586.
[80] Alonso, A.; Muñoz-Berbel, X.; Vigués, N.; Macanás, J.; Muñoz, M.; Mas, J.; Muraviev, D. N., Characterization of Fibrous Polymer Silver/Cobalt Nanocomposite with Enhanced Bactericide Activity. *Langmuir* 2011, *28* (1), 783-790.
[81] Domenech, B.; Munoz, M.; Muraviev, D. N.; Macanas, J., Polymer-stabilized palladium nanoparticles for catalytic membranes: ad hoc polymer fabrication. *Nanoscale Res. Lett.* 2011, *6*.
[82] Ruiz, P.; Munoz, M.; Macanas, J.; Turta, C.; Prodius, D.; Muraviev, D. N., Intermatrix synthesis of polymer stabilized inorganic nanocatalyst with maximum accessibility for reactants. *Dalton T.* 2010, *39* (7), 1751-1757.

ANNEX B

B1. Nanoscale Research Letters (**2011**), 6, 406.

B2. Chemical Communications (**2014**), (in press)

B3. Polymers for advanced technologies. (submitted)

Domènech et al. Nanoscale Research Letters 2011, 6:406
http://www.nanoscalereslett.com/content/6/1/406

Nanoscale Research Letters
a SpringerOpen Journal

NANO EXPRESS Open Access

Polymer-stabilized palladium nanoparticles for catalytic membranes: *ad hoc* polymer fabrication

Berta Domènech[1], Maria Muñoz[1], Dmitri N Muraviev[1] and Jorge Macanás[2*]

Abstract

Metal nanoparticles are known as highly effective catalysts although their immobilization on solid supports is frequently required to prevent aggregation and to facilitate the catalyst application, recovery, and reuse. This paper reports the intermatrix synthesis of Pd^0 nanoparticles in sulfonated polyethersulfone with Cardo group membranes and their use as nanocomposite catalytic membrane reactors. The synthesized polymer and the corresponding nanocomposite were characterized by spectroscopic and microscopic techniques. The catalytic efficiency of catalytic membranes was evaluated by following the reduction of *p*-nitrophenol in the presence of $NaBH_4$.

Introduction

The unusual physical, chemical, and catalytic properties of metal colloids (better known in nowadays as metal nanoparticles, MNPs) have attracted increasing interest of scientists and technologists during the last decade [1]. A characteristic high percentage of surface atoms and the associated quantum effects make MNPs efficient and selective catalysts for several types of catalytic reactions [2,3]. However, for most practical catalytic applications, MNPs must be immobilized on solid supports to prevent their aggregation and to facilitate the catalyst recovery [4]. In this sense, encapsulation of MNPs in polymers seems advantageous because, in addition to stabilizing and protecting effects towards MNPs, polymers offer unique possibilities for enhancing the access of reactants to the catalytic sites [5]. The *in situ* synthesis of MNPs into a polymeric membrane matrix permits to combine catalysis and membrane processes, which may result in process intensification [6,7]: destruction and separation of pollutants in a single step [7,8]. These polymer stabilized MNPs (PSMNPs) can be synthesized by various methods [1,9,10], including the intermatrix synthesis (IMS) technique [11,12]. Some common polymers such as cellulose acetate, hydrophilized polysulfone, polyacrylic acid-modified polyethersulfone, polyvinylidene fluoride, and many others, which are widely used as membrane materials, have been successfully employed for the synthesis of PSMNPs [13]. These polymers can be used as a support of metal catalysts [14,15] after a simple casting procedure. However, it is imperative to adequate the polymeric matrix for both the IMS of PSMNPs and the final application of the nanocomposites. Therefore, the development of catalytic membranes requires the use of polymers with good chemical, thermal, and mechanical stability, and these polymers also have to be easily fabricated in a suitable form for their further practical application [16].

The application of the IMS technique implies that the matrix polymer must bear some functional groups (e.g., sulfonic or carboxylic) capable to bind metal ions (PSMNP precursors). Yet, the presence of these groups is known to increase the hydrophilicity of the polymer, which can hinder, in some cases, the preparation of membranes with the required properties. For example, sulfonated poly(etheretherketone) has already proved to be a very suitable matrix for IMS of various PSMNPs [11,12], but it cannot be used for the preparation of catalytic membranes by phase inversion technique[15] due to the following reasons: (1) its high hydrophilicity and (2) quite low mechanical stability. For this reason, a compromise needs to be found for each type of application by balancing hydrophilicity and hydrophobicity. To cope with this drawback, we propose the sulfonation of polyethersulfone with Cardo group (PES-C) which has a very hydrophobic group in its skeleton (a five-member lactone ring of a phenolphthalein moiety) but whose sulfonation can be done in a simple way [16]. The resulting structure of sulfonated PES-C (SPES-C) is shown in Figure 1.

* Correspondence: Jorge.Macanas@upc.edu
[2]Department of Chemical Engineering, UPC, C/Colom, 1, 08222 Terrassa, Barcelona, Spain
Full list of author information is available at the end of the article

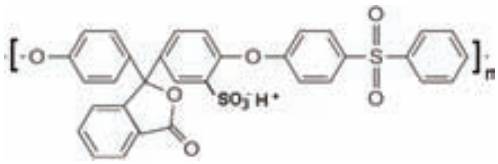

Figure 1 Structural unit of sulfonated polyethersulfone with Cardo group (SPES-C) in its acid form.

The main goal of this work is the development of palladium nanoparticles (Pd^0-NPs) by IMS technique inside SPES-C membranes for their use as catalytic membrane reactors. The characterization of the catalytic effect was performed by following the reduction of *p*-nitrophenol (4-np) in presence of $NaBH_4$ [6].

Experimental

Materials

Commercial PES-C was kindly supplied by Dr. Trong Nguyen from Université de Rouen, France. H_2SO_4, HCl, *N*-methyl-2-pyrrolidone (NMP), and *N*,*N*-dimethyl-formamide (DMF) (all from Panreac, S.A., Castellar del Vallès, Spain) organics and metal salts (4-np, NaCl, NaOH, $NaBH_4$, $CuSO_4$, Na_2SO_4, and $[Pd(NH_3)_4]Cl_2$ all from Aldrich, Munich, Germany) were used as received.

PES-C sulfonation

Sulfonation of PES-C was carried out following a procedure similar to those published elsewhere [16,17]. The polymer powder was dried at 70°C for 48 h prior to use. Then, it was dissolved (11% *w*/*v*) in concentrated sulfuric acid and mixed at constant temperature (60°C). After 5 h, the reaction medium was precipitated in a cold-water bath under strong stirring to obtain the SPES-C in its acid form. Afterward, it was neutralized with NaOH 1 M solution, filtered, washed with deionized water, and dried at 70°C (polymer in Na form).

Membrane casting

Membranes were prepared by wet phase inversion method [15] by using a polymer solution in NMP (25 wt.%). After casting, membranes were stored in deionized water.

Synthesis of Pd^0-NPs

The synthesis of Pd^0-NPs in SPES-C membranes was carried out by a two-step procedure (see below Equations 1 and 2) [11,12], consisting in the loading of sulfonic groups with $[Pd(NH_3)_4]^{2+}$ ions and their subsequent chemical reduction inside polymeric matrix by using $NaBH_4$ 0.1 M solution:

$$2R\text{-}SO_3^-Na^+ + [Pd(NH_3)_4]^{2+} \leftrightarrow (R\text{-}SO_3^-)_2[Pd(NH_3)_4]^{2+} + 2\,Na^+ \quad (1)$$

$$(R\text{-}SO_3^-)_2[Pd(NH_3)_4]^{2+} + 2\,NaBH_4 + 6H_2O \rightarrow 2R\text{-}SO_3^-Na^+ + 7H_2 + 2B(OH)_3 + 4NH_3 + Pd^0 \quad (2)$$

Polymer and nanocomposite characterization

Attenuated total reflectance Fourier transform infrared (ATR-FTIR) spectra were recorded with a Perkin Elmer Spectrum GX spectrometer (Norwalk, CT, USA).

Membrane water uptake (MWU, g H_2O/g dry membrane) was determined by a simple procedure: membrane samples stored in water were weighed (W_w), then dried in the oven for 48 h at 80°C, and weighed again (W_d). MWU was calculated by using Equation 3:

$$\mathrm{MWU} = \frac{W_w - W_d}{W_d} \quad (3)$$

The ion-exchange capacity (IEC) defined as the number of milliequivalents (meq) of ionogenic groups (e.g., SO_3^-) per gram of dry membrane (W_d) was determined by two different methodologies:

1. Indirect titration: samples were equilibrated with HCl 2 M for 24 h to convert the functional groups of the polymer into protonated form. Then, samples were equilibrated with an excess of NaCl 1 M solution for 24 h, and the resulting solutions were titrated with NaOH 4.3 mM using phenolphthalein as indicator.

2. Cu^{2+} displacement and determination: a sample of membrane in the H form (see above) was equilibrated with 20 ml of $CuSO_4$ 0.1 M solution for 20 h, washed with water several times and finally equilibrated with 20 ml of Na_2SO_4 0.5 M. The exchanged Cu^{2+} ions were analyzed by inductively coupled plasma-atomic emission spectroscopy (ICP-AES) using an Iris Intrepid II XSP spectrometer (Thermo Electron Corporation, Milford, MA, USA).

The commonly used sulfonation degree[18] (SD), which corresponds to the molar ratio of sulfonated units to the total basic units, was calculated from IEC value by Equation 4 where M_0 was 532 g/mol, and the molar mass variation (considering both the sulfonation and the conversion from H to Na form) was 102 g/mol:

$$\mathrm{SD} = \frac{M_0 \cdot 10^{-3} \cdot \mathrm{IEC}}{1 - 102 \cdot 10^{-3} \cdot \mathrm{IEC}} \quad (4)$$

In order to determine the exact metal content in the prepared nanocomposites, the membrane samples of known weight were treated with *aqua regia* to completely dissolve all MNPs. The resulting solutions were diluted and analyzed by ICP-AES. The average uncertainty was <2% in all cases.

Characterization of Pd^0-NPs

With the aim of characterizing the size and structure of Pd^0-NPs, transmission electron microscope (TEM) images were obtained by using a JEOL JEM-2011 Microscope (Jeol Ltd., Tokyo, Japan). For this purpose, a drop of samples diluted in DMF was deposited onto a Cu TEM grid, followed by solvent evaporation at room temperature.

Catalytic properties evaluation

The catalytic performance of modified SPES-C membranes was evaluated by using the reduction of *p*-nitrophenol (4-np) by $NaBH_4$ to *p*-aminophenol as a model reaction [7], which was considered to follow the pseudo-first-order kinetics. In a typical run, a given amount of $NaBH_4$ was added to 5 ml of 4-np solution (5 mM) to achieve a $NaBH_4$ concentration of 55 mM. After mixing, a piece of nanocomposite (1 cm^2) was added to the vessel. The process was monitored at 390 nm by a Pharmacia LKB Novaspec II spectrometer (Biochrom Ltd., Cambridge, UK).

Results and discussion

The ATR-FTIR-ATR spectra of both bare (PES-C) and sulfonated polymer (SPES-C) shown in Figure 2 have been used to follow the effectiveness of the sulfonation procedure. As it is clearly seen, spectra only differ by the peak at about 1,030 cm^{-1} assigned to symmetric S = O stretching due to the introduction of -SO_3H groups into the polymer chains. This fact confirms that the rest of the polymer structure is not degraded in the course of sulfonation. As it is also seen in Figure 2, the ATR-FTIR spectrum of the Pd^0-NMP containing nanocomposite also shows the same peak.

The qualitative confirmation of polymer sulfonation was also supported by the quantitative determination of the IEC and the corresponding SD values. The IEC value obtained by titration of three samples (uncertainty 95%, t = 2.92) was 0.48 ± 0.12 meq/g whereas that obtained by Cu^{2+} exchange was found to be equal to 0.31 ± 0.07 meq/g. The higher value obtained by the first method can be due to incomplete displacement of Cu^{2+} from the polymer and to the partial retention of some metal ions in the matrix when preparing samples for ICP-AES. The obtained SD values (0.27 ± 0.09 and 0.17 ± 0.05, respectively) are far from the practical limitation of 0.9, which has been reported to cause the polymer dissolution in water [18]. These results prove that a moderate SD can be achieved under mild reaction conditions corresponding to reasonable reaction temperature and time (60°C, 5 h) just by using concentrated H_2SO_4. This procedure appears to be far simpler than, for instance, the polymer modification by the metalation route [19].

The measured values of MWU for the sulfonated polymer and the corresponding nanocomposite were found to be 2.73 ± 0.13 and 3.21 ± 0.19 g H_2O/g dry membrane, respectively (three replicates in each case). These values prove that (1) even if hydrophilicity of the material is high, it does not result in the membrane dissolution, and (2) the IMS of Pd^0-NPs does not substantially affect the membrane morphology and the accessibility of water to the sulfonic groups.

The content of Pd-MNPs in the nanocomposites was found to be 156.7 ± 0.8 μmol of Pd^0 per gram of dry nanocomposite (16.68 ± 0.08 mg Pd^0/g) by analyzing eight different samples by ICP-AES. Similarly to the other studied parameters, it is worth noting the high homogeneity of samples, probably due the IMS methodology.

Figure 3 shows typical TEM images of Pd^0-NPs synthesized inside SPES-C matrix and their size distribution histograms. As it is seen, Pd forms almost spherical nanoparticles characterized by quite narrow size distribution with the most frequent diameters lying inside the 4- to 8-nm range. Particles are well separated from each other, which testifies to the high stabilizing efficiency of SPES-C matrix towards Pg-MNPs.

The results of the catalytic characterization of samples are shown in Figure 4. As it is seen, MNP-free membranes do not exhibit any catalytic activity while the membrane

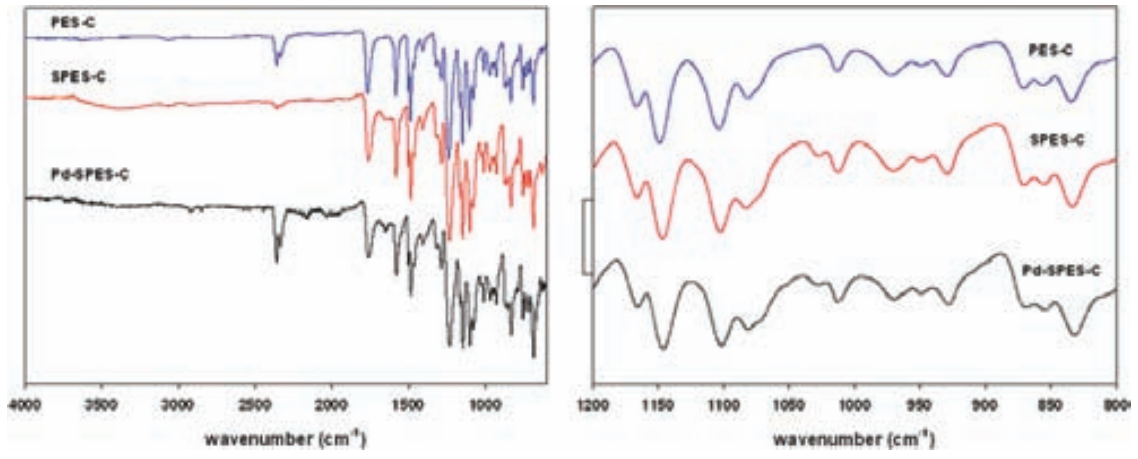

Figure 2 ATR-FTIR spectra of PES-C, SPES-C, and Pd^0-NP-SPES-C (left). Partial spectra corresponding to 800 to 1,200 cm^{-1} interval (right).

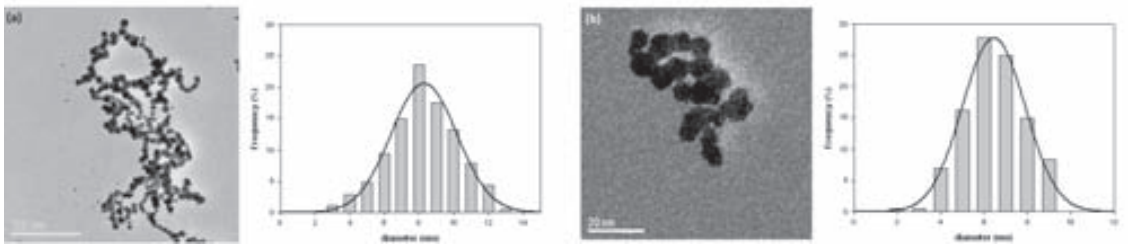

Figure 3 TEM images and size distribution histograms of two Pd^0-MNP samples prepared in the same way.

samples containing Pd^0-NPs show a clearly pronounced catalytic effect, which is confirmed by a quite fast absorbance decay. However, the attenuation only followed a linear trend after approximately 1 h. In order to understand this issue, it is important to consider that Pd is a classical hydrogen-storage metal [20,21]. Thus, the observed induction period can be associated with hydrogen loading (evolved from the decomposition of $NaBH_4$) into the Pd-NPs, which competes with the catalytic reaction. Once the absorption of hydrogen has reached a saturation value (after the induction/activation period), the catalytic reaction prevails and the reaction rate follows pseudo-first-order kinetics at high extend. In fact, Pd^0-NPs can already be partially loaded by hydrogen after the second IMS step (see Equation 2).

From a practical point of view, more than 90% of [4-np] can be easily reduced within less than 4 h through a single reaction step. This can be considered as the experimental confirmation of the suitability of this kind of catalytic membranes for decontamination applications. An apparent rate constant (k_{app}) of [4-np] reduction has been estimated by assuming pseudo-first-order kinetics (see Equation 5). The k_{app} value was found to be 0.0132 ± 0.0002 s^{-1}.

$$\ln\left(\frac{\mathrm{Abs}_t}{\mathrm{Abs}_0}\right) = -k_{app} \cdot t \tag{5}$$

The possibility to reuse nanocomposite catalytic membranes was also evaluated. Figure 4 (right) shows the decrease of the normalized absorbance vs. time for four consecutive cycles, which testifies to the decrease of the reaction rate and the increase of the activation time after each cycle. This can be explained either by possible poisoning of the catalyst due to the generation of by-products of the 4-np reduction, which can interfere with the catalyst surface [7], or (and most probably) by a stronger competition between hydrogen absorption and catalytic reactions, after the initial discharge in the first cycle. It must be pointed out that the loss of catalytic activity cannot be explained by the leaching of Pd^0-NPs from the matrix to the aqueous solution as no change of Pd content in nanocomposite membranes before and after catalytic cycles has been detected. Moreover, the absorbance of reacting solutions did not keep decreasing

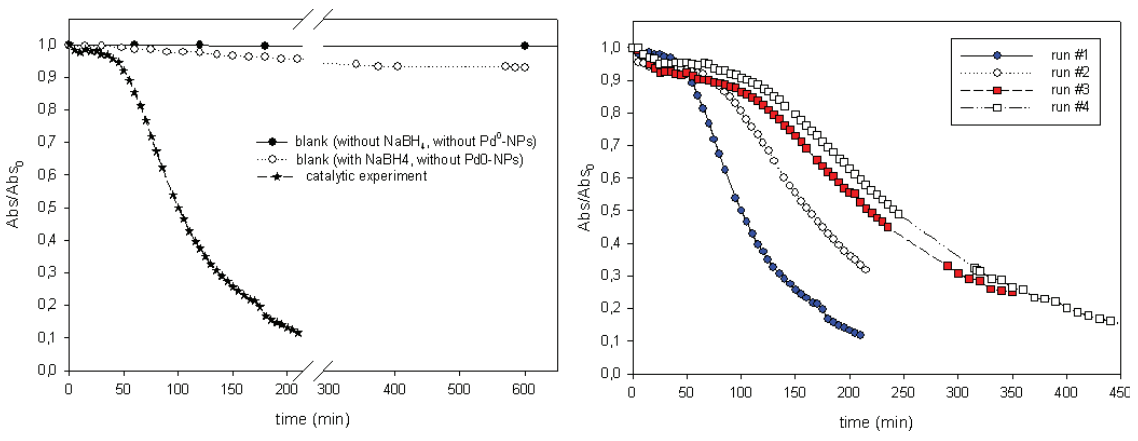

Figure 4 Catalytic performance of Pd-MNPs containing membranes (M_0 sample).

after the catalytic membrane was removed, even when stored overnight.

It has been reported that some polymer-encapsulated catalytic MNPs do aggregate after catalytic reactions [22]. However, due to the presence of the polymeric matrix, this mechanism might not be applicable for Pd^0-SPES-C nanocomposites.

As it can be seen in Figure 4 (right), the decrease in catalytic activity diminishes after each catalytic cycle if one takes into account the slope of the absorbance vs. time plot. The difference between the first and second cycles is much higher than that corresponding to third and fourth cycles. This fact may suggest that after few cycles, the catalytic efficiency could be preserved, although at a lower value when compared with the first run. However, this point requires a stricter experimental confirmation if membranes operate under a pressure gradient.

Conclusions

Polyethersulfone with Cardo group was easily sulfonated and used as a suitable matrix for IMS of palladium nanoparticles. Pd^0-NPs were well separated from each other, which indicates the high stabilizing efficiency of the polymer. Synthesis of Pd-MNPs by IMS resulted not only in the formation of catalyst NPs but also in their additional activation due to dissolution of H_2 inside Pd-MNPs. The membrane morphology is not affected by IMS of Pd-MNPs inside the polymeric matrix; however, further investigations are required to determine if the membrane transport processes are affected by the presence of MNPs. The obtained nanocomposite material exhibits a high catalytic activity, although an induction period is needed before reaction starts and the catalytic efficiency is not maintained with time. Further experiments are required in order to explain the deactivation effect observed when running consecutive catalytic cycles.

Acknowledgements

We thank ACC1O for VALTEC09-02-0058 grant within the "Programa Operatiu de Catalunya" (FEDER). The Ministry of Science and Innovation of Spain is acknowledged for the financial support to J. Macanás, and D.N. Muraviev. Prof. Trong Nguyen is acknowledged for supplying the polythersulfone Cardo. Special thanks are given to Servei de Microscopia from Universitat Autònoma de Barcelona.

Author details

[1]Analytical Chemistry Division, Chemical Department, Universitat Autònoma de Barcelona, 08193 Bellaterra, Barcelona, Spain [2]Department of Chemical Engineering, UPC, C/Colom, 1, 08222 Terrassa, Barcelona, Spain

Authors' contributions

BD carried out the experimental part concerning the polymer preparation and characterization, the nanocomposite synthesis and characterization, and the catalytic evaluation. BD also contributed in drafting the manuscript.. MM and DNM participated in the interpretation of the results. JM conceived the study, participated in its design and coordination, and wrote the main part of the manuscript. All authors read and approved the final manuscript.

Competing interests

The authors declare that they have no competing interests.

Received: 5 November 2010 Accepted: 1 June 2011
Published: 1 June 2011

References

1. Wang D, Song Y, Wang J, Ge X, Wang Y, Stec AA, Richard HT: **Double in situ approach for the preparation of polymer nanocomposite with multi-functionality.** *Nanoscale Res Lett* 2009, **4**:303.
2. Campelo JM, Luna D, Luque R, Marinas JM, Romero AA: **Sustainable preparation of supported metal nanoparticles and their applications in catalysis.** *Chem Sus Chem* 2009, **2**:18.
3. Astruc D, Fu F, Aranzaes JR: **Nanoparticles as recyclable catalysts. The frontier between homogeneous and heterogeneous catalysis.** *Angew Chem Int Ed* 2005, **44**:7852.
4. Kidambi S, Bruening ML: **Multilayered polyelectrolyte films containing palladium nanoparticles: synthesis, characterization, and application in selective hydrogenation.** *Chem Mater* 2005, **17**:301.
5. Kidambi S, Dai J, Li J, Bruening ML: **Selective hydrogenation by Pd nanoparticles embedded in polyelectrolyte multilayers.** *J Am Chem Soc* 2004, **126**:2658.
6. Dotzauer DM, Bhattacharjee S, Wen Y, Bruening ML: **Nanoparticle-containing Membranes for the catalytic reduction of nitroaromatic compounds.** *Langmuir* 2009, **25**:1865.
7. Macanás J, Ouyang L, Bruening ML, Muñoz M, Remigy JC, Lahitte JF: **Development of polymeric hollow fiber membranes containing catalytic metal nanoparticles.** *Catal Today* 2010, **156**:181.
8. Wu L, Ritchie SMC: **Enhanced dechlorination of trichloroethylene by membrane-supported Pd-coated iron nanoparticles.** *Environ Prog* 2008, **27**:218.
9. Kishore P, Viswanathan B, Varadarajan T: **Synthesis and characterization of metal nanoparticle embedded conducting polymer-polyoxometalate composites.** *Nanoscale Res Lett* 2008, **3**:14.
10. Selvaganesh S, Mathiyarasu J, Phani K, Yegnaraman V: **Chemical synthesis of PEDOT-Au nanocomposite.** *Nanoscale Res Lett* 2007, **2**:546.
11. Muraviev DN, Ruiz P, Muñoz M, Macanás J: **Novel strategies for preparation and characterization of functional polymer-metal nanocomposites for electrochemical applications.** *Pure Appl Chem* 2008, **80**:2425.
12. Muraviev DN, Macanás J, Farre M, Muñoz M, Alegret S: **Novel routes for inter-matrix synthesis and characterization of polymer stabilized metal nanoparticles for molecular recognition devices.** *Sens Actuators B* 2006, **118**:408.
13. Smuleac V, Bachas L, Bhattacharyya D: **Aqueous-phase synthesis of PAA in PVDF membrane pores for nanoparticle synthesis and dichlorobiphenyl degradation.** *J Membr Sci* 2010, **346**:310.
14. Yu ZK, Xu Y, Liao SJ, Liu R: **Catalytic behaviors and gas permeation properties of palladium-containing phenolphthalein poly(ether sulfone).** *J Appl Polym Sci* 1996, **61**:599.
15. Mulder M: *Basic Principles of Membrane Technology* Kluwer Academic Publishers, Dordrecht, The Netherlands; 1996.
16. Blanco JF, Nguyen QT, Schaetzel P: **Novel hydrophilic membrane materials: sulfonated polyethersulfone.** *Cardo J Membr Sci* 2001, **186**:267.
17. Jia L, Xu X, Zhang H, Xu J: **Permeation of nitrogen and water vapor through sulfonated polyetherethersulfone membrane.** *J Polym Sci B: Polym Phys* 1997, **35**:2133.
18. Li L, Wang Y: **Sulfonated polyethersulfone Cardo membranes for direct methanol fuel cell.** *J Membr Sci* 2005, **246**:167.
19. Kerres J, Ullrich A, Hein M: **Preparation and characterization of novel basic polysulfone polymers.** *J Polym Sci A: Polym Chem* 2001, **39**:2874.
20. Schlapbach L, Züttel A: **Hydrogen-storage materials for mobile applications.** *Nature* 2001, **414**:353.
21. Vogel W, He W, Huang QH, Zou Z, Zhang XG, Yang H: **Palladium nanoparticles "breathe" hydrogen; a surgical view with X-ray diffraction.** *Int J Hydrogen Energ* 2010, **35**:8609.
22. Narayanan R, El-Sayed MA: **Catalysis with transition metal nanoparticles in colloidal solution: nanoparticle shape dependence and stability.** *J Phys Chem B* 2005, **109**:12663.

doi:10.1186/1556-276X-6-406
Cite this article as: Domènech *et al.*: Polymer-stabilized palladium nanoparticles for catalytic membranes: *ad hoc* polymer fabrication. *Nanoscale Research Letters* 2011 **6**:406.

ChemComm

COMMUNICATION

View Article Online
View Journal

Uncommon patterns in Nafion films loaded with silver nanoparticles†

Cite this: DOI: 10.1039/c4cc01285b

Received 18th February 2014,
Accepted 12th March 2014

DOI: 10.1039/c4cc01285b

www.rsc.org/chemcomm

Berta Domènech,[a] Maria Muñoz,[a] Dmitri N. Muraviev[a] and Jorge Macanás*[b]

Nafion has been frequently used for the synthesis of nanoparticles by taking advantage of its so-called cluster-network structure. Unexpectedly, the synthesis of AgNPs inside Nafion 117 was found to produce NPs organization, resulting in a regular pattern that could reveal the real morphology of the polymer.

Nafion is a poly(perfluorosulfonic) acid membrane, known for its cation exchange properties as well as for its thermal and chemical stability.[1] It has been extensively used for a variety of applications,[2–4] and it is still the benchmark material against which most results are compared.[4,5] The chemical structure of the Nafion-117 membrane consists of a polytetrafluoroethylene (PTFE) backbone and a regularly spaced pendant side chain terminated by a sulfonate ionic group.[2,5] The unique behaviour of Nafion is explained by the lack of chemical cross-linking that provides a dynamic morphology,[1,6] which is responsible for phase segregation into hydrophilic and hydrophobic domains.[7]

Over the last 40 years many attempts have been made to precisely define the chemical structure of Nafion. Although there have been several models under debate[8,9] (*i.e.* Fujimura's core–shell model, Dreyfus' local-order model, Haubold's sandwich-like model, Rubatat's rodlike model, Litt's lamellar model and Kreuer's film-like morphology), the pioneering cluster-network model proposed by Gierke *et al.*[10] is frequently reported in the literature for justifying Nafion properties, especially ion and water transport and ion permselectivity.[1,11] According to this model, polymer chains form reverse micelles in which sulfonate groups are lined in the wall encapsulating 4–5 nm water cavities connected by channels of *ca.* 10 Å size.[1,11] However, nowadays there is quite an agreement regarding the inaccuracy of this model as it is based on the limited structure property information that was available at the time.[4]

Taking into account Gierke's model, cavities defined by water clusters were suggested for use as nanoscale reactors in the formation of nanoparticles (NPs). Using this simple concept new composite materials can be prepared, in which the polymeric matrix controls the NPs size and avoids aggregation, preserving many of their special properties (*i.e.* catalytic and photocatalytic).[12,13] Accordingly, several studies were prompted for the synthesis of metal, metal oxide or metal sulphide NPs in such cavities.[14–19] Synthesis generally involved ion exchange of metal ions in the membrane matrix followed by a chemical reaction (*i.e.* reduction or precipitation) producing NPs in the polymeric matrix. Still, very often the sizes of the formed NPs were much larger than the size of water clusters[16–18] (ESI,† S1, Table S1). This paradox was sometimes rationalized in terms of additional hydration of ionic clusters or to polymer chain reorganization due to the incorporation of NPs. In addition to the NPs size disagreement, the NPs location was not always consistent with a simple template procedure (ESI,† S1, Table S1).[14,18] As a rule of thumb, it is generally accepted that anionic reagents (*i.e.* BH_4^-, S^{2-}) are repelled due to the Donnan exclusion effect (DEE)[20] and NPs are formed on the surface of the polymer whereas neutral reagents (*i.e.* thioacetamide, formamide) or gases can freely diffuse through the matrix.[16,21]

Besides, the embedment of NPs can be regarded differently: the incorporation of NPs in the matrix can reveal the true morphology of the ionic channels of the membrane, behaving as a sort of nanometric staining agent. So, direct microscopy imaging of Nafion and related ionomer membranes embedded with nanoscale objects can provide new insight into the membrane structural domains and properties.[18,22]

In our previous reports of intermatrix synthesis inside polymer films and resin beads,[23] the NPs location was consistent with the DEE approach: NPs were mostly located on the surface of the samples, as can be clearly seen in transmission electron microscopy (TEM) images of Nafion with Pd-NPs (ESI,† S2, Fig. S2).[13] However, when carrying out the synthesis of Ag-NPs using a loading–reducing procedure (described in ESI,† S3) and analysing the corresponding TEM images, it was revealed that the adjacent but not aggregated Ag-NPs followed a general pattern of almost

[a] *Chemistry Department, Universitat Autònoma de Barcelona, UAB, 08193 Bellaterra, Barcelona, Spain*
[b] *Department of Chemical Engineering, Universitat Politècnica de Catalunya, UPC, C/Colom, 1, 08222 Terrassa, Spain. E-mail: jorge.macanas@upc.edu; Tel: +34 937398239*

† Electronic supplementary information (ESI) available: Experimental section, TEM and FESEM images, *etc*. See DOI: 10.1039/c4cc01285b

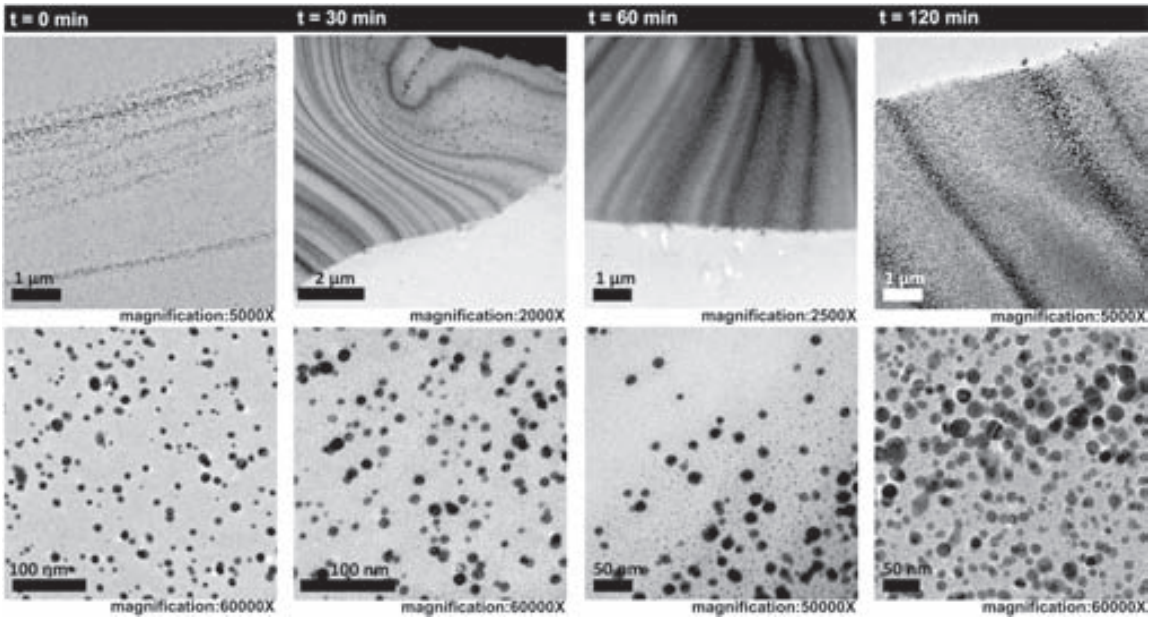

Fig. 1 Patterns observed of TEM images for Nafion samples containing Ag-NPs treated by ultrasound at different times.

parallel stripes (Fig. 1). In order to discard any artifact, samples were also analysed by high-resolution field emission scanning electron microscopy (FE-SEM), giving the same results (ESI,† S4, Fig. S4). Furthermore, when Ag-NPs-Nafion nanocomposites were introduced into an ultrasonic bath for different periods of time (ESI,† S3), TEM images showed that the stripes got coarser and more separated while the average diameter of Ag-NPs varied linearly with time (Fig. 2, ESI,† S5, Fig. S5.1 and S5.2). Regarding the metal content, it was 51.8 mg Ag g^{-1} dry membrane (s = 1.5) for the as-prepared samples and almost constant after the ultrasound treatment since Ag release was lower than 1% after 2 h.[23c]

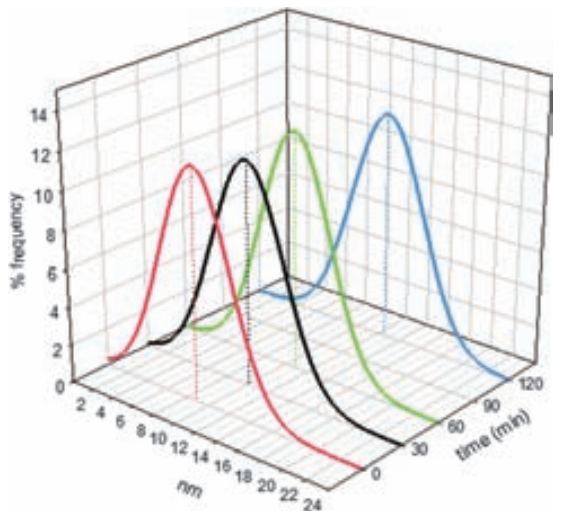

Fig. 2 Evolution of the distribution of nanoparticles diameter due to the duration of the ultrasound treatment.

To the best of our knowledge, this kind of images has never been published before for Nafion nanocomposites.

However, these patterns occurring during material deposition have been demonstrated experimentally more than a century ago and are known as Liesegang rings (LRs) or bands.[24,25] LRs form when a soluble reactant (typically an ion) diffuses from the periphery of a medium (often a gel) uniformly filled with a second soluble reactant (typically another ion) to produce an insoluble substance. The gel medium would be the Nafion film loaded with Ag^+ whilst BH_4^- would be the reactant that diffuses through.

In order to discern why such nanostructures were obtained, several factors were taken into account: (i) the Nafion structure; (ii) membrane hydration and membrane pre-treatment; (iii) reducing agent diffusion; (iv) Ag^+ mobility and (v) ultrasound effects.

First, since the stripes are quite parallel instead of circular, the development of such LR-like bands would be in agreement with Litt's and Kreuer's models which describe Nafion as a multilayered structure in which the ionic domains are defined as hydrophilic micelle layers separated by thin hydrophobic PTFE-like lamellar crystallites (ESI,† S6, Fig. S6).[4,9] Swelling of the microscopic level should occur by having water incorporation between the lamellae, thereby pushing them farther apart, which is a convenient and simple explanation for the swelling behaviour of Nafion as well as for the observed bands.

Second, Moore and Martin[26] found that Nafion pre-treatment is crucial to define the polymer morphology since it rules the hydration state of the polymer and hydration controls the extent of penetration of the ions into the polymer.[1] Water uptake measurements showed that boiling in water clearly

enhanced the ability of Nafion to absorb water when compared to the vacuum dried and as-received samples.

Third, it has been demonstrated by Pintauro *et al.*[27] that the aforementioned DEE explanation is oversimplified. They realized that anion transport through Nafion (previously boiled in water for 30 min) occurred efficiently for NaCl and the movement of Cl^- was thought to occur by co-ions moving together as a neutral particle, thus reducing the DEE. Na^+ and BH_4^- can act similarly to Na^+ and Cl^-, entering a fully hydrated region of the Nafion while single BH_4^- ions may experience limited transport. As a result, the feasibility of reducing metal ion precursors deeply past the membrane surface might be hindered and the nucleation and growth of NPs occurs near this surface.[21] As well, the decomposition of BH_4^- produces H_2, which can diffuse freely through the membrane providing additional autocatalytic reduction of Ag^+ without any electrostatic repulsion.[28]

Besides, it is worth mentioning that Ag is one of the most attractive metals for nanomaterial synthesis and many different nanostructures have already been reported (*i.e.* nanowires, nanoparticles, nanocubes).[29] This myriad of nanostructures testifies to the ability of Ag to undergo shape transformations by dissolution–precipitation processes even though the mechanisms are not fully understood.[30] Indeed, the mobility of ions inside Nafion 117 have been correlated with the membrane water-uptake[6] and Ag^+ ions (which enhance water uptake) were found to possess a very high self-diffusion coefficient (1.61×10^{-6} cm^2 s^{-1}), which provides them with a higher mobility when compared with other cations (*i.e.* Na^+, K^+, Ca^{2+}). Then, it is not surprising that Ag^+ ions were often associated with the formation of LR since their mobility aids in generating alternating regions of high and low concentration of the solid phase.

Finally, it is well-known that ultrasound offer a very attractive and fast method for the synthesis of metal NPs. Combining ultrasound with classical Ostwald ripening[31,32] it is feasible that bigger nanocrystals grow at the expense of smaller ones that get dissolved. So, the growth of stripes can be a result of and induced by dissolution–precipitation processes. (Fig. 2, ESI,† S5, Fig. S5.1 and S5.2).

The simple concept of synthesising NPs by using Nafion's cavities ends up being a very complex scenario that can give rise to uncommonly patterned nanostructures as those shown here. But, even if the observed patterns have never been reported before for Nafion nanocomposites, their existence is in agreement with the general knowledge regarding reaction–diffusion mechanisms and reinforces the idea of hydrophilic–hydrophobic lamellar domains in Nafion.

Notes and references

1 A. Eisenberg and H. L. Yeager, *Perfluorinated Ionomers Membrane, ACS Symposium Series 180*, American Chemical Society, 1982.
2 C. Heitner-Wirguin, *J. Membr. Sci.*, 1996, **120**, 1.
3 (*a*) V. Neburchilov, J. Martin, H. Wang and J. Zhang, *J. Power Sources*, 2007, **169**, 221; (*b*) C. J. Hora and D. E. Maloney, *Electrochem. Soc. Ext. Abstr.*, 1977, **77**, 1145.
4 K. Mauritz and R. Moore, *Chem. Rev.*, 2004, **104**, 4535.
5 H. Strathmann, Ion-exchange membrane separation processes, *Membrane Science and Technology*, Elsevier, 2004, series 9, p. 1.
6 A. Goswami, A. Acharya and A. K. Pandey, *J. Phys. Chem. B*, 2001, **105**, 9196.
7 J. Chou, E. W. McFarland and H. Metiu, *J. Phys. Chem. B*, 2005, **109**, 3252.
8 (*a*) M. Fujimura, T. Hashimoto and H. Kawai, *Macromolecules*, 1981, **14**, 1309; (*b*) B. Dreyfus, G. Gebel, P. Aldebert, M. Pineri, M. Escoubes and M. Thomas, *J. Phys.*, 1990, **51**, 1341; (*c*) G. Gebel and J. Lambard, *Macromolecules*, 1997, **30**, 7914; (*d*) H. G. Haubold, T. Vad, H. Jungbluth and P. Hiller, *Electrochim. Acta*, 2001, **46**, 1559; (*e*) L. Rubatat, A. Rollet, G. Gebel and O. Diat, *Macromolecules*, 2002, **35**, 4050.
9 (*a*) M. H. Litt, *Polym. Prepr.*, 1997, **38**, 80; (*b*) K. D. Kreuer and G. Portale, *Adv. Funct. Mater.*, 2013, **23**, 5390.
10 W. Y. Hsu and T. D. Gierke, *Macromolecules*, 1982, **15**, 101.
11 (*a*) W. Y. Hsu and T. D. Gierke, *J. Membr. Sci.*, 1983, **13**, 307; (*b*) T. D. Gierke, G. E. Munn and F. C. Wilson, *J. Polym. Sci., Polym. Phys. Ed.*, 1981, **19**, 1687.
12 N. Kakuta, J. M. White, A. Campion, A. J. Bard, M. A. Fox and S. E. Webber, *J. Phys. Chem.*, 1985, **89**, 48.
13 B. Domenech, M. Muñoz, D. N. Muraviev and J. Macanás, *Catal. Today*, 2012, **193**, 158.
14 P. Bertoncello, M. Peruffo and P. R. Unwin, *Chem. Commun.*, 2007, 1597.
15 (*a*) E. S. Smotkin, R. M. Brown, L. K. Radenburg, K. Salomon, A. J. Bard, A. Campion, M. A. Fox, T. E. Mallouk, S. E. Webber and J. M. White, *J. Phys. Chem.*, 1990, **94**, 7543; (*b*) Y. Zhang, D. Kang, C. Saquing, M. Aindow and C. Erkey, *Ind. Eng. Chem. Res.*, 2005, **44**, 4161; (*c*) P. Liu, J. Bandara, Y. Lin, D. Elgin, L. F. Allard and Y.-P. Sun, *Langmuir*, 2002, **18**, 10389; (*d*) N. H. Jalani, K. Dunn and R. Datta, *Electrochim. Acta*, 2005, **51**, 553.
16 (*a*) J. Wang, P. Liu, S. Wang, W. Han, X. Wang and X. Fu, *J. Mol. Catal. A: Chem.*, 2007, **273**, 21; (*b*) S. Wang, P. Liu, X. Wang and X. Fu, *Langmuir*, 2005, **21**, 11969.
17 (*a*) M. Krishnan, J. R. White, M. A. Fox and A. J. Bard, *J. Am. Chem. Soc.*, 1983, **105**, 7002; (*b*) R. Kumar, A. K. Pandey, S. Das, S. Dhara, N. L. Misra, R. Shukla, A. K. Tyagi, S. V. Ramagiri, J. R. Bellare and A. Goswami, *Chem. Commun.*, 2010, **46**, 6371.
18 (*a*) H. W. Rollins, F. Lin, J. Johnson, J. J. Ma, J. T. Liu, M. H. Tu, D. D. DesMarteau and Y.-P. Sun, *Langmuir*, 2000, **16**, 8031; (*b*) Y.-P. Sun, P. Atorngitjawat, Y. Lin, P. Liu, P. Pathak, J. Bandara, D. Elgin and M. Zhang, *J. Membr. Sci.*, 2004, **245**, 211; (*c*) H. W. Rollins, T. Whiteside, G. J. Shafer, J. J. Ma, M. H. Tu, J. T. Liu, D. D. DesMarteau and Y.-P. Sun, *J. Mater. Chem.*, 2000, **10**, 2081.
19 A. Sachdeva, S. Sodaye, A. K. Pandey and A. Goswami, *Anal. Chem.*, 2006, **78**, 7169.
20 F. G. Donnan, *J. Membr. Sci.*, 1995, **100**, 45.
21 A. Sode, N. J. C. Ingle, M. McCormick, D. Bizzotto, E. Gyenge, S. Ye, S. Knights and D. P. Wilkinson, *J. Membr. Sci.*, 2011, **376**, 162.
22 W. Kubo, K. Yamauchi, K. Kumagai, M. Kumagai, K. Ojima and K. Yamada, *J. Phys. Chem. C*, 2010, **114**, 2370.
23 (*a*) P. Ruiz, M. Muñoz, J. Macanás, C. Turtra, D. Prodius and D. N. Muraviev, *Dalton Trans.*, 2010, **39**, 1751; (*b*) J. Bastos-Arrieta, A. Shafir, A. Alonso, M. Muñoz, J. Macanás and D. N. Muraviev, *Catal. Today*, 2012, **193**, 207; (*c*) B. Domènech, N. Viguès, J. Mas, M. Muñoz, D. N. Muraviev and J. Macanás, *Solvent Extr. Ion Exch.*, DOI: 10.1080/07366299.2013.839192.
24 (*a*) R. E. Liesegang, *Naturwiss. Wochenschr.*, 1896, **11**, 353; (*b*) H. K. Henisch, *Crystals in gels and Liesegang rings*, Cambridge University Press, Cambridge, MA, 1988.
25 (*a*) D. A. Smith, *J. Chem. Phys.*, 1984, **81**, 3102; (*b*) M. I. Lebedeva, D. G. Vlachos and M. Tsapatsis, *Ind. Eng. Chem. Res.*, 2004, **43**, 3073.
26 R. B. Moore and C. R. Martin, *Macromolecules*, 1988, **21**, 1334.
27 P. Pintauro and D. Bennion, *Ind. Eng. Chem. Fundam.*, 1984, **23**, 234.
28 H. Lee, S. E. Habas, S. Kweskin, D. Butcher, G. A. Somorjai and P. Yang, *Angew. Chem., Int. Ed.*, 2006, **45**, 7824.
29 D. Muñoz-Rojas, J. Oró-Solé and P. Gómez-Romero, *J. Phys. Chem. C*, 2008, **112**, 20312 and references therein.
30 B. Y. Sun, B. Mayers and Y. Xia, *Adv. Mater.*, 2003, **15**, 641.
31 J. E. Park, M. Atobe and T. Fuchigami, *Electrochim. Acta*, 2005, **51**, 849.
32 R. Boistelle and J. P. Astier, *J. Cryst. Growth*, 1988, **90**, 14.

Electronic Supplementary Information

S.1. Literature review of NPs synthesis in Nafion.

Table S.1. Data regarding NPs synthesis in Nafion.

Nanoparticle type	Nanoparticle diameter (nm)	Reacting agent	Location	Reference
CdS	2-4	H_2S	uniform distribution	[1]
Pt	2.5	Heat treatment	uniform distribution	[2]
CdS	2.9	Thioacetamide	uniform distribution	[3]
TiO_2	3.7 ± 0.5	Boiling H_2O	uniform distribution	[4]
CdS	4.1	Na_2S	surface	[3]
Pd	5 ± 1	$NaBH_4$	uniform distribution	[5]
PbS	6.3 ± 1	Na_2S	uniform distribution	[6]
CdS	6.5 ± 1.2	Na_2S	uniform distribution	[6]
ZnO	8	Ethanol/NaOH	uniform distribution	[7]
Ag	9 ± 2	Formamide	uniform distribution	[8]
Ag_2S	10.5 ± 2.2	Na_2S	uniform distribution	[9]
Ag	13.0 ± 3.4	$NaBH_4$	uniform distribution	[9]
Ag	13.4 ± 2.2	$NaBH_4$	uniform distribution	[10]
Ag	15 ± 3	$NaBH_4$	surface	[11]
Ag	15 ± 4	$NaBH_4$	surface	[10]
CdS	ca. 1000	H_2S	uniform distribution	[12]

S.2. Nafion Pd-NPs

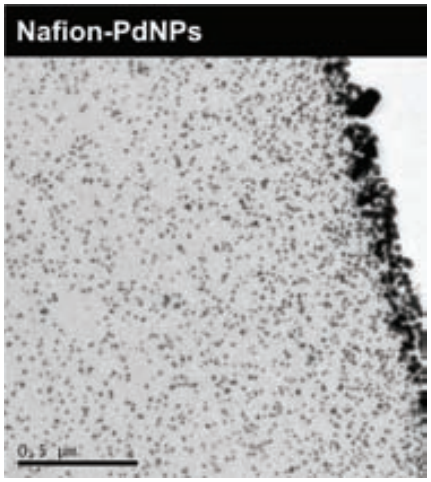

Figure S.2. TEM image of the cross-section of Nafion 117 with Pd-NPs.

S.3. Experimental.

S3.1. Materials

Nafion 117 membranes were from Sigma Aldrich, $AgNO_3$, $NaBH_4$, H_2SO_4 and H_2O_2 were all from Panreac and HNO_3 from Fisher Chemical.

S3.2. Nafion pretreatment

Commercial Nafion 117 membranes were washed twice with bidistilled water in an ultrasonic bath for 30 min. Then they were kept under stirring for 24 h in an aqueous oxidizing solution (10% of concentrated H_2SO_4 and 10% of commercial H_2O_2) to remove impurities. Afterwards, samples were washed again with boiling bidistilled water for several hours and kept in the fridge at 4 ºC.

S3.3. Synthesis of AgNPs

The synthesis of MNPs in the membranes was carried out by a two-steps procedure, Intermatrix Synthesis (IMS) [13] (equations (1) and (2)), consisting in the loading of the ionogenic groups with the correspondent metal precursor (corresponding M^{n+} to Ag^+ ions) and their subsequent chemical reduction by using $NaBH_4$ 0.5 M solution to obtain the metal nanoparticles (in this case, M^0 stands forAg^0):

$$n\ (R\text{-}SO_3^-)Na^+ + M^{n+} \leftrightarrow (R\text{-}SO_3^-)_nM^{n+} + n\ Na^+ \quad (1)$$

$$(R\text{-}SO_3^-)_nM^{n+} + n\ NaBH_4 + 3n\ H_2O \rightarrow n\ (R\text{-}SO_3^-)Na^+ + (7n/2)H_2 + n\ B(OH)_3 + M^0 \quad (2)$$

S3.4. Ultrasonic bath treatment

Samples of $1cm^2$ were deposited in a closed vessel with 10 mL of bidistilled water and placed in an ultrasonic bath during different times: 30min, 60min, 120 min. Temperature of the bath during the experiment went up from 20 ºC (initial temperature) to 40 ºC (final temperature).

S3.5. Nanocomposite characterization

With the aim of characterizing the size and structure of the obtained MNPs, Transmission Electron Microscopy (TEM) was performed by a Jeol JEM-2011 HR-TEM and Jeol JEM-1400 TEM. FE-SEM images were obtained by a Zeiss Merlin, Carl Zeiss High Resolution SEM.
Before observation, samples were deposited between two plastic sheets in an epoxy resin and ultra-thin slices were obtained using an ultra-microtome and sputtered with Carbon.
Through the image analysis of TEM micrographs it was possible to make size distribution histograms from the sample data. By measuring the diameter of up to 600 AgNPs per sample, data were fitted to a 3-parameter Gaussian curve (3) where a is the height of Gaussian peak, d_m is the position of the center of the peak (corresponding to the most frequent diameter), and σ is the standard deviation.

$$y=a\cdot\exp\left[-0.5\cdot\left(\frac{d-d_m}{\sigma}\right)^2\right] \quad (3)$$

S3.6. Metal loading

The exact metal content in the prepared nanocomposites was analysed by Inductively Coupled Plasma Mass Spectrometry (ICP-MS, Agilent 7500). Samples of 1 cm^2 were digested with 1 mL of concentrated HNO_3 (65% w/w) overnight and then diluted 1:100 with distilled water. The resulting solutions (2 replicates) were appropriately diluted for ICP-MS analyses. After Ultrasonic bath treatment, the silver release was calculated as described previously [14].

S.4. FE-SEM characterization.

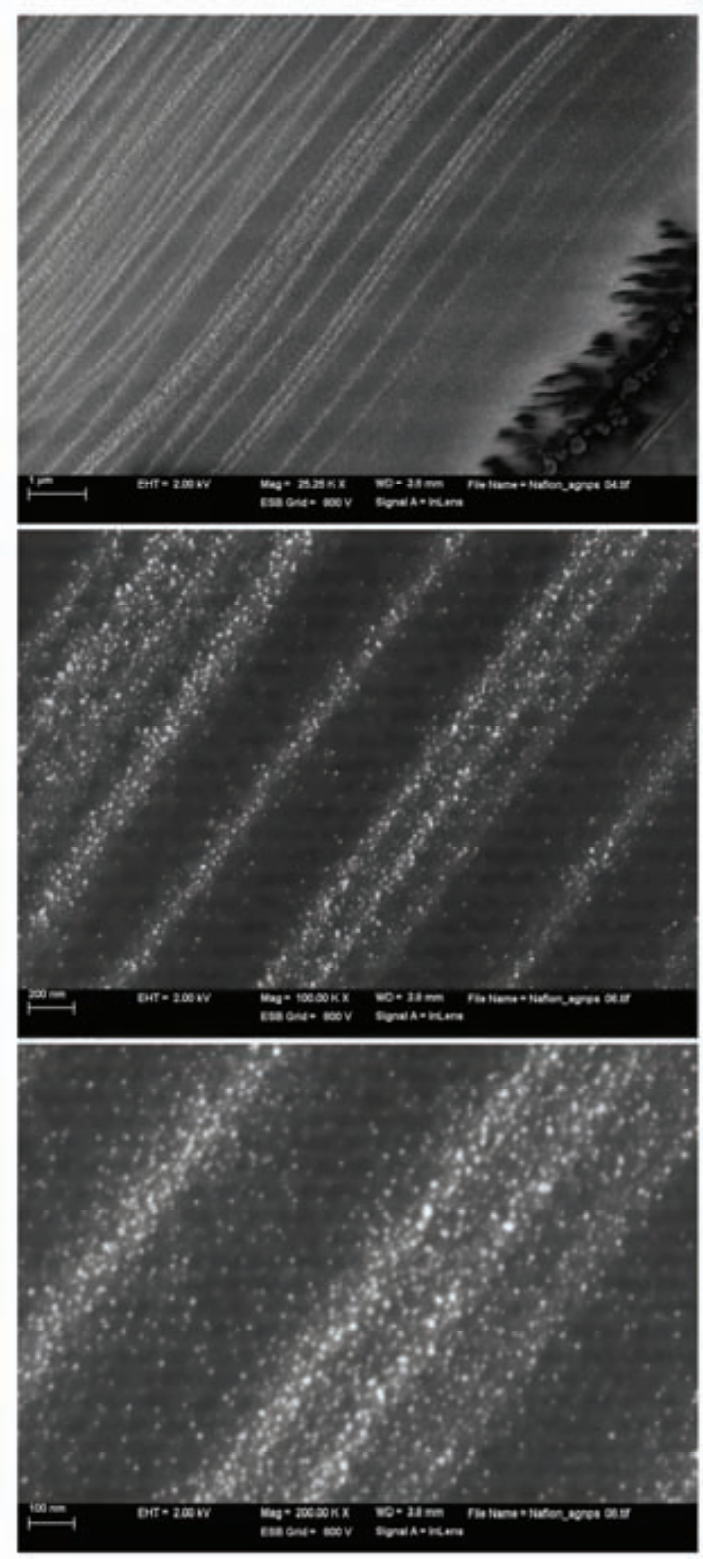

Figure S.4. FE-SEM images of the cross-section of Nafion 117 with AgNPs.

S.5. NPs size distribution.

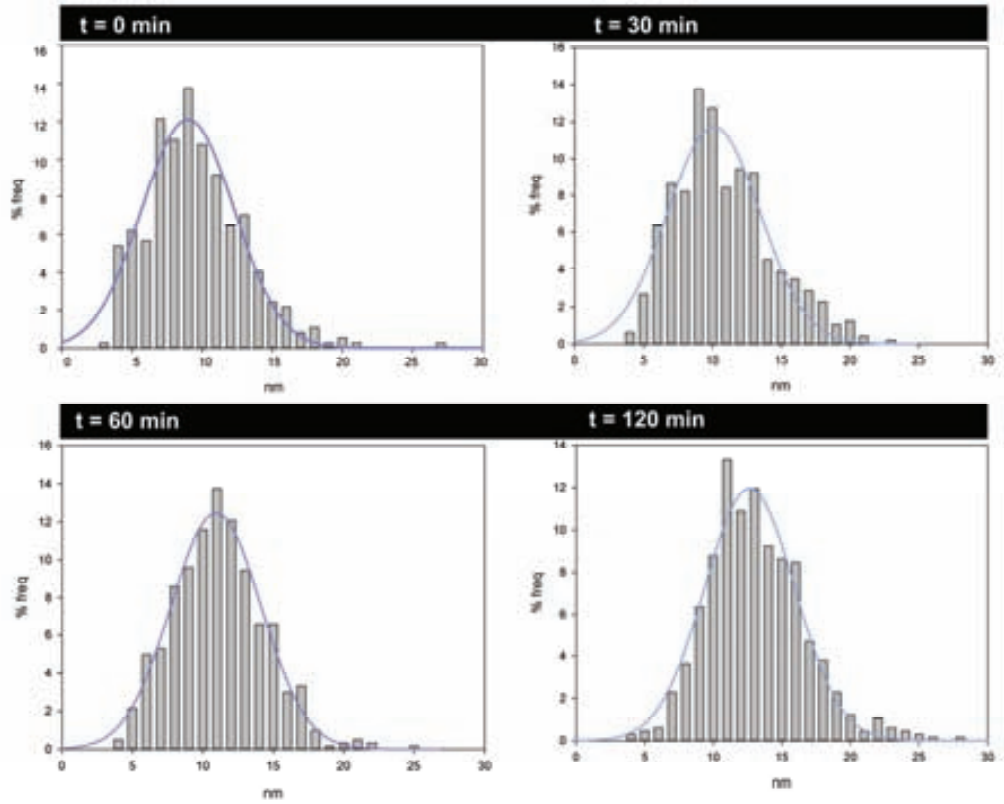

Figure S.5.1. Size distribution histograms of the nanocomposite samples after immersion in an ultrasonic bath for different times.

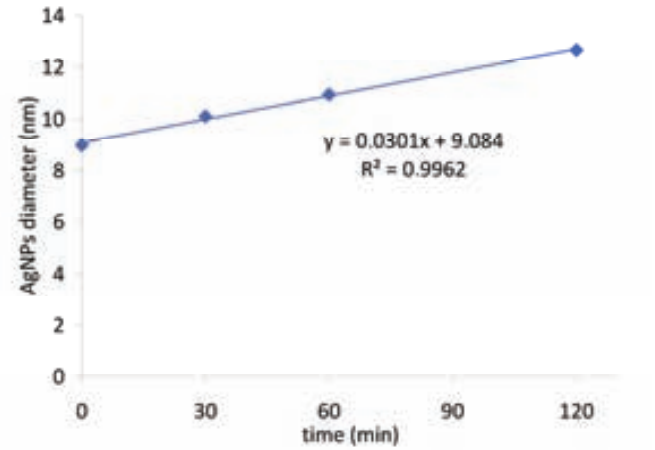

Figure S.5.2. Linear evolution of NPs diameter *vs.* time of the US treatment.

The Ag-NPs average diameter found for the original samples (without being treated by ultrasounds) was 9.0 ± 0.2 nm which is in close agreement with the water cavity size for a Nafion membrane extrapolated from data plotted in reference [15]. The content of water was considered 67 ± 6 g of water per 100 g of dry polymer form reference [16].

S.6. Schematic representation of hydrated Nafion .

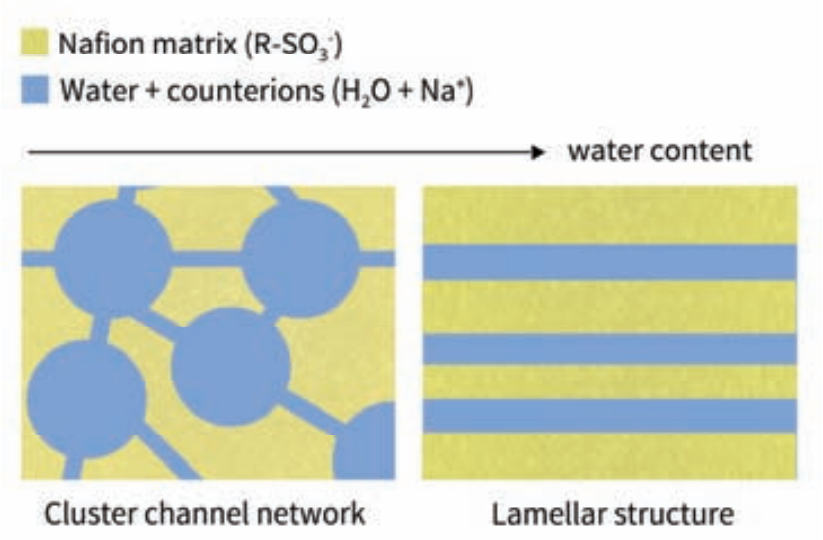

Figure S.6.1. Schematic representation of hydrated Nafion matrix.

References of the Electronic Support Information

[1] E.S. Smotkin, R.M. Brown, L.K. Radenburg, K. Salomon, A.J. Bard, A. Campion, M.A. Fox, T.E. Mallouk, S.E. Webber and J.M. White, *J. Phys. Chem*., 1990, **94**, 7543

[2] Y. Zhang, D. Kang, C. Saquing, M. Aindow and C. Erkey., *Ind. Eng. Chem. Res*., 2005, **44**, 4161.

[3] S. Wang, P. Liu, X. Wang and X. Fu., *Langmuir*, 2005, **21**, 11969.

[4] P. Liu, J. Bandara, Y. Lin, D. Elgin, L.F. Allard and Y.-P. Sun., *Langmuir*, 2002, **18**, 10389.

[5] P. Bertoncello, M. Peruffo and P.R. Unwin, *Chem. Commun.*, 2007, 1597

[6] H.W. Rollins, T. Whiteside, G.J. Shafer, J.J. Ma, M.H. Tu, J.T. Liu, D.D. DesMarteau and Y.-P. Sun, *J. Mater. Chem.*, 2000, **10**, 2081.

[7] J. Wang, P. Liu, S. Wang, W. Han, X. Wang and X. Fu, *J. Molecular Catal. A: Chemical*, 2007, **273**, 21

[8] R. Kumar, A.K. Pandey, S. Das, S. Dhara, N.L. Misra, R. Shukla, A.K. Tyagi, S.V. Ramagiri, J.R. Bellare and A. Goswami, *Chem. Commun*., 2010, **46**, 6371.

[9] H.W. Rollins, F. Lin, J. Johnson, J.J. Ma, J.T. Liu, M.H. Tu, D.D. DesMarteau, and Y.-P. Sun, *Langmuir*, 2000, **16**, 8031;

[10] Y.-P Sun, P. Atorngitjawat, Y. Lin, P. Liu, P. Pathak, J. Bandara, D. Elgin and M. Zhang, *J. Membr. Sci*., 2004, **245**, 211;

[11] A. Sachdeva, S. Sodaye, A.K Pandey and A. Goswami., *Anal. Chem*., 2006, **78**, 7169.

[12] M. Krishnan, J.R. White, M.A. Fox and A.J. Bard, *J. Am. Chem. Soc*., 1983, **105**, 7002.

[13] B. Domènech, M. Muñoz, D.N. Muraviev, J. Macanás, *Nanoscale Res. Lett*., 2011, **6**, 406.

[14] B. Domènech, N. Vigués, J. Mas, M. Muñoz, D.N. Muraviev and J. Macanás, *Solvent Extr. Ion Exc*. DOI: 10.1080/07366299.2013.839192.

[15] Gierke, T. D.; Munn, G. E.; Wilson, F. C. J. Polym. Sci., Polym.Phys. 1981, **19**, 1687.

[16] B. Domènech, M. Muñoz, D.N. Muraviev and J. Macanás, *Catal. Today*, 2012, **193**, 158.

Polymers for Advanced Technologies

Reusable polyurethane foams containing silver nanoparticles for dual-purpose water treatment.

Journal:	*Polymers for Advanced Technologies*
Manuscript ID:	Draft
Wiley - Manuscript type:	Research Article
Date Submitted by the Author:	n/a
Complete List of Authors:	Domènech, Berta; Universitat Autònoma de Barcelona, Analytical Chemistry Ziegler, Kharla; Universitat Autònoma de Barcelona, Analytical Chemistry Muñoz, Maria; Universitat Autònoma de Barcelona, Analytical Chemistry Muraviev, Dmitri; Universitat Autònoma de Barcelona, Analytical Chemistry Vigués, Núria; Universitat Autònoma de Barcelona, Department of Genetics and Microbiology Mas, Jordi; Universitat Autònoma de Barcelona, Department of Genetics and Microbiology Macanás, Jorge; Universitat Politècnica de Catalunya, Department of Chemical Engineering
Keywords:	nanocomposites, polyurethane foams, silver nanoparticles, water treatment, intermatrix synthesis

Reusable polyurethane foams containing silver nanoparticles for dual-purpose water treatment.

B. Domènech[1], K. Ziegler[1], M. Muñoz[1], D.N. Muraviev[1], N. Vigués[2], J. Mas[2], J. Macanás[3,*]

[1]*Department of Chemistry, Universitat Autònoma de Barcelona, Campus UAB, 08193 Bellaterra, Spain.*
[2]*Department of Genetics and Microbiology, Universitat Autònoma de Barcelona, UAB, 08193 Bellaterra, Barcelona, Spain*
[3]*Department of Chemical Engineering, Universitat Politècnica de Catalunya, C/Colom 1, 08222, Terrassa, Spain.*

** corresponding author: Dr. Jorge Macanás, Department of Chemical Engineering, Universitat Politècnica de Catalunya, C/Colom 1, 08222, Terrassa, Spain.*
Telephone: +34 937398239, e-mail: jorge.macanas@upc.edu

Abstract

The development of reusable dual-purpose nanocomposite foams for catalytic and biocidal water treatment is reported. Small non-aggregated silver nanoparticles were made by Intermatrix Synthesis inside a polyurethane foam, which was chosen as a suitable polymeric matrix due to its high chemical and mechanical stability and also because it is one of the most cost-effective, food-grade polymers available, being really suitable for industrial applications. The antibacterial activity of the obtained nanocomposites was evaluated against suspensions of the Gram-negative bacteria *E. coli*, showing ideal bactericide features for being applied to bacterial disinfection of water. The catalytic activity was also evaluated through a model reaction carried out at different flow conditions. The possibility to reuse the catalytic nanocomposites was evaluated in 3 consecutive cycles, and, for all of them, almost no loss in the efficiency was found. Finally, the leakage of the catalytic species to the media was evaluated during the experiments and under extreme ageing conditions (3h in an ultrasonic bath), and almost no silver was found outside the matrix, what agreed with the results obtained for the catalytic experiments.

1. Introduction

There are about 780 million people in the world (it is to say, more than one-tenth of the world population) who have no access to clean and potable water.[1] There are also an additional number of people (ca. 3.4 million) who die each year from water, sanitation, and hygiene-related causes.[2] Therefore, the importance of potable water for people in some countries dictates the need for the development of innovative technologies and materials for the production of safe potable water. And, thanks to the development of new metal nanocomposites, new approaches are being established in wastewater treatment.[3]

Yet, even if the use of Metal Nanoparticles (MNPs) seems to open a new way towards the development of new age water treatments, some environmental and health safety risks (sometimes referred as nanotoxicity or nanosafety) must be intensively considered since the threats of leaked MNPs are still unclear.[4-7]

In this sense, the synthesis of polymer-metal nanocomposites, obtained by the direct incorporation of MNPs into polymeric matrices, has demonstrated to be an attractive approach preventing MNPs escape to the reaction medium.[8,9] The superior stability of such nanocomposites (in terms of low or even negligible MNPs release) allows the possibility to reuse the active species without losing efficiency. Under this regard, several techniques can be

applied in order to obtain such nanocomposites[9,10] and among them the Intermatrix synthesis (IMS) approach[11,12] allows coping with some of the main drawbacks of nanocomposite preparation and use such as self-aggregation and Ostwald ripening.[13]
Originally, the IMS had been applied only to ion exchange polymeric matrices (fibres, thin films, membranes and resin beads),[12] but recently the successful application of this methodology to polymeric matrices without ionogenic functional groups was achieved.[14] However, further investigation was still necessary in order to completely control the MNPs synthesis. Thus, this work is focused on the IMS synthesis of silver nanoparticles (AgNPs) in a non-ionic polymeric matrix that could act as water filter, such as Polyurethane Foams (PUFs).
Polyurethanes are a broad class of materials with different properties employed in a wide range of applications.[15] Among the different possible presentations, PUFs represent ca. 80 % of the total polyurethane market.[16] Moreover, PUFs exhibit high stability against chemical degradation, high mechanical durability, ease of separation from a solution, and they are also one of the most cost-effective polymers available, what makes them really suitable for practical low-cost applications.[17]
Up to now, very few studies had been focused on the development of nanocomposite polyurethane matrices.[18-26] These publications demonstrated that the incorporation of nano-objects (i.e. metal nanoparticles, carbon nanotubes) could significantly improve the mechanical or thermal properties of polyurethane materials and their further applicability.[21, 22] Among these previous works, those undertaking the incorporation of AgNPs in PUFs[20, 23-26] proved the possibility to synthesize them either by *in-situ* or *ex-situ* approaches.[9, 12]
Nevertheless, controlling the total metal load in the final nanocomposite was sometimes a pending issue. In a previous publication[14], the likelihood to enhance the ion exchange capacity (IEC) of the pristine PUF through an acid or basic pre-treatment was evaluated. Though, new functional groups were not formed and the final value of the IEC was not significantly affected, even if these pre-treatments did have some effect in the AgNPs final size and amount loaded. By means of this work, we try to shed more light on this issue and to deeply evaluate the final properties and thereby final applications of the obtained nanocomposites.
Regarding AgNPs-PUF materials applicability, it is worthy to mention that only disinfection purposes were considered in the related literature.[23-25] With the idea of optimizing the final use of such nanocomposites, our goal was to assess a dual-purpose material as water treatment filter: as antimicrobial material and as a catalyst for the degradation of hazardous compounds in water. In this sense, the antibacterial activity was considered against suspensions of the Gram-negative *Escherichia coli*. On the other hand and in order to evaluate the additional catalytic functionality, a model reaction was carried out in different flow conditions: the reduction of p-nitrophenol (4-np) to p-aminophenol (4-ap) in the presence of $NaBH_4$ and a metallic catalyst.[27]
Finally, to be consistent with the nanotoxicity concerns, special attention was paid to the stability of the nanocomposites obtained. First, the leakage of the active species to the media was evaluated during the experiments and under extreme aging conditions and, second, the possibility to reuse catalytic nanocomposites was also evaluated in up to 3 consecutive cycles.

2. Materials and methods

2.1. Materials

Commercial open-cell Polyurethane foam (PUF) with an average density of about 18.5 $g \cdot dm^{-3}$ was obtained from Comercial del Caucho (Spain). For bacterial tests, *Escherichia coli* (CGSC 5073 K12), Luria-Bertani medium (LB) and phosphate buffered saline (PBS) from Life

Technologies were used. HNO_3 was purchased from Fisher Chemical, whereas other reagents ($AgNO_3$, $NaBH_4$, 4-nitrophenol, solvents, acetone, NaOH) were all from Panreac. Deionized water was used for all the experiments

2.2. Pre-treatment of PUFs

Foams were washed with acetone and then with distilled water to eliminate the possible commercial post-treatments applied to the material.[28] The resulting material was designated as "pristine PUF" and samples were cut out either in cubic form (1 cm^3) or in disk shape (3 cm diameter, 1 cm width, ca. 7 cm^3). Different pre-treatments were applied to these samples by their immersion in 25 mL of a reagent solution (i.e. HNO_3 1M, HNO_3 3M, NaOH 1M, and NaOH 3M) for 2h, under agitation.[14] Afterwards, samples were washed several times with distilled water.

2.3. Synthesis of AgNPs

The synthesis of AgNPs in the polymeric matrices by the IMS methodology [11] consisted of two steps: (1) loading of the material with the metal ions ($AgNO_3$ 0.4 M solution) and (2) reduction of metal ions (by using $NaBH_4$ 0.5M solution) to build zero-valent MNPs up.

2.4. Nanocomposite characterization

In order to determine the exact metal content in the prepared nanocomposites, two replicates of samples of known weight were digested with concentrated HNO_3. The resulting solutions were appropriately diluted and analysed by Inductively Coupled Plasma Mass Spectrometry (ICP-MS, Agilent 7500).

High Resolution Transmission Electron Microscopy (HR-TEM) was performed by a Jeol JEM-2011 HR-TEM, and images were used to establish the real distribution of the AgNPs in the matrix, as well as to evaluate the size and shape of the obtained MNPs. Before HR-TEM observation nanocomposite samples were embedded in an epoxy resin and ultra-thin slices were obtained using an ultramicrotome (Leica EM UC6 with a 35° diamond knife, Diatome).

By using an image processing software (Adobe Professional) it was possible to measure the size of ca. 300 AgNPs per sample and to represent the corresponding size distribution histograms. Histograms were fitted to a three parameter Gaussian curve to find out the AgNPs average diameter.

2.5. Nanocomposite stability characterization

Nanocomposite samples were treated either by long-term immersion in warm water or by ultrasounds, as specified in **Table 1**. Two replicates of cubic samples of 1 cm^3 were deposited in a vessel with 10 mL of distilled water and placed for different times in the corresponding bath: an ultrasonic cleaner (Branson 1200) or an incubator (Aquatron Infors AG, shaker incubator). As ultrasounds can heat the solution, temperature variation in the ultrasonic bath was also monitored during the experiment.

Table 1. Experimental conditions of the nanocomposites stability characterization.
(Table 1 here)

After each experiment, silver content in both solution ($n_{Ag,\ solution}$) and matrix ($n_{Ag,\ matrix}$) were analysed by ICP-MS so as to determine the release percentage (R%), see **Equation (1)**. Matrix samples were digested as aforementioned. Typically, two replicates per time and sample were analysed.

$$R\% = \frac{100 \cdot n_{Ag,\,solution}}{\left(n_{Ag,\,solution} + n_{Ag,\,matrix}\right)} \quad (1)$$

2.6. Catalytic activity

The reduction of a nitroaromatic compound in water was evaluated by monitoring a model reaction: the reduction of 4-nitrophenol (4-np) to 4-aminophenol (4-ap) by $NaBH_4$ [27]. Kinetics were followed by a UV-Vis spectrometer (Pharmacia LKB Novaspec II spectrometer, λ = 390 nm). Experiments were carried out as it is described as follows: a disk-shaped nanocomposite sample was placed in a filter holder connected to a peristaltic pump that forced the test solution (4-np 0.5 mM and $NaBH_4$ 500 mM) to pass though the nanocomposite at different flow rates: 0.4, 1.7, 4,1 and 6.8 $mL \cdot min^{-1}$. Samples were used for up to 3 cycles of catalysis to their possible reuse.

The reaction was assumed to follow pseudo-first order kinetics due to the high excess of reducing agent (1000:1) so the reaction rate was expressed as an apparent constant rate (k_{app}) as shown in **Equation (2)**, being Abs_t and Abs_0 the solution absorbance at a defined time (t) and at the beginning of the experiment, respectively.[29]

$$Ln\,(Abs_t / Abs_0) = -k_{app} \cdot t \quad (2)$$

2.7. Antimicrobial properties

The procedure to evaluate the bactericidal activity of the Ag-nanocomposites is described elsewhere.[30] *Escherichia coli* CGSC 5073 was grown overnight in LB medium at 37 ºC. An aliquot of 20mL of culture was centrifuged for 10 minutes at 10000 x g (Eppendorf 5804R centrifuge). The supernatant liquid was removed and the pellet was suspended again in 10 mL of phosphate buffer saline (PBS) at pH 7.4. The bacterial suspension was then serially diluted down to $1 \cdot 10^7$ colony forming units (CFU) per mL. The initial concentration was measured by plating on LB agar.

To determine the bactericidal properties of the as-prepared nanocomposites and bare matrices, a cubic sample was immersed in 20 mL of bacterial suspension and maintained at 37 °C with gentle agitation (160 rpm). Periodically, 100 µL of each suspension were collected at different times and counted using plating and incubation on LB LB agar at 37ºC.

Besides, in order to evaluate the possible effect of the AgNPs or Ag^+ ions released to the medium during the experiments, a cubic sample was immersed in 20 mL of PBS and maintained for 24 h at 37 °C with gentle agitation. After this time, samples were removed, and an *Escherichia coli* pellet was suspended again in the solution. Aliquots of 100 µL were collected at different times and viable microorganisms were counted after cultivation on LB medium. The bactericide activity of the material was in relation to the positive control (raw material without NPs).

Two replicates per sample were analysed and manipulations were performed under sterile conditions.

3. Results

3.1. Nanocomposite characterization

After applying the IMS procedure to the cubic samples they turned dark, directly attesting to the successful loading of the AgNPs in the polymeric matrix. A quantitative value of metal loading was obtained by ICP-MS analyses and results are shown in **Table 2**. As it can be seen, the total metal amount in the nanocomposites was found to be in the range from 12 to 22

mg Ag/g matrix depending on the sample pre-treatment, which has been found to play an important role in the metal loading capacity. In this sense, and compared to pristine PUFs (17mg/g), an acid pre-treatment caused a lower metal retention (around 13 mg/g) compared with PUFs which were immersed in alkaline solutions that were able to incorporate a higher metal amount (about 20 mg/g). In other words, pre-treatments provide a way for tuning the total metal content in nanocomposite.

It was previously demonstrated [14] that the use of such pre-treatments did not affect the chemical composition of PUFs as new functional groups were not detected by Infrared Spectroscopy as the obtained spectra for treated samples was identical to the pristine PUF. Taking this into account, the observed loading differences can be attributed to the possible coordination of Ag^+ ions with lone electron pairs of nitrogen atoms of the polymeric structure: when an acid pre-treatment is applied, the nitrogen atom is mostly protonated and the formation of coordination bonds between the nitrogen and the Ag^+ is hindered. Therefore, less Ag^+ ions remain immobilized in the matrix and less AgNPs can be formed. Conversely, by a basic pre-treatment the number of binding positions is maximized.

The same idea of coordination bonds was reported by Jain *et.al* [23]. However, they incorporated *ex-situ* fabricated AgNPs into PUFs and their reasoning considered the formation of coordination bonds between the nitrogen lone pairs and the pre-formed AgNPs. Hence, it seems that the chemical structure of PUF plays an important role in both the formation and stabilization of the AgNPs.

Table 2. Ag content in cubic samples. All values are presented with their corresponding standard deviation of two replicates.

(Table 2 here)

(Figure1 here)

Figure 1. TEM images of the nanocomposite's cross section with the corresponding AgNPs diameter average.

Besides, having in mind that size, morphology and nanoparticles location are also crucial parameters to understand the properties of nanocomposites, TEM images of the cross-section were taken in order to estimate these parameters. **Figure 1** clearly shows that AgNPs were well dispersed in the matrix, without any clear agglomeration and that a narrow size distribution of the nanoparticles was observed, although the average diameter was not the same for all the samples. In fact, nanocomposites showed far larger AgNPs on the surface while smaller ones were observed inside the matrix, as is shown on the right column of **Figure 1** for the nanocomposites made of pristine PUF. The size of inner particles was in the range of 6 to 10 nm. Still, acid or basic pre-treatments seem not to dramatically affect the size and distribution of the AgNPs since there is not any well-defined correlation between the treatments applied and the average diameter.

From the results obtained up to this point, it is possible to state that the IMS methodology has been successfully applied to the synthesis of AgNPs with diameters below 10 nm in PUF and that no agglomeration of NPs was found. By using the IMS approach, the total metal content was up to ten-fold higher than the previously reported values corresponding to similar systems where *ex-situ* formed AgNPs were incorporated to PUF[21,23,25]. Moreover, comparing with other synthetic methods[10,12] it is noteworthy to mention that IMS does not require any stabilizer other than the polymeric matrix itself and that it is possible to easily tune the AgNPs loading in the nanocomposites by applying simple chemical treatments to the matrix.

3.2. Stability of the nanocomposites

Since one of the most serious concerns associated with the production and final uses of MNPs in real-life applications deals with the possibility of their uncontrollable release to the medium under treatment[5], in this work it was considered essential to evaluate the stability of the obtained nanocomposites.

To determine the eventual loss of AgNPs, cubic samples underwent different aging treatments (see **Table 1**) and the amount of metal found in solution was compared with the remaining amount in the sample. This study was limited to those treatments that involved the highest concentrations of reactants (e.g. HNO_3 3M and NaOH 3M) and results were compared with the pristine PUF nanocomposites.

As it can be observed in **Figure 2**, after 3h under aging conditions provided by sonication, the total Ag release calculated by **Equation (1)** did not exceed the 0.2% for any of the nanocomposites. On the other hand, after immersing the samples for 24h at 37 ºC, the amount of lost Ag was higher but it never exceeded 1% of the total amount of metal in the nanocomposites.

It is significant that the basic pre-treatment (NaOH 3M) allowed a better preservation of the nanoparticles inside the polymeric matrix for both aging treatments (ultrasonic or thermostatic bath with agitation). Again, this higher stability is in agreement with the Ag^+ coordination due to nitrogen atom lone electron pair, which can retain ionic species as well as AgNPs as suggested previously.[23] Accordingly, the basic pre-treatment would be preferable for a final application since it allows a higher loading of AgNPs and provides a stronger stabilization, even if all the release values are very low.

(Figure 2 here)

Figure 2. Ag release (a) after 1 and 3 h in the ultrasonic bath, and (b) after 24h at 37 ºC, 160 rpm. Results are presented with the corresponding standard deviation

Besides, the influence of the ultrasounds aging treatment on AgNPs size and size distribution was also considered and **Table 3** reports the AgNPs average diameters measured from TEM images of the different samples after different periods of time together with the original values (0 h).

Table 3. AgNPs average diameters before and after ultrasounds treatment.

(Table 3 here)

The experimental results evidenced that after ultrasonic treatment, the AgNPs average diameter slightly diminished from 6-10 nm to 4-6 nm except for one of the samples which tendency was not consistent (HNO_3 3M). The diameter shrinkage was achieved in 1 h and no further diminution was observed for a longer period (3 h). Note that samples that originally contained AgNPs of about 6 nm did not dramatically change their size whereas bigger particles (> 6 nm) became smaller.

The size change can be attributed to the loss of the larger unstable AgNPs to the medium, so that only those AgNPs that were better stabilized (the smaller ones, mainly found in the inner part of the nanocomposite) remained. Therefore, the use of ultrasounds can be understood as an interesting post-treatment for the synthesized nanocomposites, useful to remove the unstable AgNPs as well as to reduce the average diameter of AgNPs what would result in a greater catalytic surface and, accordingly, in a substantially improved reactivity. Such post-treatment will somehow guarantee that the amount of AgNPs lost to the reacting media will be minimized. Notice that these advantages can be afforded without an important reduction in the amount of immobilised silver since the AgNPs losses were extremely low (< 0.2 %).

3.3. Catalytic activity

Preliminary experimental results concerning the catalytic activity of AgNP-PUF nanocomposites were performed in batch configuration and demonstrated the ability of such nanocomposites to catalyze the reduction of 4-np to 4-ap in basic media.[14] Not dramatic differences were found for acid or basic pre-treatments even if the latter showed a shorter induction period. However, taking into account that the developed nanocomposites could be applied as reactive water filters, it was necessary to evaluate their catalytic performance in flow conditions as well as their possible reutilization

Table 4. Ag content in disk samples. All values are presented with their corresponding standard deviation of two replicates.

(Table 4 here)

Since the nanocomposite used for these catalytic experiments had to be placed in the circular filter holder showed, disk-shaped foams were cut out and nanocomposites were prepared as usual. The total metal load was evaluated by ICP-MS and results were in close agreement with the ones obtained for cubic samples, proving the high reproducibility of the IMS technique (see **Table 4**).

The catalytic activity of all the nanocomposites made of different PUF (pristine, NaOH 1M, NaOH 3M, HNO_3 1M and HNO_3 3M) was first evaluated at a constant flow rate (1.7 $mL \cdot min^{-1}$) and the corresponding results are shown in **Figure 3a**. Plotted data of normalized absorbance at 390 nm (at which the maximum absorbance of 4-np is produced) indicated that the catalytic performance was very similar for all the nanocomposites disregarding the endured pre-treatment. This situation is quite controversial since, *a priori*, one might expect that those nanocomposites with higher silver content (NaOH 1M or NaOH 3M) would have performed better. However, as no significant differences were found for the different samples it is possible to assume that all of them exceed a minimal amount of catalyst that ensured the catalytic reaction at that flow rate. The higher porosity of the PUF along with the AgNPs location are beneficial aspects for the catalytic reaction if we compare them with other systems such as Nafion nanocomposites containing AgNPs reported elsewhere.[31] Despite the fact that Nafion nanocomposites contained a higher amount of catalytic metal (ca. 52 mg/g), the dense structure of the polymeric matrix combined with a lower distribution on the surface played a negative role in the final catalytic application. So, it seems that nanocomposites based on PUF are advantageous materials.

Likewise, from a practical point of view, one can reason that those nanocomposites prepared with PUFs that undergone an acid pre-treatment could be preferable as the amount of precious metal is the lowest (ca. 11 mg/g) and the catalytic efficiency was the same. Anyhow, in terms of simplicity, the nanocomposites prepared with pristine PUF are more advantageous as they can be prepared without difficulty and without any unnecessary step.

(Figure 3 here)

Figure 3. Catalytic evaluation of the nanocomposites (a) with different pre-treatments and (b) at different flow conditions for the nanocomposite made of pristine PUF.

Consequently, once the effect of the pre-treatment was discarded, the impact of the flow conditions was evaluated by using exclusively nanocomposites made of pristine PUF (without any pre-treatment except for the acetone rinsing). Results presented in **Figure 3b** show the variation of the normalised absorbance for experiments carried out at different flow conditions: 0.4, 1.7, 4.1 and 6.8 $mL \cdot min^{-1}$. In this case, there was a remarkable effect: the higher the flow, the fastest the reaction, albeit the trend was not linear. This effect can be

explained because at higher flow conditions, a higher amount of reactants flow through the nanocomposite for the same period of time and, therefore, the conversion of reactants to products is faster.

Additionally, in order to verify the above-mentioned good results regarding AgNPs stability, the synthesized new materials were evaluated in different consecutive catalytic cycles. Results presented in **Figure 4** correspond to the 4-np reduction by $NaBH_4$ performed with nanocomposites made of pristine PUF for 3 consecutive catalytic cycles and at different flow conditions.

(Figure 4 here)

Figure 4. Comparison between catalytic cycles in different flow conditions of the nanocomposite made of pristine PUF. ■run#1, ● run#2, ◇ run#3.

As it can be clearly seen, the effect of the flow conditions in each cycle remains the same as before and it is noteworthy that almost no variation in the reaction rates between cycles was observed. The single experiment that was not perfectly consistent was that performed at 1.7 $ml \cdot min^{-1}$, what can be attributed to experimental errors.

As main conclusion of this part, the durable catalytic efficiency together with the low loss of the AgNPs to the media seems to confirm the suitability of the material for catalytic purposes.

3.4. Antimicrobial properties

The antibacterial mechanisms of AgNPs are still not completely understood nowadays but this fact has not hindered the development of many antibacterial systems that profit of the particular properties of such nanoparticles.[32]

Generally it is widely accepted that the main antibacterial effect of AgNPs or AgNPs-based materials is due to its partial oxidation and release of Ag^+.[33] After oxidation occurs, some actions can happen either simultaneously or separately: (1) disruption of adenosine triphosphate (ATP) production; (2) disturbance of DNA replication; (3) interaction with bacterial proteins; or (4) direct cell membrane damage. Several works have stated that AgNPs may increase the cell membrane permeability and, subsequently, penetrate inside cells to induce any one or the entire cascade of quoted effects.[34]

Up to now, there have been few but encouraging attempts to prepare AgNPs-containing antimicrobial materials based on PUFs.[23-25] Taking into account the previous promising results obtained by other authors using the same polymeric matrix, the catalytic nanocomposite filters were also evaluated as bactericidal filters, envisaging a dual-purpose filter for advanced water treatment.

Following a procedure described elsewhere[30,31] cubic samples (1 cm^3) of AgNPs-containing nanocomposite made of pristine PUF were exposed to the cultivation medium. Samples without AgNPs were also evaluated to ascertain any possible effect of the polymeric matrix, such as adsorption of the microorganisms on the matrix. Besides, the antibacterial properties of released silver were also estimated by using a water solution where nanocomposites were immersed for 24 h.

(Figure 5 here)

Figure 5. Cell viability versus time. Inicial dose: 10^7 CFU/mL in PBS.

In **Figure 5**, where the cell viability percentage is plotted versus time, it is possible to see that the cell population is not affected by the presence of pristine PUF without AgNPs. Even if small variations in the number of cells can be observed, they can be attributed to experimental error of CFU counting or to cell adsorption onto the polymeric matrix. As expected, the percentage of cell viability strongly decreased with time for test tubes where the solution was

in contact with AgNPs-PUF or with released AgNPs/Ag^+. In fact, nanocomposite samples (AgNPs-PUF) were able to kill the 100% of bacteria in less than 6.5 h.

From the results obtained it was possible to calculate the mortality rate, expressed as the number of CFU deactivated per second in a single milliliter of the treated solution. For the PUF-AgNPs the calculated value was ca. 1000 $CFU \cdot mL^{-1} \cdot s^{-1}$. Although in previous publications focused on the antibacterial application of AgNPs-PUF nanocomposites[23-25] this rate is not explicit, it is possible to state that the nanocomposites here-developed showed a mortality rate 3-6 fold higher. For instance, from the data reported by Phong *et al.*, the calculated mortality rate that attains the highest value was about 300 $CFU \cdot mL^{-1} \cdot s^{-1}$.[25]

This increase in the bactericidal activity could be first accredited to the higher load of AgNPs found in the nanocomposites obtained by the IMS procedure. However, when comparing the results here presented with other silver-nanocomposites prepared by the same synthetic methodology, (membranes[31], resin beads[35] and fibers[30]) the mortality rate of the AgNPs-PUF appeared to be up to 2 orders of magnitude higher. This exceptional result states not only for the synthetic methodology, but also for the suitable usefulness of the polymeric matrix employed.

Moreover, from the results obtained with the Ag released from the sample (after 24h in 20 mL of a PBS solution under gentle agitation at 37 ºC) a second conclusion can be drawn: the metal amount released to the media (either AgNPs or Ag^+) was enough to kill all the microorganisms in a short period as 2 h. This means that once the solution is not in contact with the nanocomposite (either because it is missing, deactivated, or exhausted), a remaining mortality rate of about 2500 $CFU \cdot mL^{-1} \cdot s^{-1}$ is still active. Hence, these nanocomposites can be considered as Ag reservoirs with a remaining antibacterial effect and, consequently, they can provide a residual disinfection effect prolonging the possible use of the nanocomposite filter.

4. Conclusions

In this work the preparation and use of reusable AgNPs-PUF nanocomposites as dual-purpose water filters has been evaluated. The preparation AgNPs in Polyurethane foams by the IMS methodology allowed obtaining small non-aggregated AgNPs (diameters between 6-10 nm) all over the matrix. The total metal loading of the prepared nanocomposites as well as the nanoparticle size can be tuned by applying simple acid or basic pre-treatments to the polymeric matrix.

Regarding the stability of the prepared AgNPs, they turned to be very stable as the released Ag never exceeded the 0.2 % of the initial amount after heavy aging conditions (ultrasonic bath). Among the different samples, those which underwent a basic treatment showed the higher stability, what can be explained due to the establishment of coordination bonds between de lone electron pairs of the nitrogen atom of the urethane group with either Ag^+ or AgNPs. On the other hand, after 24 h in water under agitation at 37 ºC the amount of Ag lost was found to be slightly higher, but never exceeded the 1% of the total amount of Ag in the nanocomposites.

Developed nanocomposites exhibited durable catalytic activity when evaluating the reduction of nitroaromatic compounds in water. By changing the flow conditions, the catalytic efficiency could be improved: the higher the flow, the higher the reaction rate. This trend was confirmed even after 3 consecutive catalytic cycles, showing that there were almost no losses in the catalytic efficiency after each cycle, what testifies the great suitability of the synthetic technique and of the matrix itself.

Regarding the antibacterial activity, Ag-containing nanocomposites were able to wipe out all of the microorganisms present in solution in quite short times, even shorter than other previous publications using similar nanocomposites.[21,23,25] Moreover, the bactericidal

effect of released silver can be considered as an additional contribution to the antimicrobial activity of the nanocomposites providing a residual disinfection effect.
Accordingly, and as a main conclusion, it was possible to achieve the targeted stable dual-function reusable polymer-metal nanocomposites by using a low-cost readily available polymer that can be used for high effective and low-cost new water treatments.

Acknowledgements
This work was supported by CTQ2009-14390-C02-02 from the Ministry of Science and Innovation of Spain (MCINN). Special thanks are given to Servei de Microscòpia from Universitat Autònoma de Barcelona.

References

1. UNICEF and World Health Organization, *Progress on Drinking-Water and Sanitation: 2012 Update*. UNICEF and World Health Organization , New York, **2012**.
2. A. Prüss-Üstün, R. Bos, F. Gore, J. Bartram, *Safer Water, Better Health: Costs, benefits, and sustainability of interventions to protect and promote health*, World Health Organization, Genova, **2008**.
3. M.A. Shannon, P.W. Bohn, M. Elimelech, J.G. Georgiadis, B.J. Marinas, A.M. Mayes, Nature, **2008**; 452, 7185).
4. P.J.A. Borm, D. Berube, Nano Today, **2008**; 3, 1–2.
5. Q. Li, S. Mahendra, D.Y. Lyon, L. Brunet, M.V. Liga, D. Li, P.J.J. Alvarez, Water Res., **2008**; 42, 18.
6. S.F. Hansen, A. Baun, Nat. Nanotechnol., **2012**; 7, 7.
7. P.V. AshaRani, G. Low Kah Mun, M.P. Hande, S. Valiyaveettil, ACS Nano, **2008**; 3, 2.
8. B.A. Rozenberg, R.Tenne, Prog. Polym. Sci., **2008**; 33, 1.
9. L. Nicolais,G. Carotenuto, *Metal-Polymer Nanocomposites*, John Wiley and Sons Ltd., New York, **2004**.
10. J.M. Campelo, D. Luna, R. Luque, J.M. Marinas, A.A. Romero, ChemSusChem, **2009**; 2, 1.
11. D.N. Muraviev, J. Macanás, M. Farre, M. Muñoz, S. Alegret, Sens. Actuators, B, **2006;** 118**,** 1-2.
12. B. Domènech, J. Bastos-Arrieta, A. Alonso, M. Muñoz, D.N. Muraviev, J. Macanás, in *Ion Exchange Technologies*, (Ed. A. Kilislioglu), **2012**, pp. 5-72.
13. S.B. Simonsen, I. Chorkendorff, S. Dahl, M. Skoglundh, J. Sehested, S. Helveg, J. Am. Chem. Soc., **2010**; 132, 23.
14. B. Domènech, K. Ziegler, J. Macanás, F. Carrillo, M. Muñoz, D.N. Muraviev, Nanoscale Res. Lett., **2013**; 8, 1.
15. J.E. Mark, *Physical Properties of Polymers Handbook*, Springer, New York, **2007**.
16. K.K. Uhlig, *Discovering Polyurethanes*, Hanser Publishers, Munich, **1999**.
17. J.I. Kroschwitz, A. Seidel, *Kirk-Othmer Encyclopedia of Chemical Technology*, Wiley-Interscience, John Wiley and Sons, Michigan, **2004**.
18. L. Madaleno, R. Pyrz, A. Crosky, L.R. Jensen, J.C.M. Rauhe, V. Dolomanova, A.M.M.V. de Barros Timmons, J.J. Cruz Pinto, J. Norman, Composites, Part A, **2013**; 44, 0.
19. J.G. Han, Y.Q. Xiang, Y. Zhu, J. Inorg. Organomet. Polym. Mater., **2014**; 24, 0.
20. V. Apyari, P. Volkov, S. Dmitrienko, Adv. Nat. Sci.: Nanosci. Nanotechnol., **2012**; 3, 1.
21. C.-W.Chou, S.-H. Hsu, H. Chang, H., S.-M. Tseng, H.-R. Lin, Polym. Degrad. Stab., **2006**; 91, 5.

22. H. Deka, N. Karak, R.D. Kalita, A.K. Buragohain, Polym. Degrad. Stab., **2010**; 95, 9.
23. P. Jain, T. Pradeep, Biotechnol. Bioeng., **2005**; 90, 1.
24. G. Mulongo, J. Mbabazi, P. Nnamuyomba, S. Hak-Chol, Nanosci. Nanotechnol., **2011**; 1 (2).
25. N.T.P. Phong, N.V.K. Thanh, P.H.Phuong, J. Phys.: Conf. Ser., IOP Publishing, **2009.**
26. W. Mackay, *Antimicrobial foam and method of manufacture,* Patent: US 2011/0200674 A1, United States, **2010**, pp. 13
27. J. Macanás, L. Ouyang, M.L. Bruening, M. Muñoz, M., J.-C. Remigy, J.-F. Lahitte, Catal. Today, **2010**; 156, 3-4.
28. E.A. Moawed, Anal. Chim. Acta, **2006**; 580, 2.
29. B. Domènech, M. Muñoz, D.N. Muraviev, J. Macanás, Nanoscale Res. Lett., **2011**; 6, 406.
30. A. Alonso, N. Vigués, X. Muñoz-Berbel, J. Macanás, M. Muñoz, J. Mas, D.N. Muraviev, Chem. Commun., **2011**; 47, 37.
31. B. Domènech, N. Vigués, J. Mas, M. Muñoz, D.N. Muraviev, J. Macanás, Solvent Extr. Ion Exch., **2013**; Accepted on september 2013. DOI: 10.1080/07366299.2013.839192.
32. A. Panáček, L. Kvítek, R. Prucek, M. Kolář, R. Večeřová, N. Pizúrová, V.K. Sharma, T.J. Nevěčná, R. Zbořil, R., J. Phys. Chem. B, **2006**; 110, 33.
33. E. T. Hwang, J.H. Lee, Y.J. Chae, Y.S. Kim, B.C. Kim, B.-I. Sang, M.B. Gu, Small, **2008**; 4, 6.
34. O. Choi, K.K. Deng, N.-J. Kim, L. Ross Jr, R.Y. Surampalli, Z. Hu, Water Res., **2008**; 45, 12.
35. A. Alonso, X. Muñoz-Berbel, N. Vigués, R. Rodríguez-Rodríguez, J. Macanás, M. Muñoz, J. Mas, D.N. Muraviev, Adv. Funct. Mater., **2013**; 39, 19.

TABLES

Table 1. Experimental conditions of the nanocomposites stability characterization.

Experiment	T (ºC)	Solution composition	Duration (h)
Ultrasonic bath	19-43	Deionised water	3
Thermostatic stirred bath	37	Deionised water	24

Table 2. Ag content in cubic samples. All values are presented with their corresponding standard deviation of two replicates.

Pre-treatment	HNO_3 1M	HNO_3 3M	pristine	NaOH 1M	NaOH 3M
Total metal load (mg Ag/g matrix)	12.7 ±0.2	13.4±1.5	16.7±1.4	19.6±1.0	20.0±1.3

Table 3. AgNPs average diameters before and after ultrasounds treatment.

Sample	0 h	1 h	3 h
pristine	9.4 ± 0.2	5.2 ± 0.1	4.70 ± 0.03
HNO_3 1M	6.8 ± 0.1	6.1 ± 0.4	6.4 ± 0.3
HNO_3 3M	10.4 ± 0.2	5.4 ± 0.1	8.37 ± 0.2
NaOH 1M	6.3 ± 0.2	5.0 ± 0.3	6.4 ± 0.1
NaOH 3M	9.4 ± 0.1	4.9 ± 0.4	4.34 ± 0.3

Table 4. Ag content in disk samples. All values are presented with their corresponding standard deviation of two replicates.

Pre-treatment	HNO_3 1M	HNO_3 3M	pristine	NaOH 1M	NaOH 3M
Total metal load (mg Ag/g matrix)	11.0 ±0.1	10.9±0.3	15.6±3.3	21.2±1.7	21.2±5.4

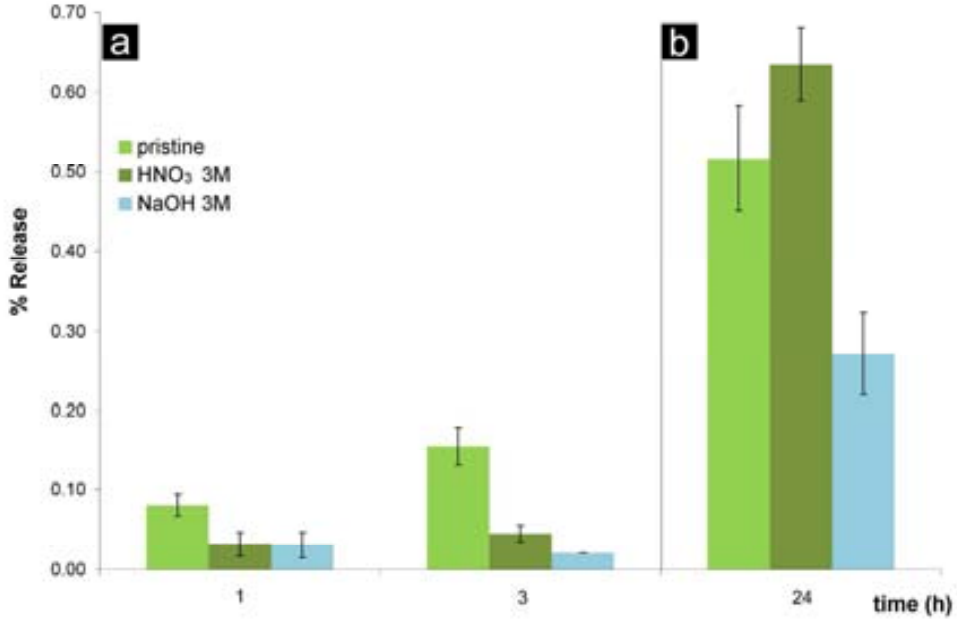

Figure 2. Ag release (a) after 1 and 3 h in the ultrasonic bath, and (b) after 24h at 37 ºC, 160 rpm. Results are presented with the corresponding standard deviation
270x180mm (300 x 300 DPI)

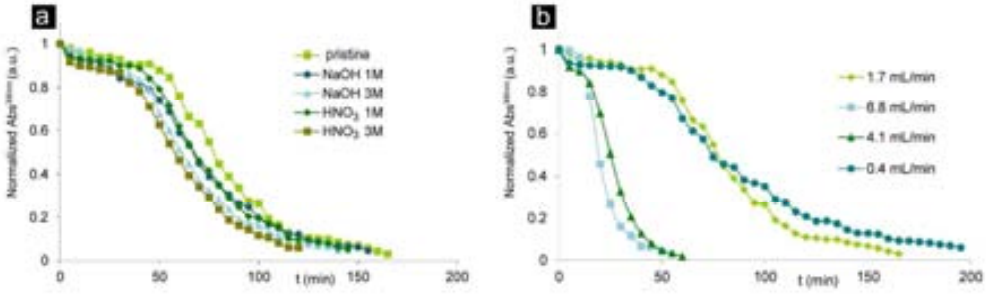

Figure 3. Catalytic evaluation of the nanocomposites (a) with different pre-treatments and (b) at different flow conditions for the nanocomposite made of pristine PUF.
480x146mm (300 x 300 DPI)

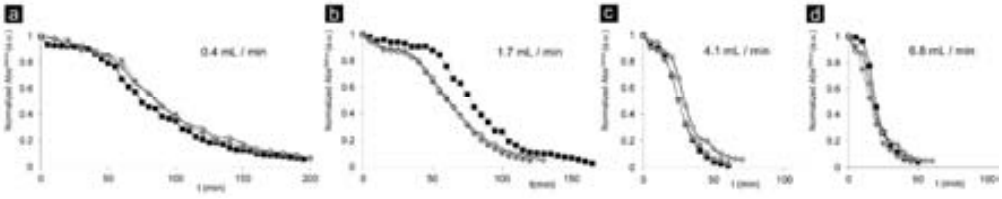

Figure 4. Comparison between catalytic cycles in different flow conditions of the nanocomposite made of pristine PUF. ν run#1, λ run#2, ↓ run#3.
713x142mm (300 x 300 DPI)

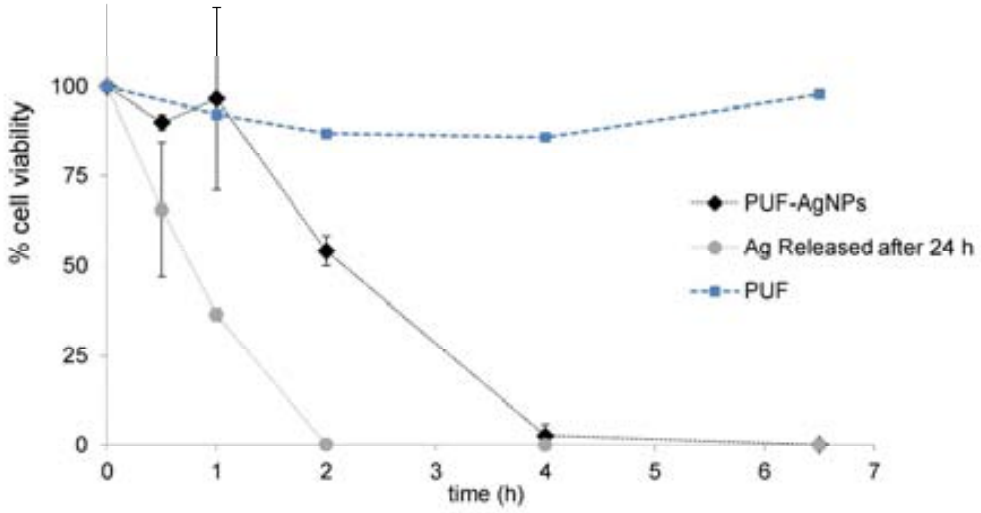

Figure 5. Cell viability versus time. Inicial dose: 107 CFU/mL in PBS.
279x163mm (300 x 300 DPI)

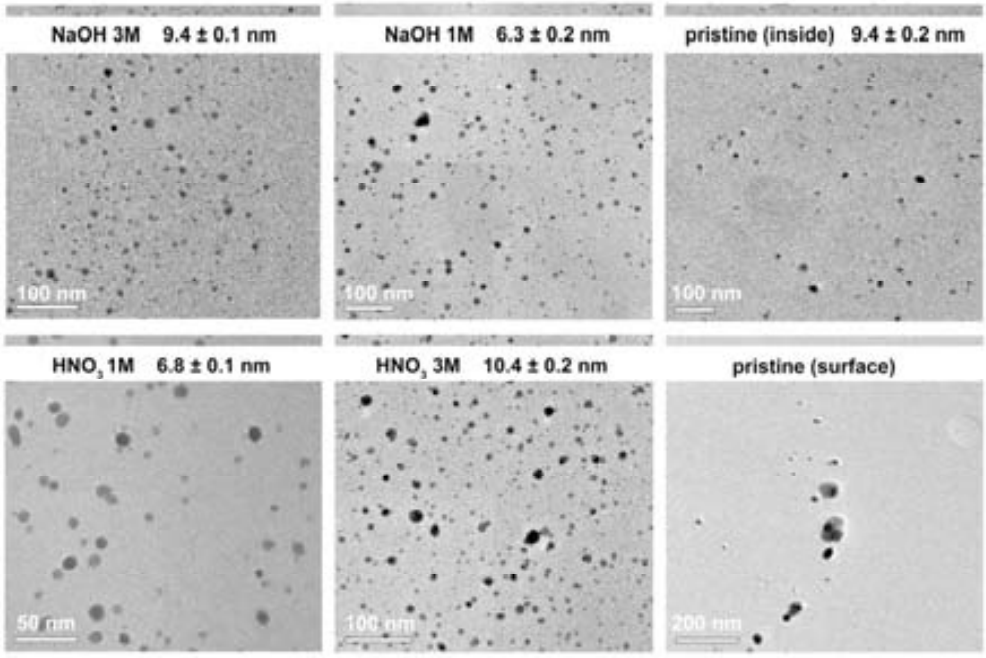

Figure 1. TEM images of the nanocomposite's cross section with the corresponding AgNPs diameter average.
137x93mm (300 x 300 DPI)

INTERMATRIX SYNTHESIS . metal nanoparticles . silver . palladium . stabilization . POLYMERIC MATRICES . membranes . sulfonation . polyethersulfone with cardo group . polyphenylsulfone. nafion . polyurethane foams . textile fibers . DUAL FUNCTION . water treatment . catalysis . nitroaromatic . biocide . escherichia coli . release . reusable . filters .